FOUNDATION DESIGN
THEORY AND PRACTICE

Foundation Design: Theory and Practice N. S. V. Kameswara Rao
 ISBN: 978-0-470-82534-1

FOUNDATION DESIGN
THEORY AND PRACTICE

N. S. V. Kameswara Rao
Universiti Malaysia Sabah, Malaysia

John Wiley & Sons (Asia) Pte Ltd

This edition first published 2011

Registered office
John Wiley & Sons (Asia) Pte Ltd, 2 Clementi Loop, # 02-01, Singapore 129809

Library of Congress Cataloging-in-Publication Data

Kameswara Rao, N. S. V.
Foundation design : theory and practice / N.S.V. Kameswara Rao.
p. cm.
Includes bibliographical references and index.
ISBN 978-0-470-82534-1 (hardback)
1. Foundations. I. Title.
TA775.K337 2010
624.1'5–dc22 2010029407

Print ISBN: 978-0-470-82534-1
ePDF ISBN: 978-0-470-82535-8
oBook ISBN: 978-0-470-82536-5
ePub ISBN: 978-0-470-82815-1

Typeset in 10/12pt Times by Thomson Digital, Noida, India.

To
Divinity
all pervading

Contents

Preface

It is well realized that 'Geotechnical Engineering is an engineering science but its practice is an art!' Foundations are essential interfaces between the superstructure and the supporting soil at the site of construction. Thus they have to be designed logically to suit the loads coming from the superstructure and the strength, stiffness and other geological conditions of the supporting soil. With an enormous increase in construction activities all over the world, structures and their foundations have become very sophisticated while the supporting soil has to accommodate these variations and complexities. This book focuses on the analysis and design of foundations using rational as well as conventional approaches. It also presents structural design methods using codes of practice and limiting state design of reinforced concrete (RCC) structures.

This book was evolved from the courses on Foundation Engineering taught by the author formerly in the Indian Institute of Technology Kanpur, India and presently in the School of Engineering and IT, Universiti Malaysia Sabah, Kota Kinabalu, Malaysia. Accordingly, the contents of the book are presented in a user-friendly manner that is easy to follow and practice.

Contents

The book consists of 12 chapters plus appendices. Chapters 1–3 present the engineering properties, tests and design parameters needed for the analysis and design of foundations. Chapter 4 discusses the conventional and rational approaches for designing different types of shallow foundations, including rafts. Methods for exact solutions using beams and plates on elastic foundations are presented in Chapter 5. Numerical methods of analysis such as finite difference method (FDM) and methods of weighted residuals (Galerkin, least squares, etc.) are discussed in Chapter 6. The finite element method (FEM) for foundation analysis is explained in Chapter 7. The design criteria for shallow foundations are presented in Chapter 8 while actual design principles are given in Chapter 12 along with structural design details. Chapter 9 discusses the design and construction of deep foundations such as piles, large diameter drilled piers, pile raft systems and non-drilled piers/caissons. The construction aspects and design of pile foundations are presented in Chapter 10. The principles of machine foundation design are discussed in Chapter 11. Chapter 12 summarizes the important provision of RCC design codes and comparative features of commonly used codes such as the Indian Code, Euro Code, and ACI Code. As mentioned earlier, detailed examples of structural design of shallow foundations are also given in this chapter.

Special Features

Every effort has been made to include the background material for easy understanding of the topics being discussed in the text. Both conventional and rational approaches to analysis and design are included. For example, the provision of RCC codes, pile design and construction, vibration theory and construction practices, as well as tests for obtaining the design parameters are included in the respective chapters. Examples of structural design of foundations are also discussed in detail. Comparative features of different RCC codes relevant to foundation design are also examined to help designers. In addition, several examples have been worked out to illustrate the analysis and design methods presented. Also, assignment problems are given at the end of each chapter for practice.

The author hopes that this book will be a very useful resource for courses on Foundation Engineering and Design, Soil-Structure Interaction, and so on, at undergraduate as well as postgraduate levels, besides being helpful to research, development and practice.

N. S. V. Kameswara Rao
January, 2010

Acknowledgments

I am happy to bring out this book on *Foundation Design: Theory and Practice* after teaching this course formerly at IIT Kanpur, India, and currently at the School of Engineering and IT, Universiti Malaysia Sabah, Kota Kinabalu, Malaysia. I express my gratitude to all my colleagues, students and authorities in both of these institutions for their cooperation and help in bringing out this book. I am extremely happy that this book is being published during the Golden Jubilee Year (2010) of IIT Kanpur, India. I am thankful to Dr. B.M. Basha, Assistant Professor, Department of Civil Engineering IIT, New Delhi (former M. Tech. student at IIT Kanpur), for his extensive help in working out the design examples (Appendix 12.C). I am grateful to Dr. John W. Bull, Newcastle University, United Kingdom, for reviewing and giving useful suggestions on Appendix 12.D – Comparative Features of Concrete Codes, included in this book. My thanks are also due to Ms. Chong Chee Siang and Mr. Ashrafur Rob Chowdhury, graduate students at Universiti Malaysia Sabah for their help in preparing the manuscript and figures. I also thank Mr. K.P. Chary, former graduate student at IIT Kanpur for helping in the preparation of the manuscript.

I am pleased to thank Dr. Rosalam Sarbatly, Dean, Mr. Radzif and Mr. Jodin, former and current Heads of the Civil Engineering Program, School of Engineering and IT, Universiti Malaysia Sabah, for their encouragement in publishing this book.

I offer my grateful salutations to my parents for their blessings. Finally, I am delighted to express my thanks to my wife Ravi Janaki, grandchildren Raaghavi and Harish, and my family members Sree, Ravi, Siva, Sarada, Krishna and Kalyani for their enthusiastic support during the preparation of this book.

N. S. V. Kameswara Rao
January, 2010

1

Introduction

1.1 Foundations, Soils and Superstructures

Foundations are essential to transfer the loads coming from the superstructures such as buildings, bridges, dams, highways, walls, tunnels, towers and for that matter every engineering structure. Generally that part of the structure above the foundation and extending above the ground level is referred to as the *superstructure*. The foundations in turn are supported by soil medium below. Thus, soil is also the foundation for the structure and bears the entire load coming from above. Hence, the structural foundation and the soil together are also referred to as the *substructure*. The substructure is generally below the superstructure and refers to that part of the system that is below ground level. Thus, the structural foundation interfaces the superstructure and the soil below as shown in Figures 1.1 and 1.2. The soil supporting the entire structure above is also referred to as subsoil and/or subgrade. For a satisfactory performance of the superstructure, a proper foundation is essential.

The manmade superstructures or facilities/utilities are expected to become very intricate and complex depending on creativity, architecture and infinite scope in modern times. However, the soil medium is mother earth which is a natural element and very little can be manipulated to achieve the desirable engineering properties to carry the large loads transmitted by the superstructure through the interfacing structural foundation (which is usually referred to as the foundation). Further, almost all problems involving soils are statically indeterminate (Lambe and Whitman, 1998) and soils have a very complex behavior, as follows:

1. Natural soil media are usually not linear and do not have a unique constitutive (stress–strain) relationship.
2. Soil is generally nonhomogeneous, anisotropic and location dependent.
3. Soil behavior is influenced by environment, pressure, time and several other parameters.
4. Because the soil is below ground, its prototype behavior cannot be seen in its entirety and has to be estimated on the basis of small samples taken from random locations (as per provisions and guidelines).
5. Most soils are very sensitive to disturbances due to sampling. Accordingly, their predicted behavior as per laboratory samples could be very much different from the *in situ* soil.

Foundation Design: Theory and Practice N. S. V. Kameswara Rao
 ISBN: 978-0-470-82534-1

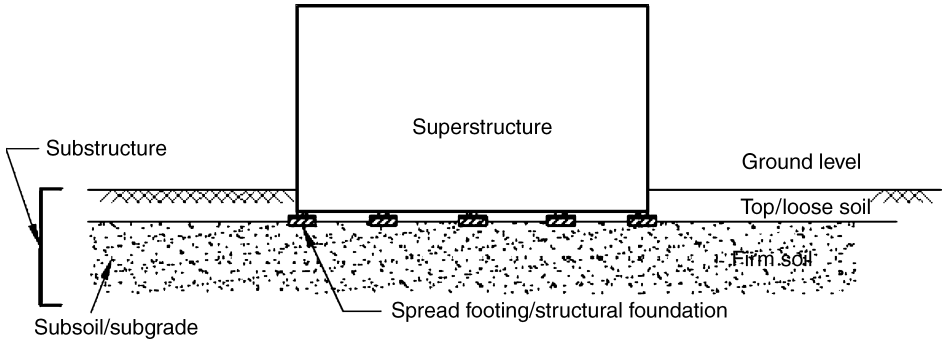

Figure 1.1 Building with spread foundations.

Thus, foundation design becomes a challenging task to provide a safe interface between the manmade superstructure and the natural soil media whose characteristics have limited scope for manipulation. Hence, the above factors make every foundation or soil problem very unique which may not have an exact solution.

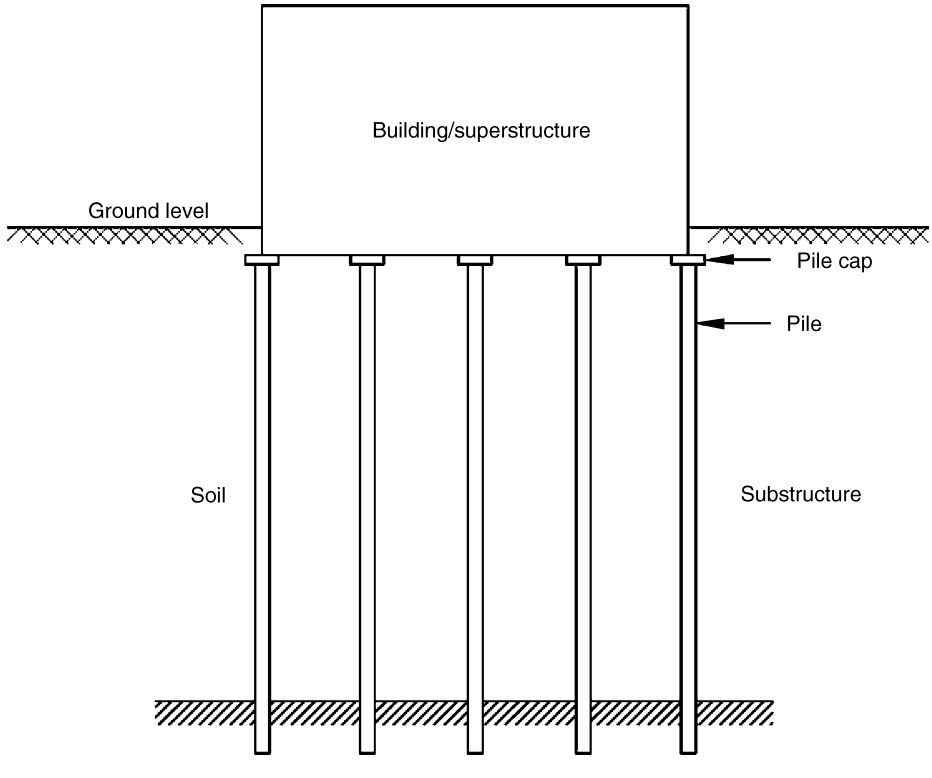

Figure 1.2 Superstructure with pile foundations.

The generally insufficient and conflicting soil data, selection of proper design parameters for design, the anticipated mode for design, the perception of a proper solution and so on require a high degree of intuition – that is, engineering judgment. Thus, foundation engineering is a complex blend of soil mechanics as a science and its practice through foundation engineering as an *art*. This may be also referred to as *geotechnique* or *geotechnical engineering*.

1.2 Classification of Foundations

Foundations are classified as shallow and deep foundations based on the depth at which the load is transmitted to the underlying and/or surrounding soil by the foundation as follows.

1.2.1 Shallow Foundation

A typical shallow foundation is shown in Figure 1.3(a). If $D_f/B \leq 1$, the foundations are called shallow foundations, where D_f = depth of foundation below ground level, and B = width of foundation (least dimension). Common types of shallow foundations are continuous wall footing, spread footing, combined footing, strap footing, grillage foundation, raft or mat foundation and so on. These are shown in Figure 4.2.

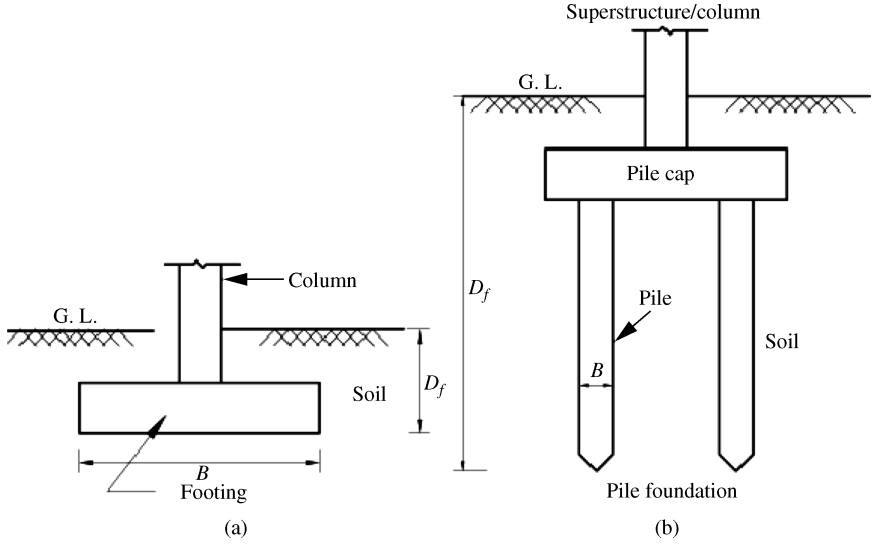

Figure 1.3 Shallow and deep foundations.

All design and analysis considerations of shallow foundations are discussed in Chapters 4–8 and 12. The shallow foundations are thus used to *spread* the load/pressure coming from the column or superstructure (which is several times the safe bearing pressure of supporting soil) horizontally, so that it is transmitted at a level that the soil can safely support. These are used when the natural soil at the site has a reasonable safe bearing capacity, acceptable compressibility and the column loads are not very high.

1.2.2 Deep Foundations

A typical deep foundation is shown in Figure 1.3(b). If $D_f/B \geq 1$, the foundations are called deep foundations such as piles, drilled piers/caissons, well foundations, large diameter piers, pile raft systems. The details of analysis and design of such foundations are discussed in Chapters 9 and 10.

Deep foundations are similar to shallow foundations except that the load coming from columns or superstructure is transferred to the soil vertically. These are used when column loads are very large, the top soils are weak and the soils with a good strength and compressibility characteristics are at a reasonable depth below ground level. Further, earth retaining structures are also classified under deep foundations.

Foundations can be classified in terms of the materials used for their construction and/or fabrication. Usually reinforced concrete (RCC) is used for the construction of foundations. Plain concrete, stone and brick pieces are also used for wall footings when the loads transmitted to the soil are relatively small. Engineers also use other materials such as steel beams and sections (such as in grillage foundations and pile foundations), wood as piles (for temporary structures), steel sheets (for temporary retaining structures and cofferdams) and other composite materials.

Sometimes, these are also encased in concrete depending on the load and strength requirements (Bowles, 1996; Tomlinson, 2001).

1.3 Selection of Type of Foundation

While engineering judgment and cost play a very important role in selecting a proper foundation for design, the guidelines given in Table 1.1 can be helpful (please see also Chapters 4–12).

1.4 General Guidelines for Design

Following broad guidelines may be useful for foundation design and construction, depending on site.

1. Footings should be constructed at an adequate depth below ground level to avoid passive failure of the adjacent soil by heaving.
2. The footing depth should be preferably below the zone of seasonal volume changes due to freezing, thawing, frost action, ground water and so on.
3. Adequate precautions have to be taken to cater for expansive soils causing swelling pressure (upward pressure on the footing).
4. The stability of the footing has to be ensured against overturning, sliding, uplift (floatation), tension at the contact surface (base of the footing), excessive settlement and bearing capacity of soil.
5. The foundation needs to be protected against corrosion and other harmful materials that may be present in the soil at site.
6. The design should have enough flexibility to take care of modifications of the superstructure at a later stage or unanticipated site conditions.

Table 1.1 Foundation types.

Types of foundation	Use	Condition of soil at site
Shallow foundations		
1. Spread footing or wall footings	Isolated/individual columns, and continuous walls	Bearing capacity is reasonably adequate for applied load.
2. Combined footings	Two to four columns on footing and/or space is limited	Compressibility of soil is acceptable.
3. Raft/mat foundations	Several rows of parallel columns; heavy column loads; used to reduce differential settlements	Soil bearing capacity is generally less than for spread footings and over half the plan area would be covered if spread footings are used. Settlement has to be acceptable.
4. Grillage foundation	Very large column loads from superstructure	Reasonable soil bearing capacity, necessary to restrict the depth of foundation to enable it to be above the ground water table.
Deep foundations		
1. Floating pile	In groups of two supporting a cap which is connected to column(s)	Surface and near surface soils have low bearing capacity and good soil is at a reasonable depth.
2. Bearing pile	Same as above	Surface and near surface soils are very weak. Good soil is at reasonable depth.
3. Drilled piers or caissons	For large column loads	Same as for piles.
Earth-retaining structures		
1. Retaining walls, bridge abutments	Permanent soil retention	Any type of soil but a specified zone in backfill is usually of controlled fill.
2. Sheeting structures (sheet pile, wood sheeting, etc.)	Temporary or permanent for excavations; marine cofferdams for underwater construction	Retain any type of soil or water.

1.5 Modeling, Parameters, Analysis and Design Criteria

All practical problems need to be reduced to physical models and behavior represented by corresponding analytical equations. The physical parameters of the system form the inputs in the mathematical equations for computing the responses. The models used should be simple enough that the physical parameters needed for computations are accurately and reliably determined using inexpensive test procedures. For example, in a foundation–soil system, the foundation can be modeled as rigid, while the soil may be assumed to be elastic. The physical parameters needed in such a model are the elasticity parameters of the soil, that is. Young's modulus of elasticity, E, and Poisson's ratio, v, of the soil. Naturally E and v have to be

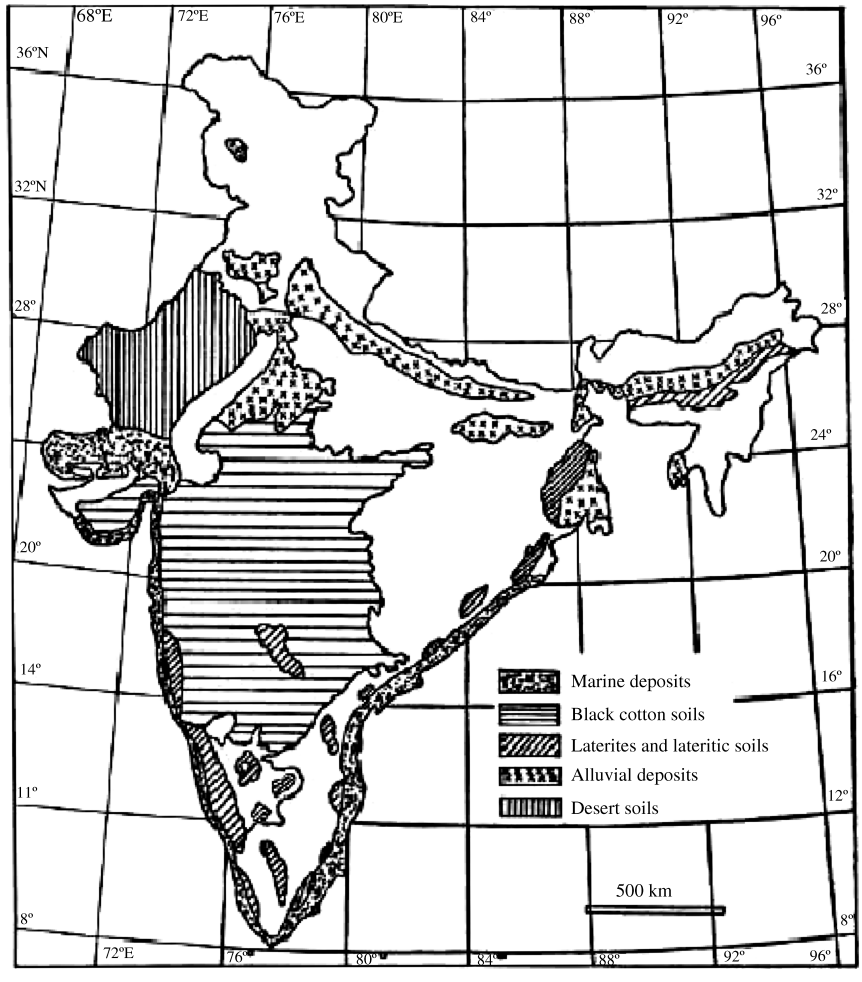

Figure 1.4 Soils of India. (Adapted from B.K. Ramiah and L.S. Chickanagappa, *Soil Mechanics and Foundation Engineering*, p. 3 (Figure 1.1), Oxford and IBH Publishing Co., New Delhi, India. © 1981.)

accurately determined for the soil under consideration as they will be needed for the computation of the responses of the system. Thus modeling, evaluation of parameters and analysis are closely linked and the solutions obtained are highly dependent on all these aspects.

The responses thus obtained have to be judged using appropriate design criteria specified either by codes or evolved from practice and/or experience.

The design process necessarily has two vital components, namely the methods of analysis and experimental data which have to be integrated with them to yield accurate results. However, both the methods and data depend entirely on the mechanism chosen for mathematical idealization of the system components. At this juncture, engineering judgment and experience is very useful. It may be noted that optimum accuracy in analysis and design can be achieved only by properly matching the data and analytical methods used. It is also obvious that any improvement in the data alone or any sophistication in the analytical methods alone can even reduce the accuracy of the results/predictions (Lambe, 1973).

1.6 Soil Maps

Most countries have prepared maps of soil deposits, based on the geological and geotechnical data available. These are very useful for a quick assessment of the project and its requirements. A map of soil deposits in India is given in Figure 1.4 (Ramiah and Chickanagappa, 1981).

2

Engineering Properties of Soil

2.1 Introduction

The physical and engineering properties of soil are necessary for foundation design, as all loads are ultimately supported by the soil media and occasionally by rock medium if present at the site. For engineering applications, soils include all earth materials, organic and inorganic, present in the zone overlying the rock crust of the planet earth.

This chapter presents the engineering properties of soils relevant to foundation design, such as simple soil properties, strength and compressibility characteristics and so on. The laboratory and field tests necessary to evaluate the parameters are also discussed briefly.

However, for more detailed discussion, one may refer to classical and recent books on Soil Mechanics, Geotechnical Engineering, and Foundation Engineering, such as Terzaghi (1943), Taylor (1964), Terzaghi and Peck (1967), Ramiah and Chickanagappa (1981), Shamsher Prakash and Sharma (1990), Cemica (1994), Coduto (2001), Tomlinson (2001), Das (2002, 2007) Reese, Isenhower and Wang (2005), Budhu (2006), Salgado (2007). In the case of foundations on rock, the relevant properties of rock have to be studied, as discussed in standard rock mechanics books, such as Goodman (1989), Brady and Brown (2006), Jaeger and Cook (2007).

2.2 Basic Soil Relations

Soil is formed by the weathering of parent rock as a continuous geological process. It may be identified broadly as residual and/or transported. Residual soils are formed due to weathering of parent rock at its present location. Usually such soils consist of angular grains of different sizes. Residual soils are considered good for supporting a foundation. Transported soils are those that are formed at one location and are transported to their present location by nature, that is, wind, water, ice or gravity. They are of poor quality and are fine grained with low strength and high compressibility.

Thus, soils consist of irregular shaped particles of different sizes and shapes, that is, solids. In addition, there are voids between these particles (pores), which may be filled partly or fully by

Foundation Design: Theory and Practice N. S. V. Kameswara Rao
 ISBN: 978-0-470-82534-1

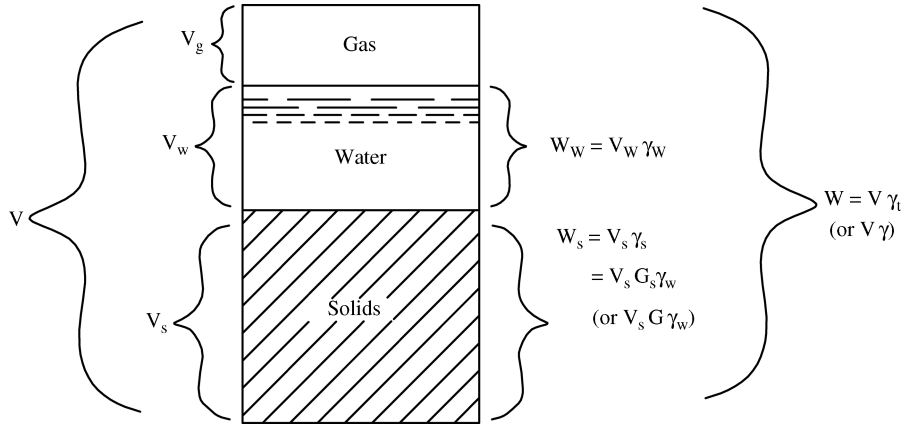

Figure 2.1 Representation of soil as a three-phase material.

air and water. Thus, the soil mass can be symbolically represented as a three phase material, as shown in Figure 2.1.The various parameters shown in the figure are defined as follows

V, W = total volume and weight of soil mass respectively
V_s, W_s = volume and weight of soil solids respectively
V_w, W_w = volume and weight of water respectively
V_g = volume of gas.

$$\begin{aligned} V_v &= V_w + V_g = \text{volume of voids} \\ V &= V_v + V_s \\ W &= W_s + W_w \end{aligned} \tag{2.1}$$

The basic parameters used in geotechnical engineering studies are void ratio, e, porosity, n, water content, w and degree of saturation, S. These are defined as follows

$$\begin{aligned} e &= \frac{V_v}{V_s} = \frac{n}{1-n} \\ n &= \frac{V_v}{V} = \frac{e}{1+e} \\ w &= \frac{W_w}{W_s} \\ S &= \frac{V_w}{V_v} \end{aligned} \tag{2.2}$$

Besides these parameters, the unit weights of the soil mass and its variations with changes in water content are important and they can be expressed as follows

$$\begin{aligned} \gamma_t &= \text{bulk/total unit weight} = \frac{W}{V} = \frac{G+Se}{1+e}\gamma_w \\ \gamma_s &= \text{unit weight of soil solids} = \frac{W_s}{V_s} \\ \gamma_w &= \text{unit weight of water} = \frac{W_w}{V_w} \end{aligned} \tag{2.3}$$

where G = specific gravity of soil solids, which varies between 2.65 and 2.85 for the majority of soils.

It can be shown from Equation (2.2) that, for a soil mass

$$Se = wG \tag{2.4}$$

Hence

$$\gamma_t = \frac{G + Se}{1 + e}\gamma_w = \frac{G(1 + w)}{1 + e}\gamma_w = \frac{1 + w}{1 + e}\gamma_s \tag{2.5}$$

When layers of soils are submerged due to ground water present at site, then the soil mass in saturated and is subjected to buoyancy. Accordingly, we can define

$$\begin{aligned}
\gamma_{\text{sat}} &= \text{saturated unit weight} = \frac{G + e}{1 + e}\gamma_w \,(\text{since } S = 100\% = 1) \\
\gamma_{\text{sub}} &= \text{submerged unit weight (buoyant unit weight)} = \gamma_{sat} - \gamma_w = \frac{G-1}{1 + e}\gamma_w \\
\gamma_{\text{dry}} &= \text{dry unit weight} = \frac{G}{1 + e}\gamma_w \,(\text{since } S = w = 0 \text{ for dry soils})
\end{aligned} \tag{2.6}$$

All these soil properties are routinely determined by standard laboratory tests and also by field tests (Lambe, 1951; Taylor, 1964).

2.2.1 Grain Size Distribution

Grain size distribution (GSD) is also a basic soil property which affects its engineering properties considerably and is used in most soil classification systems. Mechanical sieve analysis is used to determine the grain size distribution of coarse grained soils such as sands. For fine grained soils, hydrometer analysis is used for determining the distribution of grain size (Lambe, 1951; Taylor, 1964) as grain sizes less than 0.074 mm (sieve size No. 200 BS and US) are the smallest sizes that are visible to the naked eye and can be mechanically sieved. Typical sieve sizes used for sieve analysis of coarse grained soils are given in Table 2.1.

Table 2.1 Sieve sizes.

United States		British Standard		German DIN		French	
Sieve no.	mm	Sieve no.	mm	Sieve no.	mm	Sieve no.	mm
4	4.76	—		—		—	
10[a]	2.00	8[a]	2.057	—		34[a]	2.000
20	0.841	16	1.003	—		31	1.000
30	0.595	30	0.500	500	0.500	28	0.500
		36[b]	0.422	400[b]	0.400	27[b]	0.400
40[b]	0.420	—		—		—	
50	0.297	52	0.295	—		—	
60	0.250	60	0.251	250	0.250	25	0.250
80	0.177	85	0.178	160	0.160	23	0.160
100	0.149	100	0.152	125	0.125	22	0.125
200	0.074	200	0.076	80	0.080	20	0.080
270	0.053	300	0.053	50	0.050	18	0.050

[a]Limit between sand and gravel.
[b]For Atterberg's limits.

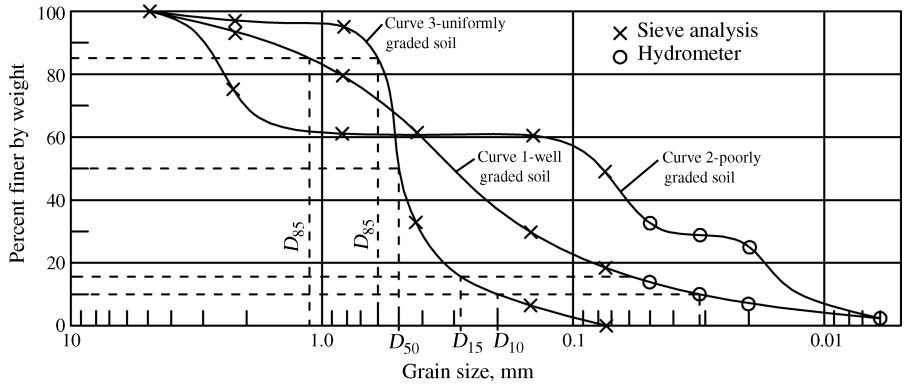

Figure 2.2 Typical grain size distribution curves.

Also typical grain size distribution curves are shown in Figure 2.2. If the curve is smooth and is spread evenly with almost constant slope as shown in curve 1, it is called a well graded soil. If the slope of the curve is wavy as shown in curve 2, it is called poorly graded. If the curve has very steep slope with most of the soil particles being of almost same size as shown in curve 3, it is called uniformly graded soil. A commonly accepted method to express the general features of the GSD curve is due to Hazen (Taylor, 1964) which uses the grain sizes D_{10} and D_{60} (respectively, diameter finer than 10 and 60%) to define the uniformity coefficient, c_u as

$$c_u = \frac{D_{60}}{D_{10}} \tag{2.7}$$

where D_{10} = effective size which is used in several engineering applications such as in permeability studies. For example, Hazen's formula (Taylor, 1964) for the coefficient of permeability, k in filter sands is

$$k = 100\,D_{10}^2 \quad \text{(using units of centimeters and seconds)} \tag{2.8}$$

GSD curves are used in almost all soil classification systems, as shown in Figures 2.3 and 2.4. A typical classification system of soils using grain sizes of particles is given in Table 2.2 (Das, 2007), besides the ones shown in Figures 2.3 and 2.4.

The general names given to various soils in the above table and figures convey additional information about their engineering behavior. For example, clays are cohesive with plasticity.

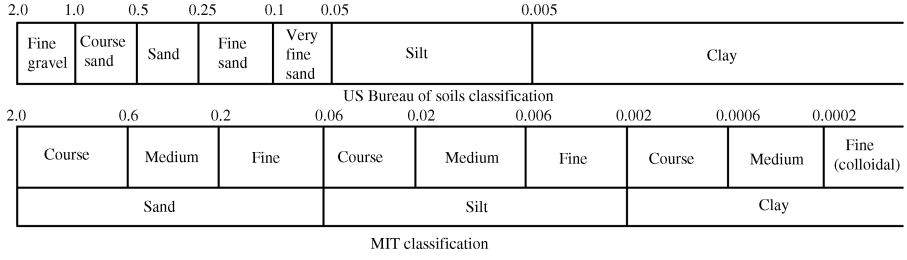

Figure 2.3 Classifications based on grain size (in mm).

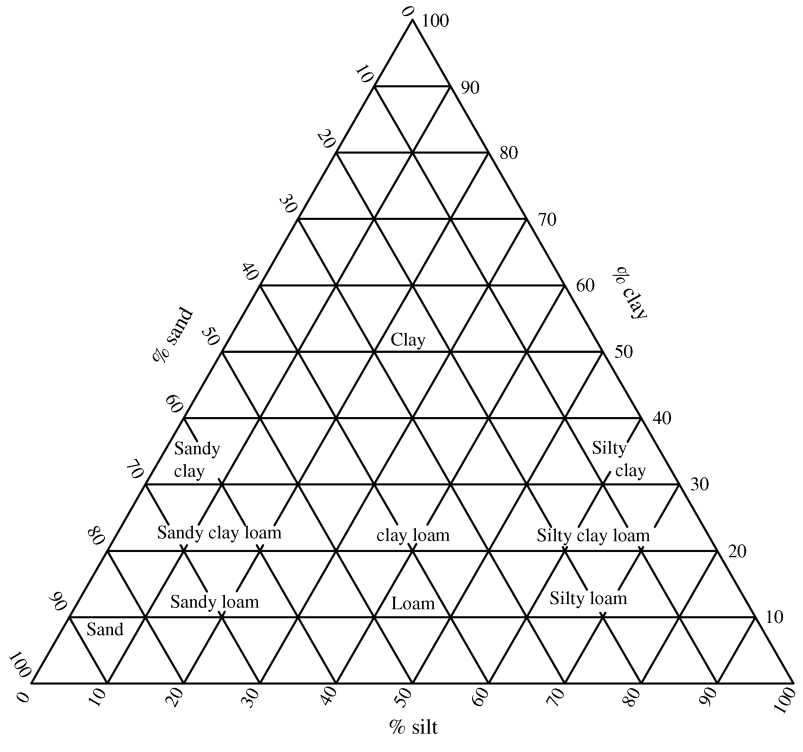

Figure 2.4 United States Bureau of Soils triangular classification chart.

The cohesion of the clay is represented by c. Similarly, sands and gravel are nonplastic with only frictional properties represented by angle of internal friction, φ. Silts have low plasticity and have cohesion and very low friction. These soils can be identified by simple tests like the dispersion test, shaking test and rolling test (Taylor, 1964).

2.2.2 *Plasticity and the Atterberg's Limits*

Plasticity (mainly in clays or cohesive soils) is a predominant feature of fine grained soils such as clays or cohesive soils. It is defined as the ability of the material or soil to undergo

Table 2.2 General classification of soils.

Soil type	Grain size (mm)	
	Unified	AASHTO
Gravel	75–4.75	75–2
Sand	4.75–0.075	2–0.05
Silt	<0.075	0.05–0.002
Clay	<0.075	<0.002

deformation/distortion/change of shape without rupture or crack. Water content affects the physical properties of clays. Atterberg (Taylor, 1964) proposed a series of tests for determining these effects which are known as Atterberg Limits (also referred to as Consistency Limits). A lot of useful empirical formulae have been developed over the years to correlate these limits to strength, compressibility and other important engineering properties of the soil. These are simple tests and are routinely conducted in the laboratories and throw lot of information on the soil for soil mechanics and foundation engineering applications. The Atterberg limits are shown in Figure 2.5.

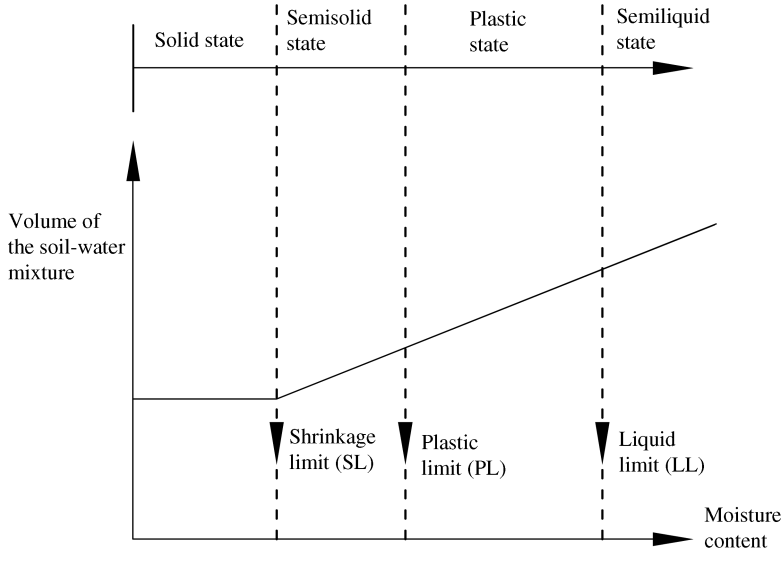

Figure 2.5 Representation of Atterberg limits.

These are briefly explained below depending on their physical state as functions of water content. If a lot of water is added to a clayey soil, it may start flowing and behave like a semiliquid state. The limit at which the soil behaves like a semiliquid is called the liquid limit (LL). This is determined in the laboratory by Casagrande's LL device and is defined as the water content at which a groove closure of 12.7 mm occurs at 25 standard blows.

If the soil is dried gradually, it behaves in a plastic, semi solid or solid state. The limit between plastic and semi solid states is called the plastic limit (PL), as shown in Figure 2.5. It is determined in the laboratory as the moisture content at which the soil shows visible cracks/ crumbles when rolled into a thread 3.18 mm in diameter.

The water content limit at which the soil changes from a semi solid to solid state is called the shrinkage limit (SL). It is also easily determined in the laboratory as the water content at which the soil does not undergo any further volume change with loss of moisture (Figure 2.5). The liquid and plastic limits of few well studied clays and silts are given in Table 2.3.

Table 2.3 Liquid and plastic limits of clay minerals and clayey soils.

Soil	LL	PL
Kaolinite	35–100	25–35
Illite	50–100	30–60
Montmorillonite	100–800	50–100
Boston clay	40–45	20–25
London clay	65–70	25–30
Loessial soils of China	25–35	15–20

The following indices are also useful in analyzing the behavior of soils.

$$\begin{aligned}
\text{Plasticity index} &= \text{PI} = \text{LL} - \text{PL} \\
\text{Liquidity index} &= \text{LI} = \frac{w - w_p}{w_L - w_p} \\
\text{Toughness index} &= \frac{I_f}{\text{PI}} \\
\text{Flow index} &= I_f = \text{slope of curve for no. of blows vs water content} \\
&\qquad \text{(Casagrande's method for determination of LL)}
\end{aligned} \tag{2.9}$$

where

w = natural water content of the soil
w_p = water content at plastic limit
w_L = water content at liquid limit.

If LI ≥ 1, it may indicate the possibility of liquefaction, that is, a loss of soil strength after a few cycles of loading and unloading resulting in liquid like behavior.

2.3 Soil Classification

Based on the Atterberg's limits and Grain size distribution, soils are classified by several agencies in most countries, like the AASHTO and Unified systems. The focus in classification is on the purpose for which the soil is used. The most popular classification is due to Casagrande and is referred to as the Unified classification. It is presented as a plasticity chart shown in Figure 2.6; Table 2.4 shows the procedure for assigning symbols for various soils.

2.4 Permeability

Since soil is porous, water can flow through the pores, which is also referred to as seepage. The ease with which water flows through the soils is represented by the coefficient of permeability of soils, k. The velocity follows Darcy's Law as

$$v = ki \tag{2.10a}$$

where

v = superficial velocity (assuming water is flowing through the entire cross section including pores and soil particles)
i = hydraulic gradient = $\frac{h}{L}$
h = loss of head between any two cross sections of flow
L = straight distance between the cross sections.

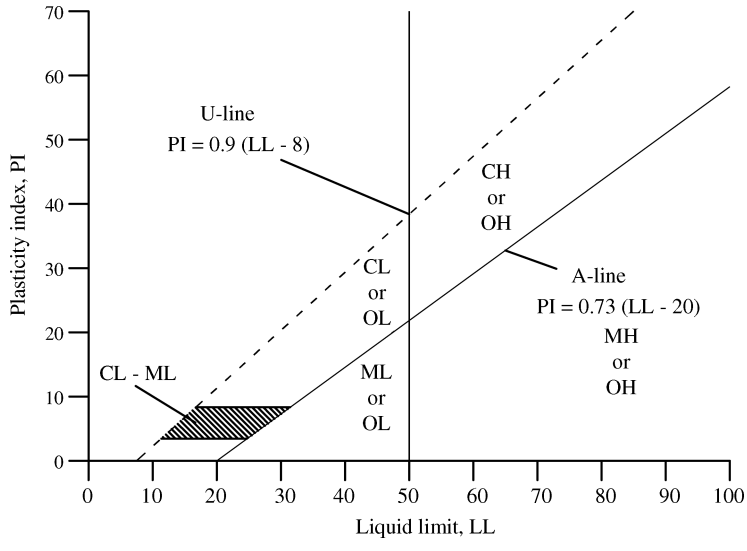

Figure 2.6 Plasticity chart.

k can be determined in the laboratory using constant head permeameter and/or variable head permeameter (Taylor, 1964). k can also be determined in the field (*in situ*) by pumping tests.

2.4.1 Quick Sand Condition and Critical Hydraulic Gradient

As the hydraulic gradient increases, the seepage force acting on the soil particles gradually increases and starts pulling the particles out in the direction of flow. This phenomenon is called the quick sand condition where the soil particles appear to be boiling. This happens when the buoyant weight or submerged weight of the soil equals the seepage force when the flow is opposite to the direction of gravity. This gradient is called critical hydraulic gradient, i_c and can be obtained as

$$\text{Seepage force} = i_c\gamma_w = \text{submerged unit weight of soil} = \frac{G-1}{1+e}\gamma_w$$

Hence

$$i_c = \frac{G-1}{1+e} \tag{2.10b}$$

This value generally ranges from 0.8 to 1.3 and it may be taken as 1.0 for average conditions in the absence of data.

2.5 Over Consolidation Ratio

A soil whose present overburden pressure is the largest pressure ever experienced by this soil is referred to as normally consolidated soil. If otherwise, it is called an over consolidated soil. The

Table 2.4 Unified soil classification system (based on material passing 75-mm sieve).

Criteria for assigning group symbols				Group symbol
Coarse-grained soils: more than 50% retained on no. 200 sieve	Gravel: more than 50% of coarse fraction retained on no. 4 sieve	Clean gravels	$C_u \geq 4$ and $1 \leq C_c \leq 3^c$	GW
		Less than 5% fines[a]	$C_u < 4$ and/or $1 > C_c > 3^c$	GP
		Gravel with fines	$PI < 4$ or plots below A line (Figure 2.6)	GM
		More than 12% fines[a,d]	$PI > 7$ or plots on or above A line (Figure 2.6)	GC
	Sand: 50% or more of coarse fraction passes no. 4 sieve	Clean sands	$C_u \geq 6$ and $1 \leq C_c \leq 3^c$	SW
		Less than 5% fines[b]	$C_u < 6$ and/or $1 > C_c > 3^c$	SP
		Sands with fines	$PI < 4$ or plots below A line (Figure 2.6)	SM
		More than 12% fines[b,d]	$PI > 7$ or plots on or above A line (Figure 2.6)	SC
Fine-grained soils: 50% or more passes no. 200 sieve	Silts and clays: liquid limit <50	Inorganic	$PI > 7$ or plots on or above A line (Figure 2.6)	CL
			$PI < 4$ or plots below A line (Figure 2.6)	ML
		Organic	$\frac{\text{Liquid limit}-\textit{oven dried}}{\text{Liquid limit}-\textit{not dried}} < 0.75$; see Figure 2.6; OL zone	OL
	Silts and clays: liquid limit 50 or more	Inorganic	PI plots on or above A line (Figure 2.6)	CH
			PI plots below A line (Figure 2.6)	MH
		Organic	$\frac{\text{Liquid limit}-\textit{oven dried}}{\text{Liquid limit}-\textit{not dried}} < 0.75$; see Figure 2.6; OL zone	OH
Highly organic soils	Primarily organic matter, dark in color and organic odor			Pt

[a]Gravels with 5–12% fines require dual symbols: GW-GM, GW-GC, GP-GM, GP-GC.
[b]Sands with 5–12% fines require dual symbols: SW-SM, SW-SC, SP-SM, SP-SC.
[c]$C_u = \frac{D_{60}}{D_{10}}$; $C_c = \frac{(D_{30})^2}{D_{60} \times D_{10}}$.
[d]When $4 \leq PI \leq 7$ and plots in the hatched area in Figure 2.6 use dual symbol GC-GM or SC-SM.
[e]When $4 \leq PI \leq 7$ and plots in the hatched area in Figure 2.6 use dual symbol CL-ML.

ratio of the past effective pressure, σ'_p, to the present overburden pressure, σ'_o, is called the over consolidation ratio (OCR), that is

$$\text{OCR} = \frac{\sigma'_p}{\sigma'_o} \tag{2.11}$$

For normally consolidation soils, OCR = 1. For over consolidation soils, OCR > 1.
If OCR < 1, it has no significance.
If OCR > 1–3, the soils are lightly over consolidated.
If OCR > 3–8 or more, the soils are heavily over consolidated.

OCR has a very significant effect in the behavior of clayey soils though its effect is marginal in sandy soils. OCR can be determined by the consolidation test (oedometer test) in the laboratory as described in Section 2.9.

2.6 Relative Density

The degree of compaction in granular soils in the field can be determined by the relative density, D_r, expressed as a percentage as

$$D_r = \frac{e_{\max} - e}{e_{\max} - e_{\min}} \tag{2.12}$$

where
$e_{\max}$ = void ratio of the soil in the loosest state
$e_{\min}$ = void ratio of the soil in the densest state
e = *in situ* void ratio.

The various void ratios can be determined in the laboratory using standard methods. The relative density can also be expressed in terms of dry unit weights as

$$D_r = \left(\frac{\gamma_d - \gamma_{d(\min)}}{\gamma_{d(\max)} - \gamma_{d(\min)}}\right) \frac{\gamma_{d(\max)}}{\gamma_d} \times 100 \tag{2.13}$$

where
γ_d = *in situ* dry density of soil
$\gamma_{d(\max)}$ = dry unit weight in the densest state (corresponding $e_{\min}$)
$\gamma_{d(\min)}$ = dry unit weight in the loosest state (corresponding $e_{\max}$).

The denseness of the soil is correlated to the relative density, D_r, as given in the Table 2.5.

Table 2.5 Denseness of soils.

Denseness	D_r (%)
Very loose	0–20
Loose	20–40
Medium	40–60
Dense	60–80
Very dense	80–100

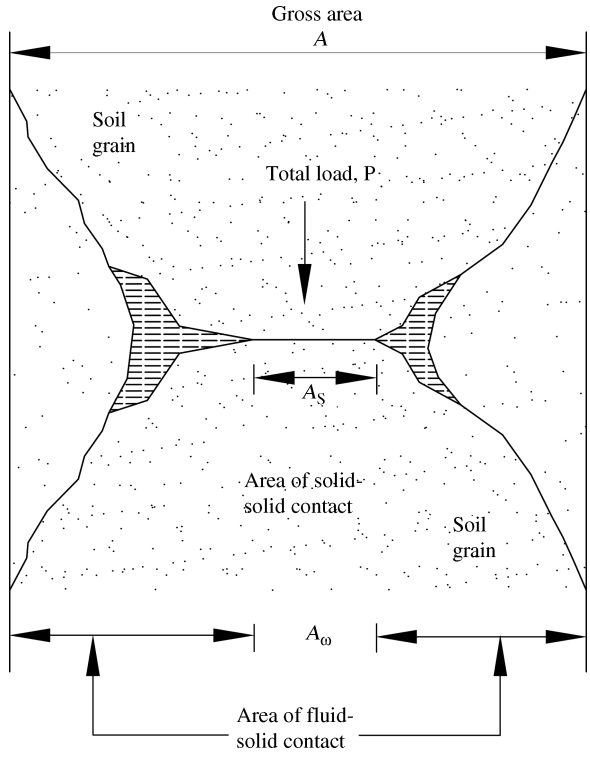

Figure 2.7 Intergranular or effective stress.

2.7 Terzaghi's Effective Stress Principle

If a soil mass shown in Figure 2.7 is subjected to a total stress, σ, then from equilibrium we can express

$$\frac{P}{A} = \sigma = (1-a)u + \sigma' \tag{2.14}$$

where $a = \frac{A_s}{A}$

A_s = contact area between solid grains
A = total area of cross section of the soil mass
u = pore water pressure
σ' = vertical component of stress of the contact (over the unit cross sectional area)
= vertical effective stress.

Usually a is negligible in comparison to 1 and hence Equation (2.14) can be expressed as

$$\sigma = \sigma' + u \tag{2.15}$$

where

σ = total stress at any point in the soil mass

σ' = effective stress (stress between the solid to solid contact)

u = pore water pressure.

This is called the effective stress principle formulated by Terzaghi (1943) and is one of the important concepts in soil mechanics and foundation engineering. It can be readily recognized that stresses and hence strains and displacements (settlements) occur only due to changes in effective stresses.

2.8 Compaction of Soils

A soil mass can be made denser by compacting with some mechanical energy (static or dynamic) and its unit weight generally increases. The dry unit weight increases with the gradual increase of water content and subsequent compaction. This is because the additional water acts as a lubricant and helps in rearranging the soil particles into a denser state of packing. The dry unit weight increases with the water content up to a maximum or limiting value beyond which it decreases with increase in water content, as shown in Figure 2.8.

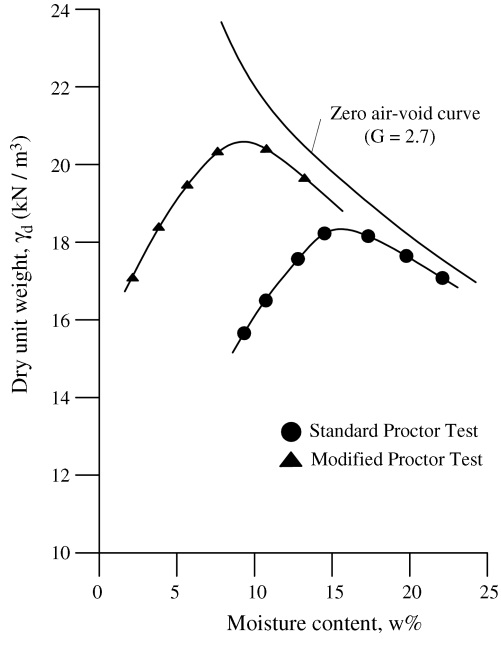

Figure 2.8 Standard and modified Proctor compaction curves for a fine grained soil.

The moisture content at which the soil reaches its maximum dry density is called the optimum moisture content (OMC).

The OMC and maximum dry density of soils can be determined by standard laboratory tests such as the standard Proctor Test (using a 2.5 kg rammer and a drop of 305 mm) and the modified Proctor Test (using a 4.54 kg rammer and a drop of 457 mm; Taylor, 1964; Das, 2002).

Typical curves from these compaction tests are shown in Figure 2.8. These results are used for specifying the methods of field compaction. Usually the field compaction is required to achieve a relative compaction (RC) of 90% or more of the max dry density obtained in laboratory using either the standard or modified Proctor test (or other tests specified by local codes), that is

$$\text{RC} = \frac{\gamma_{\text{dry(field)}}}{\gamma_{d(\max)}} = \frac{A}{1-D_r(1-A)} \tag{2.16}$$

where $A = \dfrac{\gamma_{d(\min)}}{\gamma_{d(\max)}}$

D_r = relative density defined in Equation (2.13)

Another empirical relationship between RC and D_r is given by Lee and Singh (Das, 2007) as

$$D_r(\%) = \frac{RC-80}{0.2} \tag{2.17}$$

The field compaction of soils is done by rollers such as sheep foot rollers, vibratory rollers, pneumatic rubber tired rollers, smooth wheel rollers.

2.9 Consolidation and Compressibility

When a fine grained soil or cohesive soil is subjected to loads or stresses, some or all the additional load or stress is supported by the pore water present in the soil mass initially. This excess pore pressure creates hydraulic gradients in the pore water and the water flows out (due to the soil permeability) and simultaneously transfers the load or stress to the soil particles gradually. This amounts to the gradual transfer of pore water pressure to the intergranular stress or effective stress, until the entire load or total stress becomes effective stress (as per Equation (2.15)). This simultaneously produces compression/settlement of the soil mass (as only effective stresses produce settlements). This gradual process involves simultaneously a slow escape of water, a gradual load transfer and a gradual compression of the soil mass and is called consolidation. The compressibility and consolidation characteristics of the soil are determined in the laboratory using a consolidometer/oedometer, as shown in Figure 2.9.

The saturated soil sample (usually 64 mm diameter and 25 mm thick) is placed inside the metal ring with porous stones at top and bottom to facilitate escape of water, as shown in the Figure 2.9.

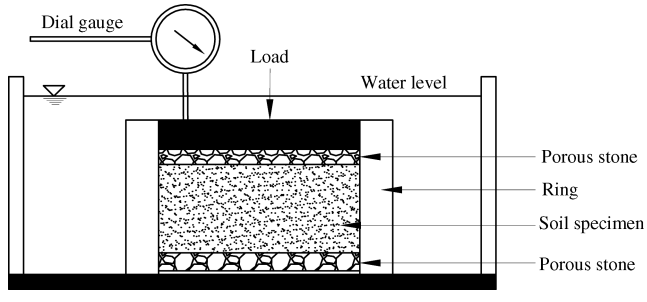

Figure 2.9 Schematic diagram of oedometer/consolidometer.

A load is applied on the specimen which becomes the total vertical stress, σ. Compression or settlement readings are taken at 15 s, 1 min, 4 min, 16 min and so on, in time ratios of four, up to 24 h or until no further settlement is noticeable, signifying the consolidation is practically complete under the present load. Then the load on the specimen is doubled and the test is repeated for several cycles to include the range of design stresses anticipated in the field. The results of these tests can be plotted as a graph of void ratio at the end of consolidation (corresponding to each applied load) versus corresponding vertical effective stress, as shown in Figure 2.10. While the total effective stress can be directly calculated by dividing the applied load by the area of cross section of the specimen, the change in void ratio (being directly proportional to the change in thickness of the sample) can be obtained as

$$\frac{\Delta e}{1 + e} = \frac{\Delta H}{H} \tag{2.18}$$

where

Δe = change in void ratio
e = void ratio (initial)
ΔH = change in thickness of the sample
H = initial thickness of the sample.

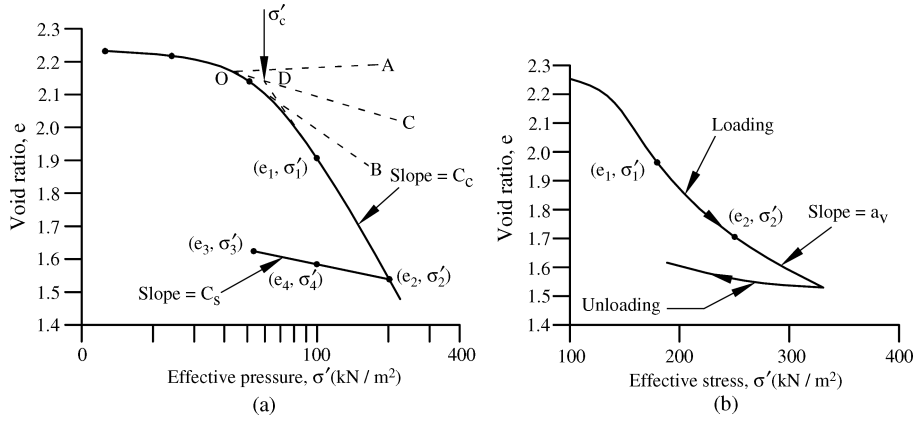

Figure 2.10 Compressibility curves for a clayey soil.

Figure 2.10(a) shows the semi log plot of e versus log σ'. Figure 2.10(b) shows the e versus σ' curve.

After completing the test up to the desired pressure, the specimen can be gradually unloaded resulting in some recovery of the compression recorded, that is, increase in thickness as shown in these figures.

2.9.1 Compressibility Characteristics and Settlement of Soils

Following compressibility characteristics can be determined from Figure 2.10:

1. Compression index, C_c
   The slope of the straight line portion of the e log σ' graph (loading part) shown in Figure 2.10(a) is called the compression index, C_c.

Accordingly

$$C_c = \frac{\Delta e}{\log \sigma_2' - \log \sigma_1'} = \frac{e_1 - e_2}{\log \sigma_2' - \log \sigma_1'} = \frac{e_1 - e_2}{\log\left(\frac{\sigma_2'}{\sigma_1'}\right)} \tag{2.19}$$

There are several correlations of compression index with the other soil parameters (Bowles, 1996). The most popular one is due to Terzaghi and Peck (1967) and is expressed as

$$C_x = 0.009(LL - 10) \tag{2.20}$$

where LL is the liquid limit of the soil.

2. Swelling index or recompression index, C_s
   This is the slope of the unloading portion of the e log σ' graph, (Figure 2.10(a)), that is

$$C_s = \frac{e_3 - e_4}{\log\left(\frac{\sigma_4'}{\sigma_3'}\right)} \tag{2.21}$$

In most cases

$$\frac{C_s}{C_c} = \frac{1}{4} \text{ to } \frac{1}{5} \tag{2.22}$$

3. The coefficient of compressibility, a_v, and the coefficient of volume decrease, m_v.
   a_v is the slope of the $e - \sigma'$ graph which is idealized as a straight line between the ranges of σ' needed for computations, as shown in Figure 2.10(b).
   Accordingly

$$a_v = -\frac{\Delta e}{\Delta \sigma_2'} = \frac{e_1 - e_2}{p_2 - p_1} \tag{2.23}$$

Also, coefficient of volume decrease

$$m_v = \frac{a_v}{1 + e} \tag{2.24}$$

Change in the thickness or settlement of the soil sample or layer (ΔH) of total thickness (H) is due to primary consolidation, S_c.

From Equations (2.18), (2.19), (2.23) and (2.24), we can write

$$\begin{aligned} S_c = \Delta H &= \frac{C_c}{1 + e} \log \frac{\sigma_2'}{\sigma_1'} = \frac{C_c H}{1 + e} \log \frac{\sigma_1' + \Delta \sigma'}{\sigma_1'} \quad \text{(a)} \\ &= \frac{a_v}{1 + e} (\sigma_2' - \sigma_1') H = \frac{a_v}{1 + e} \Delta \sigma' H = m_v \Delta \sigma' H \quad \text{(b)} \end{aligned} \tag{2.25}$$

where e and σ_1' are the initial void ratio at effective stress σ_1' and $\Delta \sigma_1'$ is the change in effective stress $= \sigma_2' - \sigma_1'$.

Similarly the increase in thickness during swelling can be calculated using the swelling index or coefficient of swelling.

4. Preconsolidation pressure, σ_p'
   This may also be called the over consolidation pressure, σ_p'. This is the maximum past effective pressure to which the soil specimen is subjected to, as mentioned in Section 2.5. It can be determined from Figure 2.10(a), as shown there. The preconsolidation pressure can be determined using Casagrande's method (Taylor, 1964) as follows.

i. Locate O on the e log σ' curve where the curve has maximum curvature, that is, smallest radius of curvature.
ii. Draw the line OA horizontally.
iii. Draw the line OB tangentially to the e log σ' curve.
iv. Draw the line OC bisecting the angle AOB.
v. Extend the straight line portion of the e log σ' curve backward to intersect line OC at D. The pressure corresponding to point D on the e log σ' curve is the preconsolidation pressure σ'_p.

2.9.2 *Time Rate of Consolidation*

The one-dimensional consolidation equation (Terzaghi, 1943) for the laboratory soil sample shown in Figure 2.9 is

$$C_v \frac{\partial^2 u}{\partial z^2} = \frac{\partial u}{\partial t} \tag{2.26}$$

where

C_v = coefficient of consolidation = $\frac{k}{\gamma_w m_v}$
u = pore water pressure
z = vertical coordinate of the soil sample
t = time parameter
k = coefficient of permeability
m_v = coefficient of volume decrease (Equation (2.24))
γ_w = unit weight of water.

The above equation was solved by Terzaghi (1943), and the following curve fitting methods were developed for determining C_v, which is useful for calculating time rate of settlements. These are:

1. Square root of time ($\sqrt{t}$) fitting method (Taylor, 1964)
2. Logarithm of time (log t) fitting method – Casagrande's method (Taylor, 1964).

From the exhaustive solution of Equation (2.26) given by Terzaghi, the most important ones used for settlement calculations are given in Figure 2.11. These are in terms of value of average degree of consolidation, U (%) versus nondimensional time factors, T where

$$U = 1 - \frac{\int_0^H u\, dz}{\int_0^H u_i\, dz} = \frac{\Delta H}{H} \tag{2.27}$$

$$T = \frac{C_v t}{\left(\frac{H}{2}\right)^2} \tag{2.28}$$

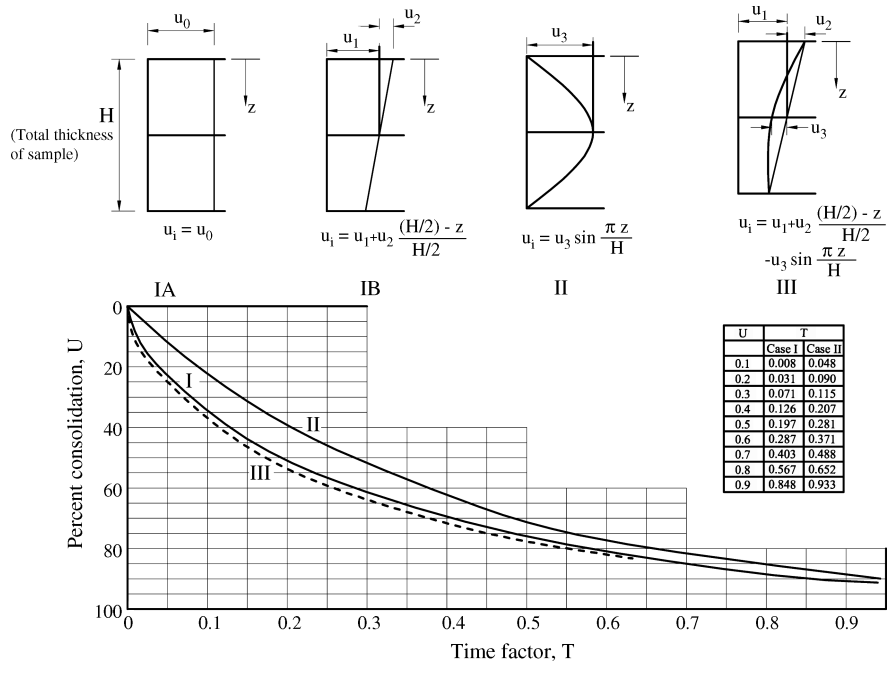

U	T	
	Case I	Case II
0.1	0.008	0.048
0.2	0.031	0.090
0.3	0.071	0.115
0.4	0.126	0.207
0.5	0.197	0.281
0.6	0.287	0.371
0.7	0.403	0.488
0.8	0.567	0.652
0.9	0.848	0.933

Figure 2.11 Consolidation curves as per Terzaghi's theory.

where

u = pore pressure at time t
u_i = initial pore pressure at $t = 0$
H = total thickness of the soil layer or sample
z = vertical coordinate
C_v = coefficient of consolidation.

Noting that the solutions shown in Figure 2.11 are close to each other, only curve 1 (case 1) is used for most of the calculations.

Using these results shown in Figure 2.11, C_v is determined using curve fitting methods developed by Taylor (1964) and Casagrande (Taylor, 1964). Taylor's method is called the square root of time ($\sqrt{t}$) fitting method and uses 90% consolidation results from experiments and theory (Figure 2.11) for comparison; that is, he compares t_{90} from experiments and $T_{90} = 0.848$ from theory (Figure 2.11).

Casagrander's method is called the logarithm of time (log t) fitting method and uses 50% consolidation results from experiments and theory (Figure 2.11) for comparison; that is, he uses t_{50} from experiments and $T_{50} = 0.197$ from theory (Figure 2.11).

The solution details and several examples are given in all standard books in Geotechnical Engineering (Taylor, 1964; Bowles, 1996; Das, 2007).

2.10 Shear Strength of Soils

Engineering materials may generally fail due to tension, compression, shear or a combination of these factors. However, soils and rocks fail essentially due to shear. The corresponding shear stress beyond which the soil fails is called the shear strength of the soil and is expressed by Coulomb's equation, that is

$$\begin{aligned} s &= c + \sigma \tan\phi = c + \sigma f \text{ (in terms of total stress components)} \\ s &= c' + \sigma' \tan\phi' = c' + \sigma' f' \text{ (in terms of effective stress components)} \end{aligned} \tag{2.29}$$

where

s = shear strength of the soil
c, c' = cohesion of the soil
φ, φ' = angle of internal friction of the soil
σ' = effective stress = $\sigma - u$ (as in Equation (2.15))
u = pore water pressure
f or f' = $\tan\phi$ or $\tan\phi'$ = coefficient of friction.

Generally shear strength parameters depending on the total stresses, that is, c and φ are used to check the stability of the supporting soil at the end of construction stage, while c' and φ' (shear strength parameters of the soil with reference to effective stress) are used for analyzing long term stability. Hence, most of the following details are presented in terms of c and φ, though they equally apply for c' and φ'.

The cohesion c of the soil is independent of the normal stress. However, the frictional component between the grains (i.e., $f = \tan\phi$) depends on the normal stress, σ. The shear strength of soils given by Equation (2.29) is shown in Figure 2.12 for different soils, such as (a) cohesive soils, (b) cohensionless soils (sands and gravels) and (c) purely cohesive soils (clays) or sometimes for end of construction analysis with $\phi = 0$ (Taylor, 1964; Terzaghi and Peck, 1967; Lambe and Whitman, 1969).

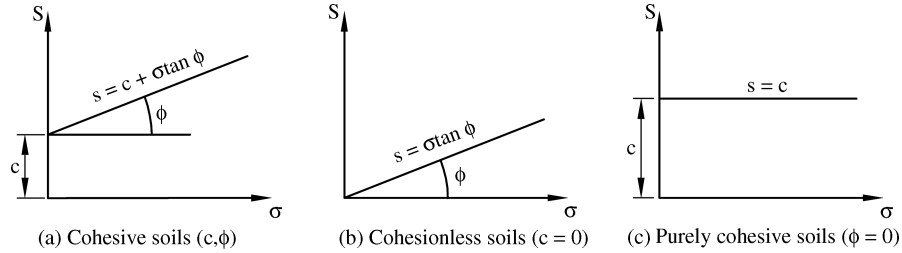

Figure 2.12 Shear strength of soils.

The shear strength parameters of the soils can be determined in the laboratory by:

1. Direct shear test for sandy soils
2. Vane shear test for clayey soils
3. Triaxial shear test for general soils and loading conditions
4. Unconfined compression test for clayey soils.

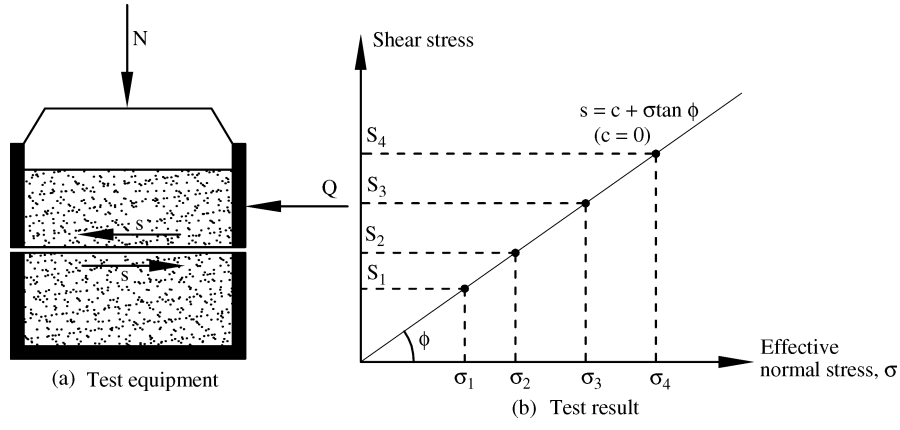

Figure 2.13 Direct shear test for sands.

Some important aspects of these tests are briefly described below while more details can be obtained from Lambe (1951), Taylor (1964), Das (2002) and other books.

2.10.1 Direct Shear Test

This test is mainly done on frictional soils/coarse grained soils/sandy soils using a shear box, as shown in Figure 2.13(a). The sandy soil is to be tested in the shear box, which is split into two halves (Figure 2.13(a)). A normal load N is applied and then a shear force, Q is applied in steps until the specimen fails along the horizontal plane dividing the two halves of the split shear box. A plot of normal stress, σ, versus shear stress, s, is drawn as shown in Figure 2.13(b), where

$$\sigma = \frac{N}{A}, \quad s = \frac{Q}{A} \tag{2.30}$$

where A is the area of the failure plane, that is, the cross sectional area of the shear box. From the graph, it can be noted that

$$\phi = \tan^{-1}\frac{s}{\sigma} \tag{2.31}$$

For sandy soils, ϕ varies from 20° to 45° increasing with relative density D_r.

2.10.2 Vane Shear Test

This test can be done both in the laboratory as well as in the field and is applicable more for cohesive soils. The vane consists of four thin plates welded to a torque rod as shown in Figure 2.14. A torque is then gradually applied at the top of the torque rod (as shown in the sketch) and the cylindrical surface of soil of height h and diameter d resists the applied torque until the soil fails. Then, the shear strength (undrained, since practically no drainage occurs

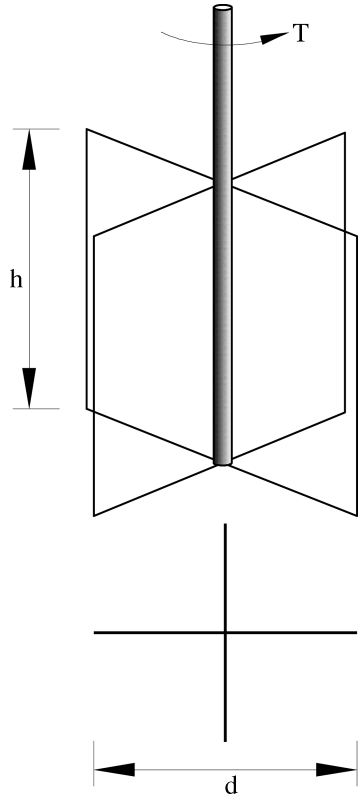

Figure 2.14 Sketch of vane shear test equipment.

during the test) can be computed by this expression

$$s = \frac{T}{\pi\left(\frac{d^2 h}{2} + \frac{\beta\, d^3}{4}\right)} \tag{2.32}$$

where

s = undrained shear strength
= cohesion, c (since $\phi = 0$ for cohesive soils)
T = torque at failure
d = diameter of the shear vane
h = height of the shear vane
β = a factor depending on the slope of the zone of resistance/shear strength at the periphery of cylindrical surface
= 1/2 for triangular mobilization
= 2/3 for uniform mobilization
= 3/5 for parabolic mobilization.

Uniform mobilization factor of 2/3 is commonly used and accordingly $s\,(=c)$ is calculated as

$$s = c = \frac{T}{\pi\left(\frac{d^2h}{2} + \frac{d^3}{6}\right)} \tag{2.33}$$

The commonly used laboratory vane size has $d = 13$ mm and $h = 25$ mm. The field vane is generally bigger and there are several sizes prescribed by standards such as ASTM (Das, 2002).

2.10.3 *Triaxial Shear Test*

This is a very comprehensive test that can be conducted on any general soil with cohesion, c, and friction, φ, components. The test set up is shown in Figure 2.15.

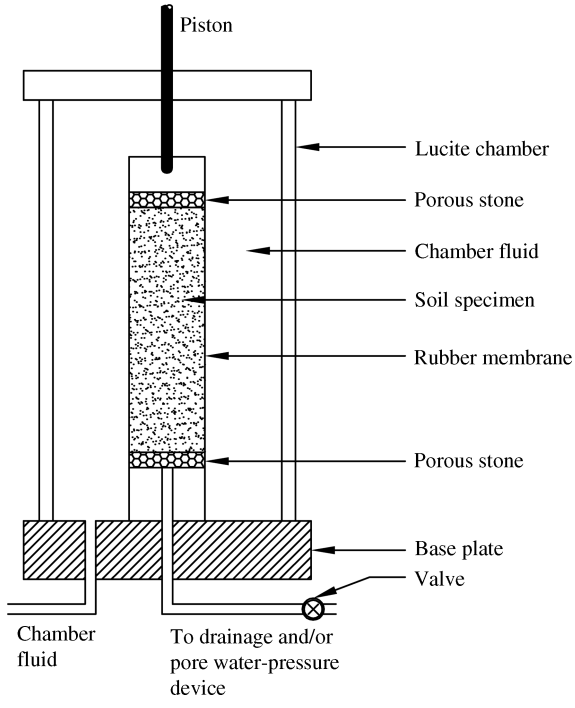

Figure 2.15 Sketch of triaxial test equipment.

In this test, a cylindrical soil specimen of standard size (around 36 mm diameter, 76 mm long; usually the length diameter ratio is 2.0 to 2.5) confined by a rubber membrane is placed in a lucite chamber. Then an all round confining pressure, σ_3, is applied to the specimen using either water (mostly) or glycerin as the chamber fluid. This is also called hydrostatic stress, all round pressure or cell pressure, σ_3. Then a vertical stress, $\Delta\sigma_1$, is applied in the vertical direction until failure. This is also called the deviator stress. Thus the normal stress in the vertical direction at failure becomes $\sigma_1 = \sigma_3 + \Delta\sigma_1$.

If drainage is allowed in the test, it is called a drained test. Otherwise, it is called an undrained test where pore pressures are developed due to the applied deviator stress. The soil specimen is

usually tested after complete saturation but also can be tested at any desired water content. Out of the several customized triaxial tests, following three main types of tests are commonly conducted in the triaxial equipment (Lambe, 1951; Lambe and Whitman, 1969).

1. Unconsolidated undrained test (UU test)
2. Consolidated undrained test (CU test)
3. Consolidated drained test (CD test).

The test results are analyzed using Mohr's circle, knowing the major and minor principal stresses, that is, σ_3 (minor principal stress) and $\sigma_1 = \sigma_3 + \Delta\sigma_1$ (major principal stress), as shown in Figure 2.16. Usually three or four samples are tested at different cell pressures, and a common envelope is drawn tangential to the circumferences of these Mohr's circles obtained for each sample using minor and major principal stresses at failure. This is called the failure envelope or Mohr–Coulomb failure envelope. These details are shown in Figure 2.16 for the above types of tests. Noting that the failure envelope represents the shear strength of the soils, as shown in Figure 2.12, the cohesion, c (or c'), and the angle of internal friction, φ (or φ'), can be determined from these figures, as marked therein.

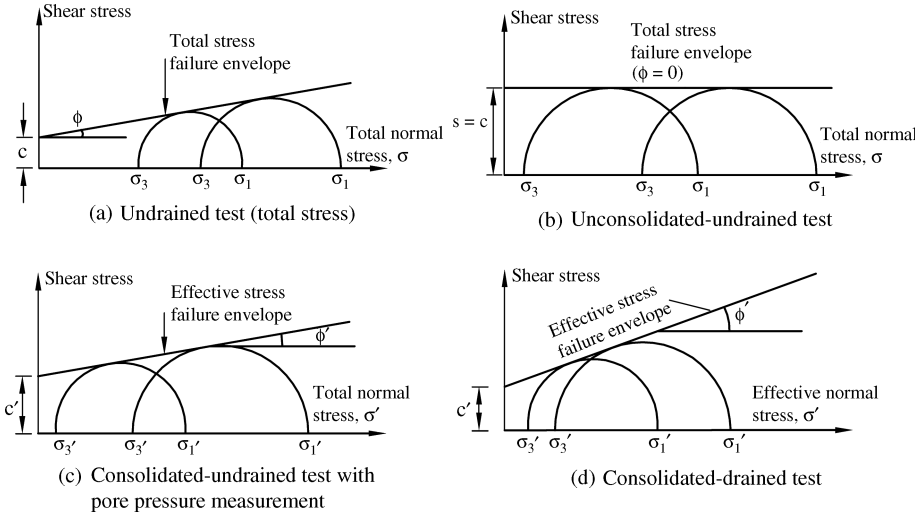

Figure 2.16 Mohr's circles and failure envelopes for different triaxial tests.

Thus, the triaxial test is very comprehensive and versatile with lots of flexibility to customize the test to simulate the design requirement. The literature available on this test is very exhaustive (Lambe, 1951; Lambe and Whitman, 1969).

2.10.4 Unconfined Compression Test

The unconfined compression test (also called the UCC test) is more relevant to cohesive soils. This is a special case of the unconsolidated undrained trixial test with no cell pressure (that is, $\sigma_3 = 0$, as shown in Figure 2.17(a)), Hence, it is called unconfined compression test since the

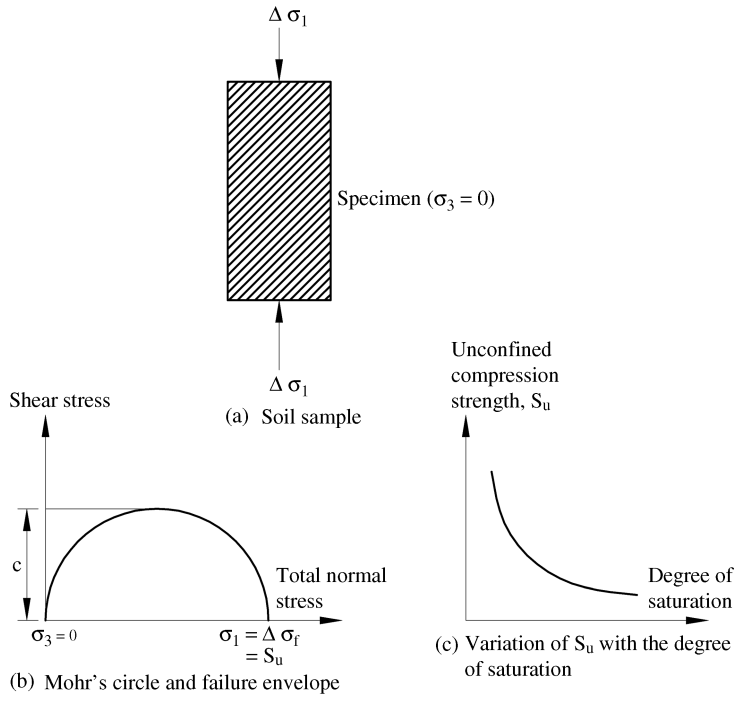

Figure 2.17 Unconfined compression test.

vertical compression stress, $\Delta\sigma_1$, is applied until failure. The corresponding Mohr's circle and failure envelope are shown in Figure 2.17(b). It may be noted that only one Mohr's circle can be drawn with $\sigma_3 = 0$ for the same soil sample, and hence only one shear strength parameter can be determined (as it requires two or more circles to draw a unique envelope tangential to these circles). Thus only cohesion can be determined as shown. Hence, it is more relevant to cohesive soils where only cohesion, c exists while friction angle, $\phi = 0$. Thus, the major principal stress $\sigma_1 = \Delta\sigma_f$ is the unconfined compression strength of the soil, usually referred to as S_u. Then, the shear strength

$$s = c = \frac{S_u}{2} \tag{2.34}$$

As can be seen from Figure 2.17(b), UCC tests are usually conducted on unsaturated soil samples. The UCC strength decreases with the increase in degree of saturation as shown in Figure 2.17(c).

2.10.5 Correlations

There are several well known correlations between the shear strength parameters, plasticity index (PI), over burden pressure and the results of various field tests (Das, 2007).

2.10.6 Sensitivity and Thixotropy

Usually the UCC strength is considerably reduced from its natural value when the soils are tested using remolded (thus disturbed) samples of most natural clays. This is called sensitivity. This is defined by the sensitivity ratio of the soil as

$$S_r = \frac{S_u(\text{undisturbed})}{S_u(\text{remolded})} \tag{2.35}$$

where S_u is the UCC strength, as explained in the previous sections. S_r values range from 1.0 to 8.0. The loss of strength is mainly attributed to the destruction of the particle structure of clays which existed prior to the disturbance or remolding.

In most clays, if a remolded soil specimen is kept in an undisturbed state (i.e., without any change in water content), it will gradually regain part of its strength with time. This phenomenon is called thixotropy. Thixotropy is a time dependent and reversible process (Taylor, 1964; Das, 2002).

2.11 Soil Exploration and Sampling

Foundation loads are supported by the soil below and it is in this context we have to know the behavior of soil layers existing at the site. This process of identifying the nature of soils and their physical properties is called soil or subsurface exploration. While carrying out the soil exploration, disturbed and undisturbed soil samples are collected for carrying out all laboratory tests discussed in the above sections. Also, some *in situ* tests are conducted while boring for soil exploration.

2.11.1 Purposes of Soil Exploration

The purposes for soil exploration are to obtain the general and necessary information needed for the project:

1. Selection of type and depth of foundation to suit the superstructure and soil at site
2. Determination of bearing capacity of the foundation
3. Determination of the settlement of the foundation due to loads
4. Locating the ground water level
5. Determination of the earth pressure against retaining walls, abutments, sheet piles and so on
6. To safeguard against construction difficulties
7. Assessing the suitability of soil and the degree of compaction of fill for base slabs, pavements, retaining walls and so on
8. Soil exploration is also needed for investigation of the safety of existing structures, that is, effect on settlement and carrying out the remedial measures if necessary for the structures to ensure safety
9. For highways and runways it is necessary for carrying out the following:
   a. The location of the roads (and runways)
   b. The location and selection of soils for fills and ground improvement, if necessary
   c. The design and location of ditches, culverts and drains
   d. The design of highway or runways
   e. The location of local construction materials when adopting them for construction.

The planning of a soil exploration should always start by obtaining preliminary information. For buildings and similar projects, the following information should be obtained first:

1. Available information of soils and existing structures
2. Reconnaissance of the area
3. Requirements of codes
4. Data for preliminary design.

After this information is obtained, a tentative exploration program is worked out. The first two or three borings should be randomly located around the entire site to disclose the general characteristics of the subsoils. As the boring operation progresses, the balance of the boring program may be revised so that the number and types of borings furnish enough data concerning the arrangement of the successive soil strata. Also sufficient number of soil samples are taken for laboratory tests from these bore holes. Some field tests are also carried out to correlate the results with the laboratory tests.

The details of the above phases of exploration are given in Taylor (1964), Teng (1964), Bowles (1996), Tomlinson (2001), Das (2007) and other books.

2.12 Site Investigation – Boring, Sampling and Testing

The site investigation phase consists of three steps, namely boring, sampling (taking soil or rock sample from the bore hole) and testing. Testing may be done both in the field and in the laboratory.

At least one soil sample may be taken at every 1.5 – 2.0 m of depth of the bore hole. A soil sampler (split spoon, Shelby tube and others) is driven into the ground to take a soil sample. The sample is visually examined and saved for laboratory test. Then, the bole hole is advanced for about 1.0 m. During the advancing of the hole, shavings and cuttings of soil brought up by the boring tools are observed. If soil shavings indicate change in soil characteristics, the depth where the change occurs needs to be recorded and additional soil samples should be taken. The sampler is again advanced to take soil sample. In such alternative sequence, the test hole is advanced and soil samples are taken. In certain critical layers, continuous sampling may have to be done.

While advancing the bole hole, water level in the test holes should be observed. Lack of information concerning the ground water level will result in inadequate designs and difficulties in construction.

2.12.1 Minimum Depth of Bore Holes

The rules established by the American Society of Civil Engineers in 1972 (Das, 2007) may be used for determining the minimum depth of boring required:

1. Determine the net increase in the effective stress, $\Delta\sigma'$, under a foundation with depth as shown in Figure 2.18, using expressions for stress distribution in soils (Chapter 3).
2. Estimate the variation of the vertical effective stress, σ'_o, with depth.
3. Determine the depth, $D = D_1$, at which the effective stress increase $\Delta\sigma'$ is equal to (1/10) p (where p = estimated net stress on the foundation).
4. Determine the depth, $D = D_2$, at which $\Delta\sigma'/\sigma'_o = 0.05$.

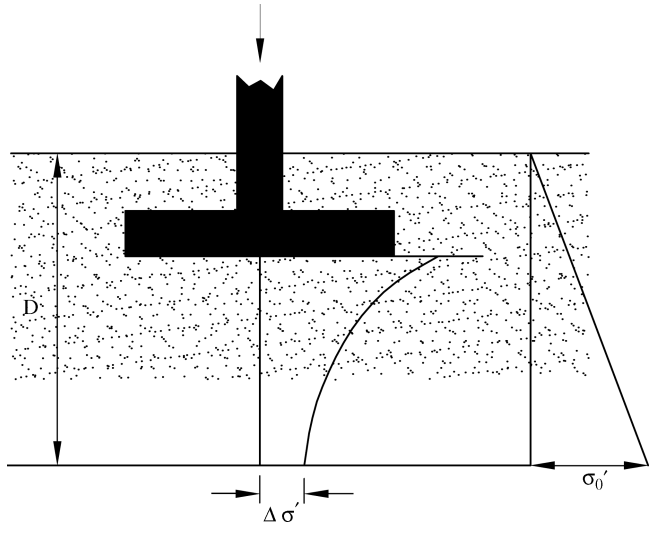

Figure 2.18 Minimum depth of bore hole.

5. Choose the smaller of the two depths, D_1 and D_2, as the approximate minimum depth of boring required, unless bedrock is encountered.

If the preceding guidelines are used, the approximate depths of boring for a building with a width of 30 m are given below in Table 2.6 (Das, 2007).

The approximate spacing of bore holes is given in Table 2.7 for planning the site investigation.

Table 2.6 Bore hole depths.

Number of stories in building	Depth of bore hole (m)
1	3.5
2	6
3	10
4	16
5	24

Table 2.7 Spacing of bore holes.

Structure/project	Bore hole spacing (m)
Multistorey building	10–30
Industrial plant (single storey)	20–60
Highways	250–500
Residential colony	250–500
Dams and dikes	40–80

The literature available on soil exploration and site investigation is extensive in terms of boring techniques, samplers and sampling techniques and other field techniques. The readers and practitioners may refer to Hvorslev (1949), Tomlinson (2001) and several other books for further details.

In addition to the laboratory tests that may be carried out on disturbed and undisturbed samples described in the earlier sections, several field tests also are carried out while boring is done at site. Some important field tests are described below. Field tests are generally more preferable because they are done *in situ* with the soil being in almost undisturbed state. However, they require lot of coordination at site and are generally expensive.

2.13 Split Spoon Sampler and Standard Penetration Test

The split spoon sampler is one of the samplers used in the field to obtain soil samples that are generally disturbed, but still representative. A standard split spoon sampler is shown in Figure 2.19. The sampler consists of a steel driving shoe, a steel tube that is split longitudinally in half, with a coupling at the top as shown in the figure. The coupling connects the sampler to the drill rod. The tube has an inside diameter of 34.93 mm and an outside diameter of 50.8 mm.

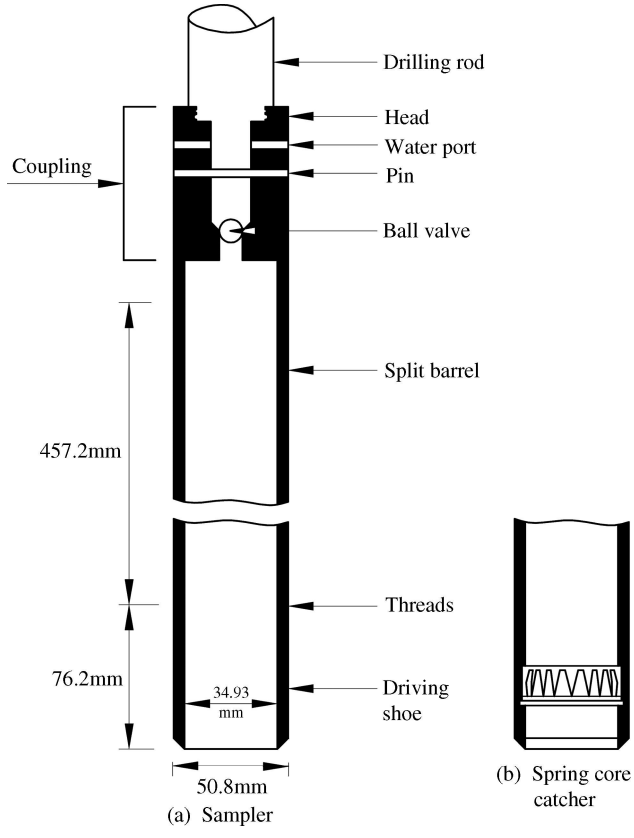

Figure 2.19 Standard split spoon sampler.

However, samplers having inside and outside diameters up to 63.5 mm and 76.2 mm, respectively, are also used. When a borehole has reached the required depth, the drill tools are removed and the sampler is lowered to that level. The sampler is then driven into the soil by hammer blows given at the top of drill rod. The standard weight of the hammer is 622.72 N, and for each blow, the hammer drops from a height of 0.762 m. The number of blows required for the spoon penetration at three intervals of 152.4 mm are recorded. The number of blows required for last two intervals are added to give the standard penetration number, N, at the depth. This number is generally referred to as the N value. The sampler is then withdrawn, and the shoe and coupling are removed. Then, the soil sample is recovered from the tube and is placed in a container and brought to the laboratory for testing. This field test is called the standard penetration test (SPT).

The soil sample is usually disturbed due to drilling and hammering. The degree of disturbance of the soil sample is expressed as

$$A_R(\%) = \frac{D_o^2 - D_i^2}{D_i^2}(100) \tag{2.36}$$

where

A_R = area ratio (ratio of disturbed area to total area of soil)
D_o = outside diameter of the sampling tube
D_i = inside diameter of the sampling tube.

When the area ratio is 10% or less, the sample generally is considered as undisturbed. For a standard split spoon sampler, with dimensions shown in Figure 2.19(a)

$$A_R = 111.5\% \tag{2.37}$$

Hence, these samples are highly disturbed. Split spoon samples generally are taken at intervals of about 1.5 m. If the material encountered in the field is sand (particularly fine sand below the water table), recovery of the sample by a split spoon sampler may be difficult. In that case, a device such as a spring cone catcher may have to be placed inside the split spoon (Figure 2.19(b)) to recover the sample.

It may be noted that several factors contribute to the variation of the standard penetration number N at a given depth for similar soil profiles. These are the SPT hammer efficiency, borehole diameter, sampling method and rod length factor (Das, 2007). A safety hammer and donut hammer are commonly used in the field. They are dropped by a rope with two wraps around a pulley.

On the basis of field observations, SPT values are standardized as a function of the input driving energy and its dissipation around the sampler into the surrounding soil as

$$N_{60} = \frac{N\eta_H\eta_B\eta_S\eta_R}{60} \tag{2.38}$$

where

N_{60} = standard penetration number, corrected for field conditions to an average energy ratio of 60%
N = measured penetration number
η_H = hammer efficiency (%)
η_B = correction for borehole diameter
η_S = sample correction
η_R = correction for rod length.

Variations of η_H, η_B, η_S and η_R are summarized by Das (2007) based on recommendations by Seed *et al.* and Skempton (Das, 2007). Besides, using it as a sampler, the split spoon sampler is useful to obtain both the disturbed soil samples for laboratory tests and also the N values (SPT). These SPT values provide several useful correlations. For example, the consistency of clayey soils can often be estimated from the standard penetration number, $N_{60,}$ as shown in Table 2.8. However, correlations for clays require tests to verify that the relationships are valid for the clay deposit being examined.

Table 2.8 Consistency of clays and approximate correlation with N_{60}.

Standard penetration number, N_{60}	Consistency	Unconfined compression strength, q_u ($=S_u$) (kN/m^2)
0–2	Very soft	0–25
2–5	Soft	25–50
5–10	Medium stiff	50–100
10–20	Stiff	100–200
20–30	Very stiff	200–400
>30	Hard	>400

There are many correlations between the standard penetration number and the undrained shear strength or cohesion of clay, c_u. On the basis of results of undrained triaxial tests conducted on insensitive clays, Stroud (Das, 2007) suggested that

$$c_u = KN_{60} \tag{2.39}$$

where

K = constant = 3.5–6.5 kN/m^2

N_{60} = standard penetration number obtained from the field.

The OCR of a natural clay deposit can also be correlated with the standard penetration number. On the basis of the regression analysis, Mayne and Kemper (Das, 2007) obtained the relationship

$$\text{OCR} = 0.193\left(\frac{N_{60}}{\sigma'_o}\right)^{0.689} \tag{2.40}$$

where σ'_o = effective vertical stress in MN/m^2

In granular soils, the value of N is affected by the effective overburden pressure, σ'_o. For that reason, the value of N_{60} obtained from field exploration under different overburden pressures should be changed to correspond to a standard value of σ'_o. That is

$$(N_1)_{60} = C_N N_{60} \tag{2.41}$$

where

$(N_1)_{60}$ = value of N_{60} corrected to standard value of σ'_o (100 kN/m^2)

C_N = correction factor

N_{60} = value of N obtained from field exploration (Equation (2.38)).

In the past, a number of empirical relations were proposed for C_N. The most commonly cited relationships are those of Liao and Whitman, and Skempton (Das, 2007).

In the following relationships for C_N, note that σ'_o is the effective overburden pressure and p_a = atmospheric pressure ($\approx$100 kN/m^2).

Liao and Whitman's correlation:

$$C_N = \frac{1}{\left(\frac{\sigma'_o}{p_a}\right)^{0.5}} \tag{2.42}$$

Skempton's correlation:

$$C_N = \left[\frac{2}{\left(1 + \frac{\sigma'_o}{p_a}\right)}\right] \tag{2.43}$$

where

σ'_o = effective overburden pressure
p_a = atmospheric pressure ($\approx$100 kN/m^2)

The other empirical correlation between the corrected standard penetration number and the relative density of sand is given in Table 2.9. There are several such empirical correlations available in literature (Das, 2007).

Table 2.9 Correlation between corrected $(N_1)_{60}$ values and the relative density in sands, D_r (%).

$(N_1)_{60}$	Approximate relative density, D_r (%)
0–5	0–5
5–10	5–30
10–30	30–60
30–50	60–95

The peak friction angle, φ', of granular soil has also been correlated with N_{60} and $(N_1)_{60}$ by several investigators. Some of these correlations are as follows:

1. Peck, Hanson and Thornburn (1974) give a correlation between $(N_1)_{60}$ and φ' in a graphical form, which can be approximated as

$$\phi'(\text{deg}) = 27.1 + 0.3(N_1)_{60} - 0.00054[(N_1)_{60}]^2 \tag{2.44}$$

Schmertmann provided an approximate correlation between N_{60}, σ'_o and φ' (Das, 2007) as

$$\phi' = \tan^{-1}\left[\frac{N_{60}}{12.2 + 20.3\frac{\sigma'_o}{p_a}}\right]^{0.34} \tag{2.45}$$

where

N_{60} = field standard penetration number
σ'_o = effective overburden pressure
p_a = atmospheric pressure with the same units as σ'_o
φ' = soil friction angle.

Although these correlations are approximate, the standard penetration test provides a good evaluation of soil properties, if interpreted properly. The primary sources of error in standard penetration tests are inadequate cleaning of the borehole, eccentric hammer strikes on the drill rod, and inadequate maintenance of water head in the borehole and so on. In addition to the split spoon sampler, there are a large number of samplers used in site investigation such as thin walled tube sampler, piston samplers and several other sophisticated samplers (Hvorslev, 1949).

2.14 Cone Penetration Test

The cone penetration test (CPT), originally known as the Dutch cone penetration test, is a versatile method that can be used to determine the soil profile and estimate the engineering properties. This is also called the static cone penetration test. In the original version, a 60° cone with a base area of 10 cm^2 was pushed into the ground at a steady rate of about 20 mm/s and the resistance to penetration (called the point resistance) was measured.

The cone penetrometers in use at present measure: (a) the cone resistance (q_c) to penetration developed by the cone, which is equal to the vertical force applied to the cone, divided by its horizontally projected area, and (b) the frictional resistance (f_c), which is the resistance measured by a sleeve located above the cone with the local soil surrounding it. The resistance is equal to the vertical force applied to the sleeve, divided by its surface area, which gives the sum of friction and adhesion.

Two types of penetrometers are used to measure q_c and f_c:

1. Mechanical friction cone penetrometer (Figure 2.20)
   The tip of the penetrometer is connected to an inner set of rods. The tip is first advanced about 40 mm, giving the cone resistance. With further pushing, the tip engages the friction sleeve. As the inner rod advances, the rod force is equal to the sum of the vertical forces on the cone and sleeve. Subtracting the force on the cone gives the side frictional resistance.
2. Electric friction cone penetrometer (Figure 2.21)
   In this equipment, the tip of the penetrometer is attached to a string of steel rods. The tip is pushed into the ground at the rate of 20 mm/s. Wires from the transducers continuously measure the cone and side resistance.

The typical results of penetrometer tests in a soil profile with point and friction resistance measurements by a mechanical friction cone penetrometer are shown in Figure 2.22.

Several correlations of CPT values with properties of soils have been developed for the point resistance (q_c) and the friction ratio (F_r) obtained from the cone penetration tests. The friction ratio is defined as

$$F_r = \frac{\text{frictional resistance}}{\text{cone resistance}} = \frac{f_c}{q_c} \tag{2.46}$$

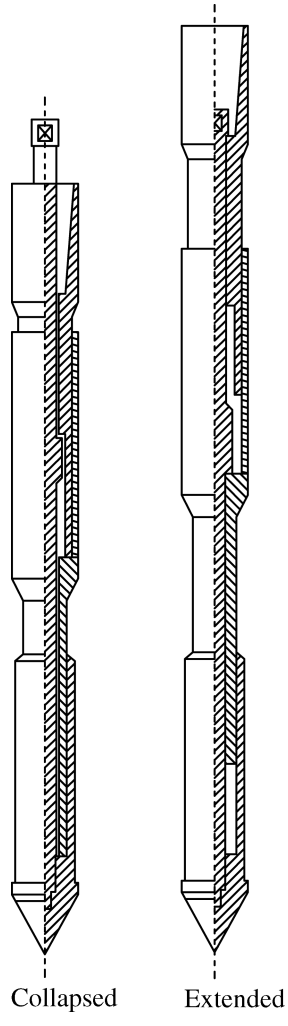

Figure 2.20 Sketch of mechanical friction cone penetrometer.

As in the case of standard penetration tests, several correlations have been developed between q_c and other soil properties (Das, 2007).

Correlation Between Relative Density (D_r) and q_c for Sand

The following relationship to correlate D_r, q_c and the vertical effective stress σ'_o is given by Kulhawy and Mayne (Das, 2007)

$$D_r = \sqrt{\left[\frac{1}{305 Q_c \mathrm{OCR}^{1.8}}\right]\left[\frac{q_c / p_a}{\left(\sigma'_{0.5} / p_a\right)^{0.5}}\right]} \tag{2.47}$$

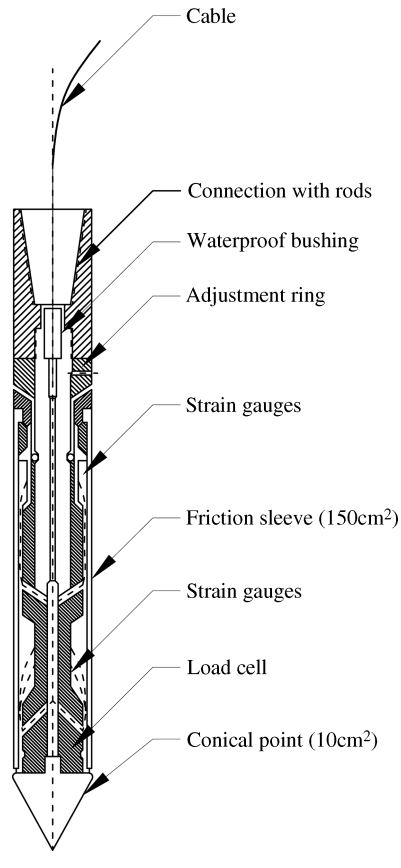

Figure 2.21 Sketch of electric friction cone penetrometer.

where

OCR = overconsolidation ratio
p_a = atmospheric pressure
Q_c = compressibility factor.

The values of Q_c are recommended as below:

1. Highly compressible sand = 0.91
2. Moderately compressible sand = 1.0
3. Low compressible sand = 1.09

Correlation Between q_c and Drained Friction Angle (φ') for Sand

A relationship between q_c/N_{60} (N_{60} = field standard penetration resistance) versus mean grain size (D_{50}) for various types of soils is shown in Figure 2.23 (Das, 2007). Several such empirical correlations are available in literatures which are useful for interpretation of soil data.

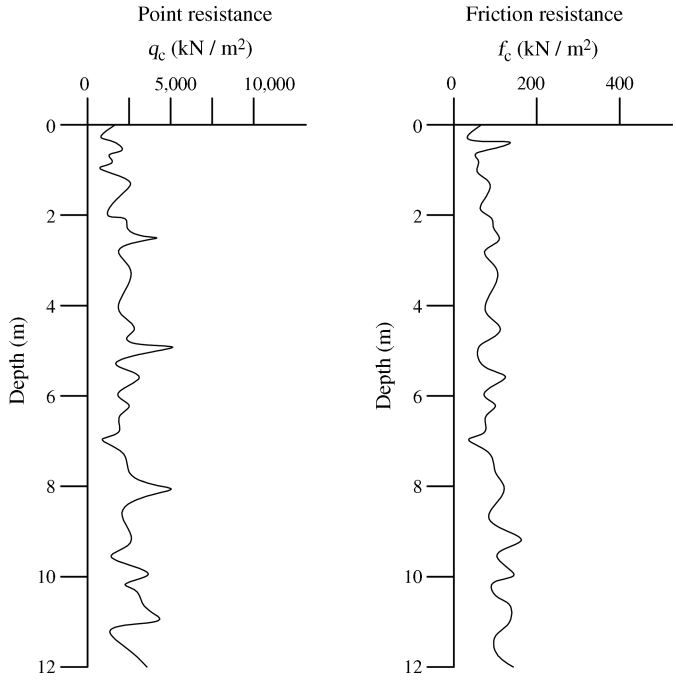

Figure 2.22 Typical results of cone penetrometer test (CPT).

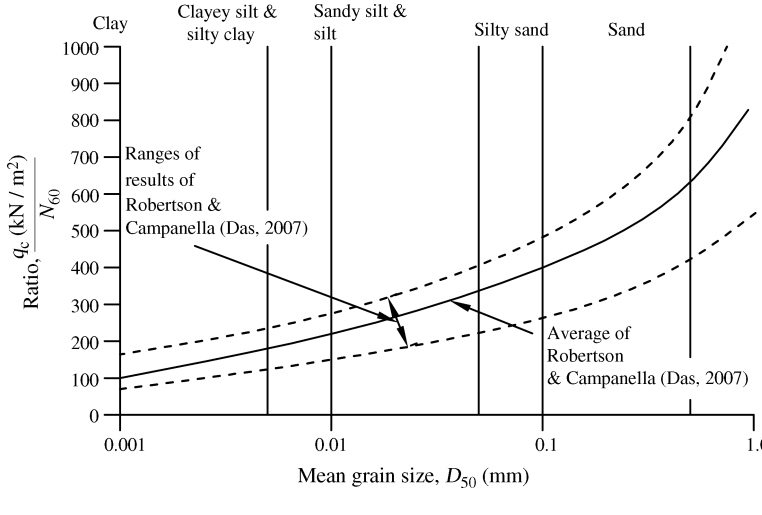

Figure 2.23 Correlation of q_c/N_{60} for different soils.

2.15 Field Vane Shear Test

The vane shear test is described in Section 2.10.2 except that the dimensions of the field vane (diameter, d, and height, h) are bigger than the laboratory vane dimensions. The *in situ* undrained shear strength can be obtained using the field vane test by the Equation (2.32). However, it may be noted that this test is more suited for predominantly cohesive soils.

2.16 Other *In Situ* Tests

In recent times, several other *in situ* static and dynamic tests are being used to correlate the engineering properties of the soil with the results of these tests. These are the dilatometer test (DMT), pressure meter test (PMT) and so on (Bowles, 1996). Plate load test and cyclic plate load test are also used to obtain the pressure – settlement curves and determine the elastic properties, coefficient of subgrade reaction, elastic settlements of the soil and these are described in detail in Chapters 3 and 4 (Kameswara Rao, 2000). Several tests are also adopted for evaluating the *in situ* elastic properties of the soil using wave propagation methods, and correlating them with soil properties of soil layers.

These are geophysical refraction survey methods, cross-hole techniques, SASW technique and so on and are described in several books on foundation dynamics and geophysics (Kameswara Rao, 1998, 2002). Ground penetration radar (GPR) is also being developed to explore the properties of soils using microwave transmission (Kameswara Rao, 1998).

2.17 Summary

Thus, brief descriptions of basic soil properties, laboratory tests, soil exploration, *insitu* field tests and correlations with engineering properties of soils are presented in this chapter.

The determination of parameters for the design of foundation, such as bearing capacity, settlement analysis, stress distribution in soils and lateral pressures are presented in the next chapter.

2.18 Examples

In all these examples, acceleration due to gravity, g, is taken as 9.8 m/s^2 and the unit weight of water, γ_w, is taken as 9.8 kN/m^3, unless stated otherwise.

Example 2.1

Derive an expression for w (water content) in terms of γ_{sub} (submerged unit weight of soil) and S (degree of saturation), and G (specific gravity). Find w, γ_s (bulk unit weight) and γ_{dry} (dry unit weight) for a soil with $S = 85\%$, $\gamma_{sub} = 9.8\,\text{kN/m}^3$, $G = 2.70$.

Solution:

$$Se = wG$$

i. $\gamma_{sub} = \dfrac{G-1}{1+e}\gamma_w, \qquad \therefore e = \dfrac{(G-1)\gamma_w - \gamma_{sub}}{\gamma_{sub}}$

$$\therefore w = \frac{Se}{G} = \frac{S}{G}\left[\frac{(G-1)\gamma_w - \gamma_{sub}}{\gamma_{sub}}\right]$$

$$\because S = 0.85,\ \gamma_{sub} = 12\,\text{kN/m}^3,\ G = 2.70,\ \gamma_w = 9.8\,\text{kN/m}^3$$

$$\therefore w = \frac{S}{G}\left[\frac{(G-1)\gamma_w - \gamma_{sub}}{\gamma_{sub}}\right] = \frac{0.85}{2.70}\left[\frac{[(2.70-1)\,(9.8)]-12}{12}\right] = 0.122$$

ii. $$e = \frac{(G-1)\gamma_w - \gamma_{sub}}{\gamma_{sub}} = \frac{[(2.7-1)(9.8)]-12}{12} = 0.388$$

$$\gamma_{bulk} = \frac{G + Se}{1+e}\gamma_w = \frac{2.7 + 0.85 \times 0.388}{1 + 0.388} \times 9.8 = 21.387\,\text{kN/m}^3$$

$$\gamma_{dry} = \frac{G}{1+e}\gamma_w = \frac{2.7 \times 9.8}{1 + 0.388} = 19.06\,\text{kN/m}^3$$

Example 2.2

A fine sand has an in-place unit weight of 18.85 kN/m^3 and a water content of 5.2%. The specific gravity of solids is 2.66. Void ratios at densest and loosest conditions are 0.38 and 0.92, respectively. Find the relative density.

Solution:

$$\gamma_t = 18.85\,\text{kN/m}^3,\ w = 5.2\%,\ G = 2.66,\ e_{\text{dense}} = 0.38,$$

$$e_{\text{loose}} = 0.92,\ \gamma_w = 9.8\,\text{kN/m}^3$$

$$\gamma_t = \frac{G(1+w)}{1+e}\gamma_w, \quad \therefore e = \frac{G(1+w)\gamma_w}{\gamma_t} - 1$$

$$\therefore e = \frac{G(1+w)\gamma_w}{\gamma_t} - 1 = \frac{2.66(1+0.052)(9.8)}{18.85} - 1 = 0.455$$

$$\text{Relative density, } D_r = \frac{e_{maz} - e}{e_{\max} - e_{\min}} = \frac{0.92 - 0.455}{0.92 - 0.38} = 0.86 = 86\%$$

Example 2.3

A 0.082 m^3 sample of soil weighs 1.445 kN. When it is dried out in an oven, it weighs 1.301 kN. The specific gravity of solids is found to be 2.65. Find the water content (w), void ratio (e), porosity (n), degree of saturation (S) and the wet and dry unit weights.

Solution:

$$V = 0.082\,\text{m}^3, \text{ Bulk weight} = 1.445\,\text{kN},$$

$$\text{After drying,} \qquad W_s = 1.445\,\text{kN}$$

$$W_w = 1.445 - 1.301 = 0.144\,\text{kN}$$

$$\therefore w = \frac{W_w}{W_s} = \frac{0.144}{1.301} = 0.11 = 11\%$$

$$\gamma_t = \frac{\text{soil weight}}{\text{sample volume}} = \frac{1.445\,\text{kN}}{0.082\,\text{m}^3} = 17.62\,\text{kN/m}^3$$

$$\because G = 2.65,\ \gamma_t = \frac{G + Se}{1 + e}\gamma_w = \frac{G(1 + w)}{1 + e}\gamma_w = \frac{2.65(1 + 0.11)}{1 + e} \times 9.8$$

$$= 17.62\,\text{kN/m}^3$$

$$\therefore \frac{2.65(1 + 0.11)}{1 + e} \times 9.8 = 17.62$$

$$e = \left[\frac{2.65(1 + 0.11)}{17.62} \times 9.8\right] - 1 = 0.636$$

$$n = \frac{e}{1 + e} = \frac{0.636}{1 + 0.636} = 0.39 = 39\%$$

$$\text{Wet unit weight} = \gamma_t = 17.62\,\text{kN/m}^3$$

$$\text{Dry unit weight} = \gamma_{dry} = \frac{G}{1 + e}\gamma_w = \frac{2.65}{1 + 0.636} \times 9.8 = 15.87\,\text{kN/m}^3$$

Example 2.4

A cylindrical sample 3.5 cm diameter and 6.0 cm long weighs 0.91 N. $S = 43\%$, $G = 2.70$, $\gamma_w = 10\,\text{kN/m}^3$. Determine w. If there had been an error of 10% in measuring the weight of the sample, what would be the percentage error in w?

Solution:

$$S = 43\%,\ G = 2.70,\ \gamma_w = 10\,\text{kN/m}^3$$

$$\text{Volume of sample} = \frac{\pi \times 3.5^2}{4} \times 6 = 57.73\,\text{cm}^3 = 57.73 \times 10^{-6}\,\text{m}^3$$

$$\text{Weight} = 0.91 \times 10^{-3}\,\text{kN}, \qquad \gamma_t = \frac{0.91 \times 10^{-3}}{57.73 \times 10^{-6}} = 15.76\,\text{kN/m}^3$$

$$\gamma_t = \frac{G + Se}{1 + e}\gamma_w, \qquad \therefore e = \frac{G\gamma_w(1 + w) - \gamma_t}{\gamma_t}$$

$$\therefore \gamma_t(1 + e) = (G + Se)\gamma_w$$

$$\therefore e(\gamma_t - S\gamma_w) = G\gamma_w - \gamma_t$$

$$\therefore e = \frac{G\gamma_w - \gamma_t}{\gamma_t - S\gamma_w} = \frac{(2.7 \times 10) - 15.76}{15.76 - (0.43 \times 10)} = \frac{11.24}{11.46} = 0.98$$

$$Se = wG, \quad \therefore w = \frac{Se}{G} = \frac{0.43 \times 0.98}{2.7} = 0.156$$

$$w = \frac{Se}{G}, \quad e = \frac{G\gamma_w(1 + w) - \gamma_t}{\gamma_t}, \quad \therefore w = \frac{S}{G}\left[\frac{G\gamma_w(1 + w) - \gamma_t}{\gamma_t}\right]$$

$$wG\gamma_t = S[G\gamma_w(1 + w) - \gamma_t] = SG\gamma_w(1 + w) - S\gamma_t$$

$$wG\gamma_t - SG\gamma_w w = SG\gamma_w - S\gamma_t$$

$$w = \frac{SG\gamma_w - S\gamma_t}{G\gamma_t - SG\gamma_w}$$

$$\partial w = \frac{[(G\gamma_t - SG\gamma_w)(-S\partial\gamma_t)] - [(SG\gamma_w - S\gamma_t)G\partial\gamma_t]}{(G\gamma_t - SG\gamma_w)^2}$$

Noting that a 10% error in weight results in a 10% error in γ_t, we have $\frac{\partial\gamma_t}{\gamma_t} = 0.1$ Then

$$\therefore \frac{\partial w}{w} = \partial\gamma_t\left[\frac{-S(G\gamma_t - SG\gamma_w) - G(SG\gamma_w - S\gamma_t)}{(G\gamma_t - SG\gamma_w)^2}\right]\frac{1}{w} = \text{Error in } w$$

$$= \partial\gamma_t\left[\frac{-S(G\gamma_t - SG\gamma_w) - G(SG\gamma_w - S\gamma_t)}{(G\gamma_t - SG\gamma_w)^2}\right] \times \frac{G\gamma_t - SG\gamma_w}{SG\gamma_w - S\gamma_t}$$

$$= \frac{\partial\gamma_t}{\gamma_t}\frac{\gamma_t[-S(G\gamma_t - SG\gamma_w) - G(SG\gamma_w - S\gamma_t)]}{(G\gamma_t - SG\gamma_w)(SG\gamma_w - S\gamma_t)}$$

$$= \frac{\partial\gamma_t}{\gamma_t}\gamma_t\left[\frac{SG\gamma_w(S - G)}{(G\gamma_t - SG\gamma_w)(SG\gamma_w - S\gamma_t)}\right]$$

$$= \frac{0.1 \times 15.76 \times [0.43 \times 2.7 \times 10 \times (0.43 - 2.7)]}{(2.7 \times 15.76 - 0.43 \times 2.7 \times 10)(0.43 \times 2.7 \times 10 - 0.43 \times 15.76)}$$

$$= -\frac{1.576 \times 11.61 \times 2.27}{(30.94 \times 4.9332)} = -0.2721$$

$$\therefore \%\text{ error in } w = 27.21\%$$

Example 2.5

An undistributed soil sample has a void ratio of 0.56, water content of 15% and specific gravity of solids of 2.64. Find the wet (total) and dry unit weights (kN/m^3), porosity and degree of saturation.

Solution:

$$e = 0.56, \quad w = 15\%, \quad G = 2.64$$

$$Se = wG \qquad \therefore S = \frac{wG}{e} = \frac{0.15 \times 2.64}{0.56} = 0.7071 = 70.71\%$$

$$\gamma_t = \frac{G(1+w)}{1+e}\gamma_w = \frac{2.64(1+0.15)}{1+0.56}9.8 = 19.07\,\text{kN/m}^3$$

$$\gamma_d = \frac{G}{1+e}\gamma_w = \frac{2.64}{1+0.56}9.8 = 16.58\,\text{kN/m}^3$$

$$n = \frac{e}{1+e} = \frac{0.56}{1+0.56} = 0.359 = 35.9\%$$

Example 2.6

Derive an expression for w (water content) in terms of γ_{sub} (submerged unit weight), degree of saturation, S, and specific gravity, G. Find S and γ_{dry} if γ_{sub} is 10 kN/m^3 and w = 22%. G = 2.70, $\gamma_w = 10\,\text{kN/m}^3$.

Solution:

$$Se = wG, \qquad \gamma_{sub} = \frac{G-1}{1+e}\gamma_w, \qquad \gamma_{sub}(1+e) = (G-1)\gamma_w$$

$$\therefore e = \frac{(G-1)\gamma_w}{\gamma_{sub}} - 1 = \frac{(G-1)\gamma_w - \gamma_{sub}}{\gamma_{sub}}$$

$$\therefore w = \frac{Se}{G} = \frac{S}{G}\left[\frac{(G-1)\gamma_w - \gamma_{sub}}{\gamma_{sub}}\right]$$

$$\gamma_{sub} = 10\,\text{kN/m}^3, \quad w = 22\%, \quad G = 2.70, \quad \gamma_w = 10\,\text{kN/m}^3$$

$$\therefore e = \frac{(G-1)\gamma_w - \gamma_{sub}}{\gamma_{sub}} = \frac{(2.7-1)10-10}{10} = 0.7$$

$$S = \frac{wG}{e} = \frac{0.22 \times 2.7}{0.7} = 0.85 = 85\%$$

$$\gamma_{dry} = \frac{G}{1+e}\gamma_w = \frac{2.7}{1+0.7} \times 10 = 15.88\,\text{kN/m}^3$$

Exercise Problems

2.1 The water content of a 100% saturated soil is 30% and the specific gravity of solids is 2.65. Determine the void ratio and unit weight (kN/m^3).

2.2 A soil sample has the following data:

i. Degree of saturation = 46%
ii. Void ratio = 0.8
iii. Specific gravity of solids = 2.70.

Find its water content and unit weight (kN/m^3).

2.3 A 0.08 m^3 sample of soil weighs 1.4 kN. When it is dried out in an oven, it weighs 1.3 kN. The specific gravity of solids is found to be 2.70. Find the water content, void ratio, porosity, degree of saturation and the wet and dry unit weights.

2.4 The unit weight of a soil sample is 18.00 kN/m^3. Its specific gravity of solids and water content are 2.70 and 15%, respectively. Find the dry unit weight, void ratio and degree of saturation.

2.5 A fine sand has an in-place unit weight of 18.75 kN/m^3 and a water content of 5.0%. The specific gravity of solids is 2.70. Void ratios at densest and loosest conditions are 0.38 and 0.92, respectively. Find the relative density.

2.6 A container with soil sample of completely saturated clay weighs 0.7 N. After drying, the weight becomes 0.62 N. The container weight is 0.35 N and the specific gravity of the soil is 2.70. Determine the void ratio, water content and porosity of the original sample.

2.7 A moist sand sample has a volume of 464 cm^3 in natural state and a weight of 8.5 N. The dry weight is 7.4 N and the specific gravity is 2.68. Determine the void ratio, the porosity, the water content and the degree of saturation.

2.8 i. A dry soil has a void ratio of 0.65, and its grains have a specific gravity of 2.70. Determine the unit weight.
ii. Sufficient water is added to the sample to give a degree of saturation of 80%. There is no change in void ratio. Determine the water content and the unit weight.

2.9 A completely saturated clay has a water content of 42% and unit weight of 18 kN/m^3. Determine the void ratio and the specific gravity.

3

Bearing Capacity, Settlement, Stresses and Lateral Pressures in Soils

3.1 Introduction

The soil which is supporting the loads transmitted by the foundation should be capable enough so that the structure–foundation–soil system is safe and stable besides being serviceable without excessive settlements. Thus, stability and settlement aspects of soil have to be analyzed to arrive at the design pressure that can be safely carried by the soil so that the foundation type, shape, size and other parameters can be selected and designed accordingly. The limiting shear resistance beyond which the soil collapses or becomes unstable is called the ultimate bearing capacity (UBC). This is also referred to as soil shear failure and results in distortions in the superstructure leading to collapse. The foundation sinks into the ground as if there is no resistance from the soil below. This type of failure is also called bearing capacity failure.

3.1.1 General and Local Shear Failure of Soils

If the soil is generally dense, the settlement of the footing that precedes the ultimate shear failure is relatively small. It is called general shear failure (GSF) as shown in Figure 3.1(a) and curve 1 of the load settlement curves. If the soil is loose, then a large settlement precedes the shear failure as shown in Figure 3.1(b) and curve 2, of the load settlement curve. Such a failure is called a local shear failure (LSF).

3.1.2 Punching Shear Failure

In some structures like liquid storage tanks and rafts supported on loose soils, there could be a base shear failure in which the base/foundation undergoes a punching failure as shown in Figure 3.1c and curve 3 of the load settlement curve.

Foundation Design: Theory and Practice N. S. V. Kameswara Rao
 ISBN: 978-0-470-82534-1

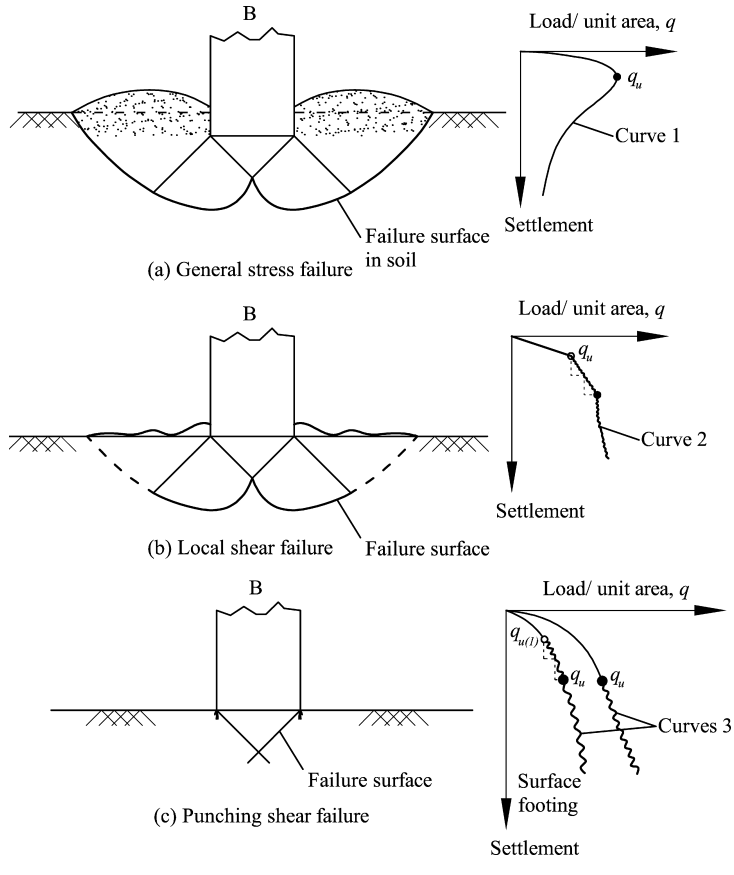

Figure 3.1 Sketches of bearing capacity failures in soil.

3.1.3 Failure Due to Large Settlements

Structural damage can also be caused by excessive settlements of the foundation–soil–system (without any shear failure of the soil) making the structure unserviceable with cracking, large distortions and misalignments in various components. The limiting soil pressure for such a failure due to large settlements is referred to as the allowable soil pressure (ASP).

In modern structures, the settlement failure is more common. The shear failures are reported mostly from embankments and similar structures/constructions. Punching shear failure is likely in liquid storage structures and raft foundations founded on soft soils.

3.1.4 Allowable or Design Soil Pressure

The criteria governing the allowable soil pressure depending on the breadth B of the foundation is shown in Figure 3.2. It can be noted from the figure, that the bearing capacity governs the allowable pressure up to certain breadth, beyond which it is the settlements that

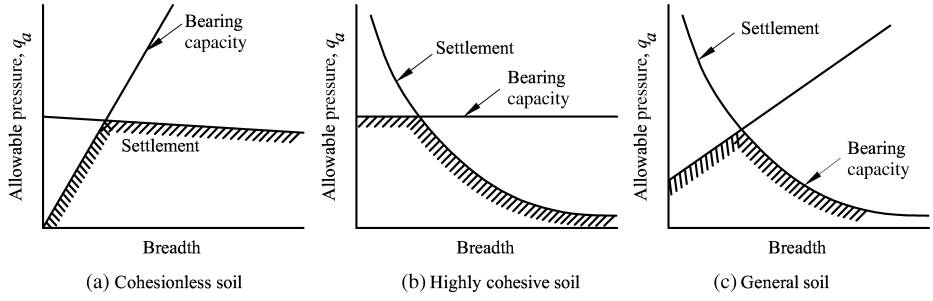

Figure 3.2 Relationships between allowable bearing pressure and breadth.

govern the design pressure, the limits, marked by the hatched region in the Figures 3.2(a)–(c) (Taylor, 1964).

These engineering parameters, that is, bearing capacity, settlement analysis, and elastic stress distribution in soils, lateral earth pressures are discussed with the focus on the applications in foundation design.

3.2 Ultimate Bearing Capacity of Shallow Foundations

3.2.1 Prandtl's Theory for Shallow Foundations

The earliest solution for ultimate bearing capacity (UBC) of soils for shallow foundations ($D_f \leq B$ in Figure 3.3) is due to Prandtl (Terzaghi, 1943; Taylor, 1964; Terzaghi and Peck, 1967) using plastic equilibrium theory with Mohr Coulomb failure criterion for the soil expressed in terms of shear strength as

$$s = c + \sigma \tan \phi \tag{3.1}$$

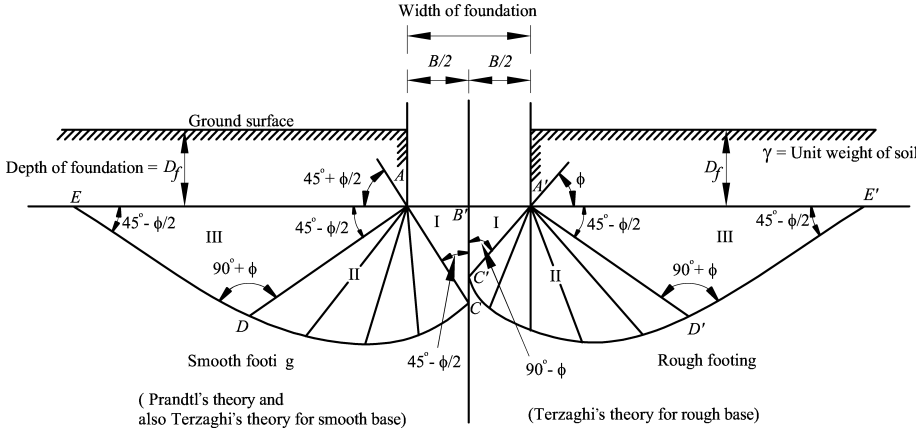

Figure 3.3 Bearing capacity theories of Prandtl and Terzaghi.

where

s = shear strength of soil

c, ϕ = cohesion and angle of internal friction of the soil

σ = normal stress.

The failure zone obtained by Prandtl for continuous or strip footing (two-dimensional cases) is shown on the left half of Figure 3.3 (keeping symmetry in view). It consists of three zones, that is, unsheared conical zone I, which moves downwards as a unit (Rankine's active zone), zone II, which is plastic with its curved boundary as a logarithmic spiral with its center at A (radial shear zone) and zone III which is forced by passive pressure upward and outward as a unit (Rankine's passive zone). Prandtl expressed the solution for ultimate bearing capacity, q_u, as

$$q_u = \left(\frac{c}{\tan\phi} + \frac{1}{2}\gamma B\sqrt{K_p}\right)(K_p e^{\pi \tan\phi} - 1) \tag{3.2}$$

where

c, ϕ = shear strength parameters of soil that is, cohesion and angle of internal friction respectively as given in Equation (3.1).

γ = unit weight of the soil.

$$K_p = \text{Rankine's passive earth pressure coefficient} = \frac{1+\sin\phi}{1-\sin\phi} \tag{3.3}$$

Prandtl's solution was originally derived for a weightless soil, except that the term $\frac{1}{2}\gamma\, B\sqrt{K_p}$ in Equation (3.2) is added later to account for the strength caused by the overburden pressure. It may further be noted that Prandtl's solution assumes that the foundation base (contact surface) is smooth.

3.2.2 Terzaghi's Theory for Shallow Foundations

Tergazhi modified Prandtl's solutions to include the weight of the soil for the foundations with smooth base as well as rough base (such as concrete foundations). He however assumed that the general shape of the various zones (I, II, III) remained the same as in Prandtl's solution, in spite of the fact that weight of the soil contained in the failure zones are included in the analysis. This amounts to a superposition of the solution of the analysis with and without body weight, which is not strictly correct since the failure envelopes in these two cases are slightly different (Terzaghi, 1943) but acceptable for practical applications. The zones of failure for the smooth and rough bases are shown on the left and right halves of the Figure 3.3. Only half the failure zones are shown for comparison in each case, noting that they are symmetric. It can be seen from Terzaghi's solution for the smooth base that the failure zones are identical to those of Prandtl while zones I, II and III are slightly different for a rough base (as shown on the right half of the Figure 3.3).

The main difference in the failure zones is the angle the failure plane of zone 1 makes with the base, that is, ϕ for a rough base as at A′ and $45 + \frac{\phi}{2}$ for a smooth base as at A. Terzaghi then

considered the equilibrium of the wedge AB'C (for a smooth base) and A'B'C' (for a rough base) and expressed the ultimate bearing capacity of a continuous or strip footing as

$$q_u = cN_c + qN_q + 0.5\gamma \quad BN_\gamma \tag{3.4}$$

where

c = cohesion of the soil
ϕ = angle of internal friction of the soil
γ = unit weight of the soil
$q = \gamma D_f$ = surcharge at the foundation base level
D_f = depth of the foundation
N_c, N_q, N_γ = nondimensional bearing capacity factors which are functions of ϕ.

These factors for the rough base are obtained by Terzaghi as

$$N_c = \cot\phi\left[\frac{e^{2(3\pi/4-\phi/2)\tan\phi}}{2\cos^2(45+\phi/2)}\right] = \cot\phi(N_q - 1) \tag{3.5}$$

$$N_q = \frac{e^{2(3\pi/4-\phi/2)\tan\phi}}{2\cos^2(45+\phi/2)} \tag{3.6}$$

$$N_\gamma = \frac{1}{2}\left[\frac{K_{p\gamma}}{\cos^2\phi} - 1\right]\tan\phi \tag{3.7}$$

where

$K_{P\gamma}$ = passive earth pressure coefficient.

For example, for $\phi = 0$, $N_c = 5.7$, $N_q = 1$, $N_\gamma = 0$ as shown in the Figure 3.4. The above bearing capacity factors are derived by Terzaghi, assuming a general shear failure of the soil

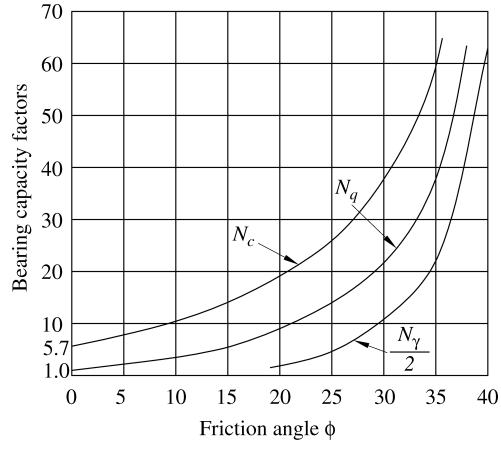

Figure 3.4 Terzaghi's bearing capacity factors for general shear failure – rough base.

(Section 3.1.1). These factors are available in the form of graphs (as shown in Figure 3.4) and also available in tabular form (Bowles, 1996; Das, 2007).

For local shear failure, Terzaghi modified the above equation as

$$q_u = c'N_c' + qN_q' + 0.5\gamma BN_\gamma' \tag{3.8}$$

where

$$c' = 2/3\, c \tag{3.9}$$

and N_c', N_q', N_γ' are bearing capacity factors given in Figure 3.4 corresponding to

$$\phi' = \tan^{-1}\left(\frac{2}{3}\tan\phi\right) \tag{3.10}$$

in which c and ϕ are the shear strength parameters of the soil as determined. The ultimate bearing capacity for foundations of other common shapes are expressed as follows.

Square foundation:

$$q_u = 1.3\, cN_c + qN_q + 0.4\gamma\, BN_\gamma \tag{3.11}$$

where B is the width of the foundation.

Circular foundation:

$$q_u = 1.3cN_c + qN_q + 0.3\gamma\, BN_\gamma \tag{3.12}$$

where B is the diameter of the foundation.

For local shear failure, Equations (3.11) and (3.12) are used with N_c', N_q', N_γ' with c′ and ϕ' given by Equations (3.9) and (3.10).

3.2.3 Modified Bearing Capacity Factors for Smooth Base

Based on laboratory and field studies, if the failure surface of zone 1 (Rankine active zone) is inclined at $45 + \frac{\phi}{2}$, as may be applicable for smooth base, the bearing capacity factors can be obtained as (Das, 2007)

$$N_c = (N_q - 1)\cot\phi \tag{3.13}$$

$$N_q = \tan^2(45 + \phi/2)\, e^{\pi \tan\phi} \tag{3.14}$$

$$N_\gamma = 2(N_q + 1)\tan\phi \tag{3.15}$$

For example, for $\phi = 0$, $N_c = 5.14, N_q = 1, N_\gamma = 0$ as per these factors.

3.2.4 Factors of Safety

The allowable bearing capacity q_{all} for purposes of foundation design is obtained as:

$$q_{\text{all}} = \frac{q_{\text{ult}}}{\text{FS}} \tag{3.16}$$

where FS = the factor of safety, usually taken as 3.

Terzaghi's bearing capacity factors are most commonly used for obtaining the UBC that is, q_{ult}, assuming rough base while the factors for smooth base and other factors available in literature are also used depending on the specific requirement. It may be observed that the differences in values of bearing capacity factors developed by various contributors are considered minor compared to the variations in soils at the same site whose parameters are not known unless tested extensively.

3.2.5 General Bearing Capacity Solutions

The basic bearing capacity equation developed by Terzaghi (Equation (3.4)) was modified by Terzaghi and others for application to general foundations to incorporate the effects of shape, depth of foundation and inclination of the applied load. The general equation can be written as

$$q_u = c\lambda_{cs}\lambda_{cd}\lambda_{ci}N_c + q\lambda_{qs}\lambda_{qd}\lambda_{qi}N_q + 0.5\,\lambda_{\gamma s}\lambda_{\gamma d}\lambda_{\gamma}N_{\gamma} \tag{3.17}$$

where

$\lambda_{cs}, \lambda_{qs}, \lambda_{\gamma s}$ = shape factors
$\lambda_{cd}, \lambda_{qd}, \lambda_{\gamma d}$ = depth factors
$\lambda_{ci}, \lambda_{qi}, \lambda_{\gamma i}$ = inclination factors
c = cohesion of the soil
N_c, N_q, N_{γ} = bearing capacity factors as described in Section 3.2.2 (commonly Terzaghi's factors given in Figure 3.4 are used though other factors are also adopted in specific situations).

These λ factors for shape, depth and inclination as given by Meyerhof (Das, 2002) are given in Table 3.1.

3.2.6 Effect of Ground Water Table

The following modifications have to be made in the computation to take into account the presence of ground water table depending on its relative location with respect to the depth of the foundation.

Case 1: If the ground water table is between 0 and D_f, as shown in Figure 3.5(a), then surcharge term q (second term of the Equations (3.4) and (3.17)) has to be computed as

$$q = \gamma(D_f - D) + \gamma_{sub}D \tag{3.18}$$

where $\gamma_{sub} = \gamma_{sat} - \gamma_w$ = submerged unit weight of soil.

Table 3.1 Meyerhof's λ factors for a rectangular footing (B = width, L = length).

Shape factors	
For $\phi = 0^\circ$:	For $\phi \geq 10^\circ$:
$\lambda_{cs} = 1 + 0.2\left(\frac{B}{L}\right)$	$\lambda_{cs} = 1 + 0.2\left(\frac{B}{L}\right)\tan^2\left(45 + \frac{\phi}{2}\right)$
$\lambda_{qs} = 1$	$\lambda_{qs} = \lambda_{\gamma s} = 1 + 0.1\left(\frac{B}{L}\right)\tan^2\left(45 + \frac{\phi}{2}\right)$
$\lambda_{\gamma s} = 1$	
Depth factors	
For $\phi = 0^\circ$:	For $\phi \geq 10^\circ$:
$\lambda_{cd} = 1 + 0.2\left(\frac{D_f}{B}\right)$	$\lambda_{cd} = 1 + 0.2\left(\frac{D_f}{B}\right)\tan\left(45 + \frac{\phi}{2}\right)$
$\lambda_{qd} = \lambda_{\gamma d} = 1$	$\lambda_{qd} = \lambda_{\gamma d} = 1 + 0.1\left(\frac{D_f}{B}\right)\tan\left(45 + \frac{\phi}{2}\right)$
Inclination factors	
$\lambda_{ci} = \left(1 - \frac{\alpha^\circ}{90^\circ}\right)^2$	
$\lambda_{qi} = \left(1 - \frac{\alpha^\circ}{90^\circ}\right)^2$	
$\lambda_{\gamma i} = \left(1 - \frac{\alpha^\circ}{\phi^\circ}\right)^2$ where α is the angle between the inclined load and the vertical direction.	

Also, the unit weight of soil, γ that appears in the third term of the bearing capacity equations should be replaced by γ_{sub}.

Case 2: When the groundwater table coincides with the bottom of the foundation (Figure 3.5(b)), the magnitude of q is equal to $\gamma\ D_f$. However, the unit weight γ in the third term of the bearing capacity Equations (3.4) and (3.17) should be replaced by γ_{sub}.

Case 3: The groundwater table is at a depth D below the bottom of the foundation (Figure 3.5(c)). In this case, compute with $q = \gamma D_f$. Also the magnitude of γ in the third term of the bearing capacity Equations (3.4) and (3.17) should be replaced by γ_{av} where

$$\gamma_{av} = \frac{1}{B}[\gamma D + \gamma(B - D)] \qquad (\text{For } D \leq B) \tag{3.19}$$

$$\gamma_{av} = \gamma \qquad (\text{For } D > B) \tag{3.20}$$

3.2.7 *Other Factors*

There are several other factors which effect the bearing capacity such as eccentric loads, layered and nonhomogeneous soils. These aspects are presented in Chapter 4.

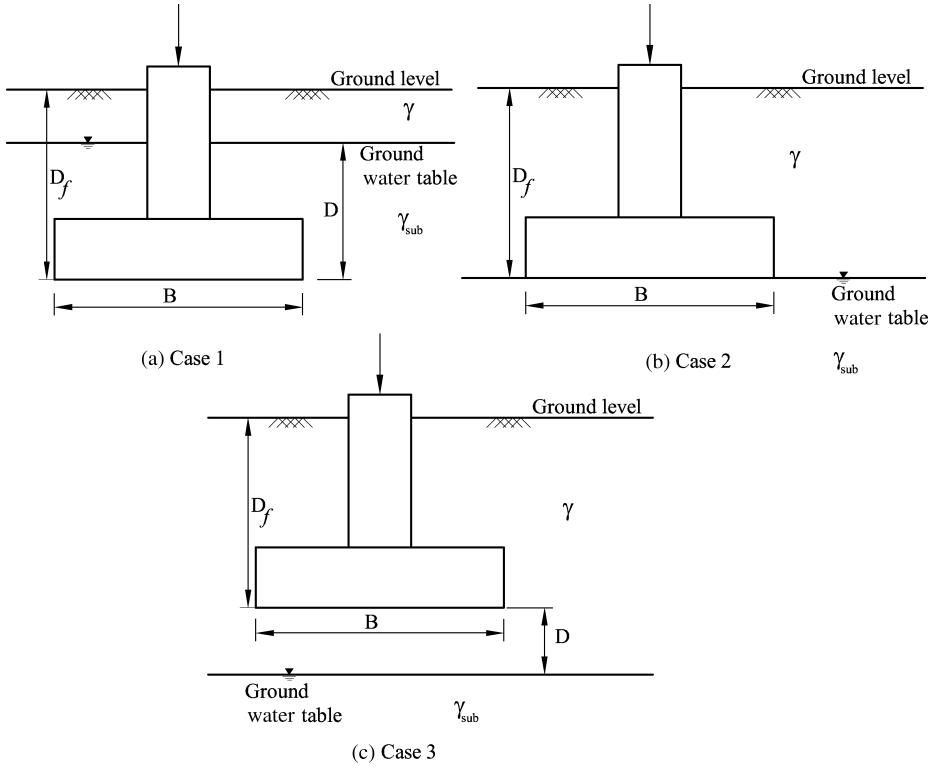

Figure 3.5 Effect of the location of groundwater table on the bearing capacity of soils.

3.3 Bearing Capacity of Deep Foundations

3.3.1 Types of Deep Foundations

When a good bearing stratum does not exist near the ground surface or at relatively shallow depths, the structural loads are transmitted to deeper strata capable of supporting such loads by means of deep foundations. Thus, deep foundations are those where $\frac{D_f}{B} > 1$ and generally >3–4 (D_f and B are the depth and width of foundation as shown in Figures 3.3 and 3.6). The main types are: pile foundations, piers or cylinder foundations and wells or caisson foundations. A pile is a slender structural member of timber, concrete and/or steel, which is driven or bored/cast *in situ* into the soil, generally for supporting vertical or lateral loads and moments. A pier is a vertical column of relatively larger cross section than a pile though similar to a pile. It transmits structural loads to a hard deeper stratum. A caisson is a hallow box or well which is sunk through ground with or no water. Subsequently it becomes an integral part of the permanent foundation.

The details of these deep foundations are discussed in Chapters 9 and 10. The evaluation of the bearing capacity of deep foundations is discussed below.

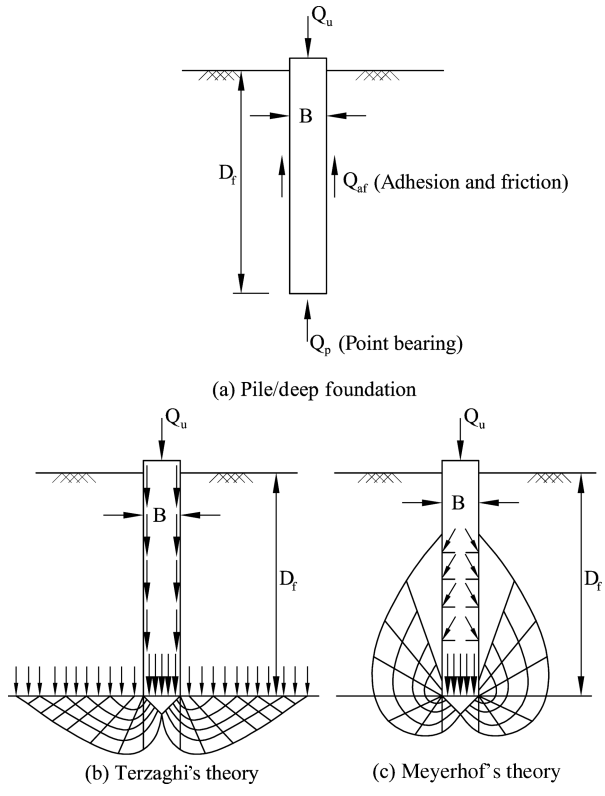

Figure 3.6 Failure zones in deep foundations.

3.3.2 Bearing Capacity

The main difference in the evaluation of bearing capacity of shallow and deep foundation is that the shear resistance along the boundary of the failure zone is neglected in the case of shallow foundations while it is included in the case of deep foundations.

The methods available in the literature (Ramiah and Chickanagappa, 1981; Bowles, 1996; Tomlinson, 2001) are quite numerous and mainly differ in conceptualizing the failure zones and mobilization of shear resistance along the boundary. The resistance offered by soil due to applied loads on a pile/deep foundation is shown in Figure 3.6(a). Terzaghi's theory considers the pattern of failure zone as shown in Figure 3.6(b) for a slender deep foundation like a pile. Thus, the bearing capacity at the base of the foundation is called point resistance or point bearing and is calculated as per shallow foundation theory (as given in Equation (3.4)). But there is an additional resistance due to friction and cohesion/adhesion along the surface of the shaft of the foundation (called the shaft resistance or shaft friction and adhesion) in contact with the surrounding soil which is added to the total capacity. Thus the total capacity of the deep foundation includes the two components, that is, point resistance and the shaft resistance. These details are discussed in detail in Chapters 9 and 10.

In a similar way, Meyerhof (Ramiah and Chickanagappa, 1981) assumed the failure zones for deep foundations as shown in Figure 3.6(c). Meyerhof further suggested that a failure zone based on Terzaghi's theory can be conceptualized for general deep foundations as shown in Figure 3.7(a).

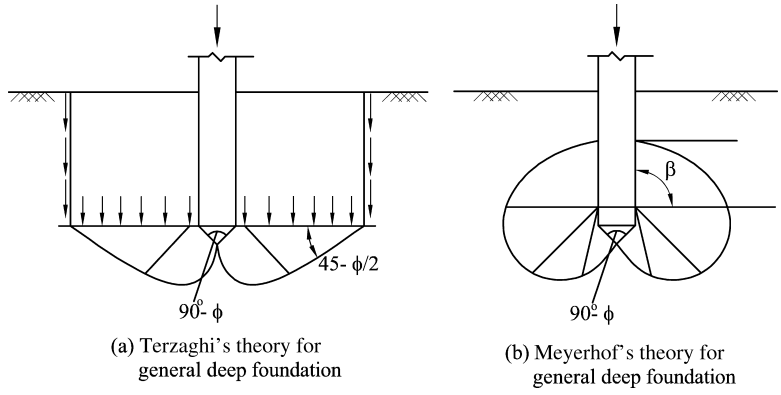

(a) Terzaghi's theory for general deep foundation

(b) Meyerhof's theory for general deep foundation

Figure 3.7 General deep foundations.

However, he assumed a general failure zone as shown in Figure 3.7(b) (similar to Figure 3.6(c)) and expressed the ultimate bearing capacity (UBC) at the base, that is, point resistance as

$$q_p = cN_{pc} + \sigma_o N_{pq} + \frac{\gamma B}{2} N_{p\gamma} \tag{3.21}$$

where

N_{pc}, N_{pq}, $N_{p\gamma}$ = Meyehof's bearing capacity factors for deep foundations
σ_o = normal stress on an equivalent free surface as defined by Meyerhof
c = cohesion
γ = unit weight of soil
D_f = depth of the foundation below ground level
B = width of the foundation.

The factors N_{pc}, N_{pq}, $N_{p\gamma}$ are given in Figures 3.8(a)–(c). The angles β, σ_o can be found from the values of the D_f/B ratio and ϕ values, as given in Figure 3.8(d).

Meyerhof also further simplified the bearing capacity factors for cohesive and cohesionless soils separately (Ramiah and Chickanagappa, 1981).

3.4 Correlation of UBC and ASP with SPT Values and CPT Values

The SPT and CPT values and their correlation with soil properties are discussed in Chapter 2. They are *in situ* tests and provide good correlation with angle of internal friction, ϕ, allowable soil pressure (ASP), settlements and so on.

3.4.1 SPT Values

The correlation of ϕ and allowable soil pressure for a 25 mm settlement with SPT values, *N*, are given in Figures 3.9(a) and (b). It may be noted that ultimate bearing capacity values for sands can be calculated using Figure 3.9(a) knowing the value of ϕ. This is different from the allowable soil pressure given in Figure 3.9(b) wherein the settlement of 25 mm is the criterion. Ultimately, the lower of the two values, that is, UBC (with FS of say 3) and ASP has to be adopted as the design pressure for foundation design. These aspects are further elaborated in Chapter 8.

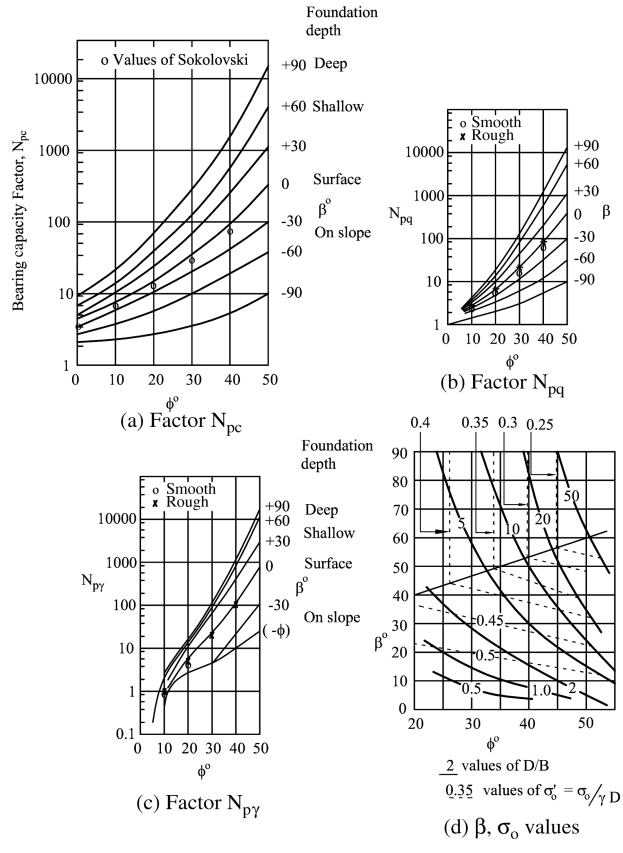

Figure 3.8 Meyerhof's bearing capacity factors.

3.4.2 Correlation to N Values

In saturated very fine or silty sands the values of N may be high if the void ratio is below the critical void ratio which corresponds approximately to $N = 15$. In such soils the equivalent value of N ($N_{\text{equivalent}}$) should be determined from the following relation, when N is greater than 15:

$$N_{\text{equivalent}} = 15 + \frac{1}{2}(N-15) \tag{3.22}$$

The value of N gives an indication of the probable mode of soil failure under a footing, (Terzaghi and Peck, 1967). Local shear failure can be assumed if $N \leq 5$ and general shear failure if $N \geq 30$. For intermediate values of N between 5 and 30, linear interpolation between the local and general shear failure values of bearing capacity factors may be used.

Gibbs and Holtz (Ramiah and Chickanagappa, 1981) showed that the effective overburden pressure also affects the penetration resistance. It was found that the effect of overburden on a cohesionless soil tend to increase the penetration resistance. Based on this finding, it was proposed to modify the penetration resistance near the ground surface to

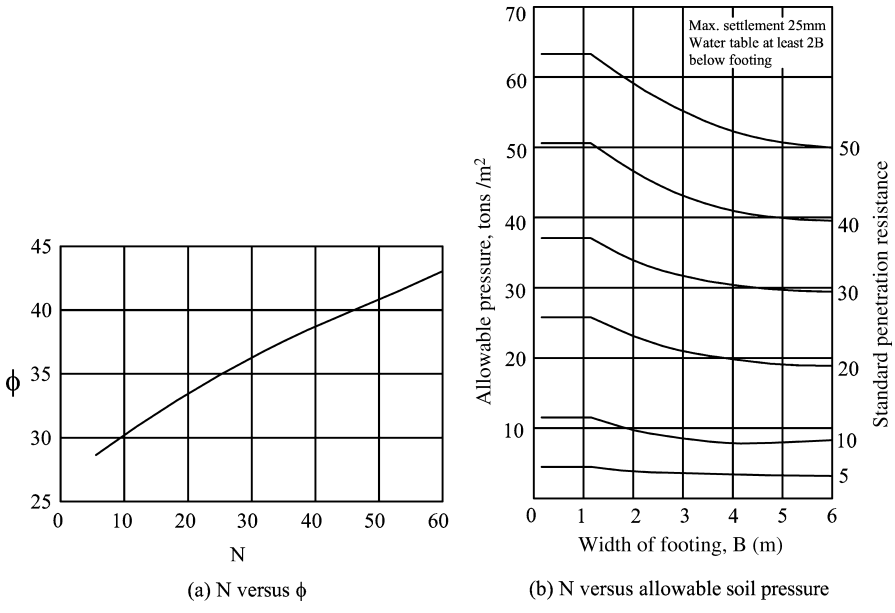

Figure 3.9 Correlation with SPT values.

include the effect of overburden pressure since the penetration resistance without this correction tends to be too small. The modification for air-dried or moist sands proposed by Gibbs and Holtz is

$$N = N^r \left\{ \frac{5}{1.422p + 1} \right\} \tag{3.23}$$

where

N = corrected value of penetration
N' = actual blow count
p = actual effective overburden pressure in kg/cm^2 (but not greater than 2.8 kg/cm^2).

Similar corrections for N values are also discussed in Chapter 2.

3.4.3 CPT Values

Meyerhof (Ramiah and Chickanagappa, 1981) correlated CPT (Delft type cone) values (that is, cone penetration resistance or static cone resistance) with SPT values as

$$q_c = 4N \tag{3.24}$$

where

q_c = resistance in kg/cm^2
N = SPT values (corrected or equivalent).

Shmertmann (Bowles, 1996) gave the following correlation of CPT values, q_c, with Terzaghi's bearing capacity factors, N_q and N_γ

$$q_c = 0.8N_q = 0.8N_\gamma \tag{3.25}$$

where

q_c = average cone resistance of the soil between a depth of $B/2$ and 1.1 B in kg/m^2
B = width of the footing in m.

For cohesive soils ($D_f/B \leq 1.5$),

$$q_{\text{ult}} \text{ for strip footing } (\text{kg/cm}^2) = 28 - 0.0052\,(300 - q_c)^{1.5} \tag{3.26}$$

$$q_{\text{ult}} \text{ for square footing } (\text{kg/cm}^2) = 48 - 0.009\,(300 - q_c)^{1.5} \tag{3.27}$$

For clayey soils,

$$q_{\text{ult}} \text{ for strip footing} (\text{kg/cm}^2) = 2 + 0.28\,q_c \tag{3.28}$$

$$q_{\text{ult}} \text{ for square footing } (\text{kg/cm}^2) = 5 + 0.34 q_c \tag{3.29}$$

3.5 UBC and Probable Settlements Using Field Plate Load Test

The plate load test is a very useful field test and is described in detail in Section 4.8 (Kameswara Rao, 2000) for evaluating the modulus of subgrade reaction, coefficient of elastic uniform compression, spring constant, and modulus of elasticity and other related parameters. This test can also be used for determining the ultimate bearing capacity, mode of failure (GSF, LSF) and probable elastic settlements as outlined below.

The plate load test is conducted at site at the proposed depth of the foundation with a standard size plate of 30 or 75 cm (diameter or side width of a circular or square shape) and at least 25 mm thickness for rigidity. The set-up and details of the test are described in Section 4.8. Typical test results can be plotted between settlement, s, and bearing pressure, $p = \frac{P}{A}$, as shown in Figure 3.10(a), where P is the load applied on the plate and A is the area of the plate. The same results can also be plotted on a log-log scale as shown in Figure 3.10(b).

3.5.1 Spring Constant from Total Deformation

The spring constant represents the force required for unit vertical deformation. In the case of soil, the value of any parameter analogous to the spring constant will necessarily depend on the type of soil, its density and moisture content, area, depth, shape of foundation and so on.

Consider the curve shown in Figure 3.10(a) obtained from the plate load test on a soil. The initial part of the curve is essentially a straight line or can be approximated to be so. This part at low bearing pressure represents elastic deformation. Since the applied pressure in most cases will be within this pressure range, it is reasonably safe to assume this as elastic deformation of

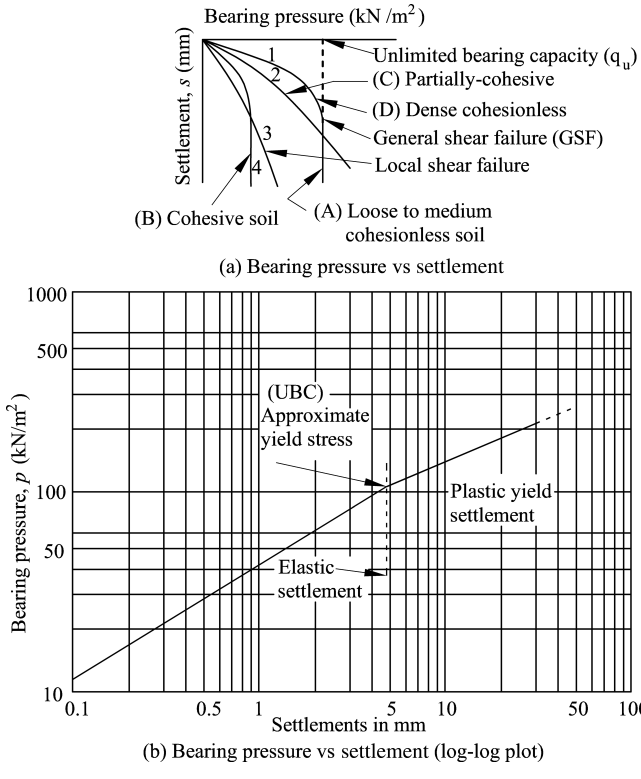

Figure 3.10 Plate load test results.

the foundation–soil system subjected to static loads. The slope of the curve represents spring constant of the soil.

Of course the plate load test curve represents the elastic characteristics for a single short-term load application for a particular area of bearing plate. The curve is likely to be different for different areas of bearing or for repeated loads or for long-term constant loading.

3.5.2 Settlement

It is well known that when two areas of different sizes are loaded, the one with larger area will show larger deformation for the same bearing pressure.

The relation between the deformation and the area at a given pressure intensity is given by several empirical expressions as follows:

1. For clays

$$s_2 = s_1 \frac{B_2}{B_1} \tag{3.30}$$

where B_1 and s_1 are the width of bearing plate and corresponding settlement at a given pressure and s_2 is the settlement of another area with width B_2 at the same pressure.

Where the modulus of elasticity, E, of a soil is constant, such as saturated clay, the settlement of area with width B and load intensity q is given by

$$s = \frac{0.6qB}{E} \tag{3.31}$$

2. **For sands:** The settlements s_2 of an area with width B_2 in meters is related to the settlement s_1 of a plate with width B_1 in meters as

$$s_2 = s_1 \left[\frac{B_2(B_1 + 0.3)}{B_1(B_2 + 0.3)}\right]^2 \tag{3.32}$$

Several authors have evolved similar empirical relationships between the settlement and area at given pressures.

From the plate bearing tests the elastic property of a soil in a given condition is generally expressed by the modulus of subgrade reaction which is usually the pressure required per unit deformation calculated at 0.5 in (12.7 mm) of deformation. The units are pounds per cubic inch in the FPS system (or N/m^3 in SI units). This term relates the stress to the total deformation. These parameters are used for carrying out static or pseudo static/dynamic analysis of foundation soil systems. The details for getting others parameters are given in Section 4.8.

A modified version of the plate load test is the cyclic plate load test which is more relevant for evaluating parameters that can be used in dynamic analysis of machine–foundation–soil (MFS) system which relates bearing stress to the elastic (recoverable) part of total deformation. This is also discussed in Section 4.8.

3.5.3 Ultimate Bearing Capacity

If it is a soil with a probable general shear failure, the *p-s* curves look like curves 1 and 4 in Figure 3.10(a). The load corresponding to the steep slope of the curve can be noted as the ultimate bearing capacity of the soil.

However, if such a steep slope is not evident as in curves 2 and 3, it could be a local shear failure. In such cases, it is difficult to determine the UBC form these curves. Then, *p-s* curves can be plotted in log-log scale as shown in Figure 3.10(b). From the plot, the pressure corresponding to the point where the two linear parts of the graph intersect, can be noted to be the ultimate bearing capacity. Of course log-log plots can also be used for soils with GSF for cross verification of the values of UBC.

These results from the standard plate load tests can be used to extrapolate the UBC, settlements and other parameters for the actual foundations using several empirical and semi-empirical relations (Ramiah and Chickanagappa, 1981; Bowles, 1996) and bearing capacity equations discussed in Section 3.2.

3.6 Elastic Stress and Displacement Distribution in Soils

Evaluation of stress in soils due to loads transmitted by foundations is necessary in many geotechnical engineering problems such as in settlement calculation (both elastic and due to consolidation), pore pressure estimation, stress transmission due to foundation loads, underground constructions and effects on adjacent structures. Following methods are commonly used to determine the stress distribution in soils due to foundation loads. These stresses will be in addition to the existing stresses due to overburden pressure and so on.

1. **Empirical method:** For a quick and approximate estimation of stresses for stability analysis of footings, the pressure under a footing may be assumed to spread like a pyramid with a slope of 2 vertical to 1 horizontal as shown in Figure 3.11. Thus, a load Q acting concentrically on a footing area of $B \times L$ is assumed to be distributed over an area of $(B+Z)(L+Z)$ at a depth Z below the footing as shown in Figure 3.11(a). If any stratum of soil is inadequate to sustain this pressure, the design bearing pressure should be reduced.

   The slopes to be assumed may depend on the soils. In loose soils, the slope can be steeper and in strong and dense soils, they could be flat. However, for elastic displacements, a logarithmically decreasing function of depth or similar functions may be used (Vlasov and

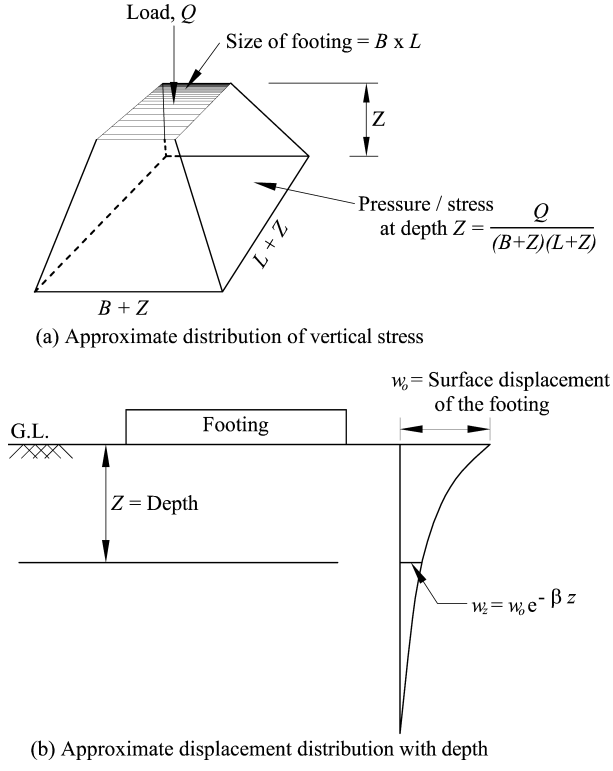

Figure 3.11 Approximate distribution of stresses and displacements below a footing.

Leontev, 1966), that is, w at depth $z = w_o e^{-\beta z}$ where w_o is the surface displacement and β is a parameter depending on soil as shown in Figure 3.11(b). β values may range from 0.5 (for clayey soils) to 2.5 (for sandy soils).

However, for more accurate evaluation, the methods described in (2) may be preferable.

2. **Methods using theory of elasticity:** For settlement and stress analysis, a more accurate approach based on elastic theory may be used. All elastic methods are developed from the Boussinesq's or Mindlin's solutions (Timoshenko and Goodier, 1951; Taylor, 1964; Harr, 1966; Bowles, 1996). Mindlin's solution is generally used for applications in piles, deep foundations, deep excavations and so on and involves intensive computations. However, Boussinesq's solution is very simple and easy to compute.

   Hence, Boussinesq's solutions are most commonly used and are presented below. Westergaard's Solution which is applicable to anisotropic soils is also presented subsequently and is also used in specific situations.

1. **Boussinesq's solutions – elastic stresses and displacements:**

   a. Vertical concentricated load on the surface: The stresses and displacements in a semi-infinite, homogeneous, isotropic and linearly elastic solid or soil medium caused by a vertical, concentrated load P applied on the surface at the origin O (Figure 3.12) are obtained by Boussinesq as follows

$$\sigma_z = \frac{3P}{2\pi}\frac{z^3}{R^5} = \frac{3P}{2\pi z^2}\frac{1}{\left(1+\frac{r^2}{z^2}\right)^{5/2}}$$

$$\tau_{\tau z} = \frac{3P}{2\pi}\frac{z^2 r}{R^5}$$

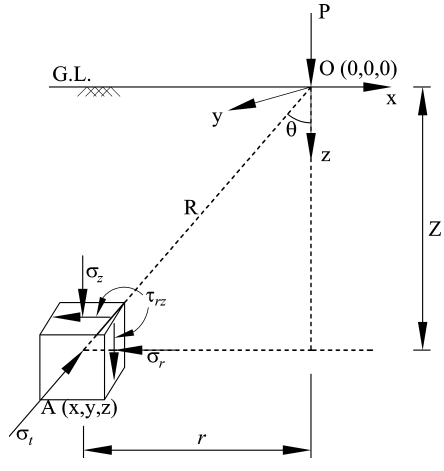

Figure 3.12 Stresses in cylindrical coordinates caused by a vertical point load on the surface of soil medium.

$$\sigma_r = \frac{P}{2\pi}\left[\frac{3zr^2}{R^5} - \frac{1-2v}{R(R+z)}\right], \quad \sigma_\theta = \frac{P}{2\pi}(1-2v)\left[\frac{1}{R(R+z)} - \frac{z}{R^3}\right]$$
$$u = \frac{P(1+v)}{2\pi E}\left[\frac{xz}{R^3} - \frac{(1-2v)x}{R(R+z)}\right]$$
$$v = \frac{P(1+v)}{2\pi E}\left[\frac{yz}{R^3} - \frac{(1-2v)y}{R(R+z)}\right] \tag{3.33}$$
$$w = \frac{P(1+v)}{2\pi E}\left[\frac{z^2}{R^3} + \frac{2(1-v)}{R}\right]$$

where

E = Young's modulus of elasticity
v = Poisson's ratio (ranges from 0 to 0.5)
R = $\sqrt{r^2+z^2} = \sqrt{x^2+y^2+z^2}$ = spherically radial distance oA
$r^2 = \sqrt{x^2+y^2}$ = cylindrically radial distance as shown
x, y, z = Cartesian coordinates of A with respect to the origin O
$\theta = \tan^{-1}{}^{r}/_{z}$ = radial coordinate as shown
u, v, w = displacements of A along the x, y, z coordinates
$\sigma_r, \sigma_\theta, \sigma_z$ = normal stresses in the r, θ, z coordinates
τ_{rz} = shear stress.

It should be noted that although both the vertical normal stress and shearing stress are independent of the elastic constants they are very much dependent on the assumptions of linear elasticity.

The vertical stress, σ_z, can be written as

$$\sigma_z = K_B \frac{P}{z^2} \tag{3.34}$$

where

$$K_B = \frac{3}{2\pi}\left[1 + \left(\frac{r}{z}\right)^2\right]^{-5/2} \tag{3.35}$$

is a dimensionless influence factor. A plot of the coefficient K_B is given in Figure 3.13. Just as in the two-dimensional case, the effects of a number of forces on the surface can be accounted for by superposition.

b. Stresses and displacement caused by a uniformly loaded rectangular surface area: For the case wherein the load consists of a uniformly distributed vertical load of intensity p over a rectangular area on the surface, Newmark (Taylor, 1964) has derived expressions for the stresses at a point below a corner of this area by integration of Equations (3.33). The expression for vertical stress is obtained as

$$\sigma_z = \frac{p}{4\pi}\left[\frac{2mn\sqrt{m^2+n^2+1}}{m^2+n^2+1+m^2n^2}\frac{m^2+n^2+2}{m^2+n^2+1} + \sin^{-1}\frac{2mn\sqrt{m^2+n^2+1}}{m^2+n^2+1+m^2n^2}\right. \tag{3.36}$$

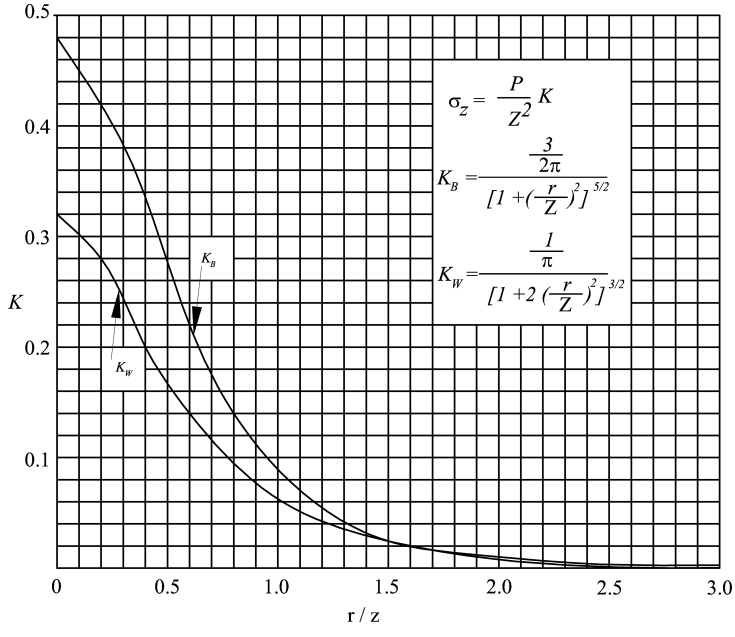

Figure 3.13 Boussinesq's and Westergaard's solutions.

where p is the uniform intensity of surface loading on a rectangle of dimensions mz by nz, and the stress σ_z occurs at distance z below the corner of this rectangular area. The second term within the bracket is an angle in radians; this angle is less than $\pi/2$ when $m^2 + n^2 + 1$ is larger than m^2n^2; otherwise it is between $\pi/2$ and π.

The above expression does not contain the dimension z, and stress depends only on the ratios m and n and the surface intensity. Newmark also developed charts for calculating vertical stress at the corner of the rectangular load using Equation (3.36). He has also developed charts for other stresses and displacements (particularly vertical displacement, w) by integrating Equation (3.33).

When the stress is desired at any point other than the corner, it may be obtained by superposition of rectangular areas to represent the loaded area, each having the point as its corner, as illustrated in Figure 3.14(a). Same procedure is applicable for other stresses and displacements as the principle of superposition is valid for linear problems.

For a point below any point K inside the rectangular area, the actual loaded area must be considered to consist of four rectangles, KK_1DK_2, KK_2EK_3, KK_3BK_4 and KK_4CK_1, the point desired being below their common corner, K. Then, the stress at any point below K is the sum of the stresses due to these four rectangular areas (since K is the common corner) by the principle of superposition.

For determination of the stress below a point such as A in Figure 3.14(a), due to loading of the rectangle BCDE, the area may be considered to be composed of four sections as follows: AHBF − AHEG + AJDG − AJCF. Each of these four rectangles has a corner at point A, and the stress below point A due to loading on each section may

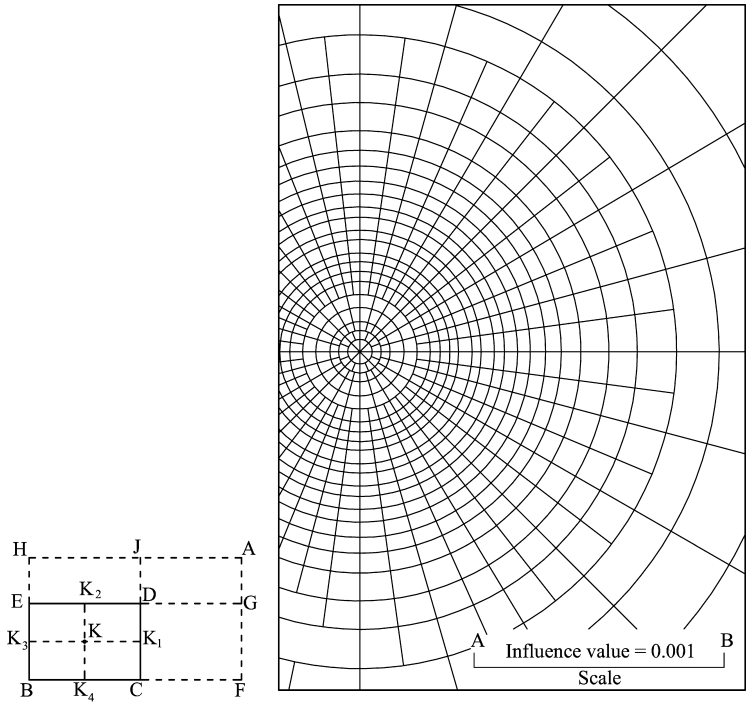

(a) Stress at any point below a rectangular area

(b) Newmark's influence chart

Figure 3.14 Stresses at any point below loaded area.

be computed. Superposition of these values, with signs as indicated above, gives the desired stress.

Out of all the stresses and displacements, the vertical stress σ_z and vertical displacement, w at any point are most commonly needed in geotechnical engineering. The expressions for point load are given in Equation (3.33). The vertical stress due to rectangular shaped load is given in Equation (3.36). Charts and expressions are also given by Newmark and others (Harr, 1966). The vertical displacement at the corner of the rectangular shaped surface load (p) was obtained by Steinbrenner (Harr, 1966) by integrating the expression for w due to point load (Equation (3.33)) as

$$w_c(z) = \frac{ap}{2E}(1-v^2)\left[A - \frac{1-2v}{1-v}B\right]$$

$$A = \frac{1}{\pi}\left(l_n \frac{\sqrt{1+m^2+n^2}+m}{\sqrt{1+m^2+n^2}-m} + m l_n \frac{\sqrt{1+m^2+n^2}+1}{\sqrt{1+m^2+n^2}-1}\right) \qquad (3.37)$$

$$B = \frac{n}{\pi}\tan^{-1}\frac{m}{n\sqrt{1+m^2+n^2}}$$

where

$m = b/a, n = z/a$

$2a$, $2b$ = dimension of the rectangular area

l_n = natural logarithm = log to the base e

$w_c(z)$ = vertical displacement below the corner

The values of A and B are available in tables (Harr, 1966) for various values of m and n. For calculating the displacements at any point other than the corner of the rectangle, similar procedure as in stresses using the principle of superposition can be adopted.

For the special case of vertical displacement at the surface, that is, $z = 0$, the above constants simplify as $B = 0$, $n = 0$ and

$$w = \frac{2ap}{E}(1-v^2)K_o \tag{3.38}$$

where K_o is a dimensionless constant.

K_o can be obtained from the above tables given in Harr (1966). In particular for a square shaped load the values of K_o for vertical displacement at center, average displacement (from the center to the edges), and for a rigid footing are 1.12, 0.95 and 0.88 respectively. Some specific values of K_o which may be useful are given in Table 3.2.

Table 3.2 K_o values for rectangular foundations.

Shape of the area ($2a \times 2b$) $m = b/a$	K_o values			
	Corner	Center	Average	Rigid foundation
Square, $m = 1$	0.56	1.12	0.95	0.88
Circular with diameter, $2a$	0.64	1.00	0.85	0.79
Rectangle				
$m = 1.5$	0.68	1.36	1.15	1.08
$m = 2.0$	0.77	1.53	1.30	1.22
$m = 5$	1.05	2.10	1.83	1.72
$m = 10$	1.27	2.53	2.25	2.12
$m = 100$	2.00	4.00	3.69	—

c. Stresses and displacements due to uniformly distributed load (UDL) on a circular area: By integrating the expressions for σ_z and w, over a circular area, Egorov (Harr, 1966) gave the general expressions and charts. In particular the expressions for σ_z and w along the center line of the circular area ($r = 0$) at any depth z can be obtained as

$$(\sigma_z)_{r=0} = p\left[1-\frac{1}{(a/z)^2+1}\right]^{3/2} \tag{3.39}$$

$$(w_z)_{r=0} = \frac{2ap(1-v^2)}{E}\left(\sqrt{1+n^2} - n + \frac{n}{2(1-v)\sqrt{1+n^2}}\right) \tag{3.40}$$

where
a = radius of the circular area
$n = {}^{z}/_{a}$
p = UDL on the circular area.

For stress and displacement at the center of the circle on the surface, that is, $r = 0$, $z = 0$, the above expressions simplify as

$$(\sigma_z)_{r=z=0} = p \tag{3.41}$$

$$(w)_{r=z=0} = \frac{2ap(1-v^2)}{E} \tag{3.42}$$

The solution of an annular foundation can be obtained by appropriate superposition that is, deducting the influence of the inner circle from the total influence of outer circle.

d. Stresses and displacement for uniform loaded areas of general shape: While strip, circular, square and rectangular shapes of foundations are more common, occasionally general shaped foundations such as L-shaped, oval shaped, foundations with cut outs, triangular and others are also used depending on the requirement. For calculating stresses and displacements due to such general shaped foundation, Newmark (Harr, 1966) developed circular influence charts using Equations (3.39) and (3.40). A chart for vertical stress is shown in Figure 3.14(b). The detailed procedure is available in standard books (Teng, 1964; Harr, 1966; Bowles, 1996).

Besides the above charts, such general problems in elasticity can be solved using numerical methods and the finite element method. The details of these methods are given in Chapters 6 and 7.

2. Westergaard's solutions: Typical clay strata usually have partings or thin lenses of coarser material within them. The material in such lenses represents the non-isotropic condition that is so common in sedimentary soils. Hence, it increases resistance to lateral strain.

An elastic solution that is based on above conditions has been obtained by Westergaard (Taylor, 1964). In this solution, an elastic material is assumed to be laterally reinforced by numerous, closely spaced, horizontal sheets of negligible thickness but of infinite rigidity, which prevent the mass as a whole from undergoing lateral strain. This material may, therefore, be viewed as representative of an extreme case of non-isotropic condition. Westergaard obtained the solution for the vertical stress caused by a point load as

$$\sigma_z = \frac{P}{z^2}\frac{\frac{1}{2\pi}\sqrt{\frac{1-2v}{2-2v}}}{\left[\frac{1-2v}{2-2v} + \left(\frac{r}{z}\right)^2\right]^{3/2}} \tag{3.43}$$

For $v = 0$, Equation (3.43) becomes

$$\sigma_z = \frac{P}{z^2} \frac{\frac{1}{\pi}}{\left[1 + 2\left(\frac{r}{z}\right)^2\right]^{3/2}} = K_w \frac{P}{z^2} \tag{3.44}$$

This expression is similar to Equation (3.34) which represents the isotropic case. A plot of K_w as function of r/z is shown in Figure 3.13.

For stresses below a uniformly loaded rectangular area, an integration of Equation (3.43) gives

$$\sigma_z = \frac{p}{2\pi} \cot^{-1} \sqrt{\left(\frac{(1-2v)}{(2-2v)}\left(\frac{1}{m^2} + \frac{1}{n^2}\right)\right) + \left(\frac{1-2v}{2-2v}\right)^2 \frac{1}{m^2 n^2}} \tag{3.45}$$

For $v = 0$, the above expression becomes

$$\sigma_z = \frac{p}{2\pi} \cot^{-1} \sqrt{\frac{1}{2m^2} + \frac{1}{2n^2} + \frac{1}{4m^2 n^2}} \tag{3.46}$$

In Equations (3.45) and (3.46), the notations are the same as those used in Equation (3.36), which is the corresponding formula for the Boussinesq case. A chart that may be used to obtain σ_z values according to Equation (3.46) is also available (Taylor, 1964).

3.7 Settlement Analysis

The design soil pressure for the foundation analysis has to be taken as the lower of the two values, that is, allowable bearing capacity (based on shear failure, presented in Section 3.2) and allowable settlement of the structure (based on settlement analysis or compressibility, presented in Chapter 2) as brought out in Section 3.1.

Foundations on granular soils will not suffer detrimental settlement if the smaller value of the two allowable pressures mentioned above is used. Footings on stiff clay, hard clay and other firm soils generally require no settlement analysis if the design provides a minimum factor of safety of 3. Soft clays, and other weak soils settle under moderate pressure and hence settlement analysis is necessary.

The total settlement of a footing on clay may be considered to consist of three parts (Teng, 1964; Bowles, 1996), that is

$$S = S_i + S_c + S_s \tag{3.47}$$

where

S = total settlement

S_i = immediate elastic settlement

S_c = settlement due to primary consolidation (for clayey soils)

S_s = settlement due to secondary consolidation (for clayey soils).

3.7.1 Immediate Settlement

After the application of load on the footing, elastic compression of the underlying soil takes place immediately causing elastic settlement of the footing. This amount can be computed by elastic theory as discussed in Sections 3.5 and 3.6. It is usually very small and can be neglected for all practical purposes.

3.7.2 Settlement Due to Consolidation

The settlement caused by consolidation is due to the slow extrusion of pore water from the fine gravel soils. The amount of final consolidation settlement S_c can be calculated using consolidation theory as discussed in Chapter 2. It may be recalled (Equation (2.25)) that

$$\begin{aligned} S_c &= \text{primary consolidation settlement calculated by Terzaghi's theory (Chapter 2)} \\ &= m_v \Delta p H \\ &= \frac{C_c}{1+e} H \log_{10} \frac{p_o + \Delta p}{p_o} \end{aligned} \tag{3.48}$$

where

m_v = coefficient of volume compressibility of the clay, determined by consolidation test $= \frac{a_v}{1+e}$
a_v = coefficient of compressibility (slope of the compressibility curve, that is, e vs. p curve, Chapter 2)
e = void ratio
Δp = vertical stress at the middle of the compressible layer due to load on footing (as per Section 3.6)
H = thickness of the compressible clay. For very thick layers, the clay thickness should be divided into several layers to obtain accurate settlement
C_c = compression index, also determined by consolidation test (Chapter 2)
p_o = vertical effective pressure due to soil overburden.

The other important expressions which need to be used in settlement analysis in addition to the details given in Chapter 2 are as follows (Taylor, 1964)

$$\begin{aligned} s &= US_c \\ T &= \frac{C_v t}{H^2} \approx \frac{\pi}{4} U^2 && \text{for U} < 60\% \text{ (approximate)} \\ T &= -0.9332 \log_{10}(1-U) - 0.085 && \text{for U} > 60\% \text{ (approximate)} \\ C_v &= \frac{k}{\gamma_w m_v} \end{aligned} \tag{3.49}$$

where

s = settlement at any particular U corresponding to time t
S_c = ultimate consolidation settlement, that is, when $U = 100\%$
U = average degree of consolidation at any time t
H = total thickness of compressible clay layer
H_{dp} = length of drainage path
$= \frac{H}{2}$ for two-way drainage and H for one-way drainage
k = coefficient of permeability
C_v = coefficient of consolidation
T = nondimensional time period
t = time coordinate
γ_w = unit weight of water

3.7.3 Settlement Due to Secondary Consolidation

When an undisturbed soil sample is tested in the consolidometer (or oedometer) the rate of volume decrease follows consolidation theory for most part of compression as described in Chapter 2. This is called primary consolidation. However, when the sample is 100% consolidated (according to the theory of consolidation) the volume decrease does not stop according to the theory, but instead the sample continues to compress at a reduced but continuous rate. This slow consolidation that takes place afterwards is called secondary consolidation. Rheological models are used to predict the secondary consolidation settlement, S_s. This is a continuous and long drawn process. Usually the magnitudes of S_s are very small in comparison to primary consolidation settlement, S_c and are not taken seriously. However, S_s values could be reasonably large for organic soils and heavy clays with high plasticity.

3.8 Lateral Earth Pressure

Lateral earth pressure determination is needed in the design of many types of structures and structural members, common examples being retaining walls of the gravity and other types, sheet pile bulkheads, basement walls of buildings and other walls that retain earth fills and excavation trenches (Figure 3.15). Often the lateral pressures are difficult to evaluate. However, lateral pressures can be estimated accurately using earth pressure theories, such as Rankine's theory, Coulomb's theory and other theories (Taylor, 1964; Teng, 1964; Das, 2007).

3.8.1 Fundamental Relationships Between Lateral Pressure and Backfill Movement

Terzaghi (Taylor, 1964) demonstrated that the lateral force on a wall varies as the wall undergoes lateral movement. The relationship between the force and the movement is shown in Figure 3.16. The ordinate of point A represent the force on a wall which has been held rigidly in place while a soil backfill is behind it. This is called Earth pressure at rest where there is no

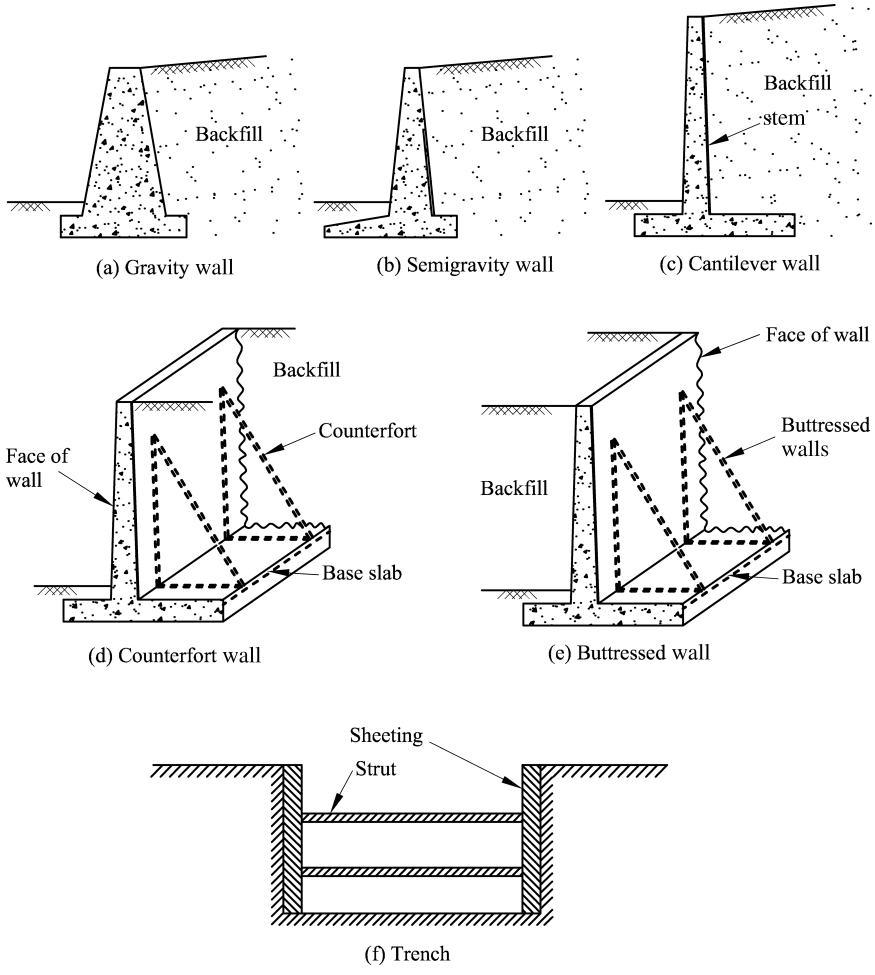

Figure 3.15 Typical retaining structures and trenches.

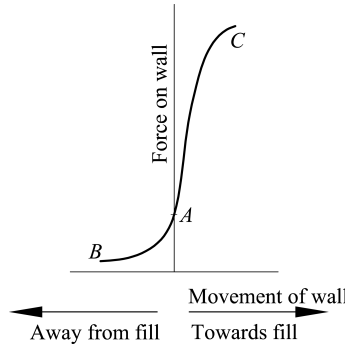

Figure 3.16 Effect of movement of a wall on the lateral thrust.

relative movement between the back fill and the soil. This is also called K_o condition where K_o is the corresponding earth pressure coefficient. K_o values are around 0.4–0.5. K_o is referred to as coefficient of earth pressure at rest.

If the wall moves in the direction away from the backfill, the force decreases and after a small movement reaches a minimum value at point B. This is called active earh pressure. The corresponding earth pressure coefficient is K_A. K_A values are around 1/3 to 1/4.

If the wall is forced against the backfill, the force between the wall and the fill increases, reaching a maximum value at C. This is called passive earth pressure. The corresponding earth pressure coefficient K_p. K_p values are around 3–4.

The earth pressures and hence the earth pressure coefficients are evaluated using several earth pressure theories (Taylor, 1964; Bowles, 1996; Das, 2002). The most popular among them are Rankine's theory and Coulomb's theory, which are discussed below. They furnish expressions for active and passive pressures and thrusts caused by a soil mass which is not subject to seepage forces. Each applies to the cross section of a long wall of constant section and gives results per unit of running length. These two theories are discussed in this and the following sections.

3.8.2 Rankine's Theory

This theory assumes a conjugate relationship between the vertical pressures and the lateral pressures on vertical plane within the soil backfill behind a retaining wall. In other words, it is assumed that the presence of the wall introduces no changes in shearing stresses at the surface of contact between the wall and the backfill, since the conjugate relationship would hold. The stresses on the wall would closely resemble those on vertical planes within the infinite slope, Rankine's theory would be more accurate were it not for changes in shearing stresses that are introduced by the presence of the wall.

In its simplest form, Rankine's method refers to the active pressures and the active thrust on a vertical wall that retains a homogeneous cohesionless fill. The backfill is at an inclination i, as shown in Figure 3.17(a). At any depth z below the surface of the fill, the pressure for the totally

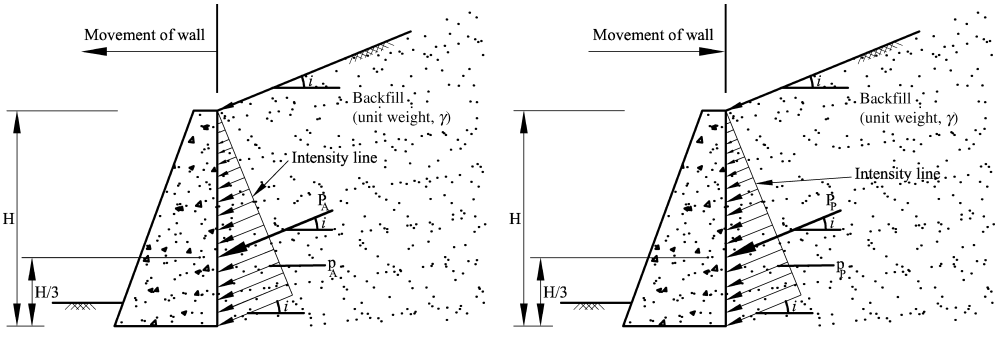

(a) Active case (b) Passive case

Figure 3.17 Rankine's earth pressures – inclined backfill.

active case acting parallel to the surface of the fill is given by

$$p_A = \gamma\, z \cos i \frac{\cos i - \sqrt{\cos^2 i - \cos^2 \phi}}{\cos i + \sqrt{\cos^2 i - \cos^2 \phi}} = K_{Ai}\gamma_z \tag{3.50}$$

The resultant thrust on the wall for either the totally active or the arching-active case is

$$P_A = \frac{1}{2}\gamma H^2 \cos i \frac{\cos i - \sqrt{\cos^2 i - \cos^2 \phi}}{\cos i + \sqrt{\cos^2 i - \cos^2 \phi}} = K_{Ai}\frac{\gamma H^2}{2} \tag{3.51}$$

where

H = height of the wall
γ = unit weight of soil
z = depth coordinate from top of the wall
K_{Ai} = active earth pressure coefficient for inclined backfill

$$= \cos i \frac{\cos i - \sqrt{\cos^2 i - \cos^2 \phi}}{\cos i + \sqrt{\cos^2 i - \cos^2 \phi}} \tag{3.52}$$

Since the pressure is of triangular distribution in the totally active case, the thrust acts at a height of 1/3 H from the base of the wall. The active pressures and the resultant thrust are expressed by Equations (3.50) and (3.51) and their directions are shown in Figure 3.17(a).

If the backfill is level (horizontal, $i = 0$), Equations (3.50)–(3.52) reduce to a simpler form

$$p_A = \gamma\, z \frac{1 - \sin\phi}{1 + \sin\phi} = \gamma\, z \tan^2\left(45 - \frac{1}{2}\phi\right) = K_A \gamma\, z \tag{3.53}$$

$$P_A = \frac{1}{2}\gamma H^2 \frac{1 - \sin\phi}{1 + \sin\phi} = \frac{1}{2}\gamma H^2 \tan^2\left(45 - \frac{1}{2}\phi\right) = K_A \frac{\gamma H^2}{2} \tag{3.54}$$

where K_A = active earth pressure coefficient for level backfill

$$= \frac{1 - \sin\phi}{1 + \sin\phi} = \tan^2\left(45 - \frac{\phi}{2}\right) \tag{3.55}$$

For this case, the p, P_A and other details are shown in Figure 3.18(a). In Rankine's Theory, the failure planes are inclined at an angle of $45 + \frac{\phi}{2}$ to the major principal plane, that is, horizontal plane in the active case. σ_1 is the major principal stress which is along vertical direction and σ_3 is the minor principal stress which is along the horizontal direction, as shown in Figure 3.18(a). A totally passive case exists if the retaining wall is pushed in that is, the wall moves towards the backfill (Figure 3.17(b)). This is Rankine's passive case

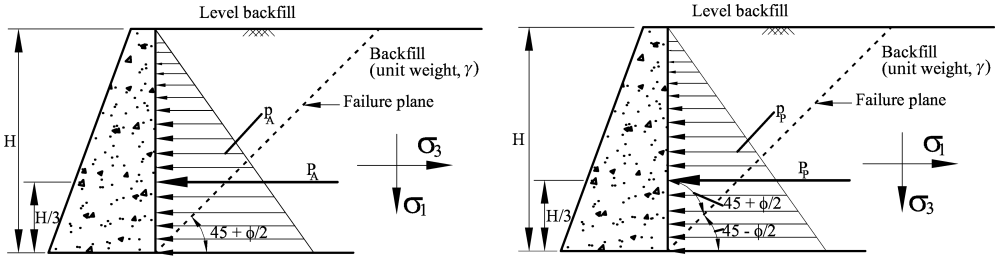

(a) Active case (b) Passive case

Figure 3.18 Rankine's earth pressures – horizontal backfill.

(Figure 3.17(b)). The lateral pressure at depth z is given by

$$p_p = \gamma\, z \cos i \frac{\cos i + \sqrt{\cos^2 i - \cos^2 \phi}}{\cos i - \sqrt{\cos^2 i - \cos^2 \phi}} = K_{pi}\, \gamma\, z \tag{3.56}$$

The expression for total passive pressure can be obtained as

$$P_p = \frac{1}{2}\gamma H^2 \cos i \frac{\cos i + \sqrt{\cos^2 i - \cos^2 \phi}}{\cos i - \sqrt{\cos^2 i - \cos^2 \phi}} = K_{pi} \frac{\gamma H^2}{2} \tag{3.57}$$

where

$$K_{pi} = \cos i \frac{\cos i + \sqrt{\cos^2 i + \cos^2 \phi}}{\cos i - \sqrt{\cos^2 i - \cos^2 \phi}} \tag{3.58}$$

The total passive pressure acts at H/3 along the line parallel to the slope of the backfill. For a horizontal backfill ($i = 0$), Equations (3.56)–(3.58) simplify as

$$p_P = \gamma\, z \frac{1 + \sin \phi}{1 - \sin \phi} = \gamma\, z \tan^2 \left(45 + \frac{1}{2}\phi\right) = K_P \gamma\, z \tag{3.59}$$

$$P_P = \frac{1}{2}\gamma H^2 \frac{1 + \sin \phi}{1 - \sin \phi} = \frac{1}{2}\gamma H^2 \tan^2 \left(45 + \frac{1}{2}\phi\right) = K_P \frac{\gamma H^2}{2} \tag{3.60}$$

where

$$K_P = \frac{1 + \sin \phi}{1 - \sin \phi} = \tan^2 \left(45 + \frac{\phi}{2}\right) = \frac{1}{K_A} \tag{3.61}$$

K_A = *active earth pressure coefficient* given in Equation (3.55).

The distribution of p_p, P_p and other details are shown in Figure 3.18(b). The major principal stress σ_1 in this passive case is along the horizontal direction (i.e., major principal plane is vertical) and the minor principal stress σ_3 is along the vertical direction (i.e., minor principal plane is horizontal). Hence, the failure planes in Rankine's passive case are at an angle of $45 + \frac{\phi}{2}$ with the vertical plane (major principal plane) or $45 - \frac{\phi}{2}$ with the horizontal plane as shown in the Figure 3.18(b).

3.8.2.1 Cohesive Soils

For cohesive soils with horizontal backfill, the active and passive earth pressures can be obtained (Teng, 1964) using Mohr's circle as

$$p_A = K_A \gamma z - 2c\sqrt{K_A} \tag{3.62}$$

$$P_A = K_A \frac{\gamma H^2}{2} - 2c\sqrt{K_A} H \tag{3.63}$$

$$p_P = K_P \gamma z + 2c\sqrt{K_P} \tag{3.64}$$

$$P_P = K_P \frac{\gamma H^2}{2} + 2c\sqrt{K_P} H \tag{3.65}$$

The p_A, P_A and effect of cohesion are shown in Figure 3.19(a). p_p,P_p and other details are shown in Figure 3.19(b). The total pressures now can be found out from the areas of earth pressure distribution shown in Figure 3.19.

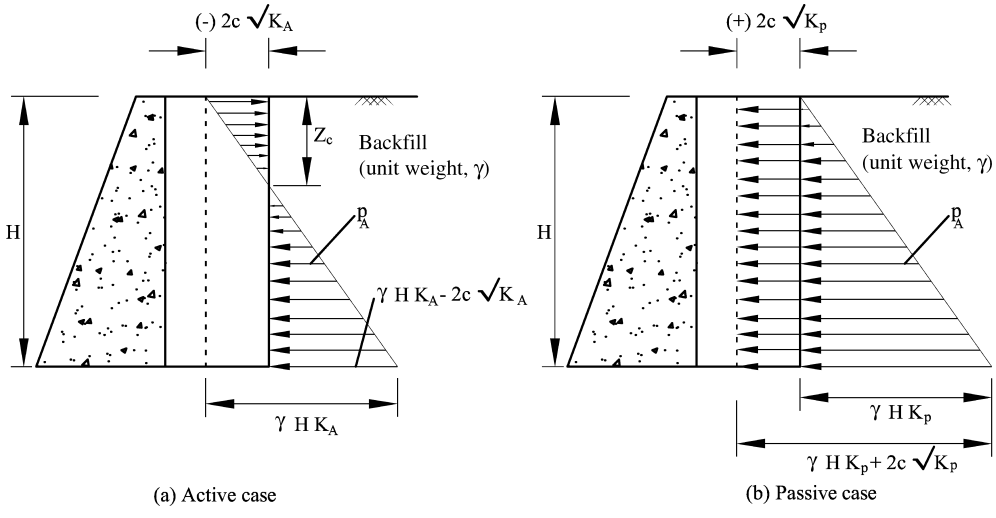

Figure 3.19 Rankine's pressures for cohesive soils – horizontal backfill.

3.8.2.2 Tension Cracks in Cohesive Soils (Active Case)

As can be seen from Equation (3.62) and Figure 3.19(a), the cohesion reduces the earth pressure intensity by an amount of $-2c\sqrt{K_A}$. Hence up to $z = z_c$, there is a tension zone in the soil and the tension cracks develop in the soil. z_c can be obtained from Equation (3.62) as the depth at which $p_A = 0$, that is

$$(p_A)_{at\ z=z_c} = 0 = \gamma z_c K_A - 2c\sqrt{K_A}$$

$$\therefore z_c = \frac{2c}{\gamma}\frac{1}{\sqrt{K_A}} = \frac{2c}{\gamma \tan\left(45 - \frac{\phi}{2}\right)} = \frac{2c}{\gamma}\tan\left(45 + \frac{\phi}{2}\right) \tag{3.66}$$

$$\text{since } \tan\left(45 + \frac{\phi}{2}\right) = \frac{1}{\tan\left(45 - \frac{\phi}{2}\right)} \tag{3.67}$$

The total lateral pressures can be obtained by computing the total areas of the earth pressure diagrams shown in Figures 3.19(a) and (b). However, in the active case, the usual practice is to neglect the negative pressure due to tensile zone up to $z = z_c$ and only calculate the net compressive pressure from z_c to H.

3.8.3 Coulomb's Theory of Earth Pressure

Coulomb's theory (Taylor, 1964; Bowles, 1996; Das, 2002) antedates Rankine's theory. It is based on the concept of a failure wedge which is bounded by the face of the wall and by a surface of failure that passes through the foot of the wall. The main assumption is that the surface of failure is a plane, and the other assumption is that the thrust on the wall acts in some known direction. Once these assumptions have been made, the resultant thrust on the wall may easily be determined by simple considerations based on principles of static equilibrium of the wedge due to the forces acting on it. This can be easily done using graphic statics in which the polygon of forces has to close for static equilibrium.

3.8.3.1 Active Case – Cohesionless Soils

The three forces acting on the wedge ABC (Figure 3.20) must be in equilibrium. The weight of the wedge W is a known force for any arbitrarily chosen trial failure plane AB. Since an active case exists, the resultant force P_F across plane AB must be at an angle of ϕ with the normal to the plane AB. The resultant force on the wall P_A (active pressure) is assumed, in the most general form of the Coulomb's theory, to be at an arbitrarily chosen obliquity α. With W known in magnitude and direction and the other two forces known in direction, the magnitude of force P_A is easily obtained by drawing the force triangle (Figure 3.20(b)). This lateral force P_A depends on the choice of failure plane, and the critical value must be found by trial corresponding to the case when P_A is maximum (Taylor, 1964). The force P_A also depends on the angle α.

However, α is usually taken as the wall friction angle, ϕ' which is slightly smaller than ϕ (angle of internal friction of soil). In the absence of enough data on the wall friction angle, α can be taken as ϕ' (i.e., $\phi' = \phi$).

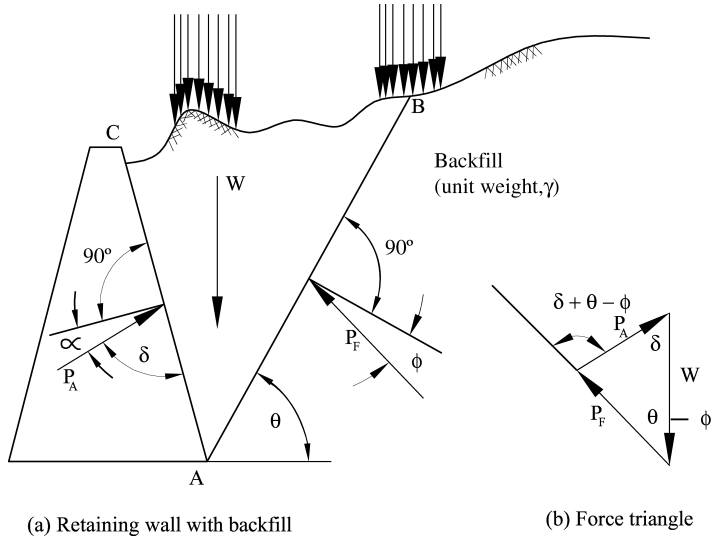

Figure 3.20 Coulomb's theory – active pressure.

In addition to the above mentioned trial method using triangle of forces, several methods such as Rebhann's method, Engesser's method, Poncelet method and Culmann's method are available in literature (Taylor, 1964; Teng, 1964) to get the critical value, P_A. However, the trial method is very general and can be used for all practical situations of backfills, retaining walls, surcharge loads, underground loads and so on.

3.8.3.2 Coulomb's Solution for Active Pressure – Simple Cases

The thrust P_A as given by Coulomb's theory for the simple case shown in Figure 3.21(a) is as follows

$$P_A = \frac{1}{2}\gamma H^2 \left[\frac{\csc\beta \sin(\beta-\phi)}{\sqrt{\sin(\beta+\phi')} + \sqrt{\dfrac{\sin(\phi+\phi')\sin(\phi-i)}{\sin(\beta-i)}}} \right]^2 \tag{3.68}$$

where ϕ is the angle of internal friction of the soil, that is also taken as the wall friction angle.

It is interesting to note that if β equals 90° and ϕ' equal i, the conditions conforms to the Rankine's theory, and Equation (3.68) reduces to Equation (3.51).

A special form of Equation (3.68) is that in which the wall is vertical, the surface of the backfill is level and $\alpha = \phi = \phi'$ (Figure 3.21(b)). Then the simplified solution is

$$P_A = \frac{1}{2}\gamma H^2 \frac{\cos\phi}{\left(1+\sqrt{2\sin\phi}\right)^2} \tag{3.69}$$

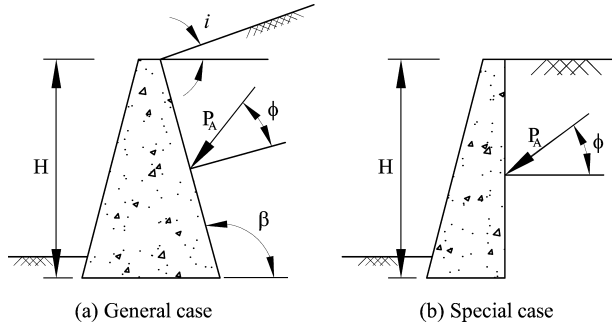

Figure 3.21 Coulomb's solutions for simple retaining walls – active case.

3.8.3.3 Coulomb's Theory for Passive Cases – Cohesionless Soils

The passive case differs from the active case in that the obliquity angles at the wall and on the failure plane are of opposite sign, as shown in Figure 3.22 along with the force triangle. Coulomb's theory uses the assumption of plane failure for the passive case, as it did for the active case, but the critical plane is that for which the passive thrust is a minimum. The critical active thrust is a maximum value. The failure plane is at a much smaller angle to the horizontal than in the active case. In general the passive thrust is several times larger than the active thrust.

The equation for the passive pressure according to Coulomb's theory for the simple case shown in Figure 3.23(a) is

$$P_P = \frac{1}{2}\gamma H^2 \left[\frac{\csc\beta \sin(\beta+\phi)}{\sqrt{\sin(\beta-\alpha)} - \sqrt{\dfrac{\sin(\phi+\alpha)\sin(\phi+i)}{\sin(\beta-i)}}} \right]^2 \tag{3.70}$$

with $\alpha = \phi' = \phi$.

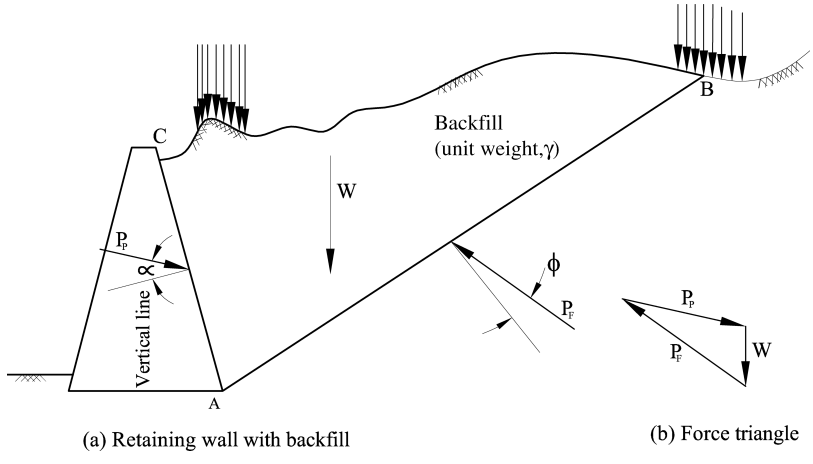

Figure 3.22 Coulomb's theory – passive pressure.

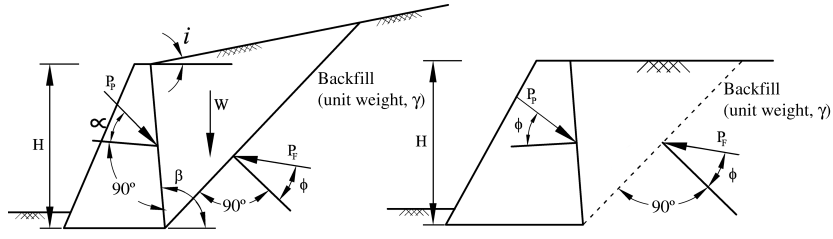

(a) General case (b) Special case

Figure 3.23 Coulomb's solutions for simple retaining walls – passive case.

For the special case with $i = 0$, $\alpha = \phi = \phi'$ and $\beta = 90^\circ$ (retaining wall with vertical face as shown in Figure 3.23(b)), Equation (3.70) further simplifies as

$$P_p = \frac{1}{2}\gamma H^2 \frac{\cos\phi}{\left(1-\sqrt{2}\sin\phi\right)^2} \tag{3.71}$$

3.8.3.4 Coulomb's Theory – Active Earth Pressure Due to Cohesive Soils

Determination of the active earth pressure in the case of cohesive backfills (soils with cohesion, c, and angle of internal friction, ϕ) is generally complex due to the uncertain movements of the wall relative to the soil. However, the general graphical solution using equilibrium of the failure wedge as per Coulomb's theory can be used in such cases of cohesive backfills (Figure 3.24(a)). All the assumptions are the same as in the case of cohesionless soils except that the shear strength along the plane of failure consists of both the adhesion component (due to cohesion) and the friction component (due to friction angle, ϕ) and is expressed as per the Mohr–Coulomb failure criterion, that is

$$s = c + \sigma_n \tan\phi$$

where

s = shear strength
σ_n = normal stress on the failure plane
c, ϕ = shear strength parameters of the soil.

While adhesion (due to c) along the failure plane ($c_{1A} = c$.OG) is taken into account, adhesion along the soil–wall interface is usually neglected. However, this also can be included if needed as it can be easily added in the polygon of forces with its magnitude ($c_{2A} = c$.OA), as shown in Figure 3.24(a).

Taking any trial wedge OGA (Figure 3.24(a)), the directions of P_{FA} and P_A are drawn as shown in Figure 3.24(a). Since ϕ and α (wall friction angle $= \phi'$) are known, and since the wedge fails by sliding down in the active case, the magnitudes and direction of adhesion along the trial failure plane C_{1A} (= c.OG) and along the well C_{2A} (= c.OA) are known. The

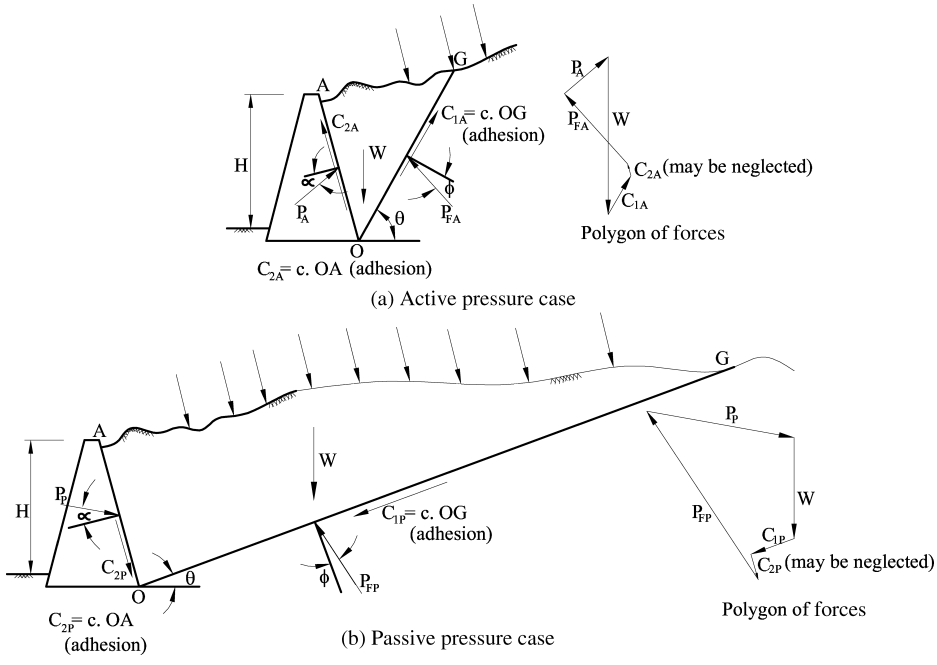

Figure 3.24 Coulomb's theory for earth pressures in cohesive soils – trial wedge method.

polygon of forces can be drawn as shown in Figure 3.24(a). Since the magnitudes of P_A and P_{FA} are the only two unknowns, they can be obtained from the polygon of forces. This gives the active pressure for this trial wedge. The trials are continued and values of P_A in each case are obtained. The maximum of these P_A values gives the actual/critical active pressure and the corresponding failure plane is the critical failure plane. As mentioned above, the adhesion along the wall–soil interface may be neglected, in which case C_{2A} can be deleted in the polygon of forces.

3.8.3.5 Coulomb's Theory – Passive Pressure Due to Cohesive Soils

The trial wedge in this case along with the forces is shown in Figure 3.24(b). It may be noted that the wedge fails by sliding up in the passive case. Correspondingly, the adhesions C_{1P} and C_{2P} along the failure plane and along the wall–soil interface are in the opposite direction to those shown in the case of active failure (opposite to direction of C_{1A} and C_{2A} shown in Figure 3.24(a)). Similarly, the passive pressure P_p and the resultant pressure due to friction P_{FP} along the trial failure plane OG are also inclined to the normals of the planes in the opposite directions by α and ϕ (Figure 3.24(b)) in comparison to the forces P_A and P_{FA} shown in Figure 3.24(a).

Then, the polygon of forces is drawn as shown in Figure 3.24(b) to determine P_P for the trial wedge. After a few trials, the minimum value P_P is taken as the passive pressure corresponding to that critical failure plane:

In this case also, the adhesion along the wall–soil interface can be neglected in which case C_{2P} can be deleted in the force polygon given in Figure 3.24(b).

3.8.3.6 Coulomb's Theory for General Cases of Retaining Walls

The above procedure of trial wedges can be used to determine the active and passive pressures on general retaining structures involving cohesive and cohesionless soils, partly or fully submerged backfills, layered backfills, surcharge loads including concentrated loads, openings, irregular wall faces and backfill surfaces and so on (Taylor, 1964; Teng, 1964; Peck, Hanson and Thornburn, 1974; Bowles, 1996).

3.8.3.7 Point of Action of the Resultant Active or Passive Pressure

The point of action of the resultant pressures (active or passive) is obtained by drawing a parallel line, GT to the failure plane AB form the center of gravity G of the failure wedge, ABC (active or passive cases) as shown in Figure 3.25.

Then, the resultant pressure (active or passive) is assumed to act at J. The direction of the pressure will be at an angle of $\alpha = \phi = \phi'$ taken appropriately that is, anticlockwise (active case) and clockwise (passive case) from the normal to the face at the point J as shown in Figure 3.25. This method can be used in the case of all practical problems involving cohesive and cohesionless soils, partially or fully submerged backfills, layered soils, surcharge loads, irregular wall faces and backfill surfaces and so on, (Taylor, 1964; Teng, 1964; Peck, Hanson and Thornburn, 1974; Bowles, 1996).

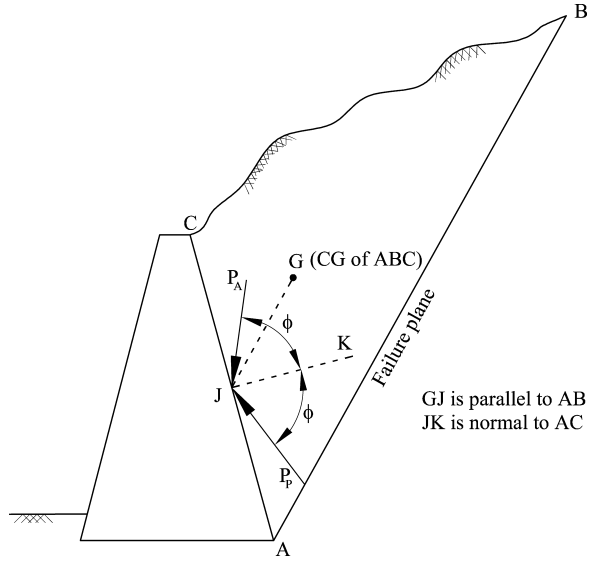

Figure 3.25 Direction and point of action of resultant active (P_A) and passive (P_P) pressures – Coulomb's theory.

3.9 Coefficient of Earth Pressure at Rest

The earth pressure at rest (Section 3.8.1) can be expressed as

$$\sigma_h = K_o \sigma_v \tag{3.72}$$

where

σ_h = lateral pressure at rest at any point
K_o = coefficient of earth pressure at rest
σ_v = vertical pressure at that point (usually the overburden pressure)
$= \gamma z$
γ = effective unit weight of the soil
z = vertical depth of the point below ground level.

It is very difficult to determine K_o for various soils and conditions. The formulae for K_o can also be derived from the theory of elasticity (Bowles, 1996) as

$$K_o = \frac{v}{1-v} \tag{3.73}$$

where v = Poisson's ratio of the soil (values range from 0 to 0.5).

The formula developed by Jaky (Bowles, 1996) for all granular materials including agricultural grains is

$$K_o = \frac{1-\sin\phi}{1+\sin\phi}\left(1+\frac{2}{3}\sin\phi\right) \tag{3.74}$$

where ϕ = angle of internal friction of the granular material.

The above formula is subsequently simplified for soils as

$$K_o = 1-\sin\phi \tag{3.75}$$

Equation (3.75) is most widely used in geotechnical engineering. There are several other formulae developed in literature (Bowles, 1996). The range of values of K_o is given in Table 3.3.

Table 3.3 Values of K_o.

Soil types	Values of K_o
Sands and gravels	0.35–0.60
Clays and silts	0.45–0.75
Overconsolidated clays	1.0

3.10 Other Theories of Lateral Pressure

There are several other theories proposed for the evaluation of lateral pressure based on analysis with assumed failure planes such as log spirals and bilinear surfaces and so on. Also solutions have been obtained using limiting equilibrium theory and method of characteristics (Harr, 1966).

However, the most widely accepted theories are due to Rankine and Coulomb and these have been discussed in the above sections.

3.11 Examples

3.11.1 Examples in Bearing Capacity (Sections 3.2 to 3.5)

Example 3.1

Compute the bearing capacity per unit area of the following footings (Figure 3.26) on a soil for which $c = 12\,\text{kN/m}^2$, $\phi = 20^o$, $\gamma_t = 17\,\text{kN/m}^2$ and $\gamma_{sub} = 10\,\text{kN/m}^2$. The depth of foundation is 1.0 m and the water table is at a depth of 3.5 m below ground level (GL). $N_c = 17.69$, $N_q = 7.44$ and $N_\gamma = 3.64$.

1. Strip footing, 3 m wide
2. Square footing, 3×3 m
3. Circular footing, 3 m diameter

Solution:

$$c = 12\,\text{kN/m}^2,\ \phi = 20^\circ,\ \gamma_t = 17\,\text{kN/m}^3,\ \gamma_{sub} = 10\,\text{kN/m}^2$$

$$\gamma_{average} \text{ for soil in cone of depression ABC}$$
$$= \frac{\gamma_t \times 2.5 + \gamma_{sub} \times 0.5}{3}$$
$$= \frac{17 \times 2.5 + 10 \times 0.5}{3}$$
$$= 15.83\,\text{kN/m}^3$$

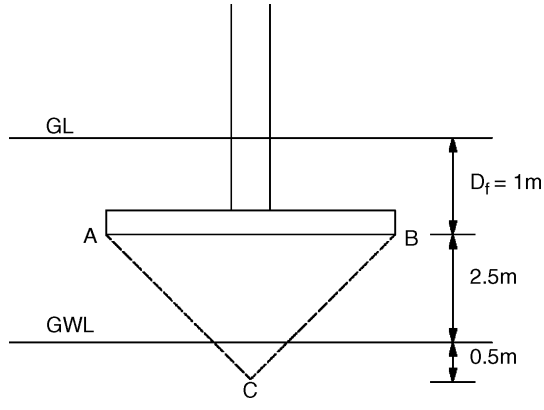

Figure 3.26 Example 3.1.

1. Strip footing, 3 m wide

$$\begin{aligned} q_u &= cN_c + qN_q + 0.5\gamma_{av.}BN_\gamma \\ &= (12 \times 17.69) + (17 \times 1 \times 7.44) + (0.5 \times 15.83 \times 3 \times 3.64) \\ &= 425.2\,\text{kN/m}^2 \end{aligned}$$

2. Square footing, 3×3 m

$$\begin{aligned} q_u &= 1.3cN_c + qN_q + 0.4\gamma_{av.}BN_\gamma \\ &= (1.3 \times 12 \times 17.69) + (17 \times 1 \times 7.44) + (0.4 \times 15.83 \times 3 \times 3.64) \\ &= 471.6\,\text{kN/m}^2 \end{aligned}$$

3. Circular footing, 3 m diameter

$$\begin{aligned} q_u &= 1.3cN_c + qN_q + 0.3\gamma_{av.}BN_\gamma \\ &= (1.3 \times 12 \times 17.69) + (17 \times 1 \times 7.44) + (0.3 \times 15.83 \times 3 \times 3.64) \\ &= 454.3\,\text{kN/m}^2 \end{aligned}$$

Example 3.2

A square footing and a circular footing are to be designed to carry a load of 120 kN at a depth of 2 m below GL in a soil with the following data. $\gamma_{soil} = 18\,\text{kN/m}^3$, $c = 10\,\text{kN/m}^3$, $\phi = 20^o$ ($N_c = 17.69$, $N_q = 7.44$ and $N_\gamma = 3.64$). Calculate their dimensions. What will be their bearing capacities if the ground water level (GWL) is 3 m below GL?

$$\gamma_{sub} = 10\,\text{kN/m}^3,\ F.S = 3$$

Solution:

$$c = 10\,\text{kN/m}^2,\ \phi = 20^o,\ N_c = 17.69,\ N_q = 7.44,\ N_\gamma = 3.64,\ \gamma = 18\,\text{kN/m}^3,$$

$$\gamma_{sub} = 10\,\text{kN/m}^3,\ D_f = 2\,\text{m}$$

$$\frac{Q_u}{Q_{all}} = F.S., \qquad Q_u = F.S.Q_{all} = 3 \times 120 = 360\,\text{kN}$$

For square footing:

$$q_u = \frac{Q_u}{area} = \frac{360}{B^2}$$

$$q_u = 1.3cN_c + qN_q + 0.4\gamma BN_\gamma$$

$$\frac{360}{B^2} = (1.3 \times 10 \times 17.69) + (18 \times 2 \times 7.44) + (0.4 \times 18 \times B \times 3.64)$$

$$\frac{360}{B^2} = 497.81 + 26.21B$$

$$26.21B^3 + 497.81B^2 - 360 = 0$$

$$\therefore B = 0.83 \text{ m}$$

For circular footing:

$$q_u = \frac{Q_u}{area} = \frac{360}{\pi B^2/4}$$

$$q_u = 1.3cN_c + qN_q + 0.3\gamma BN_\gamma$$

$$\frac{360}{\pi B^2/4} = (1.3 \times 10 \times 17.69) + (18 \times 2 \times 7.44) + (0.3 \times 18 \times B \times 3.64)$$

$$\frac{458.4}{B^2} = 497.81 + 19.66B$$

$$19.66B^3 + 497.81B^2 - 458.4 = 0$$

$$B = 0.94 \text{ m}$$

Bearing capacity if ground water level is at $D = 3$ m, below GL:

If $B < 1$ m, then bearing capacity is the same as above.

If $B > 1$ m, then γ_{average} is to be used in place of γ in the third term of bearing capacity equations that is, $0.4\gamma_{\text{av}} BN_\gamma$ for square footing and $0.3\gamma_{\text{av}} BN_\gamma$ for circular footing (Figure 3.27).

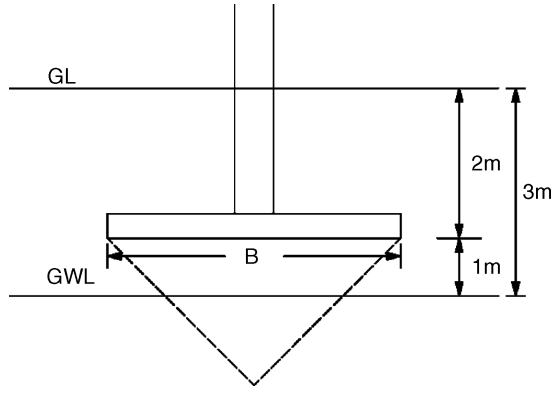

Figure 3.27 Example 3.2.

Example 3.3

Compute the bearing capacity per unit area of a continuous footing 3 m wide on a soil for which $c = 20\,\text{kN/m}^3$, $\phi = 20^o$, $N_c = 20$, $N_q = 9$, $N_\gamma = 5$, $\gamma = 19\,\text{kN/m}^3$, and $\gamma_{sub} = 12\,\text{kN/m}^3$. The depth of foundation is 3 m and the water table is at a depth of 5 m below GL (Figure 3.28).

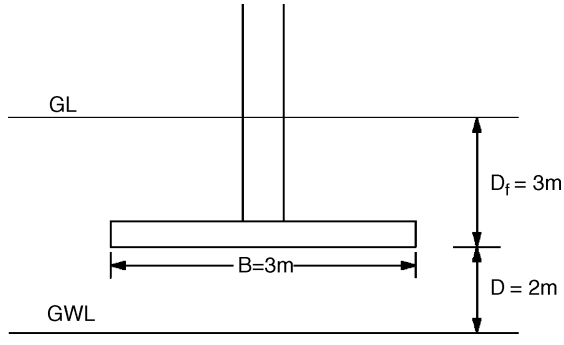

Figure 3.28 Example 3.3.

Solution:

$$c = 20\,\text{kN/m}^3,\ \phi = 20^o,\ N_c = 20,\ N_q = 9,\ N_\gamma = 5,\ \gamma = 19\,\text{kN/m}^3,$$

$$\gamma_{sub} = 12\,\text{kN/m}^3,\ D_f = 3\,\text{m}$$

$$\gamma_{av} = \frac{1}{3}[(19 \times 2) + 12] = \frac{50}{3} = 16.67\,\text{kN/m}^3 \quad \text{For } D \leq B$$

$$\begin{aligned} q_u &= cN_c + \gamma D_f N_q + 0.5\gamma_{av} B N_\gamma \\ &= 20 \times 20 + 19 \times 3 \times 9 + 0.5 \times 16.67 \times 3 \times 5 \\ &= 1038.025\,\text{kN/m}^2 \end{aligned}$$

Example 3.4

Load tests were carried out on a 0.3 m square plate and a 0.3 m diameter circular plate on a dense cohesionless sand having a unit weight of $17\,\text{kN/m}^3$. The plates were tested at a depth of 0.6 m below GL. Failure occurred at 10 kN and 7 kN for square and circular plates respectively. The settlement of the square plate was observed to be 1.5 cm just before failure. What would be the failure load per unit area of (1) 0.3×0.3 m square footing and

(2) 1.5×3.0 m rectangular footing, both located with their bases at the same depth in the same soil?

Solution:
$D_f = 0.6m,\ c = 0$ (For dense sand)

$$q_u \text{ from tests } = \frac{10}{0.3 \times 0.3}\text{kN/m}^2 \text{ for square plate}$$
$$= \frac{10}{(\pi/4) \times 0.3^2}\text{kN/m}^2 \text{ for circular plate}$$

1. For square plate: 0.3×0.3 m, $\therefore B = 0.3$ m

$$q_u = 1.3cN_c + qN_q + 0.4\gamma BN_\gamma$$
$$(1.3 \times 0 \times N_c) + (17 \times 0.6 \times N_q) + (0.4 \times 17 \times 0.3 \times N_\gamma) = \frac{10}{0.3 \times 0.3}$$
$$0.3 \times 0.3[(17 \times 0.6 \times N_q) + (0.4 \times 17 \times 0.3 \times N_\gamma)] = 10$$

$$0.918N_q + 0.1836N_\gamma = 10$$

2. For circular plate: D = 0.3 m, B = 0.3 m

$$q_u = 1.3cN_c + qN_q + 0.3\gamma BN_\gamma$$
$$(1.3 \times 0 \times N_c) + (17 \times 0.6 \times N_q) + (0.3 \times 17 \times 0.3 \times N_\gamma) = \frac{7}{\pi \times 0.3^2/4}$$
$$\frac{\pi \times 0.3^2}{4}\left[(17 \times 0.6 \times N_q) + (0.3 \times 17 \times 0.3 \times N_\gamma)\right] = 7$$

$$0.721N_q + 0.108N_\gamma = 7$$

$$N_q = \frac{\begin{vmatrix} 10 & 0.1836 \\ 7 & 0.108 \end{vmatrix}}{\begin{vmatrix} 0.918 & 0.1836 \\ 0.721 & 0.108 \end{vmatrix}} = 6.175, \qquad N_\gamma = \frac{\begin{vmatrix} 0.918 & 10 \\ 0.721 & 7 \end{vmatrix}}{\begin{vmatrix} 0.918 & 0.1836 \\ 0.721 & 0.108 \end{vmatrix}} = 23.593$$

Failure load of 2 m square footing:

$$q_u = 1.3cN_c + qN_q + 0.4\gamma BN_\gamma \text{ (note : } c = 0)$$
$$q_u = (17 \times 0.6 \times 6.175) + (0.4 \times 17 \times 2 \times 23.593) = 383.8498\,\text{kN/m}^2$$
$$Q_u = q_u \times \text{area} = 383.8498 \times (2 \times 2) = 1535.4\,\text{kN}$$

Failure load of 1.5×3.0 m rectangular footing:

$$\text{Shape factors, } \lambda_{cs} = 1 + 0.2\frac{B}{L} = 1.1 \quad (\text{Assuming } 0 \leq \phi \leq 10^\circ)$$

$$\lambda_{qs} = 1$$

$$\lambda_{\gamma s} = 1$$

$$q_u = \left[(17 \times 0.6 \times 1.0 \times 6.175) + \left(17 \times \frac{1.5}{2} \times 23.593 \times 1.0\right)\right] = 363.8\,\text{kN/m}^2$$

$$Q_u = q_u \times \text{area} = 363.8 \times (1.5 \times 3) = 1637.1\,\text{kN}$$

3.11.2 Examples in Stress Distribution in Soils (Section 3.6)

Example 3.5

Soil with unit weight of 16 kN/m^3 is loaded at the surface by a UDL of 200 kN/m^2 over:

1. Circular area of 2 m diameter
2. Annular area with 3 m outer diameter and 2 m inner diameter.

Calculate the change of vertical stress at a depth of 3 m below surface for the above two cases (Figure 3.29). What will be the total stress in both cases at that depth (= 3 m)?

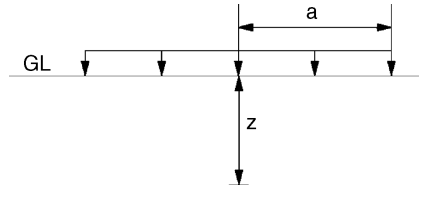

Figure 3.29 Example 3.5.

Solution:

$$\gamma_t = 16\,\text{kN/m}^2,$$

$$\sigma_z = p\left[1 - \frac{1}{\left[\left(\frac{a}{z}\right)^2 + 1\right]^{3/2}}\right]$$

1. Circular area:

$$p = 200\,\text{kN/m}^2,\ a = 1\,\text{m},\ z = 3\,\text{m}$$

$$\therefore (\sigma_z)_{z=3m} = 200\left[1-\frac{1}{\left[\left(\frac{1}{3}\right)^2+1\right]^{3/2}}\right] = 29.24\,\text{kN/m}^2$$

Total stress $= (29.24) + (3 \times 16) = 77.24\,\text{kN/m}^2$

2. Annular area:

$$p = 200\,\text{kN/m}^2,\ z = 3\,\text{m},\ a_1 = 1.5\,\text{m},\ a_2 = 1\,\text{m}$$

$$\sigma_1 = (\sigma_z)_{a=1.5m,z=3m} = 200\left[1-\frac{1}{\left[1+\left(\frac{1.5}{3}\right)^2\right]^{3/2}}\right] = 56.89\,\text{kN/m}^2$$

$$\sigma_2 = (\sigma_z)_{a=1m,z=3m} = 200\left[1-\frac{1}{\left[1+\left(\frac{1}{3}\right)^2\right]^{3/2}}\right] = 29.24\,\text{kN/m}^2$$

$$(\sigma_z)_{annular} = \sigma_1 - \sigma_2 = 56.89 - 29.24 = 27.65\,\text{kN/m}^2$$

Total stress $= (27.65) + (3 \times 16) = 75.65\,\text{kN/m}^2$

Example 3.6

A 3×3 m square footing ABCD with its CG at E, carrying a UDL of $250\,\text{kN/m}^2$ is located at ground level (GL). Assuming it as an equivalent circular footing, calculate the vertical stress at a depth of 4 m directly below the following points.

1. Center E of the square ABCD (Figure 3.30)
2. Any corner (say A; Figure 3.31)
3. What will be the stresses at the same points given in (1) and (2), that is, below E and A, if the above load is treated as a concentrated load acting at E.

Solution:

$$P = 3 \times 3 \times 250 = 2250\,\text{kN},\ p = \frac{2250}{3 \times 3} = 250\,\text{kN},\ z = 4\,\text{m}$$

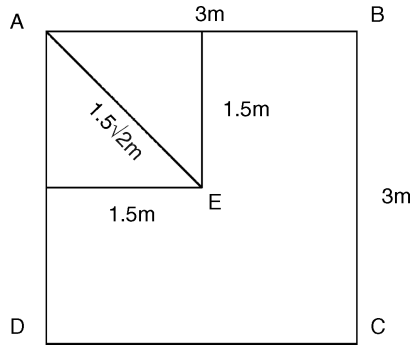

Figure 3.30 Example 3.6.

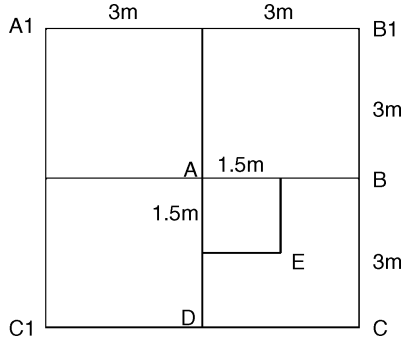

Figure 3.31 Example 3.6.

Equivalent circle:

1. Center E of the square ABCD

$$Area = 3 \times 3 = 9m^2 = \pi r^2$$

$$\therefore r = \sqrt{\frac{9}{\pi}} = 1.69\,\text{m}$$

For circular area

$$\frac{\sigma_z}{p} = \left[1 - \frac{1}{\left[1 + \left(\frac{a}{z}\right)^2\right]^{3/2}}\right]$$

$$= \left[1 - \frac{1}{\left[1 + \left(\frac{1.69}{4}\right)^2\right]^{3/2}}\right] = 0.219$$

$$\therefore (\sigma_z)_{below\ at\ 4\ m} = 0.219 \times 250 = 54.75\ \text{kN/m}^2$$

2. Corner A (4 m below)
   A is the center of the square $A_1B_1CC_1$ and corner of ABCD.

$$Area\ of\ A_1B_1CC_1 = 6 \times 6 = 36\ \text{m}^2 = \pi r^2$$

$$\therefore \text{Radius of equivalent circle, } r = \sqrt{\frac{36}{\pi}} = 3.385\ \text{m}$$

   For circle

$$\frac{(\sigma_z)_A}{p} = \left[1 - \frac{1}{\left[1 + \left(\frac{a}{z}\right)^2\right]^{3/2}}\right] = \left[1 - \frac{1}{\left[1 + \left(\frac{3.385}{4}\right)^2\right]^{3/2}}\right] = 0.556\ \text{m}$$

$$\therefore \text{stress below A due to ABCD} = \frac{1}{4}p \times 0.556 = \frac{1}{4} \times 250 \times 0.556$$

$$\therefore \sigma_{zA} = 34.75\ \text{kN/m}^2$$

3. Treating it as a concentrated load, $P = 2250$ kN
   Boussinesq's solution

$$\sigma_z = \frac{3P}{2\pi z^2}\left[\frac{1}{1 + \left(\frac{r}{z}\right)^2}\right]^{5/2} = \frac{3P}{2\pi}\frac{z^3}{R^5}$$

$$(\text{since } R^2 = \sqrt{r^2 + z^2})$$

   a. 4 m below E

$$(\sigma_z)_E = \frac{3P}{2\pi}\frac{z^3}{R^5} = \frac{3 \times 2250 \times}{2\pi}\frac{4^3}{4^5} = 67.14\ \text{kN/m}^2$$

   b. 4 m below A

$$r = 1.5\sqrt{2}\ \text{from } E, z = 4\ \text{m}, R^2 = \sqrt{r^2 + z^2} = \sqrt{(1.5\sqrt{2})^2 + 4^2} = 4.53$$

$$(\sigma_z)_A = \frac{3P}{2\pi}\frac{z^3}{R^5} = \frac{3 \times 2250 \times}{2\pi}\frac{4^3}{4.53^5} = 36.04\ \text{kN/m}^2$$

Example 3.7

A column load of 1600 kN is supported by a circular footing of radius of 4 m at the ground level. Using the expression for vertical stress at any depth z below the center of the footing, compute the stress at a depth of 6 m below the center. If the footing is converted to an annular shape with outer and inner radii as 6 and 4 m, what will be the vertical stress at the same depth of 6 m below center (Figure 3.32)? Find the vertical stress at 6 m depth below the center if the column load is treated as a concentrated load using Boussinesq's equation.

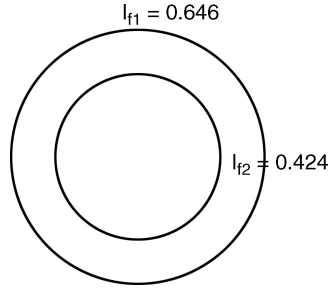

Figure 3.32 Example 3.7.

Solution:
Circular footing radius, $r = 4$ m

$$\text{Area} = \pi r^2 = \pi(4)^2 = 50.27 \text{ m}^2$$

$$p = \frac{1600}{50.27} = 31.83 \text{ kN/m}^2$$

$r = 4$ m, $z = 6$ m

$$\frac{(\sigma_z)_{\text{below center of circle}}}{p} = \left[1 - \frac{1}{\left[1 + \left(\frac{r}{z}\right)^2\right]^{3/2}}\right] = \left[1 - \frac{1}{\left[1 + \left(\frac{4}{6}\right)^2\right]^{3/2}}\right] = 0.424$$

$$(\sigma_z)_{\text{below center of circle}} = 0.424p = 0.424 \times 31.83$$

$$(\sigma_z)_{\text{below center of circle}} = 13.5 \text{ kN/m}^2$$

$r_1 = 6$ m, $r_2 = 4$ m

$$I_{f1} \text{ for } r_1 = 6 \text{ m} = \left[1 - \frac{1}{\left[1 + \left(\frac{6}{6}\right)^2\right]^{3/2}}\right] = 0.646.$$

$$I_{f2} \text{ for } r_2 = 4\,\text{m} = \left[1 - \frac{1}{\left[1 + \left(\frac{4}{6}\right)^2\right]^{3/2}}\right] = 0.424.$$

$$\text{Net } I_f = I_{f1} - I_{f2} = 0.646 - 0.424 = 0.222$$

$$\text{Area } A_1 = \pi r^2 = \pi(6)^2 = 113.10\,\text{m}^2$$

$$\text{Area } A_2 = \pi r^2 = \pi(4)^2 = 50.27\,\text{m}^2$$

$$\text{Annular area} = A_1 - A_2 = 62.83\,\text{m}^2$$

$$p = \frac{1600}{62.83} = 25.47\,\text{N/m}^2$$

$$\sigma_z = 0.222\,p = 0.222 \times 25.47 = 5.65\,\text{kN/m}^2$$

Boussinesq's solution, concentrated load P at $r = 0\,\text{m}$

$$\sigma_z = \frac{3P}{2\pi z^2}\left[\frac{1}{1 + \left(\frac{r}{z}\right)^2}\right]^{5/2} = \frac{3 \times 1600}{2\pi(6)^2}\left[\frac{1}{1 + (0)^2}\right]^{5/2} = 21.22\,\text{kN/m}^2$$

Example 3.8

Compute the vertical stress at a depth of 4 m below the center of a circular footing of radius 3 m subjected to a UDL of 30 kN/m^2. What should be the radius of footing if the influence value at a depth of 6 m is 0.3?

Solution:

$$\frac{\sigma_z}{p} = \left[1 - \frac{1}{\left[1 + \left(\frac{a}{z}\right)^2\right]^{3/2}}\right] = \left[1 - \frac{1}{\left[1 + \left(\frac{3}{4}\right)^2\right]^{3/2}}\right] = 0.488$$

$$\sigma_z = 0.488, p = 0.488 \times 30 = 14.64\,\text{kN/m}^2$$

$$\text{If } I_f = 0.3, \frac{r}{z} = \sqrt{\left[\frac{1}{(1-I_f)^{2/3}}\right] - 1} = \sqrt{\left[\frac{1}{(1-0.3)^{2/3}}\right] - 1} = 0.518$$

$$r = 0.518 \times z = 0.518 \times 6 = 3.11 \text{ m}$$

Example 3.9

A UDL of 250 kN/m^2 is acting on a rectangular foundation ABCD shown in Figure 3.33. Find the vertical stress at a depth of 4 m below the points A, B, C, D, F and G using Newmarks formula and/or charts.

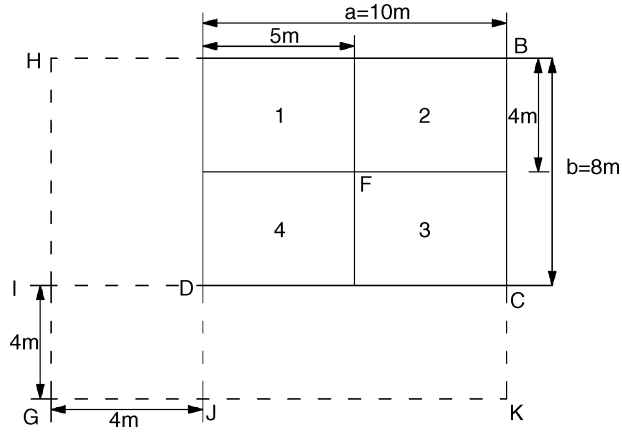

Figure 3.33 Example 3.9.

Solution:
Stresses below A, B, C and D:
A, B, C, D are corners of the rectangular footing.

$$p = 250 \text{ kN/m}^2, a = 10 \text{ m}, b = 8 \text{ m}, z = 4 \text{ m}.$$

$$m = \frac{10}{4} = 2.5, \quad n = \frac{8}{4} = 2 \qquad \therefore I_{f(A,B,C,D)} = 0.236$$

$$\therefore \text{vertical stress at 4 m below the corner A}, B, C, D = 0.236 \times 250 = 59 \text{ kN/m}^2$$

Stress below F: (interior point)
F is the corner of the four rectangles 1,2,3,4

$$\therefore (I_f)_F = I_f \text{ of } 1+2+3+4$$
$$= 4 \times I_{f(1)}$$

For rectangle 1: $a_1 = 5\,\text{m}$, $b_1 = 4\,\text{m}$, $z = 4\,\text{m}$

$$m = \frac{5}{4} = 1.25, \quad n = \frac{4}{4} = 1 \quad \therefore I_{f(A,B,C,D)} = 0.186$$

$$\therefore (I_f)_F = 4 \times 0.186 = 0.744$$

$$\therefore \text{vertical stress at 4 m below F} = 0.744 \times 250 = 186\,\text{kN/m}^2$$

Stress below G:
G is the corner of the rectangles BHGK, HAJG, CIGK, IGJD. Hence, stress can be obtained by superposition.

$$\therefore (I_f)_G \text{ due to ABCD} = (I_f)_G\,[\text{HGKB-HAJG-CIGK} + \text{IGJD}]$$

$(I_f)_G$ due HGKB $= (I_f)_I$
For rectangle HGKB: $a = 10 + 4 = 14\,\text{m}$, $b = 8 + 4 = 12\,\text{m}$, $z = 4\,\text{m}$

$$m = \frac{14}{4} = 3.5, \quad n = \frac{12}{4} = 3 \quad \therefore (I_f)_I = 0.246$$

$(I_f)_G$ due HAJG $= (I_f)_{II}$
For rectangle HAJG: $a = 4\,\text{m}$, $b = 8 + 4 = 12\,\text{m}$, $z = 4\,\text{m}$

$$m = \frac{4}{4} = 1, \quad n = \frac{12}{4} = 3 \quad \therefore (I_f)_{II} = 0.205$$

$(I_f)_G$ due CIGK $= (I_f)_{III}$
For rectangle CIGK: $a = 14\,\text{m}$, $b = 4\,\text{m}$, $z = 4\,\text{m}$

$$m = \frac{14}{4} = 3.5, \quad n = \frac{4}{4} = 1 \quad \therefore (I_f)_{III} = 0.207$$

$(I_f)_G$ due IGJD $= (I_f)_{IV}$
For rectangle IGJD: $a = 4\,\text{m}$, $b = 4\,\text{m}$, $z = 4\,\text{m}$

$$m = \frac{4}{4} = 1, \quad n = \frac{4}{4} = 1 \quad \therefore (I_f)_{Iv} = 0.209$$

$$(I_f)_G \text{ due to ABCD} = (I_f)_I - (I_f)_{II} - (I_f)_{III} + (I_f)_{IV}$$

$$= 0.246 - 0.205 - 0.207 + 0.209$$

$$(I_f)_G \text{ due to ABCD} = 0.043$$

$$\therefore \text{Stress at 4 m below G (exterior point)} = 0.043 \times 250 = 10.75\,\text{kN/m}^2$$

3.11.3 Examples in Settlement Analysis (Section 3.7)

The symbol ρ is used instead of s to refer to settlement in these examples, that is

$$\rho = s,\ \rho_u = S_c$$

where S_c = ultimate settlement due to primary consolidation

Example 3.10

After construction, the average settlement for a structure was 5 cm after 4 years. The total settlement was known to be more than 15 cm. Estimate its settlement after 16 years. Calculate the time taken for the settlement to be 10 cm.

Solution:

$$\rho = U\rho_u,\ \rho_u = m_v\, dp\, H,\ T = \frac{\pi}{4}U^2 (U < 60\%),\ T = \frac{c_v t}{(H/2)^2}$$

$$\rho_4 = 5\,\text{cm},\ t = 4\,\text{years},\ \rho_u \geq 15\,\text{cm} \quad \therefore U < 60\%$$

1. $\rho_{16} = ?,\ t = 16\,\text{years}$

$$\rho_4 : \rho_{16} = U_4 : U_{16} = \sqrt{T_4} : \sqrt{T_6} = \sqrt{t_4} : \sqrt{t_6}$$

$$5 : \rho_{16} = \sqrt{4} : \sqrt{16}, \frac{2}{4} = \frac{5}{\rho_{16}}$$

$$\therefore \rho_{16} = \frac{4}{2} \times 5 = 10\,\text{cm}$$

2. $\rho = 10\,\text{cm}, t = ?$

$$\rho_4 : 10 = \sqrt{t_4} : \sqrt{t}$$

$$\frac{5}{10} = \frac{\sqrt{4}}{\sqrt{t}}$$

$$\therefore \sqrt{t} = \frac{10}{5} \times \sqrt{4}$$

$$\therefore t = \left(\frac{10}{5} \times \sqrt{4}\right)^2 = 16\,\text{years}$$

Example 3.11

The settlement analysis for a proposed structure indicated 5 cm of settlement after 4 years, with an ultimate settlement of 10 cm. Subsequent tests indicated that the actual coefficient of compressibility (a_v) is 20% smaller and the coefficient of consolidation (C_v) is 30% smaller than the values used for the above estimate originally made. Based on these accurate values, determine the ultimate settlement and the time for 3 cm settlement.

Solution:

$$\rho_1 = 5\,\text{cm},\ t_1 = 4\,\text{years},\ \rho_{u1} = 10\,\text{cm},\ a_{v2} = 0.8a_{v1},\ C_{v2} = 0.7c_{v1}$$

$$\frac{\rho_{u1}}{\rho_{u2}} = \frac{m_{v1}}{m_{v2}} = \frac{a_{v1}}{a_{v2}} = \frac{1}{0.8}$$

$$\therefore \rho_{u2} = 0.8\rho_{u1} = 8\,\text{cm}$$

$$\frac{\rho_1}{\rho_2} = \frac{U_1\rho_{U1}}{U_2\rho_{U2}} = \frac{1}{0.8}\sqrt{\frac{T_1}{T_2}} = \frac{1}{0.8}\sqrt{\frac{C_{v1}t_1}{C_{v2}t_2}} = \frac{1}{0.8}\sqrt{\frac{1}{0.7}}\sqrt{\frac{t_1}{t_2}}$$

$$\frac{1}{0.8}\sqrt{\frac{1}{0.7}}\sqrt{\frac{t_1}{t_2}} = \frac{\rho_1}{\rho_2} = \frac{5}{3}$$

$$\sqrt{\frac{t_1}{t_2}} = \frac{5}{3} \times 0.8 \times \sqrt{0.7} = 1.1155, \frac{t_1}{t_2} = 1.1155^2,$$

$$\therefore t_2 = \frac{t_1}{1.1155^2} = \frac{4}{1.1155^2} = 3.21 \text{ years}$$

Example 3.12

The settlement analysis of a structure based on preliminary tests indicates 3 cm settlement in 4 years and an ultimate settlement of 10 cm. After detailed investigations it is found that the coefficient of permeability k is 20% higher than the one in the preliminary tests. What will be the ultimate settlement, the settlement in 5 years and the time required for 3 cm settlement of the structure, based on detailed test results?

Solution:

$$\frac{\rho_{u2}}{\rho_{u1}} = \frac{m_v dp_2 H_2}{m_v dp_1 H_1} = \frac{12 \times 1.2H_1}{2H_1} = 7.2$$

Find ρ_{u2}, ρ_2 in $t_2 = 5$ years and t_3 for $\rho_3 = 3$ cm

1. $\frac{\rho_{u2}}{\rho_{u1}} = \frac{m_v dpH}{m_v dpH} = 1, \rho_{u2} = \rho_{u1} = 10$ cm

$$\rho_u = m_v dpH$$

$$\frac{\rho}{\rho_u} = U$$

$$T = \frac{\pi}{4}U^2 \quad (\text{U} < 60\%)$$

$$T = \frac{C_v t}{(H/2)^2} = \frac{k}{\gamma_w m_v}\frac{t}{(H/2)^2}$$

$$\frac{\rho_2}{\rho_{u2}}\frac{\rho_{u1}}{\rho_1} = \frac{U_2}{U_1} = \sqrt{\frac{T_2}{T_1}} = \sqrt{\frac{\frac{k_2}{\gamma_w m_v}\frac{t_2}{H_2^2}}{\frac{k_1}{\gamma_w m_v}\frac{t_1}{H_1^2}}}$$

$$\therefore \frac{\rho_2}{\rho_1} = \sqrt{\frac{k_2 t_2}{k_1 t_1}}$$

2. $\rho_2 = ?$ in $t_2 = 5$ years

$$\rho_1 = 3\,\text{cm} \quad \text{in} \quad t_1 = 4\,\text{years}$$

$$\therefore \frac{\rho_2}{\rho_1} = \sqrt{\frac{k_2 t_2}{k_1 t_1}}, \frac{\rho_2}{3} = \sqrt{\frac{1.2k_1}{k_1}\frac{5}{4}} = \sqrt{1.5}$$

$$\therefore \rho_2 = 3 \times \sqrt{1.5} = 3.674\,\text{cm}$$

3. $\rho_3 = 3\,\text{cm}, \quad t_3 = ?$

$$\rho_1 = 3\,\text{cm} \quad \text{in} \quad t_1 = 4\,\text{years}$$

$$\therefore \frac{\rho_3}{\rho_1} = \sqrt{\frac{k_2 t_3}{k_1 t_1}}, \sqrt{\frac{1.2k_1}{k_1}\frac{t_3}{4}} = \frac{3}{3}$$

$$\therefore t_3 = \frac{1 \times 4}{1.2} = 3.33\,\text{years}$$

Example 3.13

The settlement analysis of a structure based on preliminary tests indicates 3 cm settlement in 4 years and an ultimate settlement of 10 cm. After detailed investigations, it has been found that the coefficient of consolidation, C_v, is 30% higher than the one in preliminary test. What will be the ultimate settlement, settlement in 5 years and time required for 3 cm settlement of the structure based on detailed test results?

Solution:

$$C_{v2} = 1.3C_{v1},\ \rho_{u2} = ?,\ \rho_2 = ?\ \text{when}\ t_2 = 5\,\text{years}$$

$$\rho_1 = 3\,\text{cm} \quad \text{in} \quad t_1 = 4\,\text{years},\ \rho_{u1} = 10\,\text{cm},\ c_{v1}$$

$$t_3 = ?\ \text{when}\ \rho_3 = 3\,\text{cm}$$

$$\frac{\rho_{u2}}{\rho_{u1}} = \frac{m_v dpH}{m_v dpH} = 1, \quad \therefore \rho_{u2} = \rho_{u1} = 10\,\text{cm}$$

$$\frac{\rho_2}{\rho_{u2}}\frac{\rho_{u1}}{\rho_1} = \frac{U_2}{U_1} = \sqrt{\frac{C_{v2}\dfrac{t_2}{H^2}}{C_{v1}\dfrac{t_1}{H^2}}} = \sqrt{1.3\frac{t_2}{t_1}}$$

$$\because \rho_{u2} = \rho_{u1} = 10\,\text{cm}, \quad \rho_2 = \sqrt{1.3\frac{t_2}{t_1}}\rho_1 = \sqrt{1.3\frac{5}{4}} \times 3$$

$$\therefore \rho_2 = 3.82\,\text{cm}$$

Similarly, $\rho_3 = \sqrt{1.3\frac{t_3}{t_1}}\rho_1 = \sqrt{1.3\frac{t_3}{4}} \times \rho_1$

$$t_3 = \left(\frac{\rho_3}{\rho_1}\right)^2 \times \frac{4}{1.3} = \left(\frac{3}{3}\right)^2 \times \frac{4}{1.3} = 3.08\,\text{years}$$

Example 3.14

The settlement analysis for a proposed structure indicated 5 cm of settlement in 4 years and an ultimate settlement of 10 cm. The estimated increment of pressure in the clay layer below is 2 kN/m^2. The following variations are subsequently noticed.

1. A permanent 1 m lowering of the water table will take place.
2. The compressive clay stratum is 20% thicker than assumed in the original analysis.

Compute the modified values of ultimate settlement, settlement after 2 years.

Solution:

$$\rho_u = m_v dpH$$
$$\frac{\rho}{\rho_u} = U \quad ,$$

$$T = \frac{\pi}{4}U^2(\text{U} < 60\%), \qquad T = \frac{C_v t}{(H/2)^2} = \frac{k}{\gamma_w m_v}\frac{t}{(H/2)^2}$$

$$\rho_1 = 5\,\text{cm in } t_1 = 4\,\text{years}, \ \rho_{u1} = 10\,\text{cm}$$

$$\Delta p_1 = 2\,\text{kN/m}^2, \ h_1$$

$\Delta p_2 = 2 + 10$ (due to 1 m lowering, reduction in pore pressure, $\Delta u = 10\,\text{kN/m}^2$)

$$H_2 = 1.2H_1$$

$$\rho_{u2} = ?, \ \rho_2 = ? \text{ when } t_2 = 2\,\text{years}$$

1. $\frac{\rho_{u2}}{\rho_{u1}} = \frac{m_v dp_2 H_2}{m_v dp_1 H_1} = \frac{12 \times 1.2H_1}{2H_1} = 7.2,$

$$\therefore \rho_{u2} = 7.2 \times \rho_{u1} = 7.2 \times 10 = 72\,\text{cm}$$

2. $\frac{\rho_2}{\rho_1} = \frac{U_2\rho_{u2}}{U_1\rho_{u1}} = \sqrt{\frac{T_2}{T_1}}, \frac{\rho_2}{\rho_1} = \sqrt{\frac{C_v t_2}{H_2^2}\frac{H_1^2}{C_v t_1}}\frac{\rho_{u2}}{\rho_{u1}} = \sqrt{\frac{t_2}{t_1}}\frac{H_1}{H_2}\frac{\rho_{u2}}{\rho_{u1}}$

$$\frac{\rho_2}{\rho_1} = \sqrt{\frac{t_2}{t_1}}\frac{1}{1.2} \times 7.2 = 6\sqrt{\frac{t_2}{t_1}}$$

$$\frac{\rho_2}{5} = 6\sqrt{\frac{2}{4}}$$

$$\rho_2 = 6\sqrt{\frac{2}{4}} \times 5 = 21.213\,\text{cm}$$

3.11.4 Examples in Lateral Pressures (Sections 3.8 to 3.10)

Example 3.15

A frictionless wall is shown in Figure 3.34. What is the total active earth pressure per meter of wall, by Rankine's theory and Coulomb's theory (with wall friction angle $\phi' = \phi$; use the formulae)?

$$\gamma = 17.3\,\text{kN/m}^3$$

$$\phi = 30^\circ$$

$$c = 0$$

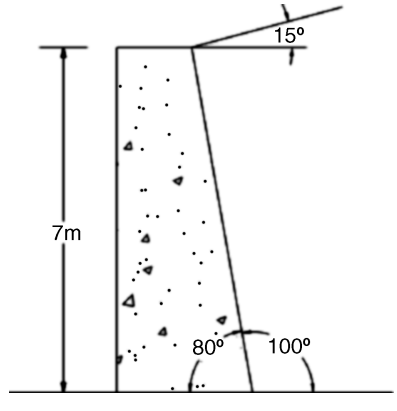

Figure 3.34 Example 3.15.

Solution:

1. By Rankine's theory (Figures 3.35 and 3.36)

$$\gamma = 17.3\,\text{kN/m}^3, c = 0, i = 15^\circ, \phi = 30^\circ$$

$$K_A = \cos i \frac{\cos i - \sqrt{\cos^2 i - \cos^2 \phi}}{\cos i + \sqrt{\cos^2 i - \cos^2 \phi}}$$

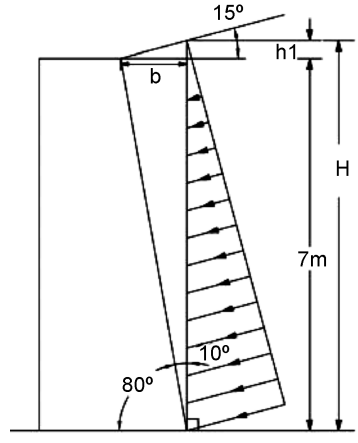

Figure 3.35 Example 3.15.

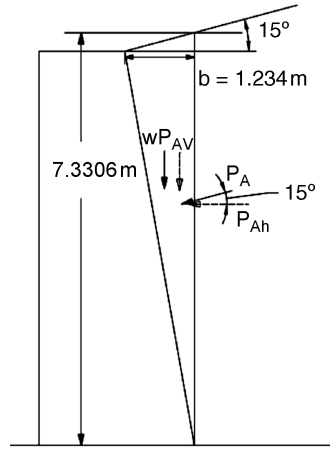

Figure 3.36 Example 3.15.

$$K_A = \cos 15^\circ \frac{\cos 15^\circ - \sqrt{\cos^2 15^\circ - \cos^2 30^\circ}}{\cos 15^\circ + \sqrt{\cos^2 15^\circ - \cos^2 30^\circ}}$$
$$K_A = \cos 15^\circ \frac{0.5381}{1.3937}$$
$$K_A = 0.373$$

$$\frac{b}{7} = \tan 10^\circ, b = 7 \tan 10^\circ = 1.234, \quad \frac{h_1}{b} = \tan 15^\circ, h_1 = 1.234 \tan 15^\circ = 0.3306$$

$$\therefore H = 7 + 0.3306 = 7.3306 \text{ m}$$

$$\text{At H} = 0, p_A = 0$$

$$\text{At H} = 7.3306 \text{ m}, p_A = H\gamma K_A - 2c\sqrt{k_A}$$
$$= (7.3306 \times 17.3 \times 0.373) - 0 = 47.3 \text{ kN/m}^2$$

Total active pressure due to lateral pressure

$$P_A = \frac{1}{2} H p_A = \frac{1}{2} \times 47.3 \times 7.3306 = 173.37 \text{ kN/m}^2$$

$$P_{Ah} = 173.37 \cos 15^\circ = 167.46 \text{ kN/m}^2$$

$$P_{Av} = 173.37 \sin 15^\circ = 44.87 \text{ kN/m}^2$$

Soil weight acting on the wall face

$$W = \frac{1}{2} \times 1.234 \times 7.3306 \times 17.3 = 78.25 \text{ kN/m}$$

$$\therefore \text{Total vertical force} = P_{av} + W$$
$$= 44.87 + 78.25$$
$$= 123.21 \text{ kN/m}^2$$

$$\text{Total horizontal force} = P_{ah} = 167.46 \text{ kN/m}^2$$

$$\therefore \text{Total resultant force} = \sqrt{123.12^2 + 167.46^2}$$
$$= 207.85 \text{ kN/m}$$

2. By Coulomb's solution (Figure 3.37)

$$\gamma = 17.3\,\text{kN/m}^3, H = 7\,\text{m}, \beta = 100^\circ, i = 15^\circ, \phi' = \phi = 30^\circ$$

$$P_A = \frac{1}{2}\gamma H^2 \left[\frac{\csc\beta\sin(\beta-\phi)}{\sqrt{\sin(\beta+\phi')}+\sqrt{\frac{\sin(\phi+\phi')\sin(\phi-i)}{\sin(\beta-i)}}}\right]^2$$

$$= \frac{1}{2}(17.3)(7)^2\left[\frac{\csc(100^\circ)\sin(100^\circ-30^\circ)}{\sqrt{\sin(100^\circ+30^\circ)}+\sqrt{\frac{\sin(30^\circ+30^\circ)\sin(30^\circ-15^\circ)}{\sin(100^\circ-15^\circ)}}}\right]^2$$

$$= \frac{1}{2}(17.3)(7)^2\left[\frac{\csc(100^\circ)\sin(70^\circ)}{\sqrt{\sin(130^\circ)}+\sqrt{\frac{\sin(60^\circ)\sin(15^\circ)}{\sin(85^\circ)}}}\right]^2 = \frac{1}{2}(17.3)(7)^2\left[\frac{0.9543}{0.87523+0.4743}\right]^2$$

$$= 211.94\,\text{kN/m}$$

The direction and point of action of P_A are shown in the Figure 3.37.

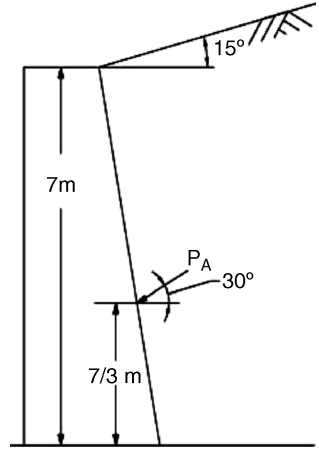

Figure 3.37 Example 3.15.

Example 3.16

Assume this is a frictionless wall (Figure 3.38). Draw the active pressure diagram and determine the total active force after the tensile crack occurs.

$$\gamma = 17.3\,\text{kN/m}^3, \phi = 30^\circ, c = 10\,\text{kN/m}^2$$

Solution:

$$K_A = \frac{1-\sin\phi}{1+\sin\phi} = \frac{1-\sin 30^\circ}{1+\sin 30^\circ} = \frac{1}{3}$$

$$\text{At H} = 0\,\text{m}, \quad p_A = H\gamma K_A - 2c\sqrt{K_A} + qK_A$$

$$p_A = \left(0 \times 17.3 \times \frac{1}{3}\right) - \left(2 \times 10 \times \sqrt{\frac{1}{3}}\right) + \left(15 \times \frac{1}{3}\right) = -6.55\,\text{kN/m}^2$$

$$\text{At H} = 7\,\text{m}, \quad p_A = H\gamma K_A - 2c\sqrt{K_A} + qK_A$$

$$p_A = \left(7 \times 17.3 \times \frac{1}{3}\right) - \left(2 \times 10 \times \sqrt{\frac{1}{3}}\right) + \left(15 \times \frac{1}{3}\right) = 33.82\,\text{kN/m}^2$$

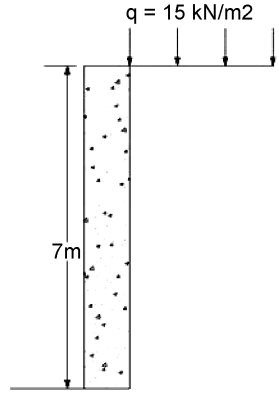

Figure 3.38 Example 3.16.

The active pressure diagram is shown in Figure 3.39

$$\frac{33.82}{7-H_c} = \frac{6.55}{H_c}$$

$$33.82\,H_c = 6.55(7-H_c)$$

$$H_c = \frac{6.55 \times 7}{33.82 + 6.55} = 1.136\,\text{m} = z_c$$

Total active force after tensile crack occurs, $P_A = 5.864 \times 33.82 \times \frac{1}{2} = 99.16\,\text{kN/m}^2$

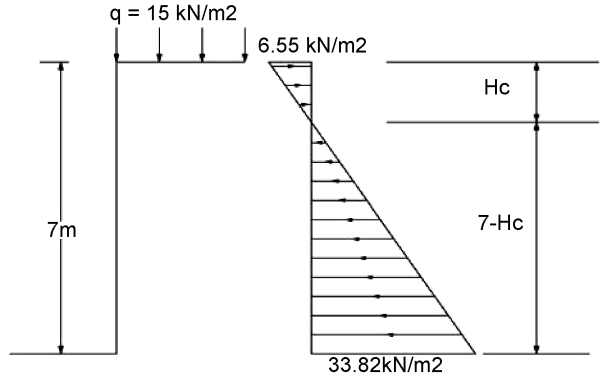

Figure 3.39 Example 3.16.

Example 3.17

A vertical wall 7.5 m high supports a level backfill of clayey sand (Figure 3.40). The samples of the backfill soil were tested, and the following properties were determined:

$$\phi = 20^\circ,\ c = 12.5\,\text{kN/m}^2,\ \gamma = 19.6\,\text{kN/m}^3$$

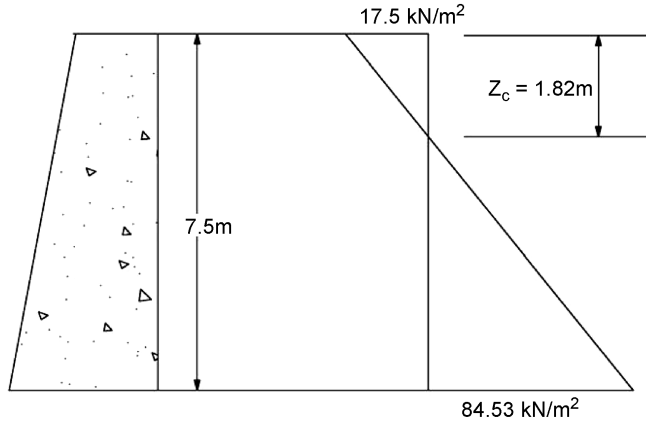

Figure 3.40 Example 3.17.

Draw the active earth pressure diagram, using Rankine theory.

Solution:

$$P_A = \gamma z K_A - 2c\sqrt{K_A}$$

$$P_P = \gamma z K_P + 2c\sqrt{K_P}$$

For $\phi = 20^\circ$

$$K_A = \frac{1-\sin\phi}{1+\sin\phi} = \frac{1-\sin 20^\circ}{1+\sin 20^\circ} = 0.49$$

$$K_P = \frac{1+\sin\phi}{1-\sin\phi} = \frac{1+\sin 20^\circ}{1-\sin 20^\circ} = 2.04$$

$$\text{At } z = 0, \quad p_A = (19.6 \times 0.49 \times 0) - (2 \times 12.5 \times \sqrt{0.49}) = -17.5\ \text{kN/m}^2$$

$$\text{At z} = 7.5\ \text{m}, \quad p_A = (19.6 \times 0.49 \times 7.5) - (2 \times 12.5 \times \sqrt{0.49}) = 54.53\ \text{kN/m}^2$$

$$z_c = \frac{17.5}{19.6 \times 0.49} = 1.82\ \text{m}$$

Example 3.18

A vertical retaining wall 8 m high supports a deposit of sand having a level backfill. Soil properties are as follows

$$\gamma = 18.84\ \text{kN/m}^3, \phi = 35^\circ, c = 0$$

Calculate the total active earth pressure per meter length of wall and point of application, by Rankine's theory and Coulomb's theory taking $\phi' = \phi$ (wall friction angle).

Solution:

1. By Rankine's theory (Figure 3.41)

$$K_A = \frac{1-\sin\phi}{1+\sin\phi} = \frac{1-\sin 35^\circ}{1+\sin 35^\circ} = 0.271$$

$$\text{At H} = 0, \quad p_A = \gamma z K_A - 2c\sqrt{K_A} = (18.84 \times 0 \times 0.271) - 0 = 0$$

$$\text{At H} = 8\ \text{m}, \quad p_A = \gamma z K_A - 2c\sqrt{K_A} = (18.84 \times 8 \times 0.271) - 0 = 40.85\ \text{kN/m}^2$$

$$P_A = \frac{1}{2} \times 40.8 \times 8 = 163.2\ \text{kN/m}$$

Point of application, $\bar{z} = \frac{8}{3} = 2.67\ \text{m}$

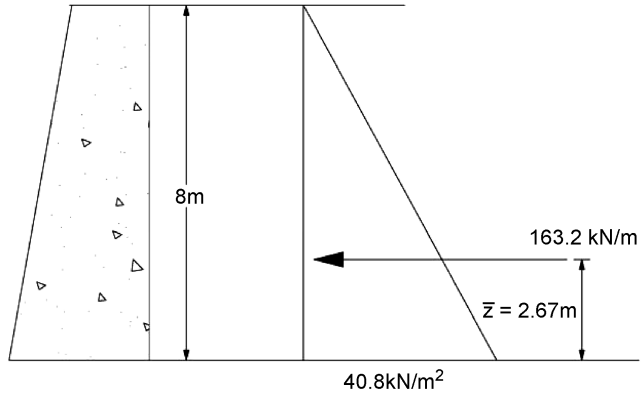

Figure 3.41 Example 3.18.

2. By Coulomb's theory (Figure 3.42)

$$\gamma = 18.84\,\text{kN/m}^3, H = 8\,\text{m}, \beta = 90^\circ, i = 0^\circ, \phi' = \phi = 35^\circ$$

$$P_A = \frac{1}{2}\gamma H^2 \left[\frac{\csc\beta \sin(\beta - \phi)}{\sqrt{\sin(\beta + \phi')} + \sqrt{\dfrac{\sin(\phi + \phi')\sin(\phi - i)}{\sin(\beta - i)}}} \right]^2$$

$$= \frac{1}{2}(18.84)(8)^2 \left[\frac{\csc(90^\circ)\sin(90^\circ - 35^\circ)}{\sqrt{\sin(90^\circ + 35^\circ)} + \sqrt{\dfrac{\sin(35^\circ + 35^\circ)\sin(35^\circ - 0^\circ)}{\sin(90^\circ - 0^\circ)}}} \right]^2$$

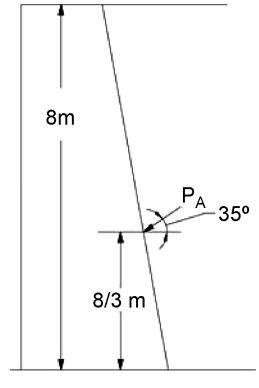

Figure 3.42 Example 3.18.

$$= \frac{1}{2}(18.84)(8)^2 \left[\frac{\csc(90)\sin(55^\circ)}{\sqrt{\sin(125^\circ)} + \sqrt{\frac{\sin(70^\circ)\sin(35^\circ)}{\sin(90^\circ)}}} \right]^2 = \frac{1}{2}(18.84)(8)^2 \left[\frac{0.8192}{0.9051 + 0.7342} \right]^2$$

$$= 150.55\,\text{kN/m}$$

The direction and point of action of P_A in the retaining wall are shown in Figure 3.42.

Example 3.19

Determine the Rankine active pressure, P_A, per unit length of the wall shown in Figure 3.43 and the location of the resultant pressure. The parameters given in Figure 3.43 are

$$H = 6\,\text{m},\ H_1 = 3\,\text{m},\ q = 15\,\text{kN/m}^2,\ \gamma_1 = 15\,\text{kN/m}^3$$

$$\gamma_2 = 18\,\text{kN/m}^3,\ c_1 = 8\,\text{kN/m}^2,\ \phi_1 = 30^\circ$$

$$c_2 = 4\,\text{kN/m}^2, \phi_2 = 36^\circ$$

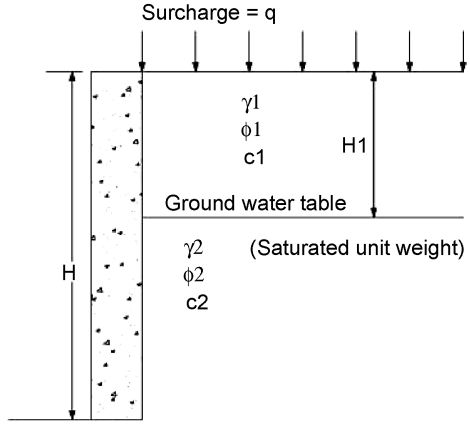

Figure 3.43 Example 3.19.

Solution (Figure 3.44):
Pressure due to soil:

$$\text{For first layer, } K_A = \frac{1-\sin\phi}{1+\sin\phi} = \frac{1-\sin 30^\circ}{1+\sin 30^\circ} = \frac{1}{3}$$

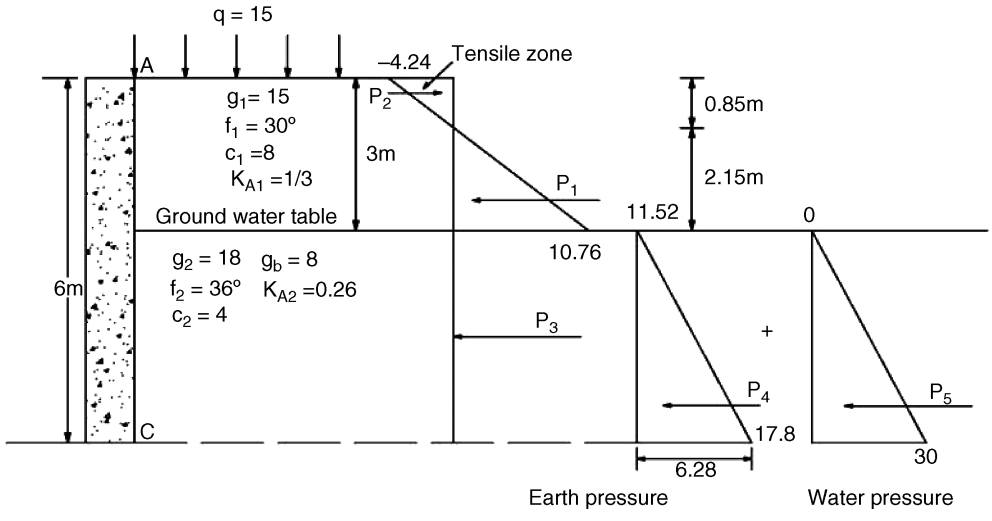

Figure 3.44 Example 3.19.

$$\text{At } H = 0, \qquad p_{A1} = H\gamma K_A - 2c\sqrt{K_A} + qK_A = 0 - (2 \times 8 \times \sqrt{1/3}) + (15 \times 1/3) = -4.24$$

$$\text{At } H = 3\,\text{m}, \qquad p_{A2} = (15 \times 3 \times 1/3) - (2 \times 8 \times \sqrt{1/3}) + (15 \times 1/3) = 10.76\,\text{kN/m}^2$$

$$\text{For second layer, } K_A = \frac{1-\sin\phi}{1+\sin\phi} = \frac{1-\sin 36^\circ}{1+\sin 36^\circ} = 0.26$$

$$\text{At } H = 3\,\text{m}, \qquad p_{A3} = (15 \times 3 \times 0.26) - (2 \times 4 \times \sqrt{0.26}) + (15 \times 0.26) = 11.52\,\text{kN/m}^2$$

$$\text{At } H = 6\,\text{m}, \qquad p_{A4} = [(15 \times 3) + (8 \times 3)] \times 0.26) - (2 \times 4 \times \sqrt{0.26}) + (15 \times 0.26)$$

$$= 17.8\,\text{kN/m}^2$$

Water pressure:

$$\text{At } H = 0, \qquad \text{At } H = 0, \quad p_w = 0$$

$$\text{At } H = 3\,\text{m}, \qquad p_w = 0$$

$$\text{At } H = 6\,\text{m}, \qquad p_w = 3 \times 10 = 30\,\text{kN/m}^2 \text{ (assuming } \gamma_w = 10\,\text{kN/m}^3)$$

$$\text{At critical depth, } z_c, p_{A1} = z_c\gamma K_A - 2c\sqrt{K_A} + qK_A = 0$$

$$z_c \times 15 \times 1/3 - 2 \times 8\sqrt{1/3} + 5 \times 1/3 = 0$$

$$z_c = \frac{2 \times 8\sqrt{1/3} - 15 \times 1/3}{15 \times 1/3} = 0.85\,\text{m}$$

Total Force (kN/m)	Lever arm from C	Moment (kNm/m)
$P_1 = \frac{1}{2} \times -4.24 \times 0.85 = -1.802$	$6 - \frac{0.85}{3} = 5.72$	-10.29
$P_2 = \frac{1}{2} \times 2.15 \times 10.76 = 11.57$	$3 + \frac{2.15}{3} = 3.72$	$+43.04$
$P_3 = 11.52 \times 3 = 34.56$	1.5	$+51.84$
$P_4 = \frac{1}{2} \times 3 \times 6.28 = 9.42$	1	$+9.42$
$P_5 = \frac{1}{2} \times 3 \times 30 = 45$	1	$+45$
$\sum P_A = 98.75$		$\sum M = 139.01$

$$\therefore \bar{z} \text{ above } C = \frac{139.01}{98.75} = 1.41 \text{ m}$$

Thus, the resultant acts at a height of 1.41 m above C.

Exercise Problems

Bearing Capacity

3.1 Compute the bearing capacity per unit area of a continuous footing 2 m wide, supported on a soil for which c = 20 kN/m^2, $\phi = 18°$ and $\gamma = 19$ kN/m^2. The depth of foundation is 2 m. The water table is at depth of 5 m below the ground surface. (Use GSF as well as LSF criteria.)

3.2 Compute the bearing capacity per unit area of a square footing 2×2 m on dense sand ($\phi = 35°$), if the depth of foundation is 1, 2 and 5 m respectively. The unit weight of the soil is 18 kN/m^2. (Use GSF as well as LSF criteria.)

3.3 A load test was made on a square bearing plate 0.3×0.3 m on the surface of a cohensionless deposit of sand having a unit weight of 17 kN/m^3. The load–settlement curve approaches a vertical tangent at a load of 18 kN. What is the value of ϕ for the sand? (Use the GSF criterion.)

3.4 A load test was made on a square plate 0.3×0.3 m on dense cohesionless sand having a unit weight of 18 kN/m^3. The bearing plate was enclosed in a box surrounded by a surcharge 0.6 m deep. Failure occurred at a load of 58 kN. What would be the failure load per unit area of the base of a square footing 2×2 m located with its base at the same depth in the same material? (Use the GSF as well as LSF criteria.)

3.5 A structure was built on a square mat foundation 30×30 m. The mat rested at the ground surface on a stratum of uniform clay which extended to a depth of 60 m. If failure occurred at a UDL of 300 kN/m^2, what was the average value of cohesion for the clay? (Use Tezaghi's charts as well as Meyerhof's charts and GSF criterion.)

3.6 (Redo problem 3.1.) Load is inclined at an angle of 15° with vertical and GWL is at a depth of 3 m below GL. $\gamma_{sub} = 10\,\text{kN/m}^3$ (Use GSF.)

3.7 (Redo problem 3.2.) $D_f = 3\,\text{m}$, depth of GWL = 2 m, inclination of the load with vertical = 10°, $\gamma_{sub} = 11\,\text{kN/m}^3$.

3.8 (Redo problem 3.3.) Depth of GWL = 4 m, surcharge on the ground surface $q_s = 30\,\text{kN/m}^2$, $\gamma_{sub} = 10.5\,\text{kN/m}^3$.

3.9 (Redo problem 3.4.) Inclination of the load on a 1.5 m square footing is 20° to the vertical, $\gamma_{sub} = 11.5\,\text{kN/m}^3$.

3.10 (Redo problem 3.5.) Depth of GWL = 10 m. Inclination of the load is 15° with vertical. $\gamma_{sub} = 12\,\text{kN/m}^3$.

Stress Distribution in Soils

3.11 A concentrated load of 1500 kN is applied to the ground surface. What is the vertical stress increment due to the load at a point 5 m below the ground surface at a horizontal distance of 3 m from the line of the concentrated load?

3.12 Soil with a unit weight of $18\,\text{kN/m}^3$ is loaded on the ground surface by a UDL of $350\,\text{kN/m}^2$ over a circular area 3 m in diameter. Determine:

a. the vertical stress increment due to the uniform load, at a depth of 4 m under the edge of the circular area
b. the total vertical pressure.

3.13 A 3 m by 4 m rectangular area carrying a uniform load of $300\,\text{kN/m}^2$ is applied to the ground surface. What is the vertical stress increment due to the uniform load at a depth of 4 m below the corner of the rectangular loaded area?

3.14 The L-shaped area shown in Figure 3.45 carries a $200\,\text{kN/m}^2$ uniform load. Find the vertical stress increment due to the load at a depth of 8 m below the following points: (a) below corner A, (b) below corner E, (c) below point G and (d) below point H.

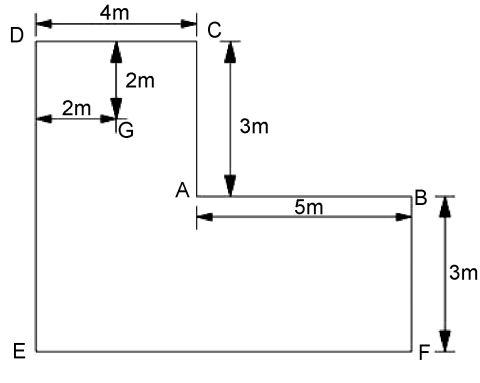

Figure 3.45 Problem 3.14.

3.15 Draw Newmark's circular influence chart with z = unit lengths = 1.0, 1.25, 1.5, 1.75, 2.0 cm.

3.16 Using the circular influence chart find the vertical stress σ_z at point A (4 m directly below the CG of the footing), due to a rectangular footing of 8×6 m on the surface supporting a total load of 1000 kN.

3.17 Check this result with the result obtained by Steinbrenner's chart, Newmark's rectangular chart and also by analytical expressions given by Newmark.

Settlement Analysis

3.18 A compressible clay layer 12 m thick has an initial void ratio (*in situ*) of 1.04. Test and computations show that the final void ratio of the clay layer after construction of a structure is 0.978. Determine the estimated primary consolidation settlement of the structure.

3.19 A foundation is to be constructed at a site where the soil profile is as shown in Figure 3.46. The base of the foundation, which is 3 m square, exerts a total load (weight of structure, foundation, and soil surcharge on the foundation) of 1200 kN. The initial void ratio *in situ* of the compressible clay layer is 1.058, and its compression index is 0.65. Find the estimated primary consolidation settlement for the clay layer.

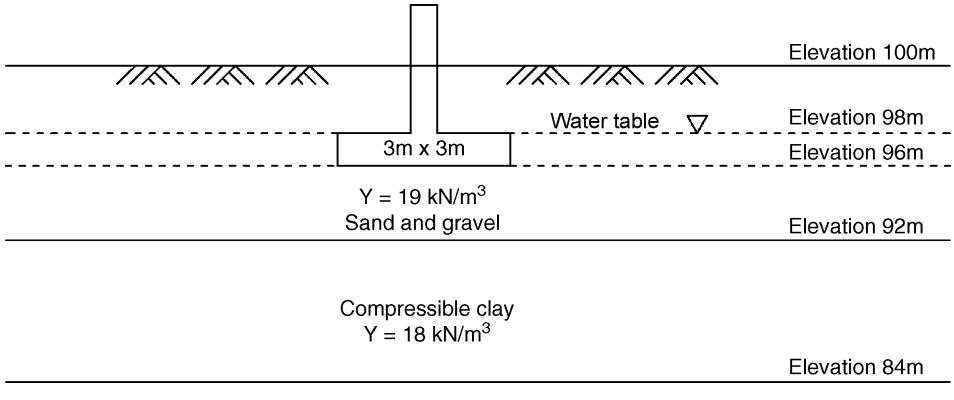

Figure 3.46 Problem 3.19.

3.20 In problem 3.19, tests and computations indicate that the coefficient of consolidation is 6.08×10^{-7} m^2/kN. Compute the time required for 90% of the expected primary consolidation settlement to take place if the clay layer is underlain by:

a. permeable sand and gravel
b. impermeable bedrock.

Lateral Pressures

3.21 What is the total active earth pressure per meter of the retaining wall in Figure 3.47 Angle of wall friction between backfill and wall is 25°. Use Coulomb's theory as well as Rankine's theory.

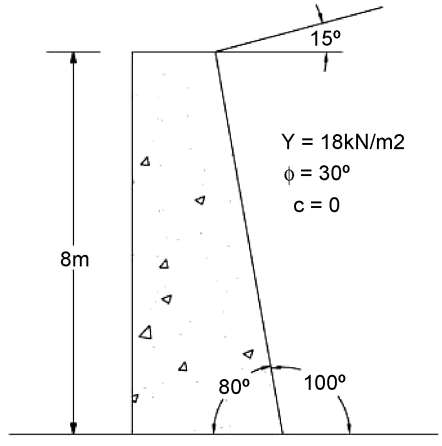

Figure 3.47 Problem 3.21.

3.22 A vertical wall 7.0 m high supports a cohesionless backfill with a horizontal surface. The backfill soil's unit weight and angle of internal friction are 17 kN/m^3 and 31°, respectively and the angle of wall friction between backfill and wall is 15°. Using trial wedges, find the total active earth pressure against the wall.

3.23 A smooth, vertical wall is 9.5 m high and retains a cohesionless soil with $\gamma = 19$ kN/m^3 and $\phi = 20°$. The top of the soil is level with the top of the wall, and the soil surface carries a UDL of 25 kN/m^2. Calculate the total active earth pressure on the wall per unit length, and determine its point of application, by Rankine's theory as well as by Coulomb's theory.

3.24 Solve problem 3.21 by Rebhann's graphical solution.

3.25 Solve problem 3.21 by Culmann's graphical solution.

3.26 Find passive pressure in problem 3.21.

3.27 Find passive pressure in problem 3.22.

3.28 Find passive pressure in problem 3.23.

4

Rational Design of Shallow Foundations

4.1 Introduction

Every engineering structure, whether it is a building, bridge, highway pavement or railway track, consists of a superstructure (above ground) and a foundation (below ground; Figure 4.1). The function of the foundation is to transmit the load from the superstructure to the soil or rock below as the case may be. A proper foundation design has to ensure that no component of either the superstructure or the foundation experiences distress of any kind in the above process of load transmission. A description of shallow foundations (also referred to as footings) is given in Section 4.2.

The conventional method of design of a footing is to assume the footing as rigid and the distribution of contact pressure at the surface of contact between the base of a foundation and the supporting soil as planar, that is, uniform or uniformly varying depending upon whether the foundation supports symmetric or eccentric loading. This assumption of planar contact pressure distribution is far from reality and therefore, to be realistic in design, the flexibility of the footing and the soil type (which together give rise to variable contact pressure distribution) should be considered (Kurian, 1992).

Due to vast growth in computing power and due to the hurdles posed by classical solutions, numerical methods (finite differences, finite element, etc.) have come to the aid of the foundation designer in the form of easy to use packages to incorporate this flexibility into the footing design.

The foundation system comprises of two components: (i) the structural part of foundation such as the footing or pile and (ii) the natural foundation, meant to indicate the soil. Similarly the design of foundation system consists of two phases. These are referred to as: (i) geotechnical (GT) design and (ii) structural design. The aim of GT design essentially is to arrive at the plan dimensions of the foundation, satisfying the *soil design parameters*, viz *bearing capacity* and *settlement*. The structural design is taken up only after its GT design is completed, which determines the footing thickness and also the quantum and location of reinforcement. However the design has to be carried out as per *local codes* of practice.

Foundation Design: Theory and Practice N. S. V. Kameswara Rao
 ISBN: 978-0-470-82534-1

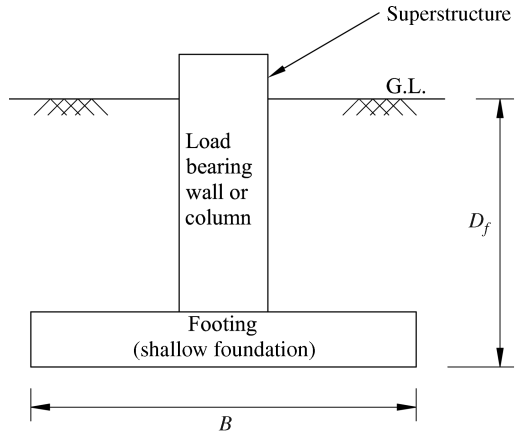

Figure 4.1 Shallow foundation (D_f/B O 1).

4.2 Shallow Foundations

Foundation structures are customarily divided into *shallow* or *deep* on the basis of their depth in relation to their width, the typical divide being the unit value for the ratio (D_f/B; Figure 4.1), that is, $D_f B \leq 1$ for shallow foundations and $D_f B > 1$ for deep foundations.

The real difference between shallow and deep foundations is based on the structural response as well as the depth to which the foundation is taken. Thus bending (flexure) is the predominant structural action in the case of shallow foundations. The behavior of deep foundations could result in axial and lateral loads besides bending moments and torsional moments. The deep foundation–soil interaction needs a detailed analysis. Shallow foundations or footings can be of several types (see Figure 4.2) and can be classified further as:

1. **Continuous (or Strip Footings)**
   These footings are primarily used for load bearing walls and are generally of rectangular cross sections.
2. **Independent (Isolated or Spread) Footings**
   These footings are generally used for individual columns and can be rectangular or trapezoidal, square or circular in shape.
3. **Strap Footings**
   These footings support more than one column or wall.
4. **Combined Footings**
   These types of footings are used for two or more columns in one row. These are generally rectangular, trapezoidal or cantilever type with two interconnected footings.
5. **Mat Foundations**
   These foundations support two-dimensional arrays (regular or irregular) of columns.

Rafts are generally used for two or more columns in several rows. These can be rectangular, square, circular, annular or octagonal in shape. Rafts also may have to be used if the allowable design soil (contact) pressure is very low.

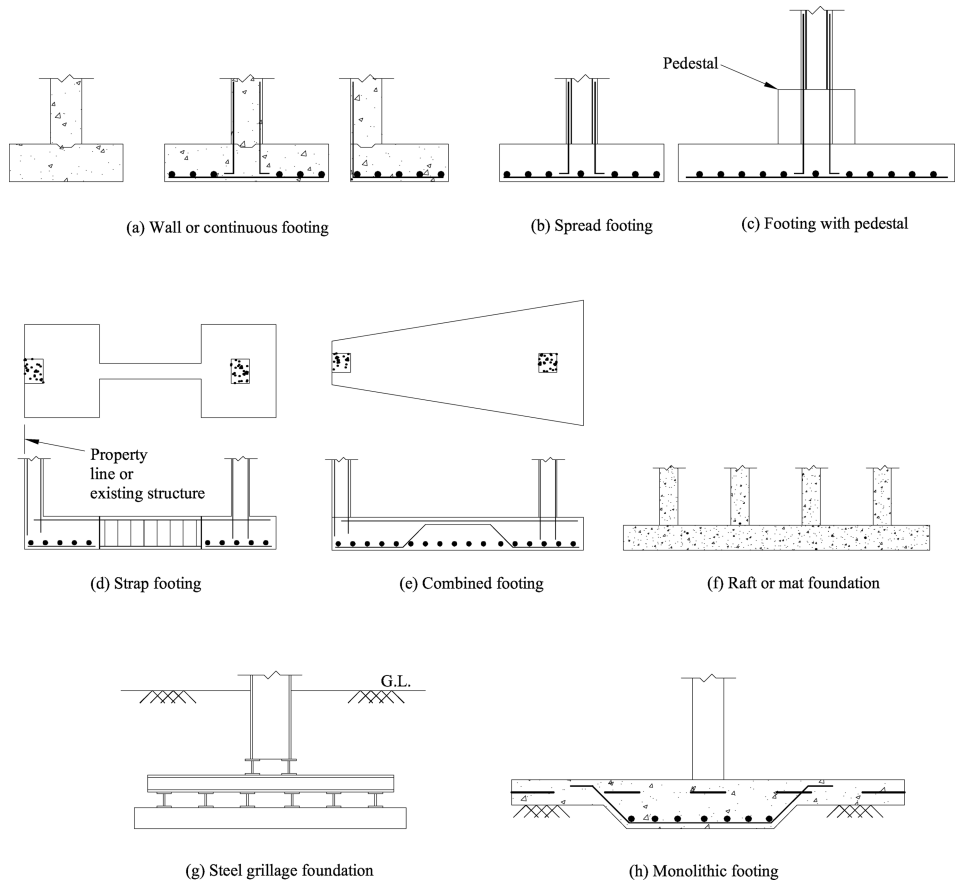

Figure 4.2 Common types of shallow foundations.

4.3 Conventional Design and Rational Design

In the conventional design of footings, the soil pressure is assumed to be uniform or linearly varying depending upon whether the foundation supports symmetric or eccentric loading. (Figure 4.3)

However the actual contact pressure distribution, which is the result of the soil foundation interaction, can be far from the assumed uniform or linear distribution. The contact pressure distribution for flexible footing could be uniform for both clay and sand. The contact pressure for rigid footings is maximum at the edges in clay and for rigid footings on sand, it is minimum at the edges. The typical distributions of immediate settlement and contact pressure for flexible and rigid footings are shown in Figure 4.4.

Hence the assumption of uniform pressure distribution results in a slightly unsafe design for rigid footings on clays as the maximum bending moment at the center is underestimated. It will give a conservative design for rigid footings on sandy soils, as the maximum bending moment is

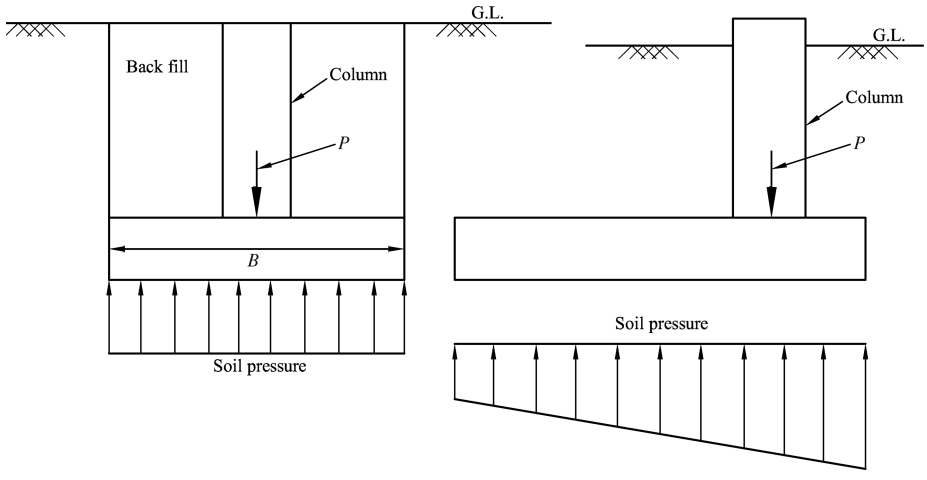

Figure 4.3 Soil contact pressures in conventional design.

overestimated. Similarly the actual bending moments and shear forces in flexible footings could be at considerable variance with the design values obtained with the assumption of uniform contact pressure distribution.

Hence the necessity for developing effective and safe design for foundations based on realistic distribution of soil pressure, obtained by a rational interaction analysis, known as *flexible* or *elastic* designs, arises from the above drawbacks (Kameswara Rao, 1969, 1971; Kurian, 1992).

4.4 Procedures for the Design of Footings

Footings may be designed as outlined below:

1. Calculate the loads applied at top of footings. Two types of loads are necessary, one for bearing capacity determination and the other for settlement analysis (Chapter 3).
2. Sketch a soil profile or soil profiles showing the soil stratification at the site. Draw an outline of the proposed foundation on the soil profile of the site (Chapter 2).
3. Mark the maximum water level from the borehole data (Chapter 2).
4. Determine minimum depth of footings (Section 4.4.1).
5. Determine the bearing capacity of supporting stratum (Chapter 3).
6. Proportion the footing sizes (Section 4.4.2).
7. Check for danger of overstressing the soil strata at greater depths (Section 4.4.3).
8. Predict the total and differential settlements (Section 4.4.4).
9. Check stability due to eccentric loading (Section 4.4.5).
10. Check uplift on individual footings and basement slabs, footings on slopes (Section 4.4.8).
11. Design the footings (Section 4.5, Chapters 5, 8, 12).
12. Check for foundation drains, waterproofing or damp proofing (Teng, 1964; Bowles, 1996; Tomlinson, 2001).

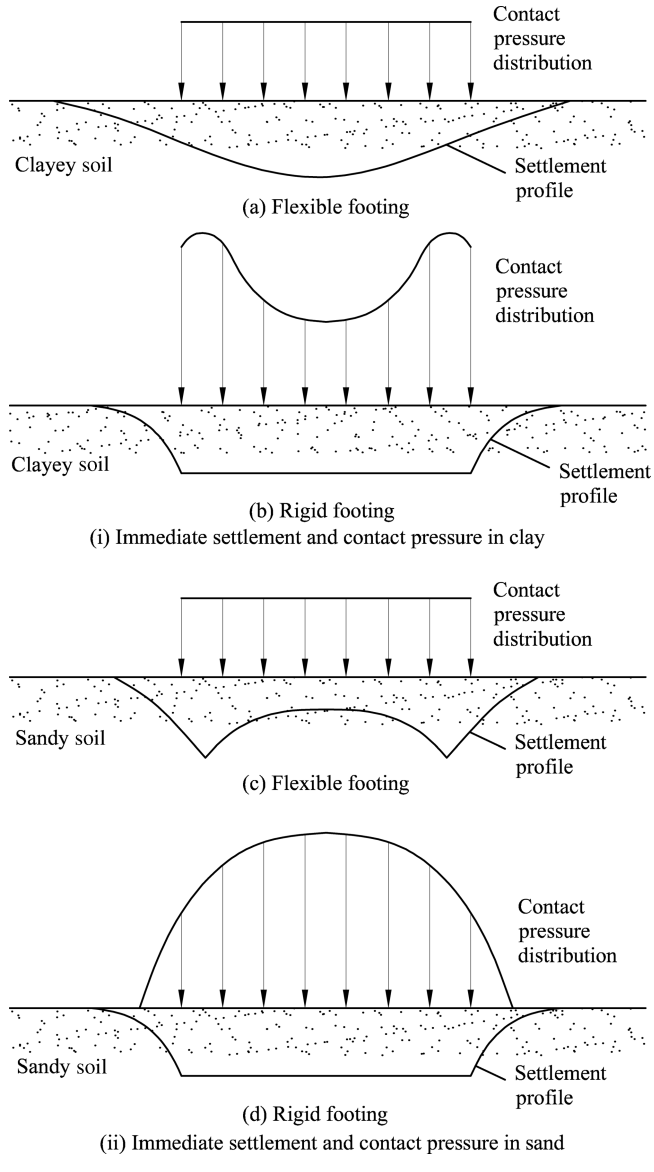

Figure 4.4 Typical distribution of immediate settlements and contact pressures in soils.

4.4.1 Depth of Footings

1. Footings should be carried below the top (organic) soil, miscellaneous fills, or weak soil. If the top soil is too deep, alternatives may be used as shown in Figures 4.5(a) and (b).
2. Footings should be carried below the depth of frost penetration. In heated buildings, the interior footings are not affected by frost, therefore they may be as high as other

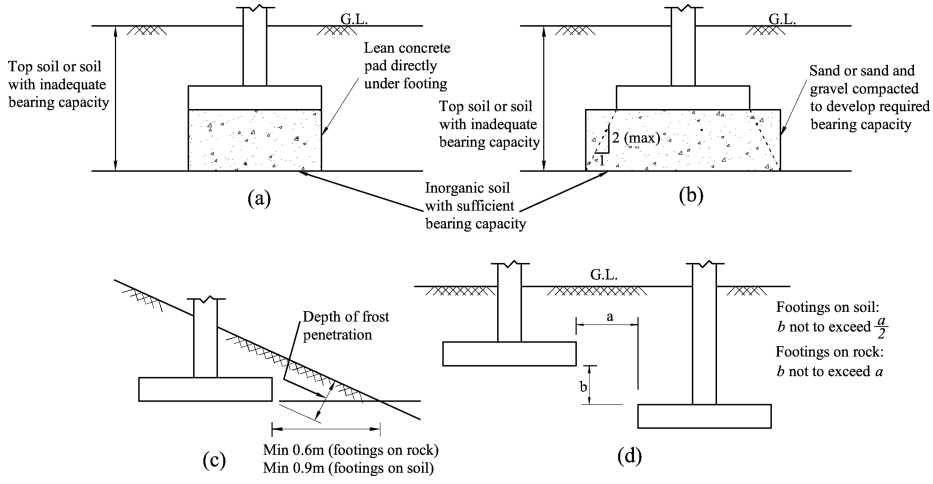

Figure 4.5 Guidelines for minimum depth of footings.

requirements permit. The minimum depths of footings are generally stipulated in the local building codes or national codes. The damage of footings and of the superstructure, due to frost action is caused by the volume expansion and contraction of water in the soil at freezing temperatures. Gravel and coarse sand above water level containing less than 3% silt, fine sand or clay particles cannot hold any water and consequently are not subject to frost damage. Other soils are subjected to frost heave within the depth of frost penetration.

3. Usually footings are not to be on the ground surface even in localities where freezing temperatures do not occur because of the possibility of surface erosion. The minimum depth of footings is usually taken as 0.5 m for one- and two-storey buildings and stores and 0.8 m for heavier constructions.
4. Footings on sloping ground should have sufficient edge distance (min. 0.6–0.9 m) as protection against erosion (Figure 4.5(c)).
5. The difference in footing elevations should not be so great as to introduce undesirable overlapping of stresses in soil. This is generally avoided by maintaining the maximum difference in elevation equal to or equal to one-half of the clear distance between two footings as shown in Figure 4.5(d). This requirement is also necessary to prevent disturbance of soil under the higher footing due to the excavation for lower footing.

4.4.2 Proportioning the Size of the Footing

Footing sizes based on allowable bearing pressures are usually satisfactory provided that a settlement analysis is made. However, the footing sizes have to be revised if the analysis indicates excessive settlement. Some designers try to minimize the differential settlement due to varying live loads by proportioning the footings such that all footings will have the same average bearing pressure under the service load. The service load is the actual load expected to act on the foundation during the normal service of the structure. In ordinary buildings, it may be

taken as dead load plus one half live loads. A larger percentage of live load should be used in warehouses and other storage type floors. This procedure is outlined below.

Let

L_{l+d} = live load + dead load for the column which has the largest live load/dead load ratio.
L_s = service load for the same column
q_a = allowable bearing pressure as determined by the principles discussed in Chapter 3.
q_d = design pressure for all footings except this one with largest live load/dead load ratio.

Then

A = area of footing supporting the column with the largest live load/dead load ratio.

$$= \frac{L_{l+d}}{q_a} \tag{4.1}$$

$$q_d = \frac{L_s}{A} \tag{4.2}$$

$$\text{Area of other footings} = \frac{\text{Service Load}}{q_d} \tag{4.3}$$

4.4.3 *Stress on Lower Strata*

1. To safeguard against overstressing soil strata at greater depths, the following methods can be used to calculate the stress at any desired depth below ground level (GL). The pressure under a footing may be assumed to spread out on a slope of 2 vertical to 1 horizontal. Thus, a load Q acting concentrically on a footing area of B × L is assumed to be distributed over an area of (B + Z) (L + Z) at a depth Z below the footing, as shown in Figure 4.6. If any stratum of soil cannot sustain this spread-out pressure, the design bearing pressure should be reduced. However, for a two layer system of clays, the procedure described in Teng (1964) gives more reliable results.
2. For settlement analysis, the above approximation may not be sufficient, and a more accurate approach based on elastic theory using Boussinesq's solution has to be used (Harr, 1966).

This gives the vertical normal stress due to a concentrated vertical load acting on the surface of semi-infinite elastic half-space (Figure 3.12) as given below.

$$\sigma_z = \frac{3Pz^3}{2\pi R^5} \tag{4.4}$$

where

σ_z = vertical stress at any point, A with coordinates x, y, z with reference to the point of application of surface load, that is, O which is the origin.
P = concentrated vertical surface load at point O (origin).
z = vertical depth of point A below the surface.

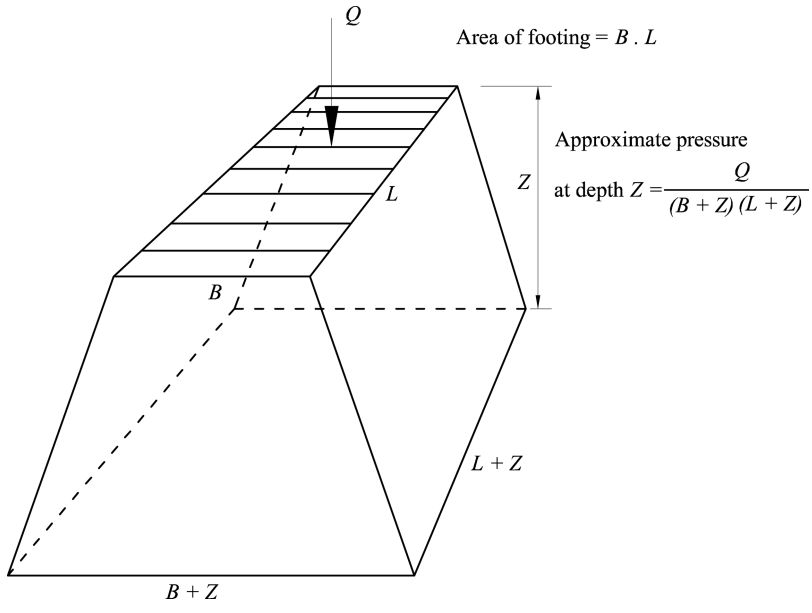

Figure 4.6 Approximate distribution of vertical pressure with depth.

x, y = coordinates along x and y (horizontal axes) of the point with reference to the point of application of load (with respect to O).

$R = \sqrt{x^2 + y^2 + z^2} = \sqrt{r^2 + z^2}$

$r = \sqrt{x^2 + y^2}$ radial distance (in plan) that is, from O to A in plan.

Based on the Boussinesq's solution, the vertical stresses due to footing of any shape and size can be computed using integration or Newmark's influence charts (Harr, 1966; Teng, 1964). The concept of pressure bulb can also be used to find the vertical pressure at any point below the surface of the soil (Chapter 10). Further details for the evaluation of stresses are discussed in Chapters 3 and 9.

4.4.4 Settlement of Footings

Footings on granular soils may not have detrimental settlement if the smaller values of the two allowable pressures (safe bearing capacity, SBC and allowable soil pressure, ASP) discussed in Chapter 3 are used. Footings on stiff clay, hard clay, and other firm soils generally require no settlement analysis if the design provides a minimum factor of safety of 3. Soft clay, compressible silt, and other weak soils will settle even under moderate pressure, and therefore settlement analysis is necessary.

The total settlement of a footing on clay may be considered to consist of three parts (Teng, 1964):

$$S = S_i + S_c + S_s \tag{4.5}$$

where

S = total settlement
S_i = immediate elastic settlement
S_c = settlement due to primary consolidation of clay
S_s = settlement due to secondary consolidation of clay

1. Immediate settlement, S_i
   Soon after the application of load on the footing, elastic compression of the underlying soil takes place causing an immediate settlement of the footing. This is also called elastic settlement and can be computed by elastic theory (Scott, 1963, Harr, 1966). However, it is usually very small and can be neglected for all practical purposes. Further details are given in Chapter 3.
2. Settlement due to primary consolidation, S_c
   The settlement caused by consolidation is due to the slow migration of water from the pores of the clay. The amount of final consolidation settlement s_o can be calculated by the following equation:

$$s_o = S_c \beta \tag{4.6}$$

   where

β = the coefficient depending on the geometry of the footing and the loading history of the clay. Values of β (given by Skempton and Bjerrum, 1957) are shown in Figure 4.7
S_c = settlement calculated by Terzaghi's theory of consolidation

$$= m_v \Delta p \, H \tag{4.7}$$

$$= \frac{C_c}{1 + e} H \log_{10} \frac{p_0 + \Delta p}{p_0} \tag{4.8}$$

where

m_v = coefficient of volume compressibility of the clay. This value is determined by consolidation test.
$= \frac{a_v}{1 + e}$
a_v = coefficient of compressibility.
e = initial void ratio of the soil at the middle of the compressible layer.
Δp = mean vertical stress at the middle of the compressible layer due to load on footing.
H = total thickness of the compressible layer. For thick layers of clay, thickness should be divided into several layers for better accuracy.
C_c = compression index, also determined by consolidation test.
p_0 = initial vertical effective pressure due to soil overburden at the middle of the compressible layer.

   The computation of settlement due to consolidation is illustrated in Chapter 3. along with all the details. Terzaghi's consolidation theory is explained in Chapter 2.
3. Settlement due to secondary consolidation S_c
   When an undisturbed soil sample is tested in the consolidometer (or odometer) the rate of volume decrease/settlement checks very closely with the theory. However, even after one

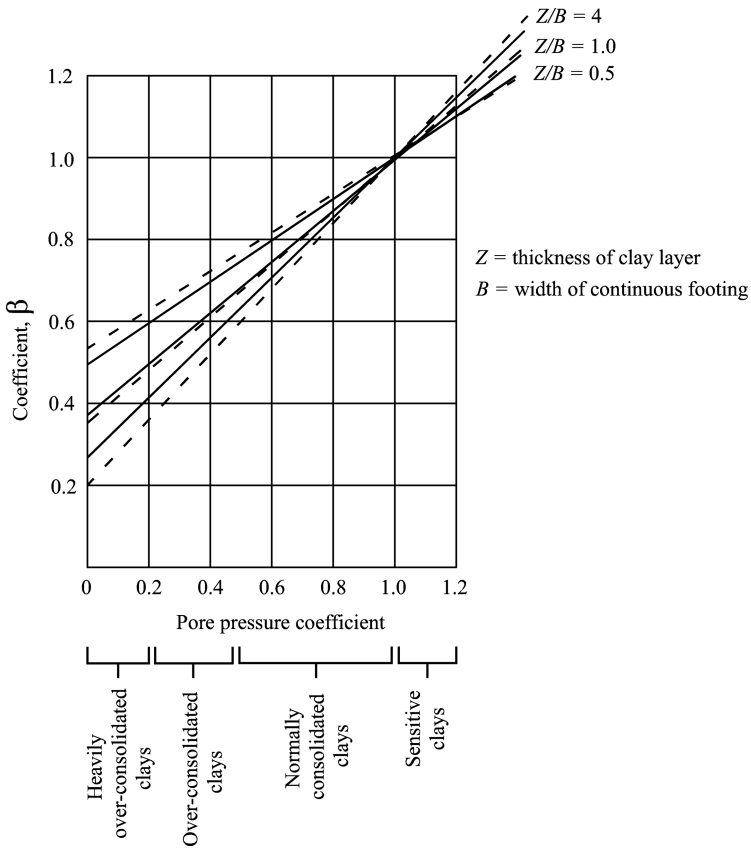

Figure 4.7 Coefficient β. (Reproduced from A.W. Skempton and L. Bjerrum, "A contribution to the settlement analysis of foundations on clay," *Géotechnique*, vol. **7**, no. 4, p. 168, © 1957, with permission from The Institution of Civil Engineers (ICE), Thomas Telford Ltd.)

hundred percent consolidation (according to the theory of consolidation), the settlement does not stop according to theory but continues to increase though at a reduced and rather constant rate. The amount of consolidation that can be computed by the consolidation theory is called primary consolidation; whereas the slow consolidation that takes place afterwards is called secondary consolidation (Chapters 2 and 3).

4.4.5 Design Considerations for Eccentric Loading

A load may become eccentric if applied off-center on the footing or if a concentric load plus a bending moment or horizontal load is applied on the column/superstructure (Figure 4.8). For the purpose of determining the pressure under the footing the moment may be removed/replaced by shifting the vertical load to a fictitious location with an eccentricity e = moment/vertical load. In the analysis of an eccentrically loaded footing, following aspects have to be considered.

1. For the purpose of conventional structural design, the pressure against the bottom of the footing, that is, contact pressure, is assumed to have a planar distribution. When the load is applied within the kern of the footing area, common flexural formulae are applicable.

$$q = \frac{Q}{A} \pm \frac{M_x}{I_x} y + \frac{M_y}{I_y} x \tag{4.9}$$

where
q = contact pressure at a given point (x, y);
Q = vertical load
A = area of footing = $L \times B$
(where L = Length of the footing and B = Breadth of the footing)
x and y = coordinates of point (at which contact pressure is calculated) with respect to the C.G of contact area.
M_x, M_y = Moments about x and y axes respectively (i.e., $M_x = Qe_y$, $M_y = Qe_x$)
e_x, e_y = eccentricities of the load along x and y axes respectively.
I_x,I_y = moments of inertia of footing area about the x and y axes respectively.

Equation (4.9) is applicable for any of the following conditions:

a. The footing is symmetrical about x and y axes.
b. The footing is symmetrical about x axis and $e_y = 0$
c. The footing is symmetrical about y axis and $e_x = 0$.

For rectangular footings, Equation (4.9) may be written in a simpler form:

$$q = \frac{Q}{A}\left(1 \pm 6\frac{e_l}{L} \pm 6\frac{e_b}{B}\right) \tag{4.10}$$

where e_l and e_b are the eccentricities of the resultant load along the length (L) and breadth (B) of the footing respectively.

When e_x, e_y or e_b, e_l exceed certain limits, Equations (4.9) and (4.10) give a negative value of q which indicates tension between the soil and bottom of footing. Unless the footing is weighed down by surcharge loads, the soil cannot be relied upon for bonding to the footing and offering tensile resistance. Therefore, the formulae given by Equations (4.9) and (4.10) are applicable only when the load is applied within a limited area which is known as the kern and is shown shaded in Figure 4.8(a). The procedure for determination of soil pressure when the load is applied outside the kern is simple in principle but laborious. Cases for rectangular and circular footings have been worked out and the kerns are shown by shaded areas in Figures 4.8(a) and (b). For footings of other shapes, the graphical method of successive trials is the simplest for practical solutions as given in Teng (1964).

The graphical method, similar to any other method, is based on the assumption that the pressure varies linearly with the distance to the neutral axis from zero at the neutral axis to a maximum at the most remote point and on the requirement of statical equilibrium that the resultant of the soil pressure should lie on the line of action of the applied load Q. The procedure is described in Teng (1964).

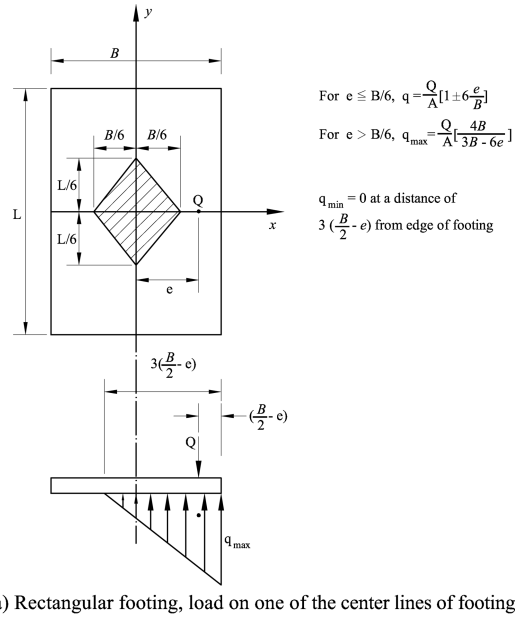

(a) Rectangular footing, load on one of the center lines of footing

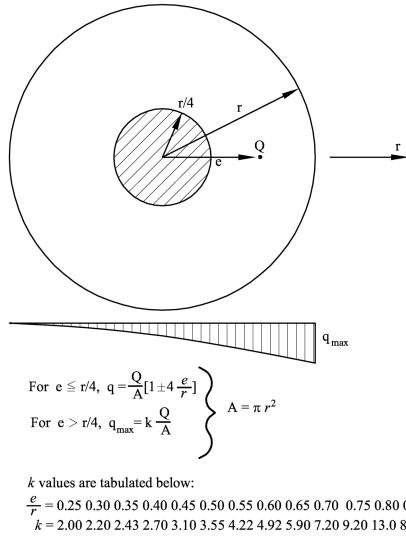

k values are tabulated below:

$\frac{e}{r}$	0.25	0.30	0.35	0.40	0.45	0.50	0.55	0.60	0.65	0.70	0.75	0.80	0.90
k	2.00	2.20	2.43	2.70	3.10	3.55	4.22	4.92	5.90	7.20	9.20	13.0	80.0

(b) Circular footing

Figure 4.8 Contact pressure distribution for eccentrically loaded footings.

For a rational/elastic/flexible design the contact pressure has to be computed from the soil structure interaction analysis using beams or plates on elastic foundation approach (Section 4.7 and Chapter 5).

2. For determination of ultimate or allowable bearing capacity of an eccentrically loaded footing, the concept of useful width is also used. By this concept, the portion of the footing

which is symmetrical about the load is considered useful and the other portion is simply assumed superfluous for the convenience of computation. If the eccentricities are e_l and e_b, as shown in Figure 4.9, the useful widths are $B - 2e_b$ and $L - 2e_l$. The equivalent area $(B - 2e_b)$ $(L - 2e_l)$ is considered as subjected to a central load for determination of bearing capacity.

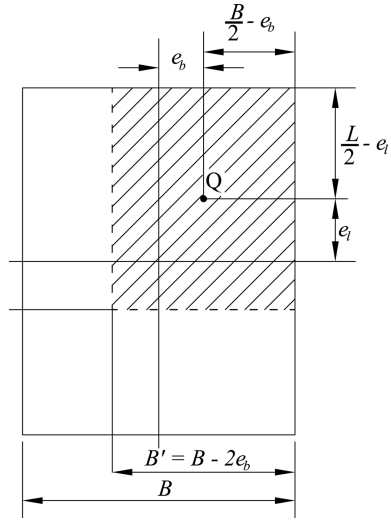

Figure 4.9 Useful widths.

The above concept simply means that the bearing capacity of a footing decreases linearly with eccentricity of load as is shown by a straight line in Figure 4.10 (AREA, 1958). In cohesive soils, this linear relationship fails, but in granular soils, however, the reduction is parabolic rather than linear (Meyerhof, 1953). Therefore the reduction factor shown in Figure 4.10 should be used for design purposes: The bearing capacity of the footing is first determined on the basis that the load is applied at the centroid of the footing. Then this bearing capacity is corrected by multiplying with the factor shown in Figure 4.10.

4.4.6 Inclined Loads

Footings may be subjected to inclined loads due to vertical and horizontal loads transmitted by the superstructure or inclined columns such as in transmission towers. The conventional method of stability analysis of footings subjected to inclined loads is as follows: the inclined load Q is resolved into a vertical component Q_V and horizontal component Q_H. The stability of the footing against ultimate failure under the vertical load is treated by the same principles for footings subjected to vertical load only, and the effect of horizontal component is ignored. Then, the stability of footing against the horizontal force is analyzed by calculating the factor of safety against sliding which is defined as the ratio between the total horizontal resistance and the horizontal force. The total horizontal resistance in

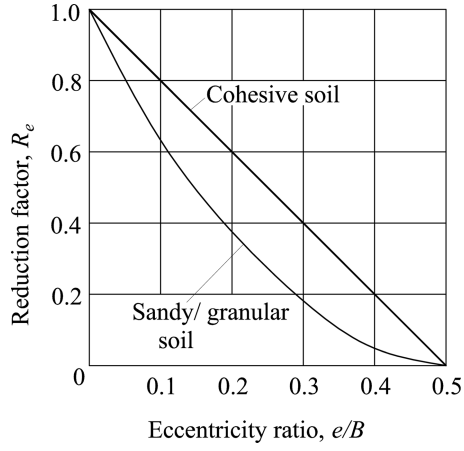

Figure 4.10 Bearing capacity of eccentric footings. (Reproduced from American Railway Engineering Association (AREA), *Manual of Recommended Practice*, Chicago Construction and Maintenance Section, Engineering Division, © 1958, with permission from The American Railway Engineering and Maintenance-of-Way Association (AREMA).)

general consists of a passive resistance of soil, P_p, and a frictional resistance R (Figure 4.11). The value of P_p can be determined by the principles of lateral earth pressure discussed in Chapter 3.

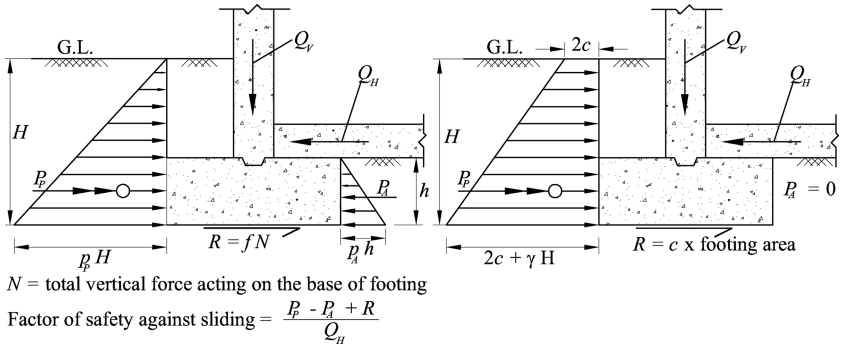

Figure 4.11 Footings subjected to inclined loads.

However for minor projects, conservative values such as those given in Table 4.1 may be used. It should be emphasized that high values of passive earth pressure P_p may not be realized for granular soils unless the backfill is well compacted in layers.

The bearing capacity theory has also been extended to the case of inclined loads (Meyerhof, 1953; Janbu, 1957). Janbu's analysis is based on Terzaghi's theory with the addition of a factor N_h to the Terzaghi's bearing capacity factors N_c, N_q. and N_γ (given in

Table 4.1 Conservative pressure values and parameters for granular and cohesive soils.

Type of granular soil	P_p psf submerged	P_p psf dry or moist	Coefficient of friction, f
Sand and/or gravel with <5% silt	210	350	0.55
Sand and/or gravel with 5% or more silt	180	250	0.45
Silt or soils containing more than 30% silt	120	150	0.35
Type of cohesive soil	**Cohesive strength c = psf**		**Unit weight, γ pcf**
Very soft clay	200		110
Soft clay	400		120
Medium stiff and hard clay	600		125

Chapter 3) and is expressed below.

$$\frac{Q + N_h Q_h}{A} = N_c c + N_q \gamma D + \frac{1}{2} N_\gamma \gamma B \tag{4.11}$$

where

Q = inclined load
Q_h = horizontal component of Q
Q_v = vertical component of Q as shown in Figures 4.12 and 4.13.

The notations and values of N_c, N_q, N_γ and N_h (Janbu, 1957) are shown in Figure 4.12.

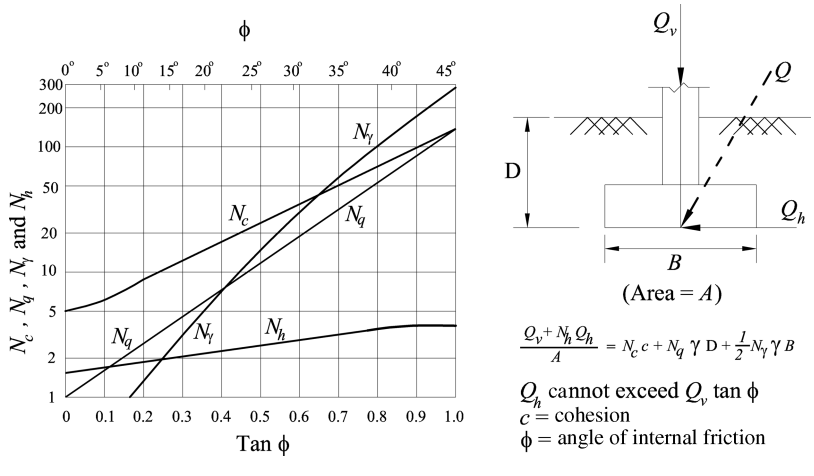

Figure 4.12 Bearing capacity of continuous footings subjected to inclined loads. (Reproduced from *Proceedings of the 4th International Conference on Soil Mechanics and Foundation Engineering*, vol. **2**, N. Janbu, "Earth pressure and bearing capacity calculations by generalized procedure of slices," pp. 207–213, August 12–24, © 1957, London, England, with permission from Elsevier.)

Meyerhof (1953) has calculated ultimate bearing capacity of footings subjected to inclined loads as given in Figure 4.13. The load is assumed to be acting vertically and the bearing capacity is determined by the normal procedure. Then it is multiplied by the reduction factor R_i, shown in Figure 4.13 to get the design value.

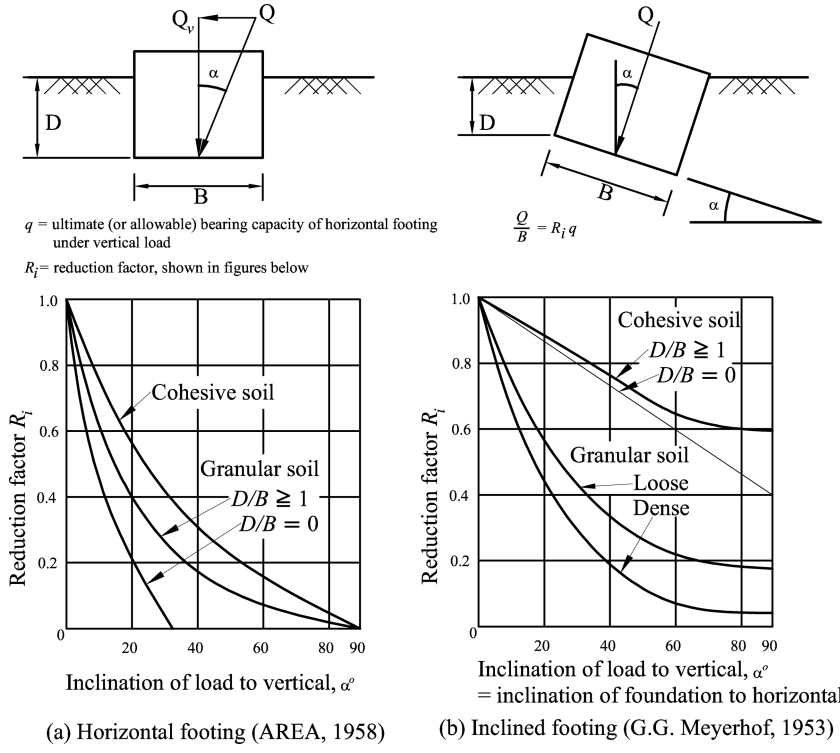

Figure 4.13 Bearing capacity of footings subjected to inclined loads.

The bearing capacity and general equations for loads including inclined loads are given in Chapter 3.

4.4.7 Footings on Slopes

The bearing capacity of footings on slopes may be determined using Meyerhof's equation (Meyerhof, 1957) as

$$q = cN_{cq} + \frac{1}{2}\gamma BN_{\gamma q} \tag{4.12}$$

The values of the bearing capacity factors N_{cq} and $N_{\gamma q}$ for continuous footings are shown in Figure 4.14. These factors vary with the slope, the relative position of the footing and the angle of internal friction of soil.

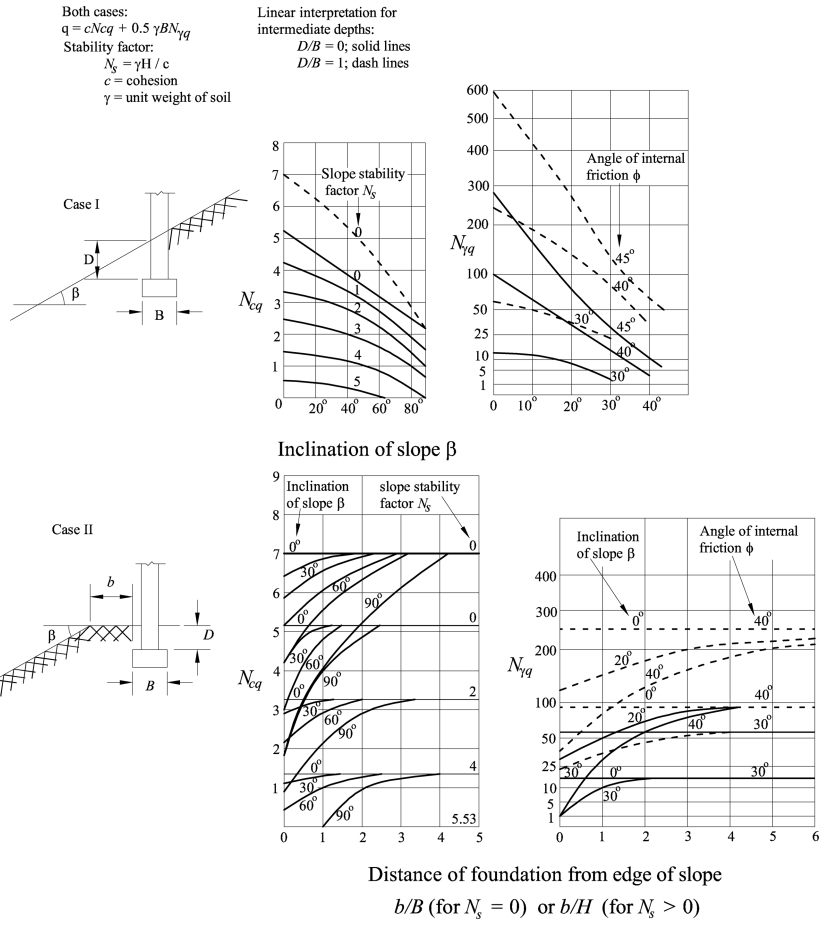

Figure 4.14 Bearing capacity of continuous footings on slopes. (Reproduced from *Proceedings of the 4th International Conference on Soil Mechanics and Foundation Engineering*, vol. **1**, G.G. Meyerhof, "The ultimate bearing capacity of foundations on slopes," pp. 384–386, August 12–24, © 1957, London, England, with permission from Elsevier.)

Before constructing footings on slopes, the stability of the slope itself must be investigated (Taylor, 1964; Das, 2001). Footings should not be constructed on slopes which are unstable. They should also be avoided on slopes where slow creep of the soil may occur. The stability of slope may be endangered by the addition of loads due to footings.

4.4.8 Uplift of Footings

The resistance of a footing against uplift is computed from the weight of the footing and the weight of soil above it. For soil below ground water level the submerged weight should be used.

As a footing is subjected to upward (pull out) load, a prism of soil is carried by the footing at the time of failure, as shown in Figure 4.15(a). The shape of the prism depends upon the characteristics of soil above the footing. Due to lack of conclusive data, no rational design rules could be developed. However, conventional method assuming a 60° prism, as shown in Figure 4.15(a) may lead to unsafe results. For footings subjected to a small uplift, the method shown in Figure 4.15(b) may be used. If a large number of footings are subjected to high uplift forces, some model tests or full sized field tests may be economically justified, in addition to detailed analysis using the finite element method (FEM).

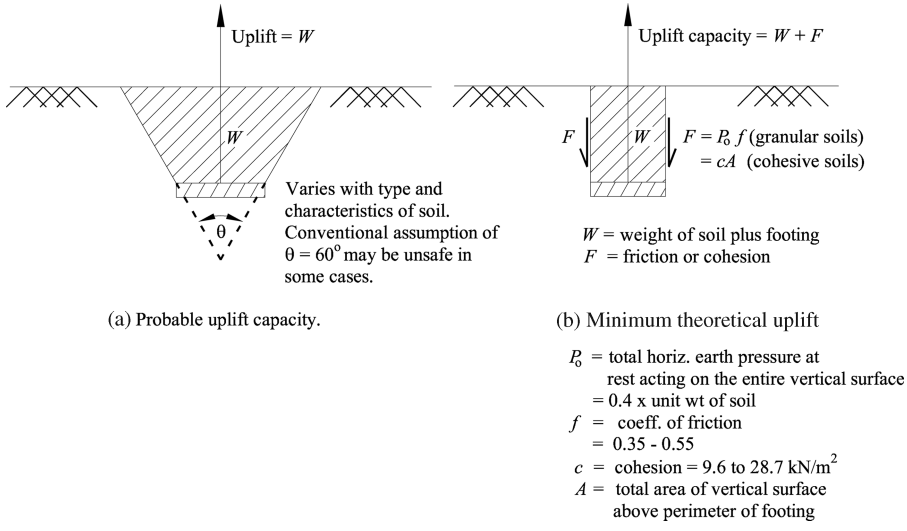

Figure 4.15 Uplift capacity of footings.

4.5 Conventional Structural Design of Footings

In practice all individual and wall footings and rafts are designed on the assumption that the distribution of the soil pressure against the bottom of the footing is linear or planar. Thus, when the load is applied at the centroid of the footing area, the unit pressure is equal to the total load divided by the footing area. In case of eccentric load, the pressure may be calculated by the procedure described in Section 4.4.5, with planar distribution of contact pressure.

By far the majority of footings are constructed of concrete and the design of such footings should follow the concrete codes prescribed. The design criteria used in practice are discussed in Chapter 8 and the principles of structural design are presented in Chapter 12.

Footings with pedestal, grillage foundations and so on are also used in some cases as per requirement.

If a pedestal is so proportioned that its height is at least equal to twice its width beyond the face of column, as shown in Figure 4.16, the critical sections for computing bending, bond and

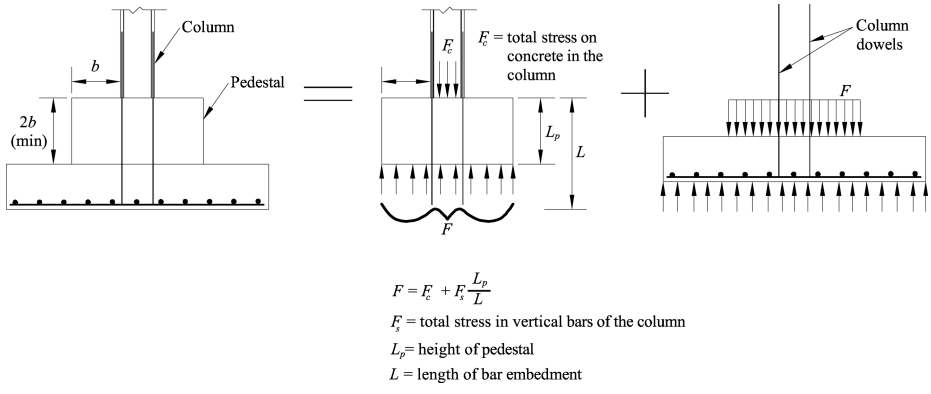

Figure 4.16 Footings with pedestal.

shear stresses are as shown in Figure 4.17 and there is no need to analyze the stresses in the pedestal. For pedestals having smaller depth/width ratio, the stresses in the pedestal must be analyzed. The analysis may be made on the assumption that the bond stress along the entire embedment of dowels below the top of the pedestal is uniformly distributed. Based on this assumption, the total stress acting on the bottom of the pedestal is equal to the total stress in the concrete of the column plus the amount of stress in the column vertical reinforcement transmitted through bond within the depth of the pedestal. Figure 4.16 illustrates the stresses acting on each element of the footing.

The members in a steel grillage are designed as cantilever beams subjected to uniformly distributed soil pressure.

4.6 Foundations in Difficult Soil Formations

There are several situations when foundations have to be constructed in difficult soils present at the site (Bowles, 1996). Precautions to be taken under a few such cases are given below.

4.6.1 Sites with Possible Soil Erosion

Foundations for bridges, retaining walls and structures near flowing water must be constructed at a depth more than the depth of erosion or scour.

4.6.2 Foundations with Susceptibility of Corrosion

If the soil is polluted such as in old garbage dumps and landfills, soils near leaking sewer lines and industrial plants or backwater areas with dead vegetation, the foundations my get corroded with time. It may be necessary to use air entrained concrete or sulfate resistant concrete in such cases. Treated timber piles are preferable to metal piles in such cases.

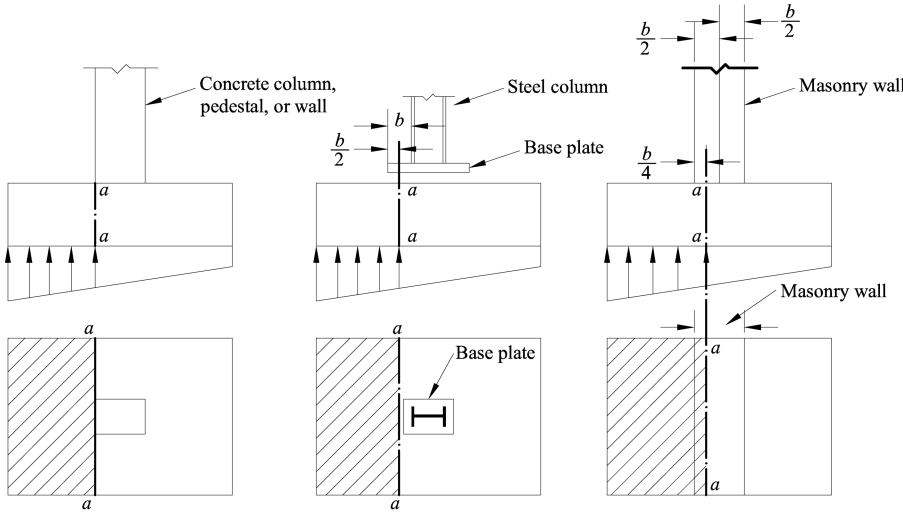

(a)

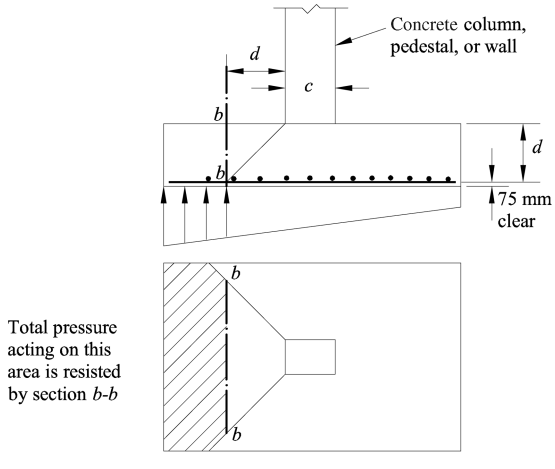

(b)

Figure 4.17 Concrete footings: (a) critical section (*a–a*) and load area for computing bond and bending stresses; (b) critical section (*b–b*) and load area for computing shear stress.

4.6.3 Sites with Water Fluctuation or Near Large-Scale Mining Operations

Special care has to be taken in the above cases due to the following reasons:

1. A raised water table may cause instability due to reduction in effective pressure and (or) making the structure floating.
2. A lowered water table may cause additional settlements due to increased effective stress.

3. Waste from ore dumps may cause large-scale subsidence.
4. Areas adjacent to mining sites might become unstable due to removal of overburden for mining.

4.6.4 Foundations in Loose Sand

Loose sand must be well compacted to improve bearing capacity and control the settlement. The foundations should be placed at a sufficient depth such that the soil beneath the footing is confined. A minimum depth as per Rankine's theory of earth pressure to ensure confinement can also be used (Taylor, 1964; Teng, 1964), that is

$$D_f = \frac{q}{\gamma}\left(\frac{1-\sin\phi}{1+\sin\phi}\right)^2 \tag{4.13}$$

where

D_f = minimum depth of foundation required for the stability of adjoining soil.
q = contact pressure
γ = unit weight of soil
ϕ = angle of internal friction of soil.

The larger of the values given by Equation (4.13) and minimum depth that is, 0.5 m as per usual practice/codes should be adopted in such cases (Section 4.4.1).

4.6.5 Foundations on Loess or Other Collapsible Soils

Such soils are generally wind blown (aeolin) deposits usually referred to as loess, sand dunes, and volcanic ash. They are loose but stable with water soluble bonding agent. Hence they collapse with loading and wetting with water resulting in large settlements. The collapse potential of such soils can be estimated (Bowles, 1996) and the following remedial measures can be adopted.

1. Compacting the soil or excavation and replacement of the soil to achieve γ_{dry} (dry unit weight of soil) $\geq 15.5\,\text{kN/m}^3$.
2. Use lime, lime-fly ash or cement as admixture during compaction.
3. Avoid wetting of such soils if at all feasible.
4. Use piles to avoid zone of collapsible soil and reaching stable stratum.

4.6.6 Foundations on Clays or Silts

Silts and clays may vary from very soft, normally consolidated to very stiff and over consolidated soils. Problems mainly occur in the case of soft deposits. Extra care should be taken to estimate the design soil pressures in terms of bearing capacity and allowable soil pressures (from allowable settlement criterion) in such cases.

4.6.7 Foundations on Expansive Soils

Such soils undergo volume changes due to wetting and drying. These are found mostly in arid and semi arid regions and contain large clay minerals. Following remedial measures may be useful in such cases.

1. Alter the expansive nature of the soil by stabilizing the soil with lime, cement or other admixtures.
2. Control the direction of expansion by allowing it to expand into cavities. A common practice is to build waffle slabs (Bowles, 1996).
3. Control the water by excavating the soil to such a depth that the weight of the soil will be sufficient to control the heave, lay a geotextile plastic fabric which is impermeable and then backfill.
4. Increase the depth of the footing such that the heave does not cause any detrimental effect. One can use belled piers with the bulged bell of sufficient depth (Bowles, 1996) or use under reamed piles.
5. Increase the surcharge load on the soil surface to counter the swell pressure caused by heaving.

4.6.8 Foundations on Garbage Land Fills or Sanitary Landfills

With the shrinking of usable normal construction sites specially in urban areas, it is becoming increasingly necessary to use former garbage/sanitary landfills for construction. Extra precautions need to be taken to safeguard against excessive settlement and bearing capacity failure. If these are not possible, pile foundations have to be adopted with noncorroding materials (Bowles, 1996). Adequate environmental protection steps may have to be taken to avoid foul smell, escaping gases due to gradual degradation of the garbage and corrosion and so on.

4.7 Modeling Soil Structure Interactions for Rational Design of Foundations

As summarized in Section 4.3, the contact pressure is taken as a uniform/linear/planar pressure for the conventional design of foundation. While all other requirements and precautions outlined in Section 4.4 are essentially the same for elastic/flexible/rational design of foundations, the use of a realistic soil–structure interaction model can make the design more rational. While the footing can be modeled as a beam (one-dimensional) or a plate or a shell (two-dimensional) and classical bending theories can be used for representing their response, the soil reaction has to be incorporated in the integrated analysis of soil–structure interaction equation by modeling the soil appropriately using different models (Crandall, 1956; Timoshenko and Krieger, 1959; Vlasov and Leontev, 1966; Kameswara Rao, 1969).

4.7.1 Elastic Foundations

The theory of elastic foundations has attracted considerable attention due to its useful application in various technical disciplines besides foundation engineering. The problems of

elastically supported structures are of interest in solid propellant rocket motors, aerospace structures, construction projects in cold regions, and several other fields. While in some problems, the structure and the elastic support, generally referred to as the *foundation*, can be physically identified, in many others the concept of structure and foundation may be of an abstract nature.

The problem of foundation–structure interaction is generally solved by incorporating the reaction from the foundation, into the response mechanism of the structure, by idealizing the foundation by a suitable mathematical model. Even if the foundation medium happens to be complex in some problems, in a majority of cases, the response of the structure at the contact surface is of prime interest and hence, it would be of immense help in the analysis, if the foundation can be represented by a simple mathematical model, without foregoing the desired accuracy. To accomplish this objective, many foundation models have been proposed and a comprehensive review pertaining to these has been given by Reissner (1937) and Kameswara Rao (1969, 1971). These are presented in Section 4.7.3.

4.7.2 Soil–Structure Interaction Equations

The foundation–soil system subjected to external loads is shown in Figures 4.18 and 4.19 depending on the geometry of the foundation that is, beam or a plate. Most of the footings can be considered as either beams (one-dimensional) or plates (two-dimensional: rectangular, squares, circular, annular or other shapes).

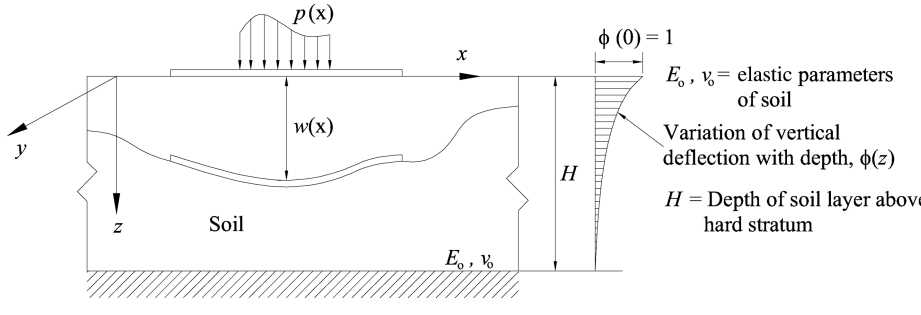

Figure 4.18 Beam on an elastic foundation.

The differential equation of bending of the beam or plate on an elastic foundation can be written as follows.

4.7.2.1 Beams on Elastic Foundations

Neglecting friction between beam and the soil medium, the governing equation can be written from bending theory as

$$EI\frac{d^4w}{dx^4} = p(x) - q(x) \tag{4.14}$$

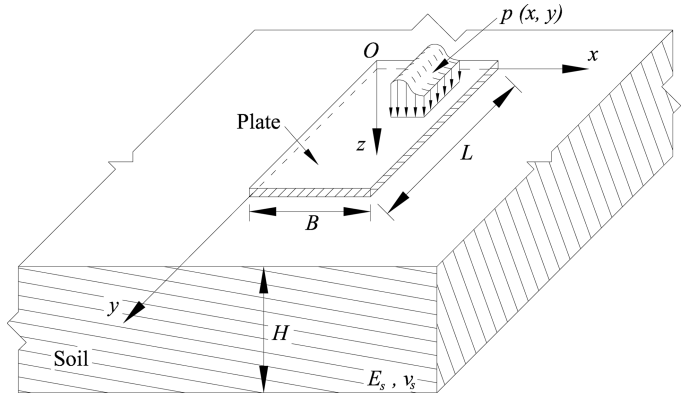

Figure 4.19 Plate on elastic foundation.

where

EI = flexural rigidity of the beam
E = modulus of elasticity of beam material
I = moment of inertia of the beam cross section

$$= \frac{h^3}{12(1-v_p^2)} \text{ per unit strip in the case of a plane strain structure (strip footing)} \quad (4.15)$$

v_p = Poisson's ratio of the strip/plane strain structure
$p(x)$ = external load applied on the footing
$q(x)$ = reaction from the supporting soil
w = vertical deflection along z axis
x, y, z = right handed coordinate system
E_s = modulus of elasticity of soil
v_s = Poisson's ratio of soil
E_0, v_0 = elastic parameters of soil defined as
$E_0 = \frac{E_s}{1-v_s^2}$ and $v_0 = \frac{v_s}{1-v_s}$ for strips (plane strain case) and three-dimensional problems.

The other parameters that can be defined for beams using classical bending theory are as follows

$$\begin{aligned} w' = \theta &= \text{slope} = \frac{dw}{dx} \\ M &= \text{bending moment} = -EI\frac{d^2w}{dx^2} \\ Q &= \text{shear force} = -EI\frac{d^3w}{dx^3} \\ q(x) &= \text{soil reaction or contact pressure} \\ &= EI\frac{d^4w}{dx^4} - p(x) \end{aligned} \quad (4.16)$$

The conventions from bending theory for bending moment (BM) and shear forces (SF) are shown below (Figure 4.20)

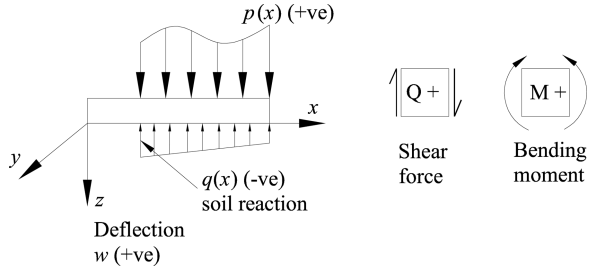

Figure 4.20 Convention sketch for bending theory of beams.

4.7.2.2 Plates on Elastic Foundations

Consider a rectangular plate on elastic foundation as shown in Figure 4.19. The assumptions usually made in the theory of bending of thin plates will be deemed to apply to this case. Friction and adhesion between the plate and the surface of the elastic foundation is neglected.

The differential equation of bending of the plate, in Cartesian coordinates, is

$$D\nabla^2\nabla^2 w(x,y) = p(x,y) - q(x,y) \tag{4.17}$$

where

∇^2 denotes the Laplace operator.

In expanded form

$$D\nabla^4 w = D\left(\frac{\partial^4 w}{\partial x^4} + \frac{\partial^4 w}{\partial x^2 \partial y^2} + \frac{\partial^4 w}{\partial y^4}\right) = p(x,y) - q(x,y) \tag{4.18}$$

where

$w = w(x, y)$ = vertical displacements of the plate surface,
$p = p(x, y)$ = distributed load on the plate,

$$D = \frac{E_p h^3}{12(1-\nu_p^2)} = \text{flexural rigidity of the plate} \tag{4.19}$$

where

E_p = modulus of elasticity of plate material
ν_p = Poisson's ratio of plate material
h = thickness of the plate
$p(x, y)$ = applied load on the plate
$q(x, y)$ = soil reaction

Although Equation (4.17) is known as the equation of bending of thin plates, it can be applied to the analysis of most rectangular plates. Further, the soil properties of an elastic foundation as shown in Figure 4.19 become

$$E_0 = \frac{E_s}{1-v_s^2}, \quad v_0 = \frac{v_s}{1-v_s} \tag{4.20}$$

where E_s and v_s are respectively the modulus of elasticity and Poisson's ratio for the material of the foundation (soil).

After $w(x, y)$ has been determined from Equation (4.17) and the boundary conditions, the reactions $q(x, y)$ can be found from Equation (4.17). The moments and shearing forces in the plate (Figure 4.21) can be computed using formulae of the theory of bending of plates as follows (Timoshenko and Krieger, 1959)

$$\begin{aligned}
M_x &= -D\left(\frac{\partial^2 w}{\partial x^2} + v_p \frac{\partial^2 w}{\partial y^2}\right) \\
M_y &= -D\left(\frac{\partial^2 w}{\partial y^2} + v_p \frac{\partial^2 w}{\partial x^2}\right) \\
M_{xy} &= H = H_x = -H_y = -D(1-v_p)\frac{\partial^2 w}{\partial x \partial y} \\
N_x &= -D\frac{\partial}{\partial x}\left(\frac{\partial^2 w}{\partial x^2} + \frac{\partial^2 w}{\partial y^2}\right) \\
N_y &= -D\frac{\partial}{\partial y}\left(\frac{\partial^2 w}{\partial x^2} + \frac{\partial^2 w}{\partial y^2}\right)
\end{aligned} \tag{4.21}$$

Following Kirchhoff (Timoshenko and Krieger, 1959; Vlasov and Leontev, 1966), the shearing forces N_x, N_y, and the torque H at the plate edges are usually replaced by the reduced

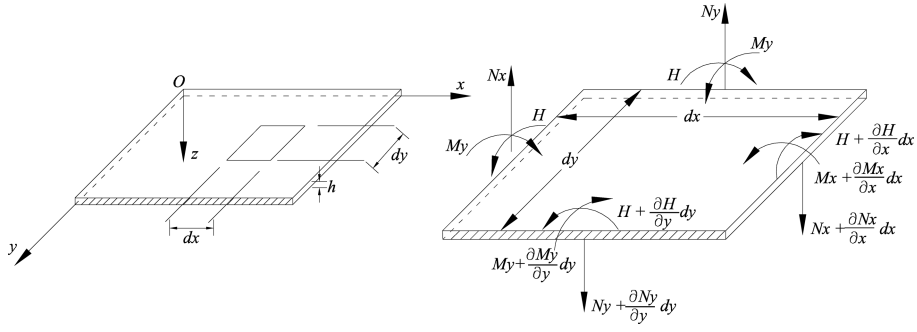

Figure 4.21 Convention sketch for plate bending.

shearing forces Q_x and Q_y which, for a rectangular plate, are

$$\begin{aligned} Q_x &= -D\left(\frac{\partial^3 w}{\partial x^3} + (2-v_p)\frac{\partial^3 w}{\partial x \partial y^2}\right) \\ Q_y &= -D\left(\frac{\partial^3 w}{\partial y^3} + (2-v_p)\frac{\partial^3 w}{\partial x^2 \partial y}\right) \end{aligned} \tag{4.22}$$

Equations (4.17) and (4.18) are valid for plates with other geometries such as circular, annular, and so on, since Lapacean operator is invariant except that its expansion in other coordinate systems has to be taken for solving the equation. For example for circular plates or annular plates, the Laplacean operator ∇^2 has the expanded form in a r,θ coordinate system as (Figure 4.22)

$$\nabla^2 = \frac{\partial^2}{\partial r^2} + \frac{1}{r}\frac{\partial}{\partial r} + \frac{1}{r^2}\frac{\partial^2}{\partial \theta^2} \tag{4.23a}$$

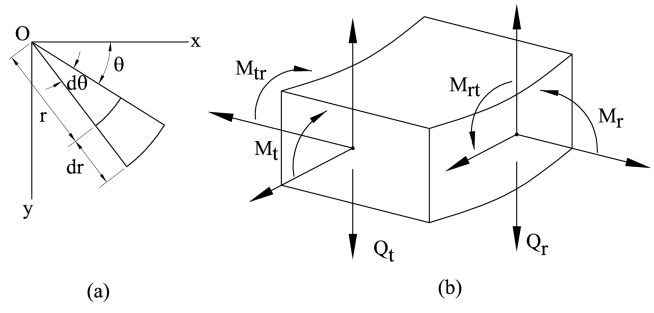

Figure 4.22 Convention sketch for circular plates.

If the load is axisymmetric, the θ coordinate can be omitted in Equation (4.23a), resulting in

$$\nabla^2 = \frac{\partial^2}{\partial r^2} + \frac{1}{r}\frac{\partial}{\partial r} \tag{4.23b}$$

However, the bending moments and shear forces take the following forms in such a situation (Timoshenko and Krieger, 1959). The convention sketch is shown in Figure 4.22.

Bending moments

$$\begin{aligned} M_r &= -D\left(\frac{\partial^2 w}{\partial x^2} + v_p\frac{\partial^2 w}{\partial y^2}\right)_{\theta=0} = -D\left[\frac{\partial^2 w}{\partial r^2} + v_p\left(\frac{1}{r}\frac{\partial w}{\partial r} + \frac{1}{r^2}\frac{\partial^2 w}{\partial \theta^2}\right)\right] \\ M_t &= -D\left(\frac{\partial^2 w}{\partial y^2} + v_p\frac{\partial^2 w}{\partial x^2}\right)_{\theta=0} = -D\left[\frac{1}{r}\frac{\partial w}{\partial r} + \frac{1}{r^2}\frac{\partial^2 w}{\partial \theta^2} + v_p\frac{\partial^2 w}{\partial r^2}\right] \\ M_{rt} &= (1-v_p)D\left(\frac{\partial^2 w}{\partial x \partial y}\right)_{\theta=0} = (1-v_p)D\left(\frac{1}{r}\frac{\partial^2 w}{\partial r \partial \theta} - \frac{1}{r^2}\frac{\partial w}{\partial \theta}\right) \end{aligned} \tag{4.23c}$$

The expressions for shear forces are as follows

$$Q_r = -D\frac{\partial}{\partial r}\left(\nabla^2 w\right)$$
$$Q_t = -\frac{D}{r}\frac{\partial}{\partial \theta}\left(\nabla^2 w\right) \tag{4.23d}$$

4.7.2.3 Soil Reaction – Contact Pressure

To solve the final form of soil–structure interaction Equations (4.14) and (4.17), the soil reaction, $q(x)$, has to be incorporated in those equations which are dependent on the beam/plate and soil characteristics and the bond at the interface. Assuming frictionless contact, and complete bond at the interface between the beam/plate and the soil, $q(x)$ can be expressed in terms of soil displacements (mainly vertical displacement for vertical loads) using different foundation models. A review of these models is given in references by Reissner (1937), Kameswara Rao (1969, 1971) and others. The important features of these models are summarized below.

4.7.3 Brief Review of the Foundation Models

The earliest formulation of the foundation model was due to Winkler, who assumed the foundation model to consist of closely spaced independent linear springs, as shown in Figure 4.23. If such a foundation is subjected to a partially distributed surface loading, q, the springs will not be affected beyond the loaded region. For such a situation, an actual foundation is observed to have the surface deformation as shown in Figure 4.24. Hence by comparing the behavior of theoretical model and actual foundation, it can be seen that this model essentially suffers from a complete *lack of continuity* in the supporting medium. The load deflection equation for this case can be written as

$$q = kw \tag{4.24}$$

where k is the spring constant and is often referred to as the *foundation modulus*, and w is the vertical deflection of the contact surface. It can be observed that Equation (4.24) is exactly satisfied by an elastic plate floating on the surface of a liquid and carrying some load which causes it to deflect. The pressure distribution under such a plate will be equivalent to the force of

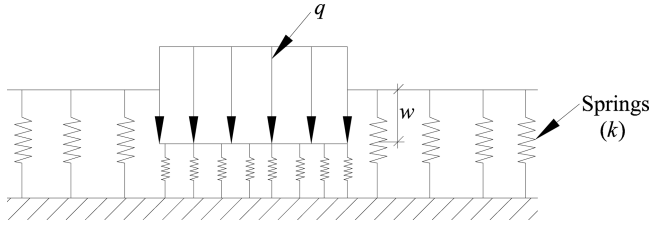

Figure 4.23 Load on Winkler's foundation.

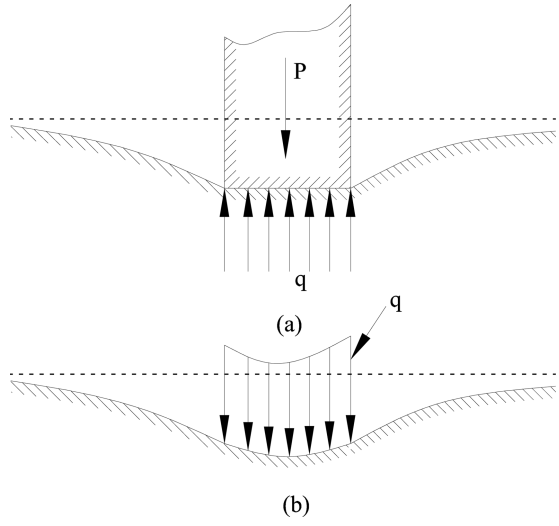

Figure 4.24 Deformation of actual foundation.

buoyancy, k being the specific weight of the liquid. With this analogy in view, the first solution for the bending of plates on a Winkler-type foundation was presented by Hertz (1884).

Also, in such a foundation model the displacements of the loaded region will be constant whether the foundation is subjected to a rigid stamp or a uniform load as can be seen from Figure 4.23. However, the displacement for these cases are quite different in actual foundations as can be noted from Figures 4.24(a) and (b). Though this model leads to some inconsistencies, being the simplest, it is amenable to an easy analysis. Through the years a large variety of solutions have been presented on this basis (Winkler, 1867; Reissner, 1937; Hetenyi, 1946, 1950; Timoshenko and Krieger, 1959; Iyengar and Ramu, 1979).

Another approach is to assume the foundation medium to be a continuous elastic solid. Though this hypothesis closely simulates the physical behavior of an actual foundation, it makes the analysis unduly complex. Despite several mathematical complexities, solutions were presented on these bases (Gorbunov-Posadov, 1949; Zimmermann, 1888), which, however, were limited to relatively simple cases. Also it was observed that the foundation performance as predicted by this theory differed from the actual behavior, probably due to the questionable assumptions of elasticity, homogeneity and isotropy of the materials, inherent in this hypothesis. As an example, in soils it has been observed that the surface displacements away from the loaded region decreased more rapidly than predicted by this theory (Kameswara Rao, 1969), and materials like soils and foam rubber hardly satisfy the basic assumptions stipulated above.

The need for bridging the gap between these two extreme and limiting cases and to arrive at a physically close and mathematically simple foundation model has been felt for some time. Several authors have proposed foundation models which involve more than one parameter for the characterization for the supporting medium.

One such attempt was presented by Filonenko–Borodich (Reissner, 1937), who modified the Winkler foundation by providing some continuity by connection top ends of the springs by a

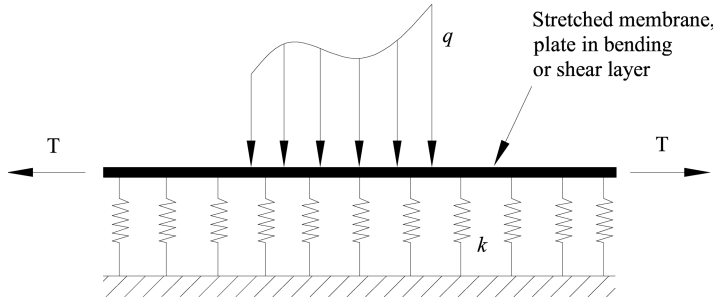

Figure 4.25 Convention sketch showing various foundation models.

stretched elastic membrane subjected to a constant tension field, T, as shown in Figure 4.25. The equilibrium in the vertical direction yields the equation

$$q = kw - T\nabla^2 w \tag{4.25}$$

where

q is the distributed vertical load applied on the surface of the soil
w is the vertical deflection of the surface
∇^2 is the Laplace operator
k and T are the two parameters characterizing the foundation.

Hetenyi (1946, 1950) achieved the continuity in the Winklers's foundation model by embedding an elastic beam in the two-dimensional case and an elastic plate in the three-dimensional case (Figure 4.25), with the stipulation that the hypothetical beam or plate deforms in bending only. In this case the relation between the load q and the deflection of the surface w can be expressed as

$$q = kw + D\nabla^4 w \tag{4.26}$$

where

D is the flexural rigidity of the embedded beam or plate
$\bigtriangledown^4$ is the bi-harmonic operator.

By providing for shear interaction between the Winkler's spring elements, Pasternak (Kameswara Rao, 1969) presented a foundation model as shown in Figure 4.25. The shear interaction between the springs has been achieved by connecting the ends of the springs to a beam or a plate (as the case may be), consisting of incompressible vertical elements, which hence deform in transverse shear only. The corresponding equation relating the load, q, and deflection, w, can be derived as

$$q = kw - \mu\nabla^2 w \tag{4.27}$$

where

μ is the shear modulus of the foundation material

∇^2 is the Laplace operator.

It can be seen that this foundation model also consists of two parameters k and μ, and is equivalent to the models proposed by Filonenko–Borodich (Equation (4.25)) and Wieghardt (Kameswara Rao, 1969).

Pasternak proposed another foundation model (Kameswara Rao, 1969) consisting of two layers of springs connected by shear layer in between as shown in Figure 4.26. The relation between the load q, and the deflection w of the surface of the foundation can be expressed as

$$\left(1 + \frac{k}{c}\right)q - \frac{\mu}{c}\nabla^2 q = kw - \mu\nabla^2 w \tag{4.28}$$

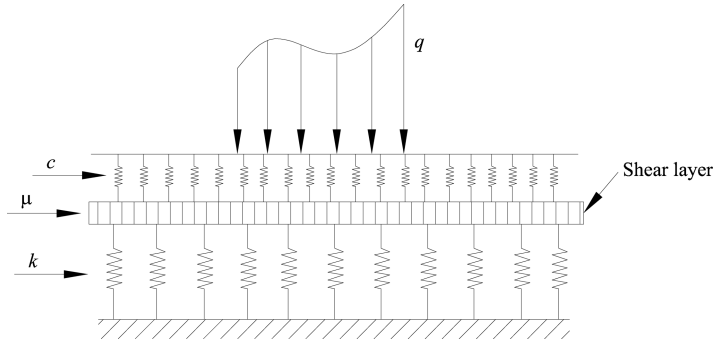

Figure 4.26 Pasternak's modified foundation model.

where

c and k are the spring constants of the upper and lower layers of springs

μ is the shear modulus of the shear layer.

Several contributions based on Pasternak-type foundations are available in the literature.

In all the above models, the Winkler's model has been modified by providing for some interaction between the spring elements and hence assuring the continuity of the foundation to some degree. In contrast to them, starting from the elastic-continuum theory, and introducing simplifying assumptions with respect to the expected stresses and (or) displacements, some models were proposed. One such contribution was from Reissner (Kameswara Rao, 1969), who assumed that the in-plane stresses σ_x, σ_y and τ_{xy} are negligible throughout the foundation layer. Also the horizontal displacements at the upper and lower surfaces of the foundation layer were assumed to be zero. Proceeding with these assumptions and solving the elastic continuum equations, the equation relating the applied distributed surface load, q, and the resulting surface

displacement, w, has been derived as

$$c_1 w - c_2 \nabla^2 w = q - \frac{c_2}{4c_1} \nabla^2 q \tag{4.29}$$

where $c_1 = \frac{E}{H}$ and $c_2 = \frac{Hv}{3}$.

E and v are the elastic constants of the foundation material and H is the thickness of the foundation layer. It can be seen that Equations (4.28) and (4.29) are similar. Also, for constant and linearly varying loads, this equation can be seen to be mathematically equivalent to Equations (4.25) and (4.27), thus establishing the similarity of the models. In this case, neglecting the in-plane stresses, it can be shown that shear stresses τ_{zx} and τ_{zy} are constant throughout the depth of the foundation for a given surface point, which is inconsistent with the actual foundation performance, especially for thick foundation layers.

Vlasov and Leontev (1966) have developed a foundation model starting from elastic-continuum theory and neglecting the horizontal displacements of the supporting medium. Using Vlasov's general variational method, the load–displacement relation can be derived as

$$q = kw - 2t_1 \nabla^2 w \tag{4.30a}$$

where

q is the distributed surface load

w is the vertical deflection.

k and t_1 are the two parameters characterizing the foundation and can be expressed in terms of the elastic constants of the material and geometric properties of the foundation layer(Vlasov and Leontev,1966). In Equation (4.30a), these parameters can be obtained as

$$k = \frac{E_0 B}{1 - v_0^2} \int_0^H \psi^2(z)\, dz \tag{4.30b}$$

$$t_1 = \frac{E_0 B}{1 - v_0^2} \int_0^H \psi^2(z)\, dz \tag{4.30c}$$

where

$E_0, v_0 = E_s, v_s$ of the soil respectively to be used for beams on elastic foundation problems (plane stress problems).

However,
$$E_0 = \frac{E_s}{1 - v_s^2}, \quad v_0 = \frac{v_s}{1 - v_s} \tag{4.30d}$$

for plates and plane strain case (strips and three-dimensional problems)

B = width of the foundation.

$\psi(z)$ is the assumed distribution function of vertical displacement with depth (preferably a function with $\psi(0) = 1$ and easy to integrate (Figure 4.18). $\psi(z)$ can be chosen as

$e^{-\beta z}$ for infinite soil layers (or layers with large depth), where β is the soil parameter, β can be chosen between 0.5 and 2.5 (0.5 for clayey soils and 1.0–2.5 for sandy soils). $\psi(z)$ can be chosen as $\frac{H-z}{H}$, linearly decreasing for soil layers of finite depth.

Comparing Equation (4.30a) and Equations (4.25) and (4.27), it can be observed that, this model is equivalent to the models proposed by Filonenko–Borodich, Pasternak and Wieghardt.

A close examination of the various models reviewed above, reveals the fact that these methods fall short for direct application to practical problems, either because the analysis is cumbersome,or, because the assumptions made for natural foundation media cannot be fully justified and often lead to some inconsistencies.

To overcome the above inconsistencies of the soil behavior, Kameswara Rao (1969, 1971) modified Vlasov and Leontev's model to account for the horizontal displacements in the elastic foundation and basic equations have been presented using Vlasov's general variational method. The resulting model is very close to elastic-continuum hypothesis and is easy for mathematical analysis and hence is expected to be useful for the solutions of many problems of practical significance.

4.7.4 Winkler's Model

After reviewing the various foundation models as outlined in Section 4.7.3, it can be seen that Winkler's model is the simplest both in terms of representation of the soil reaction at the footing soil interface as well as analysis of the resulting soil–structure interaction Equations (4.14) and (4.18), though it has inherent deficiencies as outlined in Section 4.7.3. It has an added advantage that the soil parameter used for expressing the soil reaction, that is, k (Equation (4.24)), referred to as spring constant (of the idealized springs of the Winkler's model as shown in Figure 4.23) is relatively easy to evaluate from laboratory and field experiments (Section 4.8). Thus Winkler's model is used for most of the rational analysis and design presented in this book. Thus using Winkler's model for representing the soil and using Equation (4.24) for soil reaction q the soil–structure interaction equation can be expressed as follows:

1. Beams on elastic foundations (Equation (4.14))

$$EI\frac{d^4w(x)}{dx^4} + kw(x) = p(x) \tag{4.31}$$

2. Plates on elastic foundation (Equation (4.18))

$$D\nabla^4 w(x,y) + kw(x,y) = p(x,y) \tag{4.32}$$

in which $k =$ spring or the soil constant, to be evaluated from suitable laboratory and field tests (Section 4.8).

4.8 Evaluation of Spring Constant in Winkler's Soil Model

4.8.1 Coefficient of Elastic Uniform Compression – Plate Load Test

The idea of modeling soil as an elastic medium was first introduced by Winkler and this principle is now referred to as the Winkler soil model. The subgrade reaction at any point along

the beam is assumed to be directly proportional to the vertical displacement of the beam at that point. In other words, the soil is assumed to be elastic and obeys Hooke's Law. Hence, the modulus of subgrade reaction (k_s) for the soil is given by

$$k_s = \frac{q}{w} = C_u \tag{4.33}$$

where

q is the bearing pressure at a point along the beam

w is the vertical displacement of the beam at that point.

k_s is also referred to as the coefficient of elastic uniform compression, C_u.

The main difficulty in applying the Winkler soil model is that of quantifying the modulus of subgrade reaction (k_s) to be used in the analysis, as soil is a very variable material. In practical terms, k_s can be found only by carrying out *in-situ* plate load tests or relating it in some way to elastic characteristics of the soil. The plate load test is widely used and is described in BS 1377: Part 9: 1990, IS: 1888–1982 (Jones, 1997) and so on. Plate load test is described in detail in Chapter 3, while a few important aspects are summarized below. The test set up is also shown in Figure 4.27.

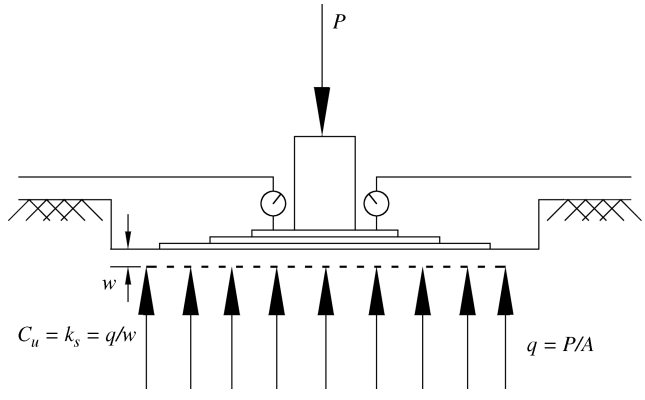

Figure 4.27 Plate load test set up.

The plate should obviously be as large as possible, consistent with being able to exert the vertical forces required. The standard plate is either a circular shape of 760 mm diameter or a square shape 760 × 760 mm, 16 mm thick, and requires stiffening by means of other circular/square plates placed concentrically above it. Invariably, a large plate does not settle uniformly. The settlement must, therefore, be monitored by means of three or four dial gauges equally spaced around the perimeter in order to determine the mean settlement. Supports for these dial gauges should be sited well outside the zone of influence of the jacking load which is measured by a proving ring. When choosing a diameter of plate to use for the test, due consideration should also be given to the limited zone of influence of the loaded plate.

Typically, the soil will only be effectively stressed to a depth of 1.25–1.50 times the diameter of the plate. This limitation can be overcome to some extent by carrying out the plate test at depth in pit, rather than on the surface. Small diameter plates are often used to overcome the practical difficulties of providing the requisite reaction/vertical forces. Terzaghi used a 305 mm square plate for evaluation.

Figure 4.28 shows a typical plot of q against w that would be obtained from a plate bearing test.

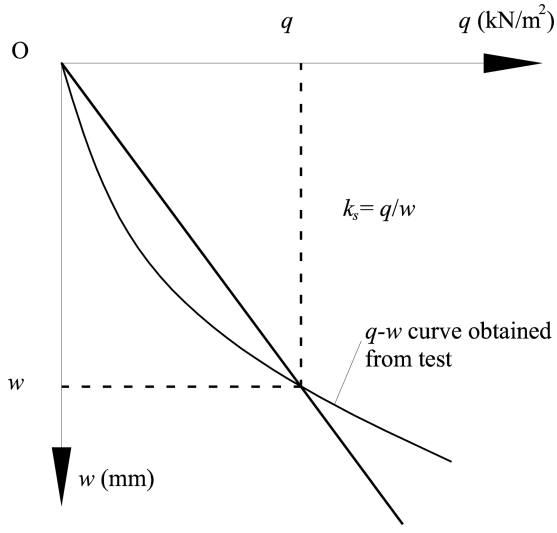

Figure 4.28 q–w curve obtained from plate load test.

In Foundation design, as distinct from pavement design, the value of k_s is the secant modulus of the graph over the estimated working range of bearing pressure as indicated in Figure 4.28. The value of the modulus of subgrade reaction (k_s) obtained from the test varies according to the size of plate used. Figure 4.29 shows the variation of k_s with plate diameter based on experimental evidence. It is apparent, therefore, that k_s depends not only on the deformation characteristics of the soil but also on the size of contact area between plate and subgrade. The variation of k_s with plate size creates an obvious difficulty in deciding which plate size should be used as the standard or reference for defining values of k_s for analysis.

Furthermore, due account must also be taken of the size and geometry of the loaded area. Terzaghi (1955) made several useful recommendations to overcome these difficulties. Basically, he first proposed reference values of k_s for sands and clays based on plate bearing tests carried out using a 305 mm square plate. He then advocated methods of conditioning these values to allow for the geometry of the base. His recommendations are presented in Section 4.8.2. As most plate bearing tests are carried out using circular plates, it is necessary to relate the performances of circular and square plates in order to follow Terzaghi's

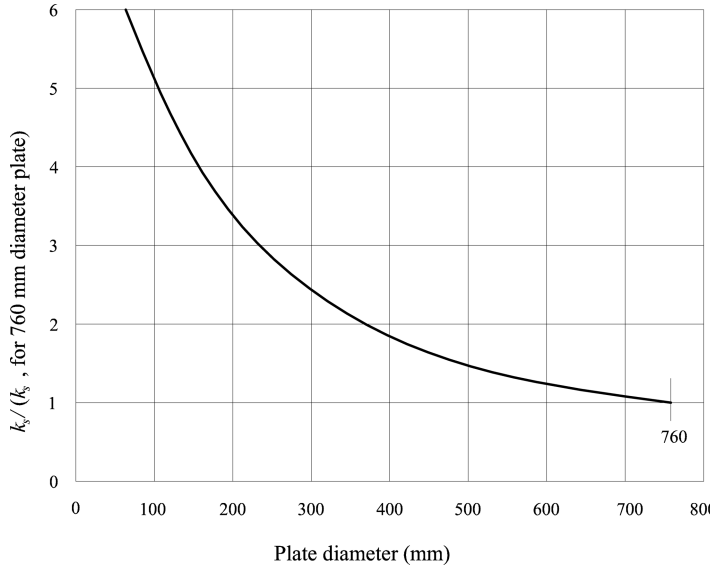

Figure 4.29 Variation of subgrade reaction ratio with plate diameter.

recommendations. The theoretical relationship between values of k_s obtained from plate bearing tests using circular and square plates can be derived as follows.

Square Plate

The mean settlement (w_{sp}) is given by

$$w_{sp} = \frac{0.95(1-v_s^2)qB}{E_s} \tag{4.34}$$

where

v_s is the Poisson's ratio of the soil
q is the average bearing pressure under plate
B is the side of square plate
E_s is the modulus of elasticity of the soil.

Circular Plate

The mean settlement (w_{cp}) for the same value of q is

$$w_{cp} = \frac{0.85(1-v_s^2)qB}{E_s} \tag{4.35}$$

where B is the diameter of the plate.

It can be noted from Equations (4.34) and (4.35) that

$$k_{sp} = 0.895\, k_{cp} \tag{4.36}$$

where the suffixes *sp* and *cp* refer to square plate and circular plate respectively.

Example 4.1

The value of k_s obtained from a plate bearing test using a 760 mm diameter plate is 120 kN/m^2/mm. Estimate the value of k_s corresponding to a test carried out using a 305 mm square plate. Assume the soil to be uniform and homogeneous.

Solution:

With reference to Figure 4.29:

k_s for circular plate with diameter of 305 mm $= 2.2 \times 120 = 264$ kN/m^2/mm
k_s for 305 mm square plate $k_{sp} = 0.895 \times 264 = 236.28$ kN/m^2/mm.

Horizontal plate load tests can also be carried out in trial pits to obtain corresponding values of the horizontal modulus of subgrade reaction (k_h) which is relevant to the analysis of laterally loaded piles, pile groups and sheet piling. More information about k_h is given in Jones (1997) and in Section 10.6. The modulus of subgrade reaction corresponding to a 305 mm square plate will henceforth be referred to as the reference value and will be denoted by k_t. Values of k_t proposed by Terzaghi for sands and clays are given in Tables 4.2 and 4.3 respectively.

Table 4.2 Terzaghi's values of k_t for sands (305 mm plate test) in kN/m^2/mm.

Type	Loose	Medium	Dense
Dry or moist sand	15	45	175
Submerged sand	10	30	105

Table 4.3 Terzaghi's values of k_t for clays (305 mm plate test) in kN/m^2/mm.

Consistency of clay	Firm to stiff	Stiff to very stiff	Hard
Uniform compressive strength (kN/m^2)	105–215	215–430	>430
Values of k_t	30	50	100

Values of k_s for long beams may also be assessed by relating them to the intrinsic parameters of the soil such as the elastic modulus (E_s), Poisson's ratio(v_s) and the California bearing ratio (CBR). E_s and $v_s$can both be derived from the results of triaxial tests. Salvadurai (1979) developed the following expressions for k_s in terms of E_s and v_s for beams having a length/breadth (L/B) ratio $\geq$10.

$$k_s = \frac{0.65\, E_s}{B(1-v_s^2)} \tag{4.37}$$

$$k_s = \frac{\pi\, E_s}{2B(1-v_s^2)\log_e\left(\frac{L}{B}\right)} \tag{4.38}$$

The two expressions are in close agreement for values of *L*/*B* in the range 10–13. Figure 4.30 plots an approximate, empirical relationship between the modulus of subgrade reaction (k_s) obtained using the standard 760 mm diameter plate and the CBR for soils that are uniform in depth (Jones, 1997).

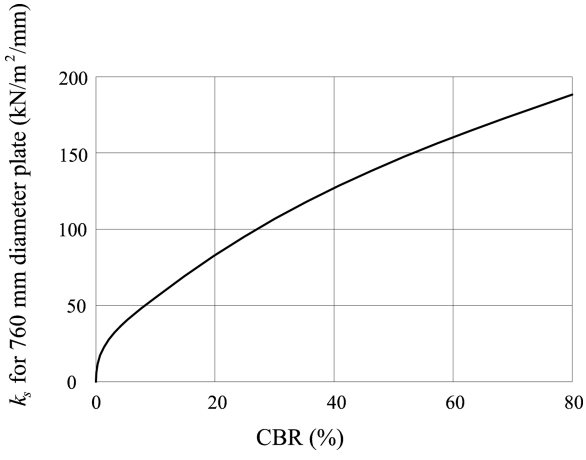

Figure 4.30 Empirical relationship between k_s and CBR value.

Example 4.2

A dense sandy soil is uniform in depth and has a measured CBR of 40%. Estimate the value of k_s that is likely to be obtained from a plate bearing test using a 305 mm square plate.

Solution:

1. Figure 4.30 gives $k_{760} = 130\,\text{kN/m}^2\text{/mm}$ (760 mm diameter plate)
2. Figure 4.29 give $k_{305} = 2.2 \times 130 = 286\,\text{kN/m}^2\text{/mm}$ (305 mm diameter plate)
3. $\therefore k_s$ corresponding to 305 mm square plate (Equation (4.36)) $= 0.895 \times 286 = 256\,\text{kN/m}^2\text{/mm}$.

4.8.2 Size of Contact Area

It is evident from Figure 4.29 that the value of modulus of subgrade reaction (k_s) varies according to the size of the plate used in the plate bearing test. Similarly k_s varies with the breadth (B) of a continuous beam resting on an elastic subgrade. This fact was first reported by Engesser (Jones, 1997) when he confirmed that the value of k_s decreases with increasing width (B) of the beam. Terzaghi (Taylor, 1964) also investigated this phenomenon and derived expressions relating k_s, k_t and B for beams supported by both cohesionless and cohesive soils as follows.

$$\text{Cohesionless soils:} \quad k_s = k_t \left(\frac{0.305 + B}{2B} \right)^2 \tag{4.39}$$

$$\text{Cohesive soils:} \quad k_s = k_t \left(\frac{0.305}{B} \right) \tag{4.40}$$

In Equations (4.39) and (4.40) the units are: k_s, k_t in kN/m^2/mm, B in meters. Both of these expressions infer that k_s for a beam 0.305 m wide is roughly equal to k_t obtained from a plate bearing test using a square plate of a side of 0.305 m.

Vesic (1961) proposed an expression for k_s in terms of E_s and v_s (of the soil) as (Bowles, 1996):

$$k_s = \frac{1}{B} \left[0.65 \sqrt[12]{\frac{E_s B^4}{E_f I_f}} \right] \frac{E_s}{1 - v_s^2} \approx \frac{E_s}{B(1 - v_s^2)} \tag{4.41}$$

where

B, I_f, E_f = width, moment of inertia of the cross section and modulus of elasticity of the footing respectively

E_s, v_s = modulus of elasticity and Poisson's ratio of the soil.

One can also adopt the expression of k (neglecting t_1) from Vlasov's elasticity model given by Equation (4.30d) with appropriate choice of $\psi(z)$ (Vlasov and Leontev, 1966).

4.8.3 Winkler's Soil Medium with or without Tension

The common assumption made in conventional methods of analyzing loaded continuous beams resting on a horizontal subgrade is that tension is not allowed to develop between the beam and the underlying subgrade. It is therefore, necessary when using beam on elastic foundation approach to condition the Winkler soil medium to detach springs which are not in compression under the action of the applied loading under consideration. However, in most other applications, tension in the springs is allowed.

Comparisons between the results of analyses carried out using these two conditions for the same foundation beam problem usually differ by only small amounts (Jones, 1997).

4.8.4 Sensitivity of Responses on k_s

When using the beam on elastic foundation concept to analyze geotechnical problems, it is imperative that a range of values of the modulus of subgrade reaction (k_s) are tested to ascertain the sensitivity of soil parameter in the analysis. Usually, the resulting bending moments and shear forces are not sensitive to changes in the value of k_s.

4.8.5 Modulus of Subgrade Reaction for Different Plate Sizes and Shapes

The same plate load test results described in Section 4.8.1 can be used for obtaining k_s of different plate sizes and shapes (some of these have been discussed in the above sections) using theory of elasticity solutions (Kameswara Rao, 2000) as follows.

For a rigid circular plate of area A on an elastic half space subjected to vertical load

$$k_s = C_u = 1.13 \frac{E}{1-v^2} \cdot \frac{1}{\sqrt{A}} \tag{4.42}$$

where

E and v are modulus of elasticity and Poisson's ratio of the soil

C_u = coefficient of elastic uniform compression/modulus of subgrade reaction.

For a rectangular plate of sides a and b on an elastic half space subjected to vertical load, k_s can be expressed as

$$k_s = c_f \frac{E}{(1-v^2)} \frac{1}{\sqrt{A}} \text{ for flexible plate} \tag{4.43}$$

$$k_s = c_r \frac{E}{(1-v^2)} \frac{1}{\sqrt{A}} \text{ for rigid plate} \tag{4.44}$$

where

A = area of the plate = ab

c_f, c_r = shape constants depending on the flexibility or rigidity of the test plate used

E, v = modulus of elasticity and Poisson's ratio of the soil medium respectively. The values of c_f and c_r are given in Table 4.4 for ready reference.

Table 4.4 Coefficients c_f and c_r.

Shape of the plate	$\frac{a}{b}$	c_f	c_r
Circular	—	—	1.13
Square	1.0	1.06	1.08
Rectangular	1.5	1.07	—
	2.0	1.09	1.10
	3.0	1.13	1.15
	5.0	1.22	1.24
	10.0	1.41	1.41

It can be seen from Table 4.4 and Equations (4.43) and (4.44), that the value of k_s is not greatly dependent on the flexibility or rigidity of the plate. It can be further observed from Equations (4.42) and (4.44) that k_s is proportional to $(A)^{-1/2}$, that is

$$\frac{k_{s_1}}{k_{s_2}} = \sqrt{\frac{A_2}{A_1}} \tag{4.45}$$

where k_{s1} is the value corresponding to a bearing plate of area A_1 and k_{s2} is the value corresponding to a bearing plate of area A_2. From Equation (4.45), it is evident that if the value of k_{s1} corresponding to a plate area A_1 is known, k_{s2} corresponding to any other plate

area A_2 can be easily evaluated. It is convenient to convert all the test results and present the values of corresponding to a bearing plate area of $10\,m^2$ (Kameswara Rao, 2000). The average values of k_s (corresponding to a plate area of $10\,m^2$) for different soils are given in Table 4.5.

These results can also be summarized as presented in Table 4.6 (Kameswara Rao, 2000).

Table 4.5 Average values of k_s for different soils (corresponding to a plate area of $10\,m^2$).

Soil description	Permissible pressure on soil (kN/m^2)	k_s (kN/m^3)
Gray plastic silty clay with sand and organic salt	98	137.34×10^2
Brown saturated silty clay with sand	147.15	196.20×10^2
Dense silty clay with some sand (above ground water level)	up to 490.5	1049.67×10^2
Medium moist sand	196.2	196.20×10^2
Dry sand with gravel	196.2	196.20×10^2
Fine saturated sand	245.25	$294.30–343.35 \times 10^2$
Medium sand	245.25	304.11×10^2
Gray fine dense, saturated sand	245.25	333.54×10^2
Loess with natural moisture content	294.3	441.45×10^2
Moist loess	196.2	461.07×10^2

Table 4.6 Values of k_s and μ for different soil categories (assuming $v_s = 0.3$).

Soil category	Soil description	Permissible pressure on soil (kN/m^2)	c_u for $A = 10\,m^2$ (kN/m^3)	Shear modulus, μ (kN/m^2)
I	Weak soils (clay and silty clays with sand in a plastic state)	Up to 147.15	98.1×10^2 196.2×10^2 294.3×10^2	100.06×10^2 201.11×10^2 301.17×10^2
II	Soils of medium strength (clays and silty clays with sand close to plastic limit)	147.15–343.35	294.3×10^2 392.4×10^2 490.5×10^2	301.17×10^2 401.23×10^2 502.27×10^2
III	Strong soils (clays and silty clays with sand of hard consistency; gravels and gravelly sand; loess and loessial soils)	343.35–490.5	490.5×10^2 583.6×10^2 686.77×10^2 784.8×10^2 882.9×10^2 981×10^2	502.27×10^2 602.33×10^2 702.40×10^2 803.44×10^2 903.50×10^2 1003.56×10^2
IV	Rocks	>490.5	$>981 \times 10^2$	$>1003.56 \times 10^2$

4.8.6 Poisson's Ratio of the Soil Medium

It is possible to evaluate Poisson's ratio (v) using dynamic test results mentioned in Chapter 2. Also Poisson's ratio can be evaluated using some simple soils tests which may result in large errors. It has been observed that in general Poisson's ratio varies from about 0.25 to 0.35 for cohesionless soils and form about 0.35 to 0.45 for cohesive soils which are capable of supporting foundation blocks. Hence, in the absence of any test data Poisson's ratio can be assumed as 0.3 for cohesionless soils and 0.4 for cohesive soils without causing any appreciable error in the analysis and design of foundations (Kameswara Rao, 2000).

This is further justifiable from the fact that the responses to foundation soil system have been found to be not much sensitive to the variations in the value of Poisson's ratio.

4.8.7 Evaluation of Young's Modulus

While it is ideal to evaluate Young's modulus (E, or shear modulus μ) from dynamic tests, often it may not be possible to do so due to physical limitations.

However, the same can be evaluated from the results of plate load test. It is obvious that E can be calculated (and hence shear modulus $\mu = E/(2(1 + v))$) from Equations (4.42)–(4.44). Knowing the value of k_s, and the shape and size of the plate used (flexible or rigid plate solutions do not make much difference, as can be seen from Table 4.4). Poisson's ratio can be assumed to be either 0.3 or 0.4 as mentioned above (Section 4.8.6).

For a square plate of 30 cm side (fairly rigid), the values of shear modulus, μ, for different soil categories listed in Table 4.6, can be computed using Equation (4.44) with $c_r = 1.08$ (from Table 4.4) and $v = 0.3$. The same are presented in Table 4.6.

4.8.8 k_s for Foundations Subjected to Dynamic Loads

For the design of foundations subjected to dynamic loads such as in machine foundations, the modulus of subgrade reaction, k_s (also referred to as the coefficient of elastic uniform compression, C_u), has to be obtained from a cyclic plate load test (instead of a plate load test) or wave propagation tests (Kameswara Rao, 2000, 1998).

4.8.8.1 Cyclic Plate Load Test

As the name itself indicates, this is a modified version of the standard plate load test as shown in Figure 4.27. The test is conducted using either standard plate (or square of circular shape of 0.305–0.760 m size or any other size) and involves several loading cycles (loading, unloading, reloading schedule), as per standard practice (Kameswara Rao, 2000). This facilitates in separating the elastic (recoverable) part of the deformation from the plastic part (irrecoverable part or permanent set) which in turn can be related to the Young's modulus of the soil.

Some Salient Features

The bearing pressure–settlement curve obtained from a typical cyclic plate load test is shown in Figure 4.31. After each load application, sufficient time is allowed to ensure

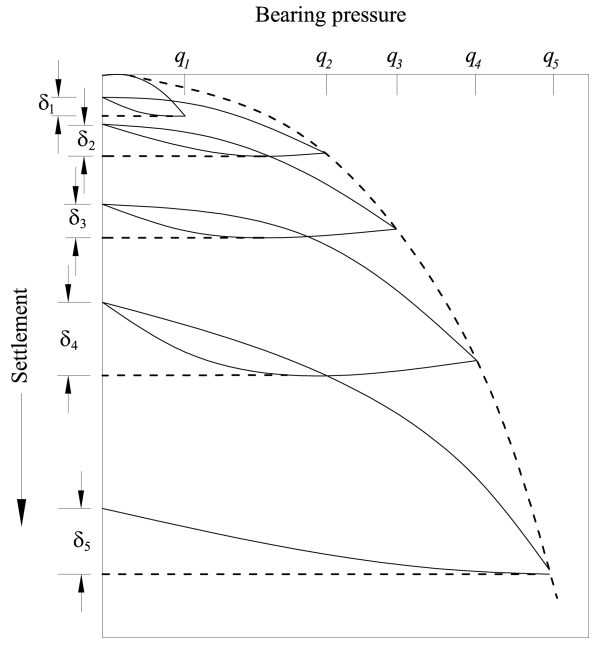

Figure 4.31 Bearing pressure-settlement curve for cyclic plate load test.

that the settlement has attained a final value for all practical purposes at that load level. In Figure 4.31, the recoverable part of the settlement (during unloading) represents the elastic part and the nonrecoverable part signifies the plastic settlement (permanent set). The elastic part of the settlement is plotted as a function of average contact pressure (bearing pressure) in Figure 4.32 and the relationship is observed to be generally linear. The slope of this curve is referred to as the modulus of subgrade reaction, k_s, or the coefficient of elastic uniform compression, C_u.

Coefficient of Elastic Uniform Compression and Spring Constant

From the curve shown in Figure 4.32, the slope referred to as the coefficient of elastic uniform compression, C_u (or k_s), can be expressed as

$$k_s = C_u = \frac{q}{w} \tag{4.46}$$

where q is the bearing pressure (load per unit area) and w is the elastic settlement and is applicable for vertical displacement. Then the spring constant (k) for vertical deformation is given by

$$k = C_u A = k_s A \tag{4.47}$$

where A = contact area of plate, that is, bearing area.

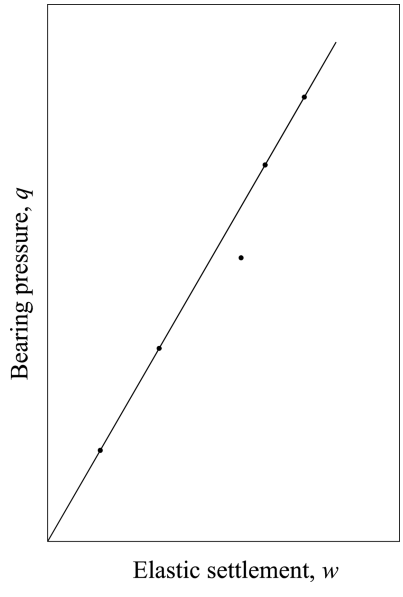

Figure 4.32 Determination of k_s/C_u from cyclic plate load test data.

All other elasticity solutions discussed in Sections 4.8.5–4.8.7 remain the same except that in dynamic situations $k_s\ (= C_u)$ obtained from cyclic plate load test discussed above has to be used instead of k_s from normal plate load test.

4.9 Soil–Structure Interaction Equations

Thus after adopting suitable foundation model for soil medium to evaluate the soil reaction as discussed in Section 4.7.3, the equation for soil–structure interaction can be written from Equation (4.14) for beams and Equation (4.18) for plates. Adopting Winkler's model due to its simplicity for analysis as well as evaluation of parameters from laboratory and field tests as described in Sections 4.7.4 and 4.8, these equations can be written by replacing the soil reaction $q(x) = kw$ and are given in Equations (4.31) and (4.32).

These are as follows, for beams on elastic foundations (Figure 4.18, Equation (4.14))

$$EI\frac{d^4w(x)}{dx^4} + kw(x) = p(x) \tag{4.48}$$

where

EI = flexural rigidity of the beam or footing
$w(x)$ = vertical deflection of the beam soil interface
k = spring constant = k_sB
k_s = modulus of subgrade reaction applicable to beams as described in Section 4.8 (for example, Equations (4.37), (4.38), (4.41) or (4.30a), whichever may be appropriate)
B = width of the beam cross section
$p(x)$ = vertical load applied on the beam/footing

For plates on elastic foundations (Figure 4.19, Equation (4.32); this equation is used for rafts, mats, square foundations, annular foundations and foundations with *L/B* ratios not more that 2–3).

$$D\nabla^4 w(x,y) + kw(x,y) = p(x,y) \tag{4.49}$$

where

D = flexural rigidity of plate = $\frac{E_p h^3}{12(1-v_p^2)}$
E_p, v_p = modulus of elasticity and Poisson's ratio of plate material
h = thickness of the plate
$\nabla^4 = \nabla^2\nabla^2$
∇^2 = Laplace operator
k = spring constant for plate
= modulus of subgrade reaction adjusted to the plate size and shape from the results of the standard plate load test as discussed in Section 4.8.5
$w(x,y)$ = vertical deflection of the plate soil interface
$p(x,y)$ = vertical load applied on the plate/footing.

For dynamic loads on elastic foundations (machine foundations), the modulus of the subgrade reaction has to be obtained preferably from cyclic plate load test or wave propagation tests as outlined in Section 4.8.8. The spring constant in such cases can then be obtained using Equation (4.47).

4.10 Summary

1. The role and types of foundations for transferring the loads to the soil stratum below is described.
2. The essential features of foundation design using conventional methods as well as rational method are highlighted.
3. Foundation design practices in difficult soils are outlined.
4. The need for soil–structure interaction analysis for rational design of foundations is presented.
5. The behavior of beams and plates on elastic foundations is discussed.
6. Various foundation models are discussed.
7. Features of Winkler's model and evaluation of necessary parameters for design from laboratory and field tests are outlined.
8. The governing equations for beams and plates on elastic foundations are presented. The expressions for the determination of all the parameters involved in the equations are discussed in detail. A few examples for the evaluation of parameters are presented.

5

Analysis of Footings on Elastic Foundations

5.1 Introduction

As mentioned in Chapter 4, the two approaches for the analysis and design of foundations are:

1. The conventional approach, which assumes the foundation to be rigid and the contact pressure at the interface to be planar.
2. The rational approach, which incorporates the flexibility of the footing as well as the soil contact pressure based on elastic theories using modulus of subgrade reaction.

The footing can be idealized as a beam (spread footings, combined footings, strap footings, wall footings, etc.) or as a plate (mat or raft foundations, circular footings, annular or ring footings and footings of general shape which are two-dimensional in plan supporting several loads from columns, walls, etc.). While several models for incorporating soil reaction in the soil–structure interaction equations (Equations (4.14) and (4.18)) are discussed in Section 4.7, the Winkler's model is used extensively in this chapter for detailed solutions and rational design due to its simplicity in analysis as well as evaluation of the soil parameters. A brief review of important contributions is presented below.

5.2 Literature Review

Analysis of footings on Winkler foundation model using analytical and numerical methods has been carried out by several pioneers in this area. Some important contributions are highlighted in this section.

5.2.1 Analytical Solutions

The earliest classical works on the subject were due to Winkler (1867), Hertz (1884), Zimmermann (1888), Reissner (1937), Hetenyi (1946), Gorbunov-Posadov (1949), Seely

Foundation Design: Theory and Practice N. S. V. Kameswara Rao
 ISBN: 978-0-470-82534-1

and Smith (1952), Timoshenko and Krieger (1959), Vlasov and Leontov (1966), and several others. Vlasov and Leontev (1966) also gave solutions to a large number of problems of beams, plates and shells on elastic foundations, idealizing the soil medium as a two parameter model which ignores the horizontal displacements in the medium. Kameswara Rao (1969, 1971) presented general solutions to beams and plates on elastic foundations using a discrete continuum model for soil, which incorporates horizontal displacements also as a modification to Vlasov's model. They presented the solutions using the versatile method of initial parameters.

Butterfield and Banerjee (Sridhar, 1999) gave solutions for settlement and contact pressure for rigid rectangular rafts. Brown (Sridhar, 1999) obtained solutions for contact pressure and bending moment in rigid, square and rectangular rafts subjected to various combinations of concentrated loads.

Fletcher and Herman (Sridhar, 1999) analyzed a beam resting on flexible elastic foundation and determined the applicability of the Winkler model and more mathematically refined models which included terms involving the derivative of the deflection without resulting in any mathematical difficulty. A procedure for finding the foundation coefficients when the elastic constants are known was developed.

Chan and Cheung (Sridhar, 1999) gave values of contact pressure for rectangular and circular rigid footings due to concentric load and eccentric loading. These solutions enable an estimate to be made of the bending moment in a rigid footing.

Dasgupta (Sridhar, 1999) considered an axially constrained beam resting on Winkler foundation and obtained solutions for beam using finite element method as well as the differential equation method. The two solutions are compared and are in close agreement to each other.

Some of the exact solutions available for beams and plates on elastic foundations are presented in the subsequent section (Section 5.3). The method of solution for general loads and moments acting on the footing, is discussed in detail using the method of initial parameters (MIP), which is very versatile (Vlasov and Leontev, 1966; Kameswara Rao, 1969, 1971).

5.2.2 Numerical Methods and Finite Difference Method

Several solutions have been presented using numerical methods such as the finite difference method (FDM), the Runge–Kutta method and iterative methods to take care of the problems not solvable by exact methods. Of these the most popular is FDM.

Malter (1958) gave solutions of beams on elastic foundations using FDM. Teng (1964) worked out several examples using FDM. Rijhsinghani (1961) presented detailed solutions for plates on elastic foundations (PEF) using FDM. There are a very large number of books and publications on FDM and its applications in soil–structure interaction analysis (Teng, 1964). Glyn Jones (1997) presented a detailed analysis of beams on Winkler's elastic foundations using finite difference theory. He also gave a number of references on the subject. He developed a software package for beams on elastic foundations (BEF). The details on the application of these methods to beams and plates on elastic foundations are given in Chapter 6.

5.2.3 Finite Element Method

The analysis of beams and plates on elastic foundations was also analyzed by various authors using the finite element method (FEM) as summarized below. Further, a detailed discussion is given in Chapter 7.

Cheung and Zienkiewicz (Sridhar, 1999) obtained the solutions for square rafts of arbitrary flexibility. The stiffness of the soil was derived from Boussinesq's equation and combined with plate bending finite elements to form a stiffness matrix for the whole system. The displacements were solved using the FEM method. The method is capable of handling both isotropic and orthotropic plates on elastic media with general loading using either a semi-infinite elastic continuum model or a linear Winkler model for the soil medium.

Cheung and Nag (Sridhar, 1999) analyzed plates and beams on an elastic continuum using the finite element method (FEM). The horizontal contact pressures at the interface between structure and foundations were incorporated in the analysis. The effects due to separation of contact surfaces and due to uplift were also investigated.

Svec and Gladwell (Sridhar, 1999) analyzed a thick plate resting on a Winkler foundation and a homogenous isotropic elastic half space, using FEM. They improved the method of Cheung and Zienkiewicz by assuming a continuous contact pressure distribution, described by a third-degree polynomial, under each plate finite element. They also developed a 10-noded triangular plate bending element specifically for contact problems.

Wood and Larnach (Sridhar, 1999) developed computer programmes using FEM for the analysis of raft foundations using both linear and nonlinear soil models. It was shown that the critical edge conditions associated with a stiff raft foundation could be correctly modeled only if a nonlinear soil analysis is used.

Fraser and Wardle (Sridhar, 1999) presented numerical solutions for the displacements and maximum bending moments for uniformly loaded raft foundations of arbitrary flexibility on a homogenous elastic layer of finite thickness overlying a rough rigid base. The solutions were obtained by FEM with the interaction between raft and finite soil layer being incorporated through the use of surface elements. Variations in raft rigidity, L/B ratio, soil layer depth and v (Poisson's ratio) can markedly effect both displacements and bending moments in raft foundations.

Ting and Mocry (Sridhar, 1999) developed a stiffness matrix for a beam on elastic foundation and element load vectors due to concentrated forces, concentrated moments, and linearly distributed forces. The stiffness and flexibility matrices were derived from the exact solution of the differential equation. The results of this finite element analysis are exact for Navier's and Winkler's assumptions.

Puttonen and Varpasuo (Sridhar, 1999) applied the boundary element method (BEM) for plates on elastic foundations. The results obtained by using a small number of boundary elements compared favorably with the results obtained by finite element mesh using SAP IV. The study was conducted by using both direct and indirect BEM, with direct BEM giving better results.

Zekai Celep (Sridhar, 1999) analyzed the behavior of elastic plates of rectangular shape on a tensionless Winkler foundation. The rectangular plate problem was investigated here by considering external uniformly distributed loads (UDLs), concentrated loads and moments without using any assumption on the shape of the contact region. The tensionless character of the foundation was taken into account by using an auxiliary function. Using Galerkin's method the problem was reduced to the solution of a system of algebraic equations.

5.3 Analysis of BEF

The governing equations for the beam–foundation interaction (Figure 4.18, Section 4.7) is derived as in Equation (4.14) as

$$EI\frac{d^4w}{dx^4} + kw = p(x) \tag{5.1}$$

where

w = vertical deflection at the interface of the beam foundation system
EI = flexural rigidity of the beam
$k = k_s b$ = spring constant of the soil idealizing it as Winkler's single parameter model
k_s = modulus of subgrade reaction to be evaluated from appropriate tests on soil outlined in Section 4.8
kw = contact pressure/soil reaction
b = width of the beam
h = depth of the beam
$p(x)$ = vertical load applied on the beam.

The Cartesian coordinates x, y, z, conventions of the classical bending theory for shear force Q, bending moment M, contact pressure $q(x)$ $(= kw)$ are shown in Figure 4.20.

The exact solution for the above problem was presented by Zimmerman (1888) and more comprehensively by Hetenyi (1946). Some of these classical solutions are presented in the following sections.

5.3.1 General Solution

The governing Equation (5.1) is an ordinary differential equation (ODE) and can be solved exactly as follows. The equation can be nondimensionalized as

$$\frac{d^4w}{d\eta^4} + 4(\lambda L)^4 w = \frac{L^4 p(x)}{EI} \tag{5.2}$$

where

$$\lambda = \sqrt[4]{\frac{k}{4EI}} = \sqrt[4]{\frac{bk_s}{4EI}} \quad (\text{units of } L^{-1}) \tag{5.3}$$

$$\eta = \frac{x}{L} = \text{dimensionless parameter} \tag{5.4}$$

L = unit length for nondimensionalization (can be taken as length of the beam for finite beams)
x = distance coordinate along the length of the beam
λL = dimensionless parameter of beam characteristics.

The characteristic Equation (ODE theory) (5.2) is

$$m^4 + 4(\lambda L)^4 = 0 \tag{5.5}$$

where

$$m = \frac{d}{d\eta} = L\frac{d}{dx}$$

The characteristic roots of Equation (5.5) are

$$m_{1,2,3,4} = \pm \lambda L(1 \pm i) \tag{5.6}$$

where $i = \sqrt{-1}$ is an imaginary constant.

The total solution of the ODE (5.1) or (5.2) can be written as

$$w = w_h + w_p \tag{5.7}$$

where

w_h = homogeneous part of the solution

w_p = particular integral part of the solution depending on the intensity of the distributed load $p(x)$ per unit length of the beam.

The homogeneous solution can be written as

$$\begin{aligned} w_h &= e^{\lambda x}(C_1 \cos \lambda x + C_2 \sin \lambda x) + e^{-\lambda x}(C_3 \cos \lambda x + C_4 \sin \lambda x) \\ &= e^{\lambda L\eta}(C_1 \cos \lambda L\eta + C_2 \sin \lambda L\eta) + e^{-\lambda L\eta}(C_3 \cos \lambda L\eta + C_4 \sin \lambda L\eta) \end{aligned} \tag{5.8}$$

where C_1 to C_4 are arbitrary constants to be determined using boundary conditions.

Equation (5.8) can also be expressed in terms of hyperbolic functions as

$$w_h = C_1F_1 + C_2F_2 + C_3F_3 + C_4F_4 \tag{5.9}$$

where C_1, C_2, C_3, C_4 are arbitrary constants to be solved uniquely from the total solution (Equation (5.7)) using the four boundary conditions at both ends of the beam (two at each end that is, 4 conditions). Functions F_1 to F_4 are called the bases of the solution and can be expressed from Equation (5.8) as

$$\begin{aligned} F_1 &= \cosh \lambda L\eta \cos \lambda L\eta \\ F_2 &= \cosh \lambda L\eta \sin \lambda L\eta \\ F_3 &= \sinh \lambda L\eta \cos \lambda L\eta \\ F_4 &= \sinh \lambda L\eta \sin \lambda L\eta \end{aligned} \tag{5.10}$$

The more commonly used boundary conditions for the beam ends are given below.

1. Free end:

$$\text{Bending moment } (B.M) = M = -EI\frac{d^2w}{dx^2} = -\frac{EI}{L^2}\frac{d^2w}{d\eta^2} = 0 \tag{5.11}$$

$$\text{Shear force } (S.F) = Q = -EI\frac{d^3w}{dx^3} = -\frac{EI}{L^3}\frac{d^3w}{d\eta^3} = 0$$

2. Simply supported end:

$$\begin{aligned} &\text{Vertical deflection} = w = 0 \\ &\text{Bending moment} \quad = M = -EI\frac{d^2w}{dx^2} = -\frac{EI}{L^2}\frac{d^2w}{d\eta^2} = 0 \end{aligned} \tag{5.12}$$

3. Fixed end:

$$\text{Vertical deflection} = w = 0$$
$$\text{Slope} = w' = \frac{dw}{dx} = \frac{1}{L}\frac{dw}{d\eta} = 0 \tag{5.13}$$

For other types of boundary conditions, one can refer to Crandall, Dahl and Lardener (1972), Jones (1997) and other books on applied mechanics. The particular integral w_p in the Equation (5.7) depends on the nonhomogenous function $p(x)$ of the ODE (Equations (5.1) and (5.2)). The various methods for obtaining the particular integral of ODE are available in any of the standard books on engineering mathematics (Kreyszigh, 1967). For example $p(x) = p(\eta) = p_0 =$ constant, w_p can be easily obtained as

$$w_p = \frac{p_0}{k} = \frac{p_0}{4EI\lambda^4} \tag{5.14}$$

For other types of continuous or discrete or partly continuous external loads acting on the footing, the normal methods used in beam bending theory can be used for getting the particular integral and the total solution. For finite beams on elastic foundations, general solution for such cases is presented using MIP in the following sections (Vlasov and Leontev, 1966; Kameswara Rao, 1969, 1971).

5.4 Infinite Beams on Elastic Foundations

Consider an infinite beam on an elastic foundation subjected to a concentrated load P at the origin ($x = 0$, without any loss of generality) as shown in Figure 5.1. Thus $p(x) = 0$ over the whole length of the infinite beam except at the origin where there is a concentrated load P. This concentrated load can be considered as a shear boundary condition rather than as an external load (as is the usual practice in applied mechanics/structural mechanics/beam theory). Also the solution can be taken in the form of Equation (5.8) to take advantage of the infinite geometry of the beam-foundation system. This essentially means that we can neglect the nonfeasible functions in the solution, that is, terms containing $e^{\lambda x}$ $(= e^{\lambda L\eta})$ have to be neglected as deflections exponentially increase with the distance x from the load, which is unrealistic along the positive x axis. Similarly $e^{-\lambda x}$ $(= e^{-\lambda L\eta})$ terms have to be neglected for the negative x axis. Hence the total solution (since $w_p = 0$ for $p(x) = p(\eta) = 0$) can be written from Equation (5.8) as

1. For $0 \leq x \leq \infty$ (along positive x – axis)

$$w = e^{-\lambda x}(C_3 \cos \lambda x + C_4 \sin \lambda x) \tag{5.15}$$

2. For $\infty \leq x \leq 0$ (along negative x-axis)

$$w = e^{\lambda x}(C_1 \cos \lambda x + C_2 \sin \lambda x) \tag{5.16}$$

Arbitrary constants C_1, C_2, C_3, C_4 have to be solved from the continuity conditions of w, $w'\left(= \frac{dw}{dx}\right)$, $M\left(= -EI\frac{d^2w}{dx^2}\right)$ and jump discontinuity in shear force $Q\left(= -EI\frac{d^3w}{dx^3}\right)$, at $x = 0$.

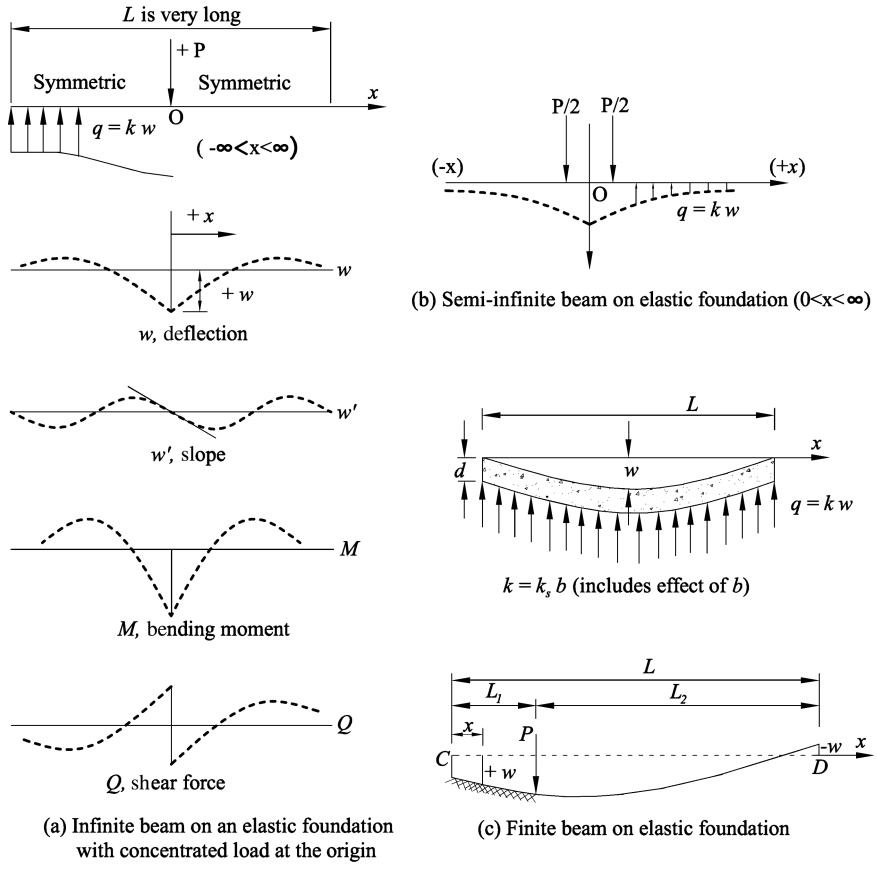

Figure 5.1 Beams on elastic foundations.

Alternatively, using the symmetry at $x = 0$, only one-half of the beam foundation system can be considered [either $+x$ axis (i.e., 0 to $+\infty$) or $-x$ axis (i.e., 0 to $-\infty$)] with half the load acting on either side of the origin as shown in Figure 5.1(b). This is equivalent to solving the problem of a semi-infinite beam on elastic foundation with the load $P/2$ acting at the origin. Considering the positive x axis for the analysis (without any loss of generality), the solution and boundary conditions in this case can be written as follows.

For $0 \leq x \leq \infty$ (along positive x axis)

$$w = e^{-\lambda x}(C_3 \cos \lambda x + C_4 \sin \lambda x) \tag{5.17}$$

Boundary conditions at $x = \infty$ are automatically satisfied by making $C_1 = C_2 = 0$ in the general solution as deflections and all other parameters become zero at infinity. Equation (5.17) satisfies these conditions and hence is a feasible solution.

Boundary conditions at $x = 0$, with symmetry of the beam at $x = 0$, we have

$$\text{Bending moment, } M = -EI\frac{d^2w}{dx^2} = 0 \tag{5.18}$$

$$\text{Shear force, } Q = -EI\frac{d^3w}{dx^3} = -\frac{P}{2} \tag{5.19}$$

Substituting for w from Equation (5.17) in (5.18) and (5.19) and putting $x = 0$, the resulting expressions are

$$C_4 = 0 \text{ and } C_3 = \frac{P}{4\lambda^3 EI} \tag{5.20}$$

Hence the solution for the deflection (Equation (5.17)) becomes

$$w = \frac{P}{4\lambda^3 EI}e^{-\lambda x}\cos \lambda x \tag{5.21}$$

Knowing the deflection, the other parameters such as slope, BM, SF and contact pressure can be written as follows

$$\text{Slope, } w' = \frac{dw}{dx} = -\frac{P}{4\lambda^2 EI}e^{-\lambda x}(\cos \lambda x + \sin \lambda x) \tag{5.22}$$

$$\begin{aligned}\text{Bending moment, } M &= -EI\frac{d^2w}{dx^2} \\ &= -\frac{P}{2\lambda EI}e^{-\lambda x}\sin \lambda x\end{aligned} \tag{5.23}$$

$$\begin{aligned}\text{Shear force, } Q &= -EI\frac{d^3w}{dx^3} \\ &= -\frac{P}{2EI}e^{-\lambda x}(\cos \lambda x - \sin \lambda x)\end{aligned} \tag{5.24}$$

$$\text{Contact pressure, } q(x) = kw = P\lambda e^{-\lambda x}\cos \lambda x \tag{5.25}$$

Typical distribution of the above parameters is shown in Figure 5.1(a). Solutions for other types of loads can be obtained in a similar manner (Hetenyi, 1946).

5.4.1 *Semi-Infinite Beams on Elastic Foundations Subjected to P at $x = 0$*

These are shown in Figure 5.1(b) for $0 < x < \infty$, and (or) $0 > -x > -\infty$. This problem has been solved already above by treating an infinite beam as the superposition of two semi-infinite beams each lying along the positive and negative x axes. Thus the solutions are exactly the same as in Equations (5.21)–(5.25) with $P/2$ being replaced by P. For example the solution for deflection in this case becomes (from Equation (5.21))

$$w = \frac{P}{2\lambda^3 EI}e^{-\lambda x}\cos \lambda x \tag{5.26}$$

Similarly the other quantities w', M, Q and $q(x)$ can be written from Equations (5.22)–(5.25).

5.5 Finite Beams on Elastic Foundations

Consider a beam of finite length on an elastic foundation subjected to transverse loads (Figure 5.1(c)). The general solution is already given by either Equation (5.8) or (5.9). For further discussion, the solution is taken (without any loss of generality) in the form of Equation (5.9) and the total solution can be obtained by adding the particular integral w_p, as given in Equation (5.7) to the homogeneous solution. Several exact solutions have been obtained for various cases of loading by Hetenyi (1946) and others. Charts and tables for a few generic solutions are available (Seely and Smith, 1952; Iyengar and Ramu, 1979). The solutions given by Seely and Smith (1952) for BM and deflection w for a finite beam (constant EI) on elastic foundation acted by a concentrated load P are shown in Figure 5.2. Each curve corresponds to a footing with P at 0, $L/12$, $L/6\ldots$ from the left end. The deflection is shown as a ratio of average deflection $w_0 = \frac{P}{Lk}$ and

$$\text{Bending moment, } M_o = \frac{P}{4\lambda} \tag{5.27}$$

where

L = length of the beam
k = spring constant of soil = $k_s b$
k_s = modulus of subgrade reaction
b = width of the beam
$\lambda = \sqrt[4]{\frac{k}{4EI}}$ as defined in Equation (5.3).

These curves are useful in practice. By superposition of the results the solutions for other loads such as multiple concentrated loads (as in combined footings), partially distributed loads and so on can be computed. This is illustrated in the following example.

Example 5.1

Obtain the responses of a footing subjected to vertical concentrated loads as shown in Figure 5.3

$$\text{Modulus of elasticity of RCC beam} = 2.8 \times 10^{10}\ \text{N/m}^2$$

$$\begin{aligned}\text{Moment of inertia} = \text{I} &= \text{bd}^3/12 \\ &= 1.2 \times 0.53/12 \\ &= 0.0125\ \text{m}^4\end{aligned}$$

Modulus of subgrade reaction (accounting for the rectangular geometry of the contact area) of soil $= 35.28 \times 10^6\ \text{N/m}^3$

Spring constant of the beam foundation system

$$\begin{aligned}k &= k_s b \\ &= 1.2 \times 35.28 \times 10^6\ \text{N/m}^2 \\ &= 4.2336 \times 10^7\ \text{N/m}^2\end{aligned}$$

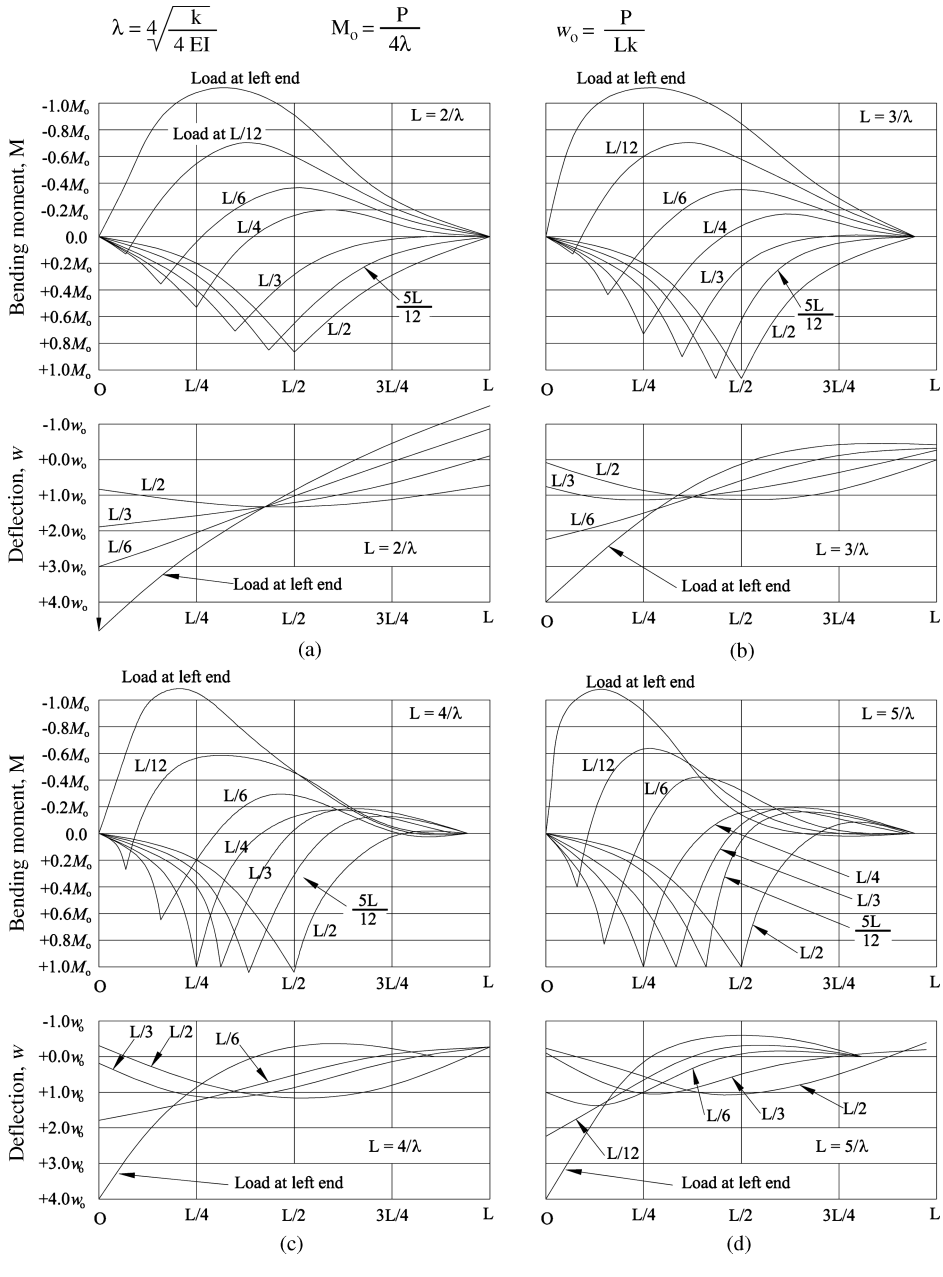

Figure 5.2 Responses of footings of finite length due to concentrated loads. (Reprinted from F.B. Seely and J.O. Smith, *Advanced Mechanics of Materials*, 2nd edition, with permission of John Wiley & Sons, Inc., New York. © 1952.)

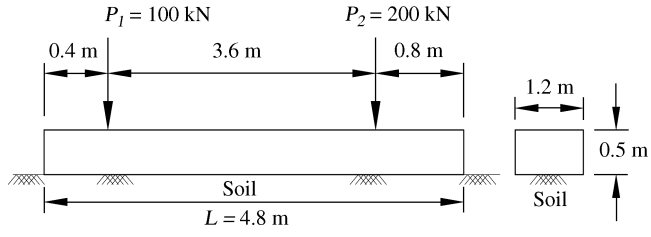

Figure 5.3 Finite beam on elastic foundation.

$$\lambda = \sqrt[4]{\frac{k}{4EI}} = \sqrt[4]{\frac{4.2336 \times 10^7}{4 \times 2.8 \times 10^{10} \times 0.0125}} = 0.417\ \text{m}^{-1}$$

$$\lambda L = 0.417 \times 4.8 = 2$$

Accordingly, the response curves given in Figure 5.2(a) are applicable for computation of responses. The 100 kN load is applied at 0.4 m (L/12) from the left end and 200 kN load is applied at 0.8 m (L/6) from the right end. The responses can now be superposed to get the total response as shown in Figure 5.4. For example the moment diagrams are superposed with curve (1) for load $P_1 = 100$ kN acting at L/12 from the left end and curve (2) for load $P_2 = 200$ kN acting at L/6 from the right end. It may be noted that curve (2) is plotted inversely for superposition as the given curves in Figure 5.2 are applicable for loads at given distances from the left end. The maximum ordinate between the two curves gives the maximum bending moment in the beam, that is, $M_{\max}$.

$$M_{\max} = (0.63P_1 + 0.32P_2)/4\lambda = (0.63 \times 100 + 0.32 \times 200)/(4 \times 0.417)$$
$$= 76.2\ \text{kN/m}$$

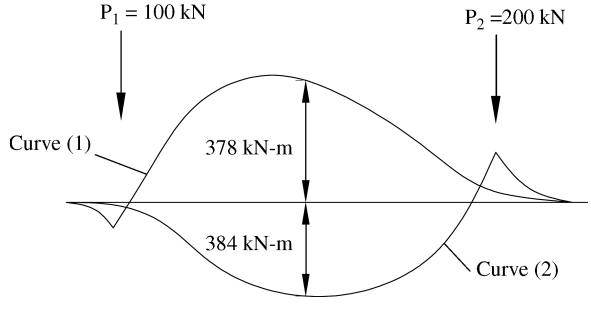

Figure 5.4 Bending moment diagram.

Similarly the deflection, slope, shear force and contact pressures can be calculated.

For other types of loads, the curves given in Figure 5.2 can be used and responses can be obtained using superposition, interpolation and approximations as may be appropriate. Design tables are also given by Hetenyi (1946), Iyengar and Ramu (1979) and others.

5.5.1 MIP for General Loads and Beam Configurations

The use of graphs and tables for obtaining responses of beams on elastic foundations has been illustrated above. However, the MIP is a powerful method for obtaining exact solutions of ODEs in general and BEF in particular. The method is presented below while the details are given in Vlasov and Leontev (1966) and Kameswara Rao (1969, 1971).

The general homogenous solution of BEF can be taken in the form of Equation (5.9), that is

$$w_h = C_1F_1 + C_2F_2 + C_3F_3 + C_4F_4 = C^TF_h \tag{5.28}$$

where

$$C^T = \{\, C_1 \quad C_2 \quad C_3 \quad C_4 \,\}$$

$$F_h = \begin{Bmatrix} F_1 \\ F_2 \\ F_3 \\ F_4 \end{Bmatrix} = \begin{Bmatrix} \cosh \lambda x \cos \lambda x \\ \cosh \lambda x \sin \lambda x \\ \sinh \lambda x \cos \lambda x \\ \sinh \lambda x \sin \lambda x \end{Bmatrix} \tag{5.29}$$

C^T, F_h are matrices. F_h is called the basis of solutions of the homogeneous ODE. Matrix C represents the four arbitrary constants to be uniquely solved from the four boundary conditions of the beam. Matrix F_h has very interesting properties for differentiation and integration which are helpful for analysis and computation. For example

$$\frac{dF_h}{dx} = \frac{1}{L}\frac{dF_h}{d\eta} = N_hF_h \tag{5.30a}$$

where

$$N_h = \begin{bmatrix} 0 & -\lambda & \lambda & 0 \\ \lambda & 0 & 0 & \lambda \\ \lambda & 0 & 0 & -\lambda \\ 0 & \lambda & \lambda & 0 \end{bmatrix} = \lambda \begin{bmatrix} 0 & -1 & 1 & 0 \\ 1 & 0 & 0 & 1 \\ 1 & 0 & 0 & -1 \\ 0 & 1 & 1 & 0 \end{bmatrix} \tag{5.30b}$$

in which $\eta = \frac{x}{L}$ is a dimensionless parameter as defined in Equation (5.4)

$$\int F_h dx = \frac{1}{2\lambda} \begin{Bmatrix} F_3 + F_2 \\ F_4 - F_1 \\ F_1 + F_4 \\ F_2 - F_3 \end{Bmatrix} = \frac{1}{2\lambda} \begin{bmatrix} 0 & 1 & 1 & 0 \\ -1 & 0 & 0 & 1 \\ 1 & 0 & 0 & 1 \\ 0 & 1 & -1 & 0 \end{bmatrix} \begin{Bmatrix} F_1 \\ F_2 \\ F_3 \\ F_4 \end{Bmatrix} = M_hF_h \tag{5.31a}$$

where

$$M_h = \frac{1}{2\lambda} \begin{bmatrix} 0 & 1 & 1 & 0 \\ -1 & 0 & 0 & 1 \\ 1 & 0 & 0 & 1 \\ 0 & 1 & -1 & 0 \end{bmatrix} \tag{5.31b}$$

The higher order derivatives can be obtained by the repeated use of Equation (5.30a), that is

$$\frac{d^2F_h}{dx^2} = \frac{1}{L^2}\frac{d^2F_h}{d\eta^2} = N_h^2 F_h \tag{5.32}$$

where

$$N_h{}^2 = N_h N_h \tag{5.33}$$

$$\frac{d^nF_h}{dx^n} = \frac{1}{L^n}\frac{d^nF_h}{d\eta^n} = N_h^n F_h \tag{5.34}$$

Matrix N_h can be noted to be symmetric about the secondary diagonal. The relevant parameters can now be expressed in terms of the basis of solutions F_h and arbitrary constants matrix C as below.

$$\left.\begin{aligned} w &= C^T F_h = F_h^T C \\ w' &= \frac{dw}{dx} = \frac{1}{L}\frac{dw}{d\eta} = F_h^T N_h^T C \\ M &= -EI\frac{d^2w}{dx^2} = -\frac{E_b I}{L^2}\frac{d^2w}{d\eta^2} = -EIF_h^T (N_h^2)^T C \\ Q &= -EI\frac{d^3w}{dx^3} = -\frac{E_b I}{L^3}\frac{d^3w}{d\eta^3} = -EIF_h^T (N_h^3)^T C \end{aligned}\right\} \tag{5.35}$$

where the superscript T denotes transpose of the matrix. Equation (5.35) can be expressed in matrix form as

$$\begin{Bmatrix} w \\ w' \\ M \\ Q \end{Bmatrix} = \begin{bmatrix} F_h^T \\ F_h^T N_h^T \\ -EIF_h^T (N_h^2)^T \\ -EIF_h^T (N_h^3)^T \end{bmatrix} C = BC \tag{5.36}$$

The four arbitrary constants to be determined from the total solution using the boundary conditions at both ends of the beam can be expressed in terms of the four relevant parameters of the beam (which are usually used in prescribing the boundary conditions at both ends of the beam) w, w', M and Q evaluated or prescribed at any point, say $x = \eta = 0$, Thus these are called initial parameters. Accordingly, putting $x = \eta = 0$ in Equation (5.36), we get

$$I_p = [B]_{x=\eta=0} C = AC \tag{5.37}$$

where I_p is called the initial parameter matrix.

From Equation (5.37), the arbitrary constants C can be expressed in terms of the initial parameters as

$$C = A^{-1} I_p = G I_p \tag{5.38}$$

Substituting for C in Equation (5.36), the beam parameters at any point along its length can be expressed in terms of the initial parameters I_p as

$$I_p = \begin{Bmatrix} w \\ w' \\ M \\ Q \end{Bmatrix} = BC = BGI_p = KI_p = K \begin{Bmatrix} w_0 \\ w'_0 \\ M_0 \\ Q_0 \end{Bmatrix} \tag{5.39}$$

These intermediate steps for deriving the matrices A, A^{-1} $(= G)$, and K $(=B\,G)$ are given in Appendix 5.A at the end of this chapter.

Matrix K is called the matrix of influence functions. Noting that N_h matrix is quite sparse and values of F_h at $x = 0$ are either 0 or 1, K can be easily obtained from Equation (5.39) as follows

$$[K] = \begin{bmatrix} K_{ww} & K_{ww'} & K_{wM} & K_{wQ} \\ K_{w'w} & K_{w'w'} & K_{w'M} & K_{w'Q} \\ K_{Mw} & K_{Mw'} & K_{MM} & K_{MQ} \\ K_{Qw} & K_{Qw'} & K_{QM} & K_{QQ} \end{bmatrix}$$

$$= \begin{bmatrix} F_1 & \frac{1}{2\lambda}(F_2 + F_3) & \frac{-1}{2\lambda^2 EI}F_4 & \frac{-1}{4\lambda^3 EI}(F_2 - F_3) \\ \lambda(F_3 - F_2) & F_1 & \frac{-1}{2\lambda EI}(F_3 + F_2) & \frac{-1}{2\lambda^2 EI}F_4 \\ 2\lambda^2 EIF_4 & \lambda EI(F_2 - F_3) & F_1 & \frac{1}{2\lambda}(F_2 + F_3) \\ 2\lambda^3 EI(F_2 + F_3) & 2\lambda^2 EIF_4 & \lambda(F_3 - F_2) & F_1 \end{bmatrix} \tag{5.40}$$

where F_1 to F_4 are the basis of solutions given by Equation (5.29). Matrix K has several interesting mathematical properties (Vlasov and Leontev, 1966; Kameswara Rao, 1969, 1971). The following two can be readily noted:

1. The matrix K is symmetric about the secondary diagonal.
2. At $x = 0$, K reduces to an identity matrix I.

Thus, Equation (5.39) gives the homogeneous solution of the beam foundation interaction, the arbitrary constants replaced by the initial parameters of the beam at the initial point (say left end, that is, $x = 0$) of the beam.

The 16 influence functions given in Equation (5.40), that is, $K_{ww}, K_{ww'}, \ldots K_{QQ}$ form a matrix for the direct linear transformation of the initial parameters w_0, w'_0, M_0, Q_0 into any derived parameters such as w, w', M, Q at any point as given by Equation (5.39). After the initial parameters are determined, the problem can be considered as solved.

Any section $x = s$ (s can be taken as zero without any loss of generality) in which w_s, w'_s, M_s, Q_s are known can be taken as initial section. The solutions of w, w', M, Q at a section x-s from the initial section can be determined by the same influence functions provided the homogeneous differential equation of bending [Equation (5.1) with $p(x) = 0$] is valid between these sections, that is, no additional loads are applied on the beam between $x = s$ and x. Accordingly

$$\begin{Bmatrix} w \\ w' \\ M \\ Q \end{Bmatrix} = K\{I_p\}_{x=s} \tag{5.41}$$

However, the argument of the influence function matrix K (with the components K_{ww}, $K_{ww'} \ldots K_{QQ}$) is $x - s$, implying that F_1, F_2, F_3, F_4 have the argument as x–s.

Knowing the initial parameters and the matrix of influence functions obtained from the homogeneous solution of BEF, the nonhomogeneous solution (including the effect of external loads, moments, changes in configurations) can be easily expressed (Vlasov and Leontev, 1966; Kameswara Rao, 1969, 1971). Brief details of this method are presented below.

5.5.2 *Effect of External Loads – General Solution of the Nonhomogeneous Equation*

For the most general case of a beam on an elastic foundation carrying arbitrary external forces and moments as shown in Figure 5.5, the solution of nonhomogeneous differential Equation (5.1) can be written as

$$\begin{Bmatrix} w \\ w' \\ M \\ Q \end{Bmatrix} = [K]\{I_p\} - \begin{Bmatrix} F_w \\ F_{w'} \\ F_M \\ F_Q \end{Bmatrix} = [K]\{I_p\} - \{PI\} \tag{5.42}$$

in which F_w, $F_{w'}$, F_M, F_Q are known functions depending on the load and its distribution. The elements of K are given in Equation (5.40). If any of the parameters w, w', M, and Q has a discontinuity at $x = s_k$ the influence of this must be taken into account for sections $x > s_k$. This influence is equal to the magnitude of the discontinuity multiplied by the corresponding

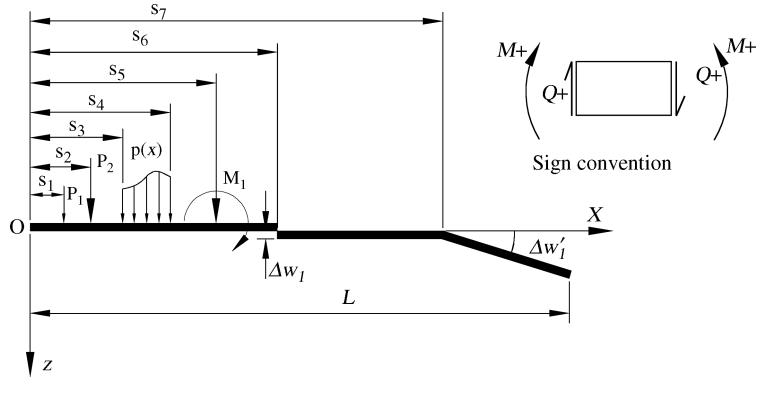

Figure 5.5 Arbitrary loading on the beam.

influence functions evaluated with the argument $(x - s_k)$. These influences are represented by functions F_w, $F_{w'}$, F_M, F_Q in Equation (5.42). This is shown by considering a beam lying on an elastic foundation with a general configuration and loading (Figure 5.5)

For $0 < x < s_1$,

$$F_w = F_{w'} = F_M = F_Q = 0 \tag{5.43}$$

At $x = s_1$, there is a discontinuity in the load and thus Q is affected. The corresponding influence functions which get affected are K_{WQ}, $K_{w'Q}$, K_{MQ}, and K_{QQ}

Therefore, $s_1 < x < s_2$

$$\begin{aligned} F_w &= P_1 \cdot (K_{wQ})_{x-s_1} \\ F_{w'} &= P_1 \cdot (K_{w'Q})_{x-s_1} \\ F_M &= P_1 \cdot (K_{wQ})_{x-s_1} \\ F_Q &= P_1 \cdot (K_{QQ})_{x-s_1} \end{aligned} \tag{5.44}$$

For $s_2 < x < s_3$

$$\begin{aligned} F_v &= P_1 \cdot (K_{wQ})_{x-s_1} + P_2 \cdot (K_{wQ})_{x-s_2} \\ F_\phi &= P_1 \cdot (K_{w'Q})_{x-s_1} + P_2 \cdot (K_{w'Q})_{x-s_2} \\ F_M &= P_1 \cdot (K_{MQ})_{x-s_1} + P_2 \cdot (K_{MQ})_{x-s_2} \\ F_N &= P_1 \cdot (K_{QQ})_{x-s_1} + P_2 \cdot (K_{QQ})_{x-s_2} \end{aligned} \tag{5.45}$$

In a similar manner, influences due to any number of concentrated loads can be taken care of. In the region $s_3 < x < s_4$, there is a distributed load $p(x)$. Accordingly for $s_3 < x < s_4$, for example

$$\begin{aligned} F_w &= P_1 \cdot (K_{wQ})_{x-s_1} + P_2 \cdot (K_{wQ})_{x-s_2} + \int_{s3}^{x} p(s)(K_{wQ})_{x-s} ds \\ F_{w'} &= P_1 \cdot (K_{w'Q})_{x-s_1} + P_2 \cdot (K_{\mathrm{w}'Q})_{x-s2} + \int_{s3}^{x} p(s)(K_{w'Q})_{x-s} ds \\ F_M &= P_1 \cdot (K_{MQ})_{x-s_1} + P_2 \cdot (K_{MQ})_{x-s2} + \int_{s3}^{x} p(s)(K_{MQ})_{x-s} ds \\ F_Q &= P_1 \cdot (K_{QQ})_{x-s_1} + P_2 \cdot (K_{QQ})_{x-s2} + \int_{s3}^{x} p(s)(K_{QQ})_{x-s} ds \end{aligned} \tag{5.46}$$

For $s_4 < x < s_5$, the equations remain the same as in Equation (5.46) with the upper limit of integration in the last term being s_4. A concentrated moment M_1 acts at $x = s_5$. Therefore, for $s_5 < x < s_6$

$$
\begin{aligned}
F_w &= P_1 \cdot (K_{wQ})_{x-s_1} + P_2 \cdot (K_{wQ})_{x-s_2} + \int_{s_3}^{s_4} p(s)(K_{wQ})_{x-s} ds - M_1 (K_{wM})_{x-s_5} \\
F_{w'} &= P_1 \cdot (K_{w'Q})_{x-s_1} + P_2 \cdot (K_{w'Q})_{x-s_2} + \int_{s_3}^{s_4} p(s)(K_{w'Q})_{x-s} ds - M_1 (K_{w'M})_{x-s_5} \\
F_M &= P_1 \cdot (K_{MQ})_{x-s_1} + P_2 \cdot (K_{MQ})_{x-s_2} + \int_{s_3}^{s_4} p(s)(K_{MQ})_{x-s} ds - M_1 (K_{MM})_{x-s_5} \\
F_Q &= P_1 \cdot (K_{QQ})_{x-s_1} + P_2 \cdot (K_{QQ})_{x-s_2} + \int_{s_3}^{s_4} p(s)(K_{QQ})_{x-s} ds - M_1 (K_{QM})_{x-s_5}
\end{aligned}
\tag{5.47}
$$

Similarly the changes in slope of the beam as well as breaks in the beam (discontinuity in deflection) and so on as shown in Figure 5.5 can be taken into account for the nonhomogeneous solution of the BEF (Vlasov and Leontev, 1966; Kameswara Rao, 1969, 1971).

Thus all the functions F_w, $F_{w'}$, F_M, F_Q can be obtained by accounting for the corresponding influence functions due to respective discontinuities in any of the parameters w, w', M and Q. Hence the complete solution of the nonhomogeneous differential Equation (5.1) is given by Equation (5.42) and the required quantities can be evaluated at any section of the beam by incorporating the particular integrals as explained above.

The initial parameters w_0, w_0', M_0, Q_0 can be obtained very simply by this method, the initial section of the beam being chosen arbitrarily. Thus by selecting one of the beam ends as initial section ($x = 0$), we automatically know two of the four parameters that is, the two boundary conditions at the left end of the beam prescribed in terms of any two of w, w', M and Q. The other two initial parameters can always be found from two equations defining the boundary conditions at the other end of the beam.

Thus, for a simply supported beam, we obtain respectively for $x = 0$ and $x = L$

$$w_o = 0, \quad M_o = 0 \tag{5.48}$$

$$w_L = 0, \quad M_L = 0 \tag{5.49}$$

$$w_L = 0 \rightarrow w_o' K_{ww'} + Q_o K_{wQ} - F_w = 0 \tag{5.50}$$

$$\mathrm{M_L} = 0 \rightarrow w_o' K_{Mw'} + Q_o K_{MQ} - F_M = 0 \tag{5.51}$$

where $K_{ww'}$, K_{wQ}, $K_{Mw'}$, K_{MQ}, F_w, F_M are determined from $x = L_i$.

Thus, the two unknown initial parameters w_0' and Q_0 can be obtained very easily from the two simultaneous Equations (5.50) and (5.51) as

$$w_0' = \frac{F_w K_{MQ} - F_M K_{wQ}}{K_{ww'} K_{MQ} - K_{Mw'} K_{wQ}} \tag{5.52}$$

$$Q_0 = \frac{F_M K_{ww'} - F_w K_{Mw'}}{K_{ww'} K_{MQ} - K_{Mw'} K_{wQ}} \tag{5.53}$$

Similarly for a free–free beam on elastic foundations, the boundary conditions are:

$$\text{At } x = 0, \quad M_o = Q_o = 0 \tag{5.54}$$

$$\text{At } x = L, \quad M_L = Q_L = 0 \tag{5.55}$$

Thus two of the IPs are known, that is, $M_L = Q_L = 0$. The remaining two IPs w_0 and w_0' can be obtained from the boundary conditions at $x = L$ of the beam as below.

Substituting Equations (5.42) and (5.54) in (5.55) gives (two of the initial parameters $M_o = Q_o = 0$ are known)

$$M_L = K_{Mw} w_o + K_{Mw'} w_o' - F_M = 0 \tag{5.56}$$

$$Q_L = K_{Qw} w_o + K_{Qw'} w_o' - F_Q = 0 \tag{5.57}$$

where $K_{Mw}, K_{Mw'}, K_{Qw}, K_{Qw'}, F_M, F_Q$ are calculated for $x = L$. Then the two IPs w_0 and w_0' can be obtained from the two simultaneous Equations (5.56) and (5.57) as

$$w_0 = \frac{F_M K_{Qw'} - F_Q K_{Mw'}}{K_{Mw} K_{Qw'} - K_{Qw} K_{Mw'}} \tag{5.58}$$

$$w_0' = \frac{F_Q K_{Mw} - F_M K_{Qw}}{K_{Mw} K_{Qw'} - K_{Qw} K_{Mw'}} \tag{5.59}$$

If the beam ends are fixed, the boundary conditions are

$$\text{At } x = 0, \quad w_o = w_o' = 0 \tag{5.60}$$

$$\text{At } x = L, \quad w_L = w_L' = 0 \tag{5.61}$$

Thus the two IPs $w_o = w_o' = 0$ being known, the remaining two IPs M_0 and Q_0 can be solved from the boundary conditions of the beam at $x = L$ as given in Equations (5.60) and (5.61). Accordingly from Equations (5.42), (5.60) and (5.61) we have these two equations

$$w_L = K_{wM} M_o + K_{wQ} Q_o - F_w = 0 \tag{5.62}$$

$$w_L' = K_{w'M} M_o + K_{w'Q} Q_o - F_{w'} = 0 \tag{5.63}$$

Then M_0 and Q_0 can be solved from the above Equations (5.62) and (5.63) as

$$M_0 = \frac{F_w K_{w'Q} - F_{w'} K_{wQ}}{K_{wM} K_{w'Q} - K_{w'M} K_{wQ}} \tag{5.64}$$

$$Q_0 = \frac{F_{w'} K_{wM} - F_w K_{w'M}}{K_{wM} K_{w'Q} - K_{w'M} K_{wQ}} \tag{5.65}$$

For beams with different combination of boundary conditions and other variations of boundary conditions, the IPs can be similarly obtained. Once the IPs are known the total solution at any cross section of the beam can be obtained as explained in detail in the above Section 5.5.2. A few examples of MIP are presented below.

Example 5.2

Obtain the solutions for BEF given in Example 5.1 (Figure 5.3). All the data is given in Example 5.1

Solution:

$\lambda = 0.417\,\mathrm{m}^{-1}$. Beam ends are free that is, $M = Q = 0$ at $x = 0$ and L. Hence, the solution at $x = 0$ becomes,

$$\begin{Bmatrix} w \\ w' \\ M \\ Q \end{Bmatrix} = [K] \begin{Bmatrix} w_0 \\ w'_0 \\ 0 \\ 0 \end{Bmatrix} - \begin{Bmatrix} F_w \\ F_{w'} \\ F_M \\ F_Q \end{Bmatrix} \tag{5.66}$$

Accordingly, for $0 < x < 0.4$ m, the solution can be obtained as follows.

Noting that $M_o = Q_o = 0$ as the beam end is free at $x = 0$ and $[K]$ is given by Equation (5.40), we can write the total solution as follows

$$\begin{Bmatrix} w \\ w' \\ M \\ Q \end{Bmatrix} = [K] \begin{Bmatrix} w_0 \\ w'_0 \\ M_0 \\ Q_0 \end{Bmatrix} = [K] \begin{Bmatrix} w_0 \\ w'_0 \\ 0 \\ 0 \end{Bmatrix} \tag{5.67}$$

For $0.4 \leq x \leq 4$, (there is load $P_1 = 100$ kN applied at $x = 0.4\,\mathrm{m} = s_1$) in which

$$\begin{aligned} F_w &= P_1 \cdot (K_{wQ})_{x-s_1} \\ F_{w'} &= P_1 \cdot (K_{w'Q})_{x-s_1} \\ F_M &= P_1 \cdot (K_{MQ})_{x-s_1} \\ F_Q &= P_1 \cdot (K_{QQ})_{x-s_1} \end{aligned} \tag{5.68}$$

where $P_1 = 100$ kN and $s_1 = 0.4$ m and K_{wQ} to K_{QQ} in Equation (5.68) have to be evaluated at $x - s_1$, that is, $x - 0.4$ m.

For $4 \leq x \leq 4.8$ m, there is another load $P_2 = 200$ kN at $s_2 = 4.0$ m. Therefore the solution is

$$\begin{Bmatrix} w \\ w' \\ M \\ Q \end{Bmatrix} = [K] \begin{Bmatrix} w_0 \\ w'_0 \\ 0 \\ 0 \end{Bmatrix} - P_1 \begin{Bmatrix} K_{wQ} \\ K_{w'Q} \\ K_{MQ} \\ K_{QQ} \end{Bmatrix}_{x-s_1} - P_2 \begin{Bmatrix} K_{wQ} \\ K_{w'Q} \\ K_{MQ} \\ K_{QQ} \end{Bmatrix}_{x-s_2} \tag{5.69}$$

Thus the total solutions for the entire BEF are given by Equations (5.66)–(5.69) with all the quantities defined except for the two initial parameters (IPs): Out of the four IPs, two of the IPs are known from boundary conditions of the beam at $x = 0$ that is, $M_o = Q_o = 0$. Hence we should now obtain the remaining IPs, w_0 and w'_0 from the boundary conditions of the beam at $x = L = 4.8$ m that is, $M_L = Q_L = 0$. These can be readily calculated from Equation (5.69) as

follows

$$M_L = K_{Mw} w_o + K_{Mw_o'} w_o' - P_1 (K_{MQ})_{L-s_1} - P_2 (K_{MQ})_{L-s_2} = 0 \tag{5.70}$$

$$Q_L = K_{Qw} w_o + K_{Qw_o'} w_o' - P_1 (K_{QQ})_{L-s_1} - P_2 (K_{QQ})_{L-s_2} = 0 \tag{5.71}$$

Solving for w_o, w_o' from the above two equations, we get

$$w_0 = \frac{[P_1 (K_{MQ})_{L-s_1} + P_2 (K_{MQ})_{L-s_2}] K_{Qw_0'} - [P_1 (K_{QQ})_{L-s_1} + P_2 (K_{QQ})_{L-s_2}] K_{Mw_0'}}{K_{Mw} K_{Qw_0'} - K_{Qw} K_{Mw_0'}} \tag{5.72}$$

$$w_0' = \frac{[P_1 (K_{QQ})_{L-s_1} + P_2 (K_{QQ})_{L-s_2}] K_{Mw} - [P_1 (K_{MQ})_{L-s_1} + P_2 (K_{MQ})_{L-s_2}] K_{Qw}}{K_{Mw} K_{Qw_0'} - K_{Qw} K_{Mw_0'}} \tag{5.73}$$

It may be noted that all the remaining K functions in Equations (5.72) and (5.73) have to be evaluated at $x = L$.

Thus all the four IPs w_0 (Equation (5.72)), w_0' (Equation (5.73)), $M_o = Q_o = 0$ are known. Hence the total solutions in different regions of the beam, that is, 0–0.4, 0.4–4.0 and 4.0–4.8 m can be computed from Equations (5.66)–(5.69). Typical response curves for these are shown in Example 5.1, Figure 5.4. The contact pressure at any point can be obtained as $q(x) = kw(x)$ for $0 \leq x \leq L$.

The solutions for other types of loads and variations in beam configurations can be similarly obtained as explained in Section 5.5.2.

Example 5.3

Obtain the responses of the BEF with the same details as in Example 5.1, but subjected to a UDL of $p_0 = 10$ kN/m length as shown below in Figure 5.6.
From Example 5.1:

$$E = 2.8 \times 10^{10} \text{ N/m}^2$$
$$I = 0.0125 \text{ m}^4$$
$$\lambda = 0.417 \text{ m}^{-1}$$

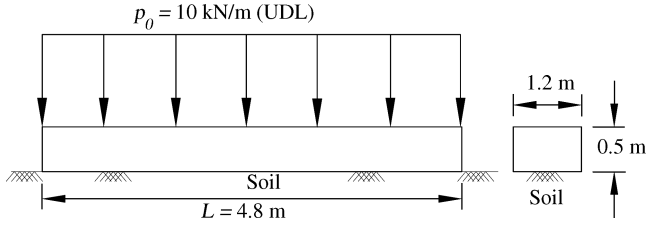

Figure 5.6 Finite beam on elastic foundation subjected to UDL.

Solution:

The solution can be expressed in terms of IPs as follows (noting $M_o = Q_o = 0$ as the beam ends $x = 0$ and $x = L$ are free). The integrals can be written directly as given in Equations (5.46) and (5.47), using Equation (5.31a) as

$$\begin{Bmatrix} w \\ w' \\ M \\ Q \end{Bmatrix} = [K] \begin{Bmatrix} w_0 \\ w_0' \\ 0 \\ 0 \end{Bmatrix} - \int_0^x p_0 \begin{Bmatrix} K_{wQ} \\ K_{w'Q} \\ K_{MQ} \\ K_{QQ} \end{Bmatrix}_{x-s} ds \tag{5.74}$$

The particular integrals for the UDL $p_o = 10\,\text{kN/m}$ are written as given in Equation (5.46). $K_{wQ}, K_{w'Q}, K_{MQ}, K_{QQ}$ are influence functions given in Equation (5.40). Equation (5.74) can be obtained after integration as given below.

$$\begin{Bmatrix} w \\ w' \\ M \\ Q \end{Bmatrix} = [K] \begin{Bmatrix} w_0 \\ w_0' \\ 0 \\ 0 \end{Bmatrix} - \frac{p_0}{2\lambda} \begin{Bmatrix} \frac{1}{2\lambda^3 EI}(F_1 - 1) \\ \frac{1}{2\lambda^2 EI}(F_3 - F_2) \\ F_4/\lambda \\ F_2 + F_3 \end{Bmatrix} \tag{5.75}$$

The unknown IPs w_0 and w_0' can be obtained from the end conditions of the beam at $x = L$ are as follows

$$M_L = \left[(K_{Mw}) w_0 + (K_{Mw'})_{x=L} w_o' - \frac{p_0 (F_4)}{2\lambda^2} \right]_{x=L} = 0 \tag{5.76}$$

$$Q_L = \left[(K_{Qw}) w_0 + (K_{Qw'}) w_o' - \frac{p_0 (F_2 + F_3)}{2\lambda} \right]_{x=L} = 0 \tag{5.77}$$

w_0 and w_0' can be computed from the above two simultaneous Equations (5.76) and (5.77). Then the total solution is given by Equation (5.75).

Alternate Method for Solution:

The solution in this case can also be obtained directly from the homogeneous solution and particular integral of the Equation (5.1) which can be obtained easily in this case of continuous UDL.

The total solution can be written from Equations (5.7), (5.9) and (5.14) as

$$w = C_1 F_1 + C_2 F_2 + C_3 F_3 + C_4 F_4 + \frac{p_0}{4EI\lambda^4} \tag{5.78}$$

where F_1 to F_4 are the basis of homogeneous solutions of ODE (Equation (5.1)), C_1 to C_4 are arbitrary constants to be calculated from the four boundary conditions at both ends of the beam, that is

$$\text{at } x = 0, \quad M_o = Q_o = 0 \tag{5.79}$$

$$\text{at } x = L, \quad M_L = Q_L = 0 \tag{5.80}$$

Substituting Equation (5.78) in the expressions M and Q as given in Equation (5.11) and applying the boundary conditions as in Equations (5.79) and (5.80), we get four nonhomogeneous simultaneous equations with C_1 to C_4 as unknowns. These can be directly solved and the responses at any section along the length of the beam can be computed from Equation (5.78).

5.5.3 Method of Superposition with MIP

The method of initial parameters becomes more involved in calculations when large numbers of loads are acting on the beam. To simplify the computations in such cases, the following modification can be made.

Using the same principle as outlined in previous sections, after determining the influence functions the expression for the parameters, namely $w(x)$, $w'(x)$, $M(x)$, $Q(x)$ can be determined for a single point load and for a given set of boundary conditions.

Then by the method of superposition the solution for other point loads also can be obtained.

Similar procedures can be adopted for UDLs and also for moments.

Thus, in the solution process, there is no need to calculate the particular integral at the end of the beam to determine the initial parameters. The derived expressions can be easily used and computational efficiency can be achieved.

5.5.4 General Comments on Exact Solutions of BEF

The exact solutions of BEF for different loads, beam configurations are given in Hetenyi (1946), Seely and Smith (1952), Iyengar and Ramu (1979) and several others. These solutions can also be obtained using MIP as presented in Section 5.5. The procedure involves several manipulations and could be laborious as well as computationally intensive. Hence for practical problems involving several loads, variable characteristics of footing and soil, numerical methods such as finite difference method (FDM) and finite element method are used which allow considerable flexibility besides the availability of software packages (Bowles, 1996; Jones, 1997; Sridhar, 1999). These are discussed in Chapters 6 and 7.

5.5.5 Approximate Categorization of BEF for Simplification and Idealization of Analysis

For purposes of possible simplifications in analysis BEF are approximately categorized as below. (Bowles, 1996) based on the dimensionless parameter λL and analyzed accordingly.

1. If $\lambda L < \pi/4$, the beam can be treated as rigid.
2. If $\pi/4 < \lambda L < \pi$, the beam is of medium length and can be analyzed as a finite beam.
3. If $\lambda L > \pi$, the beam can be analyzed as a long beam, that is, a semi-infinite or infinite beam.

However, Bowles (1996) observes that these criteria have limited application because of the number of loads and their locations along the length of the beam.

5.6 Plates on Elastic Foundations

Plates are structural elements extending in two dimensions in the horizontal plane that is, along x and y axes. The convention of the dimensions and axes for PEF are shown in Figures 4.19 and 4.21 (rectangular plates). If the plates extend along the r and θ directions, they are called circular plates and the conventions are shown in Figure 4.22. Due to several reasons (discussed in Chapters 2 and 3) such as poor supporting soil, two-dimensional geometry of columns/loads being transferred to the foundation, footings have to be analyzed as PEF.

Considering rectangular plates, the analysis can be carried out depending on the *L/B* ratio (L = length, B = breadth of plate, Figure 4.19) and the idealization, that is, the *L/B* ratio can be used as a guideline for further simplification in analysis as follows.

1. If $L/B > 5$, the footing can be analyzed as a beam (Crandall and Dahl, 1972)
2. If $L/B < 3$, the footing has to be analyzed as a plate.
3. If $3 < L/B < 5$, the footing can be analyzed as either a plate or a beam depending on the practical considerations and engineering judgment.

5.6.1 Analysis of Rectangular PEF

Idealizing the foundation as per Winkler's hypothesis, Hertz (1884) was probably the first to analyze plates on elastic foundations. A variety of solutions were latter developed starting from the same hypothesis. Using the various modified foundation models reviewed in Section 4.7.3, several solutions were also reported (Vlasov and Leontev, 1966; Reissner, 1937). Treating the foundation as elastic continuum, few results are available for relatively simple problems of plates on elastic foundations.

In the following sections, the general methods to solve the problems of rectangular and circular plates on elastic foundations are presented using the Winkler's foundation model for the soil. However, exact solutions such as Levy type and Navier type (Timoshenko and Krieger, 1959) are feasible for rectangular plates with simple boundary conditions. However Vlasov's general variational/Kantorovich method (Vlasov and Leontev, 1966; Kameswara Rao, 1969), Galerkin's method and other energy methods, numerical methods such as FDM (Crandall, 1956) and FEM (Sridhar, 1999) can be used for general boundary conditions of plates and loads acting on them. The method of initial parameters has also been developed for plate problems, thus facilitating an easy approach to analyze the action of arbitrary external loads (Vlasov and Leontev, 1966; Kameswara Rao, 1969). Some exact methods are outlined below in the case of vertical loads acting on plates on elastic foundations. It may however be realized that the exact solutions are available in few simple cases and one may have to apply FDM, FEM and other numerical methods for many practical problems in general (Chapters 6 and 7).

5.6.2 Bending of Rectangular PEF

Consider a plate lying on an elastic foundation (Figures 4.19 and 4.21), carrying an arbitrary external load $p(x,y)$. It is assumed that the plate satisfies the assumptions of the classical bending theory. Also the friction and adhesion at the contact between the plate and the foundation is neglected, hence stipulating that the plate transfers only vertical reaction to the foundation. Typical rectangular plates are shown in Figures 5.7 and 5.8.

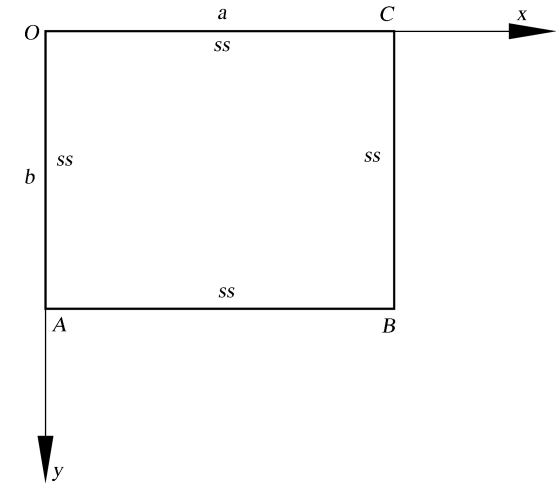

Figure 5.7 Plate with all edges simply supported (Navier's solution).

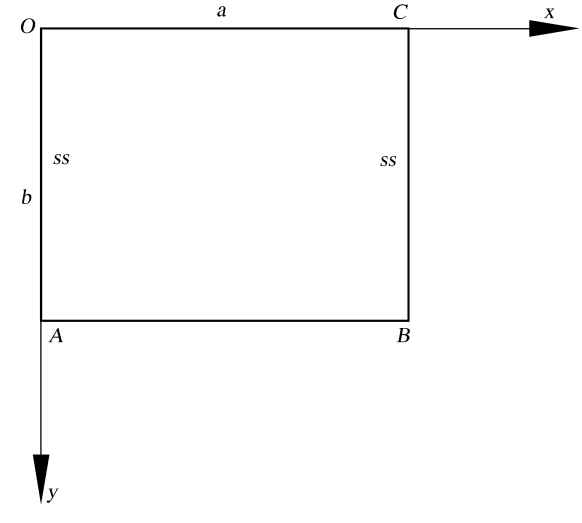

Figure 5.8 Plate with two opposite edges simply supported (Levy's solution).

The governing PEF equation (in Cartesian coordinates) is given by Equations (4.18) and (4.49), as

$$\begin{aligned} D\,\nabla^4 w\,(x,y) &= p(x,y) - q(x,y) \\ &= p(x,y) - kw(x,y) \end{aligned} \tag{5.81}$$

that is

$$D\,\nabla^4 w + kw = p(x,y) \tag{5.82}$$

where

$$\nabla^4 = \frac{\partial^4}{\partial x^4} + 2\frac{\partial^4}{\partial x^2 \partial y^2} + \frac{\partial^4}{\partial y^4} \tag{5.83}$$

and D is the flexural rigidity of the plate, given by

$$D = \frac{E_p h^3}{12\,(1-v_p^2)} \tag{5.84}$$

in which E_p and v_p are the Young's modulus and the Poisson's ratio of the plate material and h is the thickness of the plate. k is the spring constant for the plate geometry as explained in Section 4.8.5.

$q(x,y)$ is the soil reaction and $w(x,y)$ is the vertical deflection of the plate – soil interface.

The bending moments and shear forces (Figure 4.21) in the plate can be written as (Equations (4.21) and (4.22))

$$\begin{aligned} M_x &= -D\left(\frac{\partial^2 w}{\partial x^2} + v_p \frac{\partial^2 w}{\partial y^2}\right) (a) \\ M_y &= -D\left(\frac{\partial^2 w}{\partial y^2} + v_p \frac{\partial^2 w}{\partial x^2}\right) (b) \end{aligned} \tag{5.85}$$

$$\begin{aligned} M_{xy} &= -D(1-v_p)\frac{\partial^2 w}{\partial x \partial y} \qquad (c) \\ N_x &= -D\frac{\partial}{\partial x}\left(\frac{\partial^2 w}{\partial x^2} + \frac{\partial^2 w}{\partial y^2}\right) (d) \\ N_y &= -D\frac{\partial}{\partial y}\left(\frac{\partial^2 w}{\partial x^2} + \frac{\partial^2 w}{\partial y^2}\right) (e) \end{aligned} \tag{5.86}$$

The quantities N_x, N_y, N_{xy} can be combined to get the Kirchhoff shear (Timoshenko and Krieger, 1959) as

$$\begin{aligned} Q_x &= -D\left\{\frac{\partial^3 w}{\partial x^3} + (2-v_p)\frac{\partial^3 w}{\partial x \partial y^2}\right\} (a) \\ Q_y &= -D\left\{\frac{\partial^3 w}{\partial y^3} + (2-v_p)\frac{\partial^3 w}{\partial x^2 \partial y}\right\} (b) \end{aligned} \tag{5.87}$$

Boundary Conditions:

The commonly applicable boundary conditions at the four plate edges can be written as per classical thin plate bending theory as follows:

1. Simply supported or hinged edges

$$\begin{aligned} w = 0, \quad \frac{\partial^2 w}{\partial x^2} = 0 \quad \text{along} \quad x = 0 \quad \text{and} \quad x = a \\ w = 0, \quad \frac{\partial^2 w}{\partial y^2} = 0 \quad \text{along} \quad y = 0 \quad \text{and} \quad y = b \end{aligned} \tag{5.88}$$

2. Clamped edges

$$w = 0, \quad \frac{\partial w}{\partial x} = 0 \quad \text{along} \quad x = 0 \quad \text{and} \quad x = a$$

$$w = 0, \quad \frac{\partial w}{\partial y} = 0 \quad \text{along} \quad y = 0 \quad \text{and} \quad y = b \tag{5.89}$$

3. Free edges

$$\begin{aligned}
M_x &= \frac{\partial^2 w}{\partial x^2} + v_p \frac{\partial^2 w}{\partial y^2} = 0 && \text{along } x = 0 \text{ and } x = a \\
Q_x &= \frac{\partial^3 w}{\partial x^3} + (2 - v_p) \frac{\partial^3 w}{\partial x \partial y^2} = 0 && \text{along } x = 0 \text{ and } x = a \\
M_y &= \frac{\partial^2 w}{\partial y^2} + v_p \frac{\partial^2 w}{\partial x^2} = 0 && \text{along } y = 0 \text{ and } y = b \\
Q_y &= \frac{\partial^3 w}{\partial y^3} + (2 - v_p) \frac{\partial^3 w}{\partial x^2 \partial y} = 0 && \text{along } y = 0 \text{ and } y = b
\end{aligned} \tag{5.90}$$

The boundary conditions of the plate edges could be any combination of the above. The boundary conditions for other types of plate edges are given in standard books on the theory of plates (Timoshenko and Krieger, 1959).

5.6.2.1 Methods of Solution

Navier type or Levy type of solutions can be obtained for Equation (5.81), which are exact but these are feasible for simple boundary conditions along the plate edges. For plates with arbitrary boundary conditions many approximate methods such as Rayleigh's method, the Rayleigh–Ritz method, Galerkin's method and Kantorovich's method (Timoshenko and Krieger, 1959; Crandall, 1956; Vlasov and Leontev, 1966) are available. In this section the general solution of Equation (5.81) is presented using Navier and Levy type analysis.

5.6.2.2 Navier's Solutions

If all the four edges of the plate, that is, $x = 0$ and a, $y = 0$ and b are simply supported as shown in Figure 5.7, the boundary conditions at the edges can be expressed as in Equation (5.88). Solutions using double Fourier sine series which satisfies all the four boundary conditions can be obtained as follows. Accordingly

$$w = \sum_{m=1}^{\infty} \sum_{n=1}^{\infty} A_{mn} \sin \frac{m\pi x}{a} \sin \frac{n\pi y}{b} \tag{5.91}$$

where the Fourier coefficients A_{mn} have to be obtained from Equation (5.82). Substituting Equation (5.91) in Equation (5.82) and using orthogonal properties of sine functions and

Fourier theory, A_{mn} can be obtained as

$$A_{mn} = \frac{4}{ab\left[\pi^4\left(\frac{m^2}{a^2} + \frac{n^2}{b^2}\right)^2 + \frac{k}{D}\right]} \int_0^a \int_0^b \frac{p(x,y)}{D} \sin\frac{m\pi x}{a} \sin\frac{n\pi y}{b} dxdy \tag{5.92}$$

where $p(x, y)$ is the distributed load applied on the plate.

Knowing the applied load $p(x, y)$, the double integral in Equation (5.92) can be evaluated and A_{mn} can be obtained. Then the total solution for w and other quantities such as moments, shear forces, slopes and so on can be calculated from Equation (5.91) (using Equations (5.85)–(5.87)). The contact pressure $q(x, y)$ at any point can be obtained as $q(x, y) = kw$.

Example 5.4

If a plate simply supported on all four edges carries a UDL of $p(x, y) = p_o$, calculate the deflections $w(x,y)$ of the plate.

Solution:

By substituting $p(x, y) = p_o =$ constant in Equation (5.92), we get

$$\begin{aligned} A_{mn} &= \frac{4}{ab\left[\pi^4\left(\frac{m^2}{a^2} + \frac{n^2}{b^2}\right)^2 + \frac{k}{D}\right]} \frac{4p_o ab}{mn\pi^2 D} \\ &= \frac{16p_o}{\pi^2 Dmn\left[\pi^4\left(\frac{m^2}{a^2} + \frac{n^2}{b^2}\right)^2 + \frac{k}{D}\right]} \end{aligned} \tag{5.93}$$

Thus the deflection can be expressed from Equation (5.91) as

$$w(x,y) = \sum_{m=1,3,\ldots} \sum_{n=1,3,\ldots} \frac{16p_o \sin\frac{m\pi x}{a} \sin\frac{n\pi y}{b}}{\pi^2 Dmn\left[\pi^4\left(\frac{m^2}{a^2} + \frac{n^2}{b^2}\right)^2 + \frac{k}{D}\right]} \tag{5.94}$$

We can get the slopes, bending moments, shear forces and the contact pressure by substituting the solution for w (Equation (5.94)) in Equations (5.85)–(5.87) and $q(x,y) = kw$. The solution procedure for other types of transverse loads such as concentrated loads, UDL and so on can be easily obtained from Equations (5.91) and (5.92) (Timoshenko and Krieger, 1959).

5.6.2.3 Levy's Solutions

If any two opposite edges of the PEF are simply supported as shown in Figure 5.8, Levy's solutions can be obtained using single Fourier series in the direction of the simply supported

edges thus satisfying the boundary conditions given in Equation (5.88), Assuming that the edges $x = 0$ and $x = a$ are simply supported, the solution of Equation (5.82) can be written as

$$w(x, y) = \sum_{m=1,\infty} Y_m(y) \sin \frac{m\pi x}{a} \tag{5.95}$$

The above Levy's solution satisfies the boundary conditions exactly along the plate edges $x = 0$ and a. This type of solution has the advantage that the boundary conditions along $y = 0$ and b can be of general nature as given in Equations (5.88)–(5.90) or any other prescription. Substituting Equation (5.95) in Equation (5.82) and using Fourier series procedure, we get the following ODE in $Y_m(y)$ (Timoshenko and Krieger, 1959), as

$$\frac{d^4 Y_m}{dy^4} - \frac{2m^2\pi^2}{a^2} \frac{d^2 Y_m}{dy^2} + \left(\frac{m^4\pi^4}{a^4} + \frac{k}{D}\right) Y_m = f_m(y) \quad m = 1, 2, 3, \ldots \tag{5.96}$$

where

$$f_m(y) = \frac{2}{a} \int_0^a \frac{p(x, y)}{D} \sin \frac{m\pi x}{a} \, dx \quad m = 1, 2, 3, \ldots \tag{5.97}$$

$Y_m(y)$ can be exactly solved from Equation (5.96) as an ODE with the homogeneous solution containing four arbitrary constants and a particular integral corresponding to the quantity $f_m(y)$. These four arbitrary constants can be solved from the four boundary conditions of the remaining plate edges at $y = 0$ and b in a similar manner as discussed for BEF in Section 5.3. Also the MIP can be developed for general loading and other variations as in Section 5.5.1 (Vlasov and Leontev, 1966, Kameswara Rao, 1969).

Example 5.5

Obtain the Levy type solution for a plate with its edges simply supported along $x = 0$ and a and general boundary conditions along $y = 0$ and b and subjected to an UDL, p_o = constant.

Solution:

The solution is assumed as in Equation (5.95) which results in Equation (5.96) where

$$f_m(y) = \frac{2p_0}{aD} \int_0^a \sin \frac{m\pi x}{a} dx = \frac{4p_0}{\pi D m}, \quad m = 1, 3, 5, \ldots \tag{5.98}$$

The total solution of Equation (5.96) can be expressed as

$$Y_m(y) = Y_{mh} + Y_{mp} \tag{5.99}$$

where

Y_{mh} = homogeneous solution
Y_{mp} = particular integral.

Since $f_m(y)$ is given by Equation (5.98), Y_{mp} can be obtained as

$$Y_{mp} = \frac{4p_0}{\pi Dm\left[\frac{m^4\pi^4}{a^4} + \frac{k}{D}\right]}, \quad m = 1, 3, 5, \ldots \tag{5.100}$$

The homogeneous solution can be obtained as

$$Y_{mh} = C_{1m}F_{1m} + C_{2m}F_{2m} + C_{3m}F_{3m} + C_{4m}F_{4m}, \quad m = 1, 3, 5, \ldots \tag{5.101}$$

where C_{1m} to C_{4m} are the arbitrary constants and F_{1m} to F_{4m} are the basis of solutions of the ODE (Equation (5.96)). They can be obtained from the characteristic roots of the ODE, that is, roots of

$$D_c^4 - \frac{2m^2\pi^2}{a^2}D_c^2 + \left(\frac{m^4\pi^4}{a^4} + \frac{k}{D_c}\right) = 0, \quad m = 1, 3, 5, \ldots \tag{5.102}$$

where D_c is the differential operator $= d/dy$.

Thus knowing the total solution (Equation (5.99)), the four arbitrary constants C_{1m} to C_{4m} can be uniquely solved by applying the four boundary conditions at the plate edges $y = 0$ and b as given in Equations (5.88)–(5.90). These have to be solved for each harmonic ($m = 1, 3, 5, \ldots$) and then the series solution can be obtained as expressed by Equation (5.95). Also the MIP can be developed for general applications as in BEF (Section 5.5.1).

5.6.2.4 PEF with Other General Boundary Conditions

A solution for plates with general boundary conditions (other than the Navier and Levy type discussed above), can be obtained using Galerkin's method (Crandall, 1956) or Vlasov's general variational method (Vlasov and Leontev, 1966; Kameswara Rao, 1969) and a general MIP can be developed. But these methods are laborious and computationally intensive. Hence numerical methods such as FDM and FEM are used for such problems which can incorporate the practical situations of various parameters of the problems easily. These are discussed in Chapters 6 and 7.

5.6.3 Circular PEF

Circular and ring shaped (annular) footings are used to support foundations for tanks, columns in a circular geometry, tower foundations, piers, and so on. The procedure for calculating the contact pressure assuming the footing to be rigid and contact pressure to be planar is given in (Section 4.4.5). Once the contact pressure is calculated, the bending moments of all the forces from above and from below (contact pressures) are calculated by taking moments about any cross section. Similarly, the shear forces at any cross section can be calculated by summing up all the forces from above and below. These can be used in the conventional analysis and design of circular footings.

To take care of the flexibility of the footing, the footing is analyzed as a circular plate on an elastic foundation. The governing equation is given in Equation (4.18) with the operator ∇^2

given in Equation (4.23) and the convention sketch is shown in Figure 4.22. The bending equation is rewritten for an axially symmetric loading (omitting terms of θ in Equation (4.23)) as

$$\left(\frac{d^2}{dx^2} + \frac{1}{r}\frac{d}{dr}\right)\left(\frac{d^2w}{dr^2} + \frac{1}{r}\frac{dw}{dr}\right) = \frac{p-kw}{D} \tag{5.103}$$

In the particular case of a plate loaded at the center with a concentrated load P, p is equal to zero over the entire surface of the plate except as a concentrated load at the center. By defining

$$\frac{k}{D} = \frac{1}{l^4} \tag{5.104}$$

Equation (5.103) becomes

$$l^4\left(\frac{d^2}{dr^2} + \frac{1}{r}\frac{d}{dr}\right)\left(\frac{d^2w}{dr^2} + \frac{1}{r}\frac{dw}{dr}\right) + w = 0 \tag{5.105}$$

where l has the dimension of length.

To simplify analysis, the following dimensionless quantities are defined

$$\frac{w}{l} = z\frac{r}{l} = x \tag{5.106}$$

Then Equation (5.105) becomes

$$\left(\frac{d^2}{dx^2} + \frac{1}{x}\frac{d}{dx}\right)\left(\frac{d^2z}{dx^2} + \frac{1}{x}\frac{dz}{dx}\right) + z = 0 \tag{5.107}$$

Equation (5.107) can be written as

$$\Delta\,\Delta\, z + z = 0 \tag{5.108}$$

where

$$\Delta = \frac{d^2}{dx^2} + \frac{1}{x}\frac{d}{dx}$$

This is a linear differential equation of the fourth order, the general solution of which can be represented in the following form

$$z = A_1X_1(x) + A_2X_2(x) + A_3X_3(x) + A_4X_4(x) \tag{5.109}$$

where A_1 to A_4 are constants of integration and the functions X_1 to X_4 are four independent solutions of Equation (5.108).

The details of solution are given by Hertz (1884) and Timoshenko and Krieger (1959). Typical results of an infinite circular plate on an elastic foundation subjected to a concentrated load, P at the origin are presented in Figure 5.9.

5.6.3.1 Boundary Conditions for a Finite Circular Plate

The boundary conditions at the edge of the plate $r = a$ can be expressed as follows (Timoshenko and Krieger, 1959):

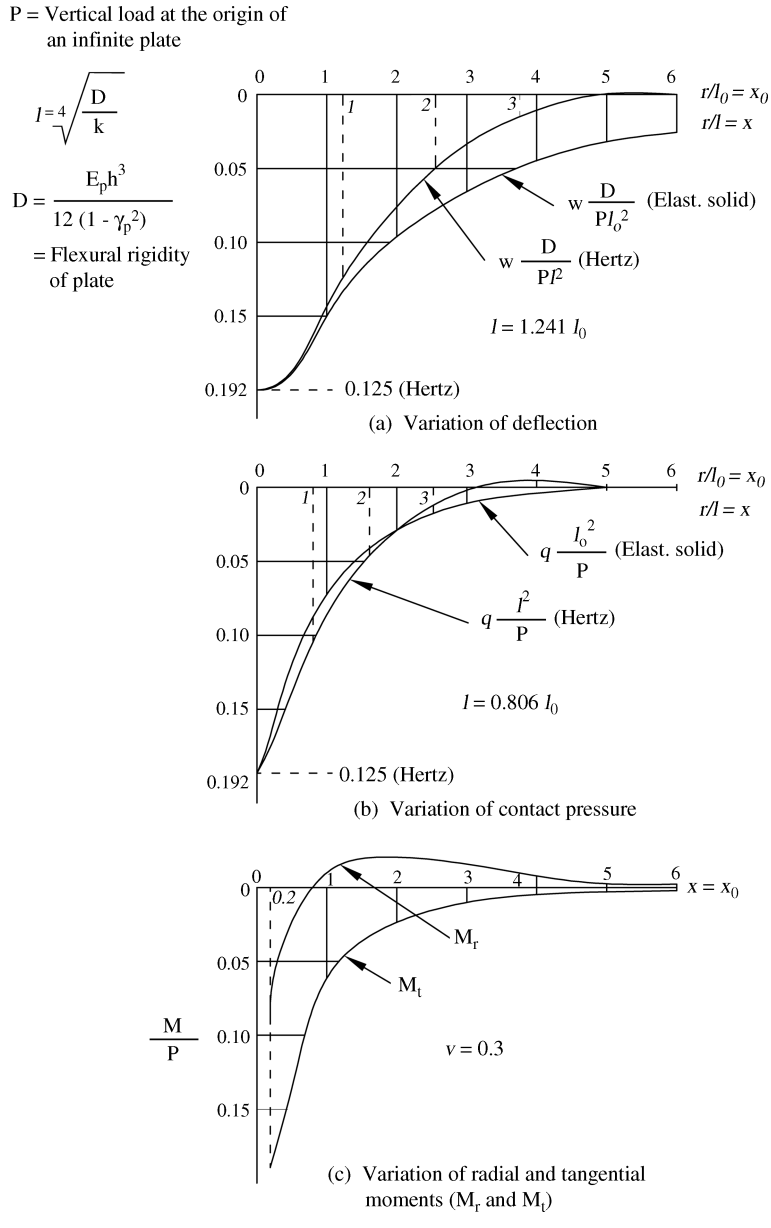

Figure 5.9 Response of an infinite plate on elastic foundation due to a concentrated load.

1. Simply supported edge (hinged edge)

$$\text{w} = 0, \quad M_r = \frac{d^2w}{dr^2} + \frac{v_p}{r}\frac{dw}{dr} = 0 \tag{5.110}$$

2. Fixed edge (clamped edge)

$$\text{w} = 0, \quad \text{slope}, \quad \theta_r = \frac{dw}{dr} = 0 \tag{5.111}$$

3. Free edge

$$\text{Radial BM}, M_r = \frac{d^2w}{dr^2} + \frac{v_p}{r}\frac{dw}{dr} = 0 \tag{5.112}$$

$$\text{Edge shear force}, Q_r = \frac{d^3w}{dr^3} + \frac{1}{r}\frac{d^2w}{dr^2} - \frac{1}{r^2}\frac{dw}{dr} = 0$$

The conditions at $r = 0$ are to be satisfied by ensuring that the solutions are finite at the singular point of symmetry, that is, at the origin $r = 0$.

Thus it can be observed that analysis of circular plates is also mathematically laborious and it is convenient to use numerical methods such as FDM and FEM to deal with practical problems because of their flexibility to be able to incorporate a wide class of loads, geometrical configurations and non-uniform situations. These are discussed in Chapters 6 and 7.

5.7 Summary

The analysis of beams, rectangular and circular plates on elastic foundations are discussed with Winkler's foundation model to account for the soil reaction. Exact solutions for BEF are derived. A solution by the method of initial parameters is presented in detail. A few examples are discussed. For PEF, Navier's and Levy's solutions for simple boundary conditions along plate edges are presented. Typical solutions for circular plates on elastic foundations are given. Some useful solutions for circular and annular plates are given in Appendix 12.B. Some structural design examples are also illustrated in Appendix 12.C.

To solve general problems of beams and plates on elastic foundations it may be necessary to use numerical methods such as FDM and FEM which are presented in Chapters 6 and 7.

Exercise Problems

The problem assignments are organized as follows.

Exercise Problems	Section(s)	Topic(s)
5.1–5.3	5.4, 5.4.1	Infinite BEF Semi-infinite BEF
5.4–5.17	5.5, 5.5.1	Finite BEF, MIP
5.18–5.20	5.5, 5.5.3	Finite BEF
5.21–5.26	5.6, 5.6.2	Rectangular PEF

5.1 Obtain the solutions of (a) an infinite beam and (b) a semi-infinite beam on elastic foundations subjected to a moment M_0 at the origin. Derive the expressions for deflection, slope, BM, SF and the contact pressure. Show that infinite beam solutions can be obtained by superposing semi-infinite beam solutions.

5.2 If a concentrated load is applied as shown in Figure 5.10 to a semi-infinite BEF, derive the responses of the beam at salient points and sketch the variations.

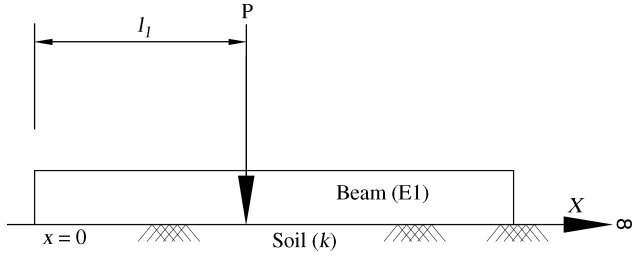

Figure 5.10 Problem 5.2.

5.3 If a concentrated moment M_0 is applied to the semi-infinite BEF as shown in Figure 5.11, derive the expressions for the responses at salient points and sketch the variations.

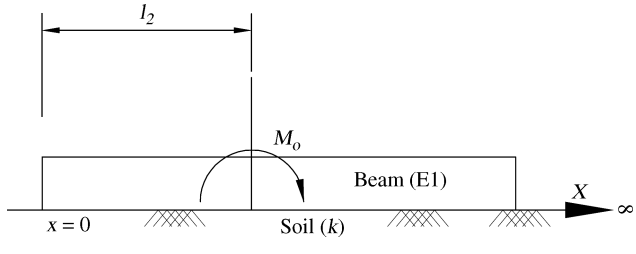

Figure 5.11 Problem 5.3.

Problems 5.4–5.10

Using MIP, obtain all the responses of the following problems (5.4–5.10) of BEF.

$$\text{Data given :} \quad P_1 = 150\,\text{kN},\ P_2 = 200\,\text{kN}, M_o = 500\,\text{kNm},\ p_o = 10\,\text{kN/m},$$
$$\phi_o = 15^\circ,\ \text{L} = 10\,\text{m},$$

$$l_1 = \frac{L}{12},\ l_3 = \frac{L}{6},\ b = 1.5\,\text{m},\ d = 0.5\,\text{m},\ \lambda L = 0.3,\ E = 3 \times 10^{10}\,\text{N/m}^2$$

5.4 Problem given in Figure 5.12

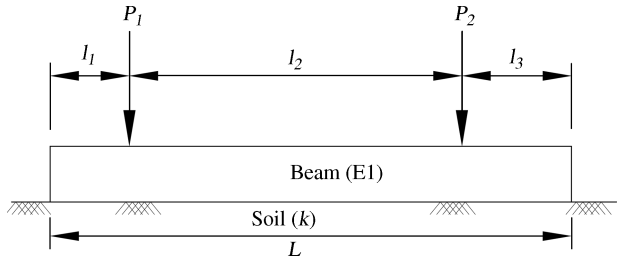

Figure 5.12 Problem 5.4.

5.5 Problem given in Figure 5.13

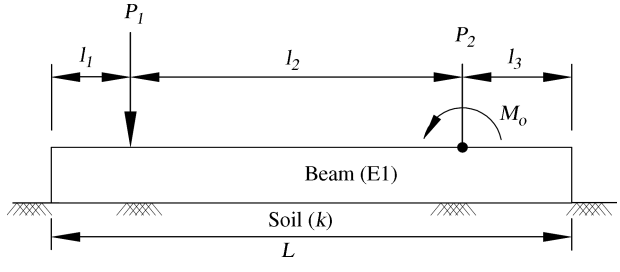

Figure 5.13 Problem 5.5.

5.6 Problem given in Figure 5.14

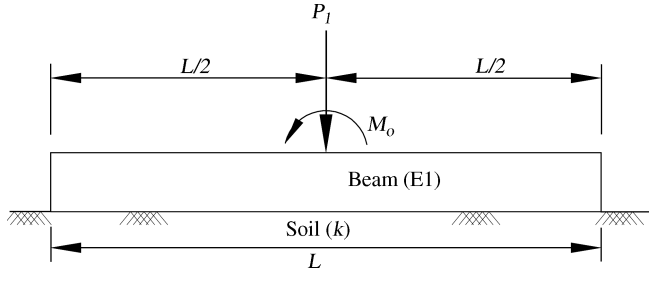

Figure 5.14 Problem 5.6.

5.7 Problem given in Figure 5.15

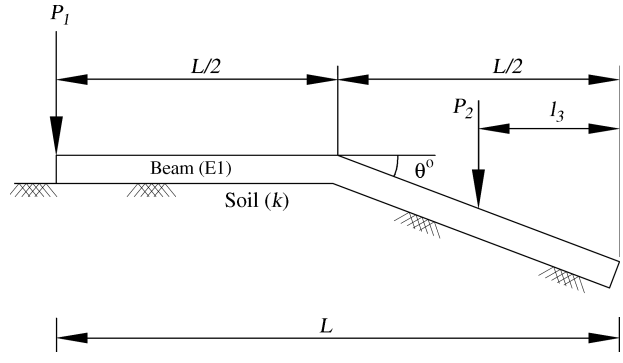

Figure 5.15 Problem 5.7.

5.8 Problem given in Figure 5.16

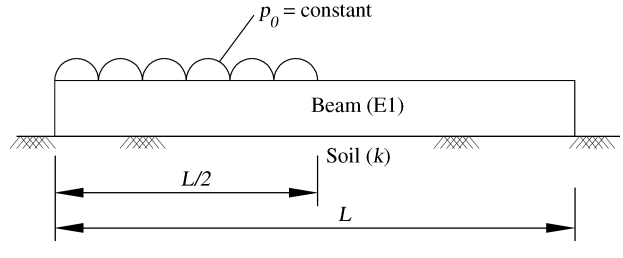

Figure 5.16 Problem 5.8.

5.9 Problem given in Figure 5.17

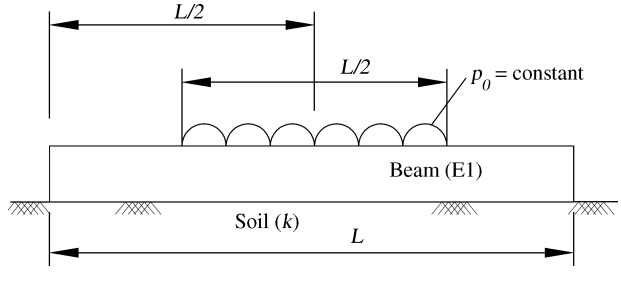

Figure 5.17 Problem 5.9.

5.10 Problem given in Figure 5.18

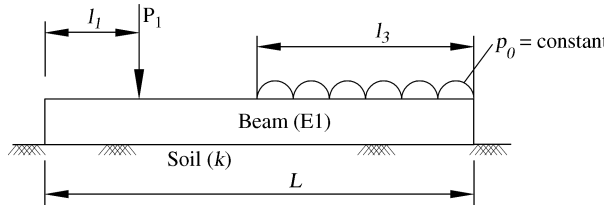

Figure 5.18 Problem 5.10.

5.11–5.17 Obtain the solutions of problems 5.4–5.10 using the principle of superposition.

5.18–5.20 Obtain the solutions of problems 5.4 and 5.5 with the following modifications. M_0 is to be replaced by a couple, that is, by two equivalent concentrated loads separated by distance of 1 m. Use Seely and Smith's (1952) response curves.

5.21 Obtain Navier's solutions for a PEF (Figure 5.7) with the following loads

$P_1 = 100$ kN acting at $a/4$, $b/4$

$a = 8$ m, b = 10 m, $h = 0.5$ m

$E = 2.5 \times 10^{10}$ N/m^2, $v_p = 0.3$.

Assume simply supported edges along the four sides OA, OC, BC, AB (Figure 5.7).

5.22–5.26 Obtain Levy's solutions for the plate shown in Figure 5.8 with the load data given below.

$P_1 = 150$ kN acting at $a/2$, $b/4$

$a = 6$ m, $b = 8$ m, $h = 0.6$ m

$E_p = 4.5 \times 10^{10}$ N/m^2, $v_p = 0.2$.

Use the following boundary conditions. Edges OA, BC are simply supported.

1. OC and AB are simply supported (Problem 5.22).
2. OC and AB are free (Problem 5.23).
3. OC and AB are fixed (Problem 5.24).
4. OC is simply supported and AB is free (Problem 5.25)
5. OC is free and AB is fixed (Problem 5.26).

Appendix 5.A Matrix of Influence Functions (Method of Initial Parameters)

The various matrices needed in developing the method of initial parameters (MIP) as discussed in Section 5.5, are given below for computation wherever necessary.
Homogeneous solution:

$$w_h = \begin{Bmatrix} w \\ w' \\ M \\ Q \end{Bmatrix} = C^T F_h \tag{5.A.1}$$

$$C^T = \{ C_1 \quad C_2 \quad C_3 \quad C_4 \} \tag{5.A.2}$$

$${F_h}^T = \{ F_1 \quad F_2 \quad F_3 \quad F_4 \} \tag{5.A.3}$$

$$\begin{aligned} F_1 &= \cosh \lambda x \cos \lambda x \\ F_2 &= \cosh \lambda x \sin \lambda x \\ F_2 &= \sinh \lambda x \cos \lambda x \\ F_2 &= \sinh \lambda x \sin \lambda x \end{aligned} \tag{5.A.4}$$

Derivatives:

$$\frac{dF_h}{dx} = N_h \quad F_h\,, \quad \frac{d^n F_h}{dx^n} = N_H^n \quad F_h \tag{5.A.5}$$

where

$$N_H = \lambda \begin{bmatrix} 0 & -1 & 1 & 0 \\ 1 & 0 & 0 & 1 \\ 1 & 0 & 0 & -1 \\ 0 & 1 & 1 & 0 \end{bmatrix} \tag{5.A.6}$$

$$N_H^2 = N_H . N_H = \lambda^2 \begin{bmatrix} 0 & 0 & 0 & -2 \\ 0 & 0 & 2 & 0 \\ 0 & -2 & 0 & 0 \\ 2 & 0 & 0 & 0 \end{bmatrix} \tag{5.A.7}$$

$$N_H^3 = N_H^2 N_H = N_H N_H N_H = \lambda^3 \begin{bmatrix} 0 & -2 & -2 & 0 \\ 2 & 0 & 0 & 2 \\ -2 & 0 & 0 & -2 \\ 0 & -2 & 2 & 0 \end{bmatrix} \tag{5.A.8}$$

$$\begin{Bmatrix} w \\ w' \\ M \\ Q \end{Bmatrix} = \begin{Bmatrix} F_h^T \\ F_h^T N_h^T \\ -EIF_h^T (N_h^2)^T \\ -EIF_h^T (N_h^3)^T \end{Bmatrix} C = BC \tag{5.A.9}$$

$$B = \begin{bmatrix} F_1 & F_2 & F_3 & F_4 \\ \lambda(F_3 - F_2) & \lambda(F_1 + F_4) & \lambda(F_1 - F_4) & \lambda(F_2 + F_3) \\ 2EI\lambda^2 F_4 & -2EI\lambda^2 F_3 & 2EI\lambda^2 F_2 & -2EI\lambda^2 F_1 \\ 2EI\lambda^3(F_2 + F_3) & -2EI\lambda^3(F_1 - F_4) & 2EI\lambda^3(F_1 + F_4) & 2EI\lambda^3(F_2 - F_3) \end{bmatrix} \tag{5.A.10}$$

$$B_{at\ x=0} = A = \begin{bmatrix} 1 & 0 & 0 & 0 \\ 0 & \lambda & \lambda & 0 \\ 0 & 0 & 0 & -2EI\lambda^2 \\ 0 & -2EI\lambda^3 & 2EI\lambda^3 & 0 \end{bmatrix} \tag{5.A.11}$$

$$A^{-1} = G = \begin{bmatrix} 1 & 0 & 0 & 0 \\ 0 & \dfrac{1}{2\lambda} & 0 & -\dfrac{1}{4EI\lambda^3} \\ 0 & \dfrac{1}{2\lambda} & 0 & \dfrac{1}{4EI\lambda^3} \\ 0 & 0 & -\dfrac{1}{2EI\lambda^2} & 0 \end{bmatrix} \tag{5.A.12}$$

Matrices of influence functions:

$$K = BG = \begin{bmatrix} K_{ww} & K_{ww'} & K_{wM} & K_{wQ} \\ K_{w'w} & K_{w'w'} & K_{w'M} & K_{w'Q} \\ K_{Mw} & K_{Mw'} & K_{MM} & K_{MQ} \\ K_{Qw} & K_{Qw'} & K_{QM} & K_{QQ} \end{bmatrix}$$

$$= \begin{bmatrix} F_1 & \dfrac{(F_2 + F_3)}{2\lambda} & \dfrac{-F_4}{2\lambda^2 EI} & \dfrac{F_3 - F_2}{4\lambda^3 EI} \\ \lambda(F_3 - F_2) & F_1 & -\dfrac{(F_2 + F_3)}{2\lambda EI} & \dfrac{-F_4}{2\lambda^2 EI} \\ 2\lambda^2 EIF_4 & \lambda EI(F_2 - F_3) & F_1 & \dfrac{(F_2 + F_3)}{2\lambda} \\ 2\lambda^2 EI(F_2 + F_3) & 2\lambda^2 EIF_4 & \lambda(F_3 - F_2) & F_1 \end{bmatrix} \tag{5.A.13}$$

K is the matrix of influence functions and is symmetric about the secondary diagonal. Also at $x = 0$, K reduces to the identity matrix.

6

Numerical and Finite Difference Methods

6.1 Introduction

The analysis of beams and plates on elastic foundations is presented in Chapter 5. It is observed that the exact solutions are available in relatively simple cases of loading, uniform cross sectional properties of the footing and soil and simple boundary conditions (particularly in the case of plates). A few exact solutions are given which are computationally intensive and laborious. Hence it may not be feasible to apply them for many practical problems of footing – soil interaction and design. In recent times, due to easy availability of powerful PCs and computers, software packages and advances in numerical and finite element methods (Teng, 1964; Bowles, 1996; Jones, 1997; Crandall, 1956; Sridhar, 1999), the analysis and design of BEF and PEF are carried out using these methods which are easily adaptable and flexible for practical applications. Numerical methods like the Runge–Kutta methods, method of weighted residuals (Crandall, 1956) and several others can be applied to solve BEF and PEF problems.

Some of these methods are described below, along with illustrations.

6.2 Trial Solutions with Undetermined Parameters

Among several numerical methods that are available in literature to solve the equilibrium problems (Crandall, 1956), this method is more popular because of its simplicity and flexibility. The method involves a trial solution which, because of undetermined parameters or functions, represents a whole family of possible approximations. There are several criteria for picking out the *best* approximation among the family of solutions. There are, however, some differences when we have an equilibrium problem that is equivalent to an extremum problem.

Consider the system of equations in the domain D as

$$L_{2m}[\psi] = f, \text{ with the boundary conditions,} \quad B_i[\psi] = g_i \quad i = 1, \ldots, m \tag{6.1}$$

Foundation Design: Theory and Practice N. S. V. Kameswara Rao
 ISBN: 978-0-470-82534-1

in which the boundary conditions are linear in ψ. Furthermore, let the trial solution have the linear form

$$\psi = \varphi_0 + \sum_{j=1}^{r} c_j \varphi_j \tag{6.2}$$

where the φ_j values are linearly independent known functions in the domain D and the c_j values are undetermined parameters. There are two basic types of criteria for fixing the c_j. In the first, the c_j are chosen so as to make weighted averages of the residual vanish, and in the other the c_j are chosen so as to give a stationary value to a functional Φ which is related to the system of Equation (6.1). In either case, applying the criterion results in a set of r simultaneous equations for the determination of c_j. These may therefore be considered as methods for reducing a continuous equilibrium problem to an approximately equivalent equilibrium problem with r degrees of freedom.

Boundary Conditions

For the weighted residual methods, we select the trial solution so that it satisfies all the boundary conditions of Equation (6.1). This is accomplished by choosing the functions φ_j in Equation (6.2) so as to satisfy the following boundary conditions:

$$\begin{aligned} &B_i\,[\varphi_o] = g_i \quad i = 1, \ldots, m \\ &B_i\,[\varphi_j] = 0 \quad\;\; i = 1, \ldots, m, \quad j = 1, \ldots, r \end{aligned} \tag{6.3}$$

Then ψ of Equation (6.2) satisfies all the boundary conditions for arbitrary c_j values.

In the case of the stationary functional method, it is enough if ψ satisfies only the essential boundary conditions. This is accomplished by taking

$$\begin{aligned} &B_i\,[\varphi_o] = g_i \quad i = e_1, e_2, \ldots \\ &B_i\,[\varphi_j] = 0 \quad\;\; i = e_1, e_2, \ldots; \quad j = 1, \ldots, r \end{aligned} \tag{6.4}$$

Weighted-Residual Methods

When the trial solution given by Equation (6.2) which satisfies Equation (6.3) is inserted in Equation (6.1), the equation gives the residual R as

$$R = f - L_{2m}[\psi] = f - L_{2m}\left[\varphi_0 + \sum_{j=1}^{r} c_j \varphi_j\right] \tag{6.5}$$

For the exact solution the residual is identically zero. Within a trail family of solutions, a *close* approximation may be described as one which makes R as small as possible. To achieve this, the following criteria can be considered (Crandall, 1956) as requirements so that various weighted averages of R should vanish if not R itself:

Collocation Method

The residual Equation (6.5) is set equal to zero at r points in the domain D. This provides r simultaneous algebraic equations for solving c_j. The location of the points is arbitrary but is usually chosen such that D is covered more or less uniformly by a simple pattern.

Subdomain Method

The domain D is subdivided into r sub domains, usually according to a simple pattern. The integral of the residual Equation (6.5) over each subdomain is then set equal to zero to provide r simultaneous equations for solving c_j.

Galerkin's Method

In this method, weighted integrals are taken over the entire domain using each of the known function $\phi_k (k = 1 \ldots r)$ and are equated to zero, that is, the r integrals

$$\int_D \varphi_k R \, dD \; (k = 1, \ldots, r) = 0 \tag{6.6}$$

These provide r equations for solving c_j. The weighing functions here are the same functions used in constructing ψ.

Method of Least Squares

The integral of the square of the residual is minimized with respect to the undetermined parameters to provide r simultaneous equations. If L_{2m} is a linear operator, then

$$\frac{\partial}{\partial c_k} \int_D R^2 \, dD = -2 \int_D R L_{2m}[\varphi_k] \, dD = 0, \quad k = 1, \ldots, r \tag{6.7}$$

The resulting r simultaneous equations are used to solve c_j.

6.2.1 Stationary Functional Method

Let Φ be a functional such that the extremum problem for Φ is equivalent to the equilibrium problem that is, Equation (6.1). *The Ritz Method* (Crandall, 1956) consists in treating the extremum problem directly by inserting the trial family of Equation (6.2) into Φ and setting

$$\frac{\partial \Phi}{\partial c_j} = 0 \quad j = 1, \ldots, r \tag{6.8}$$

These r equations are solved for c_j and the corresponding function ψ then represents an approximate solution to the extremum problem. It is an approximate solution because it gives Φ a stationary value only for these variations of ψ which are contained within the trail family. This solution is not in general an extremum if more general variations are permitted.

An advantage of the stationary functional method is that admissible functions for the extremum problem need satisfy only essential boundary conditions. This simplifies the selection of the trial family (Equation (6.2)) whenever the conditions (Equation (6.4)) are less restrictive than Equation (6.3).

6.2.2 General Comments

It should be emphasized that the most important (and most difficult) step in all these methods is the selection of the trial family, Equation (6.2). The purpose of the above criteria is merely to pick the *best* approximation out of a given family. Good results cannot be obtained if good

approximations are not included within the trial family. Theoretically, if enough independent φ_j are included in Equation (6.2), good approximations must be contained within the family; however, the principal attraction of these methods lies in the possibility of obtaining good approximations with a limited number of adjustable parameters.

Consideration should be given to symmetry or any other special characteristics of the solution which may be known.

When the system of Equation (6.1) is linear, the equations for the c_j obtained by any of the weighted residual methods are also linear. The matrix of the coefficients of the c_j is always symmetric in the least squares method but is generally nonsymmetric for the other three methods.

When the functional Φ is quadratic, the Ritz method leads to symmetric linear equations for the c_j. When it is known that the true solution minimizes Φ, then the value of Φ may be used as a measure of the relative accuracy of approximations; that is, the lower the value of Φ, the better the approximation.

For a particular trial family like Equation (6.2) which satisfies all the boundary conditions of a linear equilibrium problem, the four weighted residual criteria generally produce slightly different approximations. If there is an equivalent extremum problem and the Ritz method is applied to the same trial family, the approximation obtained turns out to be identical with that obtained by the Galerkin criterion. Thus Galerkin's method provides the optimum weighted residual criterion in the sense that the approximation so obtained is one which renders Φ stationary for all variations within the given trial family.

There are differences in the amounts of computation required to be carried out using these methods. Collocation, which involves only evaluation of functions, is usually substantially quicker than the other methods which involve integration. Whether or not this is an important consideration depends on how the resulting simultaneous equations are to be solved.

Example 6.1

Analyze the BEF shown in Figure 6.1 for the special case when $k = \frac{EI}{L^4}$

$$EI\frac{d^4w}{dx^4} + kw = p \tag{6.9}$$

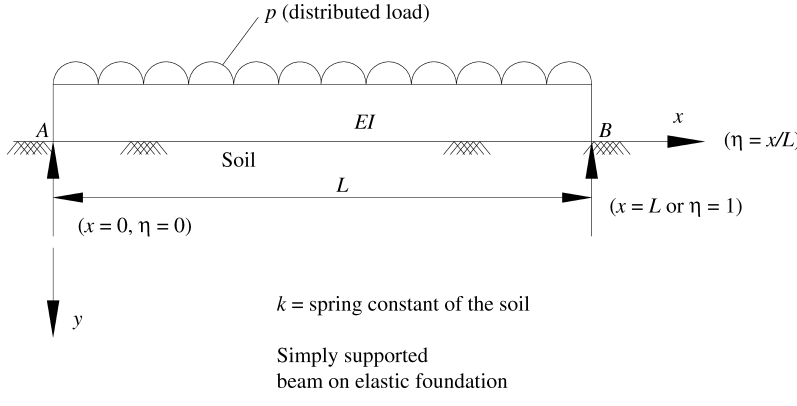

Figure 6.1 Simply supported beam on elastic foundation.

The boundary conditions for simply supported ends are

$$\begin{aligned} w &= 0 \\ M &= -EI\frac{d^2w}{dx^2} = 0 \text{ at } x = 0 \text{ and } x = L \end{aligned} \tag{6.10}$$

Equations (6.9) and (6.10) can be expressed in nondimensional form as

$$\frac{d^4\psi}{d\eta^4} + \psi = 1 \quad \text{in the domain} \quad \eta = 0 \quad \text{to} \quad 1 \tag{6.11}$$

$$\text{where} \quad \eta = \frac{x}{L} \quad \text{and} \quad \psi = \frac{EIw}{pL^4} \tag{6.12}$$

and making $k = \frac{EI}{L^4}$ for this particular problem for illustration as a special case.

Also the boundary conditions given by Equation (6.10) become

$$\psi = \frac{d^2\psi}{d\eta^2} = 0 \quad \text{at} \quad \eta = 0 \quad \text{and} \quad 1 \tag{6.13}$$

Now consider first a trial family with two undermined parameters which satisfies all the boundary conditions for the simply supported ends at $x = 0$ and $x = L$ as shown in Figure 6.1, that is, at $\eta = 0$ and $\eta = 1$.

$$\psi = c_1 \sin \pi\eta + c_2 \sin 3\pi\eta \tag{6.14}$$

Since the boundary conditions are homogeneous, there is no φ_o. The residual of the Equation (6.11) with this trial solution can be obtained as

$$R = 1 - \frac{d^4\psi}{d\eta^4} - \psi = 1 - c_1(\pi^4 + 1)\sin \pi\eta - c_2\,(81\pi^4 + 1)\sin 3\pi\eta \tag{6.15}$$

Treating this residual by the weighted-residual methods leads to simultaneous equations for c_1 and c_2. Thus if, using *collocation*, we can make $R = 0$ at $\eta = \frac{1}{4}$ and $\eta = \frac{1}{2}$, the resulting equations are

$$\begin{aligned} \frac{\pi^4 + 1}{\sqrt{2}}c_1 + \frac{81\pi^4 + 1}{\sqrt{2}}c_2 &= 1 \\ (\pi^4 + 1)c_1 - (81\pi^4 + 1)c_2 &= 1 \end{aligned} \tag{6.16}$$

Solving the two simultaneous equations, Equation (6.16), we get $c_1 = 0.012267$, $c_2 = 0.000026$

Then, the solution is given by Equation (6.14).

If instead, using the *subdomain method*, we can make the integral of R over the ranges $0 < \eta < 1/4$ and $1/4 < \eta < 1/2$ to be zero, then the resulting equations are

$$\begin{aligned} \frac{\pi^4 + 1}{\pi}\frac{\sqrt{2} - 1}{\sqrt{2}}c_1 + \frac{81\pi^4 + 1}{\pi}\frac{\sqrt{2} + 1}{3\sqrt{2}}c_2 &= \frac{1}{4} \text{ (for the region } 0 < \eta < 1/4) \\ \frac{\pi^4 + 1}{\sqrt{2}\pi}c_1 - \frac{81\pi^4 + 1}{3\sqrt{2}\pi}c_2 &= \frac{1}{4} \text{ (for the region } 1/4 < \eta < 1/2) \end{aligned} \tag{6.17}$$

Solving the above simultaneous equations, we get

$$c_1 = 0.013624,\ c_2 = 0.000029$$

The solution is then given by Equation (6.14).

If we use the *Galerkin method*, we can write

$$\begin{aligned} \int_0^1 R \sin \pi\eta \, d\eta &= \frac{2}{\pi} - \frac{\pi^4 + 1}{2} c_1 = 0 \\ \int_0^1 R \sin 3\pi\eta \, d\eta &= \frac{2}{3\pi} - \frac{81\pi^4 + 1}{2} c_2 = 0 \end{aligned} \tag{6.18}$$

By solving the above two simultaneous equations, we get $c_1 = 0.012938$, $c_2 = 0.000054$. If we use the *method of least squares,* we obtain the same equations as in the Galerkin method (for this example only). This can be easily verified.

6.2.3 Trial Solutions with Undetermined Functions

The above procedures transformed a continuous problem into an approximately equivalent lumped-parameter system. There are procedures which may be used to replace a two-dimensional continuous problem with an equivalent system consisting of a finite number of one-dimensional problems. This involves selecting a trial family of the form

$$\psi = \sum_{j=1}^{r} c_j \varphi_j \tag{6.19}$$

where the φ_j are linearly independent known functions in the two-dimensional domain (say in x, y coordinates) and c_j are undetermined functions of a single variable functions of say y alone. φ_j can be a known function of say x alone, or of both x and y. If the φ_j are suitably chosen and suitable boundary conditions are imposed on the c_j, then Equation (6.8) will give r simultaneous ordinary differential equations for determining the c_j by applying the weighted-residual technique or by the calculus of variations to a related functional.

The first method of this type was described by Kantorovich and is equivalent to Galerkin's method (Crandall, 1956).

6.2.4 Observations

From the above discussion, it appears that Galerkin's method and Kantorovich's method are preferable in solving BEF and PEF due to inherent advantages, as mentioned in the previous sections.

6.3 Finite Difference Method

The finite difference method (FDM) is straightforward and may be successfully applied to a large class of problems. Though the methods are simple, they result in much larger number of equations for the system (Crandall, 1956; Teng, 1964; Jones, 1997).

The basic approximation involves the replacement of a continuous domain D by a pattern of discrete points within D as shown in Figure 6.2. Instead of obtaining a continuous solution for ψ defined throughout D we find approximations to ψ only at these isolated points. Intermediate values, derivatives, or integrals may be obtained from the discrete solution by interpolation.

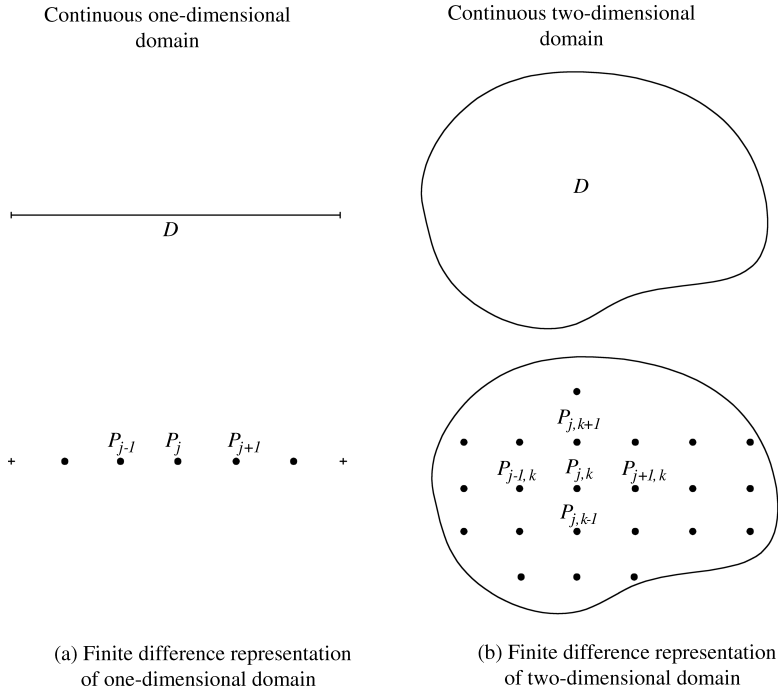

Figure 6.2 Finite difference representation of continuous domains.

The governing equation and boundary conditions for the continuous domain are reduced to those for the discrete replacement, physically or mathematically. In the first approach, the discrete system is modeled with lumped physical characteristics of the continuous system. The governing equations are then obtained by directly applying them to the lumped-parameter model. In the mathematical approach the continuous system is reduced to a discrete system by simply replacing derivatives with finite difference approximations.

As examples of the physical approach, a continuous elastic foundation under a beam can be replaced by a number of discrete springs of such stiffness and with such spacing that the resulting displacement of the beam is unaltered to a large extent.

The governing equations are then obtained by writing the equilibrium equations for the beam at each spring. Though the physical approach is qualitatively useful, the mathematical procedure using finite difference method is simpler and more flexible.

Either procedure leads to a system of n simultaneous algebraic equations if n discrete points are involved. These equations are linear or nonlinear depending on whether the original continuous system is linear or nonlinear. The resulting simultaneous equations can be solved using standard methods like Gauss elimination and so on (Crandall, 1956).

The finite difference operation for a node j in the domain D is written for the first derivative $\frac{d\psi}{dx}\left(\text{or } \frac{dy}{dx}\right)$. This can then be recursively used to derive higher-order derivatives $\left(\frac{d^2\psi}{dx^2}\right)_j$, $\left(\frac{d^3\psi}{dx^3}\right)_j$, $\left(\frac{d^4\psi}{dx^4}\right)_j$ and so on. The different methods commonly used for FD approximation of $\frac{d\psi}{dx}$ at node j are shown in Figure 6.3. These are:

1. Forward differences, using unknown functions at nodes j, and $j + 1$ (error is of the order of h).
2. Central differences, using unknown functions at $j - 1$ and $j + 1$ (error is of the order of h^2).
3. Backward differences, using unknown functions at nodes $j - 1$ and j (error is of the order of h).

From Figure 6.3, it can be clearly seen that the central difference scheme is more accurate and unbiased than the other two alternatives (Southwell, 1946; Salvadori and Baron, 1952; Crandall, 1956). This can also be shown using Taylor's series/Maclaurin's series expansion of a variable (Salvadori and Baron, 1952; Scott, 1963). Accordingly, the theory and applications in the following sections are presented using the central difference scheme only.

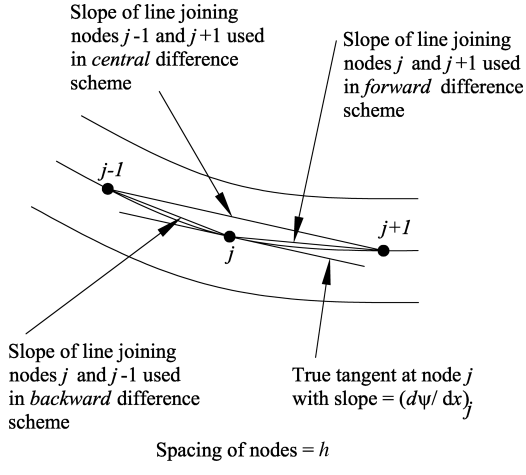

Figure 6.3 Approximation of $d\psi/dx$ using backward, forward and central differences.

6.3.1 Finite Difference Operators

For replacing differential equations with finite-difference relations, several basic finite difference operators in one, two and three dimensions can be derived. While FD operators can be derived with unequal spacing between nodes (say h) in one, two, three dimensions, it

can be shown (Scott, 1963) that the operators with equal spacing between all nodes in the domain are more accurate (error is of the order of h^2) than those with the unequal spacing (error is of the order of h). Hence, all the operators presented here are with equal spacing between nodes. In one dimension we consider only the case of equally spaced points and in two dimensions we consider only the square network or lattice. In both cases, the spacing dimension can be taken as h without any loss of generality. Three-dimensional operators can be similarly derived as a simple extension of the two-dimensional operators and are not presented here. Triangular and hexagonal lattices also are used depending on the problem (Southwell, 1946).

In Figure 6.2(a) let the points . . ., P_{j-1}, P_j, P_{j+1}. . . be separated by a distance h, and let the value of ψ (x) at P_j be denoted by ψ_j. Then for instance, the first derivative at P_j may be approximated by the following finite-difference expression

$$\left(\frac{d\psi}{dx}\right)_j = \frac{\psi_{j+1} - \psi_{j-1}}{2h} + O(h^2) \tag{6.20}$$

This relation may be represented pictorially by a finite difference operator (FDO) as shown in Figure 6.4.

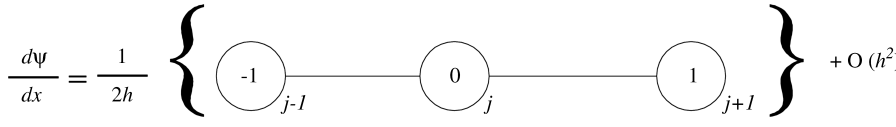

Figure 6.4 FD operator for first derivative in one dimension – central difference.

The numbers in the circles (Figure 6.4) represent the multipliers that are to be applied to the values of ψ at these stations. The corresponding formulae for the first four derivatives and the integral by Simpson's rule are given in Figure 6.5 in the form of FD operators.

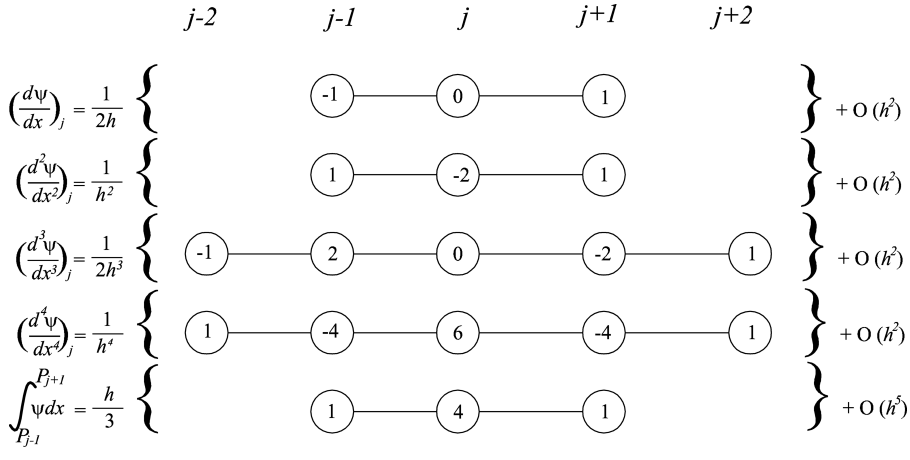

Figure 6.5 FD operators for one-dimensional derivatives and integrals.

Similar formulae for approximating partial derivatives can easily be obtained. The most commonly used FD operators for square networks of spacing h are shown in Figure 6.6. The integration formula given is the two-dimensional form of Simpson's rule.

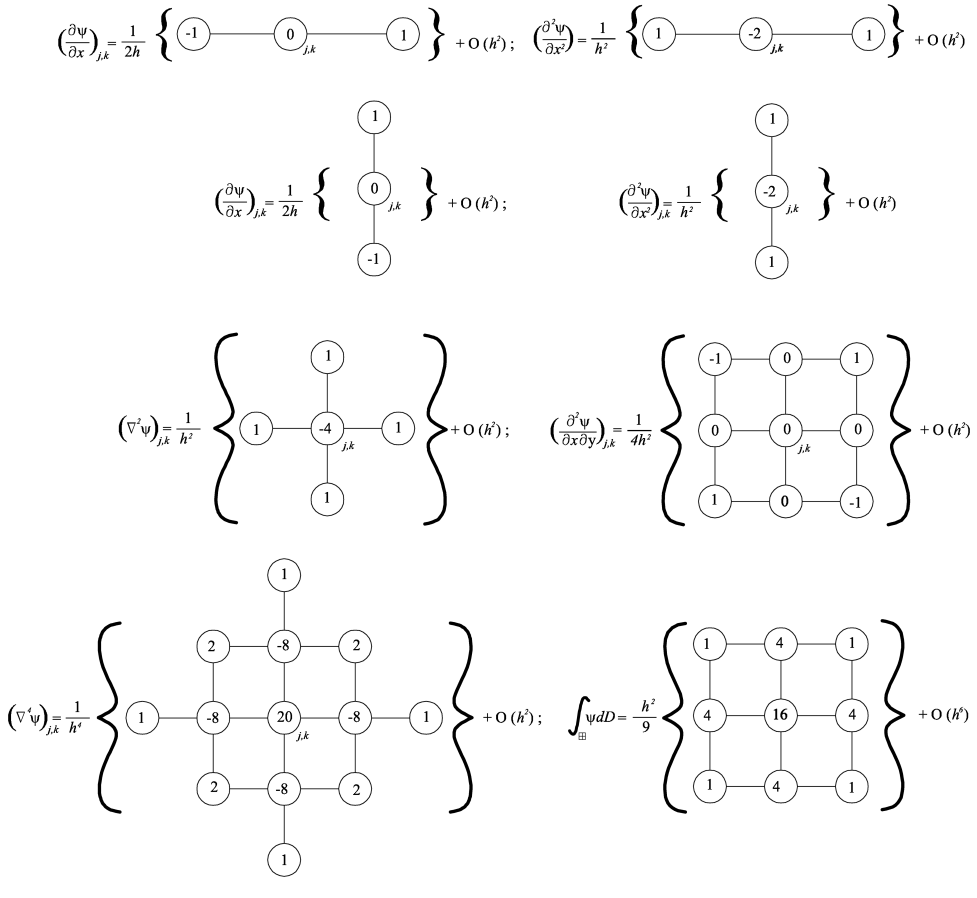

Figure 6.6 FD operators in two dimensions for partial derivatives and integrals.

6.3.2 *Application to Engineering Problems*

The process of converting the continuous differential equation and boundary conditions of a given problem into algebraic equations for a discrete approximation using FD is as follows. As soon as the appropriate basic FD operators are available, the conversion is straight forward. At each internal point the finite-difference approximation to the governing differential equation provides an algebraic equation in terms of the values at the neighboring points. Exceptional situations can arise near the boundaries, where it is possible that not all the neighboring points of a FDO will lie within domain D. It is then necessary to introduce finite-difference

approximations to the given boundary conditions in terms of fictitious points beyond D and then eliminate these fictitious values in terms of the values that lie inside D using boundary conditions. These fictitious points are shown in Figures 6.7–6.9 for illustration. The procedure to deal with such cases is illustrated in the following example.

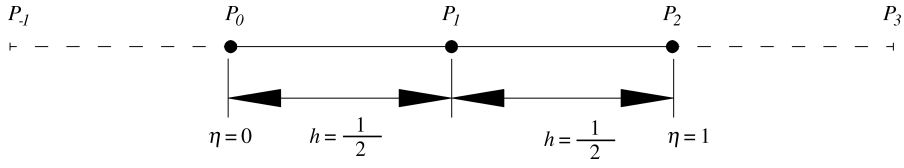

Figure 6.7 FD model for BEF with one internal and two fictitious nodes.

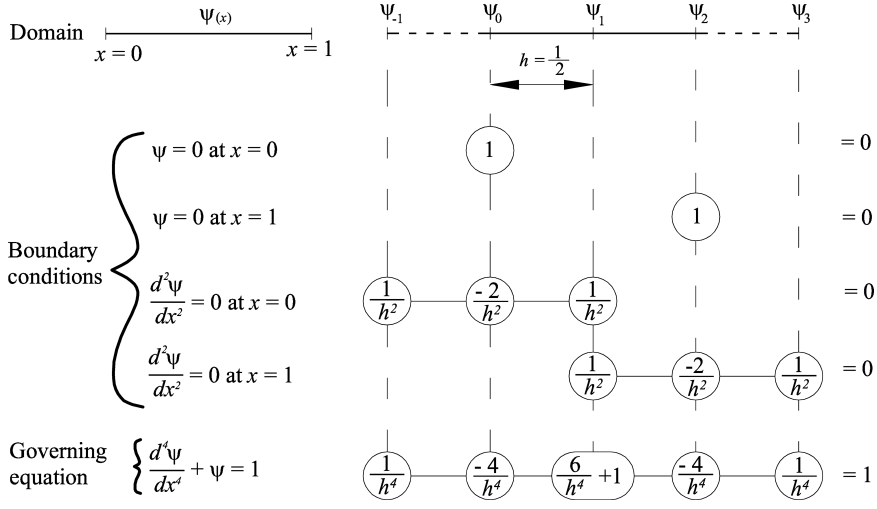

Figure 6.8 Model of BEF with one internal node.

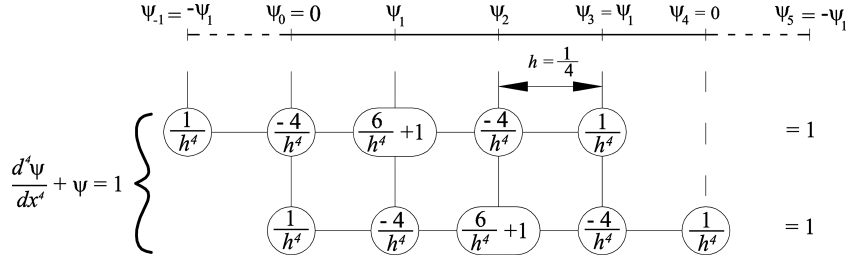

Figure 6.9 FD model of BEF with three internal modes.

Example 6.2

Obtain FD solution for the BEF shown in Figure 6.1 with data given in Example 6.1.

Consider the beam on elastic foundation, as shown in Figure 6.1 (Example 6.1). The governing equations and boundary conditions are given in Equations (6.9) and (6.10). These are nondimensionalized as given in Equations (6.11) and (6.12). Thus, the domain $0 < x < L$ is converted to a nondimensional domain $0 < \eta < 1$ where $\eta = x/L$. This nondimensionalization is only for convenience of computation and the equation can also be directly discretized in terms of x. Then the continuous domain $0 < \eta < 1$ is replaced by a discrete domain by discretizing at the single point P_1 at $\eta = 1/2$ as shown in Figure 6.7 (variable x in the figure can be read as η for this example). To accommodate the FDO (Figure 6.5) two additional points P_{-1} and P_3 are needed outside the domain at $\eta = -1/2$ and $\eta = 3/2$ which are called fictitious points. Now the problem is converted to the one of solving a one degree of freedom system for ψ_1 at point P_1 (since $\psi_0 = \psi_2 = 0$ from simply supported boundary conditions given by Equations (6.10) and (6.13)). An algebraic equation for ψ_1 can be obtained by combining finite difference approximations to the differential equation and boundary conditions given in Equations (6.11) and (6.12). This can be obtained as shown in Figure 6.8 (variable x in the figure can be read as η for this example) where FDOs are written with the aid of Figure 6.5.

The finite difference discretization of boundary conditions provide us with enough equations to fix the boundary values $\psi_0 = \psi_2 = 0$ and to eliminate the fictitious values ψ_{-1} and ψ_3 since according to the third and fourth line of Figure 6.8, $\psi_{-1} = \psi_3 = -\psi_1$. Inserting these values into the fifth line of the figure and setting $h = 1/2$ gives

$$-16\psi_1 + 0 + [(6)(16) + 1]\psi_1 + 0 - 16\psi_1 = 1 \tag{6.21}$$

from which $\psi_1 = -0.01538$. Instead of a continuous deflection curve we get only an approximation to the deflection at the center. It may be noted that in spite of the FD approximation, the solution ψ_1 is only 20% larger than the exact solution $\psi_1(\eta = 1/2) = 0.01288$ (Crandall, 1956).

Finer Discretization – BEF Discretization with Three Internal Nodes

The problem given in Example 6.2 is discretized with three internal nodes with spacing $h = 1/4$ as shown in Figure 6.9 (variable x in the figure can be read as η for this example). Because of symmetry we have $\psi_3 = \psi_1$. The boundary nodes and the fictitious nodes outside the boundary can be analyzed as before. The results of applying the boundary conditions are indicated directly on the figure. The FDOs corresponding to the differential equation is written twice, centered on P_1 and P_2. These lead to the simultaneous equations

$$\begin{aligned} -256\psi_1 + 0 + 1537\psi_1 - 1024\psi_2 + 256\psi_1 &= 1 \\ 0 - 1024\psi_1 + 1573\psi_2 - 1024\psi_1 + 0 &= 1 \end{aligned} \tag{6.22}$$

which have the following solution

$$\begin{aligned} \psi_1 &= 0.00965 \\ \psi_2 &= 0.01352 \end{aligned} \tag{6.23}$$

This solution provides approximation to ψ at the center and quarter points. Although giving more detail than the previous approximation, this is still not close to the continuous solution. However, the error at the center is now only 5%.

This procedure can be extended to finer and finer subdivisions. The treatment at the boundaries is always the same, independent of the number of internal points. If there are n independent ψ_j values in the domain, the FDO corresponding to the differential equation is written n times centered on n points P_j corresponding to the independent ψ_j. This provides n simultaneous equations from which the ψ_j can be obtained.

6.3.2.1 Two- and Three-Dimensional Problems

The FDM is similar for application to two- and three-dimensional problems in Cartesian and cylindrical polar coordinates. As the dimensionality increases, the nodal unknowns increase and interpretation of boundary conditions becomes more cumbersome. The method is illustrated in two dimensions for application to plates on elastic foundations in Section 6.10. For general application of FDM problems in two and three-dimensional problems, readers may refer to Salvadori and Baron (1952), Crandall (1956), Southwell (1956) and so on.

6.3.3 Errors in FD

The errors in finite-difference approximations are extensively studied in numerical analysis. The early mathematical convergence proofs are being reexamined from the practical viewpoint of numerical analysis.

It is generally understood that the error for FD with central difference scheme is of the order of h^2 while for forward and backward differences it is of the order of h. Also for equal intervals of discretization, that is, h, for the central difference scheme the error is of the order of h^2, while for unequal intervals it is of the order of h only. Detailed analysis of errors in FD are discussed in Salvadori and Baron (1952), Crandall (1956), Southwell (1956) and other standard books on numerical analysis.

It may also be noted that the interval, h, represents the fineness of the mesh for FD discretization. It affects the two kinds of errors, that is, discretization error [O (h^2)] and the round off error in opposite directions. The discretization error decreases with decreasing h, while the round off error generally increases. (Salvadori and Baron, 1952; Crandall, 1956)

6.3.4 Improvizations of FDM – Iterative Methods, Relaxation, h^2 Extrapolation and so on

To help in faster solution which can be carried out even without computers several improvizations such as iterative methods, relaxation methods, and so on have been developed (Salvadori and Baron, 1952; Teng, 1964). For improving the accuracy, procedures like h^2 extrapolation method have been also developed (Crandall, 1956). Details may be referred to in the above references and in other standard books on numerical analysis.

6.4 FDM Applications to General BEF Problems

The application of FDM to BEF results in direct relationships between deflection, slope, bending moment, shear force and loading in terms of the derivatives $\frac{dw}{dx}$, $\frac{d^2w}{dx^2}$, $\frac{d^3w}{dx^3}$ and $\frac{d^4w}{dx^4}$ of the deflection w of the beam. Finite difference theory leads to approximations to these derivatives, at the discretised nodes along the beam, in terms of the unknown deflections at these and adjacent points as explained in Section 6.3. The theory is much simplified and more accurate if the nodes are equally spaced along the length of the beam, that is, h is kept constant over the entire domain.

Once the derivatives have been expressed in finite difference form, they are applied to each node in turn using the simple theory of bending. This process relates the deflections at each of the nodes to the externally applied loads, such as uniformly distributed loads (UDLs), uniformly varying loads (UVLs), moment and point loads. These loads are all combined to form an equivalent system of loads at nodes for solution. Support conditions, boundary conditions and prescribed displacements can be accounted for by modifying the finite difference equations, as explained in the following sections.

The resulting system of equations is then solved for the unknown deflections. Once these deflections have been computed, it is a simple matter to calculate the magnitude of bending moments, shear forces and reactions and other derived quantities.

Thus, finite difference theory affords an extremely versatile and powerful method of analysis to solve BEF problems. More importantly, the number of unknowns to achieve an acceptable degree of accuracy is much less in comparison to other similar procedures.

6.4.1 Representation of Derivatives Using Central Differences

Consider the case of a beam on an elastic foundation as shown in Figure 6.10 (along with the right handed Cartesian coordinate system x, y, z). The interval between all adjacent nodes is equal to h.

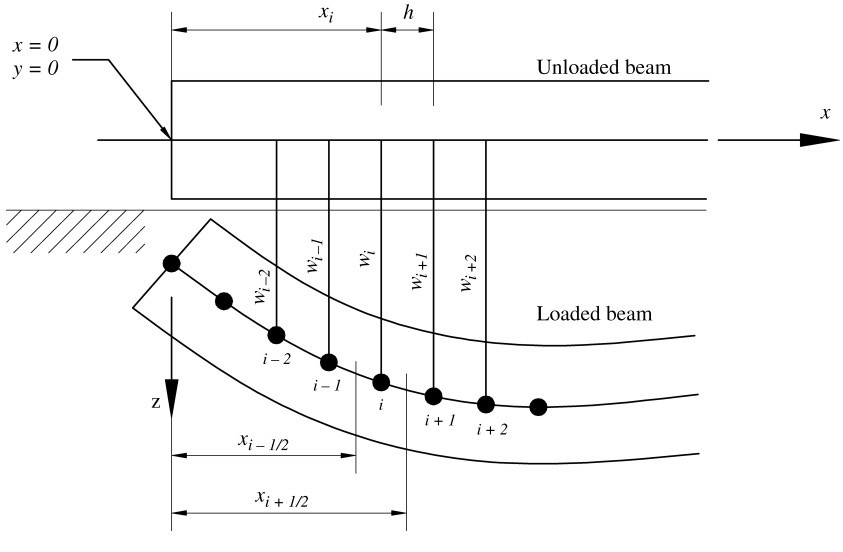

Figure 6.10 FD model of BEF.

The finite difference expressions for the derivatives of the vertical deflection w at distance x from the left-hand side of the beam, are much simplified if the nodes are equally spaced along the length (L) of the beam in addition to giving higher accuracy.

The governing differential equation has already been derived in Chapter 4 and exact and analytical solution methods have been discussed in Chapter 5.

The general form of the equation, for beams with non-uniform EI on elastic foundations (Crandall, Dahl and Lardener, 1972), is

$$\frac{d^2}{dx^2}\left(EI\,\frac{d^2w}{dx^2}\right) + kw = p(x) \tag{6.24a}$$

where EI, w, k, x, $p(x)$ are all beam, foundation parameters as defined in Equations (4.14)–(4.16). For a prismatic beam (beam with uniform cross section and flexural rigidity, EI), Equation (6.24a) becomes Equation (4.48), that is

$$EI\frac{d^4w}{dx^4} + kw = p(x) \tag{6.24b}$$

The derivatives $\frac{dw}{dx}, \frac{d^2w}{dx^2}, \frac{d^3w}{dx^3}, \frac{d^4w}{dx^4}$ at any node i can be expressed in terms of w at i and its adjacent nodes as discussed in Section 6.3 and shown as FDOs in Figure 6.5. The general procedure for the solution of Equations (6.24a) and (b) using finite difference method is already illustrated in Example 6.2 (Section 6.3). The applications of the various steps for general loads and beam configurations that may occur in practice are discussed in the following sections. These can also be obtained by logical application of FDM and FD operators to these problems. However the following details may help in dealing with the wide variations in the problems of BEF.

6.4.2 *Representation of Applied Loads*

The FDM explained in Section 6.3 relates the unknown nodal deflections to the applied loads and moments. For the purposes of analysis, it is convenient to replace the applied loads by an equivalent system of nodal point loads. The method of evaluating the equivalent nodal point loads for a beam on an elastic foundation can be demonstrated by considering the parts of a loaded beam between nodes $i-1, i$ and $i+1$, the nodes being placed at equal intervals h. Let the beam be loaded with a varying load having an intensity of $p(x)$ kN/m at a distance of x from the left-hand end of the beam as shown in Figure 6.11. The equivalent nodal point loads can be calculated on the basis of their being equal and opposite to the total reactions at each node had the beam consisted of a series of simply supported beams spanning between the nodes. This approximate approach is sufficiently accurate for most practical purposes.

It follows, therefore, that the magnitude of the equivalent point load at node i is

$$P_i = \frac{1}{h}\int_{x_{i-1}}^{x_i} p_x(x - x_{i-1})\,dx + \frac{1}{h}\int_{x_i}^{x_{i+1}} p_x(x_{i+1} - x)\,dx \tag{6.25}$$

In the simple case of a continuous, uniformly distributed load of intensity p_0 this expression reduces to

$$P_i = p_0 h \tag{6.26}$$

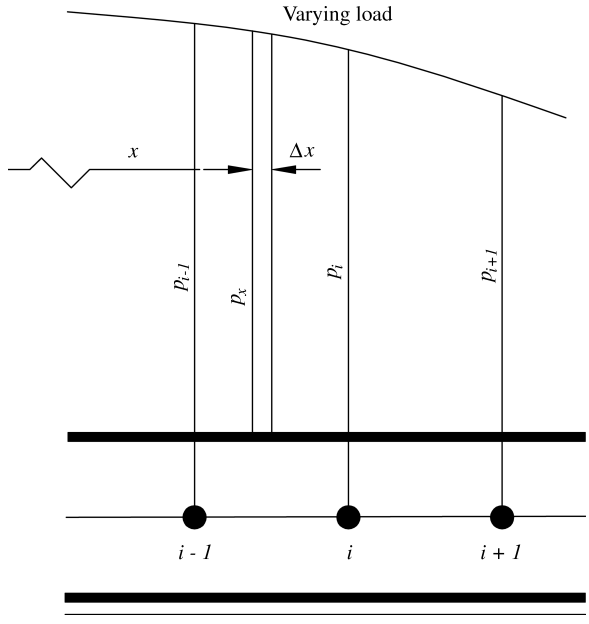

Figure 6.11 Varying load on BEF.

A similar approach can be used for idealizing the effects of the subgrade reaction by treating it as an upward acting load system. In this case, however, the equivalent nodal point loads are directly proportional to the deflection at the nodes. The other types of loads such as point loads, moments can be taken into analysis in the same way. The equivalent point loads acting on the beam are taken as being equal and opposite of the resulting nodal reactions.

Each of different load types (point loads, uniformly varying/distributed loads and couples) can now be considered separately in order to derive expressions for converting them to an equivalent point load system. It is assumed that downward acting loads are positive and upward acting loads are negative.

6.4.3 Equivalent Nodal Loads

6.4.3.1 Concentrated Loads

Figure 6.12 shows part of a beam between nodes $i-1$ and $i+1$ loaded with a point load P_x at a distance x from the left-hand end of the beam. The equivalent point load, P_i, at node i is calculated from

$$P_i = \frac{1}{h}\sum_{x=x_{i-1}}^{x<x_i} P_x\,(x - x_{i-1}) + \frac{1}{h}\sum_{x>x_i}^{x=x_{i+1}} P_x\,(x_{i+1} - x) + \sum P_i \qquad (6.27a)$$

This expression applies for the possibility of applied point loads being coincident with node i. Every effort should be made to ensure that nodes coincide with the positions of applied point loads to optimize the accuracy of the solution by avoiding truncation errors.

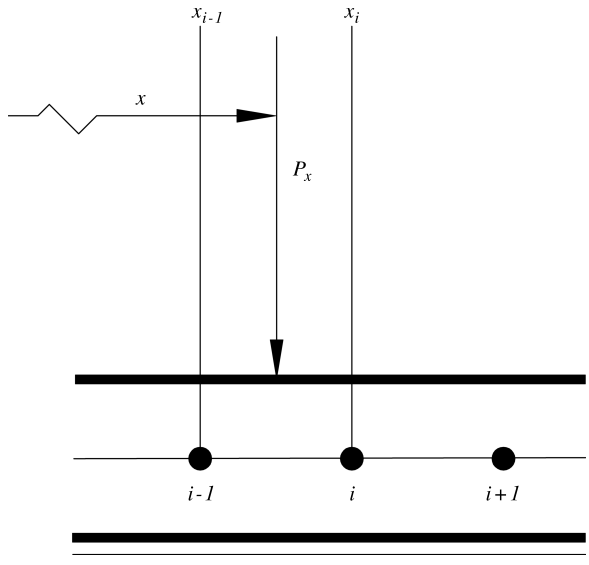

Figure 6.12 Point load on BEF.

Alternative Method

Another practical and common approach is to distribute P_x at i and $i-1$ in proportion to the proximity to the other node (as per reactions of a beam simply supported at i and $i-1$), that is

$$\begin{aligned} P_i &= \frac{P_x(x-x_{i-1})}{h} \\ P_{i-1} &= \frac{P_x(x_i-x)}{h} \end{aligned} \tag{6.27b}$$

6.4.3.2 Uniformly Distributed and Uniformly Varying Loads

A uniformly distributed load (UDL) can be considered as a special case of a uniformly varying load (UVL). General expressions for converting the latter to a system of equivalent nodal point loads therefore cover all cases of uniformly distributed loading. Consider part of a beam loaded with a UVL extending from $x = x_1$ to $x = x_2$ (Figure 6.13), where x is measured from the left-hand end of the beam and the constant rate of change of the UVL is

$$p' = \frac{(p_2-p_1)}{(x_2-x_1)} \tag{6.28}$$

Then

$$P_{i-1} = \frac{(x_i-x_1)^2}{6h}[3p_1 + p'(x_i-x_1)] \tag{6.29}$$

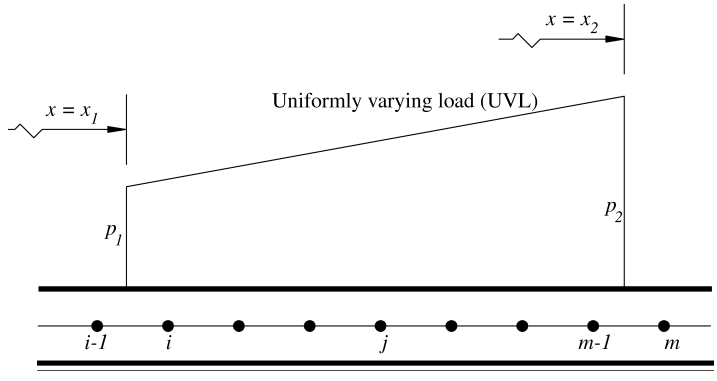

Figure 6.13 UVL on BEF.

$$P_i = p_1\,(x_i - x_1) + 0.5p'(x_i - x_1)^2 - P_{i-1} + \frac{h}{6}[3p_1 + p'(3x_i - 3x_1 + h)] \tag{6.30}$$

Applying Equation (6.30) to an intermediate node j, the equivalent point load P_j can be obtained as

$$P_j = [p_1 + p'(x_j - x_1)]\,h \tag{6.31}$$

At nodes m and $m-1$, the corresponding expressions for the equivalent point load reduces to

$$P_m = \frac{(x_2 - x_{m-1})^2}{6h}[3p_1 + p'(x_{m-1} - 3x_1 + 2x_2)] \tag{6.32}$$

$$P_{m-1} = [p_2 - 0.5p'(x_2 - x_{m-1})](x_2 - x_{m-1}) - P_m + \frac{h}{6}[3p_1 + p'(3x_{m-2} - 3x_1 + 2h)] \tag{6.33}$$

When a discontinuity occurs in the UVL between intermediate nodes $j-1$ and j, the equivalent nodal point loads can be calculated by considering the UVL to consist of two separate parts, each similar to that shown in Figure 6.14(a). Equations (6.29)–(6.33) are then applied to each part of the UVL in turn to determine the equivalent point load at each node. At nodes $j-1$ and j, care must be taken in summing the loads resulting from both parts of the UVL.

Alternative Method

Calculate the total load coming at the node by finding the resultant load distributed up to $h/2$ on either side of the node as shown in Figure 6.14(b).

Accordingly the total load at i becomes

$$P_i = \frac{p_1 + p_2}{2}h \tag{6.34}$$

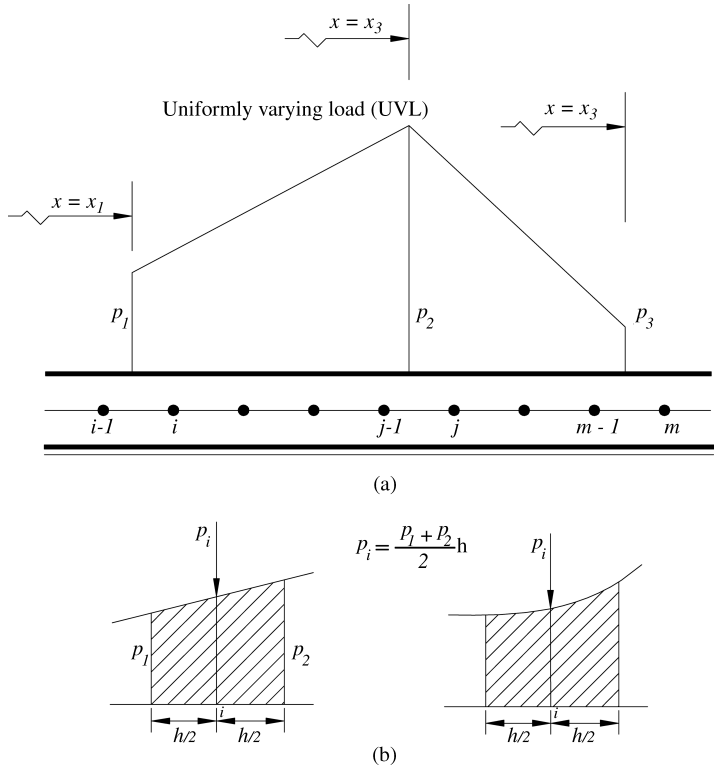

Figure 6.14 (a) UVL with discontinuity; and (b) alternative method for nodal load calculation.

6.4.3.3 Moments Applied on BEF

Moments may be applied at nodes or in between nodes. As in the case of point loads, every effort should be made in the FD discretization to ensure that nodes coincide with the points of application of the moments in order to avoid truncation errors in the final solution. The sign convention for applied moments are taken as positive or clockwise moment as shown. When a positive M is applied between two nodes $i-1$ and moments i (Figure 6.15) the equivalent nodal point loads at nodes $i-1$ and i are given by

$$P_1 = P_{n-1} = + \frac{M}{h} \tag{6.35}$$

$$P_2 = P_n = -\frac{M}{h} \tag{6.36}$$

If the positive moment M is applied at either end of the beam, as indicated in Figures 6.16(a) and (b) the equivalent nodal point loads at nodes $i-1$ and I are also given by Equations (6.35) and (6.36) above.

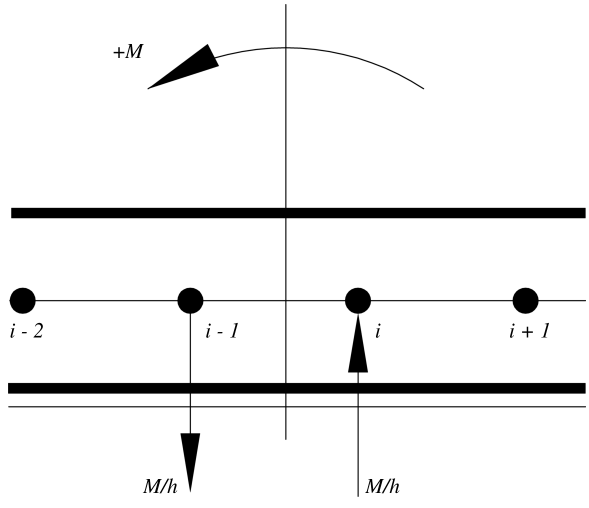

Figure 6.15 Moment applied between nodes of BEF.

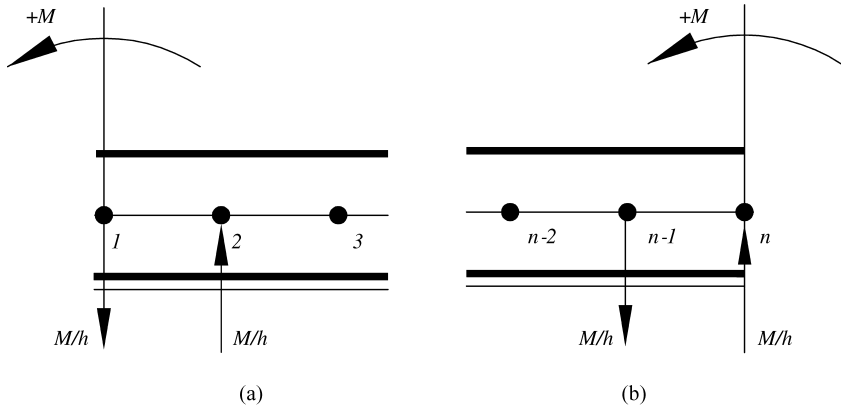

Figure 6.16 Moment applied at ends of BEF.

When a positive M is applied at an internal node i (Figure 6.17) it is replaced with equivalent point loads acting at nodes $i-1$ and i given by Equations (6.37a) and (6.37b) respectively.

$$\begin{aligned} P_{i-1} &= +\frac{M}{2h} \qquad \text{(a)} \\ P_i &= -\frac{M}{2h} \qquad \text{(b)} \end{aligned} \tag{6.37}$$

6.4.4 *Subgrade Reaction and Contact Pressures*

In the Winkler model, the subgrade reaction consists of a series of discrete spring reactions, each acting at a node position. These reactions are directly proportional to the deflections at

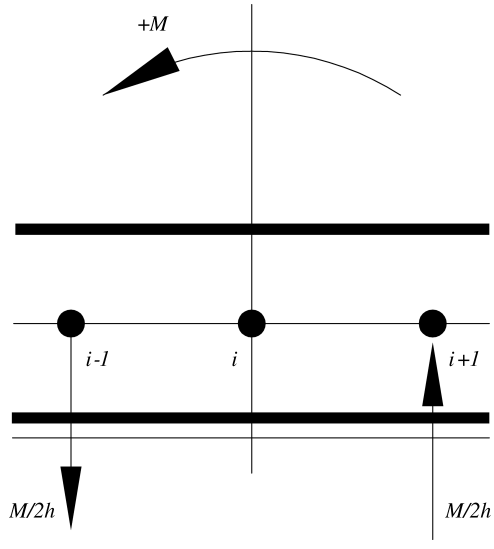

Figure 6.17 Positive moment applied at an internal node of BEF.

the respective nodes. While these reactions are normally negative, that is, acting upwards, they can also be positive (acting downwards) if tension between the beam and foundation is allowed.

The spring reactions at the nodes are given by

$$\begin{aligned} &\text{end node 1} && : && 0.5k_1w_1h \\ &\text{internal node } i\ (1 < i < n) && : && k_iw_ih \\ &\text{end node } n && : && 0.5k_nw_nh \end{aligned}$$

where the values of k are measured in kN/m^2.

Referring to Section 4.8, it is evident that at node i, $k_i = k_{si}b_i$, where k_{si} is the modulus of subgrade reaction (in kN/m^3) and b_i is the breadth of the beam at node i. When node i coincides exactly with a sudden change in the width of the beam (Figure 6.18) the effective width b_i at node i may be taken as $0.5\ (b_L + b_R)$ for the purposes of practical calculations.

If the change of width is continuous, the beam width can be taken as the average width up to $\frac{h}{2}$ on either side (stepped approximation) as shown in Figure 6.19.

The treatment of sudden change in k_s is shown diagrammatically in Figure 6.20. If the sudden change occurs at a node i (Figure 6.20), then $k_{s,i}$ is taken as $0.5\ (k_{iL} + k_{iR})$. When the change occurs between two nodes, there is a truncation effect.

6.4.5 FD Analysis for BEF Problems

The FD analysis of a beam on an elastic foundation is carried out by relating the unknown nodal deflections to the applied loading and then solving the resulting system of simultaneous equations for the unknown deflections. These deflections can then be used to calculate the

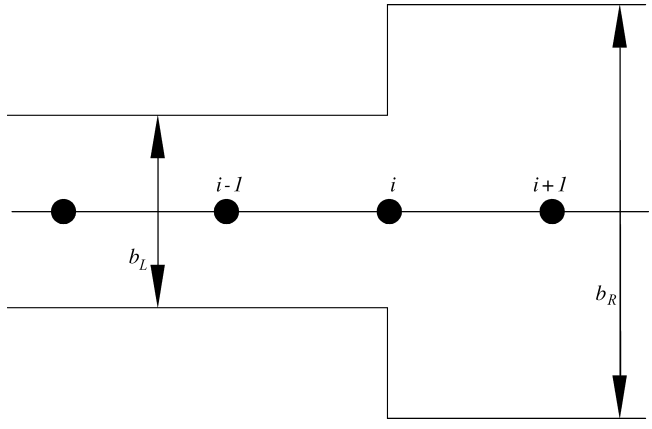

Figure 6.18 Sudden change of beam width at a node (plan).

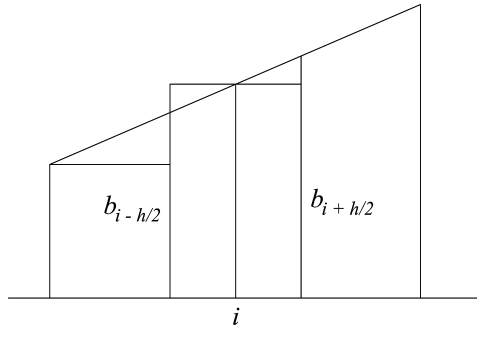

Figure 6.19 Continuously varying beam width at node *i*.

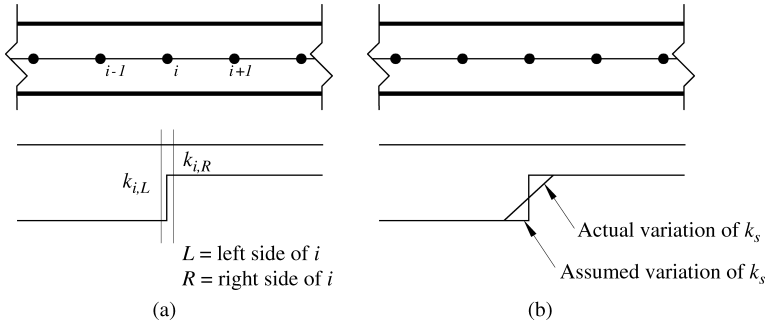

Figure 6.20 Sudden change in modulus of subgrade reaction at a node.

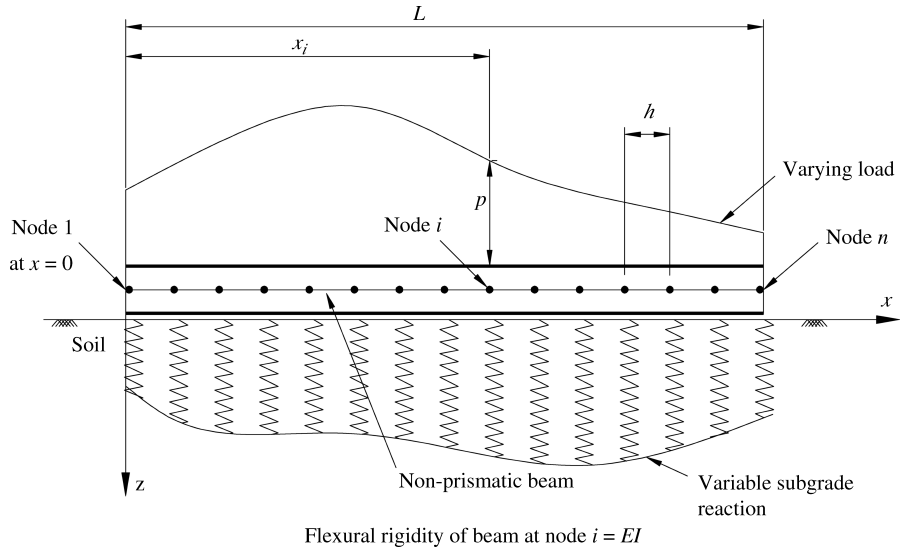

Figure 6.21 Non-prismatic beam on a variable elastic foundation subjected to general loads.

bending moments, shear forces and other reactions. As mentioned earlier, this can readily account for sudden or gradual variations in the flexural rigidity of the beam, subgrade reaction and applied loads and so on. Finite difference theory also enables various support conditions to be easily modeled, thereby allowing almost any combination of loading and support condition (s) to be investigated.

Consider the general case of a loaded non-prismatic beam on a variable elastic foundation (Figure 6.21). The length of the beam is L and the node spacing is h. The governing differential equation derived in Chapter 4 is

$$\frac{d^2}{dx^2}\left(EI\frac{d^2w}{dx^2}\right) = \frac{d^2}{dx^2}(-M) = p - kw \tag{6.38}$$

where $k = k_s b$ (kN/m^2), k_s is the modulus of subgrade reaction (kN/m^3) and b is the breadth of beam (m), M is the bending moment in the beam and I is the moment of inertia of the beam cross-section about its neutral axis.

At node i

$$EI_i\left(\frac{d^2w}{dx^2}\right)_i = -M_i \tag{6.39}$$

$$-\left(\frac{d^2M}{dx^2}\right)_i = p_i - k_i w_i \tag{6.40}$$

where $k = k_{s,i} b_i$ and $k_{s,i}$ is the modulus of subgrade reaction at node i and b_i is the breadth of beam at node i. Using central differences, substitution for $\left(\frac{d^2w}{dx^2}\right)$, given by FDOs in Figure 6.5,

into Equation (6.40) gives

$$M_i \cong -\frac{EI_i(w_{i-1}-2w_i + w_{i+1}}{h^2} \tag{6.41}$$

Likewise

$$M_{i-1} \cong -\frac{EI_{i-1}\,(w_{i-2}-2w_{i-1} + w_i)}{h^2} \tag{6.42}$$

$$M_{i+1} \cong -\frac{EI_{i+1}(w_i-2w_{i+1} + w_{i+2})}{h^2} \tag{6.43}$$

Applying the same FD operator for the second derivative now in terms of $M = -EI\frac{d^2w}{dx^2}$ given by Equation (6.38) results in

$$-\frac{(M_{i-1}-2M_i + M_{i+1})}{h^2} \cong p-k_iw_i$$

Replacing p_ih by the equivalent point load P_i, as explained in Section 6.4 we have

$$-\frac{(M_{i-1}-2M_i + M_{i+1})}{h} \cong P_i-k_iw_ih \tag{6.44}$$

Substituting the values of M_i, M_{i-1}, and M_{i+1} given by Equations (6.41)–(6.43), we get

$$\frac{E}{h^3}\,[I_{i-1}w_{i-2}-2(I_{i-1} + I_i)w_{i-1} + (I_{i-1} + 4I_i + I_{i+1})\,w_i$$
$$-2(I_i + I_{i+1})w_{i+1} + I_{i+1}w_{i+2}] \cong P_i-k_iw_ih \tag{6.45}$$

This can be rewritten as

$$\frac{E}{h^3}\left[I_{i-1}w_{i-2}-2\,(I_{i-1} + I_i)\,w_{i-1} + \left(I_{i-1} + 4I_i + I_{i+1} + \frac{k_ih^4}{E}\right)w_i\right.$$
$$\left.-2(I_i + I_{i+1})w_{i+1} + I_{i+1}w_{i+2}\right] \cong P_i \tag{6.46}$$

If the beam is of uniform cross-section with a flexural rigidity of EI, Equation (6.46) reduces to

$$\frac{EI}{h^3}\left[w_{i-2}-4w_{i-1} + \left(6 + \frac{k_ih^4}{EI}\right)w_i-4w_{i+1} + w_{i+2}\right] \cong P_i \tag{6.47}$$

For a uniform beam, Equation (6.47) can be also written directly from FDOs given in Figure 6.5 which can be readily verified.

6.5 Boundary Conditions

In dealing with boundary conditions, the end nodes and the interior nodes next to them require special consideration when the finite difference analysis of the loaded beam is to be carried out. It is convenient, to express the FD approximation of the load deflection equation for node *i*. The value of *i* can, take the value of 1, 2, *n*–1 or *n*, where *n* is the total number of nodes used in the discretization.

Equation (6.46) can be modified and applied to nodes at the ends of the beam by introducing fictitious nodes, if required, beyond the ends of the beam and considering different end conditions (free, simply supported, encastre, restrained). This is illustrated in Example 6.2, Section 6.3.2. In each case, the ends of the beam will be allowed to deflect freely or deflect by a prescribed amount. This amount can be zero, of course. Load deflection equations are developed in this chapter for the boundary nodes assuming free displacements at the ends of the beam. These same equations can then be used to satisfy the conditions for end nodes with prescribed displacements by substitution of the appropriate values.

6.5.1 Free Ends

Consider the case when node i is at the left-hand end of the beam (Figure 6.22), the bending moment at node i is zero, that is, $M_i = 0$. The bending moment at node $i + 1$ due to the equivalent point load at node i and the subgrade reaction is

$$M_{i+1} = -P_i h + 0.5 k_i w_i h^2$$

Equation (6.43) expresses M_{i+1} in terms of deflections w_i, w_{i+1}, w_{i+2}, hence

$$\frac{EI_{i+1}(w_i - 2w_{i+1} + w_{i+2})}{h^3} \cong P_i - 0.5 k_i w_i h \tag{6.48}$$

Rearranging the equation we get

$$\frac{E}{h^3}\left[\left(I_{i+1} + \frac{0.5 k_i h^4}{E}\right) w_i - 2I_{i+1} w_{i+1} + I_{i+1} w_{i+2}\right] \cong P_i \tag{6.49}$$

Hence, substituting $i = 1$ (end node at the left-hand end of the beam as shown in Figure 6.22(a)) gives

$$\frac{E}{h^3}\left[\left(I_2 + \frac{0.5 k_1 h^4}{E}\right) w_1 - 2I_2 w_2 + I_2 w_3\right] \cong P_1 \tag{6.50}$$

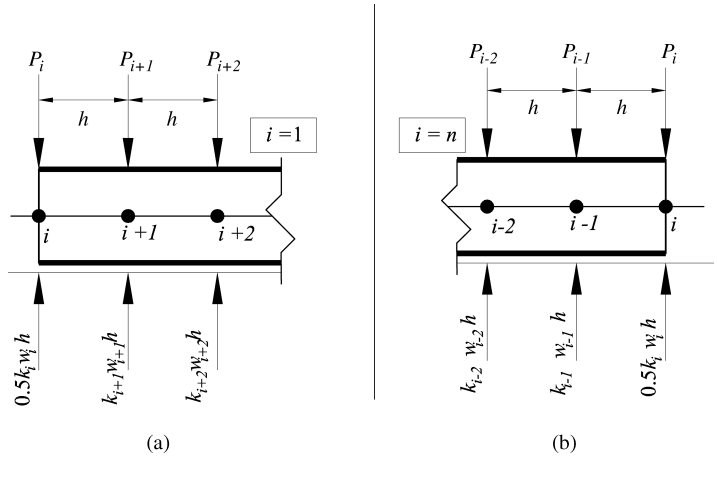

Figure 6.22 Free ends: (a) nodes at left end of beam; (b) nodes at right end of beam.

The corresponding expression for a node i at the right-hand end of the beam (Figure 6.22b) is

$$\frac{E}{h^3}\left[I_{i-1}w_{i-2}-2I_{i-1}w_{i-1}+\left(I_{i-1}+\frac{0.5k_ih^4}{E}\right)w_i\right]\cong P_i \tag{6.51}$$

Accordingly, substituting $i=n$, where n is the total number of nodes, gives

$$\frac{E}{h^3}\left[I_{n-1}w_{n-2}-2I_{n-1}w_{n-1}+\left(I_{n-1}+\frac{0.5k_nh^4}{E}\right)w_n\right]\cong P_n \tag{6.52}$$

When node i is the penultimate node at the left-hand end of the beam (Figure 6.23(a)), we have $M_{i-1}=0$.

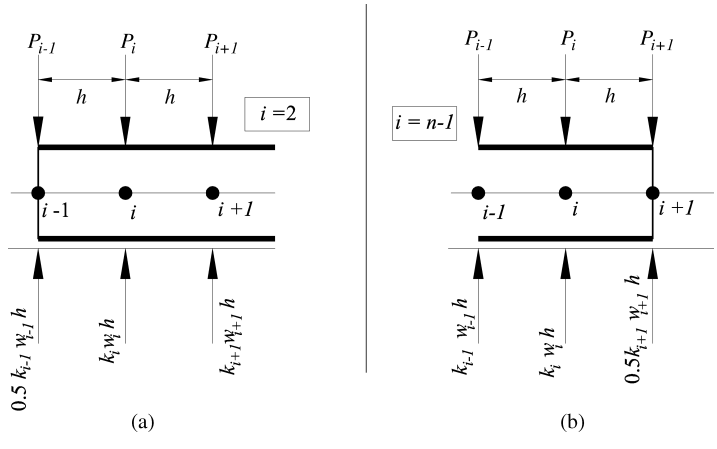

Figure 6.23 Free ends, penultimate nodes: (a) left end; (b) right end.

Substituting $M_{i-1}=0$ into Equation (6.44) yields

$$\frac{-(-2M_i+M_{i+1})}{h}\cong P_i-k_iw_ih$$

Further substitution for M_i and M_{i+1} in terms of the unknown deflections, as given by Equations (6.42) and (6.43) respectively, results in

$$\frac{E}{h^3}\left[-2I_iw_{i-1}+\left(4I_i+I_{i+1}+\frac{k_ih^4}{E}\right)w_i-2(I_i+I_{i+1})w_{i+1}+I_{i+1}w_{i+2}\right]\cong P_i \tag{6.53}$$

Substituting $i=2$ (penultimate node at the left-hand end of the beam) gives

$$\frac{E}{h^3}\left[-2I_2w_1+\left(4I_2+I_3+\frac{k_2h^4}{E}\right)w_2-2(I_2+I_3)w_3+I_3w_4\right]\cong P_2 \tag{6.54}$$

The corresponding expression for a penultimate node i at the right-hand end of the beam (Figure 6.23(b)) is

$$\frac{E}{h^3}\left[I_{i-1}w_{i-2}-2(I_{i-1}+I_i)w_{i-1}+\left(I_{i-1}+4I_i+\frac{k_ih^4}{E}\right)w_i-2I_iw_{i+1}\right]\cong P_i \qquad (6.55)$$

Hence, the substitution of $i=n-1$ in Equation (6.55) (for the penultimate end) gives

$$\frac{E}{h^3}\left[I_{n-2}w_{n-3}-2(I_{n-2}+I_{n-1})w_{n-2}+\left(I_{n-2}+4I_{n-1}+\frac{k_{n-1}h^4}{E}\right)w_{n-1}-2I_{n-1}w_n\right]\cong P_{n-1} \qquad (6.56)$$

6.5.2 *Simply Supported Ends*

If simply supported ends are allowed to deflect freely, they are similar to the cases of free ends already considered in Section 6.5.1. It is appropriate, therefore, to consider only prescribed displacements at the end nodes. Logically, it follows that the load deflection equations for these nodes are the same as those on beams with free ends. This can be easily proved for instance, by considering the left-hand end of a beam where the simple support is at the end and node i is the penultimate node (Figure 6.24(a)). The boundary condition is $M_{i-1}=0$.

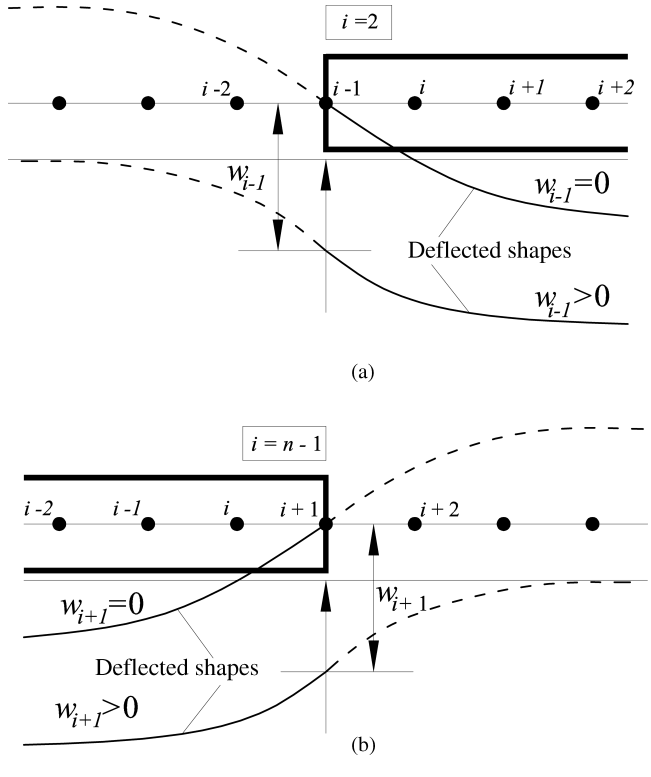

Figure 6.24 Simply supported ends: (a) left end; (b) right end.

This condition is satisfied if the beam is considered to be continuous with a fictitious beam having flexural rigidities (EI), support conditions and loadings that are all mirrored about the horizontal and vertical axes passing through, node *i*–1 as indicated in Figure 6.24(a). It follows that $w_{i-2} = 2w_{i-1} - w_i$. The substitution of this value into Equation (6.46) for node *i* give exactly the same result as that obtained for the penultimate node of a beam with a free left-hand end. Equations (6.47)–(6.56), therefore, apply equally to boundary nodes of beams with simply supported ends having prescribed displacements.The penultimate node at the right end (Figure 6.24(b)) can be similarly analyzed.

6.5.3 *Fixed Ends*

These can also be referred to as *encastre ends*.

Considering the left-hand end of the beam, we have

$$w_{i-1} = w_{i+1},\ w_{i-2} = w_{i+2},\ I_{i-1} = I_{i+1},\ \text{ and }\ I_{i-2} = I_{i+2}$$

Substituting these values into Equation (6.46) and halving the left-hand side of the equation to account for this node being an end node gives

$$\frac{E}{h^3}\left[\left(2I_i + I_{i+1} + \frac{0.5k_ih^4}{E}\right)w_i - 2(I_i + I_{i+1})w_{i+1} + I_{i+1}w_{i+2}\right] \cong P_i \tag{6.57}$$

Substituting $i = 1$ for this node yields (Figure 6.25(a))

$$\frac{E}{h^3}\left[\left(2I_1 + I_2 + \frac{0.5k_ih^4}{E}\right)w_1 - 2(I_1 + I_2)w_2 + I_2w_3\right] \cong P_1 \tag{6.58}$$

The corresponding equation (to Equation (6.57)) for node i at the right-hand end of the beam is

$$\frac{E}{h^3}\left[\left(I_{i-1} + 2I_i + \frac{0.5k_ih^4}{E}\right)w_i - 2(I_i + I_{i-1})w_{i-1} + I_{i-1}w_{i-2}\right] \cong P_i \tag{6.59}$$

Substituting $i = n$, where n is the total number of nodes, gives (Figure 6.25(b))

$$\frac{E}{h^3}\left[\left(I_{n-1} + 2I_n + \frac{0.5k_nh^4}{E}\right)w_n - 2(I_n + I_{n-1})w_{n-1} + I_{n-1}w_{n-2}\right] \cong P_n \tag{6.60}$$

When there is no displacement at node 1, the deflection is simply $w_i = 0$ ($i = 1$ or n). As with other boundary conditions, the penultimate nodes at each fixed end must also be considered, that is, node 2 and node $n - 1$.

Considering the penultimate node *i* at the left-hand end of the beam, as shown in Figure 6.25, we may note

$$w_{i-2} = w_i \ \text{ and } \ I_{i-2} = I_i$$

Substituting these values into Equation (6.46), we get

$$\frac{E}{h^3}\left[-2(I_{i-1} + I_i)w_{i-1} + \left(2I_{i-1} + 4I_i + I_{i+1} + \frac{k_ih^4}{E}\right)w_i - 2(I_i + I_{i+1})w_{i+1} + I_{i+1}w_{i+2}\right] \cong P_i \tag{6.61}$$

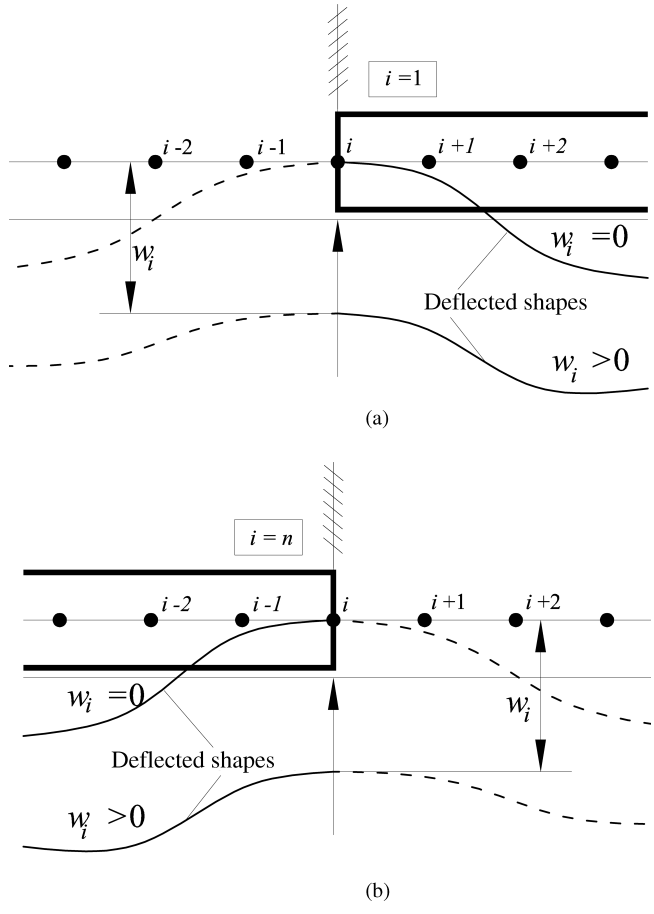

Figure 6.25 Fixed ends, end nodes: (a) left end; (b) right end.

Substituting $i = 2$ gives

$$\frac{E}{h^3}\left[-2(I_1 + I_2)\, w_1 + \left(2I_1 + 4I_2 + I_3 + \frac{k_2 h^4}{E}\right) w_2 - 2\,(I_2 + I_3) w_3 + I_3 w_4\right] \cong P_2 \quad (6.62)$$

When $w_1 = 0$, the above Equation (6.62) becomes

$$\frac{E}{h^3}\left[\left(2I_1 + 4I_2 + I_3 + \frac{k_2 h^4}{E}\right) w_2 - 2(I_2 + I_3) w_3 + I_3 w_4\right] \cong P_2 \quad (6.63)$$

The corresponding equation for the penultimate node i at the right hand end of the beam when $w_i > 0$ is

$$\frac{E}{h^3}\left[-2(I_i + I_{i+1}) w_{i+1} + \left(2I_{i+1} + 4I_i + I_{i-1} + \frac{k_i h^4}{E}\right) w_i - 2(I_{i-1} + I_i) w_{i-1} + I_{i-1} w_{i-2}\right] \cong P_i \quad (6.64)$$

Substituting $i = n-1$ in the above Equation (6.64) gives

$$\frac{E}{h^3}\left[-2(I_{n-1} + I_n)w_n + \left(2I_n + 4I_{n-1} + I_{n-2} + \frac{k_{n-1}h^4}{E}\right)w_{n-1}\right.$$
$$\left.-2(I_{n-2} + I_{n-1})w_{n-2} + I_{n-2}w_{n-3}\right] \cong P_{n-1} \tag{6.65}$$

When $w_n = 0$, Equation (6.65) simplifies as

$$\frac{E}{h^3}\left[\left(2I_n + 4I_{n-1} + I_{n-2} + \frac{k_{n-1}h^4}{E}\right)w_{n-1} - 2(I_{n-2} + I_{n-1})w_{n-2} + I_{n-2}w_{n-3}\right] \cong P_{n-1} \tag{6.66}$$

In addition to the above, we can also prescribe other types of boundary conditions and internal restraints. These also can be taken care of easily by FDM (Jones, 1997).

6.6 Calculation of Bending Moments

Bending moments can be calculated at each of the nodes along the beam. It is assumed that the bending moments vary linearly between the nodes. Thus, if a large number of nodes are used in the analysis (finer discretization), the results will in general be more accurate.

6.6.1 Boundary Nodes

The bending moments at a free end or simply supported end is obviously zero unless a couple is applied at the end. In the case of a fixed left-hand end, Figure 6.25(a), the bending moment at end node 1 is calculated from Equation (6.41) as follows

$$M_1 = -\frac{2EI_1(w_2 - w_1)}{h^2} \tag{6.67}$$

If $w_1 = 0$, then this simplifies to

$$M_1 = -\frac{2EI_1 w_2}{h^2} \tag{6.68}$$

At the right-hand end of the beam, (Figure 6.25(b)), the corresponding equations for end node n (n is the number of nodes) are

$$M_n = -\frac{2EI_n(w_{n-1} - w_n)}{h^2} \tag{6.69}$$

When $w_n = 0$, this reduces to

$$M_n = -\frac{2EI_n w_{n-1}}{h^2} \tag{6.70}$$

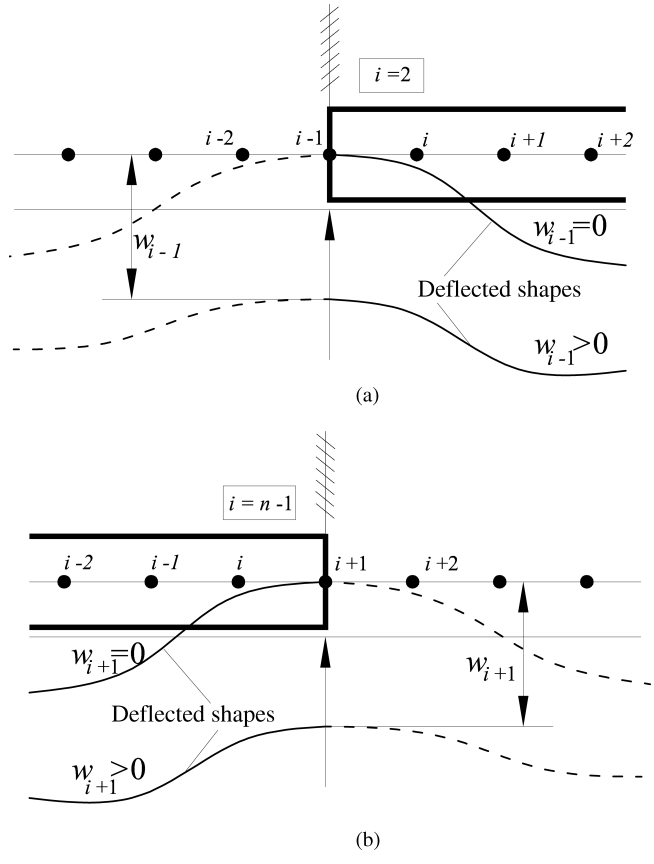

Figure 6.26 Fixed ends, penultimate nodes: (a) left end; and (b) right end.

6.6.2 *Internal Nodes*

In this context, an internal node i is defined as one numbered $2 < i < n-1$, where n is the number of nodes. The bending moment at a free internal node is generally calculated using Equation (6.41) which gives

$$M_i \cong -\frac{EI_i(w_{i-1} - 2w_i + w_{i+1})}{h^2} \tag{6.71}$$

While this equation also applies at an internal support, with or without vertical displacement, it does require some modification (Jones, 1997). Locations requiring modification include:

1. A free internal node where several moments M (kNm) are applied.
2. An internal fixed support, with and without a vertical displacement.
3. An internal simple support having a rotational restraint, with and without a vertical displacement.

6.7 Shear Forces

Using finite difference method we can compute deflections and bending moments at the nodes along the beam. Bending moments between nodes are assumed to vary linearly. Consequently, the shear forces between nodes are constant as indicated in Figure 6.27. A smoothing of the shear force diagram is achieved by joining the average values of shear forces between nodes as shown in Figure 6.27. Modifications are then only required at nodes affected by physical point loads, applied couples and support reactions (Jones, 1997). Defining $Q_{i,L}$ as the shear force immediately to left of node i, $Q_{i,R}$ as the shear force immediately to right of node i, and Q_i is the average shear force at node i, the FD expressions for shear forces are given below.

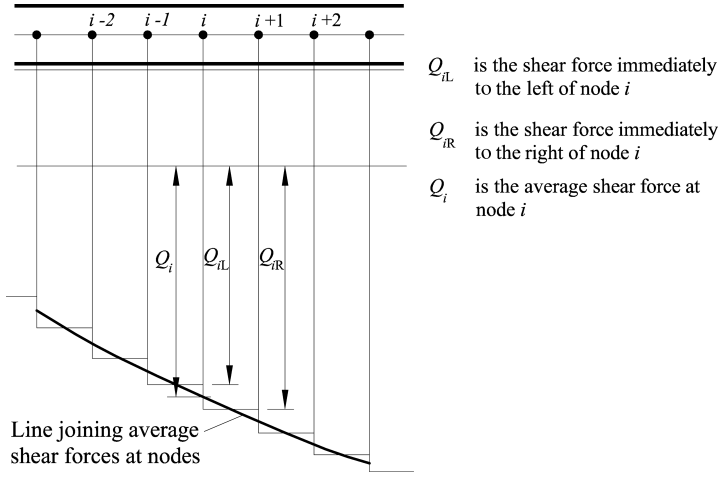

Figure 6.27 Shear forces between nodes (constant).

6.7.1 Boundary Nodes

Consider the general case of the two end nodes (numbered 1 or n; Figure 6.28). The reactions R_1 and R_n occur at simple supports, fixed supports or simple supports with rotational restraint. Clearly, if either end is free, the reaction at that end is zero. Consequently, the shear force at node 1, Q_1, at the extreme left-hand end of the beam is given by

$$Q_1 = R_1 - \sum P_1 \tag{6.72}$$

where R_1 is the support reaction at node 1, and $\sum P_1$ is the algebraic sum of all vertical point loads acting at node 1.

Likewise, at the right-hand end node n, the shear force (Q_n) is given by

$$Q_n = -R_n + \sum P_n \tag{6.73}$$

where R_n is the support reaction at node n, and $\sum P_n$ is the algebraic sum of all vertical point loads acting at node n.

Expressions for R_1 and R_n are given in Section 6.8.

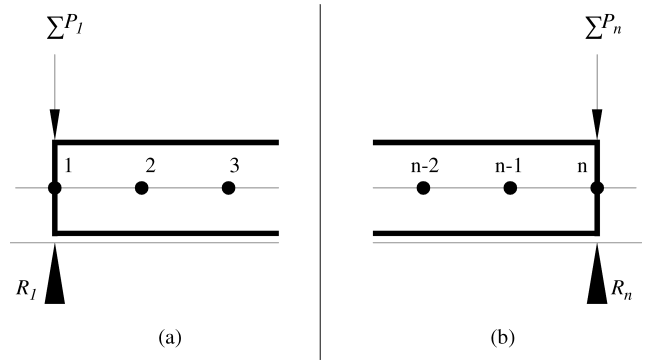

Figure 6.28 Boundary nodes, end nodes: (a) left end; (b) right end.

In the case of the two penultimate nodes (numbered 2 and $n-1$ respectively), as shown in Figure 6.29, the shear forces acting immediately to the left and right of the node are given by:

$$\text{Node 2(left)}\ Q_{2,L} = \frac{(-M_{1,R} + M_{2,L} - M_{2,R} + M_{3,L})}{2h} - 0.5\left(P_{2,L} + P_{2,R} - \sum P_2\right) \quad (6.74)$$

where $M_{1,R}$ is the bending moment acting immediately to right-hand side of node 1, $M_{2,L}$ is the bending moment acting immediately to left-hand side of node 2, $M_{2,R}$ is the bending moment acting immediately to right-hand side of node 2, $M_{3,L}$ is the bending moment acting immediately to left-hand side of node 3, $P_{2,L}$ is the equivalent point load acting at node 2 derived from point loads and/or moments acting to the left of node 2, $P_{2,R}$ is the equivalent point load acting at node 2 derived from point loads and/or moments acting to the right of node 2, and $\sum P_2$ is the algebraic sum of all vertical point loads acting at node 2.

$$\text{Node 2(right)}\ Q_{2,R} = Q_{2,L} - \sum P_2 \quad (6.75)$$

Similarly, at the right-hand penultimate node $n-1$, the corresponding equations are:

$$\text{Node n}-1\text{(left)}\ Q_{n-1,L} = -\frac{(-M_{n,L} + M_{n-1,R} - M_{n-1,L} + M_{n-2,R})}{2h} - 0.5\left(P_{n-1,L} + P_{n-1,R} - \sum P_{n-1}\right) \quad (6.76)$$

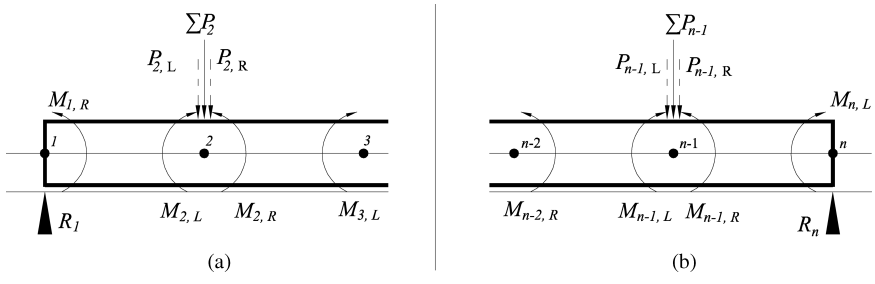

Figure 6.29 Boundary nodes, penultimate nodes: (a) left end; (b) right end.

where $M_{n,L}$ is the bending moment acting immediately to left-hand side of node n. $M_{n-1,R}$ is the bending moment acting immediately to right-hand side of node $n-1$, $M_{n-1,L}$ is the bending moment acting immediately to left-hand side of node $n-1$, $M_{n-2,R}$ is the bending moment acting immediately to right-hand side of node $n-2$, $P_{n-1,L}$ is the equivalent point load acting at node $n-1$ derived from point loads and/or moments acting to the left of node $n-1$, $P_{n-1,R}$ is the equivalent point load acting at node $n-1$ derived from point loads and/or moments acting to the right of node $n-1$, and $\sum P_{n-1}$ is the algebraic sum of all vertical point loads acting at node $n-1$.

$$\text{Node n}-1\,(\text{right})\ Q_{n-1,R} = Q_{n-1,L} - \sum P_{n-1} \tag{6.77}$$

6.7.2 *Internal Nodes*

Consider an internal node i at a point along a loaded beam supported only by the subgrade, that is, with no point support of any kind at node i. The constant shear force ($Q_{i,L}$) between internal nodes $i-1$ and i is given by

$$Q_{i,L} = \frac{(M_i - M_{i-1})}{h} \tag{6.78}$$

Substituting the values of M_i and M_{i-1} given by Equations (6.41) and (6.42) respectively gives

$$Q_{i,L} = -\frac{E}{h^3}\left[-I_{i-1}w_{i-2} + (2I_{i-1} + I_i)w_{i-1} - (I_{i-1} + 2I_i)w_i + I_i w_{i+1}\right] \tag{6.79}$$

Similarly, the shear force between nodes i and $i+1$ is given by

$$Q_{i,R} = \frac{(M_{i+1} - M_i)}{h} \tag{6.80}$$

Hence, substituting the values of M_i and M_{i+1} given by Equations (6.41) and (6.43) respectively results in

$$Q_{i,R} = -\frac{E}{h^3}\left[-I_i w_{i-1} + (2I_i + I_{i+1})w_i - (I_i + 2I_{i+1})w_{i+1} + I_{i+1}w_{i+2}\right] \tag{6.81}$$

The average shear force at node i is therefore

$$Q_i = 0.5\,(Q_{i,L} + Q_{i,R})$$

that is

$$Q_i = \frac{E}{2h^3}\left[I_{i-1}w_{i-2} - 2I_{i-1}w_{i-1} - (I_{i+1} + I_{i-1})w_i + 2I_{i+1}w_{i+1} - I_{i+1}w_{i+2}\right] \tag{6.82}$$

This equation takes into account the effects of uniformly distributed and varying loads but requires modification for the effects of point loads and applied moments.

If the beam is prismatic with a flexural rigidity of EI, Equation (6.82) reduces to

$$Q_i = \frac{EI}{2h^3}\left[w_{i-2} - 2w_{i-1} + 2w_{i+1} - w_{i+2}\right] \tag{6.83}$$

Consider now an internal node i (Figure 6.30), where there is a total physical point load of $\sum P_i$ and equivalent point loads of $P_{i,L}$ and $P_{i,R}$, due only to other physical point loads acting between nodes $i-1$ and $i+1$. The values of $Q_{i,L}$ and $Q_{i,R}$ at node i due to these point loads are

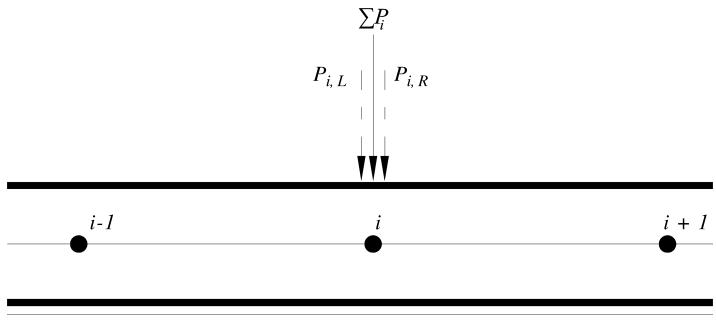

Figure 6.30 Internal node with actual and equivalent point loads.

given by

$$Q_{i,L} = \frac{E}{2h^3}[I_{i-1}w_{i-2} - 2I_{i-1}w_{i-1} - (I_{i+1} + I_{i-1})w_i + 2I_{i+1}w_{i+1} - I_{i+1}w_{i+2}]$$
$$-0.5\left(P_{i,L} - P_{i,R} - \sum P_i\right) \tag{6.84}$$

$$Q_{i,R} = Q_{i,L} - \sum P_i \tag{6.85}$$

Moments at and (or) between nodes will influence the values of the resulting nodal displacements and, the values of the shear forces. Values of the shear forces given by Equation (6.82) must be modified for nodes local to each of the acting moments (Jones, 1997).

6.8 Vertical Reactions

Expressions for vertical reactions acting at boundary and intermediate supports, coinciding with nodes, are given below. In each case, the vertical displacement at a support may be zero, prescribed or free. In the latter case (i.e., free end), the reaction at the support is zero.

6.8.1 Supports at Boundary Nodes

6.8.1.1 BEF with Simply Supported Ends

If the BEF is simply supported at one or both of the boundary nodes (numbered 1 and n), as shown in Figure 6.31, the vertical reactions R at these nodes are expressed in terms of the equivalent nodal point loads P (including the physical point loads acting at the nodes), as:

Reaction at node 1

$$R_1 = P_1 - \frac{E}{h^3}\left[\left(I_2 + \frac{0.5k_1h^4}{E}\right)w_1 - 2I_2w_2 + I_2w_3\right] \tag{6.86}$$

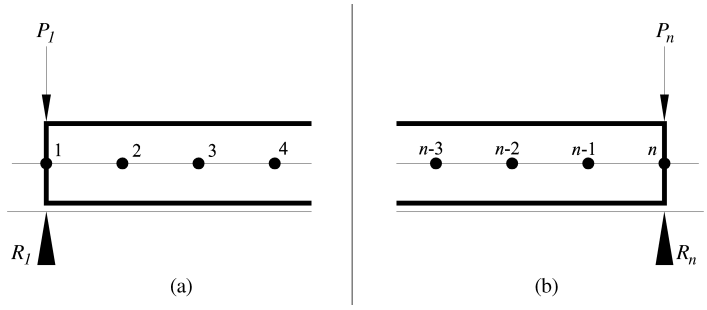

Figure 6.31 Simple supports at boundary nodes.

If $w_1 = 0$, this expression reduces to

$$R_1 = P_1 - \frac{EI_2}{h^3}(-2w_2 + w_3) \tag{6.87}$$

Reaction at node n

$$R_n = P_n - \frac{E}{h^3}\left[I_{n-1}w_{n-2} - 2I_{n-1}w_{n-1} + \left(I_{n-1} + \frac{0.5k_n h^4}{E}\right)w_n\right] \tag{6.88}$$

When $w_n = 0$, this becomes

$$R_n = P_n - \frac{E}{h^3}\left[I_{n-1}w_{n-2} - 2I_{n-1}w_{n-1}\right] \tag{6.89}$$

6.8.1.2 BEF with Fixed Supports

When the boundary supports are fixed (Figure 6.32), the corresponding expressions for the reactions are as follows

$$R_1 = P_1 - \frac{E}{h^3}\left[\left(2I_1 + I_2 + \frac{0.5k_1 h^4}{E}\right)w_1 - 2(I_1 + I_2)w_2 + I_2 w_3\right] \tag{6.90}$$

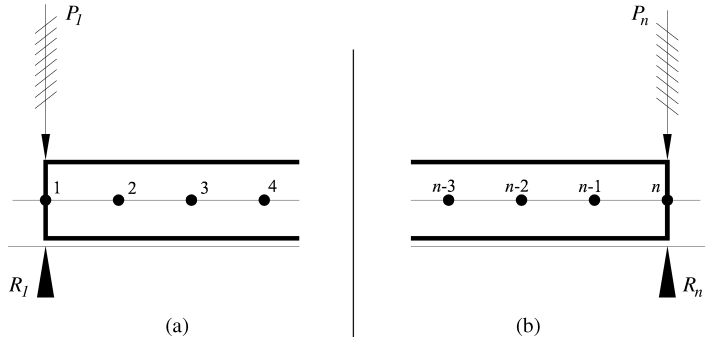

Figure 6.32 Fixed end supports at boundary nodes: (a) left end; (b) right end.

Again if $w_1 = 0$, then

Similarly
$$R_1 = P_1 - \frac{E}{h^3}[-2(I_1 + I_2)w_2 + I_2 w_3] \tag{6.91}$$

$$R_n = P_n - \frac{E}{h^3}\left[\left(I_{n-1} + 2I_n + \frac{0.5k_n h^4}{E}\right)w_n - 2(I_{n-1} + I_n)\, w_{n-1} + I_{n-1}w_{n-2}\right] \tag{6.92}$$

When $w_n = 0$, this becomes

$$R_n = P_n - \frac{E}{h^3}[-2(I_{n-1} + I_n)\, w_{n-1} + I_{n-1}w_{n-2}] \tag{6.93}$$

6.8.1.3 Simple Supports with Rotational Restraint

When the boundary supports are simple supports with a rotational restraint of τ (kNm/radian; Figure 6.33), the corresponding reactions are given by (Jones, 1997)

$$R_1 = P_1 - \frac{E}{h^3}\left[\left(I_1(1 + \xi_1) + I_2 + \frac{0.5k_1 h^4}{E}\right)w_1 - (I_1(1 + \xi_1) + 2I_2)w_2 + I_2 w_3\right] \tag{6.94}$$

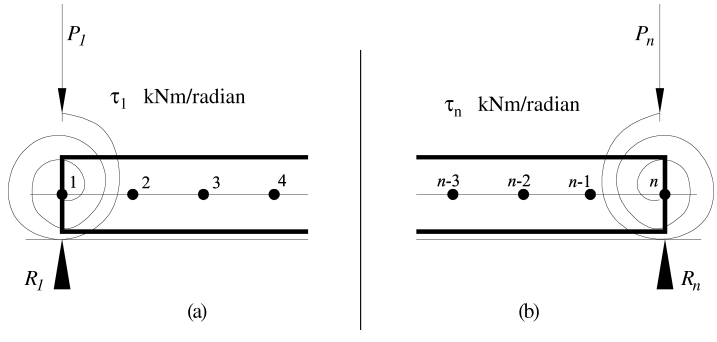

Figure 6.33 Simple supports with rotational restraint at boundary nodes: (a) left end; (b) right end.

where

$$\xi_1 = \frac{\tau_1 - \left(\frac{2EI_1}{h}\right)}{\tau_1 + \left(\frac{2EI_1}{h}\right)} \tag{6.95}$$

If $w_1 = 0$, the above Equation (6.94) simplifies as

$$R_1 = P_1 - \frac{E}{h^3}[-(I_1(1 + \xi_1) + 2I_2)\, w_2 + I_2 w_3] \tag{6.96}$$

Note: If $\xi_1 = -1$ (simple support with no rotational restraint), Equation (6.96) yields the same result as Equation (6.87). Similarly, if $\xi_1 = +1$ (fixed support), Equation (6.96) yields the same result as Equation (6.91).

Similarly reaction at the right end node (n) is

$$R_n = P_n - \frac{E}{h^3}\left[\begin{array}{l} I_{n-1}w_{n-2} - (2I_{n-1} + I_n(1 + \xi_n))w_{n-1} \\ + \left(I_{n-1} + I_n(1 + \xi_n) + \dfrac{0.5k_nh^4}{E}\right)w_n \end{array}\right] \tag{6.97}$$

where

$$\xi_n = \frac{\tau_n - \left(\dfrac{2EI_n}{h}\right)}{\tau_n + \left(\dfrac{2EI_n}{h}\right)} \tag{6.98}$$

When $w_n = 0$, Equation (6.97) becomes

$$R_n = P_n - \frac{E}{h^3}\left[I_{n-1}w_{n-2} - (2I_{n-1} + I_n(1 + \xi_n))w_{n-1}\right] \tag{6.99}$$

6.8.2 Internal Supports

In each of the cases shown in Figure 6.34, the reaction R_i is given by

$$R_i = P_i - \frac{E}{h^3}\left[\begin{array}{l} I_{i-1}w_{i-2} - 2(I_{i-1} + I_i)w_{i-1} \\ + \left(I_{i-1} + 4I_i + I_{i+1} + \dfrac{k_ih^4}{E}\right)w_i - 2(I_i + I_{i+1})w_{i+1} + I_{i+1}w_{i+2} \end{array}\right] \tag{6.100}$$

6.9 Simplification for Prismatic Beams

The FD analysis presented in Sections 6.5–6.8 are for nonprismatic beams on soils with variable spring constants. If the flexural rigidity, EI, of the beam is constant throughout the length of the beam, then the beam is called a *prismatic beam*. For such beams on uniform soils (k_s and hence $k = k_sb$ are constant over the entire contact area), the expressions for various parameters presented in the above Sections 6.5–6.8 become quite simple and are summarized below.

6.9.1 FDO for Prismatic BEF

The FD analysis of BEF is illustrated with discretization using one and three internal nodes earlier in Section 6.3.2 and Example 6.2 for simple configurations. However, the same is extended to BEF with large number of internal nodes in this section.

The FDO for such a beam on elastic foundation at any node i is given in Equation (6.47) as below:

$$\frac{EI}{h^3}\left[w_{i-2} - 4w_{i-1} + \left(6 + \frac{kh^4}{EI}\right)w_i - 4w_{i+1} + w_{i+2}\right] \approx P_i \tag{6.101}$$

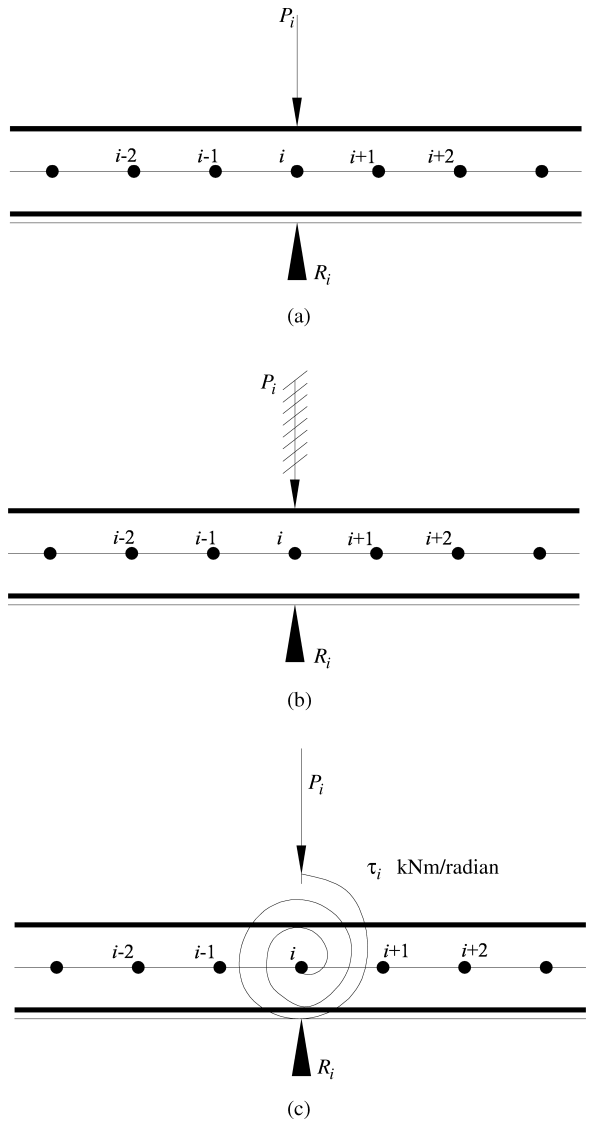

Figure 6.34 Internal supports: (a) simple; (b) fixed; (c) simple with rotational restraint.

where the parameters and nodes are defined also in Figures 6.10, 6.21 and 6.35. It may be recalled that the finite difference representation of the governing equation can be very easily written using FDOs given in Figures 6.5 and 6.8. The above equation is valid for all internal nodes except the two nodes, that is, end node and penultimate nodes near the two ends (1 and 2 for left end and $n-1$ and n for right end) as discussed in Section 6.5 and shown in Figures 6.35. This is because the FDO for the fourth derivative at any node i can be expressed in terms of two nodes on either side of the node as shown in Figure 6.5. Hence, the finite difference representation of BEF equation at these end nodes involves fictitious nodes -1 and -2 (for

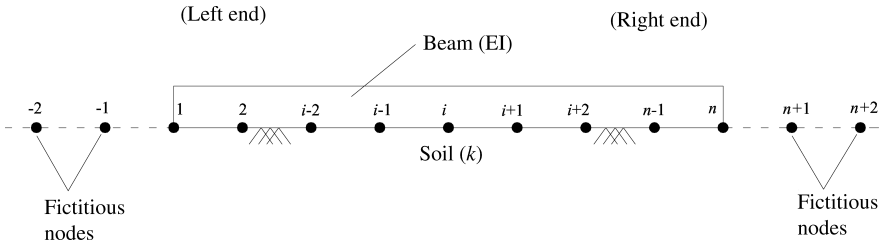

Figure 6.35 Finite difference notation for BEF.

nodes 1 and 2 for left end) and $n + 1$, $n + 2$ (for nodes $n - 1$ and n for right end). These fictitious nodes are beyond the domain of the beam ($0 \leq x \leq L$) and hence have to be calculated using boundary conditions at these ends as discussed in Section 6.5. Accordingly these are simplified depending on the boundary conditions and are summarized below for prismatic beams on elastic foundations.

6.9.2 Free Ends

Boundary conditions at $x = 0$ and L are $M = 0$ and $Q = 0$ which give the values at the fictitious nodes -1 and -2 (left end) as

$$w_{-1} = 2w_1 - w_2 \text{ and } w_{-2} = 4w_1 - 4w_2 + w_3 \tag{6.102}$$

$$w_{n+1} = 2w_n - w_{n-1} \text{ and } w_{n+2} = w_{n-2} - 4w_{n-1} + 4w_n \tag{6.103}$$

Replacing these values of w at the fictitious nodes -1 and -2 located outside the domain of BEF with the values of w at the nodes within the domain of BEF given by Equations (6.102) and (6.103), the governing FDO for BEF that is, Equation (6.101) can be expressed at nodes 1 and 2 as follows

$$\begin{aligned}
\text{At node 1}: &\quad \frac{EI}{h^3}\left[\left(2 + \frac{kh^4}{EI}\right)w_1 - 4w_2 + 2w_3\right] = P_1 && \text{(a)}\\
\text{At node 2}: &\quad \frac{EI}{h^3}\left[-2w_1 + \left(5 + \frac{kh^4}{EI}\right)w_2 - 4w_3 + w_4\right] = P_2 && \text{(b)}\\
\text{At node } n-1: &\quad \frac{EI}{h^3}\left[w_{n-3} - 4w_{n-2} + \left(5 + \frac{kh^4}{EI}\right)w_{n-1} - 2w_n\right] = P_{n-1} && \text{(c)}\\
\text{At node } n: &\quad \frac{EI}{h^3}\left[2w_{n-2} - 4w_{n-1} + \left(2 + \frac{kh^4}{EI}\right)w_n\right] = P_n && \text{(d)}
\end{aligned} \tag{6.104}$$

6.9.3 Simply Supported Ends

Boundary conditions at $x = 0$ and L are $w = 0$ and $M = 0$.

Since w is known (prescribed as 0) at $x = 0$ and L, the FDO for governing equation of BEF is not required at nodes 1 and n (Figure 6.35). It is required to be written at nodes 2 and $n - 1$. Hence only one fictitious node at each end is required that is, nodes -1 and $n + 1$. The values

of w at these fictitious nodes can be written by noting that $M = 0$ at $x = 0$ and L as

$$w_{-1} = -w_2 \text{ and } w_1 = 0 \tag{6.105}$$

$$w_{n+1} = -w_{n-1} \text{ and } w_n = 0 \tag{6.106}$$

The governing FDOs for BEF can then be written from Equation (6.101) as

$$\begin{aligned} &\text{At nodes 1 and } n: \quad \text{FDO is not required as } w_1 = w_n = 0 \\ &\text{At node 2}: \quad \frac{EI}{h^3}\left[\left(5 + \frac{kh^4}{EI}\right)w_2 - 4w_3 + w_4\right] = P_2 \qquad \text{(a)} \\ &\text{At node } n-1: \quad \frac{EI}{h^3}\left[w_{n-3} - 4w_{n-2} + \left(5 + \frac{kh^4}{EI}\right)w_{n-1}\right] = P_{n-1} \qquad \text{(b)} \end{aligned} \tag{6.107}$$

6.9.4 Fixed Ends

Boundary conditions at $x = 0$ and L are $w = 0$ and slope, $w' = 0$

Since w is known (prescribed as 0), the FDO for governing equation of BEF is not required at nodes 1 and n (Figure 6.35). It is required to be written at nodes 2 and $n - 1$. Hence only one fictitious node at each end is required that is, nodes -1 and $n + 1$. The values of w at these fictitious nodes can be written by noting that $w' = 0$ at $x = 0$ and L as

$$w_{-1} = w_2 \text{ and } w_1 = 0 \tag{6.108}$$

$$w_{n+1} = w_{n-1} \text{ and } w_n = 0 \tag{6.109}$$

The governing FDOs for BEF can then be written from Equation (6.101) as:

$$\begin{aligned} &\text{At nodes 1 and } n: \quad \text{FDO is not required as } w_1 = w_n = 0 \\ &\text{At node 2}: \quad \frac{EI}{h^3}\left[\left(7 + \frac{kh^4}{EI}\right)w_2 - 4w_3 + w_4\right] = P_2 \qquad \text{(a)} \\ &\text{At node n}-1: \quad \frac{EI}{h^3}\left[w_{n-3} - 4w_{n-2} + \left(7 + \frac{kh^4}{EI}\right)w_{n-1}\right] = P_{n-1} \qquad \text{(b)} \end{aligned} \tag{6.110}$$

6.9.5 Solutions of Simultaneous Equations

As explained in Sections 6.4–6.9, the BEF equation (Equation (6.101)) can be represented at each node (except at those nodes where the deflections are prescribed as per boundary conditions) as an algebraic equation in terms of the values of the function (w) at the neighboring nodes. The resulting system of simultaneous equation will be nonhomogenous and consistent with the number of unknowns (the nodal values of the function/deflection) depending on the number of intervals (i.e., h) into which the beam is discretised and resulting nodes where the function is not prescribed and hence governed by Equation (6.101). Standard procedures and efficient algorithms like Gauss elimination technique and so on (Crandall, 1956; Kreyszig, 1967) can be used to solve these simultaneous equations uniquely. With the deflections obtained from these solutions, the slope, the bending moment and the shear force can be obtained by using FD representation of these quantities as explained in the above sections. The

contact pressure (soil reaction) can be calculated at any point by multiplying the deflection, w with the spring constant k as $q(x) = kw$. The values of any of the above BEF parameters at any point intermediate between nodes is computed by interpolation (Crandall, 1956) and also explained in the earlier sections. These parameters can be graphically plotted for the entire domain (length L of the beam) for further analysis and design noting salient values like the maximum and minimum values, and their locations and so on. These are discussed in Chapter 12. A few examples of FD analysis of BEF are presented below.

Example 6.3

Analyze BEF with free edges given in Figure 6.36 using FDM

Length of the beam, $L = 6$ m
Width, $b = 1$ m
Depth, $d = 0.5$ m
Modulus of subgrade reaction, $k_s = 10^4$ kN/m^3
Spring constant, $k = k_s b = 10^4$ kN/m^2

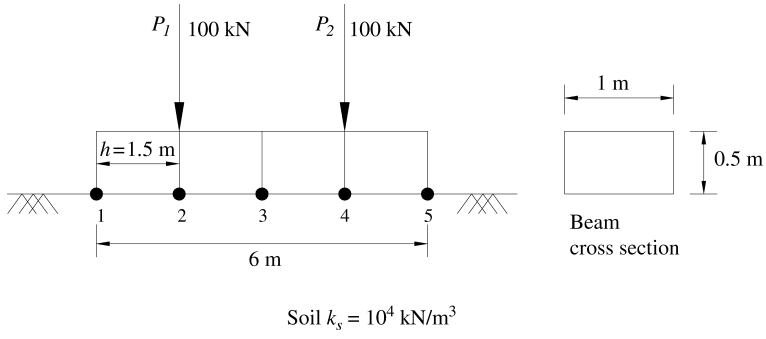

Figure 6.36 BEF with applied loads.

Divide the beam into four equal intervals of 1.5 m each for FDM discretization, that is

$$h = 1.5 \text{ m},\ E \text{ of concrete} = 20 \times 10^6 \text{ kN/m}^2$$

$$I = \frac{bd^3}{12} = \frac{1 \times 0.5^3}{12} = 0.01 \text{ m}^4$$

$$EI = 20 \times 10^6 \times 0.01 = 20 \times 10^4 \text{ kNm}^2$$

$$\lambda = \sqrt[4]{\frac{k}{4EI}} = \sqrt[4]{\frac{10^4}{4 \times 20 \times 10^4}} = 0.334 \text{ m}^{-1}$$

$$\lambda L = 6 \times 0.334 = 2.004$$

$$\frac{kh^4}{EI} = 0.2531$$

Symmetry in the BEF can be used noting that the deflections of the beam will be symmetric about node 3, that is

$$w_1 = w_5, \quad w_2 = w_4$$

Hence, if we can solve for w_1, w_2, w_3, the remaining parameters can be calculated easily.

FDO for the governing equations at nodes 1, 2 and 3 can be written using Equations (6.104) and (6.101) as follows (taking into account the boundary conditions at the free edges $x = 0$ and L).

$$\text{Node 1}: \quad \frac{EI}{h^3}\left[\left(2 + \frac{kh^4}{EI}\right)w_1 - 4w_2 + 2w_3\right] = 0$$

which can be written as

$$2.2531w_1 - 4w_2 + 2w_3 = 0 \tag{6.111}$$

$$\text{Node 2}: \quad \frac{EI}{h^3}[-2w_1 + 5.2531w_2 - 4w_3 + w_4] = 100$$

which can be simplified (noting $w_4 = w_2$ by symmetry) as

$$-2w_1 + 6.2531w_2 - 4w_3 = 1.686 \times 10^{-3} \tag{6.112}$$

$$\text{Node 3}: \quad \frac{EI}{h^3}[w_1 - 4w_2 + 6.2531w_3 - 4w_4 + w_5] = 0$$

which is simplified (noting $w_4 = w_2$, $w_5 = w_1$) as

$$2w_1 - 8w_2 + 6.2531w_3 = 0 \tag{6.113}$$

w_1, w_2, w_3 can now be solved from the Equations (6.111)–(6.113) as follows

$$\begin{aligned} w_1 &= w_5 = 3.062 \times 10^{-3}\ \text{m} \\ w_2 &= w_4 = 3.427 \times 10^{-3}\ \text{m} \\ w_3 &= 3.406 \times 10^{-3}\ \text{m} \end{aligned} \tag{6.114}$$

The contact pressures at these nodes can be obtained by noting that $q_i = k_i w_i$ as

$$\begin{aligned} q_1 &= q_5 = 30.6\ \text{kN/m} \\ q_2 &= q_4 = 34.27\ \text{kN/m} \\ q_3 &= 34.06\ \text{kN/m} \end{aligned} \tag{6.115}$$

The bearing pressure can be obtained by dividing Equation (6.115) by the width of the footing, that is, $b = 1\text{m}$ as

$$\begin{aligned} q_{b1} &= q_{b5} = 30.6\ \text{kN/m}^2 \\ q_{b2} &= q_{b4} = 34.27\ \text{kN/m}^2 \\ q_{b3} &= 34.06\ \text{kN/m}^2 \end{aligned} \tag{6.116}$$

From conventional analysis (Figure 6.37), the bearing pressure is uniformly equal to

$$q_{b1} \text{ to } q_{b5} = q_{bo} = \frac{200}{6 \times 1} = 33.33 \text{ kN/m}^2$$

$$\text{Soil reaction} = q_o = q_{bo} \times b = 33.33 \text{ kN/m}$$

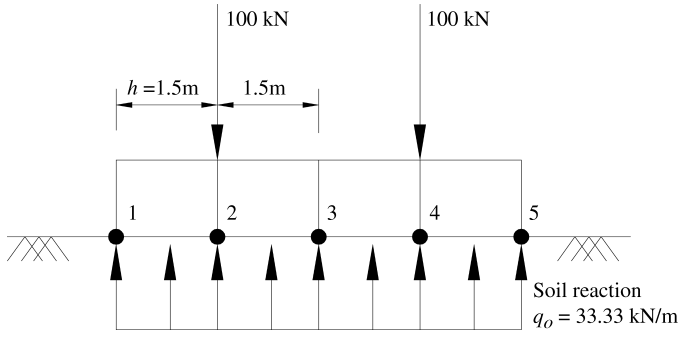

Figure 6.37 Conventional analysis.

From conventional analysis (assuming the beam to be rigid and the contact pressure to be uniform as shown in Figure 6.37) the deflections all along the beam will be the same, that is

$$w_1 = w_2 = w_3 = w_4 = w_5 = \frac{(100 + 100)}{k \times b \times L} = \frac{200}{10^4 \times 1 \times 6} = 3.33 \times 10^{-3} \qquad (6.117)$$

The bending moment can be calculated at various nodes using FD discretization as below (using BEF approach)

$$M_1 = M_5 = 0 \text{ (Free edges)}$$

$$M_2 = M_4 = -EI\left[\frac{d^2w}{dx^2}\right]_{2,4} = -\frac{EI}{h^2}[w_3 - 2w_2 + w_1]$$

$$= -\frac{20 \times 10^4}{1.5^2}[3.406 - 2 \times 3.427 + 3.062] \times 10^{-3}$$

$$= 34.3 \text{ kNm}$$

$$M_3 = -EI\left[\frac{d^2w}{dx^2}\right]_3 = -\frac{EI}{h^2}[w_2 - 2w_3 + w_4] = -\frac{2EI}{h^2}[w_2 - w_3]$$

$$= -\frac{2 \times 20 \times 10^4}{1.5^2}[3.427 - 3.406] \times 10^{-3}$$

$$= -3.73 \text{ kNm}$$

From conventional analysis these values can be obtained by taking the moments of all the loads (including applied load and soil reaction) to the left or right of the section. These can be obtained for comparison as follows (Figure 6.37)

$$M_1 = M_5 = 0$$

$$M_2 \text{ (from left)} = M_4 = \frac{33.33 \times 1.5^2}{2} = 37.5 \text{ kNm}$$

$$M_3 \text{ (from left)} = \frac{33.33 \times 3^2}{2} - 100 \times 1.5 = -0.015 \text{ kNm}$$

The shear forces at the nodes can be calculated from the finite difference expressions as follows (using BEF approach)

$$\begin{aligned} &Q_1 = Q_5 = 0 \text{ (free edges)} \\ &Q_2 \text{ (from left)} = Q_4 = -EI\left[\frac{d^3w}{dx^3}\right]_{2,4} = -\frac{EI}{2h^3}[-w_{-1} + 2w_1 - 2w_3 + w_4] \end{aligned} \tag{6.118}$$

where w_{-1} denotes the deflection at the fictitious node needed for the FD approximation

From Equation (6.102)

$$w_{-1} = 2w_1 - w_2 \text{ and from symmetry } w_4 = w_2 \tag{6.119}$$

Substituting these values in Equation (6.118) we get

$$\begin{aligned} Q_2 = Q_4 &= -\frac{EI}{2h^3}[-2w_1 + w_2 + 2w_1 - 2w_3 + w_2] = -\frac{EI}{2h^3}[2w_2 - 2w_3] \\ &= -\frac{20 \times 10^4}{1.5^3}[3.427 - 3.406] \times 10^{-3} = -1.244 \text{ kN} \\ Q_3 &= -EI\left[\frac{d^3w}{dx^3}\right]_3 = -\frac{EI}{2h^3}[-w_1 + 2w_2 - 2w_4 + w_5] = -\frac{EI}{2h^3}[0] = 0 \end{aligned} \tag{6.120}$$

From conventional analysis (Figure 6.37) these values at any point can be calculated by summing up all the forces acting on the beam either from the left or right side.

Accordingly these values are

$$\begin{aligned} &Q_1 = Q_5 = 0 \\ &Q_2 \text{ (from left)} = Q_4 = 33.33 \times 1.5 = 50 \text{ kN} \\ &\qquad\qquad\qquad\qquad = -50 \text{ kN (from right)} \\ &Q_3 = 0 \end{aligned} \tag{6.121}$$

The value of Q_2 given by Equation (6.120) differs considerably from the value given by conventional analysis Equation (6.121). This is because, the FD expressions assume that the concentrated loads are distributed uniformly on either side of the node up to $h/2$ as shown in Figure 6.38, that is, $100/1.5 = 66.67$ kN/m, as shown. If the shear force to the left is calculated from this equivalent applied load of 66.67 kN/m, using conventional

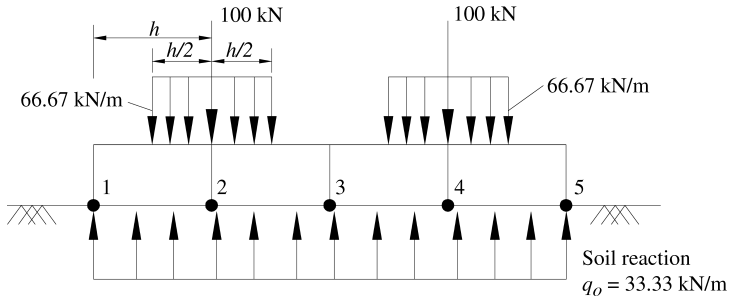

Figure 6.38 Example 6.3.

analysis, we get

$$Q_2 = Q_4 = 33.33 \times 1.5 - 66.67 \times 0.75 = 0$$

which is close to the value given in Equation (6.120).

These values can be compared using exact solutions given by Seely and Smith (1952) (Figure 5.2). Using the curves given in Figure 5.2(a) (corresponding to $L = \frac{2}{\lambda}$ and location of the load at $L/4$ from each end as applicable to this problem), these values can be obtained as follows

$$\begin{aligned} M_1 &= M_5 = 0 \\ M_2 &= M_4 = (0.5 + 0.1)\frac{P}{4\lambda} = \frac{0.6 \times 100}{4 \times 0.334} = 45 \text{ kNm} \\ M_3 &= 0 \end{aligned}$$

Similarly the other parameters can be calculated.

6.10 FDM for Rectangular Plates on Elastic Foundations

If the supporting soil is weak or made up or the loads are large, it may not be feasible to provide isolated footings to transmit the loads from the superstructure to the soil below.

If the calculation of the total area of individual or combined footings based on settlement or bearing capacity requirements shows it to be greater than one-half the area of the building itself, it may be economical if mat foundation are used.

In the conventional analysis, the mat is assumed to be rigid and the contact pressure is assumed as planar as discussed in Chapter 4. The distribution of stresses and displacements in the mat and underlying soil is a three-dimensional problem in which there is a considerable degree of interaction between structure (including the mat) and soil. The analysis of mat foundations can also be carried out treating the mat as a plate resting on elastic Winkler medium, which is considered more rational. The governing equation and conventions are given in Equations (4.17)–(4.23) and Figures 4.19, 4.21 and 4.22 for PEF problems. The analytical methods of solution are presented in Chapter 5. Noting that these solutions are of limited practical use, numerical methods including FDM and FEM may have to be used due to their flexibility and adaptability. FDM which is conceptually simple and results in smaller system of unknowns (though less flexible than FEM) is discussed below for the analysis of PEF. The

PEF problem is essentially two-dimensional and can be considered as a simple extension of BEF discussed in Sections 6.4–6.9. Accordingly the concepts of FDM are essentially same and are presented below.

Figures 4.19 and 4.21 show the rectangular PEF with convention of coordinates and the parameters. From Equation (4.49), the governing partial differential equation for rectangular PEF is

$$D\left[\frac{\partial^4 w}{\partial x^4} + 2\frac{\partial^4 w}{\partial x^2 \partial y^2} + \frac{\partial^4 w}{\partial y^4}\right] + kw = p(x) \tag{6.122}$$

that is

$$D\,\nabla^4 w + kw = p(x)$$

that is

$$\nabla^4 = \nabla^2(\nabla^2) \tag{6.123}$$

where ∇^4 is called the bi-harmonic operator.

D is the flexural rigidity of the plate
$w =$ vertical deflection at the contact surface between the plate and the soil foundation.

For the application of FDM, the plate is divided into a two-dimensional lattice as shown in Figure 6.2(b) preferably with equal intervals for efficient computation (though not essential) of say $h \times h$ along both x and y directions. The FDOs for two-dimensional partial derivatives are given in Figure 6.6. Equation (6.122) can now be discretized using FDOs given in Figure 6.6, thus converting a continuous partial differential equation (PDE) into algebraic equation at any node j, k in terms of the deflections at the neighboring nodes. The rest of the procedure for representation of applied loads and moments, modulus of subgrade reaction, k_s (Chapter 4 for PEF), boundary conditions (Equations (5.88)–(5.90)), fictitious nodes, boundary nodes, internal nodes and then calculation of bending moments, shear forces are simple extensions of FDM for BEF (Section 6.4–6.9). However FDOs given in Figure 6.6 have to be used for PEF instead of FDOs given in Figure 6.5 used for BEF. In view of the increasing complexity of these expressions, these are to be carried out using computers (with customized or commercial software packages) for general application. However, the FDM is explained below for a plate on elastic foundations (Figure 4.19) with all the four edges free (i.e., along $x = 0$, a and $y = 0$, b).

6.10.1 PEF with Free Edges

The governing equation is given by Equation (6.122) and the boundary conditions for free edges are given by Equation (5.90), that is

At $x = 0$ and a

$$\begin{aligned} M_x &= -D\left(\frac{\partial^2 w}{\partial x^2} + \nu_p \frac{\partial^2 w}{\partial y^2}\right) = 0 \\ Q_x &= -D\left[\frac{\partial^3 w}{\partial x^3} + (2-\nu_p)\frac{\partial^3 w}{\partial x \partial y^2}\right] = 0 \end{aligned} \tag{6.124}$$

At $y = 0$ and b

$$M_y = -D\left(\frac{\partial^2 w}{\partial y^2} + v_p \frac{\partial^2 w}{\partial x^2}\right) = 0$$
$$Q_y = -D\left[\frac{\partial^3 w}{\partial y^3} + (2-v_p)\frac{\partial^3 w}{\partial x^2 \partial y}\right] = 0 \tag{6.125}$$

where v_p is the Poisson's ratio of the plate and Q_x and Q_y are the edge shears which are different from the shear force at the interior points (Timoshenko and Krieger, 1959).

The FDO for the governing PDE, Equation (6.122) can be written using FDOs for partial derivatives given in Figure 6.6 for all the nodes except for suitable modifications at penultimate, ultimate and corner nodes depending on the boundary conditions. The procedure is similar to the method followed for BEF in Sections 6.4–6.9. Since the governing equation is having fourth order partial derivatives in x and y coordinates, the corresponding FDOs (Figure 6.6) at any node i, j need two nodes on either side of i, j along x and y direction as shown in Figure 6.39(a). Thus the FDO for the governing equation (using FDOs given in Figure 6.6) can be obtained as in Figure 6.39(b).

Thus, the difference equation for the governing equation of PEF (Equation (6.122)) at any interior node 0, (including the soil reaction) can be written as

$$20w_o - 8(w_t + w_b + w_r + w_l) + 2(w_{tl} + w_{lr} + w_{bl} + w_{br}) + (w_{tt} + w_{bb} + w_{ll} + w_{rr}) + \frac{kh^4 w_o}{D} = \frac{p_o h^4}{D} + \frac{P_o h^2}{D} \tag{6.126}$$

where $p_o(x,y)$ is the distributed load and P_0 is the concentrated load at node 0. The notations w_l, w_t ... represent deflection at points l, t and so on.

The moments and shear force for any interior point can be computed from the following equations and their corresponding FDOs as given below.

$$M_x = -D\left[\frac{\partial^2 w}{\partial x^2} + v_p \frac{\partial^2 w}{\partial y^2}\right] = -\frac{D}{h^2}\left[(w_l - 2w_0 + w_r) + \frac{v_p}{h^2}(w_t - 2w_0 + w_b)\right] \tag{6.127}$$

$$M_y = -D\left[\frac{\partial^2 w}{\partial y^2} + v_p \frac{\partial^2 w}{\partial x^2}\right] = -\frac{D}{h^2}\left[(w_t - 2w_0 + w_b) + \frac{v_p}{h^2}(w_l - 2w_0 + w_r)\right] \tag{6.128}$$

$$N_x = -D\left[\frac{\partial^3 w}{\partial x^3} + \frac{\partial^3 w}{\partial x \partial y^2}\right] = -\frac{D}{2h^3}[-w_{ll} + 2w_l - 2w_r + w_{rr} + w_{tl} - w_{tr} - 2(w_l - w_r) + w_{bl} - w_{br}] \tag{6.129}$$

Notations: w_a , w_t ..... = deflection at point a, t, ...
h = size of the grid
P = concentrated load at point O
υ = Poisson's ratio

Flexural rigidity of PEF = $D = \dfrac{E\,t^3}{12\,(1-\upsilon^2)}$; t = thickness of mat

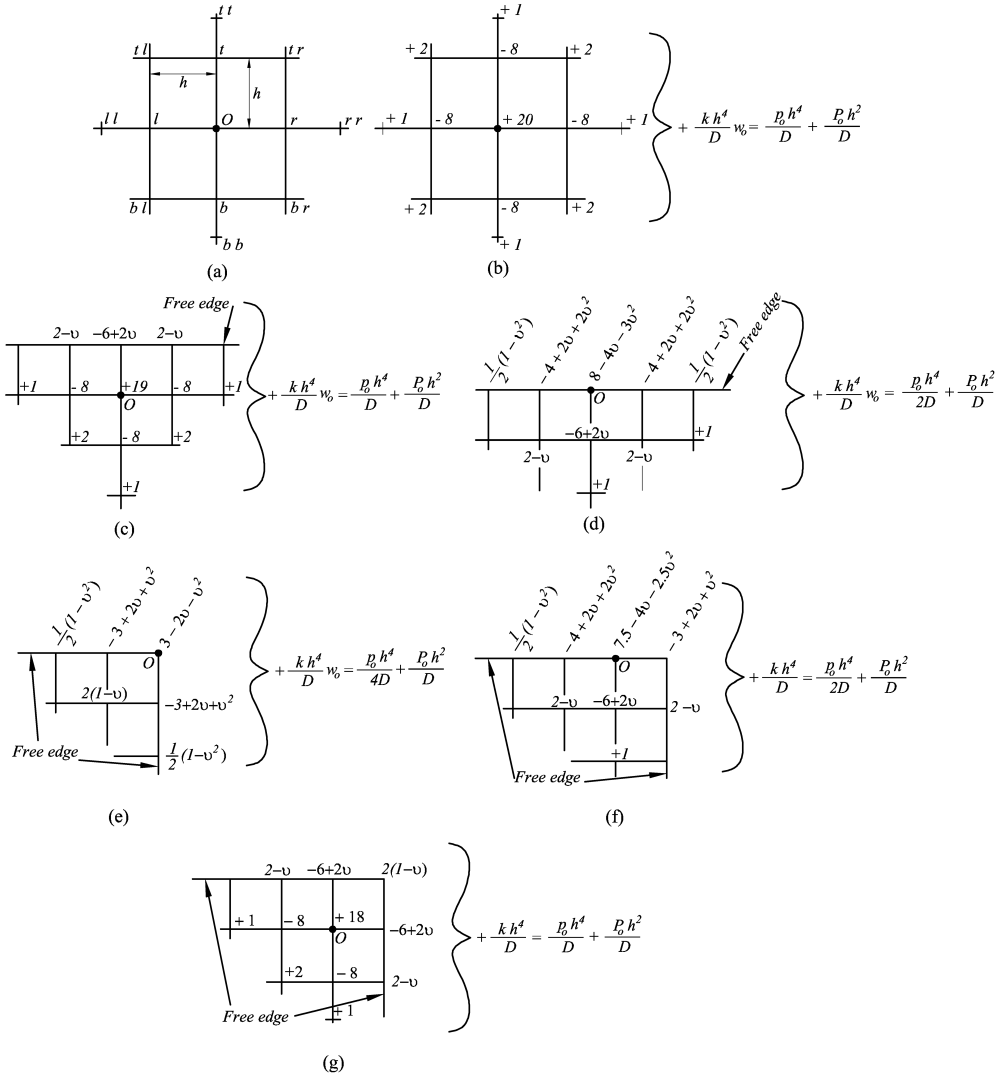

Figure 6.39 Finite difference equations for analysis of PEF.

$$N_y = -D\left[\frac{\partial^3 w}{\partial y^3} + \frac{\partial^3 w}{\partial x^2 \partial y}\right]$$
$$= -\frac{D}{2h^3}[-w_{tt} + 2w_l - 2w_b + w_{bb} + w_{tl} - w_{bl} - 2(w_t - w_b) + w_{tr} - w_{br}] \quad (6.130)$$

The edge shears Q_x and Q_y (Equations (6.124) and (6.125)) can be written in terms of FDOs as follows

$$Q_x = -D\left[\frac{\partial^3 w}{\partial x^3} + (2 - \nu_p)\frac{\partial^3 w}{\partial x \partial y^2}\right]$$
$$= -\frac{D}{2h^3}\left[-w_{ll} + 2w_l - 2w_r + w_{rr} + (2 - \nu_p)\left\{w_{tl} - w_{tr} - 2w_l + 2w_r + w_{bl} - w_{br}\right\}\right] \quad (6.131)$$

$$Q_y = -D\left[\frac{\partial^3 w}{\partial y^3} + (2 - \nu_p)\frac{\partial^3 w}{\partial x^2 \partial y}\right]$$
$$= -\frac{D}{2h^3}\left[-w_{tt} + 2w_t - 2w_b + w_{bb} + (2 - \nu_p)(w_{tl} - w_{bl} - 2w_t + 2w_b + w_{tr} - w_{br})\right] \quad (6.132)$$

The Equations (6.126)–(6.132) can be written at all interior nodes, that is, nodes which have two more adjacent nodes within the domain along x and y directions. At penultimate, ultimate and corner nodes, we have to introduce fictitious nodes located beyond the domain along x and y directions as may be necessary and solve for the values of these fictitious nodes in terms of the values of the adjacent nodes within the domain using the two or four boundary conditions depending on their locations, that is, penultimate, ultimate, corner nodes. This is the same method followed in BEF and explained in detail in Sections 6.4–6.9 above. In two dimensions such as for PEF, this procedure is somewhat more cumbersome than BEF, though it does not make much difference in the efforts to arrive at the system of equations if one uses computers and software packages. Then these values of deflections at the fictitious nodes need to be replaced in the governing FDO, that is, Equation (6.126) for all such effected nodes (penultimate, ultimate, corner nodes) by the values obtained in terms of the deflections at the nodes within the domain. Then the resulting system of simultaneous equations with nodal deflections (within the domain) as unknowns become a consistent and nonhomogeneous system which can be uniquely solved using methods like Gauss elimination and so on (Crandall, 1956; Kreyszig, 1967). It may also be noted that the FDO for the governing equation need not be written at all those nodes whose deflections are specified or known, that is, simply supported and fixed edges with zero or specified deflections.

These manipulations have been carried out by Rijhsinghani (Teng, 1964) for PEF with free edges. The governing FDOs for the PEF to be used for interior penultimate points on the edges

and boundaries (in both directions), corner points and other points on the boundary have been worked out (after accounting for fictitious points wherever needed as mentioned above) by Rijhsinghani (Teng, 1964) and are given in Figures 6.39(c)–(g). The note about adding $\frac{kh^4}{D}$ to the FDOs to account for the soil reaction is mentioned in the figure. Once the system of equations are arrived at and solved for the deflections, the design parameters of the PEF such as bending moments and shear forces (Equations (6.124)–(6.132)) can be calculated using the corresponding FDOs, as given in Equations (6.127)–(6.132). The contact pressure (soil reaction) at any node (i, j) is computed by multiplying deflection with k_s, that is, $q_{i,j}\,(x, y) = k_{i,j} w_{i,j}$. These values for points intermediate to the nodes can be computed using interpolation (Crandall, 1956). The example worked out by Rijhsinghani (Teng, 1964) is presented with some changes in dimensions.

Example 6.4

Analyze the plate on elastic foundation using FDM with the following data. A square footing 1.2×1.2 m is subjected to a concentrated load at the center, $P = 100$ kN.

Thickness $t = 12$ cm, $E_p = 30 \times 10^6$ kN/m^2, $v_p = 0.15$, Interval $h = 15$ cm (in both directions, $k_s = 10^5$ kN/m$^3 = k$ for plates).

Solution:

$$D = \frac{E_p t^3}{12(1-v_p^2)} = 4.42 \times 10^3 \text{ kNm}$$

$$\frac{kh^4}{D} = 0.01145$$

$$\frac{Ph^2}{D} = 5.09 \times 10^{-4} \text{ m}$$

The PEF is divided into grids of 15 cm as shown in Figure 6.40, with nodal numbers indicated therein. Due to symmetry in both directions, only 15 unknowns at these nodes are needed for solution, though there are 64 nodes totally. The governing FDO equations are arranged in Table 6.1. The solutions of the deflections are given at the bottom line of the table. With these values, all the parameters required for the design including soil reaction can be calculated using Equations (6.124)–(6.132). For example, the moment M_x at node 2 can be calculated using Equations (6.124) and (6.127) as

$$(M_x)_2 = -\frac{D}{h^2}\left[(w_1 - 2w_2 + w_3) + v_p(w_6 - 2w_2 + w_6)\right] = 7.37 \text{ kNm/m} \qquad (6.133)$$

The bending moments M_x and M_y have been computed along the center line of the footing and are graphically shown in Figure 6.41. These values are compared with the values obtained by conventional analysis (shown by dotted line) in the figure.

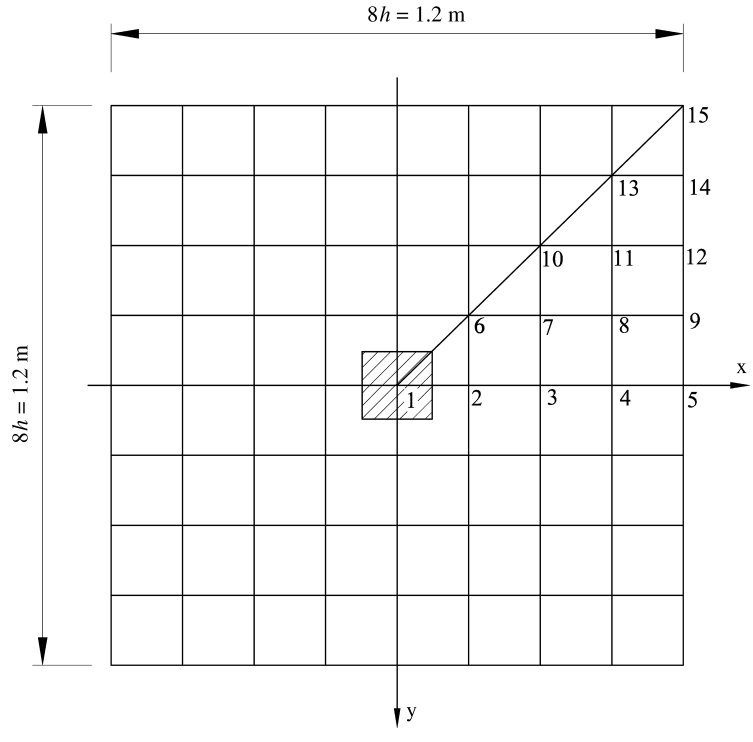

Figure 6.40 FD discretization of PEF.

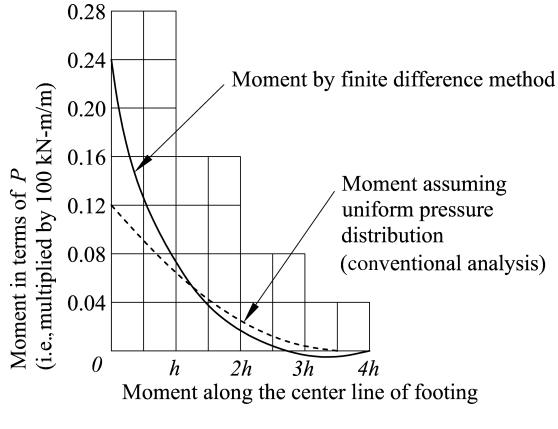

Figure 6.41 Comparison of BMs M_x and M_y along the center line of PEF.

Table 6.1 Difference equations for points/nodes 1, 2, 3, . . ., 15.

Equation	w															
	w_1	w_2	w_3	w_4	w_5	w_6	w_7	w_8	w_9	w_{10}	w_{11}	w_{12}	w_{13}	w_{14}	w_{15}	Constant
1	20.01	−32.00	4.00	0.00	0.00	8.00	0.00	0.00	0.00	0.00	0.00	0.00	0.00	0.00	0.00	5.09×10^{-2}
2	−8.00	25.01	−8.00	1.00	0.00	−16.00	6.00	0.00	0.00	0.00	0.00	0.00	0.00	0.00	0.00	0
3	1.00	−8.00	20.01	−8.00	1.00	4.00	−16.00	4.00	0.00	8.0	0.00	0.00	0.00	0.00	0.00	0
4	0.00	1.00	−8.00	19.01	−5.70	0.00	4.00	−16.00	3.70	0.00	2.00	0.00	0.00	0.00	0.00	0
5	0.00	0.00	1.00	−5.70	7.34	0.00	0.00	3.70	−7.31	0.00	0.00	0.98	0.00	0.00	0.00	0
6	2.00	−16.00	4.00	0.00	0.00	22.01	−16.00	2.00	0.00	2.00	0.00	0.00	0.00	0.00	0.00	0
7	0.00	3.00	−8.00	2.00	0.00	−8.00	23.01	−8.00	3.00	0.00	0.00	0.00	0.00	0.00	0.00	0
8	0.00	0.00	2.00	−8.00	1.85	1.00	−8.00	20.01	−5.70	2.00	−8.00	1.85	1.00	0.00	0.00	0
9	0.00	0.00	0.00	1.85	−3.66	0.00	1.00	−5.70	7.83	0.00	1.85	−3.66	0.00	0.49	0.00	0
10	0.00	0.00	2.00	0.00	0.00	2.00	−16.00	4.00	0.00	20.01	−16.00	2.00	2.00	0.00	0.00	0
11	0.00	0.00	0.00	1.00	0.00	0.00	3.00	−8.00	1.85	−8.00	21.01	−5.70	−8.00	2.85	0.00	0
12	0.00	0.00	0.00	0.00	0.00	0.00	0.00	1.85	−3.66	1.00	−5.70	7.34	1.85	−3.66	0.49	0
13	0.00	0.00	0.00	0.00	0.00	0.00	0.00	2.00	0.00	2.00	−16.00	3.70	18.01	−11.40	1.70	0
14	0.00	0.00	0.00	0.00	0.00	0.00	0.00	0.00	0.49	0.00	2.85	−3.66	−5.70	8.70	−2.68	0
15	0.00	0.00	0.00	0.00	0.00	0.00	0.00	0.00	0.00	0.00	0.00	0.98	1.70	−5.36	2.68	0
Deflection	9.33	8.77	7.94	7.09	0.00	8.40	7.70	6.92	6.16	7.15	6.46	5.77	5.86	5.22	4.60	10^{-4} m

6.11 FDM for Circular and Annular Plates on Elastic Foundations

Circular and annular shaped footings are commonly used for towers, chimneys, water tanks, silos and other structures with circular geometry. The closed form solutions are very few and are of limited practical use as mentioned in Chapter 5. FDM and FEM can be used conveniently for analysis of such foundations. Though FDM can be used for plates and rings with axially symmetric loading, the procedure becomes very cumbersome for nonsymmetric geometry (sector shaped) and nonsymmetric loads. In such cases the equations in radial coordinates (r,θ) can be transformed into rectangular coordinates as given by Scott (1963) and the standard FDOs developed for Cartesian coordinates given in Figures 6.5 and 6.6 can be conveniently used for FDM applications. The method can obviously be used also for problems with axial symmetry with much easier coordinate transformations as explained by Scott (1963), Southwell (1946), Salvadori and Baron (1952), and Timoshenko and Krieger (1959). Scott (1963) gives the basic transformations and FDOs for other geometries like triangular and hexagonal meshes and so on. As these are essentially similar to FDM for Cartesian coordinate problems, the reader may refer to the above references for details. Jones (1997) analyzes the axially symmetric PEF by treating the circular plate as an assembly of several sectors. He then considers each sector as a BEF with linearly varying cross section and the FDM equations given in Sections 6.3–6.9 are readily applicable for solving these problems.

Bowles (1996) presented FEM and also FEM like method referred to as finite grid method (FGM) and gave examples of rectangular, circular, ring-shaped (annular) footings on elastic foundations. Since these methods are based mainly on FEM concepts, these are presented in Chapter 7. Further it may be noted that these methods are computationally more intensive than FDM as the number of unknowns are usually very large and need computerized procedures and (or) software packages.

6.12 BEF Software Package

Jones (1997) developed a general purpose interactive and user friendly software package using FDM and Winkler models for soil. He presented several examples of BEF, circular, and ring-shaped and axially symmetric footings, laterally loaded piles, pile foundations, pile group analysis and a variety of problems in soil structure interaction whose behavior can be simplified to that of a general BEF.

6.13 Summary

This chapter presents numerical and finite difference methods which are very useful to solve problems of BEF and PEF. The flexibility of these methods make them quite adaptable to analyze several problems of practical significance such as spread footings, combined footings, footings with varying size, varying soil characteristics, general loads, moments, circular and ring-shaped foundations, mat foundations (rafts) with rectangular and square shapes, laterally loaded piles and so on (Jones, 1997). Software packages such as BEF (Jones, 1997) are available for easy application using computers/PCs.

Exercise Problems

The problem assignments are organized as follows:

Exercise Problems	Sections	Topics
6.1–6.8	6.2	Trial solutions with undetermined parameters
6.9–6.15	6.3–6.9	Prismatic BEF
6.15, 6.17	6.11	Circular and ring-shaped Footings
6.18, 6.19	6.10	Rectangular footings

6.1–6.4 Analyze the following BEF problem shown in Figure 6.42 using

1. Galerkin's approach
2. Least squares method
3. Collocations method
4. Subdomain approach.

$L = 6\,\text{m}, l_1 = 2\,\text{m}, l_2 = 1\,\text{m}, P_1 = 200\,\text{kN}, P_2 = 100\,\text{kN}$, both ends are free.

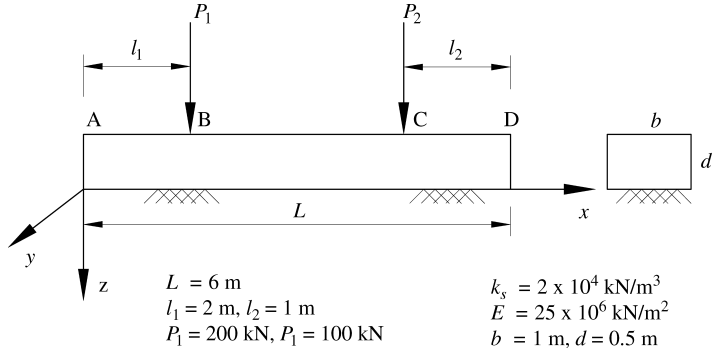

Figure 6.42 Problems 6.1–6.4.

6.5–6.8 Repeat problems 6.1–6.4 with the following loads on the beam as shown in Figure 6.43. $l_1 = l_2 = 1\,\text{m}$, $p_0 = 30\,\text{kN/m}$

6.9 Solve the BEF given in Figure 6.42 by FDM with three nodes.

6.10 Solve the BEF given in Figure 6.43 by FDM with four nodes with symmetry.

6.11–6.12 Solve the BEF problems given in Figures 6.42 and 6.43 using FDM with all the data remaining the same except that k_s varies linearly from $20 \times 10^6\,\text{kN/m}^3$ at $x = 0$ to $30 \times 10^6\,\text{kN/m}^3$ at $x = L$.

6.13 Solve problem given in Figure 6.42 using FDM if moments $M_1 = 200\,\text{kNm}$ and $M_2 = 100\,\text{kNm}$ are applied at B and C in addition to P_1 and P_2.

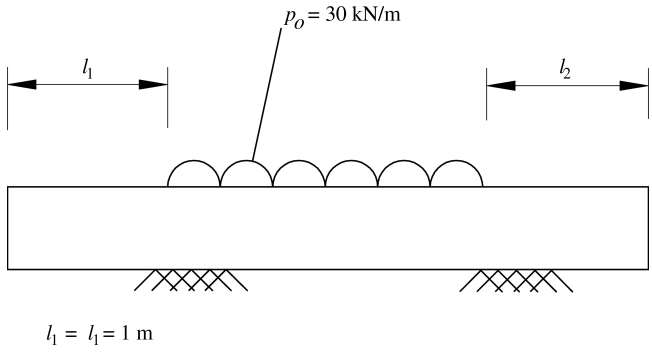

Figure 6.43 Problems 6.5–6.8.

6.14–6.15 Solve the problems given in Figures 6.42 and 6.43 with all the data remaining the same except that the width of the beam varies from $b = 0.5$ m at $x = 0$ to $b = 1.5$ m at $x = L$, that is, the footing is trapezoidal in shape. Use FDM.

6.16 Analyze the circular footing with the following data by FDM by dividing the footing into 12 sectors and applying it to any one sector (all the sectors will have identical behavior). The footing section and soil data are given as in Figure 6.44. The footing is free at its outer edge. $P_1 = 100$ kN/m (annular line load) acting along a circle with radius 2.5 m. $k_s = 2 \times 10^4$ kN/m^3, E (concrete) $= 32 \times 10^6$ kN/m^2, v (concrete) $= 0.2$, depth of footing, $d = 1$m.

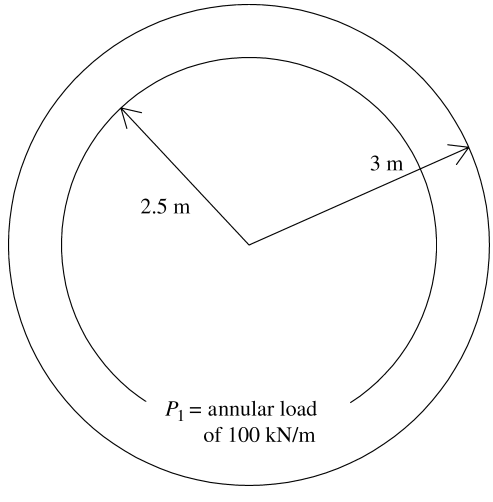

Figure 6.44 Problem 6.16.

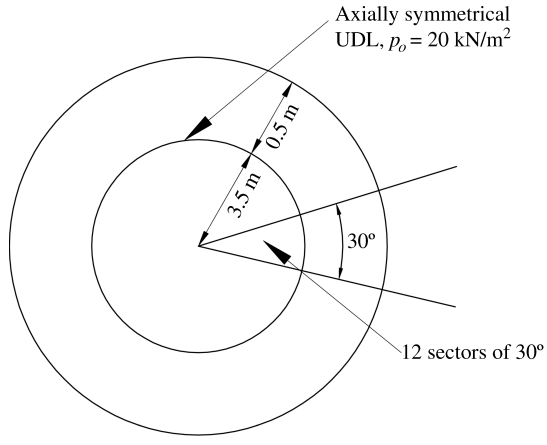

Figure 6.45 Problem 6.17.

.

6.17 Analyze the ring foundation shown in Figure 6.45 using FDM. The ring footing is supporting a udl of 20 kN/m^2 all around. $k_s = 10^4$ kN/m^3, $E = 30 \times 10^6$ kN/m^2, $v_p = 0.2$, depth of footing, $d = 0.8$ m. Divide the ring into 12 sectors.

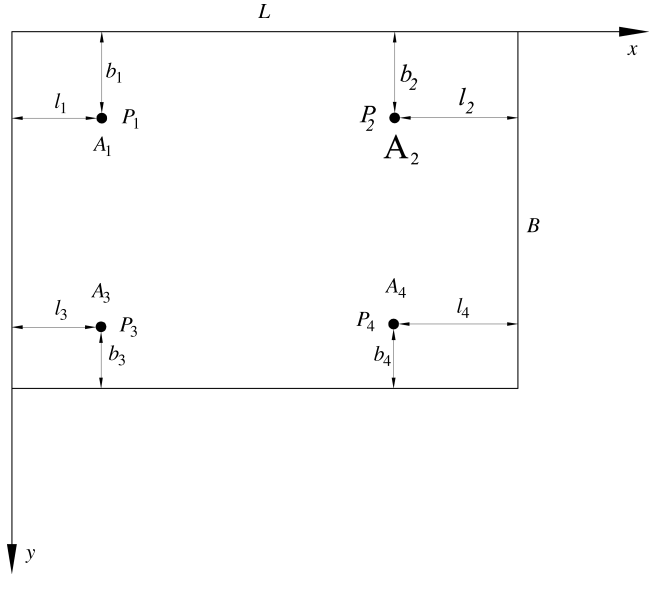

Figure 6.46 Problem 6.18.

6.18 Analyze the following mat foundation/PEF with free edges shown in Figure 6.46 taking symmetry for simplification wherever possible.

1. $E = 25 \times 10^6 kN/m^2$, $v_p = 0.1$
2. Thickness of the mat = 0.4 m
3. Concentrated loads P_1, P_2, P_3, $P_4 = 150$ kN, $L = 8$ m, $B = 6$ m
4. l_1 to $l_4 = b_1$ to $b_4 = 1$ m
5. Divide the mat into a grid with $h = 2$ m in both directions.

6.19 Analyze the above problem with udl, applied on the area ABCD of the mat (Figure 6.46).

7

Finite Element Method

7.1 General Philosophy

The finite element method was originally developed in the aircraft industry to facilitate a refined (approximate) analysis of complex airframe structures. Though the procedure was developed as a concept of structural analysis, the wider basis of this method makes it applicable to a variety of field problems such as soil structure interaction, elasticity, structural analysis, heat conduction, fluid flow and so on. In general this method is applicable to almost all problems where a variational formulation of the physical phenomenon is feasible. The important characteristics of the finite element procedure are: (1) the method is a general one based on an approximate solution of an extremum problem (which makes it applicable to many problems) and (2) unlike the Ritz process, physical quantities which have an obvious meaning are chosen as the parameters (Zienkiewicz, 1971).

Because of its origin and development as a tool for structural analysis, let us first examine the basic philosophy as applied to problems in structural mechanics. The method in its popular form is essentially a generalization of standard procedure in structural analysis known as direct stiffness analysis. The basic concept involved is that every structure may be considered to be an assemblage of finite number of individual structural components or elements. In many engineering problems, analysis of stress and strain in elastic continua is required. In all such problems the number of interconnections between any finite element isolated by some imaginary boundaries and the neighboring elements is infinite. However to make the analysis feasible by this method, the continuum is idealized as an assemblage of one, two or three dimensional elements of proper shape and size, with a finite number of inter connections. It is to be noted that this approximation of discretization is purely of a physical nature and that there need be no approximation in the mathematical analysis of the substitute system. This feature distinguishes the finite element technique from finite difference methods in which the exact equations of the actual physical system are solved by approximate mathematical procedures. Another important attribute of the finite element method is its capacity for treating arbitrary material properties, such as nonhomogeneity, anisotropy, nonlinearity, and so on, as all of the

Foundation Design: Theory and Practice N. S. V. Kameswara Rao
 ISBN: 978-0-470-82534-1

material properties of the original system can be retained in the discrete elements used in the substitute system. Before we actually go into the finite element procedure let us briefly recapitulate some of the structural analysis concepts involved.

Let Figure 7.1 represent a two dimensional structure assembled from individual components and interconnected at the nodes designated (1) to (n). The joints at the nodes are pinned. Considering the element (a) in Figure 7.1 and knowing its characteristics, the forces at the associated nodes 1, 2 and 3 can be uniquely determined using the displacement of these nodes, the distributed load, p, and its initial strain if any. The initial strain may be due to temperature, shrinkage or simply an initial lack of fit. Let the forces and displacements be defined by components (U, V and u, v) in a common coordinate system.

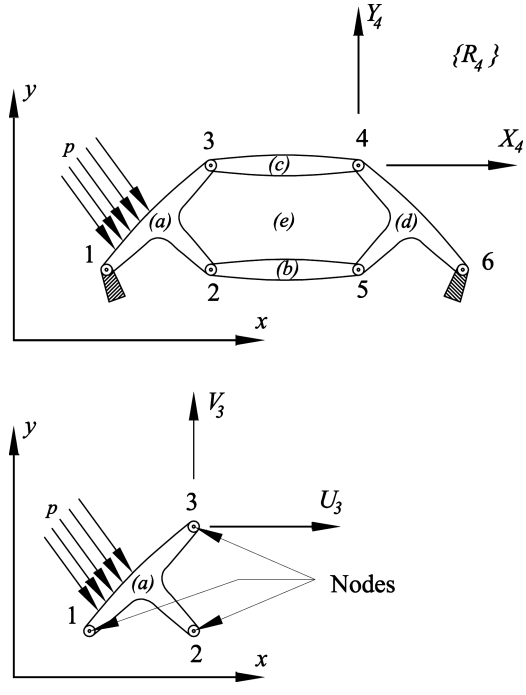

Figure 7.1 A typical structural assemblage using interconnected elements.

The forces at the nodes of element (a) in Figure 7.1 can be written in matrix form as

$$\{F\}^a = \begin{Bmatrix} F_1 \\ F_2 \\ F_3 \end{Bmatrix} = \begin{Bmatrix} U_1 \\ V_1 \\ U_2 \\ V_2 \\ U_3 \\ V_3 \end{Bmatrix} \tag{7.1}$$

and the corresponding nodal displacements as

$$\{\delta\}^a = \begin{Bmatrix} \delta_1 \\ \delta_2 \\ \delta_3 \end{Bmatrix} = \begin{Bmatrix} u_1 \\ v_1 \\ u_2 \\ v_2 \\ u_3 \\ v_3 \end{Bmatrix} \tag{7.2}$$

Assuming elastic behavior, the characteristic relationship between the forces and the displacements of the element are of the form

$$\{F\}^a = [K]^a\{\delta\}^a + \{F\}^a_p + \{F\}^a_{\varepsilon_0} \tag{7.3}$$

The first term represents the forces due to displacements at the nodes, $\{F\}^a_p$ represents the nodal forces required to balance any distributed loads acting on the element and $\{F\}^a_{\varepsilon_0}$ represent the nodal forces required to balance any initial strains. Similarly stresses, σ, at any specified point or points of the element can be written in terms of nodal displacements as

$$\{\sigma\}^a = [S]^a\{\delta\}^a + \{\sigma\}^a_p + \{\sigma\}^a_{\varepsilon_0} \tag{7.4}$$

Then the matrix $[K]^a$ is known as the element stiffness matrix and $[S]^a$ as the element stress matrix. To get the complete solution of the structural assembly, just as the one shown in Figure 7.1, the two conditions to be satisfied are

1. Displacement compatibility
2. Equilibrium.

By listing the nodal displacements for all the elements of the structural assembly, the first condition is taken care of. As can be seen, the overall equilibrium has already been satisfied within each element, as expressed by Equations (7.3) and (7.4). Hence by writing down the equilibrium conditions at the nodes, the resulting equations will contain the displacements as unknowns. Once these are solved, the rest of the analysis for forces, stresses and so on is obvious. Let us now proceed to the study of the finite element procedure.

7.2 Finite Element Procedure

This can be divided into three phases:

1. Structural idealization
2. Evaluation of the element properties
3. Structural analysis of element assemblage.

The structural idealization is the process of subdivision of the original system into an assemblage of discrete segments of proper sizes and shapes. Judgment is required as the results can be valid only to the extent that the behavior of the substitute structure simulates the actual structure. In general better results can be achieved by finer subdivision.

The objective of the second phase is to find the stiffness or the flexibility of the element, which is an important step in the analysis and will be discussed later.

The third phase is a standard structural problem as has been briefly outlined earlier. The individual element configurations are of no concern. The same techniques apply to systems of one-, two- or three-dimensional elements or any combinations of these. The essential problem is to satisfy the three conditions of equilibrium, compatibility and force–deflection relationships. Either of the basic approaches of structural analysis, known as the *force method* and the *displacement method*, or *hybrid methods* can be used. However, the displacement method is preferred as it is simpler for formulation and computer programming. The fundamental steps involved are:

1. Evaluation of the stiffness properties of the individual structural elements, expressed in any convenient local (element) coordinate system.
2. Transformation of the element stiffness matrix from the local coordinates to a form relating to global coordinates system of the complete structural assemblage. This can be done as explained in Section 7.2.2.
3. Superposition of the individual element stiffnesses contributing to each nodal point to obtain the total assemblage nodal stiffness matrix $[K]$.
4. Formulation and solution of the equilibrium equations expressing the relationship between the applied nodal forces $\{R\}$ and the resulting nodal displacements $\{\delta\}$ as

$$\{R\} = [K]\{\delta\} + \{F\}_p + \{F\}\,\varepsilon_o \tag{7.5}$$

5. Evaluation of the element deformations from the computed nodal displacements by kinematic relationships and determination of element forces from the element deformations by means of the element stiffness matrices.

7.2.1 Finite Element Deformation Patterns

In the analysis of framed structures, the evaluation of the element stiffnesses can be done by simple procedure. The stiffness characteristics of two- and three-dimensional elements cannot be obtained by equivalent methods because of several obvious reasons. To quote the more important one, the results obtained using element stiffness properties defined in this way would differ greatly from the stresses and deflections of the actual continuum. Hence, in order that the finite element idealization may represent the behavior of the continuum closely, the deformation patterns which may develop in the element have to be prescribed. The choice of the proper deformation pattern is the critical step in the evaluation of element stiffness.

Another important point to be considered while prescribing the deformation patterns is the compatibility. It is not always easy to ensure displacement compatibility between adjacent elements. The compatibility condition on such common boundary lines may be violated, though within each element it is obviously satisfied due to uniqueness of displacements implied in its functional representation. However for the simple triangular plane stress elements it is easy to prescribe fully compatible deformation patterns.

Also, by concentrating the equivalent forces at the nodes, equilibrium conditions are satisfied in the overall sense only; and local violations of equilibrium conditions within each element and on its boundaries usually arise. But the artificial boundary forces are local,

self-equilibrating effects which have little influence on the general behavior of the structure (Zienkiewicz and Taylor, 1989).

To ensure convergence of the solution by this method the displacement function chosen should satisfy the following criteria:

1. The displacement function chosen should be such that it does not permit straining of an element to occur when the nodal displacements are caused by a rigid body displacement.
2. The displacement function has to be of such a form that if nodal displacements are compatible with a constant strain condition such constant strain will in fact be obtained.

7.2.2 Transformation of Coordinates

It is generally convenient to compute the characteristics of an individual element in a local coordinate system best suited to the geometry of the element. Then these can be easily transformed into any convenient global coordinate system chosen for the whole systems for obtaining the global characteristics. Then the total assemblage to represent the system can be obtained by superposing the individual element characteristics and assembling them. A different coordinate system may conveniently be used for every element to facilitate the computation. It is easy to transform the coordinates of the displacement and force components of Equations (7.1)–(7.3) to any other global coordinate system. It is necessary to do so before an assembly of the structure can be made.

Let a prime superscript denote the local coordinate system in which the element properties have been evaluated and let the global coordinate system necessary for assembly be nonprimed. The displacement components can be transformed by a suitable matrix of direction cosines $[L]$ as

$$\{\delta'\}^a = [L]\{\delta\}^a \tag{7.6a}$$

Equating the work done by the forces in both coordinate systems as force components must perform the same amount of work, we have

$$(\{F\}^a)^T\{\delta\}^a = \left(\{F'\}^a\right)^T\{\delta'\}^a$$

Inserting Equation (7.6a) in the above equation, we get

$$(\{F\}^a)^T\{\delta\}^a = \left(\{F'\}^a\right)^T[L]\{\delta\}^a$$

that is

$$\{F\}^a = [L]^T\{F'\}^a \tag{7.6b}$$

The stiffnesses which may be available in local coordinates can be transformed to global ones as follows. The force displacement relationship in local coordinates can be written from Equation (7.3) as

$$\{F'\}^a = [k']^a\{\delta'\}^a \tag{7.6c}$$

Substituting Equations (7.6a) and (7.6b) in Equation (7.6c), we have

$$\{F\} = [L]^T[k']^a[L]\{\delta\}^a = [k]^a\{\delta\}^e$$

Hence

$$[k]^a = [L]^T[k'][L] \tag{7.6d}$$

where k' and k are element stiffness matrices in local and global coordinates.

Similarly the reverse transformations from global to local coordinates can also be done as follows.

Noting that $[L]^{-1} = [L]^T$ (since direction cosine matrix L is an orthonormal matrix), from Equations (7.6a)–(7.6d)

$$\{\delta\}^a = [L]^{-1}\{\delta'\}^a = [L]^T\{\delta'\} \tag{7.6e}$$

$$\{F'\}^a = [L]\{F\}^a \tag{7.6f}$$

$$[k']^a = [L][k]^a[L]^T \tag{7.6g}$$

7.3 Formulation of Finite Element Characteristics (Stiffness Analysis)

The stiffness of any arbitrary element of the assemblage can be evaluated using the assumed deformation patterns. Besides providing boundary compatability, the number of displacement functions chosen must agree with the number of degrees of nodal displacement freedom of the element. The procedure of stiffness analysis will be illustrated with a simple plane stress analysis of a thin slice, but the extension to other problems is straightforward.

Consider the region shown in Figure 7.2 subdivided into triangular elements. The following are basic operations:

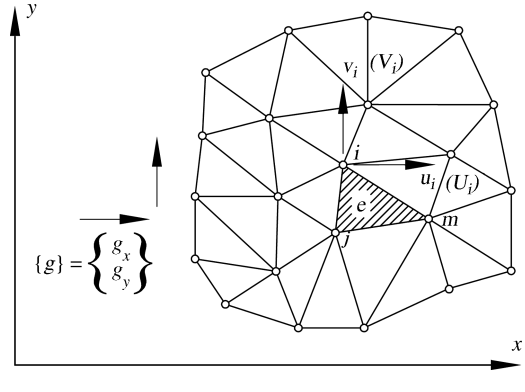

Figure 7.2 Finite element discretization of a plane stress problem.

1. Consider a typical element (e) of the assembly, associated with nodes i, j, m and straight line boundaries.

   Let the displacements of any point within the element be defined by $f(x,y)$, as

$$\{f\} = [N]\{\delta\}^e = \begin{bmatrix} N_i & N_j & N_m \ldots \end{bmatrix} \begin{Bmatrix} \delta_i \\ \delta_j \\ \delta_m \\ \cdot \\ \cdot \\ \cdot \end{Bmatrix} \tag{7.7}$$

   where components of $[N]$ are functions of position and $\{\delta\}^e$ represents a listing of nodal displacements for a particular element.
2. In the case of plane stress, for example $\{f\} = \begin{Bmatrix} u(x,y) \\ v(x,y) \end{Bmatrix}$ which represent horizontal and vertical displacements of a point within the element and $\{\delta_i\} = \begin{Bmatrix} u_i \\ v_i \end{Bmatrix}$, the displacements of node i. The displacement functions should satisfy internal compatability and also maintain boundary compatability as far as possible, as cited earlier. The strains can be evaluated as

$$\{\varepsilon\} = [B]\{\delta\}^e$$

   For the plane stress case, for instance

$$\{\varepsilon\} = \begin{Bmatrix} \varepsilon_{xx} \\ \varepsilon_{yy} \\ \gamma_{xy} \end{Bmatrix} = \begin{Bmatrix} \dfrac{\partial u}{\partial x} \\ \dfrac{\partial v}{\partial y} \\ \dfrac{\partial u}{\partial y} + \dfrac{\partial v}{\partial x} \end{Bmatrix} = [B]\{\delta\}^e \tag{7.8}$$

   Knowing N_i, N_j and N_m, $[B]$ can be easily found.
3. Assuming linear elastic behavior, the stress–strain relation for the particular case of plane stress can be expressed as

$$\{\sigma\} = \begin{Bmatrix} \sigma_x \\ \sigma_y \\ \tau_{xy} \end{Bmatrix} = [D]\{\{\varepsilon\} - \{\varepsilon_0\}\} - \{\sigma_0\} \tag{7.9}$$

   where $\{\varepsilon_0\}$ and $\{\sigma_0\}$ are the initial strains and stresses if any.

   The matrix $[D]$ will be the usual isotropic stress–strain matrix relationship and is written as

$$[D] = \frac{E}{1-v^2} \begin{Bmatrix} 1 & v & 0 \\ v & 1 & 0 \\ 0 & 0 & \dfrac{1-v}{2} \end{Bmatrix} \tag{7.10}$$

   It may be noted that $[D]$ matrix for the cases of plane strain, 3-D problems, orthotropic materials, axisymmetric problems will be different and are available in standard books/ manuals on FEM (Zienkiewicz, 1971).

4. Equivalent nodal forces: the nodal forces which are statically equivalent to the boundary stresses and distributed loads on the element are represented as

$$\{F\}^e = \begin{Bmatrix} F_i \\ F_j \\ F_m \\ \vdots \end{Bmatrix} \tag{7.11}$$

The number of components of (F_i) should be the same as the components of $\{\delta_i\}$ and be designated in the appropriate, corresponding directions.

The distributed loads $\{p\}$ are defined as those acting on a unit volume of material within the element with directions corresponding to those of the displacements $[\delta]$ at that point.

For the plane stress case

$$\{F_i\} = \begin{Bmatrix} U_i \\ V_i \end{Bmatrix} \quad \text{and} \quad \{p\} = \begin{Bmatrix} X \\ Y \end{Bmatrix} \tag{7.12}$$

where U, V correspond to the directions of displacements u and v and X and Y are the body force components along x and y directions.

To make the nodal forces statically equivalent to the actual boundary stresses and distributed loads, the simplest procedure is to impose a virtual nodal displacement and to equate the external and internal work done by the various forces and stresses during that displacement.

Taking the virtual displacement at the nodes as $\left\{\bar{\delta}\right\}^e$, from Equations (7.7) and (7.8) we have

$$\left\{\bar{f}\right\} = [N]\left\{\bar{\delta}\right\}^e \text{ and } \{\bar{\varepsilon}\} = [B]\left\{\bar{\delta}\right\}^e \tag{7.13}$$

Then work done by the nodal forces over the corresponding virtual displacements can be written as

$$\left\{\left\{\bar{\delta}\right\}^e\right\}^T \{F\}^e \tag{7.14}$$

The internal work done per unit volume by the stresses and distributed forces is

$$\{\varepsilon\}^T\{\sigma\} - \left\{\bar{f}\right\}^T\{p\} \tag{7.15}$$

From Equation (7.13), the same can be written as

$$\left\{\left\{\bar{\delta}\right\}^e\right\}^T \left\{[B]^T\{\sigma\} - [N]^T\{p\}\right\} \tag{7.16}$$

Equating external work done to the total internal work obtained by integrating over the volume of the element we have

$$\left\{\left\{\bar{\delta}\right\}^e\right\}^T \{F\} = \left\{\left\{\bar{\delta}\right\}^e\right\}^T \left[\int^{Vol} [B]^T\{\sigma\} d(Vol) - \int^{vol} [N]^T\{p\} d(vol)\right] \tag{7.17}$$

As this is identically true for any virtual displacement we have from the above

$$\begin{aligned}\{F\}^e &= \int [B]^T\{\sigma\}d(Vol) - \int [N]^T\{p\}d(Vol) \\ &= \int [B]^T[D][B]d(Vol)\{\delta\}^e - \int [B]^T[D]\{\varepsilon_0\}d(Vol) - \int [N]^T\{p\}d(Vol)\end{aligned} \tag{7.18}$$

(from Equations (7.7) and (7.8)).

This relation can be identified to be the typical characteristic of any structural element as seen earlier (see Equation (7.3)). By comparison of Equations (7.3) and (7.18), the stiffness matrix and other parameters can be written as

$$[k]^e = \int [B]^T[D][B]d(Vol) \tag{7.19}$$

$$\{F\}_p^e = -\int [N]^T\{p\}d(Vol) \tag{7.20}$$

$$\{F\}_{\varepsilon_0}^e = -\int [B]^T[D](\varepsilon_0)d(Vol) \tag{7.21}$$

$$\{F\}_{\sigma_0}^e = \int [B]^T\{\sigma_0\}\, d(Vol) \text{ (in case there is an initial stress } \sigma_0) \tag{7.22}$$

If initially the system is in equilibrium with residual stresses $\{\sigma_0\}$, then the forces given by Equation (7.22) will be equal to zero after assembling the elements to form the total system.

All these relations are quite general. The total solution of the assembly of the finite elements, now follows the standard structural procedures. In general, external concentrated forces may exist at the nodes and the matrix

$$\{R\} = \begin{Bmatrix} R_1 \\ R_2 \\ . \\ R_n \end{Bmatrix} \tag{7.23}$$

will be added to the consideration of equilibrium at the nodes as given in Equation (7.5). Solving for the nodal displacements from these equations the stresses at any point can be got from Equations (7.8) and (7.9), that is

$$\{\sigma\} = [D][B]\{\delta\}^e - [D]\{\varepsilon_0\} + \{\sigma_0\} \tag{7.24}$$

This equation can be identified to be similar to Equation (7.4) and by comparison, the stress matrix can be written as

$$\{S\}^e = [D][B] \tag{7.25}$$

The initial stress due to initial strain is

$$\{\sigma\}_{\varepsilon_0}^e = -[D]\{\varepsilon_0\} \tag{7.26}$$

All the above equations are very general and can be interpreted depending on the problem. For example, if it is of an elastic continuum problem, then the displacements, strains, stresses and forces have the same meaning mentioned in the above sections. However, if it is a beam or a plate or solid of other shapes and responses the generalized displacements can be interpreted as vertical deflections, slopes, curvatures and generalized forces could be interpreted as bending moments, shear forces and so on. Accordingly, FEM can also be used for analyzing several field problems such as heat conduction, seepage, steady and unsteady fluid flow, current and magnetic field problems and so on (Zienkiewicz, 1971; Desai and Abel, 1972; Canale and Chapra, 1989; Bowles, 1996). These are in addition to solid mechanics problems of general shapes, constitutive relationships (linear and nonlinear) external loads and so on, wherever the problems involve minimization of an extremum problem such as minimization of energy (as in the case of elasticity problems).

However, for problems where such a minimization process is not either easily identifiable or difficult to formulate, an alternate formulation of FEM can be carried out using Galerkin's method of weighted residuals wherein the residues are minimized (Crandall, 1956; Zienkiewicz, 1971; Zienkiewicz and Taylor, 1989). This procedure makes FEM very versatile and adaptable to all problems where governing equations are known with proper boundary conditions and (or) initial conditions. All these details are very well explained in standard books on FEM as well as in the large number of general purpose software packages such as SAP, NASTRAN, ANSYS, ABAQUS and so on.

Using the general equations discussed in Sections 7.1–7.3, we can derive the relevant expressions for the bending of beams and plates which are needed to analyze BEF and PEF.

7.4 Beam Elements

Consider a beam element with two nodes according to the bending theory, as shown in Figure 7.3 which shows a uniform beam element subjected to the transverse distributed force

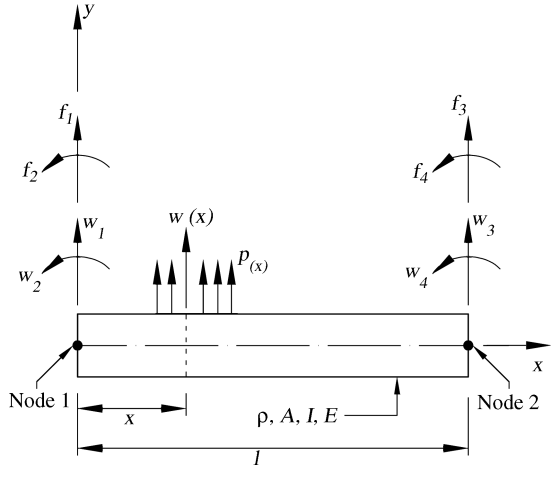

Figure 7.3 Beam element.

$p(x)$. In this case, the joints undergo both translational and rotational displacements, so the unknown joint displacements are labeled as w_1, w_2, w_3 and w_4. Thus, there will be linear joint forces f_1 and f_3 corresponding to the linear joint displacements w_1 and w_3 and rotational joint forces (bending moments) f_2 and f_4 corresponding to the rotational joint displacements w_2 and w_4 respectively. The transverse displacement within the element can be expressed as

$$w(x) = \sum_{i=1}^{4} N_i(x) w_i = [N]\{\delta\} \tag{7.27}$$

where $N_i(x)$ are shape functions and δ is the matrix of nodal displacements of the element, that is, w_1, w_2, w_3, w_4.

Noting that $w(0) = w_1,\ \frac{dw(0)}{dx} = w_2,\ w(l) = w_3,\ \frac{dw(l)}{dx} = w_4$

$N_i(x)$ must satisfy the following boundary conditions

$$N_1(0) = 1,\ N_1(l) = 0,\ \frac{dN_1}{dx}(0) = 0, \quad \frac{dN_1}{dx}(l) = 0 \tag{7.28}$$

$$N_2(0) = 0,\ N_2(l) = 0,\ \frac{dN_2}{dx}(0) = 1, \quad \frac{dN_2}{dx}(l) = 0 \tag{7.29}$$

$$N_3(0) = 0,\ N_3(l) = 1,\ \frac{dN_3}{dx}(0) = 0, \quad \frac{dN_3}{dx}(l) = 0 \tag{7.30}$$

$$N_4(0) = 0,\ N_4(l) = 0,\ \frac{dN_4}{dx}(0) = 0, \quad \frac{dN_4}{dx}(l) = 1 \tag{7.31}$$

Since four conditions are known for each $N_i(x)$, we can assume a polynomial involving four constants (a cubic equation) for $N_i(x)$, that is,

$$N_i(x) = a_i + b_i x + c_i x^2 + d_i x^3, \quad i = 1, 2, 3, 4 \tag{7.32}$$

Substituting the four sets of boundary conditions of Equations (7.28)–(7.31) into Equation (7.32), the shape functions are obtained as

$$N_1(x) = 1 - 3\left(\frac{x}{l}\right)^2 + 2\left(\frac{x}{l}\right)^3 \tag{7.33}$$

$$N_2(x) = x - 2l\left(\frac{x}{l}\right)^2 + l\left(\frac{x}{l}\right)^3 \tag{7.34}$$

$$N_3(x) = 3\left(\frac{x}{l}\right)^2 - 2\left(\frac{x}{l}\right)^3 \tag{7.35}$$

$$N_4(x) = -l\left(\frac{x}{l}\right)^2 + l\left(\frac{x}{l}\right)^3 \tag{7.36}$$

Now, the displacements within the finite beam element can be written from Equation (7.27) as

$$\begin{aligned} w(x) \;=\; & \left(1-3\frac{x^2}{l^2}+2\frac{x^3}{l^3}\right)w_1+\left(\frac{x}{l}-2\frac{x^2}{l^2}+\frac{x^3}{l^3}\right)lw_2 \\ & +\left(3\frac{x^2}{l^2}-2\frac{x^3}{l^3}\right)w_3+\left(-\frac{x^2}{l^2}+\frac{x^3}{l^3}\right)lw_4 \end{aligned} \tag{7.37}$$

We may also note that the strain matrix ε consists of only the curvature in the case of the beam and the corresponding σ matrix refers to the bending moment. Hence

$$\{\varepsilon\} = -\frac{\partial^2 w}{\partial x^2} = [B]\{\delta\}$$

$[B]$ from Equations (7.33)–(7.36) can be obtained as

$$\begin{aligned} [B] \;&=\; \left\{B_i, B_j\right\} = -\frac{d^2}{dx^2}\left\{N_i\, N_j\right\} \\ &= \frac{1}{l^2}\left\{\,6-12\frac{x}{l} \quad 4-6l\left(\frac{x}{l}\right) \quad -6+12\left(\frac{x}{l}\right) \quad 2-6l\left(\frac{x}{l}\right)\right\} \end{aligned} \tag{7.38}$$

$$\{\sigma\} = M = EI\frac{d^2 w}{dx^2} = D\{\varepsilon\} \tag{7.39}$$

where

$$[D] = EI$$

Then the stiffness matrix can be obtained from Equation (7.19) as

$$[K] = \int_0^l B^T DB\, dx = EI\int_0^l B^T B\, dx \tag{7.40}$$

Substituting for B and N from Equations (7.38) and (7.33)–(7.36) in Equations (7.40) and (7.20) and integrating the resulting expressions, we get

$$[K] = \frac{EI}{l^3}\begin{bmatrix} 12 & 6l & -12 & 6l \\ 6l & 4l^2 & -6l & 2l^2 \\ -12 & -6l & 12 & -6l \\ 6l & 2l^2 & -6l & 4l^2 \end{bmatrix} \tag{7.41}$$

and

$$f_i = \int_0^l p(x)N_i(x)\, dx \quad i = 1, 2, 3, 4 \tag{7.42}$$

However another simpler and alternate method to express the equivalent nodal forces due to $p(x)$ applied on the beam (or concentrated loads applied in between the nodes), is to distribute the

resultant force at both the nodes judiciously (depending on the proximity of the applied forces to the node under consideration) as mentioned in the following two alternatives:

1. Prorate loads to adjacent nodes using a simple beam model
2. Prorate loads to adjacent nodes as if the element has fixed ends so that the values include fixed end moments and shears (vertical forces). This is more accurate but involves cumbersome computations.

Accordingly alternative 1 is preferable because of its simplicity.

Equations (7.41) and (7.42) can also be directly derived by writing the expressions for bending strain energy and virtual work done by the virtual displacements of the element (Rao, 1982).

The corresponding generalized forces at the two nodes from the force matrix F of the element are

$$\{F\}^e = \begin{Bmatrix} F_1 \\ F_2 \end{Bmatrix} = \begin{Bmatrix} Q_1 \\ M_1 \\ Q_2 \\ M_2 \end{Bmatrix} = [K] \begin{Bmatrix} w_1 \\ w_2 \\ w_3 \\ w_4 \end{Bmatrix} + \begin{Bmatrix} f_1 \\ f_2 \\ f_3 \\ f_4 \end{Bmatrix} \tag{7.43}$$

where $[K]$ and $\{f\}$ are given by Equations (7.41) and (7.42).

It may be noted that Q and M are shear forces and bending moments and are given by

$$\begin{aligned} M &= EI\frac{d^2w}{dx^2} \\ Q &= -EI\frac{d^3w}{dx^3} \end{aligned} \tag{7.44}$$

at nodes 1 and 2. It may be noted that Equations (7.44) differ from Equations (4.16) due to change in conventions as shown in Figure 4.20 and Figure 7.3.

7.4.1 *Incorporating Soil Reaction for BEF Analysis*

The soil reaction using Winkler's model is expressed as (Chapter 4)

$$q(x) = kw$$

The corresponding soil reactions at the two nodes of the beam (Figure 7.3) can be incorporated as nodal forces either at the time of formulating the stiffness matrix of the beam element or while assembling the global stiffness matrix of the beam for applying equilibrium equations as follows:

1. Incorporating soil reactions in the element stiffness matrix for BEF (Bowles, 1996). Noting that the soil reaction has to be converted into equivalent nodal forces at the nodes of the beam element, the corresponding node soil spring (stiffness) to be added to the diagonal element of the beam stiffness matrix, that is, K_{11} and K_{33} in Equation (7.43).

   The soil spring stiffness (noting that the units should be FL^{-1}) can be expressed from the soil reactions at the nodes as

$$Q_{s1} = k_1 w_1 = \frac{l}{2} b k_s w_1$$
$$Q_{s2} = k_2 w_3 = \frac{l}{2} b k_s w_3 \tag{7.45}$$

where

b = width of the beam
k_s = modulus of subgrade reaction (FL^{-3})
l = length of the element
k_1, k_2 = equivalent soil spring stiffnesses at nodes 1, 2

$$= \frac{l}{2} b k_s \tag{7.46}$$

w_1, w_3 = vertical displacements at nodes 1, 2
Q_{s1}, Q_{s2} = equivalent soil reactions at nodes

By adding terms k_1 and k_2 to the corresponding beam stiffness elements k_{11} and k_{33} in the K matrix given by Equation (7.41), the stiffness matrix for BEF element can be written as

$$[K]_{\text{bef}} = \frac{EI}{l^3} \begin{bmatrix} 12 + \dfrac{k_1 l^3}{EI} & & \text{Symmetric} & \\ 6l & 4l^2 & & \\ -12 & -6l & 12 + \dfrac{k_2 l^3}{EI} & \\ 6l & 2l^2 & -6l & 4l^2 \end{bmatrix} \tag{7.47}$$

where k_1 and k_2 are given in Equation (7.46)

The global stiffness matrices will thus include the contributions of soil reaction coming from the adjacent elements at that node.

2. Another alternative method is to incorporate the soil reactions at the nodes directly while assembling the global stiffness matrix. This method is essentially the same as mentioned above except that Equation (7.41) is used for K instead of Equation (7.47) for K_{bef}. Thus the soil reactions are directly added at the nodes as external forces, that is, contributions form either side of the node are taken into account (Bowles, 1996).

The rest of the FEM is the same that is, assembling the total beam in terms of global stiffness matrix (using the element stiffness matrices given by Equations (7.47) or (7.41), satisfying the equilibrium equations at the nodes, solving for unknown nodal displacements from the resulting simultaneous equations and computing the bending moments, shear forces either from element characteristics or from finite difference approximation in terms of known displacements (Chapter 6), as outlined in Section 7.2.

7.5 Plate Elements for Bending Theory

7.5.1 Introduction

Foundations which have comparable dimensions along both directions (length and breadth) need to be analyzed as plates on elastic foundations (PEF) in the rational approach. The exact

solutions and the numerical and FDM solutions for PEF have been discussed in Chapters 5 and 6. The details for applying FEM to PEF are discussed in the following sections using classical bending theory of plates. The FEM approach is the same as presented in the earlier Section 7.4 except that the plate problem is two-dimensional.

The state of deformation of a plate can be described entirely by the lateral displacement w of the middle plane of the plate. Continuity conditions between elements have now, however, to be imposed not only on this quantity but on its derivatives. This is to ensure that the plate remains continuous and does not *kink*. At each node, therefore, three conditions of equilibrium and continuity need to be imposed.

Determination of suitable shape functions is now much more complex. Indeed, if complete slope continuity is required on the interfaces between various elements, the mathematical and computational difficulties often rise disproportionately fast. It is, however, relatively simple to obtain shape functions which, while preserving the continuity of w, may violate the slope continuity between elements, though naturally not at the node where continuity is imposed. If such functions satisfy the *constant strain* criterion, then convergence may still be found. Accordingly nonconforming shape functions are usually adapted. The solution with such shape functions gives bounds to the correct answer, but on many occasions it yields an inferior accuracy. For practical applications using nonconforming shape functions presented below are preferable.

The simplest type of element shape is a rectangle and this will be discussed. Triangular and quadrilateral elements present some difficulties and are used for solutions of plates of arbitrary shape and shell problems (Zienkiewicz, 1971; Rao, 1982).

7.5.2 *Displacement Formulation of the Plate Problem*

Displacement of a plate, under the usual thin plate theory, is uniquely specified once the deflection, w, is known at all points. This can be written in general form similar to Equation (7.7) as

$$w = [N]\{\delta\}^e \tag{7.48}$$

in which the shape functions are dependent on Cartesian coordinates x, y and $\{\delta\}^e$ lists the element (nodal) parameters.

The generalized *strains* and *stresses* have to be specified in such a way that their scalar product gives the internal work in the manner discussed in Section 7.3. Thus we define the strain as (Figure 7.4)

$$\{\varepsilon\} = \begin{Bmatrix} -\dfrac{\partial^2 w}{\partial x^2} \\ -\dfrac{\partial^2 w}{\partial y^2} \\ 2\dfrac{\partial^2 w}{\partial x \partial y} \end{Bmatrix} \tag{7.49}$$

This is similar to Equation (7.8)

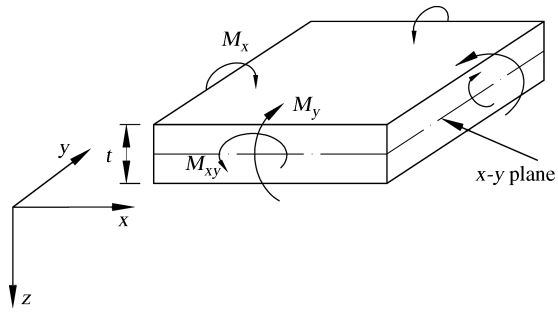

Figure 7.4 Stresses in plate bending.

The corresponding *stresses* are in fact the usual bending and twisting moments per unit lengths in x and y directions, as given below

$$\{\sigma\} = \begin{Bmatrix} M_x \\ M_y \\ M_{xy} \end{Bmatrix} \tag{7.50}$$

This is similar to Equation (7.9)

As true strains and stresses vary linearly across the plate thickness these can be found from such expressions as

$$\sigma_x = \frac{6M_x}{t^2} z, \text{ etc} \tag{7.51}$$

where z is measured from the plate midplane and t is the thickness of the plate.

The product of Equations (7.49) and (7.50) will be equal to the internal work expression exactly. As the strains are now defined by second derivatives, the continuity criterion requires that the shape functions be such that both w and its slope normal to the interface between elements be continuous.

The criterion of constant strain requires that any constant arbitrary value of second derivative should be reproducible within the element.

To ensure at least an approximate satisfaction of slope continuity three displacement components are considered as nodal parameters: the first is the actual displacement w in the z direction, the second is a rotation about the x axis (θ_x) and the third is a rotation about the y axis $\left(\theta_y\right)$. Figure 7.5 shows these rotations with their positive directions; and their magnitudes are shown by vectors directed along the axes.

Now we can write the generalized *displacement* matrix at each node (similar to Equation (7.2)) as

$$\{\delta_i\} = \begin{Bmatrix} w_i \\ \theta_{xi} \\ \theta_{yi} \end{Bmatrix} = \begin{Bmatrix} w_i \\ -\left(\dfrac{\partial w}{\partial y}\right)_i \\ \left(\dfrac{\partial w}{\partial x}\right)_i \end{Bmatrix} \tag{7.52}$$

The nodal *forces* corresponding to these displacements can be interpreted as a direct force and two moments

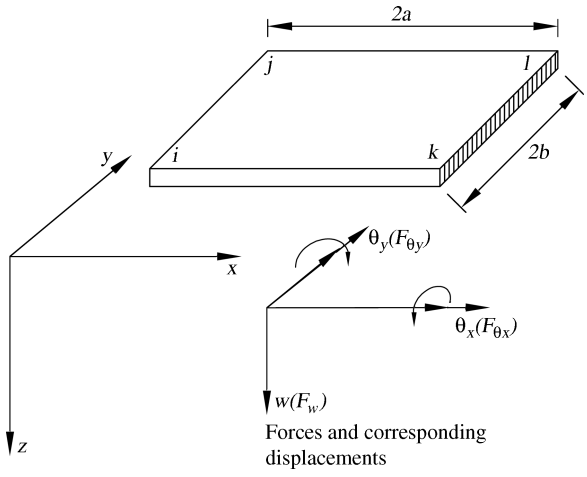

Figure 7.5 A rectangular plate element.

$$\{F_i\} = \begin{Bmatrix} F_{wi} \\ F_{\theta\, xi} \\ F_{\theta\, yi} \end{Bmatrix} \tag{7.53}$$

as shown in Figure 7.5.

The stiffness and other element matrices will be obtained in the usual manner by the expressions of Section 7.3 once the [B] matrix has been determined.

From Equations (7.48) and (7.49) it follows that

$$[B_i] = \begin{Bmatrix} -\dfrac{\partial^2}{\partial x^2}[N_i] \\ -\dfrac{\partial^2}{\partial y^2}[N_i] \\ 2\dfrac{\partial^2}{\partial x \partial y}[N_i] \end{Bmatrix} \tag{7.54}$$

The elasticity matrix [D] is similar to the usual definition as mentioned in Equation (7.10). Accordingly

$$\{\sigma\} \equiv \{M\} = [D](\{\varepsilon\} - \{\varepsilon_0\}) + \{\sigma_0\} \tag{7.55}$$

For an isotropic plate this is expressed as (Timoshenko and Krieger, 1959)

$$[D] = \frac{Et^3}{12(1-v^2)} \begin{bmatrix} 1 & v & 0 \\ v & 1 & 0 \\ 0 & 0 & \left(\dfrac{1-v}{2}\right) \end{bmatrix} \tag{7.56}$$

where E and v = Young's modulus of elasticity and Poisson's ratio of the plate material respectively.

t = the thickness of the plate.

For an orthotropic slab with principal directions of orthotropy coinciding with the x and y axes, four constants are needed to define the behavior, that is

$$[D] = \begin{bmatrix} D_x & D_1 & 0 \\ D_1 & D_y & 0 \\ 0 & 0 & D_{xy} \end{bmatrix} \tag{7.57}$$

These can be related to the appropriate elastic constants of the material (Timoshenko and Krieger, 1959), but it is more convenient to leave them in the above form as the plate theory is often used to solve grillage problems. In such cases the constants must be related to the properties of the grillage. Clearly, for a most complete case of anisotropy, six constants at most are needed to define $[D]$ since the matrix always has to be symmetric (Zienkiewicz, 1971).

7.5.3 *Continuity of Requirement for Shape Function*

To ensure the continuity of both w and its normal slope across an interface we must have both w and $\frac{\partial w}{\partial n}$ uniquely defined by values along such an interface.

However, it is impossible to specify simple polynomial expressions for shape functions ensuring full compatibility when only w and its slopes are prescribed at nodes (Zienkiewicz, 1971; Rao, 1982).

If any functions satisfying the compatibility are found with the three nodal variables, they must be such that at corner nodes they are not continuously differentiable and the cross derivative is not unique (Zienkiewicz, 1971).

The difficulties of finding compatible displacement functions led to several attempts at ignoring the complete slope continuity while still continuing with the other necessary criteria. Proceeding with the idea that the imposition of slope continuity at node must, in the limit, lead to complete slope continuity, several very successful elements have been developed. The convergence of some of these can be demonstrated and proved by other means. In view of their simplicity, they are usually adopted for applications as discussed below.

7.5.4 *Nonconforming Shape Functions*

Consider a rectangular element of a plate *ijkl* coinciding with the x, y planes as shown in Figure 7.5. At each node displacements $\{\delta\}$ are introduced. These have three components: the first a displacement in the z direction, w the second a rotation about the x axis, (θ_x), the third a rotation about the y axis (θ_y).

The nodal displacements are defined by Equation (7.52) while the element displacement will be given by the listing of the four nodal displacements, that is

$$\{\delta\}^e = \begin{Bmatrix} \delta_i \\ \delta_j \\ \delta_k \\ \delta_l \end{Bmatrix} \tag{7.58}$$

A polynomial expression is conveniently used to define the shape functions in terms of the twelve parameters. Certain terms must be omitted from a complete fourth-order polynomial.

Writing

$$w = \alpha_1 + \alpha_2 x + \alpha_3 y + \alpha_4 x^2 + \alpha_5 xy + \alpha_6 y^2 + \alpha_7 x^3 + \alpha_8 x^2 y + \alpha_9 xy^2 + \alpha_{10} y^3 + \alpha_{11} x^3 y + \alpha_{12} xy^3 \tag{7.59}$$

has certain advantages. In particular, along any $x =$ constant or $y =$ constant line, the displacement w varies as a cubic. The element boundaries or interfaces are composed of such lines. As a cubic is uniquely defined by four constants, the two end values of slopes and displacements at the ends of the boundaries therefore define the displacements uniquely along this boundary. As such end values are common to adjacent elements, continuity of w is imposed all along any interface.

It can be observed that the gradient of w normal to any of the boundaries varies along it in a cubic way (consider, for instance, $\frac{\partial w}{\partial x}$ along a line on which x is constant). As on such lines only two values of the normal slope are defined, the cubic is not specified uniquely and, in general, a discontinuity of the normal slope occurs. The function is thus *nonconforming*.

The constants α_1 to α_{12} can be evaluated by writing down the twelve simultaneous equations linking the values of w and its slopes at the nodes when the coordinates take up their appropriate values. For instance

$$\begin{aligned} w_i &= \alpha_1 + \alpha_2 x_i + \alpha_3 y_i + \text{etc.} \\ \left(-\frac{\partial w}{\partial y}\right)_i &= \theta_{xi} = -\alpha_3 + \text{etc.} \\ \left(\frac{\partial w}{\partial x}\right)_i &= \theta_{yi} = \alpha_2 + \text{etc.} \end{aligned} \tag{7.60}$$

The 12 equations can be written, in matrix form, as

$$\{\delta\}^e = [C]\{\alpha\} \tag{7.61}$$

where $[C]$ is a 12×12 matrix depending on nodal coordinates and $\{\alpha\}$ is a vector of the 12 unknown constants given by

$$\{\alpha\} = [C]^{-1}\{\delta\}^e \tag{7.62}$$

This inversion can be carried out by computer or, if an explicit expression is desired for the stiffnesses and so on, it can be performed algebraically (Zienkiewicz, 1971).

It is now possible to write the expression for the displacement within the element in a standard form as

$$\{f\} = w = [N]\{\delta\}^e = [P][C]^{-1}\{\delta\}^e \tag{7.63}$$

where

$$[P] = \left(1, x, y, x^2, xy, y^2, x^3, x^2 y, xy^2, y^3, x^3 y, xy^3\right) \tag{7.64}$$

An explicit form of the above expression was derived by Melosh (Zienkiewicz, 1971).

The expressions can be written simply in terms of normalized coordinates as described by Zienkiewicz (1971). This can be written for any node as

$$[N_i] = PC^{-1} = \frac{1}{2}\begin{bmatrix} (\xi_0 + 1)(\eta_0 + 1)(2 + \xi_0 + \eta_0 - \xi^2 - \eta^2), \\ a\xi_i(\xi_0 + 1)^2(\xi_0 - 1)(\eta_0 + 1), \\ b\eta_i(\xi_0 + 1)(\eta_0 + 1)^2(\eta_0 - 1) \end{bmatrix} \tag{7.65}$$

where

$$\xi = \frac{(x - x_e)}{a}, \quad \eta = \frac{(y - y_e)}{b}$$
$$\xi_0 = \xi \cdot \xi_i, \quad \eta_0 = \eta \cdot \eta_i \tag{7.66}$$

The matrix $[B]$ is obtained directly from Equation (7.59) or from Equation (7.65) by use of Equation (7.54). Writing the expressions for $\{\varepsilon\}$, we have

$$\{\varepsilon\} = \begin{Bmatrix} -2\alpha_4 & -6\alpha_7 x & -2\alpha_8 y & -6\alpha_{11} xy & \\ -2\alpha_6 & -2\alpha_9 x & -6\alpha_{10} y & -6\alpha_{12} xy & \\ 2\alpha_5 & +4\alpha_8 x & +4\alpha_9 y & +6\alpha_{11} x^2 & +6\alpha_{12} y^2 \end{Bmatrix} \tag{7.67}$$

This can be expressed as

$$\{\varepsilon\} = [Q]\{\alpha\} = [Q][C]^{-1}\{\delta\}^e; \quad \text{and } [B] = [Q][C]^{-1} \tag{7.68}$$

in which

$$[Q] = \begin{bmatrix} 0 & 0 & 0 & -2 & 0 & 0 & -6x & -2y & 0 & 0 & -6xy & 0 \\ 0 & 0 & 0 & 0 & 0 & -2 & 0 & 0 & -2x & -6y & 0 & -6xy \\ 0 & 0 & 0 & 0 & 2 & 0 & 0 & 4x & 4y & 0 & 6x^2 & 6y^2 \end{bmatrix} \tag{7.69}$$

It is of interest to note that the displacement function chosen does in fact permit a state of constant strain (curvature) to exist and therefore satisfies the criterion of convergence stated in Section 7.2.

7.5.5 *Stiffness and Load Matrices*

The standard procedure given in Section 7.3 can now be followed to obtain these matrices according to Equation (7.19)

$$[K] = \iint [B]^T [D][B]\, dx\, dy \tag{7.70}$$

Substituting B from Equation (7.68) in Equation (7.70) and taking t as constant within the element, we get

$$[K] = \left\{[C]^{-1}\right\}^T \left(\iint [Q]^T [D][Q]\, dx\, dy\right)[C]^{-1} \tag{7.71}$$

The terms not containing x and y have now been removed from the operation of integration. The term within the integration sign can be multiplied out and integrated explicitly without difficulty, if t is constant.

An explicit expression for the stiffness matrix [K] has been evaluated for the case of an orthotropic material and is given in Appendix 7.A.1 (Zienkiewicz, 1971).

The corresponding stress matrix for the internal moments of all the nodes is given in Appendix 7.A.2 (Zienkiewicz, 1971).

The external forces at nodes due to distributed loading can be approximately calculated by allocating specific areas as contributing to any node. However, it is more logical and accurate to use once again the standard expression Equation (7.20) instead of the simple approach.

If a distributed loading p is acting per unit area of an element in the direction of w then, by Equation (7.20), the contribution of these forces to each of the nodes is

$$\{F\}_p^e = -\iint [N]^T p \, dx \, dy \tag{7.72}$$

Or by Equation (7.65)

$$\{F\}_p^e = \left\{-[C]^{-1}\right\}^T \iint [P]^T p \, dx \, dy \tag{7.73}$$

The integral is again evaluated simply. It will now be noted that, in general, all three components of external force at any node have nonzero values. This is a result which the simple allocation of external loads would have missed. Appendix 7.A.3 shows the nodal load vector for a uniform loading p_0.

7.5.6 *Stiffness Matrix for Isotropic Plates*

Explicit expressions for [K], $\{\sigma\}$, $\{F\}$ matrices for isotropic plates can be obtained by substituting

$$D_x = D_y = D = \frac{Et^3}{12(1-v^2)}$$

$$D_1 = vD \tag{7.74}$$

$$D_{xy} = \frac{(1-v)}{2} D \tag{7.75}$$

in Appendix 7.A (i.e., Sections 7.A.1–7.A.3). This obvious substitution can be noted by comparing the [D] matrices of isotropic and orthotropic plates given by Equations (7.56) and (7.57).

7.5.7 *Incorporating Soil Reaction for PEF Analysis*

The soil reaction in such cases for plates on elastic foundations is incorporated in the analysis by either of the following idealizations.

1. The soil is idealized as Winkler's model and the soil reaction $q(x) = kw$ is incorporated as a resultant nodal force at all the four nodes of the rectangular plate element. This can be done either at the time of formulation of the stiffness matrix of the plate element or while

assembling the global stiffness matrix of the plate for applying equilibrium equations as follows (similar to the methods presented in Section 7.4.1 for BEF analysis).

a. Incorporating soil reaction in the element stiffness matrix for PEF (Bowles, 1996). Noting that the soil reaction has to be incorporated as nodal forces at the nodes of the plate element, the corresponding node soil *spring* (stiffness) has to be added to the diagonal elements of the plate element stiffness matrix, that is, K_{11}, K_{44}, K_{77} and K_{1010} in Equation (7.71) given by Appendix 7.A.1.

   Accordingly

$$Q_{si} = k_i w_i = k_s abw_i \quad i = 1, 2, 3, 4 \tag{7.76}$$

   where

   Q_{si} = nodal force due to soil reaction at node i.
   a, b = half of the dimensions of the rectangular plate element (Figure 7.5) along x and y axes respectively.
   k_s = modulus of subgrade reaction.
   k_i = equivalent spring stiffness at node i for the element under consideration $= k_s ab$

   Now by adding K_i ($i = 1, 2, 3, 4$) to the corresponding plate stiffness elements K_{11}, K_{44}, K_{77}, and K_{1010} in the [K] matrix for plate element given in Appendix 7.A.1, the soil reactions get incorporated in the PEF analysis. Thus, we have

$$(K_{ii})_{\text{pef}} = K_{ii} + k_i = K_{ii} + ab\,k_s \quad i = 1, 4, 7, 10 \tag{7.77}$$

   It should be noted that the K_{ii} of the global stiffness matrix gets contributions of soil reaction from all such plate elements with i as the common node. In Equation (7.77), a and b are the half dimensions of each of such elements joining at i.

b. Another alternative method is to incorporate the soil reactions at the nodes directly while assembling the global stiffness matrix (similar to BEF problems mentioned in Section 7.4.1). This can be done by computing the node spring stiffness based on the contributing plan area (Bowles, 1996) of an element to any node as shown in Figure 7.6 and is given below.

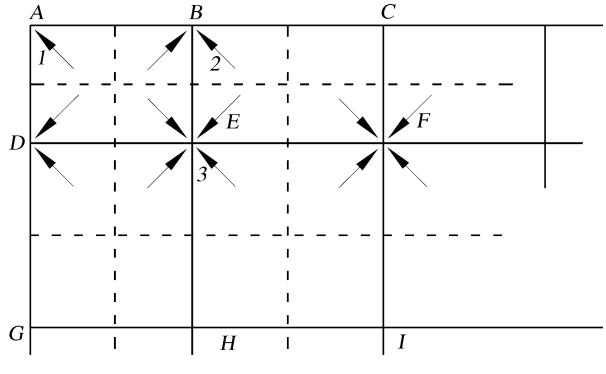

Figure 7.6 Alternate method to include soil reactions at nodes.

Contributing area:

i. Corner node (A) - ¼ of the rectangular area ABDE
ii. Side node (B, D, etc.) - ¼ of ABDE + ¼ of BCEF
iii. Interior node (E, F, etc.) - ¼ of each of the four rectangular areas joining at the common interior node. (7.78)

Then the node spring force at any node i due to soil reaction can be calculated as

$$k_i w_i = k_s \times \text{contribution area at the node } i, \text{ as indicated in Equation (7.78)} \times w_i \quad (7.79)$$

For other irregular shapes of elements, these can be expressed using judgment of the area of influence of each of the node, as outlined in Equation (7.78).

2. Soil as elastic half space. In view of the computational intensity anyway involved in FEM, soil also can be idealized as an elastic half space and the plate can be connected to it by suitable idealizations. Accordingly, the inputs for soil continuum are Young's modulus of elasticity, E_s, and Poisson's ratio, v_s. It may be noted that E_s and v_s are directly related to the modulus of subgrade reaction, k_s, as discussed in Chapter 4.

However, it may be computationally simple and preferable to use Winkler's model because of its widespread applications in footing analysis and design in practice.

The rest of the FEM is the same as indicated in Sections 7.2 and 7.4, which involves assembling global stiffness matrix for the total PEF, writing down the equilibrium equations at all the nodes, solving for unknown nodal displacements and slopes and computing the bending moments, shear forces and contact pressure (soil reaction) and so on.

7.5.8 Circular, Ring Shaped and Plates of General Shapes

The main difference in FEM for nonrectangular shapes including circular and ring shaped foundations is in discretization using finite elements to fit the shape of the prototype plate as closely as possible and to interpret displacements, strains, stresses and constitutive relationships (D matrix in Equation (7.10)) appropriately. This can even be achieved using rectangular or triangular elements with finer mesh for discretization near the boundaries which may not be strictly fitting into rectangular or triangular geometry. One can also use quadrilateral or parallelogram shaped elements. For circular and ring shaped elements, Bowles (1996) used beam elements for analysis when the problems were axisymmetric. The formulation for other cases can be done using cylindrical polar coordinates (Zeinkiewicz, 1971; Rao, 1982).

The details of analysis for such plates can be referred to in standard books on FEM (Zienkiewicz, 1971; Desai and Abel, 1972; Rao, 1982; Zienkiewicz and Taylor, 1989). The rest of the FEM procedure is the same as for rectangular plates (Section 7.5.1–7.5.7) including the incorporation of soil reaction for PEF.

7.5.9 Finite Grid Method and Boundary Element Method

These are methods similar to FEM and bring in lot of simplification in computations. The details of the finite grid method are given in Bowles (1996) and the boundary element method is given in Becker (1992).

7.5.10 General Comments on FEM

From the details outlined in this chapter, following general comments can be made.

1. The FEM is a very simple and very versatile method to deal with complex problems.
2. The procedure involves too many unknowns to be solved from simultaneous equations and is practical only if programmed on computers or software packages are used. A large number of general purpose software packages are available (SAP, STAAD, NASTRAN, ABAQUS, ANSYS, NISA and so on). Analysis is difficult to be carried out manually by hand calculators unless the unknowns are small in number (by using very few elements) and mathematical software like MATLAB® is available.
3. Since a large number of equations need to be solved in FEM the program output should always be carefully checked. A finite element computer program should be somewhat self-checking. This is accomplished by checking the input and comparing sums of input versus output forces, even in commercial software packages.
4. One should not use a very short element next to a long element. Use more finite elements and effect a transition between short and long members. Try to keep the ratio $\frac{L_{\text{long}}}{L_{\text{short}}} \leq 2$ and not more than 3.
5. The value of k_s directly affects the deflection but has very little effect on the computed bending moments at least for reasonable values of k_s.
6. Since k_s is usually estimated, the use of refined methods may give undeserved confidence in the computed results.

7.6 Summary

The general concepts of FEM are presented and expressions needed in the analysis are given in detail. The procedure is explained and versatility of FEM is reiterated. Problems of BEF and PEF are discussed including the details for incorporation of soil reaction in the analysis. The beam and plate elements are presented and approaches to deal with several complexities are outlined. General comments on the use of FEM are summarized. A few examples of BEF and PEF are illustrated.

7.7 Examples

A large number of examples of BEF and PEF using FEM are available in theses, books, papers and software packages. A few of these are presented in this section.

7.7.1 FEM Analysis of BEF

Example 7.1

Determine the distribution of bending moments and bearing pressures under the loaded, nonprismatic foundation resting on dense sand as shown in Figure 7.7. Assume that the density of concrete $= 24\,\text{kN/m}^3$, Young's modulus of elasticity of concrete, $E_c = 15\,\text{kN/mm}^2$ and $k_s = 140\,\text{kN/m}^2/\text{mm}$ (from 305 mm square plate bearing test).

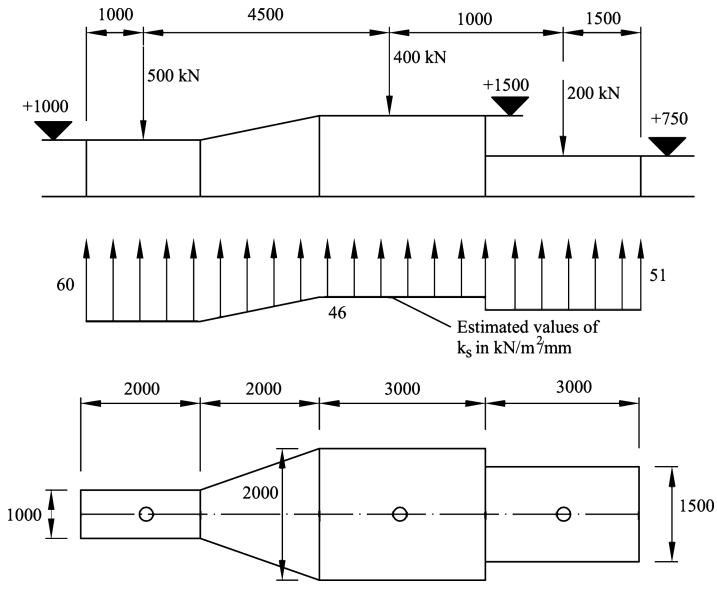

Figure 7.7 Non-prismatic foundation – loading diagram.

The results of FEM analysis using SAP-2000 package are presented in Figure 7.8 and compared with FDM results obtained by using BEF package (Jones, 1997). Tension in the soil contact pressure is not allowed in the option used in BEF package for FDM (Sridhar, 1999).

Example 7.2

Determine the bending moment distribution for the loaded foundation resting on stiff clay as shown in Figure 7.9, when k_s is discontinuous. Assume that the density of concrete $= 24\,\text{kN/m}^2$, $E_c = 15\,\text{kN/mm}^2$ and $k_s = 131\,\text{kN/m}^2/\text{mm}$ (from 305 mm square plate bearing test)

The results of FEM (using SAP 2000) are presented in Figure 7.10 and compared with FDM results. No tensile contact pressure is allowed in the FDM package.

Example 7.3

Determine the fixed end moments in the base slab of the circular tank shown in Figure 7.11. Neglect the effects of Poisson's ratio and assume: modulus of subgrade reaction of soil $k_s = 18\,\text{kN/m}^2/\text{mm}$, Young's modulus of concrete, $E_c = 15\,\text{kN/mm}^2$ and density of concrete $= 24\,\text{kN/m}^3$. The loading diagram is shown in Figure 7.11

When the tank wall is integral with the base, a simple moment distribution procedure can be adopted to calculate the bending moments induced into the wall and base.

The base slab is analyzed by assuming a wedge shaped base of length R, radius of the tank and unit breadth at the outside edge along the center line of the wall and zero breadth at the center of the tank. The only base loading that needs to be considered is an edge shear equal to

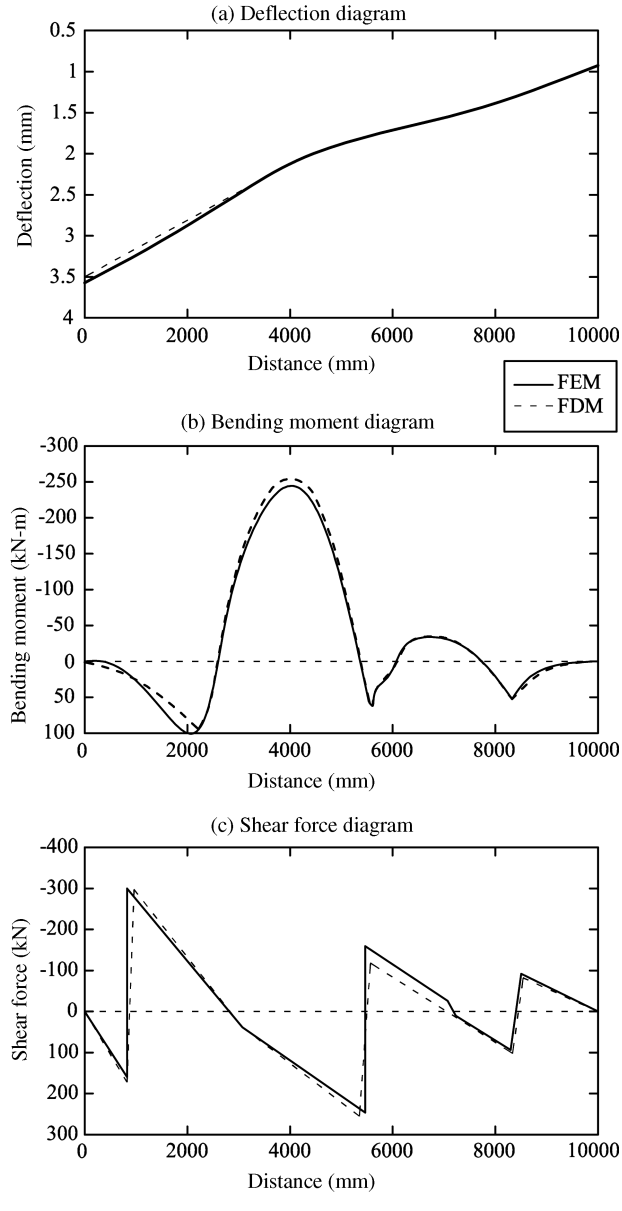

Figure 7.8 Non-prismatic foundation – deflection, bending moment and shear force diagrams.

the weight of the wall minus the weight of an equal volume of water, that is, an edge shear of $(\gamma_c - \gamma_l)Ht_w$, where γ_c is the unit weight of concrete and γ_l is the unit weight of the liquid and H and t_w are the height and wall thickness of the circular tank.

Only half of the base slab is to be analyzed because of symmetry. The results of FEM using SAP 2000 are presented in Figure 7.12 along with FDM results.

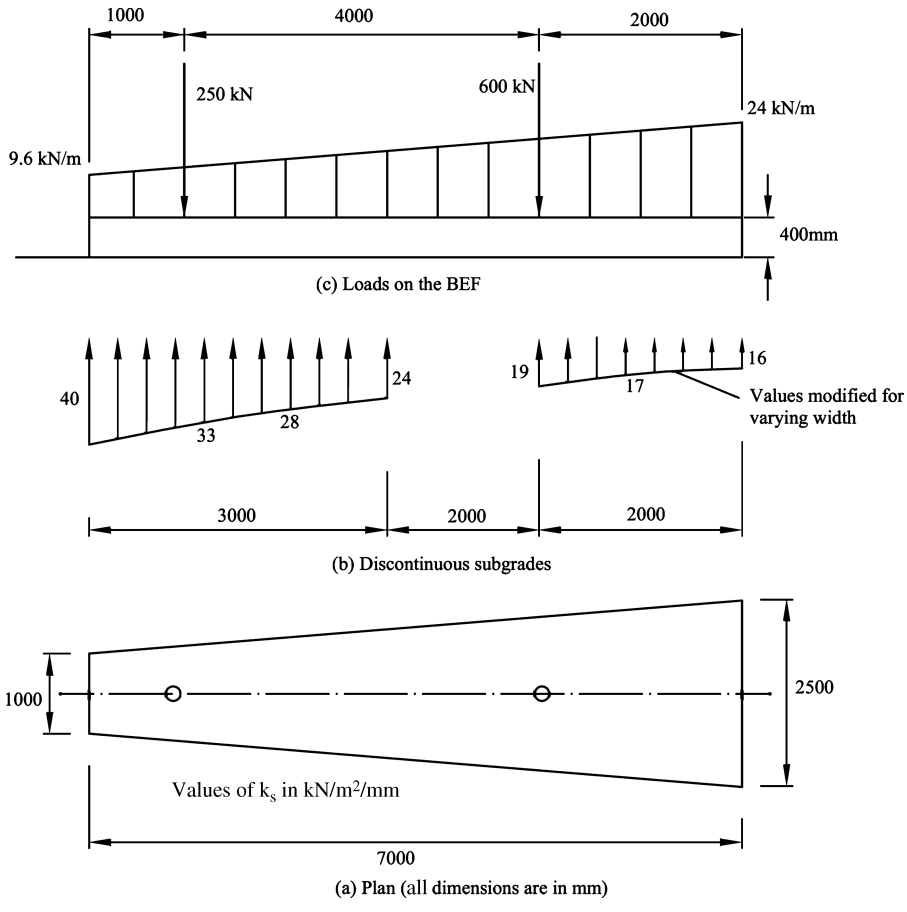

Figure 7.9 Trapezoidal foundation.

7.7.2 FEM Analysis of PEF

All the plates that are analyzed here are considered to be in the *x–y* plane and the results presented are according to this convention. In every analysis of footings idealized as plates, the self weight of the footing (which does not induce any shear or bending forces for freely supported edges) is neglected and is not taken into account during analysis. All footings considered are of uniform cross section. All plates are considered to have smooth boundaries, that is, no curved edges are present. The results presented here are from values taken from the nodal points.

Example 7.4

A $3.0 \times 3.0 \times 0.5$ m square footing with a central concentrated load of 3000 kN has been analyzed. Only one quarter of the plate has been analyzed in discretizing the plate by 64,

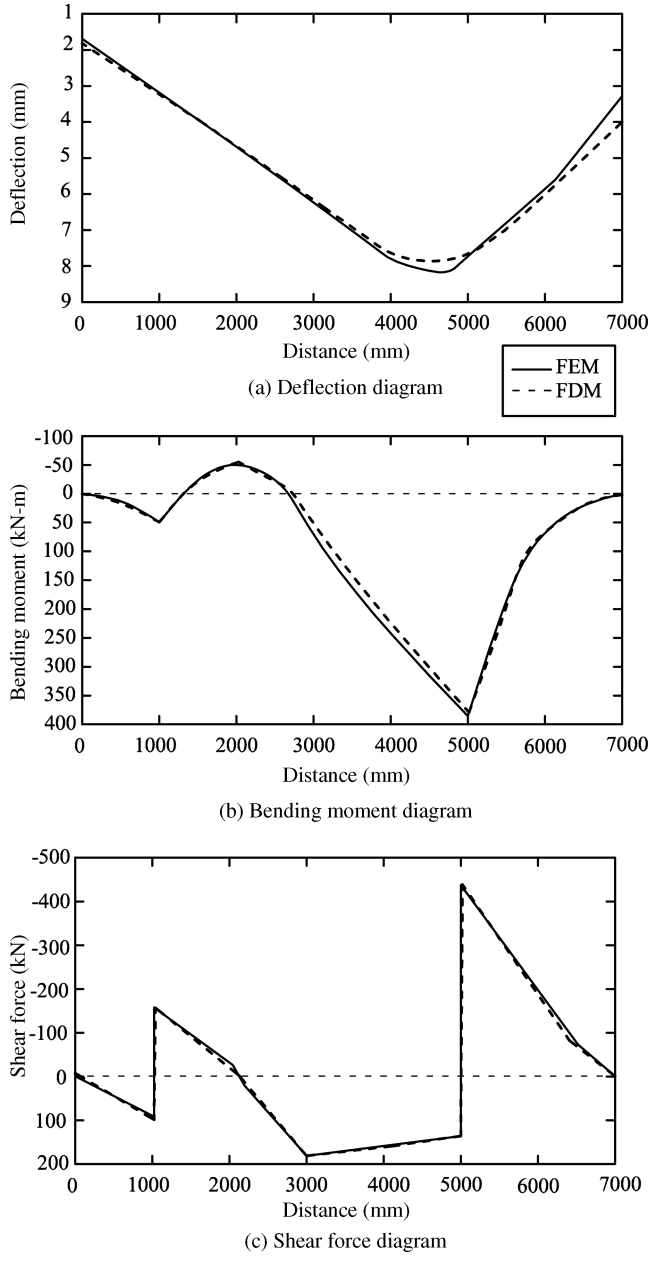

Figure 7.10 Trapezoidal foundation – discontinuous subgrade – deflection, bending moment and shear force diagrams.

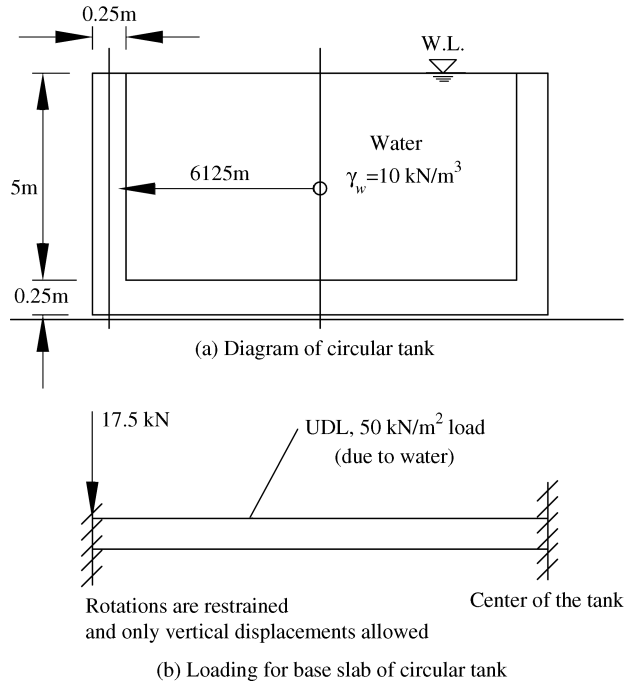

Figure 7.11 Circular tank – loading diagram.

four noded plate elements of equal length, taking advantage of symmetry. The results of this footing for $k_s = 6\,\text{MN/m}^3$ are presented in Figures 7.13 and 7.14. The properties of concrete are taken as $E_c = 25.5 \times 10^6\,\text{kN/m}^2$ and $v_c = 0.2$. The deflection diagram and M_{xx} diagram are symmetrical for the remaining part of the plate.

From Figure 7.13, the deflection diagram shows that it is not constant when seen on a large scale, as the difference in maximum and minimum deflection is about 19%. This shows the footing is neither completely flexible nor rigid. The deflected shape also shows that the plate has more deflections at the center, characteristic of the Winkler model.

From Figure 7.14, the M_{xx} diagram shows rapid decrease in bending moments close to the center and there upon the decrease is slow as we move to the edges.

Examples 7.5 and 7.6

A parametric study was conducted on a square footing resting on elastic subgrade. The influence of the following parameters on deflection, bending moment, shear force was studied. The parameters studied are:

1. Effect of k_s (modulus of subgrade reaction)
2. Effect of depth of the footing.

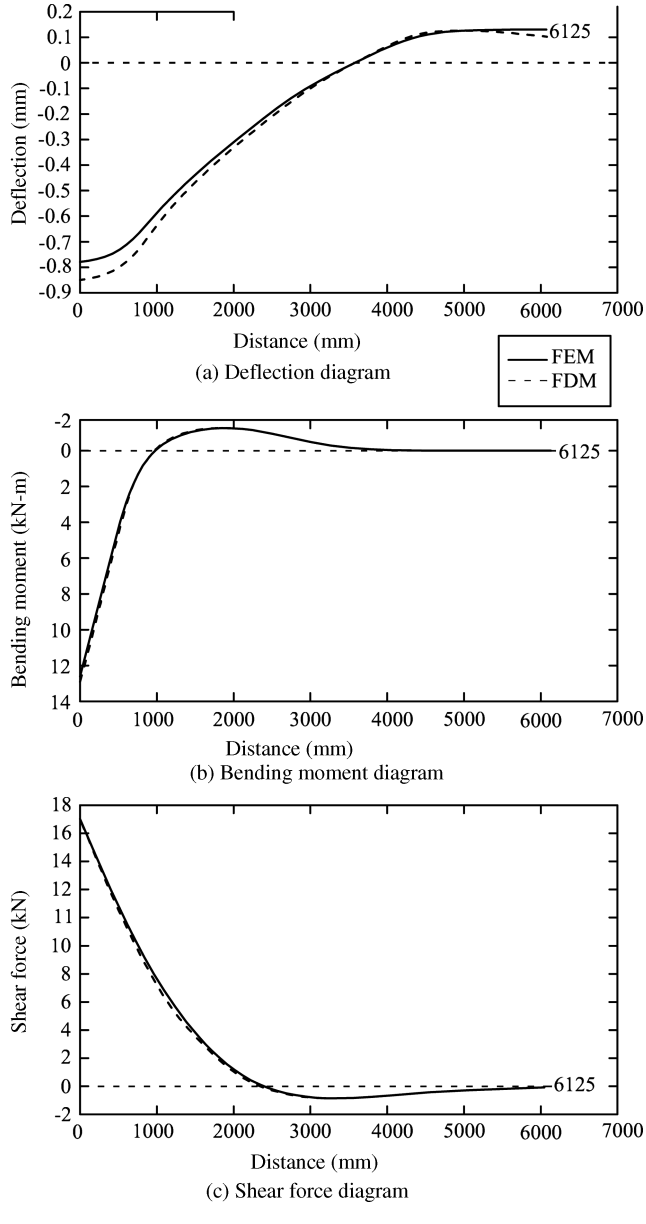

Figure 7.12 Circular tank base slab – deflection, bending moment and shear force diagrams.

Example 7.5

Effect of k_s:
A square footing of 3×3 m by 0.375 m in size is loaded centrally with 3000 kN.

The effect of k_s on deflection, bending moment and shear force is plotted in Figure 7.15. The decrease in deflection is pronounced as k_s increases. For small values of k_s and rate of decrease

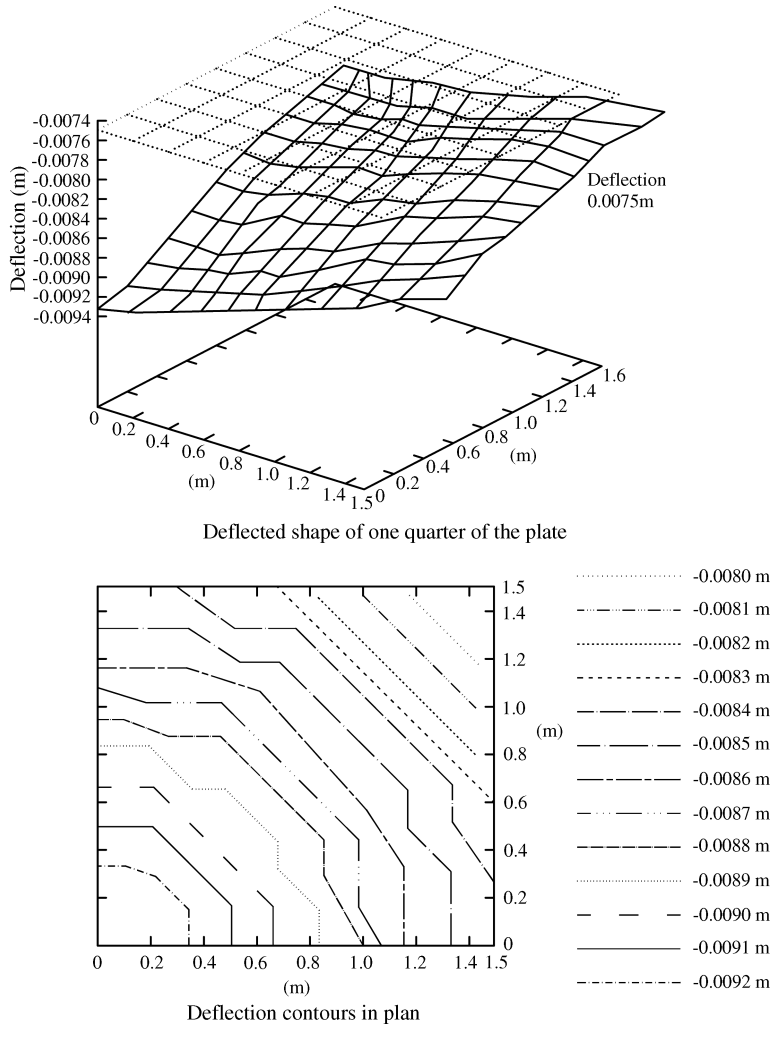

Figure 7.13 Centrally loaded square footing – deflection diagram.

is less as k_s increases, for higher values of k_s. The difference in bending moment and shear force is very small for all values of k_s except for $k_s = 300$. This result is common in all elastic analysis, due to the fact that shear force and bending moment are proportional not to deflection but to differentials (rates of change) of different orders of deflection.

Example 7.6

Effect of depth:
A square footing of side B loaded centrally with 3000 kN was analyzed for the effect of depth. The variations in deflection, bending moment and shear force for two different values of depth

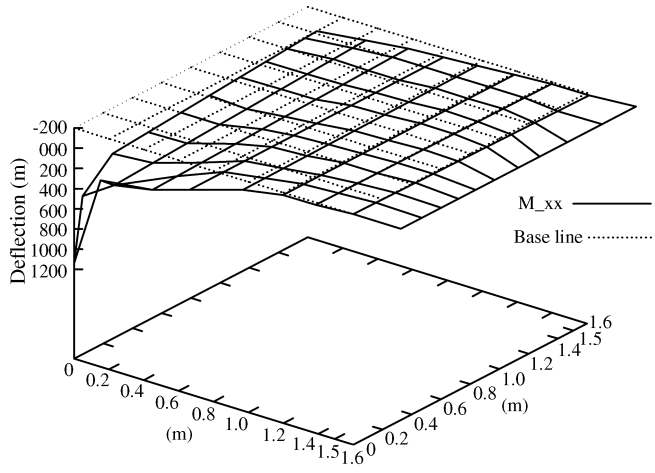

Bending moment diagram of one quarter of the plate

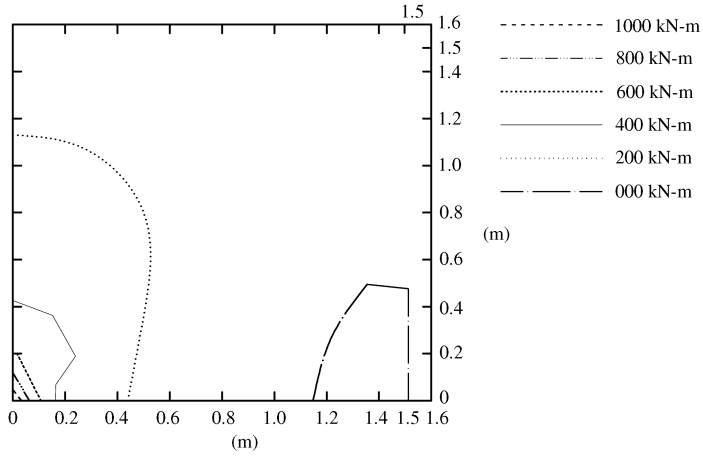

Contours of bending moment diagram

Figure 7.14 Centrally loaded square footing – M_{xx} diagram.

for $B = 2$ and 3 m are presented ($k_s = 75\,\text{MN/m}^3$) in Figures 7.16 and 7.17. The decrease in deflection amply shows the increase in rigidity of the footing as the depth increases. But though there is an increase in the depth of the footing, there is no significant increase in both the values of shear force and bending moment.

7.7.3 General FEM Examples of Soil Structure Interaction

Several examples of FEM for soil–structure interaction analysis such as laterally loaded piles, sheet pile walls, pile groups, integrated analysis of a frame–foundation–soil system are presented by Das (1977) and Sridhar (1999) to bring out its versatility and diversity.

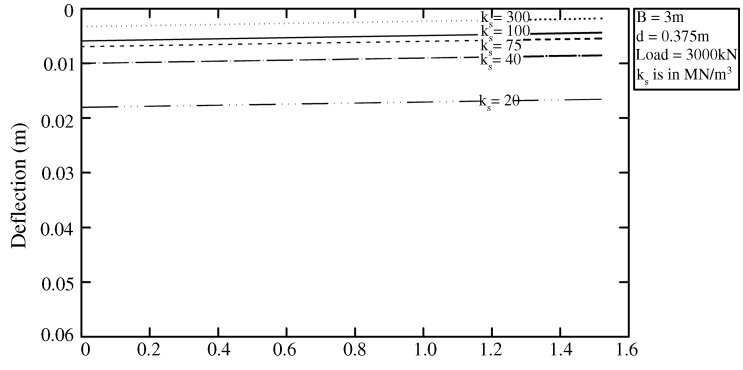

(a) Deflection diagram

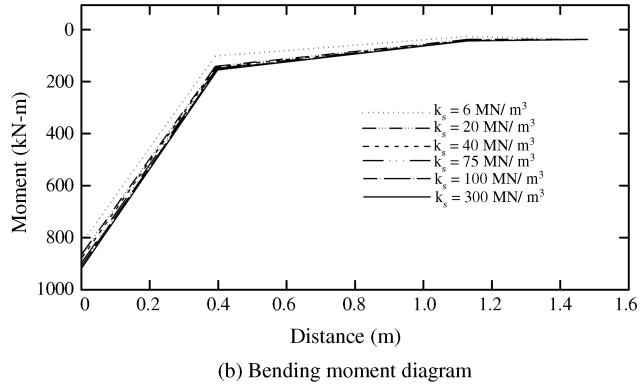

(b) Bending moment diagram

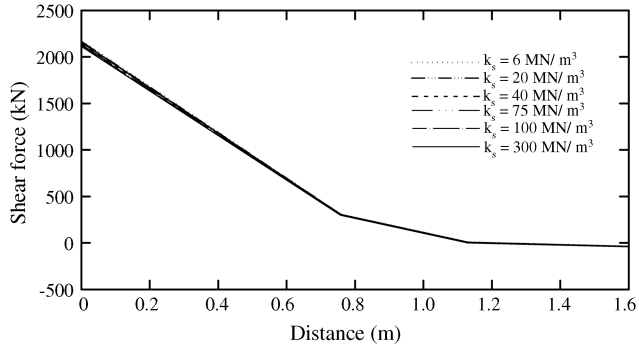

(c) Shear force diagram

Figure 7.15 Parametric study – effect of k_s.

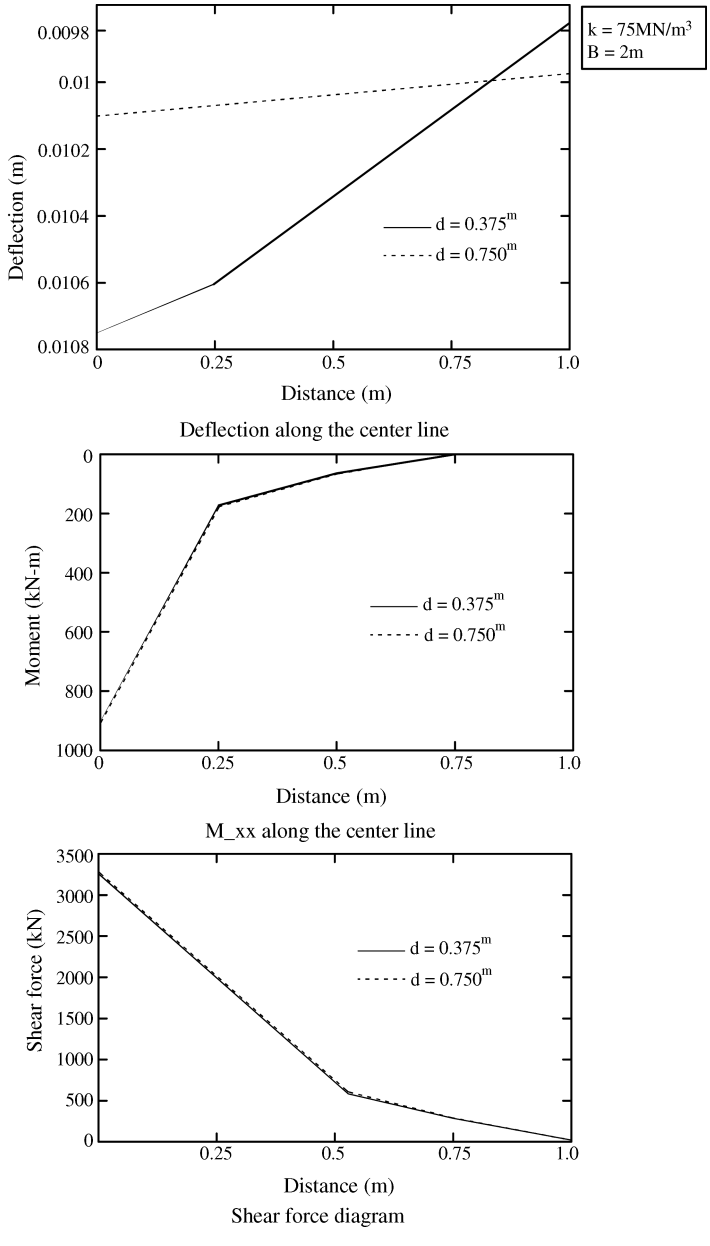

Figure 7.16 Parametric study – effect of depth for $B = 2$ m.

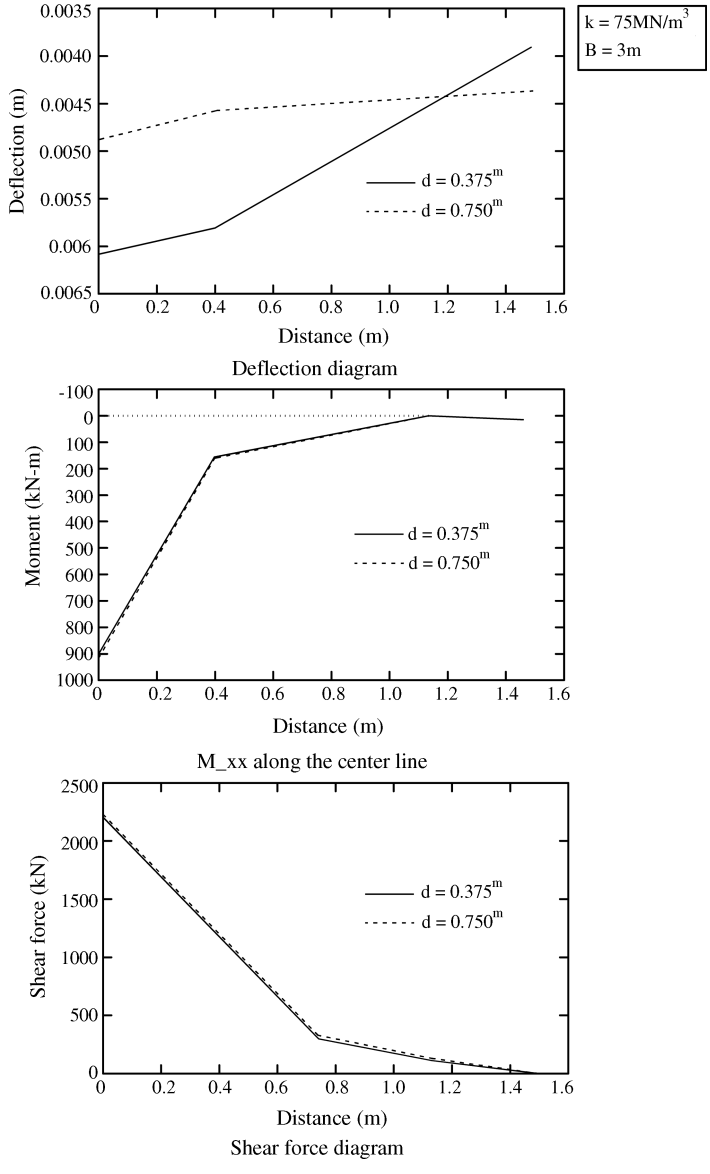

Figure 7.17 Parametric study – effect of depth for $B = 3$ m.

Exercise Problems

7.1–7.25: Redo problems 6.1–6.25 of Chapter 6 with FEM. Use 5–10 elements for manual analysis and obtain the solutions using computers and packages like MATLAB®. Also compare these analyses with finer discretization and solution using commercial FEM packages.

Appendix 7.A Stiffness and Stress Matrices for Plate Elements

7.A.1 Stiffness Matrix

Stiffness matrix for a rectangular orthotropic plate element (Figure 7.5):

$$[K] = \frac{1}{60ab}[L]\left\{D_x[K_1] + D_y[K_2] + D_1[K_3] + D_{xy}[K_4]\right\}[L]$$

with

$$\begin{Bmatrix} F_i \\ F_j \\ F_k \\ F_l \end{Bmatrix} = [K] \begin{Bmatrix} \delta_i \\ \delta_j \\ \delta_k \\ \delta_l \end{Bmatrix}$$

$$K_1 = p^{-2} \begin{bmatrix}
60 & & & & & & & & & & & \\
0 & 0 & & & & & p^{-2} = \frac{b^2}{a^2} & & & & & \\
30 & 0 & 20 & & & & & & & & & \\
30 & 0 & 15 & 60 & & & \text{Symmetrical} & & & & & \\
0 & 0 & 0 & 0 & 0 & & & & & & & \\
15 & 0 & 10 & 30 & 0 & 20 & & & & & & \\
-60 & 0 & -30 & -30 & 0 & -15 & 60 & & & & & \\
0 & 0 & 0 & 0 & 0 & 0 & 0 & 0 & & & & \\
30 & 0 & 10 & 15 & 0 & 5 & -30 & 0 & 20 & & & \\
-30 & 0 & -15 & -60 & 0 & -30 & 30 & 0 & -15 & 60 & & \\
0 & 0 & 0 & 0 & 0 & 0 & 0 & 0 & 0 & 0 & 0 & \\
15 & 0 & 5 & 30 & 0 & 10 & -15 & 0 & 10 & -30 & 0 & 20
\end{bmatrix}$$

$$K_2 = p^{2} \begin{bmatrix}
60 & & & & & & & & & & & \\
-30 & 20 & & & & & p^{2} = \frac{a^2}{b^2} & & & & & \\
0 & 0 & 0 & & & & & & & & & \\
-60 & 30 & 0 & 60 & & & \text{Symmetrical} & & & & & \\
-30 & 10 & 0 & 30 & 20 & & & & & & & \\
0 & 0 & 0 & 0 & 0 & 0 & & & & & & \\
30 & -15 & 0 & -30 & -15 & 0 & 60 & & & & & \\
-15 & 10 & 0 & 15 & 5 & 0 & -30 & 20 & & & & \\
0 & 0 & 0 & 0 & 0 & 0 & 0 & 0 & 0 & & & \\
-30 & 15 & 0 & 30 & 15 & 0 & -60 & 30 & 0 & 60 & & \\
-15 & 5 & 0 & 15 & 10 & 0 & -30 & 10 & 0 & 30 & 20 & \\
0 & 0 & 0 & 0 & 0 & 0 & 0 & 0 & 0 & 0 & 0 & 0
\end{bmatrix}$$

$$K_3 = \begin{bmatrix}
30 & & & & & & & & & & & \\
-15 & 0 & & & & & & & & & & \\
15 & -15 & 0 & & & & & \text{Symmetrical} & & & & \\
-30 & 0 & -15 & 30 & & & & & & & & \\
0 & 0 & 0 & 15 & 0 & & & & & & & \\
-15 & 0 & 0 & 15 & 15 & 0 & & & & & & \\
-30 & 15 & 0 & 30 & 0 & 0 & 30 & & & & & \\
15 & 0 & 0 & 0 & 0 & 0 & -15 & 0 & & & & \\
0 & 0 & 0 & 0 & 0 & 0 & -15 & 15 & 0 & & & \\
30 & 0 & 0 & -30 & -15 & 0 & -30 & 0 & 15 & 30 & & \\
0 & 0 & 0 & -15 & 0 & 0 & 0 & 0 & 0 & 15 & 0 & \\
0 & 0 & 0 & 0 & 0 & 0 & 15 & 0 & 0 & -15 & -15 & 0
\end{bmatrix}$$

$$K_4 = \begin{bmatrix}
84 & & & & & & & & & & & \\
-6 & 8 & & & & & & & & & & \\
6 & 0 & 8 & & & & & & & & & \\
-84 & 6 & -6 & 84 & & & & & & & & \\
-6 & -2 & 0 & 6 & 8 & & & & & & & \\
-6 & 0 & -8 & 6 & 0 & 8 & & & & & & \\
-84 & 6 & -6 & 84 & 6 & 6 & 84 & & & & & \\
6 & -8 & 0 & -6 & 2 & 0 & -6 & 8 & & & & \\
6 & 0 & -2 & -6 & 0 & 2 & -6 & 0 & 8 & & & \\
84 & -6 & 6 & -84 & -6 & -6 & -84 & 6 & 6 & 84 & & \\
6 & 2 & 0 & -6 & -8 & 0 & -6 & -2 & 0 & 6 & 8 & \\
-6 & 0 & 2 & 6 & 0 & -2 & 6 & 0 & -8 & -6 & 0 & 8
\end{bmatrix}$$

$$L = \begin{bmatrix} l & 0 & 0 & 0 \\ 0 & l & 0 & 0 \\ 0 & 0 & l & 0 \\ 0 & 0 & 0 & l \end{bmatrix} \quad \text{where} \quad l = \begin{bmatrix} 1 & 0 & 0 \\ 0 & 2b & 0 \\ 0 & 0 & 2a \end{bmatrix}$$

where the dimension of the rectangular plate are $2a \times 2b$ along x and y directions respectively and t is the thickness of the plate (Figure 7.5).

7.A.2 Stress Matrix

Stress matrix for rectangular orthotropic plate element ($p = \frac{a}{b}$):

$$
\begin{Bmatrix} M_i \\ M_j \\ M_k \\ M_l \end{Bmatrix} = \{\sigma\} = \frac{1}{4ab}
\begin{bmatrix}
6p^{-1}D_x + 6pD_1 & -8aD_1 & 8bD_x & -6pD_1 & -4aD_1 & 0 & -6p^{-1}D_x & 0 & 4bD_x & 0 & 0 & 0 \\
6pD_y + 6p^{-1}D_1 & -8aD_y & 8bD_1 & -6pD_y & -4aD_y & 0 & -6p^{-1}D_1 & 0 & 4bD_1 & 0 & 0 & 0 \\
-2D_{xy} & 4bD_{xy} & -4aD_{xy} & 2D_{xy} & 0 & 4aD_{xy} & 2D_{xy} & -4bD_{xy} & 0 & -2D_{xy} & 0 & 0 \\
-6pD_1 & 4aD_1 & 0 & 6p^{-1}D_x + 6pD_1 & 8aD_1 & 8bD_x & 0 & 0 & 0 & -6p^{-1}D_x & 0 & 4bD_x \\
-6pD_y & 4aD_y & 0 & 6pD_y + 6p^{-1}D_1 & 8aD_y & 8bD_1 & 0 & 0 & 0 & -6p^{-1}D_1 & 0 & 4bD_1 \\
-2D_{xy} & 0 & -4aD_{xy} & 2D_{xy} & 4bD_{xy} & 4aD_{xy} & 2D_{xy} & 0 & 0 & -2D_{xy} & -4bD_{xy} & 0 \\
-6p^{-1}D_x & 0 & -4bD_x & 0 & 0 & 0 & 6p^{-1}D_x + 6pD_1 & -8aD_1 & -8bD_x & -6pD_1 & -4aD_1 & 0 \\
-6p^{-1}D_1 & 0 & -4bD_1 & 0 & 0 & 0 & 6pD_y + 6p^{-1}D_1 & -8aD_y & -8bD_1 & -6pD_y & -4aD_y & 0 \\
-2D_{xy} & 4bD_{xy} & 0 & 2D_{xy} & 0 & 0 & 2D_{xy} & -4bD_{xy} & -4aD_{xy} & -2D_y & 0 & 4aD_{xy} \\
0 & 0 & 0 & -6p^{-1}D_x & 0 & -4bD_x & -6pD_1 & 4aD_1 & 0 & 6p^{-1}D_x + 6pD_1 & 8aD_1 & -8bD_x \\
0 & 0 & 0 & -6p^{-1}D_1 & 0 & -4bD_1 & -6pD_y & 4aD_y & 0 & 6pD_y + 6p^{-1}D_1 & 8aD_y & -8bD_1 \\
-2D_{xy} & 0 & 0 & 2D_{xy} & 4bD_{xy} & 0 & 2D_{xy} & 0 & -4aD_{xy} & -2D_{xy} & -4bD_{xy} & 4aD_{xy}
\end{bmatrix}
\begin{Bmatrix} \delta_i \\ \delta_j \\ \delta_k \\ \delta_l \end{Bmatrix}
$$

7.A.3 Load Matrix

Load matrix for a rectangular element orthotropic (Figure 7.5) under uniform load p_o:

$$\begin{Bmatrix} F_i \\ F_i \\ F_k \\ F_t \end{Bmatrix} = 4p_o ab \begin{Bmatrix} 1/4 \\ -b/12 \\ a/12 \\ 1/4 \\ b/12 \\ a/12 \\ 1/4 \\ -b/12 \\ -a/12 \\ 1/4 \\ b/12 \\ -a/12 \end{Bmatrix}, \quad \{F_i\} = \begin{Bmatrix} F_{wi} \\ F_{\theta xi} \\ F_{\theta yi} \end{Bmatrix}$$

8

Parameters and Criteria for Foundation Design

8.1 Introduction

The foundation, being an important interface between the superstructure and the soil, has to safely transfer the large loads and moments coming from the superstructure to the soil at site. While the superstructure loads depend on the needs of the project, the soil capacities are limited to its natural properties at site though minor manipulations are possible using suitable but expensive ground improvement methods. Thus the foundation design needs a very judicial selection of parameters and design methods and acceptability criteria. Some of these aspects are discussed in this chapter while the specific considerations for shallow foundations and pile foundations are presented in Chapters 4–7 and 9–12.

8.2 Design Considerations

There are many aspects to be considered for a proper design of foundations, as outlined in Chapters 1–3, besides the specific requirements of the particular type of foundation being designed, as discussed in subsequent chapters. These are broadly classified as follows:

1. Requirements of the project and choice of superstructures.
2. Loads and moments coming from the superstructures.
3. Selection of suitable site.
4. Soil properties at the chosen site.
5. Bearing capacity, settlement and compressibility, stress distribution and lateral pressure where necessary.
6. Choice of the foundations based on items 2, 4, and 5, as follows:
   a. Shallow foundations; spread footings, combined footings, strip footings, mat/raft foundations.
   b. Deep foundations; piles and pile groups, piers (including large diameter piers), well foundations, that is, caissons, pile–raft systems and others.

Foundation Design: Theory and Practice N. S. V. Kameswara Rao
 ISBN: 978-0-470-82534-1

c. Foundations subjected to vibratory/dynamic loads. In addition to the normal requirement for static loads, additional criteria regarding resonance, dynamic amplitudes, additional pressures/loads at interfaces, natural frequency, noise due to vibration and so on, have to be considered for these foundations. These are discussed in Chapter 11.

7. Geotechnical aspects for the design of the selected type of foundations, that is, guided by items 2, 4, 5, 6 as per codes and practices.
8. Structural design of the foundation based on items 6 and 7 as per standard codes and practices.
9. Criteria for assessment as per codes, practices and assessment of the structure designed with respect to criteria based on item 8.
10. Acceptability of the design if the foundation designed satisfies the criteria specified based on item 8.
11. If the foundation does not satisfy the specified criteria, it has to be redesigned or the soil properties have to be improved to meet the requirements until the soil and foundation requirements are acceptable with specified factors of safety.

The items mentioned in 7, 8 and 9 are presented in the following sections while most of the other aspects are described in the respective chapters of this book.

8.3 Codes, Practices and Standards

All designs, whether foundations, soils or structures, have to meet prescribed codes, practices and standards. These are developed as per national, provincial, city and local requirements and have to be complied with for acceptable design and construction practices. Since these are country-specific, only a few of the most commonly adopted criteria for the design of foundations are described below.

8.4 Design Soil Pressure

For any foundation design, one of the basic parameters to be computed is the design soil pressure, that is, the safe pressure that can be borne by the soil when the foundations transmit the superstructure loads to the soil below. This depends on many foundation factors, such as shape, size, depth and type, as described in Chapter 3. Even the parameters for design depend on the method of analysis, that is, conventional or rational methods, as presented in Chapter 4. While the specific requirements have to be closely studied, broadly the design soil pressure can be obtained using either the bearing capacity criterion or settlement/differential settlement criterion. Settlements to be considered are the long term consolidation settlements and bearing capacity relates to shear/or punching shear failure, as discussed in Chapter 3.

The design pressure also depends on breadth of the foundation, as explained in Section 3.1 (Figure 3.2). Thus, the design pressure is the lower of the allowable/safe bearing capacity (SBC) value or punching shear (based on shear failure with factor of safety of 3) and the allowable soil pressure (ASP) based on allowable maximum settlement or differential settlement (based on consolidation theory), as per prescribed criteria. The details of evaluation of these values are discussed in Chapters 2 and 3. The following sections present some more details to provide clarity for the determination of these values.

8.5 Gross and Net Values of the Safe Bearing Capacity and Allowable Soil Pressure

It needs to be noted that Terzaghi's ultimate bearing capacity equations are developed based on gross soil pressure, ($q_{ult} = q_u$) which includes all loads above the foundation level. Thus it is the gross pressure that can be considered by the foundation including the overburden pressure and is based on shear strength of the soil at the foundation level.

However, the settlements are caused only by net increase of effective pressure over the existing overburden pressure. Thus, the ASP is based on net pressure and is based on consolidation settlement/differential settlement considerations.

8.6 Presumptive Bearing Capacity

These are the design soil pressure values recommended by various national or local building codes and standards. These are somewhat arbitrary and are termed presumptive because it is presumed that the soil can support the load safely without shear failure or undue total/differential settlements. These can be used only as a helpful guide for preliminary design of foundations and should be supplemented and verified by laboratory tests, field tests and analysis. Some typical values are given in Tables 8.1 and 8.2 (IS: 1904–1966, 1966; Ramiah and Chickanagappa, 1981; Bowles, 1996).

Table 8.1 Typical values of safe bearing capacity.

Cohesionless soils		Cohesive soils	
Description	Safe bearing capacity (t/m^2)	Description	Safe bearing capacity (t/m^2)
1. Gravel, sand and gravel, compact and offering high resistance penetration when excavated by tools	45	1. Soft shale, hard or stiff clay in deep bed, dry	45
2. Coarse sand, compact and dry	45	2. Medium clay readily indented with a thumb nail	25
3. Medium sand, compact and dry	25	3. Moist clay and sand clay mixture which can be indented with strong thumb pressure	15
4. Fine sand, silt (dry lumps easily pulverized by the fingers)	15	4. Soft clay indented with moderate thumb pressure	10
5. Loose gravel or sand gravel mixture; loose coarse to medium sand and dry	25	5. Very soft clay which can be penetrated several inches with the thumb	5
6. Fine sand, loose and dry	10	6. Black cotton soil or other shrinkage or expansive clay in dry condition (50% saturation)	15

(Reproduced from B.K. Ramiah and L.S. Chickanagappa, *Soil Mechanics and Foundation Engineering*, p. 394 (Table 4.12), Oxford and IBH Publishing Co., New Delhi, India. © 1981.)

Table 8.2 Summary of presumptive/safe bearing capacities from some building codes (in kN/m^2).

Soil description	Chicago, 1995	National Board of Fire Underwriters, 1976	BOCA 1993[a]	Uniform Building Code, 1991
Clay, soft	75	100	100	100
Clay, medium stiff	175	100	—	100
Clay, stiff	210	—	140	—
Sand, compact and clean	240	140–400	140	200
Sand, compact and silty	100	140–400	—	—
Inorganic silt compact	125	140–400	—	—
Sand, loose and fine	—	140–400	140	210
Sand, loose and coarse, or sand–gravel mixture, or compact and fine	—	140–400	240	300
Gravel, loose and compact coarse sand	300	140–400	240	300
Sand–gravel, compact	—	140–400	240	300

[a]Building Officials and Code Administrators International, Inc.

8.6.1 *Design Loads and Factors of Safety*

While a factor of safety of 3 is used for safe bearing capacity with respect to all dead loads, the following factors of safety (Table 8.3) for various combinations of dead and live loads may be used (Ramiah and Chickanagappa, 1981; Bowles, 1996).

Table 8.3 Design loads and factors of safety.

Design load	Factor of safety for safe bearing capacity
$K_D DL + K_L.LL + K_W.WL + K_S.SL + HL$	3
$K_D.DL + K_L.LL + K_W.WL + HL$	2
$K_D.DL + K_L.LL + K_E E + K_S S$	2

where K_D, L_L, K_W, K_S, K_E are reduction factors specified by codes for particular combination of loads, and DL = dead load, LL = live load, WL = wind load, SL = Snow load, HL = Hydrostatic load, E = earthquake load.

However, the designers should be aware of the factor of safety adopted in foundation design and provisions of codes of practice and standards.

8.7 Settlements and Differential Settlements

The total settlement of a structure consists of three components as given in Equation (3.47) (Section 3.7), that is

$$S = S_i + S_c + S_s$$

where

S_i = immediate/elastic settlement
S_c = settlement due to primary consolidation
S_s = settlement due to secondary consolidation

Out of these, usually the consolidation (primary) settlement S_c is the most important part of the total settlement as discussed in Section 3.7. Though there may not be a collapse or shear failure of the soil due to large settlement, the structures and foundations may become unserviceable. Further tilting and cracking of beams and slabs may occur due to differential settlements. These are shown in Figure 8.1. If the foundation of structure settles uniformly as shown in Figure 8.1(a), there may not be any structural damage. However, if one part settles differentially with respect to other parts of the foundation, as shown in Figures 8.1(b) and (c), then the structure undergoes distortion and the connecting beams, slabs and interfaces may crack and the floors may become unusable. For example a building with rigid components undergoes a uniform settlement (Figure 8.1(a)). Figure 8.1(b) shows a uniform tilt, where the entire structure rotates. Figure 8.1(c) shows a common situation of non-uniform settlement, namely *dishing*. Non-uniform settlement results from: 1. uniform stress acting upon a homogeneous soil, or 2. non-uniform bearing stress, or 3. nonhomogeneous subsoil conditions. As shown in Figure 8.1 the differential settlement Δs between two points is the larger settlement minus the smaller one. Differential settlement is also characterized by angular distortion $\frac{\delta}{L}$ which is the differential settlement between two points divided by the horizontal distance between them and may be referred to as a ratio.

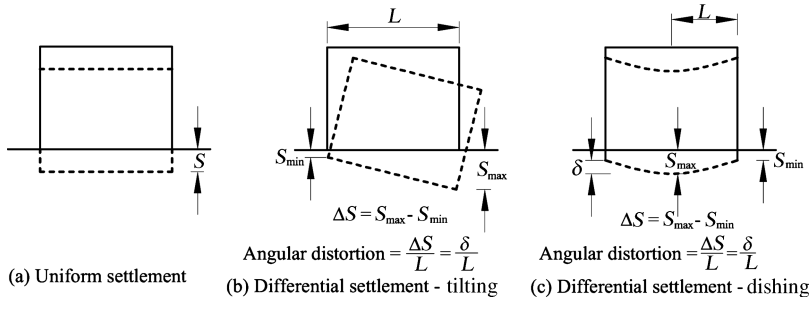

Figure 8.1 Settlement and differential settlement.

The amount of settlement a structure can withstand is called the allowable settlement or permissible settlement. This depends on many factors, including the type, size, location and intended use of the structure and the pattern, rate, cause and source of settlement. Tables 8.4 and 8.5 give typical values of allowable settlements and differential settlements.

8.7.1 Total Settlement

Generally the amount of total settlement is not a problem of concern. But it is primarily a question of serviceability. However, there are situations where large total settlements can cause

Table 8.4 Permissible settlement as per Indian Standards.

Criterion	Permissible settlement (cm)
Angular distortion: office buildings, flats and factories	Differential settlement (as a ratio) should not exceed 1/500–1/1000
Maximum differential settlement:	
Clays	4.0
Sands	2.5
Maximum total settlement:	
Isolated footings on clay	6.5
Isolated footings on sand	4.0
Raft foundations on clay	6.5–10.0
Raft foundation on sand	4–6.5

(Reproduced from B.K. Ramiah and L.S. Chickanagappa, *Soil Mechanics and Foundation Engineering*, p. 406 (Table 4.27), Oxford and IBH Publishing Co., New Delhi, India. © 1981.)

serious problems, for example, a tank on soft clay near a waterfront can settle below the water level. The allowable total settlements are given in several building codes and the values specified by IS: 1904–1966 are illustrated in Table 8.4. The table also gives a range of values for permissible differential settlement.

8.7.2 *Differential Settlement*

It is usually the differential settlement (rather than the total settlement) that is important in the designing of a foundation as the consequences of differential settlement are more detrimental. The magnitude of differential settlement is affected greatly by the nonhomogeneity of natural soils and also by the ability of foundation to bridge over soft soil. Theoretical settlement should be computed for various points in a structure, such as center, corner, lightest and heaviest column locations, in order to compute differential settlement. The allowable angular distortions in buildings have been given in several codes and research reports (Ramiah and Chickanagappa, 1981; Bowles, 1996; Das, 2007). Some useful values given by Skempton (1956) are presented in Table 8.5.

Table 8.5 Permissible maximum total and differential settlements of buildings (in cms).

Criterion	Isolated foundations	Rafts
Angular distortion		1/300
Greatest differential settlement (cm)		
Clays		4.44 (3.81)
Sands		3.17 (2.54)
Maximum settlement (cm)		
Clays	7.5 (6.35)	7.5–12.5 (6.35–10.0)
Sands	5.0 (3.81)	5.0–7.5 (3.81–6.35)

Note: The values in parenthesis take into account a safety factor of 1.25.
(A.W. Skempton and D.H. MacDonald, "The allowable settlements of buildings," *Proceedings of the Institution of Civil Engineers*, London, part III, vol. **5**, pp. 759–760, © 1956, with permission from The Institution of Civil Engineers (ICE), Thomas Telford Ltd.)

8.8 Cracks Due to Uneven Settlement

Uneven settlement creates cracks in connecting structural components such as beams and slabs. Even connecting walls and slabs develop cracks due to these uneven settlements. The cracks usually develop in the diagonal direction though vertical cracks are also possible. They may start from top if one end of the wall settles more than the next, as shown in Figures 8.2(a) and (b). If the middle part of the wall settles more than the ends, then cracks may start from the bottom, as shown in Figure 8.2(c). The cracks developed in walls due to differential settlement in nonhomogeneous soils are shown in Figure 8.3. The cracks in walls developed by causes other than settlements such as shrinkage are usually irregular or may terminate before reaching the edges of the wall, as shown in Figure 8.4.

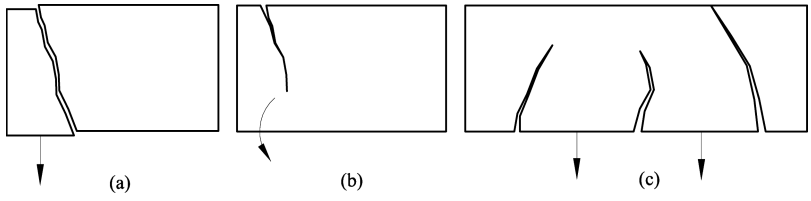

Figure 8.2 Sketches showing the nature of differential settlement and cracks.

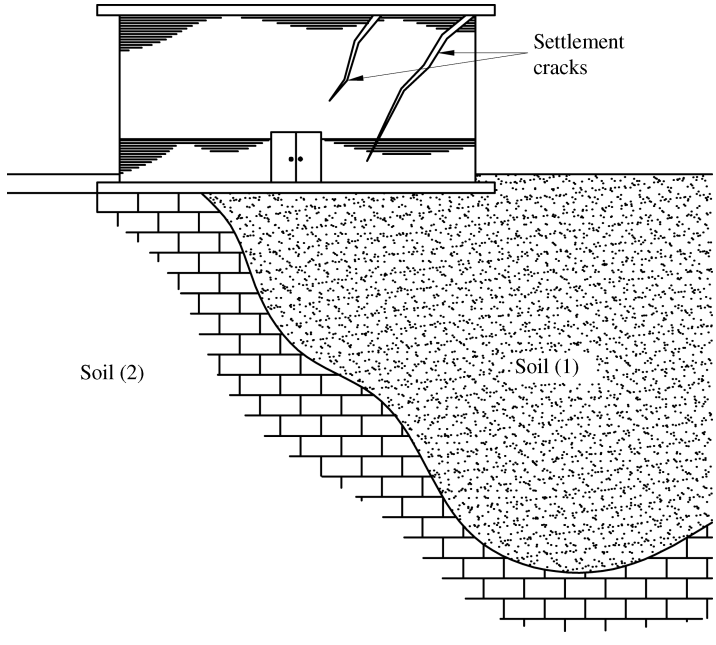

Figure 8.3 Differential settlement due to nonhomogeneous soils.

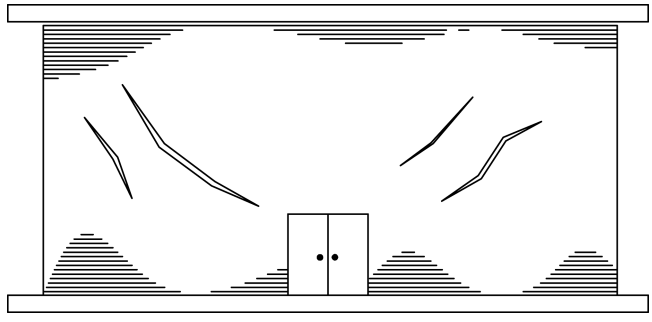

Figure 8.4 Sketch showing wall cracks not caused by foundation settlement.

8.9 Suggestions to Reduce Large Differential Settlements

As pointed out in the above section, large differential settlements are more detrimental than the individual settlement to structures and foundations. To safeguard against large differential settlements, the following alternatives in design could be helpful

1. Use a raft foundation with or without stiffening beams in one or more directions.
2. Reduce the net pressure transmitted to the soil by providing deep basements.
3. Use piles, piers or basement slab foundations, pile–raft systems to transfer large loads from the superstructure to strong deeper soils with low compressibility.
4. Provide jacking pockets or brackets in columns to relevel the alignment of the superstructure when necessary.
5. Provide additional loads on lightly loaded parts of the structure if feasible.

9

Deep Foundations – Piles, Drilled Piers, Caissons and Pile-Raft Systems

9.1 Introduction

Deep foundations are those where $\frac{D_f}{B} > 1$, usually greater than 3–4 (where D_f and B are the depth and width of the foundations as shown in Figure 3.6). These are needed when the soil at shallow depths is unable to support the loads being transferred by foundations or the low strength of soils need very large-sized shallow foundations which become uneconomical and unviable. Accordingly, deep foundations have to be adopted to transfer the loads to deeper soil strata capable of supporting such large loads coming from the superstructure. The bearing capacity for such deep foundation can be determined by including the shear strength of the soil all along the boundary of the failure zone, as explained in Section 3.3.

The most commonly used deep foundations are piles and pile groups. Others include piers, well foundations, caissons (which are used to resist very large loads coming from superstructures such as bridges), heavy industrial and offshore structures. Occasionally, pile-raft systems are also used to support large loads of multistoried buildings. A pile is a relatively slender member made of timber, concrete, steel or composite material usually either driven into the soil or placed/bored into the soil to provide vertical or lateral support or for other engineering functions. A caisson or a well foundation is a hollow box type structure which is sunk slowly into the soil with or without water and gets integrated with the superstructure subsequently. Pile-raft systems are foundations consisting of piles connected by a raft and can effectively control differential settlements (Section 8.9). In such systems the load is expected to be shared primarily by piles and partly by the raft. The important details of these deep foundations are presented in the following sections, while the specific details including the design of piles and pile groups are discussed in Chapter 10.

Foundation Design: Theory and Practice N. S. V. Kameswara Rao
 ISBN: 978-0-470-82534-1

9.2 Piles

Piles made of the following material are used in constructions. The different types of piles, their advantages, disadvantages and composition/applications are summarized in Table 9.1

Table 9.1 Common piles and their applications.

Type of pile	Advantages	Disadvantages	Applications
Timber (plain and treated)	Low cost per unit length of pile	Small bearing capacity	Foundations with moderate load
	Timber is resilient and suitable for absorption of impact load	Untreated piles above ground water may last more than 25 years but are not permanent	Protection of waterfront structures from damage by floating objects
		Prone to damage by hard driving	Timber trestles and bents
			Foundations for temporary structures
Precast concrete (normal and prestressed, pipe piles)	Fairly large bearing capacity	Must be reinforced to withstand handling stresses	Trestles and bridge bents
	Permanent foundations	Requires space for casting and storage	Waterfront structures (docks, piers, bulkheads, etc.)
	Can be treated for sea water installation and corrosion	Takes time to set and cure before installation	Foundations for bridges
		Requires heavy equipment for handling and transportation	Prestressed piles if large bearing capacity is needed
		Incurs large cost in cutting off extra lengths or adding more lengths	
Cast *in situ* concrete (with or without curing, under-reamed piles, pedestal piles)	Large bearing capacity	Difficult to ensure the uniformity of underground concreting	Foundations for buildings, bridges and so on, of moderate to heavy loads
	Permanent foundations		
	Can be treated for corrosion and installation		
	Easy to alter pile lengths		

Table 9.1 (*Continued*)

	Damage due to handling or driving can be eliminated May be installed by pre-excavation, thus eliminating vibration due to driving		
Composite	Relatively low cost, permanent foundations	Small bearing capacity	Foundations for buildings, bridges, and so on, of moderate loads where the upper part of the piles are above ground water
		Joints between two parts constitute a weak point, prone to damage due to driving	
Steel (pipe piles as well as other cross sections such as H shape)	Large bearing capacity	Possibility of damage from corrosion and electrolysis	For large structures and heavy loads
	Can penetrate through stiff layer or boulders	Expensive unless the bearing stratum can develop large pile capacity	Trestles and bridge bents
	Small volume displacement of soil Can stand rough handling	Less effective as friction piles or compaction piles	

9.2.1 Timber Piles/Plain Timber Piles

Piles of timber treated with preservatives are used mostly for short-term requirements and can not carry large loads like temporary supports and so on. These are to be driven at site and the load carrying capacity is limited to the compressive strength of the wood. Accordingly

$$Q_{\text{all}} = A_p f_w \tag{9.1}$$

where

Q_{all} = allowable pile load based on strength of the wooden pile/structure
A_p = area of cross-section of pile
f_w = allowable compressive strength of wood

However Q_{all} should be also determined based on soil properties and the lower of the two values should be used for design.

9.2.2 *Concrete Piles*

These are of two types, that is, precast piles and cast *in situ* piles.

1. **Precast piles:** These are reinforced concrete piles and are transported to the site after casting at the yard. They may also be cast at site depending on convenience and costs. They are usually of square, octagonal or circular shapes with uniform cross-section, as shown in Figure 9.1. If required they may also be tapered along length. Pipe or hollow piles may also be used for economy of material as well as improving the load carrying capacity, though they are more common in steel piles (Figure 9.2). Usually a conical end section is provided for the pile which is also called a shoe (Figure 9.2(a)). Sometimes, a flat base is also used, depending on the method of pile installation (Figure 9.2(b)).

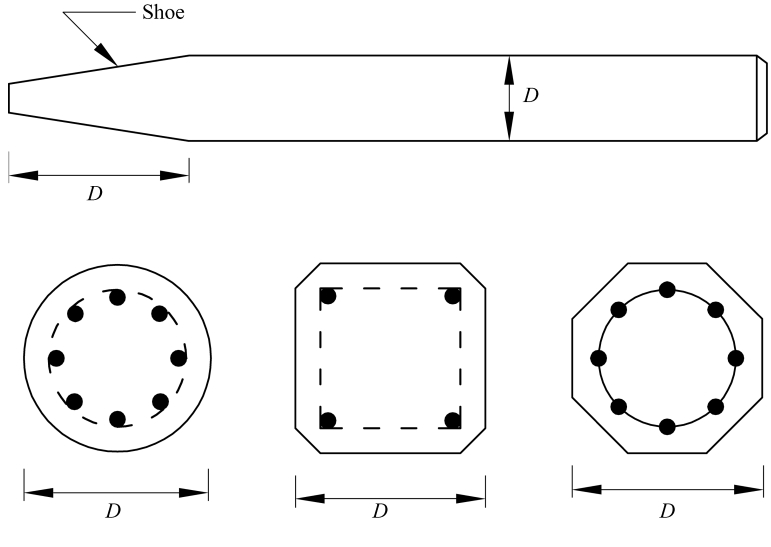

Figure 9.1 Precast concrete piles with reinforcement.

2. **Cast *in situ* piles:** These are also called bored piles. These are constructed by boring a hole in the soil and then casting the concrete *in situ* usually with reinforcement. These are widely used and provided by several organizations. They can be cased (shell type), uncased,

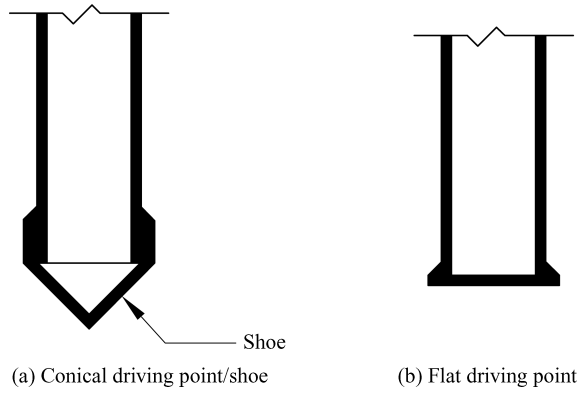

Figure 9.2 Pipe pile.

under-reamed and pedestal type of piles. Generally a bore hole is drilled while advancing the steel casing to protect the soil from caving in. Then the drill is withdrawn, the reinforcement is lowered into the bored hole and concrete is cast in place. If the casing is left in place, it is called a cased pile. If the casing is withdrawn gradually while concreting is done, it is called an uncased pile.

Sometimes to take care of uplift pressures and swelling pressures in expansive soils, the bulb type enlargement is made either by cutting or scooping the soil out at one or two locations along the depth of the pile. These are called under-reamed piles (Figures 9.3(a) and (b)). If the enlargement is made at the base of the pile, it is called a pedestal pile (Figure 9.3(c)). These piles

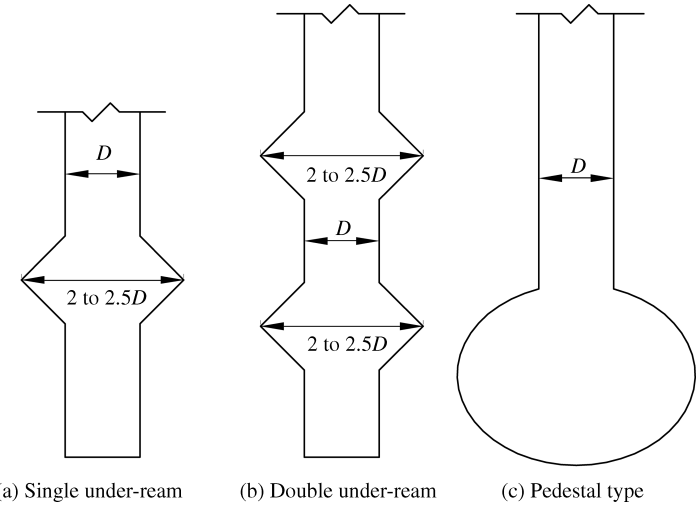

Figure 9.3 Under-reamed and pedestal type of piles.

can be tapered or of uniform cross section. Tapered piles are preferred for frictional resistance (friction piles) and for compaction of soil strata (compaction piles).

9.2.3 Composite Piles

Such piles are made by combining two portions of the pile, each of a different material, that is, timber, steel and concrete. These are used in cases where the required length of piles is greater than that available for the bored piles. It is difficult to form proper joints between the two portions of the piles. Also the capacity of the piles may be limited to the capacity of the weaker portion of the pile. Hence they are rarely used.

9.2.4 Steel Piles

A steel pile may be a rolled section, such as an H-shape or a fabricated shape (such as a box) or a flat sheet. The length of such piles can be extended as per requirement by jointing/welding additional length of pile. H-shaped steel piles are commonly used. Pipe piles (also called hollow piles) are also used in constructions which have the advantage of low material and higher capacity. They can be of large diameters and lengths. Hollow piles of larger capacities (of the order of 10 000 kN) are being used as foundations for bridge, piers and so on. Piles are made of seamless or welded pipes and can be driven close ended or open ended. The hollow portion may be filled with concrete or soil if necessary. Pipe piles can be driven to larger depths either by drop hammers or by static pressure.

9.3 Functions of Piles

Depending on their applications, piles may be broadly categorized as:

1. Point bearing piles
2. Friction piles
3. Piles to resist uplift forces
4. Anchor piles
5. Compaction piles
6. Fender piles
7. Dolphins and others.

Among these, analyses for load carrying functions are considered primarily for discussion in this chapter.

9.4 Design of Pile Foundations

The design of pile foundations can be done as per following steps:

1. Calculate the total load acting on the pile. The loads to be used for bearing capacity analysis and the loads for the settlement analysis have to be identified.

2. Sketch the soil profile and the soil properties up to a depth beyond the expected maximum length of piles. Locate the ground water level in the sketch.
3. Determine the type and length of the pile with alternatives.
4. Evaluate the pile capacity.
5. Establish the number and spacing of piles based on the pile capacity and loads to be supported. Establish the pile group and the number of piles in each group and size of the pile cap.
6. Check the stresses transmitted to lower strata, particularly if there is a weak layer of soil below the bottom of the piles.
7. Carry out the structural design of piles and pile cap.
8. Carry out settlement analysis of the pile group.
9. Check for uplift pressure and lateral load capacity of each pile group.
10. Plan for proper pile load tests for verifying the computed values.

The details of loads (vertical and lateral) on piles and design are presented in detail in Chapter 10. The input for the pile design such as length, diameter and pile capacity determination, settlement analysis and so on are discussed in the following sections.

9.5 Type and Length of Piles

The selection of type, length and capacity of piles depend on the soil condition at site and the load to be supported. Usually the people in the execution of piling projects have a better idea because of their experience. The preliminary selection is based on estimates. However, pile load tests have to be conducted to verify and confirm the estimated values before the actual construction begins. Otherwise these values have to be revised for design. Following guidelines may be helpful in selecting the type and length of the piles.

1. **Point/End Bearing Piles:** If pile resists/supports the superstructure loads through the bearing capacity at its base (or point), they are called point/end bearing piles. Such piles are used if the base is resting on a strong soil or bedrock and soil in between may be selectively loose. Thus the length of the piles depends on depth of the soil stratum where the pile base/point rests. The determination of the bearing capacity is discussed in the next section.
2. **Friction and Adhesion Piles:** If the pile resistance to superstructure load is through friction and adhesion developed along the shaft surface in contact with the surrounding soil, then, the piles are called friction piles. Such piles are used where there is no hard stratum of soil at reasonable depth for founding the pile point to get the advantage of point bearing capacity. The length needed of such piles can be computed based on soil properties and the magnitude of the loads to be supported. These aspects are discussed in the following section.
3. **Combined Point Bearing and Friction Piles:** These piles may resist/support the superstructure loads partly by end/point bearing capacity and partly by friction and adhesion developed along its shaft.
4. **Compaction Piles:** If piles are used to compact granular soils near the ground surface and improve the relative density, they are called compaction piles. These are also termed as granular piles (sand piles), stone columns, micro piles (concrete piles) and are of shorter

length. Such piles are used for general ground improvement of soft granular soils up to shallow depths as compaction may be needed only up to the required depth.

5. **Other Piles:** Piles are also used as anchor piles, fender piles, dolphins and other purposes based on their application. The design of such piles is based on requirements and special practices.

9.6 Pile Load Capacity

As mentioned earlier, the load carrying capacity of piles is governed both by its structural strength and the supporting soil properties. Obviously, the smaller of the two values should be used for the design. Usually, the pile capacity based on soil properties governs the design except probably in timber piles. However, the methods for determination of these values are similar in all these types of piles. The capacity of piles based on structural strength can be obtained by multiplying the area of pile cross section with the allowable compressive strength of the material of the pile as given for timber pile in Equation (9.1). The pile capacity determination based on soil properties is done using: (a) dynamic pile driving formula, (b) static methods, (c) correlation with field penetration tests such as SPT and CPT and (d) prototype pile load tests at site.

9.6.1 Dynamic Pile Driving Formulae and Wave Equation

These formulae have been developed for driven piles (precast type) using dynamic principles. A drop/falling hammer is used to drive the pile to the desired depth or until refusal. It is assumed that the kinetic energy of the hammer falling from a height is used partly to drive the pile into the soil and partly as a loss due to damping and so on. Using the dynamic penetration of the pile, several empirical formulae have been developed by various professional bodies and manufacturers (Teng, 1964; Ramiah and Chickanagappa, 1981; Bowles, 1996; Das, 2007). The simplest of such formula is the Engineering News Record (ENR) formula as expressed below

$$R = \frac{2E}{S + C} \tag{9.2}$$

where

R = resistance of soil, in pounds
S = pile penetration per blow, in inches
E = driving energy = weight × stroke of the hammer, in foot-pound force (for drop hammers or single action hammers)
C = empirical constant = 0.1 for steam hammers and 1.0 for drop hammers.

The above formula is obtained using a factor of safety = 6.

Similarly there are other formulae that are also used for driven piles such as Pacific Coast Uniform Building Code formula, Janbu's formula, Danish formula, AASHTO formula, Hiley's formula, Indian National Building Code formula and many others.

Since most of these formulae are empirical and involve several parameters which are difficult to quantify, the evaluation of pile capacity may have a large range of variation. Thus their utility may be limited.

9.6.2 *Static Method*

These methods are developed for piles and deep foundations using the soil properties in which they are founded. They assume equilibrium of the pile under the applied loads and resistance offered by the soil in terms of point bearing capacity and the friction and adhesion of the shaft. A single pile subjected to a vertical load and the mechanism of load transfer to the soil is shown in Figure 9.4. Thus the load is transferred to the soil partly as point bearing pressure at its base and partly as friction and adhesion along the surface of the shaft. Hence the ultimate load carrying capacity of the pile can be obtained from its static equilibrium equation as

$$\begin{aligned} Q_u &= Q_p + Q_{af} \\ &= A_p q_p + A_s S_{af} \end{aligned} \tag{9.3}$$

where

Q_u = ultimate load capacity of the pile
Q_p = point/end bearing capacity
A_p = area of the pile tip
q_p = unit point bearing capacity of the pile
Q_{af} = resistance due to adhesion and friction along the shaft of pile
A_s = surface area of the shaft of embedded length of pile in soil

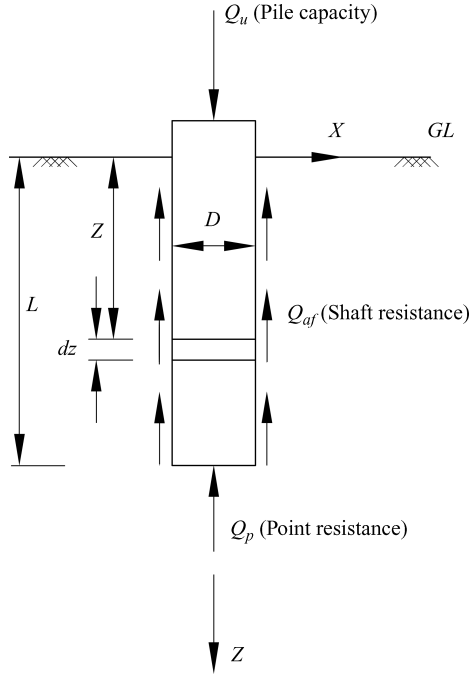

Figure 9.4 Pile capacity.

S_{af} = average unit shaft resistance due to adhesion and friction over the entire depth (A_s and S_{af} refer to only that portion of the pile embedded in soil contributing to shaft resistance.)

q_p can be obtained using Terzaghi's or Meyerhof's bearing capacity theory (for deep foundation) as explained in Section 3.3.

Using Terzaghi's theory for simplicity, q_p is given as

$$\begin{aligned} q_p &= 1.3cN_c + qN_q + 0.3\gamma DN_\gamma \quad \text{(circular footing of diameter } D\text{)} \\ q_p &= 1.3cN_c + qN_q + 0.4\gamma BN_\gamma \quad \text{(square footing of width } B\text{)} \end{aligned} \tag{9.4}$$

where

N_c, N_q, N_γ = Terzaghi's bearing capacity factors
q = surcharge load/overburden at the base of the pile
$= \gamma L + q_o$
γ = unit weight of soil
L = length of the pile embedded in soil
q_o = surcharge load on the surface (if any)
D = diameter for circular pile
B = width for square pile
c = cohesion/adhesion of soil
φ = angle of internal friction of soil

For piles of other shapes, the general bearing capacity equation (Equation (3.17)) can be used. Q_{af} can be estimated using the principles of mechanics and lateral earth pressure distribution along the embedded length of the shaft. Accordingly

$$Q_{af} = \sum \Delta z\, a_s s_{at} = \int_o^L a_s s_{af}\, dz \tag{9.5}$$

where

Δz = increment of length of pile shaft at any depth z
a_s = perimeter of pile shaft surface at depth $z = \pi d$
d = diameter of the pile at depth z
s_{af} = shear strength of soil at depth z, that is, unit resistance of the shaft due to adhesion/cohesion and friction

$$\begin{aligned} &= c + \sigma_n \tan\delta \\ &= c + K_o(\gamma z + q_o)\tan\delta \end{aligned}$$

where

δ = angle of friction between the soil and pile shaft
σ_n = normal stress to the surface of shaft at depth z (horizontal stress at depth $z = K_o(\gamma z + q_o)$)
γz = vertical overburden stress at depth z
K_o = lateral earth pressure coefficient as discussed in Section 3.8. This is usually taken as coefficient of earth pressure at rest.
q_o = surcharge pressure on the surface of the soil (if any)

In Equation (9.5), the summation sign ($\sum$) can be used for piles in layered soils and integration can be used for soils with uniform or continuously varying properties.

For a concrete pile of uniform diameter D (i.e., $d = D$), embedded in soil up to a length L, the shaft friction can be obtained by integration as

$$Q_{af} = \int_0^L \pi D \Delta z s_{af} = \int_0^L \pi D(c + \sigma_n \tan\delta) dz \tag{9.6}$$

Hence

$$\begin{aligned} Q_{af} &= \pi D \int_0^L \{(c + K_o(\gamma z + q_o)\} \tan\delta) dz \\ &= \pi D L \left[c + K_o \left(\frac{\gamma L}{2} + q_o \right) \tan\delta \right] = A_s(c + K_o \bar{q} \tan\delta) \end{aligned} \tag{9.7}$$

where

c = average cohesion of the soil in which the pile is embedded.
$\bar{q}$ = effective average (at mid height) vertical stress
that is, at mid height of the soil layer.

If $q_o = 0$, Equation (9.7) becomes

$$Q_{af} = A_s \left[c + K_o \frac{\gamma L}{2} \tan\delta \right] = A_s(c + K_o \overline{q} \tan\delta) \tag{9.8}$$

$$= A_s(S_{af})_{\text{average}} \tag{9.9}$$

From Equation (9.8) it may be noted that $(S_{af})_{\text{at z = L/2}}$ is the average shear strength corresponding to the soil at the mid depth of the embedded pile length L, if the soil is uniform and the pile is of uniform diameter. For layered soils with and without ground water, tapered piles and piles of other shapes, Q_{af} can be obtained by simple piecewise integration of Equation (9.5).

Equations (9.7) and (9.8) can also be written for layered soils (say n layers) with different soil characteristics as

$$Q_{af} = \sum_{i=1}^{n} Q_{af\ i} = \sum_{i=1}^{n} \pi D_i (L_i c_i + K_{oi} \bar{q}_i L_i \tan\delta_i) \tag{9.10}$$

where n is the total number of soil layers up to which the pile is embedded and the suffix denotes the corresponding soil characteristics of i-th layer.

In Equation (9.10), the term $\bar{q}_i L_i$ can also be interpreted as the area of the overburden pressure diagram in the i-th layer and $\sum_{i=1} \bar{q}_i L_i$ is the total area of the overburden pressure diagram in all layers up to the tip of the pile.

Usually if values of δ are not known, it is assumed to be same as angle of internal friction of the soil. Also, the most conservative analysis assumes K_o = coefficient of earth pressure at rest (Section 3.8) and can be taken as

$$K_o = 1 - \sin\phi \tag{9.11}$$

However, several modifications have been suggested to evaluate Q_{af} based on Equations (9.8)–(9.10), as discussed below.

9.6.3 The α Method

Tomlinson (1977) suggested that Equation (9.8) may be modified since full cohesion/adhesion may not be mobilized at the shaft soil interface during load transfer as observed by Peck, Hanson and Thornburn (1974). Accordingly, he suggested the general equation in any soil layer as

$$Q_{af} = A_s(\alpha\, c + \overline{q} K \tan\delta) \tag{9.12}$$

where

α = adhesion coefficient as given in Figure 9.5

c = average cohesion of the soil layer under consideration (average over depth of pile embedded in that layer)

$\bar{q}$ = effective average (or mid height) vertical stress $= \frac{\gamma L}{2} + q_o$

q_o = surcharge pressure on surface, if any

K = coefficient of lateral earth pressure

$$= \text{ranges from } K_o = 1-\sin\phi \text{ to about } 1.75 \tag{9.13}$$

$$= (1-\sin\phi)\sqrt{OCR}, \text{ for overconsolidated clays} \tag{9.14}$$

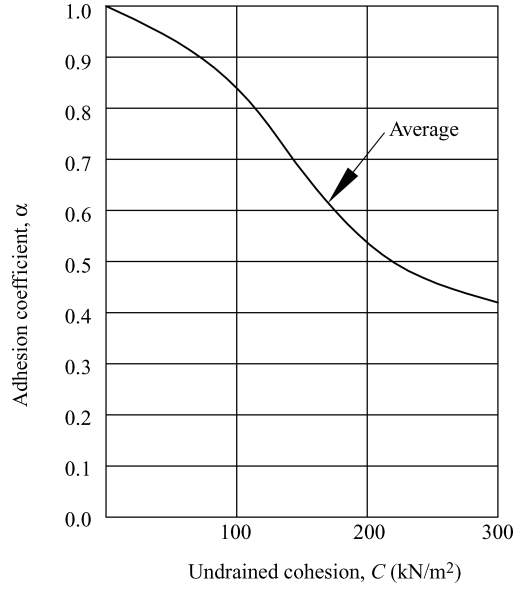

Figure 9.5 Average values of the adhesion coefficient, α.

δ = effective friction angle between soil and pile material, may be taken as φ in the absence of other data
A_s = area of embedded shaft surface in the soil layer under consideration
OCR = over consolidation ratio.

9.6.4 The β Method

This is suggested by Burland (Bowles, 1996) and is similar to the α method. The Equation (9.9) for shaft resistance can be expressed (assuming $q_o = 0$) as

$$Q_{af} = A_s \beta \frac{\gamma L}{2} \tag{9.15}$$

where

$$\beta = K \tan \phi' \tag{9.16}$$

φ' = drained friction angle of remolded clay or soil
$c = 0$ (for remolded clays)

$$K = 1 - \sin \phi' \text{ (for normally consolidated clays)} \tag{9.17}$$

$$= (1 - \sin \phi') \sqrt{OCR} \text{ (for over consolidated clays)} \tag{9.18}$$

L = embedded length of the pile in the soil layer under consideration.

9.6.5 The λ Method

Vijayvergia and Focht (Das, 2007) suggested a slightly different expression (assuming surcharge load, $q_o = 0$) for the shaft resistance of piles as

$$Q_{af} = A_s \lambda \left(\frac{\gamma L}{2} + 2c \right) \tag{9.19}$$

where
c = mean undrained shear strength (i.e., $\varphi = 0$ condition)
λ = coefficient given in Figure 9.6 (Das, 2007)
A_s = surface area of the embedded shaft.

9.6.6 Allowable Pile Capacity

In view of the several methods available for the determination of pile capacity, the designers choose the method that suits the site conditions most. However, a simple approach can be adopted using the static approach discussed in Section 9.6.2 with a factor of safety ranging from

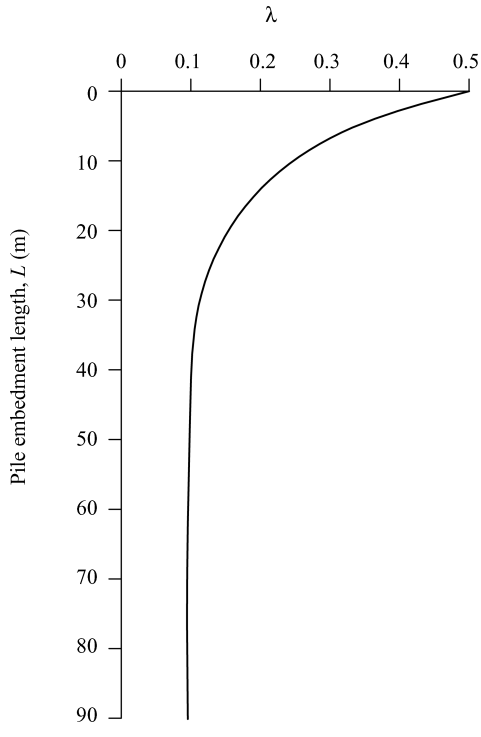

Figure 9.6 Values of λ with pile embedment length.

2.5 to 4.0 (preferably 3.0) to evaluate the allowable pile capacity, that is

$$Q_{all} = \frac{Q_u}{F.S.} \tag{9.20}$$

where

Q_{all} = allowable pile capacity
Q_u = ultimate pile capacity
$F.S.$ = Factor of safety (2.5–4.0, preferably 3.0)

9.6.7 Pile Load Tests

Load tests on piles may be conducted for determining and (or) verifying the pile capacity in the vertical direction (compressive loads or uplift loads) as well as in the horizontal direction (lateral loads). The vertical pile load test is conducted normally and other parameters required or deduced from these tests results. Though the lateral load test on piles is conducted occasionally, it is very difficult and expensive. However, the test set up for all these tests are similar except for the direction of loading. Hence, the vertical load test on piles is described below.

The test set up for vertical load test on piles is similar to plate load test as discussed in Sections 3.5 and 4.8. The test is also useful to verify the pile capacity computed by other methods such as those mentioned in the preceding sections (Ramiah and Chickanagappa, 1981; Bowles, 1996).

The test pile is driven/cast *in situ* at the site under consideration up to the design depth. The rest of the procedure of load application and measurements of displacement is the same as described in Sections 3.5 and 4.8 for plate load test. The results are plotted as load versus settlement as shown in Figure 9.7. The plot is similar to the plot for plate load test (Section 3.5).

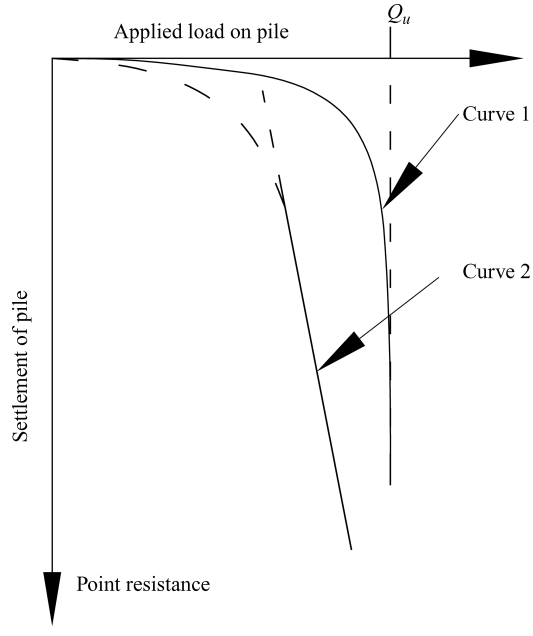

Figure 9.7 Load test on piles.

The test is conducted up to failure, as may be observed from the steep load–settlement curve 1 in Figure 9.7 or up to a large settlement with gradually varying slope of the load-settlement plot, as shown in curve 2. The ultimate pile capacity can be obtained directly for load tests with results as in curve 1 as indicated in the Figure 9.7. Then the allowable load is calculated by dividing the ultimate load with a factor of safety (say 3) or as that load corresponding to a specified value of settlement.

In cases of load test with results obtained as in curve 2, the ultimate load cannot be clearly identified. In such cases, the allowable load is determined by any prescribed criteria using displacements. For example the allowable load may be taken from any one of the following criteria.

1. One-half to one-third of the final load which causes a total settlement equal to 10% of the pile diameter or least dimension of the pile cross section.
2. Two-thirds of the final load which causes a total settlement of 12 mm
3. Two-thirds of the final load which causers a net settlement (residual settlement after removal of all the load/unloading) of 6 mm.

Usually the design values from the pile load tests are chosen as per the codes and practices. There are a few other methods available in literatures besides the methods prescribed in codes. However the above methods are useful for practical applications of design.

9.6.8 Correlation with SPT and CPT Values

The values of unit point resistance of piles, q_p and the shaft resistance, s_{at} are also correlated to the field tests, that is, SPT and CPT. The correlations are summarized by Das (2007) as given in Table 9.2. N_{60} values mentioned in the table are the average SPT values of the soil near the tip of the pile, that is, soil from $10D$ above and $4D$ below the tip of the pile where D is the diameter of the pile.

Table 9.2 Correlation with SPT values.

Soil type	Type of pile	Correlation
Sand		$q_p = 19.7\, p_a N_{60}^{0.36}$
Sand	Cast *in situ*	$q_p = 3p_a$
Sand	Bored pile	$q_p = 0.1 p_a N_{60}$
Gravely sand	Bored pile	$q_p = 0.15 p_a N_{60}$
All types of soil	Driven pile	$q_p = 0.3 p_a N_{60}$

where p_a = atmospheric pressure = 100 kN/m^2.

The unit point resistance of the pile, q_p is correlated to CPT values by Meyerhof and others (Ramiah and Chickanagappa, 1981) as

$$q_p = nq_c \tag{9.21}$$

where

q_p = unit point resistance of pile
n = coefficient ranging from 2/3 to 1.5 with average value taken as 1
q_c = unit resistance of Dutch cone penetrometer.

Similarly, for driven piles, the skin friction s_{at} is correlated with the skin friction q_f of the shaft of the penetrometer as

$$s_{af} = n\, q_f \tag{9.22}$$

where

s_{af} = unit shaft resistance
q_f = skin friction of the Penetrometer shaft
n = coefficient varying from 1.25 to 3.0
= 2.0 (average value)
= 1.0 (for small displacement piles such as steel H-piles).

Once q_p and s_{af} are obtained from Equations (9.21) and (9.22), pile capacity can be determined using Equation (9.3).

9.7 Lateral Load Capacity of Piles

Lateral loads due to wind, load transfer in framed structures, earthquakes, hydrostatic pressure, movement of vehicles and over head cranes and so on are transferred from the superstructure to the pile foundations in many cases. Thus piles have to resist lateral loads in addition to vertical loads. Lateral loads also occur due to twisting moment transmitted by the superstructure as discussed in Chapter 10. Detailed analysis of lateral loads as well as all other loads and moments transferred to the piles/pile groups have been presented in Chapter 10. Lateral pile response analysis and determination of lateral pile capacity have also been presented therein (Chapter 10). However a few details are given in subsequent sections.

The problem of response of piles is a complex phenomenon involving three-dimensional considerations. However to simplify the analysis, the problem is usually analyzed using semi-empirical approaches and (or) beams on elastic foundation (BEF) approach (Chapter 10). The responses also depend on the flexural rigidity of pile and analysis is broadly categorized as rigid pile or elastic pile analysis. The responses of rigid piles and elastic piles due to lateral loads are shown in Figures 9.8 and 9.9 respectively. The general analysis using BEF approach is given in detail in Chapters 4–7 and 10. The general solutions of elastic piles are given in Chapter 10. The practical design of piles subjected to general loads and moments are presented therein. These solutions are also available in terms of design tables, charts for ready use (Hetenyi, 1950; Teng, 1964; Iyengen and Ramu, 1979; Ramiah and Chickanagappa, 1981).

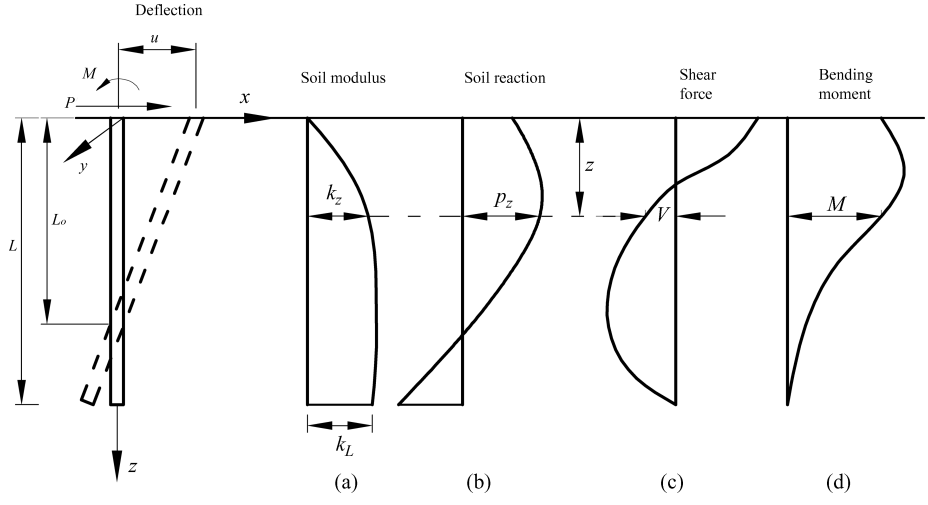

Figure 9.8 Response of rigid piles due to lateral loads.

9.8 Stresses on Lower Strata Due to Pile Foundations

The stress distribution in soil layers due to pile loads is very complicated and can be attempted using FEM and so on. However, stresses caused due to the pile loads need to be checked at some depths particularly if there are weak soil layers present below these foundations. Hence the

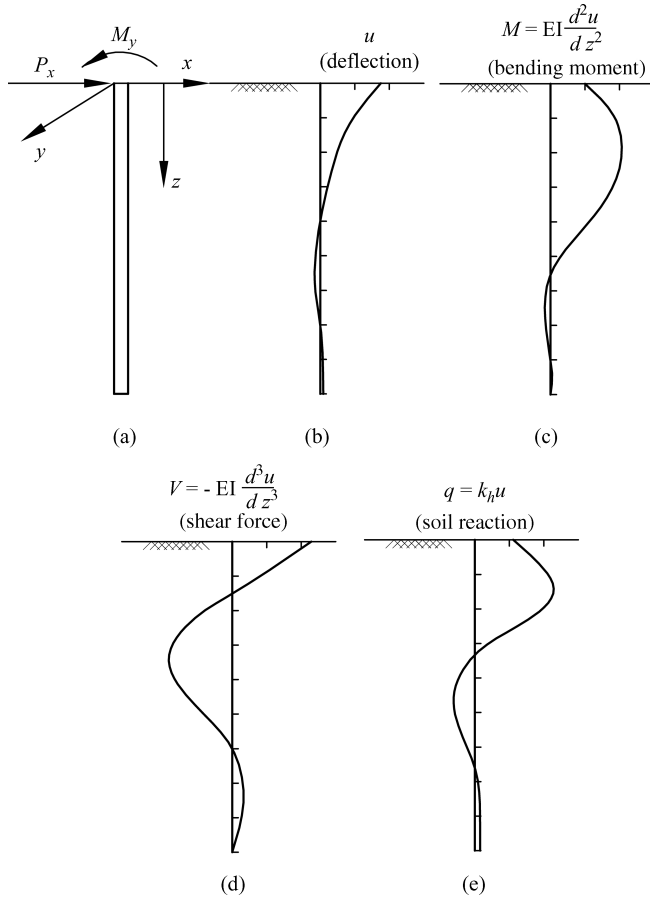

Figure 9.9 Response of elastic piles due to lateral loads.

following approximate and empirical methods are suggested for judicious application. These are shown in Figure 9.10.

1. The method for pile group with point bearing piles is shown in Figure 9.10(a). The pile group is treated as rigid foundation at the bottom of the weak soil as shown. Then the total load on pile group is assumed to spread out (in a pyramidal shape) at a 60° angle or in a slope of 2 vertical to 1 horizontal from the fictitious footing. The stresses at any depth can be easily computed using this approximate dispersion of load along the depth.
2. The approximate dispersion of the loads for pile groups with friction resistance is shown in Figure 9.10(b). The loads are assumed to spread out like a pyramidal with 60° angle (or 2 : 1 slope) starting at the top of the soil layer offering friction support. In this case the pile group is treated as a rigid footing at the top of the frictional soil layer.
3. Another alternative method for friction pile group is suggested by Peck, Hanson and Thornburn (1974) is shown in Figure 9.10(c). In this method, the load is assumed to spread

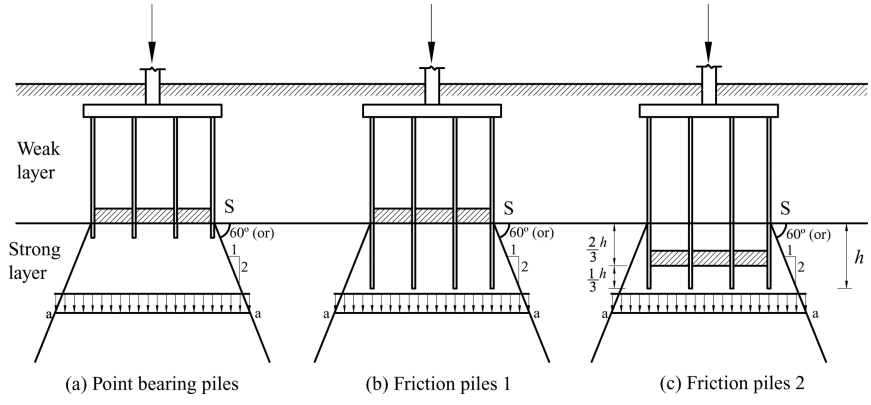

Figure 9.10 Stresses in lower strata due to pile groups – approximate methods.

out from a depth $h/3$ measured from the pile tip where h is the length of pile embedded in the soil layer offering frictional resistance as shown in the figure. Since it is known that greater penetration would bring the load to a lower level, this method appears to be more realistic.

The above methods are approximate and the settlement calculated using the above methods are smaller than the actual values measured in the field in some cases. If the calculated stress exceeds the allowable bearing capacity of any weak layer below (if present), the design should be revised either by reducing the pile load, or by increasing the pile spacing or by extending the piles up to a deeper layer below.

9.9 Settlement Analysis

As explained in Chapter 3 (Section 3.7), the total settlement of any foundation consists of the three components expressed as

$$S = S_i + S_c + S_s \tag{9.23}$$

where

S = total settlement
S_i = immediate elastic settlement
S_c = settlement due to primary consolidation
S_s = settlement due to secondary consolidation

Out of these, the elastic settlement, S_i can be determined using the solutions given in Section 3.6 and also explained in Section 10.8 in detail. Usually its magnitude is very small and may be neglected. Similarly the secondary consolidation is not significant as mentioned in Section 3.7. The primary consolidation settlement, S_c is important both due its magnitude and effect on superstructure and has to be computed if there is a compressible soil (cohesive soil) layer below the tip of pile group. The settlement, S_c is evaluated using Terzaghi's consolidation

theory as presented in Section 3.7 and is expressed (Equation (3.48)) as

$$S_c = m_v \Delta p H = \frac{C_c}{1+e} H \log_{10} \frac{p_o + \Delta p}{p_o} \tag{9.24}$$

where

$$m_v = \frac{a_v}{1+e} = \text{coefficient of volume decrease} \tag{9.25}$$

Δp = change in stress at middle of the compressible soil layer due to applied load on pile foundation.
H = total thickness of the compressible layer
a_v = coefficient of compressibility
C_c = compression index
p_o = existing/initial overburden pressure at the middle of the compressible soil layer
e = existing/initial void ratio of the compressible soil.

Other useful expressions of the computation concerning consolidation theory are given in Equation (3.49). Coefficient a_v and C_c can be obtained from the consolidation/compressibility test, H, p_o and e can be obtained from the field exploration and laboratory tests. The change of stress of the middle of the compressible layers can be obtained using any of the three approximate methods of stress distribution discussed in the previous section, that is, Section 9.8. Out of these, the use of the method shown in Figure 9.10(c) is commonly used for friction piles (Peck, Hanson and Thornburn, 1974; Das, 2007).

If the compressible layer is either very large or it consists of several layers with different thicknesses and properties, the total thickness is divided into smaller layers of suitable thickness. Then, the settlement S_{ci} for each layer is calculated from Equation (9.24) using the properties and thickness of that layer and the total settlement can be obtained as

$$S_c = \sum_{i=1}^{n} S_{ci} \tag{9.26}$$

where the suffix indicate the layer i of the compressible soil. The change in stress Δp, is computed at the middle of each layer for substitution in Equation (9.24).

The charts and expression such as those of Newmark can also be used (Chapter 3) for calculating Δp with the relocation of the pile group as a fictitious rigid foundation at the suggested depth as explained in the previous Section 9.8.

9.10 Design of Piles and Pile Groups

The practical considerations and detailed design of piles and pile groups as well as construction aspects are presented in Chapter 10.

9.11 Drilled Piers or Drilled Caissons

These are also called drilled shafts or drilled caissons or large diameter piers or large diameter bored piles with or without under-ream at bottom. These are bored cylindrical holes filled with

concrete. They are essentially piles but with large diameters ($\geq$750 mm). The bore hole may be drilled with or without casing. The casing if used can be left as part of the structure or withdrawn gradually during concreting. The bottom of the pier or caisson may be enlarged or under-reamed or belled out either manually or by machine which facilitates a larger bearing area and hence higher bearing capacity (Teng, 1964; Ramiah and Chickanagappa, 1981; Bowles, 1996; Das, 2007). A few types of these drilled piers or caissons are shown in Figure 9.11. The drilled piers or caissons consist of a shaft with or without bell and a cap as shown. The drilled piers are used where the soil is weak and the loads are too large and vibrations have to be avoided (i.e., to avoid effect of vibrations such as in driven piles).

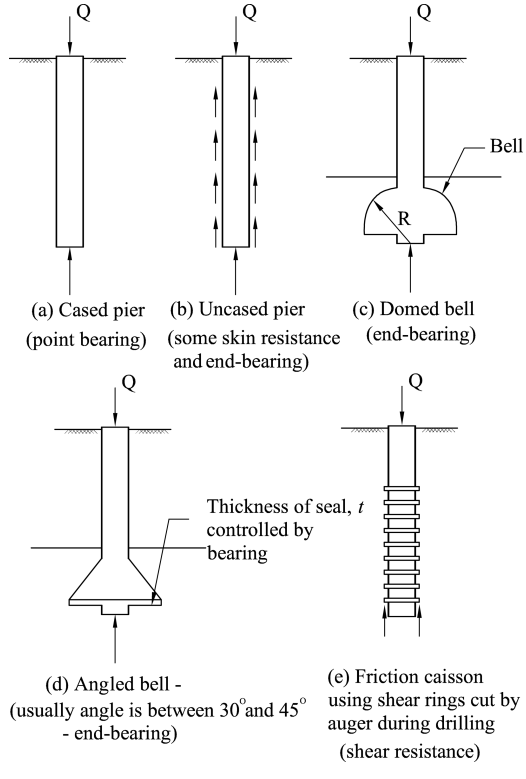

Figure 9.11 Types of drilled piers.

The term caisson is also referred to the non-drilled type of large prefabricated box-type structure which may be round or rectangular in shape. They are discussed in the next section.

Drilled piers and caissons are extensively used for bridge piers, abutments, other massive structures, docks, harbors and offshore structures. They are highly specialized type of deep foundations used only for major projects. Their foundations have several advantages but they

need very careful and skilled construction operations. The drilled piers are also used in underpinning works.

9.11.1 Construction of Drilled Piers

In the earlier methods like Chicago method and Gow's method, the drilling used to be done manually. The shaft excavations are presently done mechanically using augers. When the excavation reaches the load bearing stratum, the augers are replaced by under-reaming tools to construct the bell, if required. Casing is used to prevent caving in of soil as the bore hole is advanced deeper into the soil. Sometimes drilling mud/bentonite slurry can be used in drilling through sandy and gravely soils instead of casing. The bottom of the hole must be inspected physically by descending to the bottom to make sure that the load bearing stratum has been reached and also that the under reaming is properly done. The construction details are very elaborate and these are carried out only by specialized construction agencies (Tomlinson, 1977, 2001).

9.11.2 Other Design Details

The following are the steps involved in the design of drilled piers or drilled caissons:

1. The loads coming on top of the foundation are calculated. The weight of the pier is not usually included.
2. Establish the water level and soil profile at the location of the pier.
3. Identify the bearing stratum, that is, depth up to which the pier has to be constructed. Calculate the allowable bearing capacity.
4. Check for the safety of stresses in weak soil layers if present below the pier.
5. Check for settlements.
6. Design the shaft, bell (if required) and the cap.
7. Check lateral load capacity, bending stresses and eccentricity.
8. Check for the uplift force.

Most of the above steps are similar to those used in the pile foundations since drilled piers are essentially large diameter piles. However a few additional approaches used in practice are given below.

9.11.3 Bearing Capacity and Shaft Resistance

The total pier capacity consists of point bearing and shaft resistance as explained in Section 9.6. The same methods used for piles can also be used for piers and other deep foundations. The pier is essentially designed as a compression member, that is, as a composite column. In compressive soils, the negative skin friction or downward drag force along the shaft of the pier has to be considered in the design. A few additional methods available in literature (Ramiah and Chickanagappa, 1981) for the determination of the pier capacity are given below.

9.11.3.1 Ultimate Bearing Capacity of Drilled Caissons

The expression is given by Skempton (Ramiah and Chickanagappa, 1981) as

$$q_u = cN_c \tag{9.27}$$

where

q_u = ultimate bearing capacity
c = cohesion
N_c = 7.7–9.0 with an average value of 8.4 depending on the depth to diameter ratio of the pier.

The allowable bearing capacity, q_{all} can be written with $N_c = 8.4$ as

$$q_{all} = \frac{q_u}{F.S.} = \frac{8.4c}{3} = 2.8c \tag{9.28}$$

Similarly there are other formulae such as those given by Cooke and Whitaker and others (Ramiah and Chickanagappa, 1981; Bowles, 1996; Das, 2007).

9.11.3.2 Drilled Piers in Sands and Gravely Soils

The formulae given by Teng (1964) for the allowable bearing pressure based on shear failure and settlement criteria are as follows

$$q_1 = \frac{N^2 BW}{100} + \frac{100 + N^2}{30} LW' \tag{9.29}$$

$$q_2 = 7(N-3)\left(\frac{B + 0.3}{2B}\right)^2 W' \tag{9.30}$$

where

q_1 = allowable soil bearing pressure (t/m^2) with factor of safety = 3 using shear failure criterion
q_2 = allowable soil pressure in (t/m^2) for a maximum settlement of 2.5 cm
N = SPT values for 30 cm penetration
B = diameter of caisson bottom (m)
L = depth of caisson in meters (if $L \geq B$ use B in calculations)
W, W' = reduction factors for water level.

The lower of the q_1 and q_2 values has to be taken as the allowable design pressure.

9.11.3.3 Shaft Friction of Drilled Piers

The methods used for piles can be suitably adopted for the determination of shaft friction of drilled piers, and are given in Section 9.6.

Additional empirical formulae given by Meyerhof (Ramiah and Chickanagappa, 1981) and others for piers in sandy soils are given below

$$Q_f = 0.7\gamma D L^2 \tan\phi \tag{9.31}$$

where

Q_f = ultimate shaft friction in sandy soils
γ = average unit weight of soil (if the soil is submerged, use submerged unit weight)
L = depth of pier below ground level
D = diameter of pier shaft
φ = angle of internal friction of soil.

Meyerhof (Ramiah and Chickanagappa, 1981) has also given a correlation between shaft friction and SPT and CPT values as

$$S_{aF} = 0.01N \leq 0.5\,\text{kg/cm}^2 \tag{9.32}$$

$$= f_c \leq 0.5\,\text{kg/cm}^2 \tag{9.33}$$

where

S_{aF} = ultimate shaft resistance (kg/cm^2)
N = SPT value
f_c = value of frictional component from CPT

9.11.4 Stresses in Lower Strata

Stresses in lower strata have to be checked if there is a weak soil layer below the depth of foundation. The approximate methods used for piles as given in Section 9.8 can be used for drilled piers also.

9.11.5 Other Design Considerations

Design considerations such as settlement analysis, lateral load capacity, bending moment due to wind, water and other lateral loads, can be analyzed using the similar approaches used for piles as given in Sections 9.6–9.9.

9.11.6 Construction Problems

Drilled piers are used for major projects and construction process is very elaborate, difficult and time-consuming. Hence only specialized agencies carry out such construction. The problems during construction are quite a few, as mentioned below:

1. Dewatering problems
2. Casing problems
3. Concreting problem particularly under water environment
4. Alignment problems
5. Tilting of piers
6. Exacting quality control requirements.

Detailed procedures for design and construction are also given in books on bridges, construction, structural design, geotechnical engineering and so on.

9.12 Non-Drilled Caissons

As mentioned earlier, these are prefabricated box-type structures which may be round or rectangular in shape, as shown in Figure 9.12. These are partially or fully filled with concrete and constructed at site. Sometimes they are partially constructed at a convenient place and towed to the site for completing the construction. They are sunk through water and soft soil to provide a dry work place.

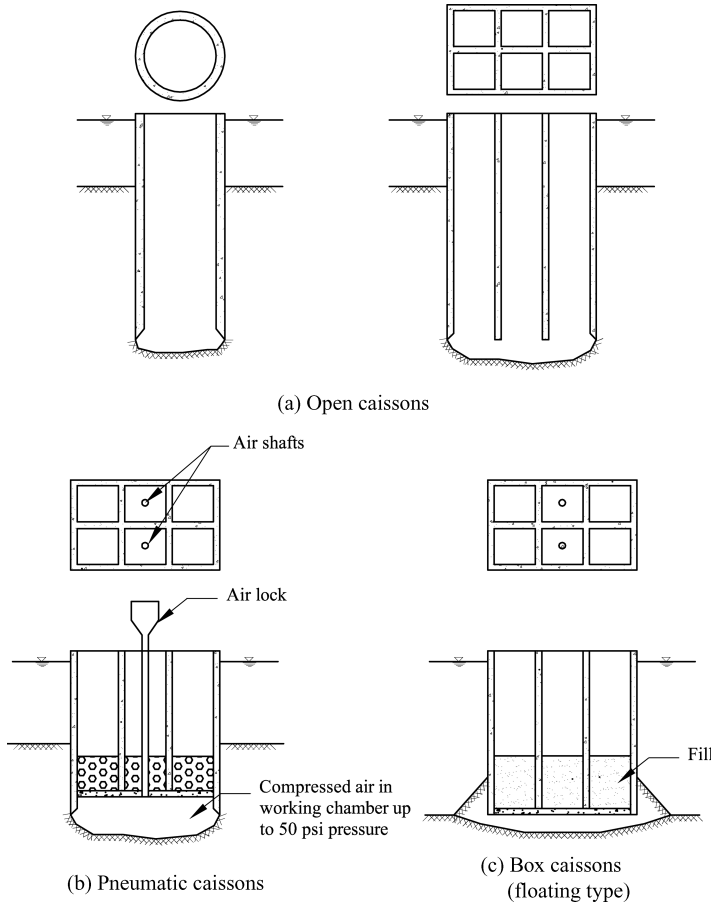

Figure 9.12 Types of caissons.

Non-drilled caissons can be advantageous under the following situations:

1. Drilling is difficult and hence drilled piers are not feasible.
2. Massive foundations are required at or below the river beds which can resist large forces due to floating objects, scour, and so on (as in bridge foundations).
3. Large lateral forces need to be resisted.

As in drilled piers, non-drilled caissons are very expensive.

9.12.1 Types of Caissons

The following types of caissons are used.

1. **Open Caissons:** These are structures which are open at top and bottom (i.e., well foundations). Upon reaching the final depth, a concrete seal of 2–5 m thick is cast through water (if present) to seal the bottom. After the seal has matured, the water present inside the caisson is pumped out and filled with concrete.
2. **Box Caissons (Floating Caissons):** These are made of concrete with the top being open and the bottom closed. These are cast on land and towed to the site like barges. They are sunk slowly by filling the inside with sand, gravel, water and concrete. Sometimes the bottom is made of wood to make it float for towing purposes.
3. **Pneumatic Caissons:** In this type of caisson, the top is sealed and compressed air is used to prevent water from entering the inside working chamber. This will help in sinking and concreting in dry condition. On reaching the required depth, the chamber is filled with concrete.

9.12.2 Design Considerations – Bearing Capacity and Shaft Friction

The heavy loads coming on to the caisson are borne both by end bearing capacity (treating it as a rigid foundation at that depth) and skin friction of the portion sunk/embedded in the soil. The formulae for deep foundations and piles can be used to determine these values. Additionally the following empirical correlations can also be used.

For caissons in granular soils

$$q_p = 0.064N^2BW + 0.192(100 + N^2)LW' \tag{9.34}$$

For caissons in cohesive soils

$$q_p = cN_c \tag{9.35}$$

where

q_p = ultimate bearing capacity of the caisson
N = SPT value
B = width of the caisson (m)
L = depth of the caisson (m)
W, W' = reduction factors for water level
c = cohesion (t/m^2)
N_c = bearing capacity factor

The allowable bearing pressure on bed rock should not exceed that for the concrete bed. Half of the shaft friction for deep caissons is assumed for design. The caissons are designed to have enough weight to overcome the skin friction. The shaft friction can be evaluated using the same methods used for piles (Section 9.6).

9.12.3 Concrete Seal

A concrete seal is placed at the bottom of an open caisson that forms a part of the caisson foundation. The seal may be designed as a thick plate subjected to the pressure caused by the maximum vertical load. The thickness of the seal is given by the following expressions (Ramiah and Chickanagappa, 1981).

1. *For round caissons, assuming the edge is fixed*

$$t = \left(\frac{6qR^2}{8f_c}\right)^{1/2} \tag{9.36}$$

2. *For round caisson with simply supported edge*

$$t = \left(\frac{3qR^2(3+v)}{8f_c}\right)^{1/2} \tag{9.37}$$

3. *For rectangular caissons with simply supported edges*

$$t = \left(\frac{6\beta\, q\, B^2}{f_c}\right)^{1/2} \tag{9.38}$$

4. *For rectangular caissons with fixed edges*

$$t = \left(\frac{6\,\alpha\, qB^2}{f_c}\right)^{1/2} \tag{9.39}$$

where

t = thickness (cm)
f_c = allowable concrete stress (kg/cm^2): use $0.1\,f_c'$ for a safety factor $\cong$1.5 and $f_c' = 28$ days cylinder strength
v = Poisson's ratio = 0.15 for concrete
q = soil pressure (kg/cm^2)
R = radius of circular caisson (cm)
B = width of rectangular caisson (cm)
A = length of rectangular caisson (cm).

The α and β factors for use in the above equations are given below in Table 9.3.

Table 9.3 α and β factors.

A/B	1	1.2	1.4	1.6	1.8	2.0	3.0	∞
α	0.051	0.064	0.073	0.078	0.081	0.083	0.083	1/12 at edge in B direction
β	0.048	0.063	0.075	0.086	0.095	0.102	0.119	1/8 at center

9.13 Pile-Raft Systems

Foundations for heavy structures on weak soils are usually on piles and (or) pile-raft systems. These are also called basement raft supported piles or piled basements (Poulos, 2001; Tomlinson, 2001). Pile-raft systems are shown in Figure 9.13. The pile groups are connected together to a raft (can also be used as a basement floor) instead of separate pile caps for each column. The piles also stiffen the raft and reduce the differential settlements and tilting. When piles are founded on a compressible soil like clays, the pile-raft system settles gradually resulting in a gradual build up of pressure at the bottom of the raft. Thus, there is a gradual transfer of the total load to the raft and a reduction in the load carried by the piles. The soil beneath the raft (located at a relatively shallow depth) is then compressed, causing a partial load

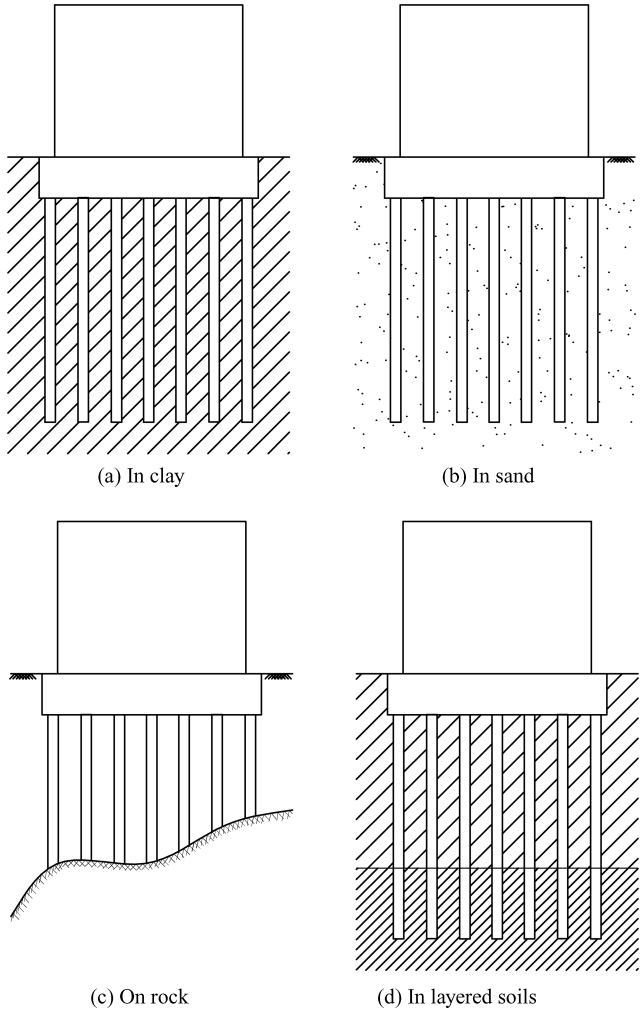

Figure 9.13 Piled basements in various soil conditions.

transfer back to the piles. This is a continuous interaction process with the total load being shared by the raft and the piles.

Hence the piles must be designed to carry the full superstructure load initially, but the raft should be designed to carry a portion of the total load due to the subsequent load transfer process. To apportion these loads between the raft and the piles over a period of time is very difficult as it is a complex three-dimensional time-dependent problem. Several case studies carried out indicate varying load-sharing percentages. For example, the results of the study conducted by Hooper (1973, 1979) for the load shared between raft and piles and the settlements are shown in Figure 9.14. It can be seen from the figure that after the construction (40 months) piles and raft carried about 60% and 40% of the superstructure load. After that more loads got transferred to the piles from the raft and the percentages of total load shared by piles and raft became 66% and 34%, respectively.

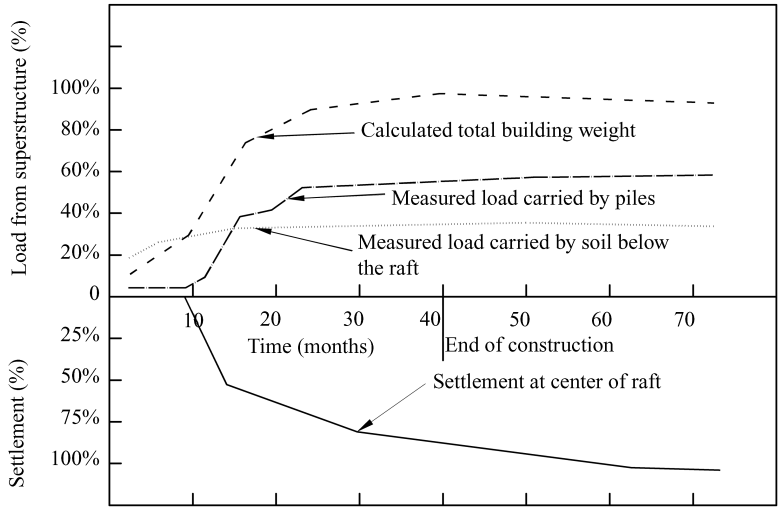

Figure 9.14 Load sharing between piles and raft.

9.13.1 Analysis of Pile-Raft Systems

There are several parameters that affect the responses of pile-raft systems to applied loads (Poulos, 2001). These are also identified by Clancy and Randolph (1996) and are given below in Table 9.4.

With such large number of parameters and wide ranging values for practical applications, it is very difficult to carry out a general analysis and present appropriate correlations. However detailed FEM analysis can be carried out for specific problems whose applicability has to be looked into judiciously in view of the complex nature of input values of parameters and large scale computations. Clancy and Randolph (1996) presented selectively simple methods to carry out the preliminary design of the pile-raft systems. However, they recommend that a detailed FEM analysis with proper inputs of the parameters of pile, soil and raft is essential to arrive at a final design.

Table 9.4 Significant dimensionless parameters for the analysis of pile-raft systems.

Dimensionless parameters	Expression	Practical range of values
Pile slenderness ratio	$\frac{L_p}{D_p}$	10–100
Pile spacing ratio	$\frac{s_p}{D_p}$	2.5–8
Pile–soil stiffness	$K_{ps} = \frac{E_p}{E_s}$	100–10 000
Aspect ratio of raft dimensions	$\frac{L_r}{B_r}$	1–10
Raft–soil stiffness	$K_{rr} = \frac{4E_rB_rt_r^3(1-v_s^2)}{3\pi E_sL_r^4(1-v_r^2)}$	0.001–10

where L_p, D_p, s_p, E_p = pile parameters – length, diameter, spacing and modulus of elasticity.
E_s, v_s = soil parameters – modulus of elasticity and Poisson's ratio, respectively.
L_r, B_r, t_r, E_r, v_r = raft parameters – length, width, thickness, modulus of elasticity and Poisson's ratio, respectively.

9.13.2 General Observations

Pile-raft systems or basement rafts are very useful in minimizing the differential settlements in structures. The piles have to be designed to carry full superstructure loads initially and the raft has to be designed to carry a part of the total load resisted by the contact pressure at the bottom of the raft. The determination of this pressure acting on the raft involves an extensive FEM analysis with reasonably reliable input parameters of the pile, soil, raft and their three-dimensional interaction. However a few simple methods are available (Clancy and Randolph, 1996) to carry out the preliminary design. Generalization of the behavior of such systems may not be practicable. Lot of research is being carried out on the subject in the areas of analysis, design and field measurements which may be helpful in practice.

9.14 Examples

Examples	Topic	Sections
9.1 to 9.3	Pile capacity	9.6, 9.10
9.4 to 9.7	Stresses in soils and settlement of pile groups	9.7, 9.8, 9.9

Example 9.1

A square concrete pile (0.6×0.6 m) 16 m long is embedded in a cohesive soil with $c = 25\,\text{kN/m}^2$, $\varphi = 20^{\phi}$, $\gamma_t = 18\,\text{kN/m}^3$, calculate the ultimate load as well as the allowable load that can be carried by the pile using Terzaghi's theory (Figure 9.15).

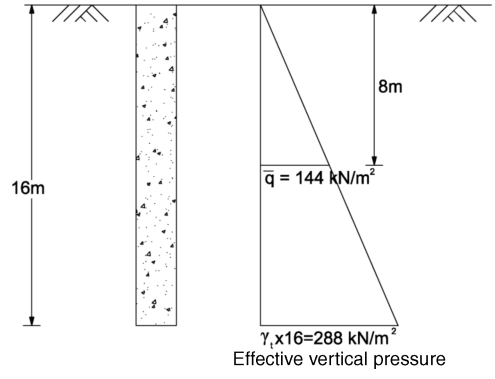

Figure 9.15 Example 9.1.

Solution:

$\gamma_t = 18\,\text{kN/m}^3$, $c = 25\,\text{kN/m}^2$, $\phi = 30^\circ$, Assume adhesion coefficient, $\alpha = 1.0$

$$K = K_o = 1-\sin\phi = 1-\sin 30^\circ = 0.5$$
$$\delta = \phi = 30^\circ,\ \tan\delta = \tan\phi = \tan 30^\circ = 0.5773$$
$$A_p = \textit{area of pile} = 0.6 \times 0.6 = 0.36\,\text{m}^2$$
$$\text{Perimeter of pile shaft} = 4 \times 0.6 = 2.4\,\text{m}$$

From Equation (9.3)

$$Q_u = Q_p + Q_{at} \tag{9.40}$$

From Equations (9.8) and (9.9)

$$\begin{aligned} Q_u &= A_p q_p + A_s S_{at} \\ &= A_p q_p + A_s(\alpha c + K_o \overline{q} \tan\delta) \end{aligned} \tag{9.41}$$

For $\phi = 30^\circ$, Terzaghi bearing capacity factors are
$N_c = 37.16$, $N_q = 22.46$, $N_\gamma = 19.13$

$$\begin{aligned} q_p &= 1.3cN_c + \gamma D_f N_q + 0.4\gamma B N_\gamma \\ &= 1.3 \times 25 \times 37.16 + 18 \times 16 \times 22.46 + 0.4 \times 18 \times 0.6 \times 19.13 \\ &= 1207.7 + 6468.5 + 82.6 = 7758.8\,\text{kN/m}^2 \end{aligned} \tag{9.42}$$

Assuming $\alpha = 1$

$$\begin{aligned} S_{at} &= c + K_o \overline{q} \tan\delta = 25 + (0.5 \times 144 \times 0.5773) \\ &= 66.6\,\text{kN/m}^2 \end{aligned}$$

$\therefore$ From Equation (9.41)

$$Q_u = [(0.36 \times 7758.8) + (2.4 \times 16 \times 66.6)] = 5350.56\,\text{kN}$$

$$\text{Allowable total capacity of pile (FS} = 3) = \frac{5350.56}{3} = 1783.5\,\text{kN}$$

Example 9.2

Compute the total pile capacity of a circular pile (0.5 m diameter) of length 20 m embedded in a soil with $c = 20\,\text{kN/m}^2$, $\varphi = 20^{\phi}$, $\gamma_t = 19\,\text{kN/m}^3$, $\gamma_{sub} = 12\,\text{kN/m}^3$. The GWL is at a depth of 5 m below the GL (Figure 9.16).

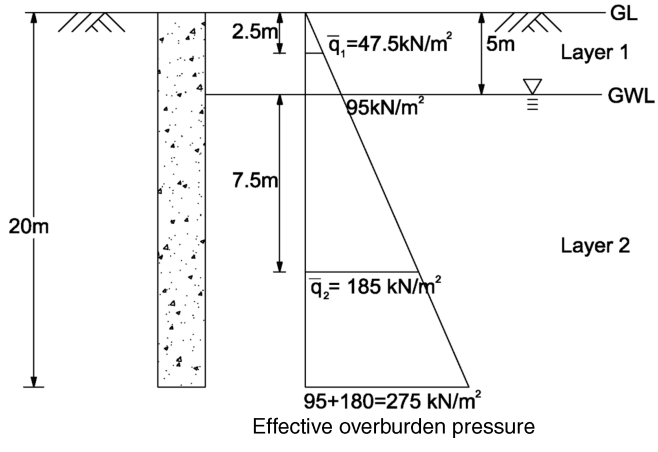

Figure 9.16 Example 9.2.

Solution:

$$\text{Pile diameter,} \quad D_p = 0.5\,\text{m},$$

$$A_p = \frac{\pi \times 0.5^2}{4} = 0.196\,\text{m}^2 \quad ,$$

$$\text{Perimeter of pile} = \pi \times D_p = 1.57\,\text{m}$$

Soil parameters: layer 1, soil above GWL

$$\gamma_t = 19\,\text{kN/m}^3,\ c = 20\,\text{kN/m}^2,\ \phi = 20^{\circ},\ \text{depth of layer} = 5\,\text{m}$$

$$K = K_o = 1 - \sin\phi = 1 - \sin 20^{\circ} = 0.66$$

$$\delta = \phi = 20^{\circ},\ \tan\delta = \tan\phi = \tan 20^{\circ} = 0.364$$

$$\bar{q}_1 = \text{overburden pressure at mid depth(i.e. 2.5 m below GL)}$$
$$= 2.5 \times 19 = 47.5\,\text{kN/m}^2$$

Layer 2, all properties are the same except $\gamma_{sub} = 12\,\text{kN/m}^3$, depth of layer $= 15\,\text{m}$.

$$\begin{aligned}\overline{q}_2 &= \text{effective overburden pressure at mid depth of layer 2 (i.e. 12.5m below } GL)\\ &= [(5 \times 19) + (7.5 \times 12)] = 185\,\text{kN/m}^2\end{aligned}$$

Ultimate pile capacity, Q_u

$$Q_u = Q_p + Q_{at} = A_p q_p + A_s(\alpha c + K_o \overline{q} \tan\delta) \tag{9.43}$$

Using Terzaghi's bearing capacity factors for the soil at the end of pile

$$c = 20\,\text{kN/m}^2,\ \phi = 20^\circ,\ N_c = 17.69,\ N_q = 7.74,\ N_\gamma = 3.64$$

Point resistance

$$\begin{aligned}q_p &= 1.3cN_c + (\gamma_1 D_{f1} + \gamma_2 D_{f2})N_q + 0.3\gamma_2 D_p N_\gamma\\ &= [(1.3 \times 20 \times 17.69) + ((19 \times 5 + 12 \times 15)7.44) + (0.3 \times 12 \times 0.5 \times 3.64)\\ &= 459.9 + 2046 + 6.6 = 2512.5\,\text{kN/m}^2\end{aligned}$$

Ultimate point bearing load of pile

$$\begin{aligned}Q_p &= A_p q_p\\ &= 0.196 \times 2512.5 = 492.45\,\text{kN}\end{aligned} \tag{9.44}$$

Shaft resistance in layer 1: assuming $\alpha = 1$

$$\begin{aligned}S_{at1} &= c_1 + K_o \overline{q}_1 \tan\delta = 20 + (0.66 \times 47.5 \times 0.364) = 31.4\\ Q_{at1} &= \pi D_p L_1 S_{at1} = 1.571 \times 5 \times 31.4 = 246.7\,\text{kN}\end{aligned} \tag{9.45}$$

In layer 2: assuming $\alpha = 1$

$$\begin{aligned}S_{at2} &= c_2 + K_o \overline{q}_2 \tan\delta = 20 + (0.66 \times 185 \times 0.364)\\ &= 64.4\\ Q_{at2} &= \pi D_p L_2 \cdot S_{at2} = 1.571 \times 15 \times 64.4 = 1517.6\,\text{kN}\end{aligned} \tag{9.46}$$

Total shaft resistance

$$Q_{at} = Q_{at1} + Q_{at2} = 246.7 + 1517.6 = 1764.3\,\text{kN}$$

Total ultimate pile load capacity

$$Q_u = Q_p + Q_{at1} + Q_{at2} = 492.5 + 1764.3 = 2256.8\,\text{kN}$$

$$Q_{allowable} = \frac{2256.8}{3} = 752.3\,\text{kN}$$

Example 9.3

A square pile (0.8×0.8 m) 18 m long is cast in a two-layered soil as shown in Figure 9.17. Calculate the allowable load that can be carried by the pile (FS = 3).

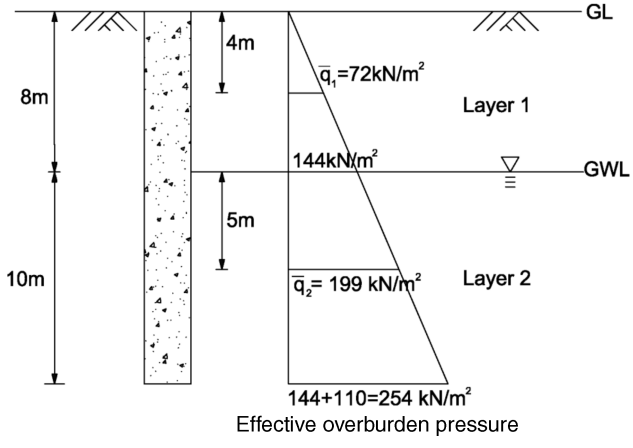

Figure 9.17 Example 9.3.

Layer 1: $\gamma_1 = 18\,\text{kN/m}^3$, $c_1 = 0$, $\phi_1 = 15^\circ$, $\delta = \phi_1$
Layer 2: $\gamma_{sub} = \gamma_2 = 11\,\text{kN/m}^3$, $c_2 = 18\,\text{kN/m}^2$, $\phi_2 = 12^\circ$, $\delta = \phi_2$

Solution:

Layer 1: $K_1 = K_{o1} = 1 - \sin\phi_1 = 1 - \sin 15^\circ = 0.74$, $\tan\delta_1 = \tan\phi_1 = \tan 15^\circ = 0.268$
Layer 2: $K_2 = K_{o2} = 1 - \sin\phi_2 = 1 - \sin 12^\circ = 0.792$, $\tan\delta_2 = \tan\phi_2 = \tan 12^\circ = 0.213$

This is like a drilled pier without under-ream/bell.

$$\begin{aligned} A_p &= \text{area of pile} \\ &= 0.8 \times 0.8 = 0.64\,\text{m}^2 \end{aligned}$$

$$\begin{aligned} \text{Perimeter of pile} &= 4 \times 0.8 \\ &= 3.2\,\text{m} \end{aligned}$$

$$Q_u = Q_p + Q_{at1} + Q_{at2}$$

$$= A_p q_p + A_{s1} S_{at1} + A_{s2} S_{at2} \tag{9.47}$$

Point bearing
Using Terzaghi's theory for end bearing in layer 2

$$c_2 = 18\,\text{kN/m}^2,\ \phi_2 = 12^\circ,\ N_c = 10.76,\ N_q = 3.29,\ N_\gamma = 0.85$$

$$\begin{aligned} q_p &= 1.3 c_2 N_c + (\gamma_1 D_{f1} + \gamma_2 D_{f2}) N_q + 0.4 \gamma_2 B N_\gamma \\ &= [(1.3 \times 18 \times 10.76) + ((144 + 110)3.29) + (0.4 \times 11 \times 0.8 \times 0.85)] \\ &= 251.8 + 835.7 + 3 = 1090.5\,\text{kN/m}^2 \end{aligned}$$

$$Q_p = A_p q_p = 0.64 \times 1090.5 = 697.9\,\text{kN/m}^2 \tag{9.48}$$

Shaft resistanceIn layer 1: assume $\alpha = 1$

$$\begin{aligned} Q_{at1} &= A_{s1}[c_1 + K_{o1}\bar{q}_1 \tan\delta_1] = 3.2 \times 8[0 + 0.74 \times 72 \times 0.268] \\ &= 25.6(14.28) = 365.5\,\text{kN} \end{aligned} \tag{9.49}$$

In layer 2: assume $\alpha = 1$

$$\begin{aligned} Q_{at2} &= A_{s2}[c_2 + K_{o2}\bar{q}_2 \tan\delta_2] = 3.2 \times 15[18 + (0.792 \times 199 \times 0.213)] \\ &= 48(18 + 33.57) = 2475.4\,\text{kN} \end{aligned} \tag{9.50}$$

Total ultimate pile load capacity

$$\begin{aligned} Q_u &= Q_p + Q_{at1} + Q_{at2} \\ &= 697.9 + 365.5 + 2475.4 \\ &= 3538.8\,\text{kN} \end{aligned}$$

$$Q_{allowable} = \frac{3538.8}{3} = 1179.6\,\text{kN}$$

Example 9.4

A pile group (4 × 4 m square) shown below is to carry a load of 2500 kN. The length of the piles is 20 m embedded in soil as shown in Figure 9.18. Compute the primary consolidation settlement.

Solution:
The piles are embedded into the strong layer of sandy soil up to 18 m (ignoring the length in weak soil). Referring to Section 9.8, Figure 9.10(c), the superstructure load is approximately carried to a fictitious rigid footing at a depth of $\frac{2}{3} \times 18 = 12$ m in the stronger sandy soil, that is, level CD. Using the approximate dispersion of load downward to deeper layer with slope of $2V:1H$ as shown, the change in vertical stress at mid depth of compressible clay layer 4, that is, EF can be written as

$$(\Delta p)_{EF} = \frac{2500}{(EF) \times (EF)} = \frac{2500}{17 \times 17} = 8.65\,\text{kN/m}^2$$

where

$$EF = 4 + \frac{13}{2} + \frac{13}{2} = 17$$

The existing over burden pressure at the midlevel, EF, of the clay layer

$$p_o = 2 \times 15 + 6 \times 18 + 16 \times 11 + 3 \times 12 = 350\,\text{kN/m}^2$$

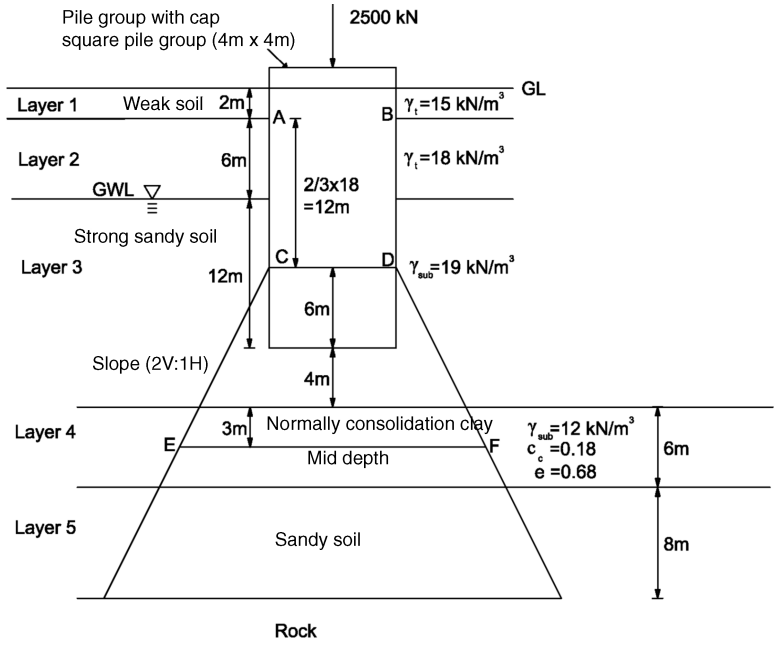

Figure 9.18 Example 9.4.

The consolidation settlement due to the clay layer can be obtained using Equation (9.24) as

$$S_c = \frac{C_c}{1+e} H \log_{10} \frac{p_o + \Delta p}{p_o} = \frac{0.18}{1+0.68} \times 6 \times \log_{10} \frac{3.50 + 8.65}{3.50} = 6.894\,\text{mm}$$

Example 9.5

If in the above problem the clay compression index, $a_v = 0.22 \times 10^{-3}\ \text{m}^2/\text{kN}$, calculate the consolidation settlement.

Solution:

$$S_c = m_v \Delta p H = \frac{a_v}{1+e} \Delta p.H = \frac{0.22 \times 10^{-3}}{1.68} \cdot 8.65 \cdot 6 = 6.796 \times 10^{-3}\, m = 6.796\,\text{mm}$$

Example 9.6

In Example 9.4, if the dimensions of the pile cap are 8 m × 6 m, what will be the consolidation settlement (Figure 9.19)?

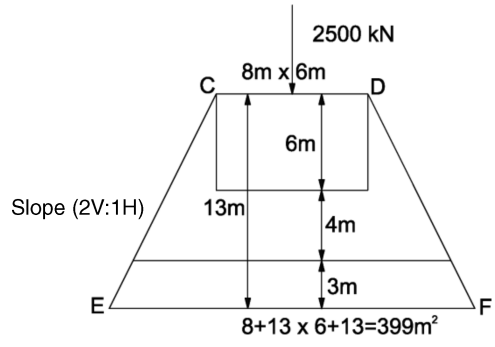

Figure 9.19 Example 9.6.

Solution:
In this case, the load on the fictitious footing CD (8×6 m) gets dispersed as a pyramid (with slope $2V:1H$).At the mid depth of compressible layer (EF)

$$\begin{aligned}&\text{Area of dispersion}\\&= (8 + 13) \times (6 + 13)\\&= 399\,\text{m}^2\end{aligned}$$

Hence, change in pressure at EF

$$\Delta p = \frac{2500}{399} = 6.27\,\text{kN/m}^2$$

Initial overburden pressure will remain the same (i.e.,$p_o = 350\,\text{kN/m}^2$). Then, the consolidation settlement can be obtained using Equation (9.24) as

$$\begin{aligned}S_c &= \frac{C_c}{1+e} H \log_{10} \frac{p_o + \Delta p}{p_o} = \frac{0.18}{1 + 0.68} \times 6 \times \log_{10} \frac{350 + 6.27}{350}\\&= 4.98 \times 10^{-3}\, m = 4.98\,\text{mm}\end{aligned}$$

Using the value of a_v, the settlement can be computed as

$$S_c = m_v \Delta p H = \frac{a_v}{1+e} \Delta p.H = \frac{0.22 \times 10^{-3}}{1.68} \times 6.27 \times 6 = 4.93 \times 10^{-3}\, m = 4.93\,\text{mm}$$

Example 9.7

In Example 9.4, soil layer 5 was subsequently identified as a compressible soil with $\gamma_{sub} = 11\,\text{kN/m}^3$, $C_{c2} = 0.14$, $e_2 = 0.53$, $a_{v2} = 0.12 \times 10^{-3}\,\text{m}^2/\text{kN}$. What is the consolidation settlement due to the two compressible clay layers 4 and 5 (Figure 9.20)?

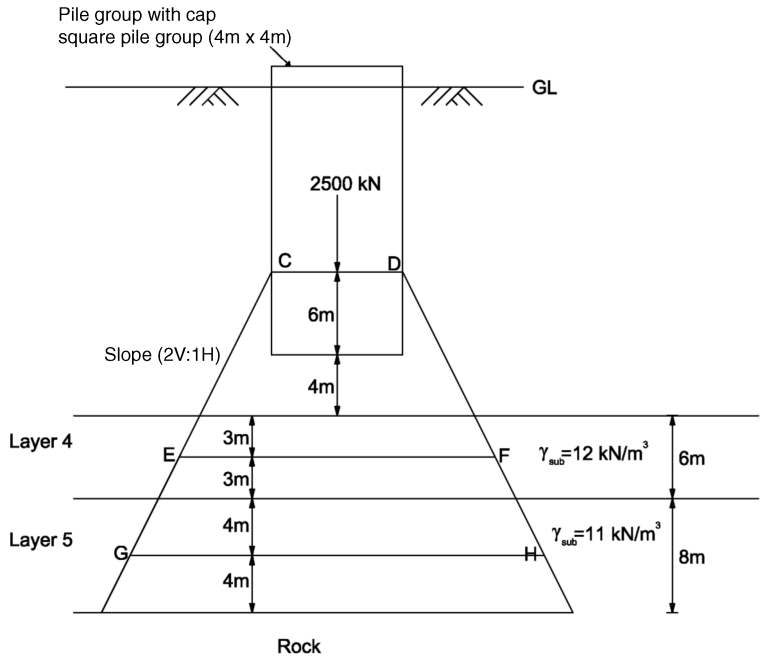

Figure 9.20 Example 9.7.

Solution:
With all other data remaining the same as in Example 9.4, the dispersion of the load from the fictitious level CD of the foundation, is as shown above. Settlement due to layer 4: all computations are the same as in Example 9.4: Accordingly

$$S_{c4} = 6.894\,\text{mm (using } C_{c1}) \tag{9.51}$$

$$= 6.796\,\text{mm (using } a_v, \text{ Ex. 9.5}) \tag{9.52}$$

Now the settlements due to compressible layer 2 have to be added, as explained in Section 9.9 (Equation (9.26)).

Settlement due to layer 2:
The change in pressure Δp_2 at mid depth of layer 2 (level GH) has to be calculated. Accordingly from the dispersion, the load gets dispersed over an area of $(4 + 20)m \times (4 + 20)m$, that is, 24×24 m.

$$\Delta p_2 = \frac{2500}{24 \times 24} = 4.34\,\text{kN/m}^2$$

Existing overburden pressure at level GH

$$(p_o)_2 = (p_o)_1(atEF) + 3 \times 12 + 4 \times 11 = 350 + 36 + 44 = 430\,\text{kN/m}^2$$

$$\therefore S_{c5} = \frac{C_{c2}}{1+e} H \cdot \log \frac{p_{o2} + \Delta p_2}{p_{o2}} = \frac{0.14}{1 + 0.53} \cdot 8 \cdot \log \frac{430 + 4.34}{430} \tag{9.53}$$

$$= 0.732 \times 4.36 \times 10^{-3} = 3.19 \times 10^{-3}\,\text{m} = 3.19\,\text{mm}$$

Settlement by using a_v can be computed as

$$S_{c5} = \frac{a_{v2}}{1 + e_2}\Delta p_2.H = \frac{0.12 \times 10^{-3}}{1.53} \times 8 \times 4.34 = 2.72 \times 10^{-3}\,\text{m} = 2.72\,\text{mm} \quad (9.54)$$

$$\begin{aligned}\text{Total settlement (using } C_c) &= S_{c4} + S_{c5} \quad \text{(from Eq. 1 and 3)} \\ &= 6.894 + 3.19 = 10.084\,\text{mm}\end{aligned}$$

$$\begin{aligned}\text{Total settlement (using } a_v) &= S_{c4} + S_{c5} \quad \text{(from Eq. 2 and 4)} \\ &= 6.796 + 2.72 = 9.516\,\text{mm}\end{aligned}$$

Exercise Problems

9.1 A concrete pile is 18 m long and 450 × 450 mm in cross section. The pile is fully embedded in sand. Given: for sand $\boldsymbol{\gamma_{sub} = 17.3\ \text{kN/m}^3}$ and $\boldsymbol{\phi = 30^\circ}$. Calculate:

a. The ultimate point load, Q_p by Terzaghi's method and compare with Meyorhof's method.
b. The total frictional resistance. Use $K_o = 1.3$ and $\delta = 0.8\phi$.

9.2 A pipe pile (closed end) that has been driven into a layered sand is shown in Figure 9.21. Calculate:

a. The ultimate point load by Terzaghi's method.
b. The ultimate frictional resistance, Q_{at}, $K_o = 1.4$ and $\delta = 0.7\phi$
c. The allowable load of the pile – use FS = 3.

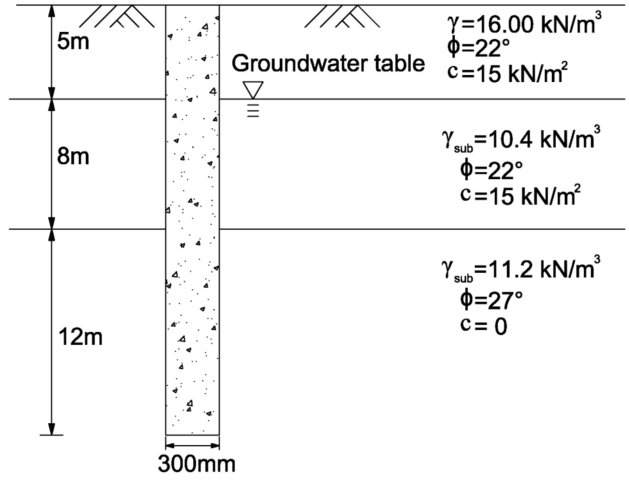

Figure 9.21 Problem 9.2.

9.3 A circular concrete pile 500 mm diameter is shown in Figure 9.22. Determine the allowable load that the pile can carry (FS = 3). Use the α method for determination of the skin resistance, γ.

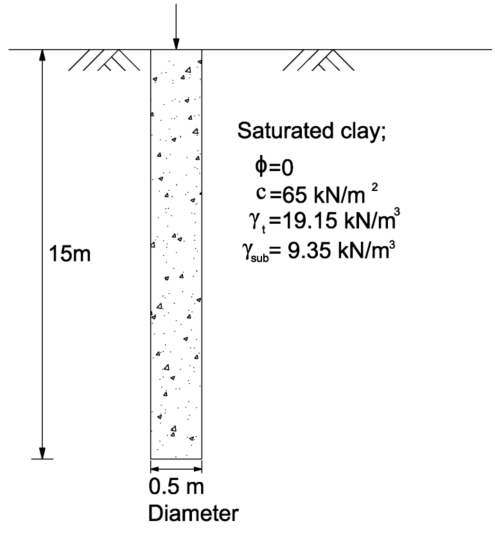

Figure 9.22 Problem 9.3.

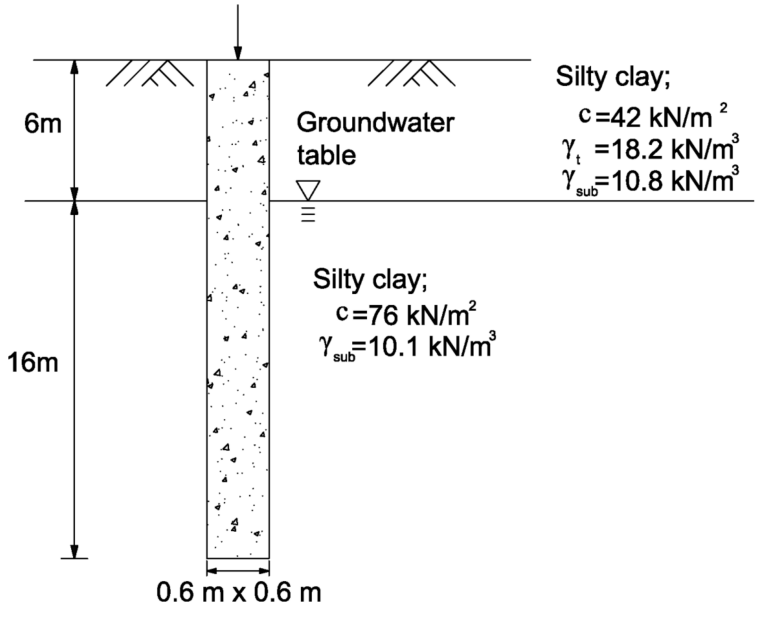

Figure 9.23 Problem 9.5.

9.4 For the pile shown in Figure 9.22, determine the ultimate skin resistance by using the λ method.

9.5 A concrete pile 600×600 mm in cross section is shown in Figure 9.23. Calculate the ultimate skin resistance by using the β method. Use $\phi = 0^\circ$ for all clays. All clays are normally consolidated.

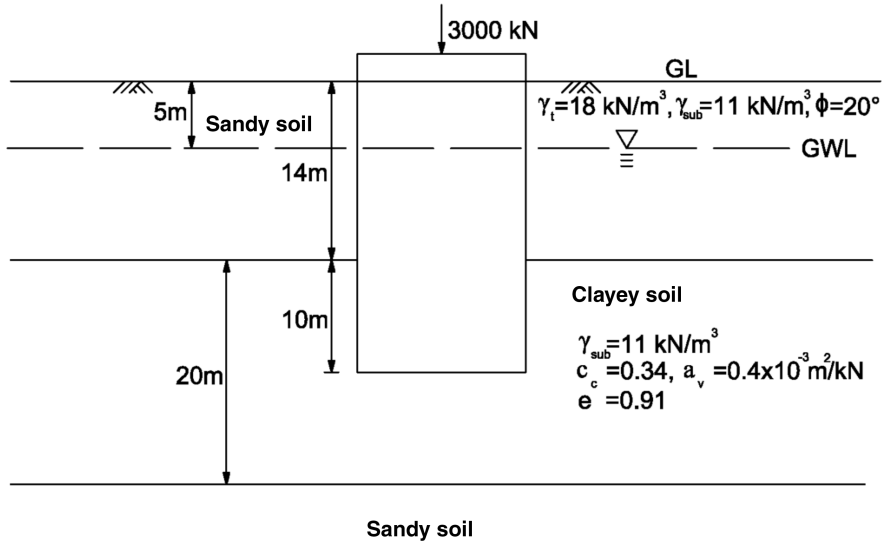

Figure 9.24 Problem 9.6.

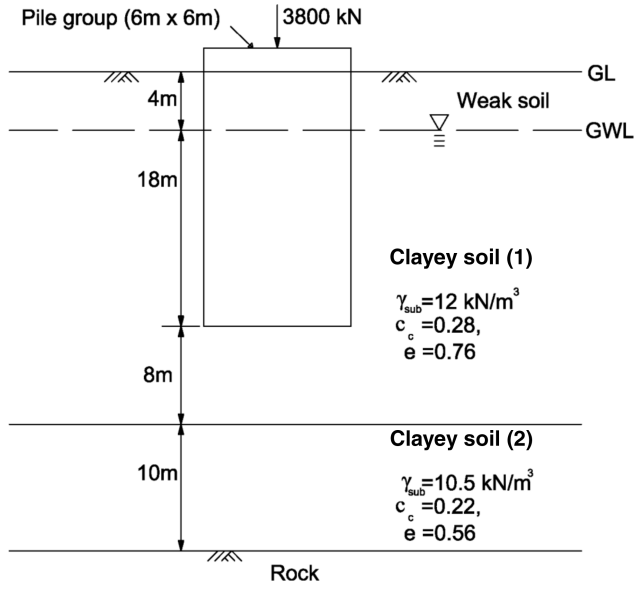

Figure 9.25 Problem 9.8.

9.6 If a pile group and pile cap with an overall plan dimensions of 5×8 m is subjected to a total load of 3000 kN as shown in Figure 9.24, compute the consolidation settlement of the group. Length of embedded piles $= 24$ m.

9.7 A circular pile group with a diameter of 8 m in plan is subjected to a total load of 3200 kN in a soil with details as shown in Figure 9.24. Compute the consolidation settlement.

9.8 A square pile group with overall dimension of 6×6 m in plan is constructed in a soil, as shown in Figure 9.25. Compute the consolidation settlement. Length of embedment is 22 m.

9.9 If the pile group in problem 9.8 is rectangular in plan of size 6×8 m with the soil data being the same as shown in Figure 9.25, calculate the consolidation settlement.

9.10 If the pile group in Figure 9.25 is circular in plan of 10 m diameter, calculate the consolidation settlement.

10

Design of Piles and Pile Groups

10.1 Introduction

Piles are structural members made of timber, concrete, steel or other materials which are used to transmit loads from superstructure to deeper soil strata. These are referred to as deep foundations as the foundation level is much below the depth of shallow foundations (Chapter 4). The definitions, classifications and details of pile foundations are given in Chapter 9. The situations where pile foundations may have to be used are indicated below.

10.2 Use of Pile Foundations

Pile foundations may be used for the following situations:

1. To transfer loads through water or soft soil to a suitable bearing stratum (end bearing or point bearing piles).
2. To transfer loads in a relatively weak soil by means of *skin friction* along the length of the piles (friction piles).
3. To compact granular soils (thus increasing their bearing capacity) (compaction piles).
4. To carry the foundation beyond the depth of scour to provide safety in the event the soil is eroded away.
5. To anchor down the structures subjected to uplift due to water pressure or excessive moments (tension piles or uplift piles).
6. To provide anchorage against horizontal forces from sheetpiling walls or other pulling forces (anchor piles).
7. To shield water front structures against impact from ships or other floating objects (fender piles and dolphins).
8. To carry large horizontal or inclined loads (batter piles).

10.3 Types of Piles and Pile Groups

Piles may be classified according to their installation, composition or function. The details are given in Chapter 9. Generally piles are used in groups to carry the large loads coming from the

Foundation Design: Theory and Practice N. S. V. Kameswara Rao
 ISBN: 978-0-470-82534-1

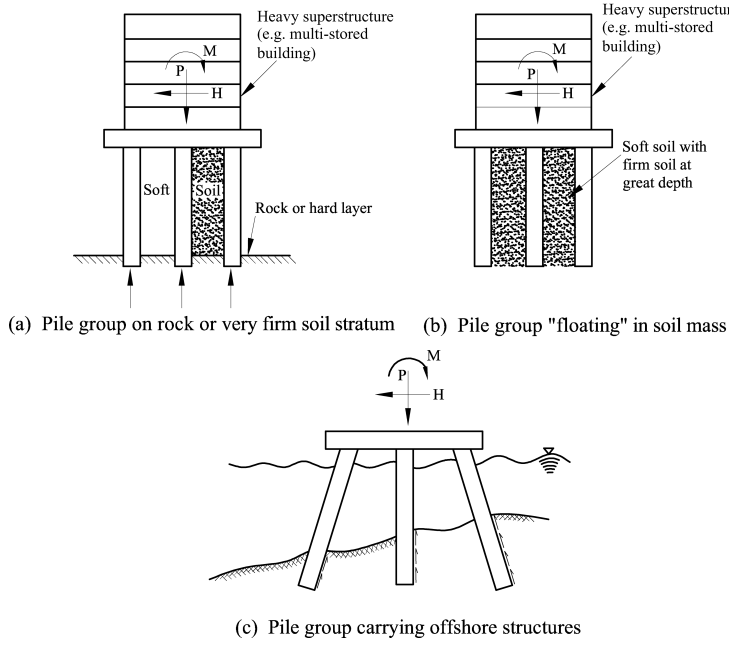

Figure 10.1 Pile groups carrying heavy superstructures.

superstructure as shown in Figure 10.1. The group may consist of three or more piles in general, and two piles occasionally. The minimum spacing (center to center) of piles suggested by a few building codes are given in the following Table 10.1 (Bowles, 1996).

Table 10.1 Minimum spacing of piles.

Type of pile	BOCA, 1993	NBC, 1976	Chicago, 1974
Friction	$2D$ or 1.75 H $\geq$ 760 mm	$2D$ or 1.75 H $\geq$ 760 mm	$2D$ or 1.2 H $\geq$ 760 mm
Point bearing	$2D$ or 1.75 H $\geq$ 610 mm	$2D$ or 1.75 H $\geq$ 610 mm	

where D: pile diameter; H: diagonal distance for rectangular shaped piles.

Optimum spacing between piles, s, generally recommended for use is $2.5D$ to $3.5D$ or $2H$ to $3H$. For pile groups carrying lateral and/or dynamic loads, larger spacing is more efficient. Though maximum spacing between piles is not prescribed in building codes, spacing up to $8D$ to $10D$ are used depending on the design and economy.

10.4 Efficiency of Pile Groups

The typical stresses/soil pressures produced from shaft friction or end bearing of a single pile and a group of piles are shown in Figure 10.2. If piles are used in groups, there may be an overlap of stresses, as shown in Figures 10.2(b), (d) and (e), if the spacing is too close. If the overlap is large, the soil may fail in shear or settlement will be very large. Though the overlapping zone of stresses obviously decreases with increased pile spacing, it may not be feasible since the pile cap size becomes too large and hence expensive.

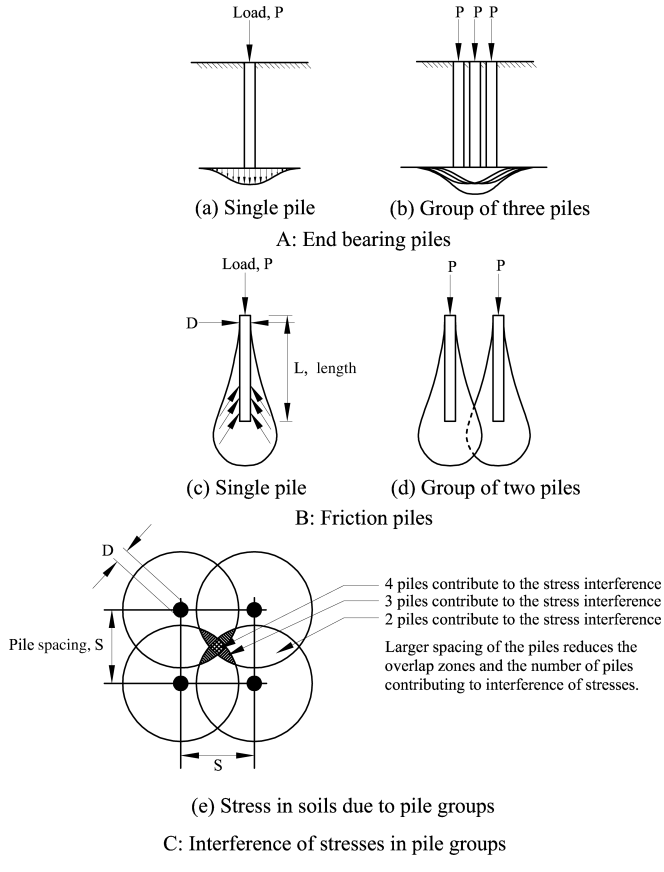

Figure 10.2 Stresses in soil due to loads on single pile and pile groups.

It is a common practice to calculate the capacity of a pile group by means of an efficiency factor η given as

$$\eta = \frac{\text{ultimate load capacity of pile group}}{\text{sum of ultimate load capacities of individual piles}} \tag{10.1}$$

Several empirical efficiency formulae are used to relate group efficiency to pile spacings for piles in cohesive soils (Poulos, 1980), as follows:

1. Converse–Labarre formula (Poulos, 1980)

$$\eta = 1 - \frac{\varsigma\left[\frac{(n-1)m + (m-1)n}{mn}\right]}{90} \tag{10.2}$$

where $\varsigma = \tan^{-1}(d/s)$
m = number of columns of piles in the group
n = number of rows of piles in the group

d = diameter of the pile
s = spacing of the piles in the group.

This equation can only be applied to rectangular groups with regular arrangement, that is, m, n and s can be identified.

2. Feld's rule, which reduces the calculated load capacity of each pile in a pile group by 1/16 for each adjacent pile taking no account of the pile spacing (Ramiah and Chickanagappa, 1981).
3. There is another empirical rule (Iyer, 1995) in which the calculated load capacity of each pile is reduced by a proportion α for each adjacent pile where

$$\alpha = \frac{1}{8}\frac{d}{s} \tag{10.3}$$

where d = diameter of the pile and s = spacing of the piles

For pile groups in sands it is fairly well established that the group efficiency may often be greater than 1. The axial capacity of a pile group may be calculated in much the same way as that for a single pile, the only difference being that the failure of the pile group as a block has now to be considered as shown in Figure 10.3 and discussed in subsequent sections.

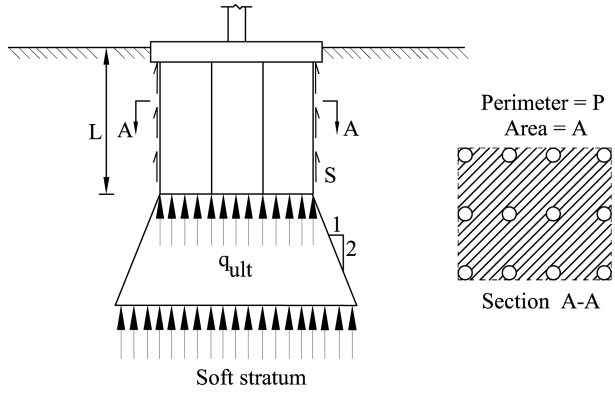

Figure 10.3 Maximum capacity of pile group.

10.5 Analysis and Design of Pile Foundations

Due to the wide variety of choices of piles based on materials, methods of construction, pile capacity assessment, applications, site conditions and so on, methods of analysis and design also vary in some details but mainly follow the usual laws of mechanics. The usual methods followed are discussed below.

10.5.1 Loads and Pile Configuration

The pile group can be designed and analyzed for any number of loads coming on the structure. However, a configuration of the pile group has to be selected (as an initial guess) in accordance with the loads that the pile group has to cater for. This is achieved by a set of heuristics inherent

in any design process. The first section gives the handling of the loads to make it more amenable for the choice of a pile group, the second section deals with how an initial selection of a pile group is made and the final section deals with the checks imposed on the group and how a final selection is made.

10.5.2 Loads

The loads are specified in the form of a point of action of the load, the x, y and z components of the forces and the x, y and z components of the moments. The axis that is chosen by the user to specify the loads is not important since the loads are transformed so that the origin passes through the C.G. of the pile group (C.G. of cross sectional area of piles).

There are distinct advantages of transforming the axis so that the origin passes through the C.G. of the pile group (C.G. of cross sectional area of piles). These advantages are listed below.

1. The major advantage of such a transformation is the alignment of the pile group. Once the loads have been so transformed, the pile group can be placed so that the length and breadth of the pile group are in conformity with the spatial distribution of the loads. An alignment in variation to this would result in a pile group spread over an extent that is much more than is required.
2. It is also preferable to make the center of the pile group coincide with the center of the load system to minimize the difference in loads coming on the individual piles in the group. This is very important in order to optimize the piles used.
3. Such a transformation also helps in the competitions.

The piles in the group can all be defined with the center of pile group at the origin. A pile group with the right handed Cartesian coordinate system is shown in Figure 10.4. The process of transformation is achieved by first rotating the loads about the origin. The loads are then laterally shifted so that the center of the load system coincides with the origin. In such a case, the loads and moments also have to be suitably transformed. Sometimes due to excessive moments or

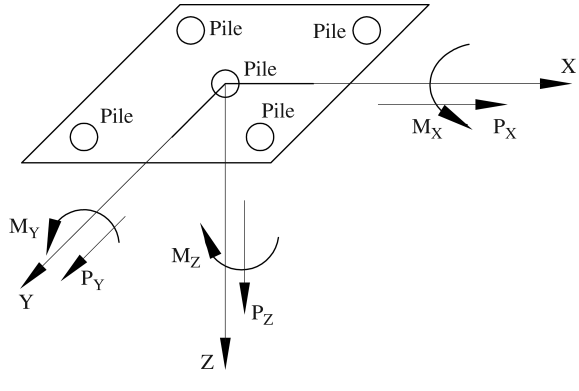

Figure 10.4 Pile group subjected to general loads and moments.

excessive differences in the loads, the center of the force system may be very far away from the geometric center of the points of application of the loads. In such a case the center has to be limited to the middle third of the area over which the loads are spread or else the moments coming on the pile cap may become excessive.

10.5.3 Pile Configuration

The number of piles can be easily selected on the basis of the axial and lateral loads on the system and the axial and lateral capacities of the piles. There are two criteria which govern the initial selection of the pile configuration:

1. The pile group should be oriented such that the length of the group lies in the direction perpendicular to the axis having a greater moment. Since the piles have now been oriented with respect to the loads, this leaves us to choose only between two perpendicular directions.
2. The pile group should be oriented such that the length of the group lies as far as possible along the length of the load system.

On the basis of these two criteria an initial number is assigned according to which we can choose an appropriate length to width ratio of the group.

10.5.4 Checks Imposed on the Pile Group

Checks are imposed on the selected pile group in stages. Initially a check for the extent of the load and the pile group is imposed in order to ensure that the loads do not come on the pile cap at a point outside the pile group. This would result in excessive moments in the pile cap. It is assumed that all loads P_x, P_y, and P_z transmitted from the superstructure are shared by piles in the group in proportion to their areas of cross section.

Next, checks are imposed such that the individual piles have adequate factors of safety against axial load, lateral load, moments and combined axial and lateral load. The axial load coming on a pile is calculated by the expression

$$P_{zi} = \frac{P_z A_i}{\sum A_i} \pm \frac{M_x y_i A_i}{I_{xx}} \mp \frac{M_y x_i A_i}{I_{yy}} \tag{10.4}$$

where

P_{zi} is the axial load coming on the i-th pile

n is number of piles in the group

P_z is the resultant of all the vertical loads

M_x is the resultant moment about the x axis

M_y is the resultant moment about the y axis.

A_i is the area of cross section of the i-th pile. If A_i is the same for all the piles ($i = 1$ to n) in the group, then $\frac{A_i}{\sum A_i} = \frac{1}{n}$ and the first term on the right hand side (RHS) of Equation (10.4) simplifies as $\frac{P_z}{n}$.

x_i, y_i are the x, y coordinates of the i-th pile with respect to the origin (C.G. of pile group). x, y, z are the right handed coordinate axes as shown in Figure 10.4.

I_{xx}, I_{yy} and I_{zz} are the moments of inertia of the pile group about the x, y and z axes respectively. I_{xx} , I_{yy} and I_{zz} are obtained as given below (using parallel axes theorem and neglecting the moments of inertia of the pile cross sections about their own axes).

$$\begin{aligned} I_{xx} &= A_1 y_1^2 + A_2 y_2^2 + \cdots + A_n y_n^2 = \sum A_i y_i^2 \\ I_{yy} &= A_1 x_1^2 + A_2 x_2^2 + \cdots + A_n x_n^2 = \sum A_i x_i^2 \\ I_{zz} &= I_{xx} + I_{yy} = \sum A_i r_i^2 \end{aligned} \tag{10.5}$$

where

$$r_i^2 = x_i^2 + y_i^2$$

The lateral loads coming on any pile along x and y direction (horizontal axes) can be expressed as

$$P_{hxi} = \frac{P_x A_i}{\sum A_i} - \frac{M_z y_i A_i}{I_{zz}} \tag{10.6}$$

$$P_{hyi} = \frac{P_y A_i}{\sum A_i} + \frac{M_z x_i A_i}{I_{zz}} \tag{10.7}$$

Thus the resultant horizontal load on the *i*-th pile is

$$P_{hi} = \sqrt{P_{hxi}^2 + P_{hyi}^2} \tag{10.8}$$

where

P_{hxi} is the lateral load coming on the *i*-th pile in the *x* direction.
P_{hyi} is the lateral load coming on the *i*-th pile in the *y* direction.
P_x is the resultant of all the horizontal loads in the *x* direction.
P_y is the resultant of all the horizontal loads in the *y* direction.
M_z is the torsional moment about the *z* axis.
x_i, y_i are the *x* and *y* coordinates of the *i*-th pile with respect to the origin (C.G. of pile group).
A_i is the area of the *i*-th pile. If A_i is the same for all the piles ($i = 1$ to n) in the group, then $A_i / \Sigma A_i = 1/n$ and the first term on the right hand side (RHS) of Equations (10.6) and (10.7) simplifies as $\frac{P_x}{n}$ and $\frac{P_y}{n}$ respectively.
I_{zz} is the torsional moment of inertia of the pile group.

The safety against combined axial and lateral load can be checked by treating the pile as a column under combined axial and lateral load.

After this the pile group is checked for group capacities. Finally a check on the settlements of the individual piles as well as on the pile group is made.

It is possible, that after all these checks there are several alternative designs feasible. In order to make a final choice a representative economic analysis is made. Three factors are considered in the economic analysis:

1. The quantity of concrete
2. The quantity of steel
3. Additional costs per unit length of the pile which could be interpreted as the cost of installation of the pile.

10.6 Lateral Capacity of Piles

Deep foundations subjected to lateral loads should be designed so that they satisfy the following conditions (Iyer, 1995):

1. The pile or drilled shaft should be able to carry the imposed load with an adequate margin of safety against failure in bending.
2. The deflection of the foundation under the load should not be larger than the tolerable deflection for the structure it supports.
3. The soil around the pile or shaft should not be loaded so heavily that it reaches its ultimate load carrying capacity.

10.6.1 Single Pile

A single pile with the lateral load is shown in Figure 10.5. There are different design philosophies prevalent for the estimation of the lateral load carrying capacity of a single pile.

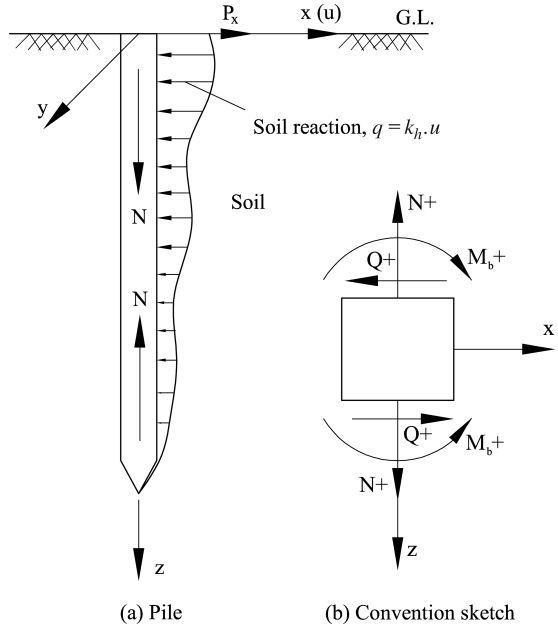

Figure 10.5 Single pile subjected to lateral/horizontal load.

1. **Conventional Statical Approach**
   The simplest method of estimating the ultimate lateral resistance of a floating pile is to consider the statics of the pile by drawing an approximate soil resistance profile along the length of the pile. Brom's (1964) theory is an application of this approach in which simplifications are made to the ultimate soil resistance distribution along the pile and also full consideration is given to restrained or fixed-headed piles as well as unrestrained or free headed piles. For a general distribution of soil resistance with depth the method given by Brinch Hansen and Christensen (1961), described in detail by Tomlinson (1977), may be used.

2. **Subgrade Reaction Approach**
   This approach is based on the assumption that the soil reaction q is proportional to the deflection of the pile. The ratio of the soil reaction to the deflection is called the modulus of subgrade reaction, k_s, which is a function of the modulus of elasticity, E_s (further details are given in Chapter 4). Solutions have been developed for E_s constant with depth (Hetenyi, 1946) and also for variation of E_s with depth and for layered soils.
3. ***p–y* Curves**
   The subgrade reaction approach is only applicable to the deflection of pile within the elastic compression of soil caused by the lateral loading of piles. The p – y curves developed by Reese (Tomlinson, 1977) represent the deformation of the soil at any given depth below the soil surface for a range of horizontally applied pressures from zero to the stage of yielding of the soil in ultimate shear.
4. **Characteristic Load Method**
   The characteristic load method described by Duncan, Evans and Ooi (1994), like the *p–y* curve approach, takes into account the nonlinearity in the soil response to a lateral load. It gives nondimensional characteristic loads and moments as a means of normalizing the soil response. Curves are then given for the estimation of the ratio of applied load to the characteristic load and applied moment to the characteristic moment for different levels of deflections.

10.6.2 Additional Considerations

The lateral load carrying capacity of a single pile depends not only on the horizontal modulus of subgrade reaction of the surrounding soil but also on the structural strength of the pile shaft against bending consequent upon application of a lateral load. While considering lateral load of piles, effect of other coexistent loads including the axial load on the pile should be taken into consideration for checking the structural capacity of the shaft. Values of modulus of horizontal subgrade reaction are given for different types of soils in the codes and are given in Tables 10.2 and 10.3. Also the fixity lengths for the various values of the modulus of subgrade reaction are given in the form of graphs in Figures 10.6(a) and (b) (Part 1 of IS: 2911–1984, 1984).

Table 10.2 Typical values of n_h as defined in Figure 10.6(a).

Soil type	n_h (kg/cm^3)[a]	
	Dry	Submerged
Loose sand	0.26	0.146
Medium sand	0.775	0.526
Dense sand	2.076	1.245
Very loose sand under repeated loading	—	0.041

[a]kg is in units of force.

The concept of the fixity length of a pile can also be used to calculate the approximate bending moments caused by the lateral loads in piles to avoid the cumbersome calculations of the BEF approach (Section 10.6.4). This fixity length approach is used by several designers and is illustrated in Sections 10.14 and 10.15.

Table 10.3 Typical values of K_h for preloaded clays.

Unconfined compression strength (kg/cm^2)[a]	Range of values of K_h (kg/cm^2)[a]	Probable values of K_h (kg/cm^2)[a]
2–4	7–42	7.73
10–20	32–65	48.79
20–40	65–130	97.73
40	—	195.46

[a]kg is in units of force.

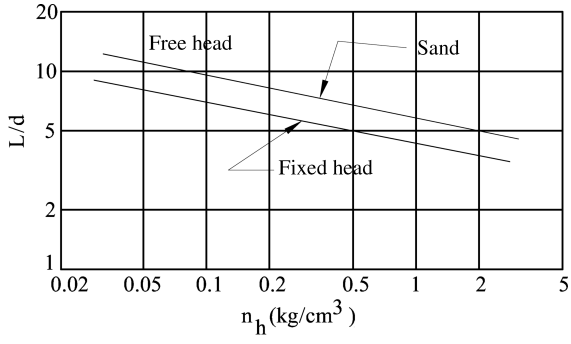

L = equivalent length of cantilever giving the same deflection at ground level as the actual pile.
d = diameter of the pile.
n_h = constant to be taken from Table 10.2 for calculation of L / d in sands.
* kg is in force units.

(a) L/d versus n_h for equivalent length in sand

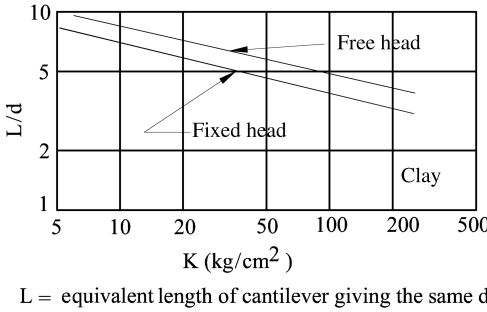

L = equivalent length of cantilever giving the same deflection at ground level as the actual pile.
d = diameter of the pile.
* kg is in force units.

(b) L/d versus K for equivalent cantilever length in clay

Figure 10.6 Fixity length of piles subjected to lateral loads.

This is an approximate approach which needs to be used with caution after verifying with local practices and codes. From the distribution of shear force and bending moment diagrams shown in Figures 9.8 and 9.9, such a simplification as illustrated in Sections 10.14 and 10.15 appears to be reasonable. However, it should be verified by the BEF approach or other methods.

It may be also noted that maximum BM due to lateral loads in piles is used mainly to compute the reinforcement needed in the pile in combination with the vertical load as in a column. It does not affect any other parameters of pile design, once the maximum allowable lateral load of individual pile is decided. Further, the construction agencies have usually their customized procedures to ensure the allowable maximum bending moment in individual piles (both for driven piles as well as cast *in situ* piles).

10.6.3 Methods of Analysis

In most cases consideration of bending moments and deflections govern design, because the ultimate load carrying capacity of the soil is reached only at very large deflections. The statical approach does not consider the load–deflection response.

The method of *p–y* curves requires a great deal of time to develop the input and is highly computer-intensive.

The characteristic load method works only for uniform soil conditions, that is, it assumes that the pile is embedded in the same type of soil throughout its length. Hence the method that can be adopted is one based on the beam on elastic foundation approach described by Vlasov and Leontev (1960), Kameswara Rao (1971). The method is explained in detail in Chapters 4 and 5. Since the method suggested by Brinch-Hansen is much more easy to apply for the case of a short pile it may be used in preference to the beam on elastic foundation approach. This method is given in Section 10.6.5.

10.6.4 Beam on Elastic Foundation Approach

This approach is discussed in detail in Chapters 4 and 5. However, a brief discussion is presented below with focus on laterally loaded piles.

Noting that the axis of the pile is along the z direction as shown in Figure 10.5, the governing equation for a beam on Winkler foundation can be expressed (Chapter 4) by the differential equation (Hetenyi, 1946) as

$$E_p I_p \frac{d^4u}{dz^4} + k_h u = p \tag{10.9}$$

where

E_p is the Young's modulus of the material of the pile

I_p is the moment of inertia of the cross-section of the pile

u is the lateral/horizontal displacement of the pile

p is the load distribution on the pile, that is, external lateral load applied along lateral (x axis) direction

k_h is the modulus of subgrade reaction in the horizontal direction.

Vesic (1961) analyzed an infinite (horizontal) beam on an elastic foundation and compared the results with those obtained by the use of Winkler's hypothesis. He concludes that the problem of bending of beams resting on a semi-infinite elastic subgrade can be treated with reasonable accuracy with the use of the concept of a coefficient of subgrade reaction. He has an expression for the value of k_h, which can be adopted for piles as

$$k_h = \frac{1.3}{B} \sqrt[12]{\frac{E_s B^4}{E_p I_p}} \frac{E_s}{1-\nu_s^2} \tag{10.10}$$

where B is the beam width and E_s, ν_s are elastic constants of the soil.

$E_p I_p$ are, respectively, the modulus of elasticity and moment of inertia of the cross section of the pile about the axis of bending.

The expression for k_s in the vertical direction is given in Equation (4.41).

The differential equation needs to be used for piles which are subjected to both axial loads and lateral loads as applicable to a beam–column (Hetenyi, 1946), that is, Equation (10.9) needs to be modified to also take into account the axial load.

Accordingly, the modified equation is

$$E_p I_p \frac{d^4u}{dz^4} - N\frac{d^2u}{dz^2} + k_h u = p \tag{10.11}$$

where N is the axial load on the beam–column/pile which actually varies with depth due to the friction on the surface of the pile. For the case when $N = 0$, Equation (10.11) reduces to Equation (10.9). For the case when N varies with depth, numerical solutions can be obtained as described in Chapters 6 and 7. For the case when $N = 0$, exact or numerical solutions can be obtained using methods discussed in Chapters 5–7. For the case when $N =$ constant again exact solutions can be obtained by the methods described in Chapter 5 (including the method of initial parameters). However for the case when $N =$ constant, initial steps for obtaining the exact solutions as described in Chapter 5 are presented below.

The characteristic equation of the ODE that is, Equation (10.11) is

$$E_p I_p m^4 - Nm^2 + k_h = 0 \tag{10.12}$$

The roots of characteristic equation are

$$m_{1,2,3,4} = \pm(\alpha \pm i\beta) \tag{10.13}$$

where

$$\alpha = \sqrt{\lambda^2 + \frac{N}{4E_p I_p}} \tag{10.14}$$

$$\beta = \sqrt{\lambda^2 - \frac{N}{4E_p I_p}} \tag{10.15}$$

in which

$$\lambda = \sqrt[4]{\frac{k_h}{4EI}}$$

Hence the homogeneous solution for Equation (10.11) can be written as

$$u_h = C_1F_1 + C_2F_2 + C_3F_3 + C_4F_4 = C^TF = F^TC \tag{10.16}$$

C is the matrix of constant coefficients which have to be solved from the boundary conditions. C can be expressed in a matrix form as

$$C = \begin{Bmatrix} C_1 \\ C_2 \\ C_3 \\ C_4 \end{Bmatrix}$$

F is the basis of solution and is given by

$$F = \begin{Bmatrix} F_1 \\ F_2 \\ F_3 \\ F_4 \end{Bmatrix} = \begin{Bmatrix} e^{\alpha z}\cos\beta z \\ e^{-\alpha z}\cos\beta z \\ e^{\alpha z}\sin\beta z \\ e^{-\alpha z}\sin\beta z \end{Bmatrix} \tag{10.17}$$

The derivative of the basis of solutions for the homogeneous solution can be expressed as

$$\frac{d\{F\}}{dz} = [N_H]\,\{F\} \tag{10.18}$$

where N_H is given by

$$N_H = \begin{bmatrix} \alpha & 0 & -\beta & 0 \\ 0 & -\alpha & 0 & -\beta \\ \beta & 0 & \alpha & 0 \\ 0 & \beta & 0 & -\alpha \end{bmatrix} \tag{10.19}$$

The parameters, that is, displacement u, slope u', moment M_b and shear force Q at any point can be expressed as

$$\begin{aligned} u &= \{C\}^T\{F\} \\ u' &= \frac{du}{dz} = \{C\}^T[N_H]F\} \\ M_b &= EI\frac{d^2u}{dz^2} = E_fI_f\{C\}^T[N_H]^2F\} \\ Q &= -EI\frac{d^3u}{dz^3} = -E_fI_f\{C\}^T[N_H]^3F\} \end{aligned} \quad or \quad \begin{Bmatrix} u^+ \\ u' \\ M_b \\ Q \end{Bmatrix} = BC \tag{10.20}$$

Hence

$$\begin{Bmatrix} u \\ u' \\ M_b \\ Q \end{Bmatrix}_{z=0} = [B]_{z=0}\{C\} \tag{10.21}$$

If we refer to the matrix on the left of the equality as $\{I_p\}$, the matrix of initial parameters, we can write

$$\{I_p\} = [B]_{z=0}\{C\} = [A]\{C\} \tag{10.22}$$

Hence the $\{C\}$ matrix can be written as

$$\{C\} = [A]^{-1}\{I_p\} = [G]\{I_p\} \tag{10.23}$$

From Equations (10.20), we get

$$\{I_p\} = [B]\{C\} = [B][G]\{I_p\} = [K]\{I_p\} \tag{10.24}$$

The total solution can be given by

$$u_T = u_h + u_p$$

where u_h and u_p are the homogenous solution and particular integral. The details of obtaining the total solution from now on will be the same as given in Chapter 5.

Equations (10.20)–(10.24) are similar to Equations (5.35)–(5.39) in Chapter 5, except that the basis of solutions F_1 to F_4 (Equation (10.17)), the coordinate axes and the direction of the displacement are different. The general solutions can be obtained as given in Section 5.5.

For example, if the parameters at any point (say $z = l$) are represented as $\{F_p\}$, they can be written as

$$\{F_p\} = [K]\{I_p\} - \{F_{\text{part}}\} \tag{10.25}$$

where $\{F_{\text{part}}\}$ is the matrix of functions depending on the external load. These can be obtained by multiplying the relevant terms of the $[K]$ matrix by the force applied. For the case of a lateral load at the head of the pile the terms of the $\{F_{\text{part}}\}$ can be obtained as

$$\begin{aligned} F_u &= P_x(K_{1,4}) \\ F_{u'} &= P_x(K_{2,4}) \\ F_M &= P_x(K_{3,4}) \\ F_Q &= P_x(K_{4,4}) \end{aligned} \tag{10.26}$$

where P_x is the lateral force applied at the head of the pile.

For a layered soil profile one could proceed down the length of the pile by expressing the final parameters, at the bottom of the layer, in terms of the initial parameters, at the top of the layer, and considering these final parameters as the initial parameters for the subsequent layer. Proceeding in this fashion one could express the parameters at the bottom of the pile in terms of the parameters at the top of the pile.

10.6.4.1 Infinitely Long Beam

For a pile with a lateral load applied at its head, the deflection and slope, tend to zero with increasing depth as is for a beam with a concentrated load as we move away from the point of application of the load. Hetenyi (1946) has found that this distance can be expressed as $1.5\pi/\lambda$.

Hence if we were to consider a pile with length greater than $1.5\pi/\lambda$ as a infinitely long pile, we could determine the parameters at the top of the pile. Once these have been determined, we could proceed from top to bottom and calculate the lateral carrying capacity as the sum of the soil reaction over the length given by $(k_h u)$ from top to bottom.

10.6.5 Short Piles – Brinch Hansen's Method

For short piles Brinch Hansen (Brinch Hansen and Christensen (1961)) suggested a simple method for calculating the lateral load capacity as shown in Figure 10.7. The resistance of the pile to rotation about the point x in Figure 10.7 is given by the sum of the moments of the soil resistance above and below this point. The passive resistance diagram is divided into a convenient number of n horizontal elements of depth L/n. The unit passive resistance of an element at depth z below the ground surface is then given by

$$p_z = p_{oz}K_{qz} + cK_{cz} \tag{10.27}$$

where p_{oz} is the effective overburden pressure at depth z, c is the cohesion of the soil at depth z, and K_{qz} and K_{cz} are the passive earth pressure coefficients for the frictional and cohesive components respectively at depth z (Figure 10.8).

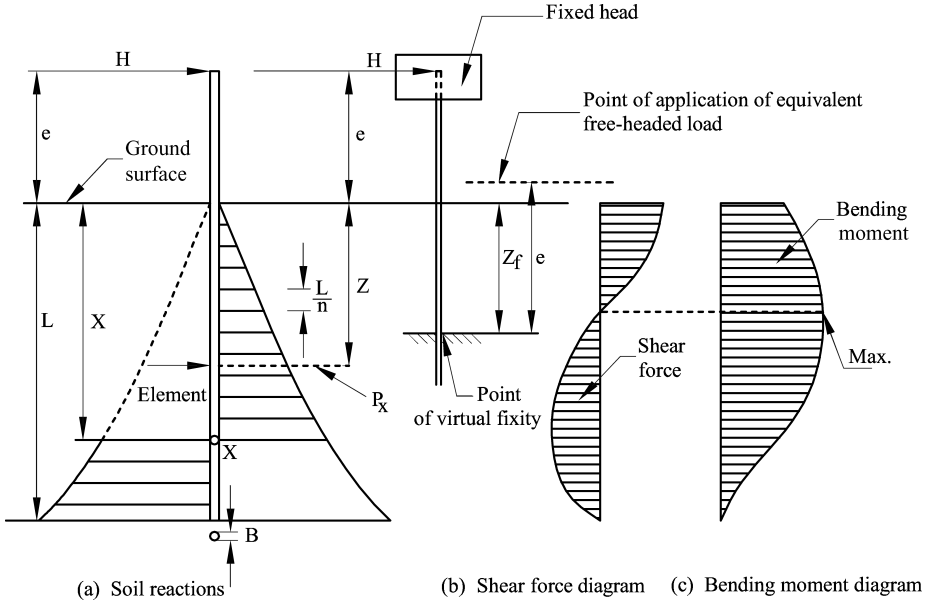

Figure 10.7 Brinch-Hansen's method for short piles.

The total passive resistance on each horizontal element is $p_z(L/n)B$ and by taking the moments about the point of application of the horizontal load, we get

$$\sum M = \sum_{z=0}^{z=x} p_z \frac{L}{n}(e + z)B - \sum_{z=x}^{z=l} p_z \frac{L}{n}(e + z)B \tag{10.28}$$

where B is the width/diameter of the pile cross section. The point of rotation has to be obtained by trial and error and it is correctly obtained when $\sum M = 0$. Having obtained the center of rotation from Equation (10.28), the ultimate lateral resistance of the pile to the horizontal force

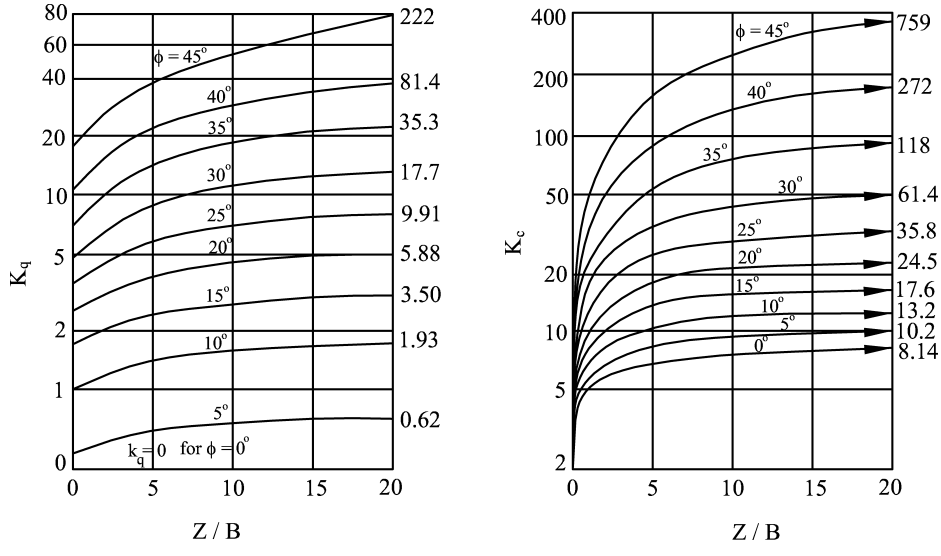

Figure 10.8 Brinch-Hansen's coefficients K_q and K_c.

H_u can be obtained by taking moments about the point of rotation, that is

$$H_u(e + z) = \sum_{0}^{x} p_z \frac{L}{n} B(x + z) + \sum_{x}^{x+L} p_z \frac{L}{n} B(z - x) \tag{10.29}$$

The ultimate bending moment, which occurs at the point of zero shear, should not exceed the ultimate moment of resistance M_u of the pile shaft. However it is quite often found that M_u is exceeded. For cases where this does take place the ultimate lateral load carrying capacity is calculated on the basis of a scheme suggested by Carter and Kulhawy which is reported by Randolph (1981) and Randolph *et al.* (1992).

10.6.6 Structural Checks

It has to be checked that the solution obtained does not violate either the maximum deflection criterion, the limiting moment criterion or the maximum permissible shear force criterion. The maximum permissible lateral deflection of the pile would depend on the use to which the superstructure is to be put and hence is user-defined criterion. The maximum moment of a pile section can be calculated from the shape, dimensions and quantity of reinforcement steel in the pile section by the limit state theory. The minimum quantity of steel to be used as longitudinal reinforcement for bored piles is given as 0.4% of the cross-sectional area of the pile or as required to cater for handling stresses (Part 1 of IS: 2911–1984, 1984). The minimum quantity of steel to be used as longitudinal reinforcement in a driven pile is given as (IS: 2911–1984, Part 1, Section 3) as follows:

1. For piles of length $<30\times$ the least width – 1.25%
2. For piles with a length 30–40$\times$ the least width – 1.5%
3. For piles with a length $>40\times$ the least width – 2.0%.

10.7 Pile Group

In the estimation of the lateral load capacity of a pile group an approach similar to that adopted for the calculation of vertical load capacity can be taken. The group capacity of a group of piles is the smaller of the following two values, that is:

1. n times the lateral load capacity of a single pile.
2. The lateral load capacity of an equivalent single block containing the piles in the group and the soil in between them.

10.7.1 Methods Available

The concept of efficiency factor for lateral loading, like one for vertical loading, has been suggested by Poulos (1980). He has attempted to plot curves of group efficiency versus spacing/pile diameter.

Instead, Randolph *et al.* (1992) suggested (avoiding calculations based on efficiency factors) a method taking into account the shear stresses developed on the soil between two piles as shown in Figure 10.9. They gave the expression

$$P_u = 2K\sigma'_v s \tan \phi' \tag{10.30}$$

where

K = earth pressure coefficient
σ'_v = effective vertical stress
ϕ' = angle of internal friction
s = spacing between piles.

However, they state that the value of K to be used in the above expression is open to question.

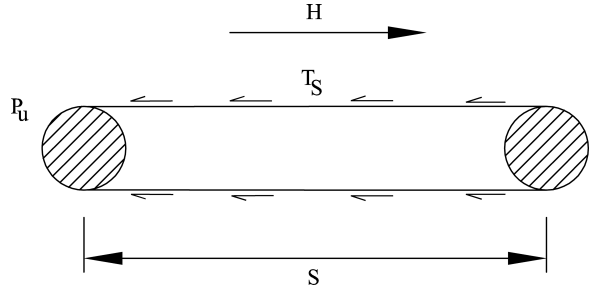

Figure 10.9 Plan view of block failure of piles under lateral load.

10.8 Settlement of Piles

The settlement of a pile is the sum of the immediate or elastic settlement and long-term or consolidation settlement. Only the immediate or elastic settlement of the pile/pile group is

discussed in this section along with discussion on the implications of soil pile interaction. The evaluation of primary consolidation settlement of pile groups is discussed in detail in Sections 9.8 and 9.9.

The total settlement of a single pile under axial load consists of the following components:

1. Elastic compression of the pile
2. Movement of pile relative to the surrounding soil
3. Settlement of surrounding soil due to pile load; this comprises of elastic deformation and consolidation settlement
4. Settlement of soil under the pile tip (elastic as well as consolidation)
5. Creep of pile material under constant axial load.

The settlement of a pile group is more complex because of overlapping of stresses in the soil introduced by the closely spaced piles. Under equal axial load per pile, the pile group generally settles more than a single pile due to the stress overlapping (Figure 10.2). The procedures for settlement analysis varies with the type of piles and the soil conditions, as discussed below.

10.8.1 Point-Bearing Piles on Bedrock

If the pile tips are on the rock and if the rock is not soft, the net settlement of a pile is generally not more than a few millimeters after deduction of rebound. However, well designed and constructed buildings supported on piles driven to solid hard rock have been subjected to total settlements several times as much as the net settlement of the test pile. The larger settlements are thought to be the result of one or more of the following factors:

1. Small uplift of piles due to driving of adjacent piles
2. Long-term creep of pile material under constant load
3. Overlapping of stresses in soil
4. Negative skin friction as a result of disturbance of clay due to pile driving.

However, the total net settlement of well designed and constructed pile foundations on rock generally will not be so large as to cause concern, unless the bedrock is soft. In this case, quantitative analysis is very difficult and in practice it can only be estimated by judging from the characteristics of the rock core samples and local experience, if available.

10.8.2 Point-Bearing Piles in Sand and Gravel

The settlement of a single pile driven in granular soils can be readily determined by load test since the settlements of such soils take place immediately after load application. However, the test must be so made to differentiate or eliminate the skin friction. The settlement of a pile group is considerably greater than that of a single point-bearing pile as discussed above. For a group of piles having the customary pile spacing, the tentative relationship shown in Figure 10.10 may be used. Pile groups closely located should be considered as one large cluster if they are connected to different pile caps.

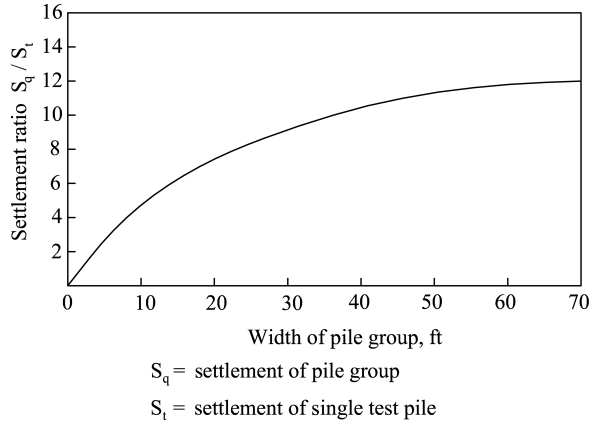

Figure 10.10 Settlement of group of point-bearing piles in sand. (Reproduced from *Proceedings of the 3rd International Conference on Soil Mechanics and Foundation Engineering*, vol. **3**, A.W. Skempton, "Discussion: settlement of pile group in sand," p. 172, August 16–27, © 1953, Zürich, Switzerland, with permission from Geotechnik Schweiz, formerly SGBF Swiss Society for Soil and Rock Mechanics.)

Also, there could be the possibility of additional settlement due to layer or layers of weak soil below the compact or hard layer which supports the pile caps. The stress in lower layers may be approximated by the 60° distribution method as discussed in Section 9.8.

10.8.3 Point-Bearing Piles on Hard Clay

Settlement of a single pile or a group of piles driven to hard clay cannot be determined by practical means. A very rough idea as to the order of magnitude of settlement may be obtained by laboratory tests on the basis of broad assumptions, approximations, and simplifications. Records of existing pile foundations are the most valuable information, if available.

Load tests on such piles usually give optimistic results because an extremely long time is necessary for consolidation. The process of consolidation may be accelerated if the tip of the test pile is provided with porous material and the excess water is drained out during the test. Even so, a load test may require long time for complete consolidation. Such lengthy load test is not feasible in all construction projects. Therefore, if pile load tests are conducted for the purpose of determining the ultimate bearing capacity, the load settlement relationship as established by the tests must be interpreted very carefully.

10.8.4 Friction Piles in Sand and Gravel

The load–settlement relationship of a single friction pile in granular soils can be determined reliably by pile load test. The time required for the test is relatively brief since settlement in such soils takes place shortly after load application.

If the settlement of the test pile is acceptable, the settlement of a pile group in such soils will be of no concern. This is because the granular soil between the piles is compacted by displacement of the piles and becomes locked in between as a dense mass. The settlement

probably approaches that of a pier foundation having a depth and base area equal to those of the pile group.

10.8.5 Friction/Adhesion Piles in Clays

The settlement of a single friction pile in clay cannot be determined within a short period because of the long time taken for consolidation. With elaborate laboratory tests, the settlement may be computed by elastic theory (Seed and Reese, 1957). There is no accurate method for determination of settlement of friction piles in clays. In practice an approximate settlement analysis may be made by the aid of consolidation on the assumption that the clay is subjected to vertical stresses determined by the methods given in Sections 9.8 and 9.9.

Driving piles in clay considerably effects the engineering properties of the clay. The pile driving operation disturbs the clay surrounding each pile, several centimeters thick around the pile surface. The clay in this zone loses a part of its strength due to disturbance. Immediately the disturbed clay begins to loose water due to the stresses setup by volume displacement. If the clay in this disturbed zone is very sensitive, it may lose a large part of its strength and becomes unable even to support the soil above. Hence, it begins to consolidate under its own weight. The strength is usually regained very rapidly as a result of water expulsion. Some 90% or more of its original undisturbed strength may be regained. Eventually the clay in the disturbed zone may become stronger than the original soil. In practice the full load is never applied until several months after pile driving, and hence, the damage due to driving disturbance does not affect the useful strength of the soil. However there are doubtful cases where the clay may not regain its full strength or may not regain it rapidly enough. In either case, laboratory tests of the undisturbed and disturbed samples need to be conducted and analyzed.

10.8.6 Settlement Under Axial Load – Single Pile

The existing methods of analysis can be broadly categorized as given below (Poulos, 1980):

1. The *load transfer method* developed by Coyle and Reese (1966), uses relationships between pile resistance and pile movement measured at various points along the pile. In this method the pile is divided into a finite number of segments. Assuming a tip movement, the movement of the pile segment at midheight is estimated from load transfer/shear strength versus pile movement curves and the elastic deformation equation in an iterative manner. Thus one proceeds up the length of the pile to obtain the load and displacement of the pile head. From a series of such calculations load–settlement curves can be plotted.
2. *Analyses based on elastic theory* have been carried out by many investigators, such as Butterfield and Banerjee (1971), Randolph and Wroth (1978), and Poulos and Davis (1980). In these analyses the pile is divided into a number of uniformly loaded elements and a solution is obtained by imposing the compatibility constraints between the displacement of the soil and the pile. The displacements of the pile are obtained by considering the compressibility of the pile under axial loading and the soil displacements in most cases are obtained by using Mindlin's equations for the displacement of a soil mass caused by a loading within the mass.

3. *Finite element solutions* have been described by Ellison *et al.*, Desai, Lee and Balaam *et al.*, among others (Iyer, 1995).

10.8.7 Settlement Under Axial Load – Pile Group

The settlement of a pile group is the sum of the immediate or elastic settlement ρ_i and the long-term or consolidation settlement ρ_c. The general equation for the calculating ρ_i for a flexible foundation at the ground surface level (discussed in Chapters 3 and 4) is

$$\rho_i = q_n 2B\left(\frac{1-v^2}{E_u}\right) I_f \tag{10.31}$$

where

ρ_i is the settlement at the center of the flexible loaded area
q_n is the net foundation pressure
B is the width of an equivalent flexible raft
v is the Poisson's ratio
I_f is an influence factor
E_u is the deformation modulus for the undrained loading conditions.

10.8.8 Methods of Computation

It can be seen from Equation (10.31) that the values of I_f depends on the ratios H/B and L/B of the pile group, where H = depth of the compressible soil layer, B = width of the pile group, L = length of the pile group.

However, it may be more convenient to use the expression given by Janbu, Bjerrum and Kjaernsli (Tomlinson, 1977) to obtain the average immediate settlement of a foundation at depth D below the surface where the equivalent raft foundation is to be located.

The base of the equivalent raft for different cases of soil conditions is as shown in Figures 10.11 and 10.12. In layered soils with different values of the deformation modulus E_u in each layer, the strata below the base of the equivalent raft are divided into a number of representative horizontal layers and an average value of E_u is assigned to each layer as shown in Figure 10.13. The dimensions L and B in Figure 10.13 are determined on the assumption that the load is spread to the surface of each layer at an angle of 30° from the edges of the equivalent raft. The total settlement of the pile foundation is then the sum of the average settlements

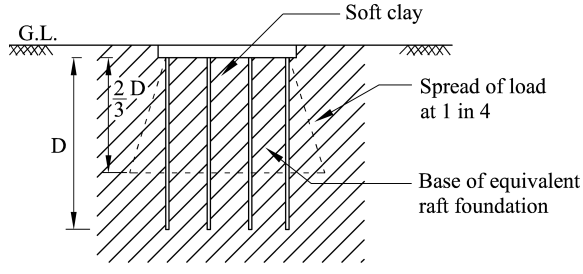

Figure 10.11 Base of equivalent raft in sandy soils for pile groups.

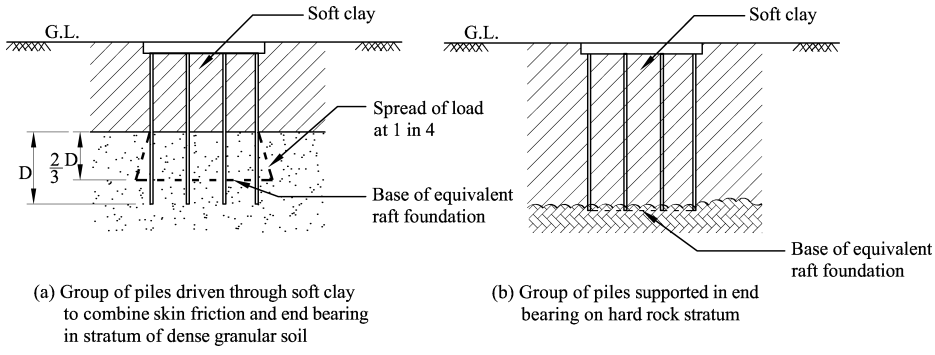

Figure 10.12 Base of equivalent raft for soft soils.

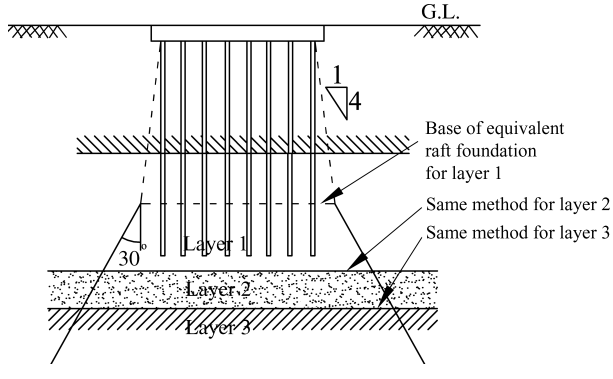

Figure 10.13 Load distribution beneath pile group in layered soils.

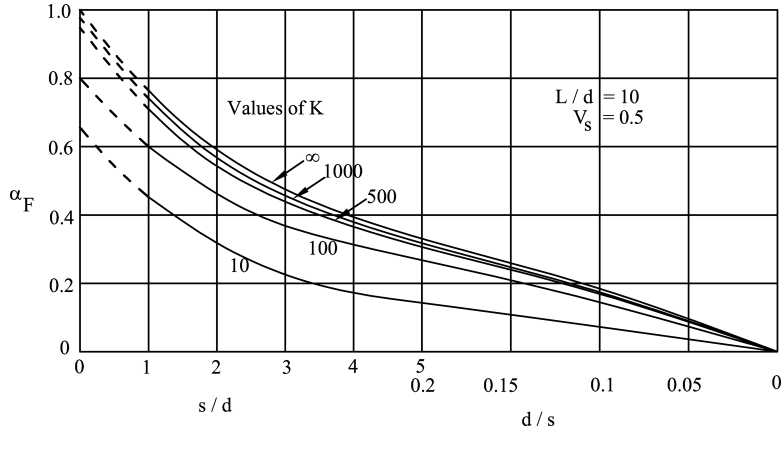

Figure 10.14 Interaction factors for floating piles, $L/d = 10$.

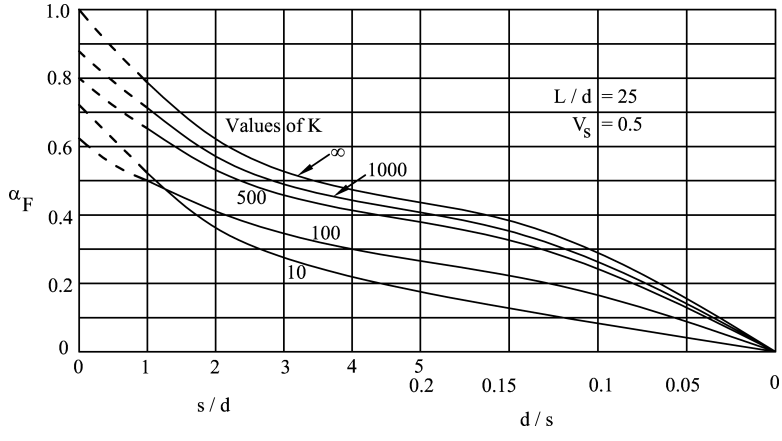

Figure 10.15 Interaction factors for floating piles, $L/d = 25$.

calculated for each soil layer from Equation (10.31). The computation of the settlement of a group of piles is often done by the application of influence factors. There are many such influence factors in literature given by Skempton, Pitchumani and D'Appolonia, Poulos, Randolph and Wroth (Iyer, 1995). Influence factors (α_F) were obtained by Poulos by the integration of the Mindlin's equation for the vertical displacement in a semi-infinite mass resulting from an interior vertical loading and are given in Poulos and Davis (1980). These are given in Figures 10.14–10.17 for various L/d and s/d ratios where $L =$ length of the pile, $d =$ diameter of pile and $s =$ spacing of the piles. The charts are given for different values of soil stiffness K at a value of Poisson's ratio of the soil $v_s = 0.5$.

In these figures, $K = (E_p I_p)/(E_s L^4)$

where

$E_p I_p =$ flexural rigidity of the pile
$E_s =$ modulus of elasticity of soil
$L =$ embedded length of pile.

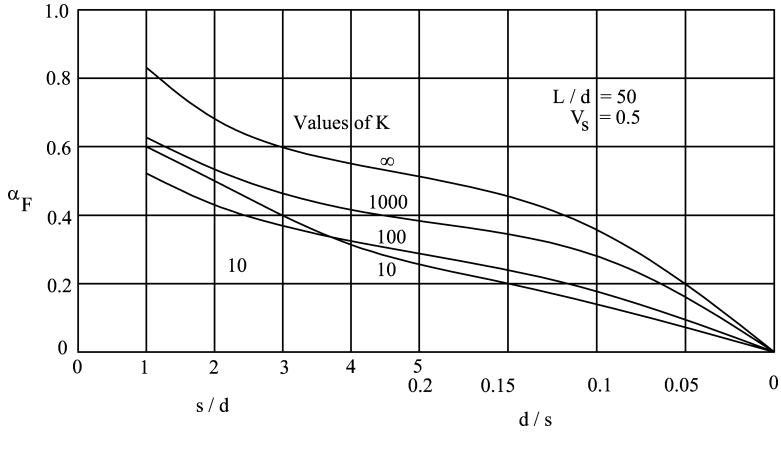

Figure 10.16 Interaction factors for floating piles, $L/d = 50$.

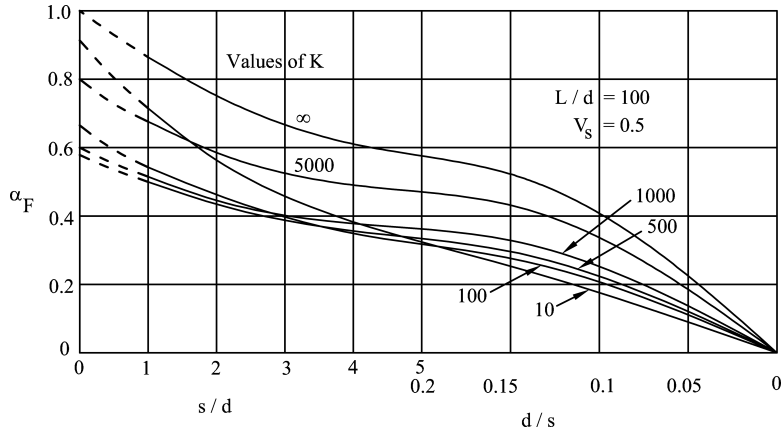

Figure 10.17 Interaction factors for floating piles, $L/d = 100$.

Since these values are obtained for a load acting in a semi-infinite media, curves for correction factor N_h for the effect of finite layer are given in Figure 10.18.

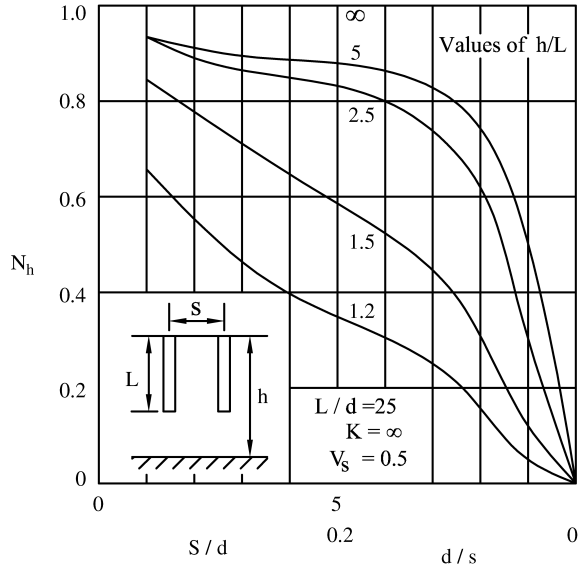

Figure 10.18 Correction factor N_h to interaction factors for the effect of finite layer depth.

Also, since these curves are plotted for a Poisson's ratio of 0.5, curves for correction factor N_v for the effect of Poisson's ratio are given in Figure 10.19.

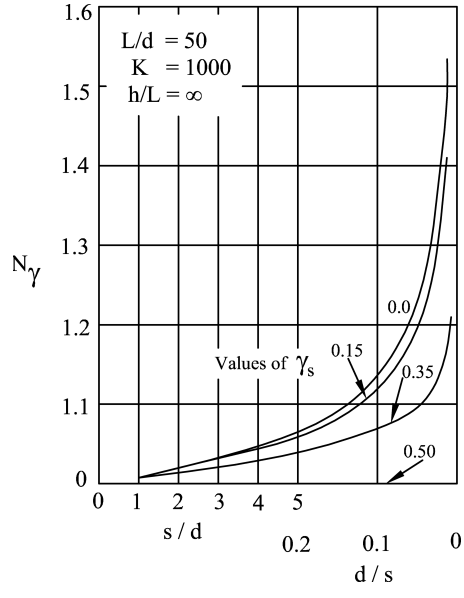

Figure 10.19 Correction factor N_v to interaction factors for the effect of Poisson's ratio.

10.9 Settlement Under Lateral Load

The lateral load capacity of the pile can be computed by the beam on elastic foundation approach on the basis of the permissible lateral deflections, as discussed in Section 10.6.4.

10.10 Design of Pile Caps

Pile caps are almost invariably made of reinforced concrete and are designed as individual footings subjected to the column loads plus the weight of the pile cap and the soil above the cap. Under a concentric load, all piles in the same group are assumed to take equal axial loads. Theory, model tests, and field measurements have proved that piles in one group do not take equal loads. Instead, the center piles take less than the outer piles and the corner piles are subjected to maximum loads. The soil under the pile cap is not assumed to offer any support. Wherever the conditions permit, the piles should be arranged in the most compact geometric form in order to keep the stresses in the pile cap to the minimum (Teng, 1964). The criteria for the structural design of the pile caps are illustrated in Figure 10.20.

Under an eccentric loading or a concentric loading plus a moment, the pile cap is designed in accordance with the following assumptions:

1. Pile cap is perfectly rigid.
2. Pile heads are hinged to the pile cap; therefore, no bending moment is transmitted from pile cap to piles.
3. Piles are short, elastic columns. Therefore, deformations and stress distribution are planar.

These assumptions permit the use of elastic theory for calculation of the pile loads and the stresses in the pile cap, as explained in Section 10.5.

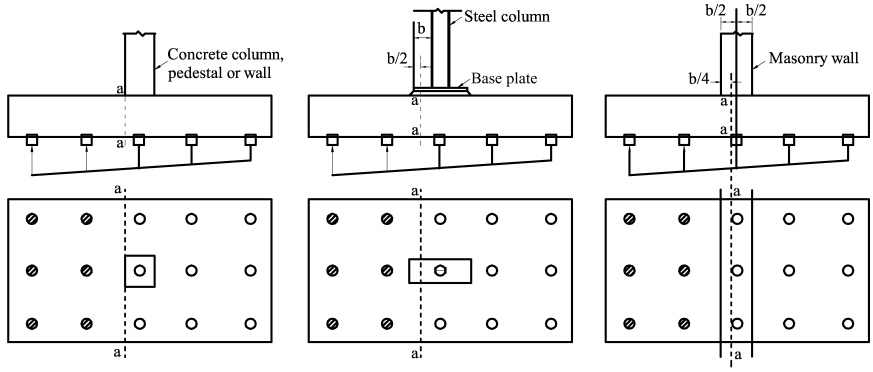

(a) Critical section (a-a) and pile reactions for computing bond and bending stresses

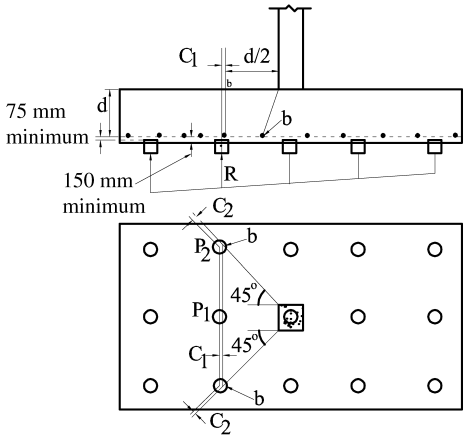

For computation of shear on section b-b:

Reaction on pile $P_1 = R\left(\frac{1}{2} \pm \frac{C_1}{6}\right)$

Reaction on pile $P_2 = R\left(\frac{1}{2} \pm \frac{C_1}{6}\right)\left(\frac{1}{2} \pm \frac{C_2}{6}\right)$

$C_1 \leq 150$ mm

$C_2 \leq 150$ mm

use + sign when it is outside the section, and - sign when inside the section

(b) Critical section (b-b) and pile reactions for computing shear (diagonal tension) stress

Figure 10.20 Critical sections for the design of pile cap.

Pile caps, similar to spread footings, may have pedestals, stepped or sloping tops. One cap may also support more than two columns.

Pile caps should be large enough to have a minimum edge distance of 100–150 mm of concrete beyond the outside face of the exterior piles. In difficult driving conditions where the actual locations of piles may deviate considerably from the required, the edge distance should be increased to provide for such field variations. Ordinarily the piles are embedded at least 150 mm into the cap and the reinforcing bars are placed at a clear distance of 75 mm above the pile head. Therefore the effective depth d of a pile cap is generally about 250 mm less than the total depth *d* of the pile cap.

10.11 Uplift

When piles are required to resist uplift force in excess of the dead load of the structure, the following steps must be taken:

1. The piles must be anchored sufficiently into the cap, the cap tied to the column and the cap designed for the uplift stresses.

2. Concrete piles must be reinforced with longitudinal steel for the full net uplift. Splices in all types of piles should be designed for the full uplift.
3. Uplift resistance of a pile is not necessarily a function of its bearing capacity under compression. For friction piles in soft clay, the capacities against compression and uplift are about equal. A friction pile in granular soils may not have an uplift resistance approaching its bearing capacity. Except for friction piles in soft clays, the uplift capacity of the pile must be determined by pull out tests. When large uplift forces are anticipated, pedestal type piles may be beneficial.

The total uplift resistance of a pile group is calculated as the smaller of the following two values:

1. Uplift resistance of a single pile × number of piles in the group.
2. Uplift resistance of the entire group as a block (Figure 10.21).

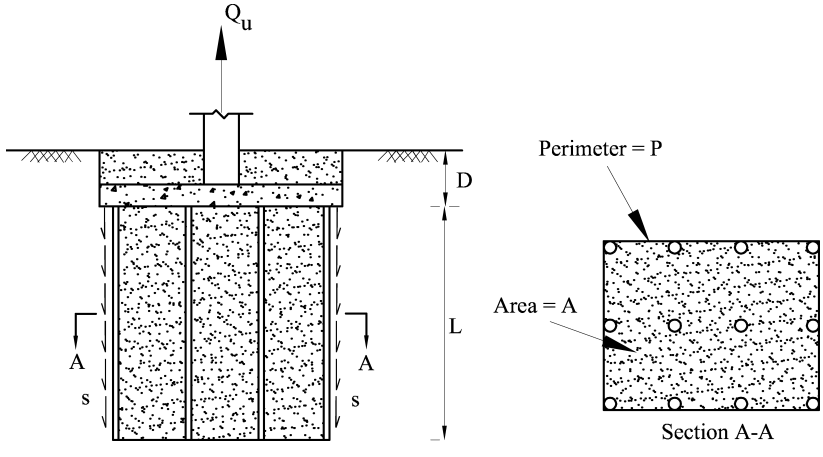

Figure 10.21 Uplift capacity of pile group.

10.12 Batter Piles

When piles are subjected to excessive lateral loads, it might be more economical and desirable to provide batter piles. Common batter varies from 1 horizontal:12 vertical to 5 horizontal:12 vertical. When batter exceeds 3 horizontal:12 vertical, special driving equipment is necessary and hence may be very costly.

The usual assumption in the design of batter piles is that the pile is capable of resisting the same axial load as a vertical pile of the same type and size and driven to the same stratum. There are several methods for analysis of pile foundations involving batter piles. Some of these are given below:

1. The most conservative method is one that provides enough batter piles to resist all the horizontal force. The capacity of a batter pile in resisting a horizontal force is assumed, in

this case, to be equal to the horizontal component of the pile capacity along the direction of batter. This method certainly requires more piles than necessary for a given condition and is not commonly used.

2. A commonly used method of analysis is known as Culmann's graphical method, as shown in Figure 10.22. Piles are grouped according to their slopes. It assumes that all piles are subjected to axial load only and that piles in each group are subjected to equal axial load. Based on these assumptions, the center of reactions can be located. Culmann's method may be described step by step as follows:
   a. Sketch a profile of the pile foundation and locate the center line of each group of parallel piles.
   b. Draw the resultant *R* of all external forces applied on the pile foundation. *R* intersects the center line of the pile group 1 (vertical piles) at point *a*.
   c. Center line of group 2 and center line of group 3 intersect at *b*. Connect *ab*.
   d. Resolve *R* into components *V* and *B*. *V* is vertical and *B* is parallel to line *ab*.
   e. Group 1 is subjected to total axial force *V*. Group 2 and Group 3 are subjected to force *B*.
   f. Resolve force *B* into axial loads along center line of group 2 and center line of group 3.

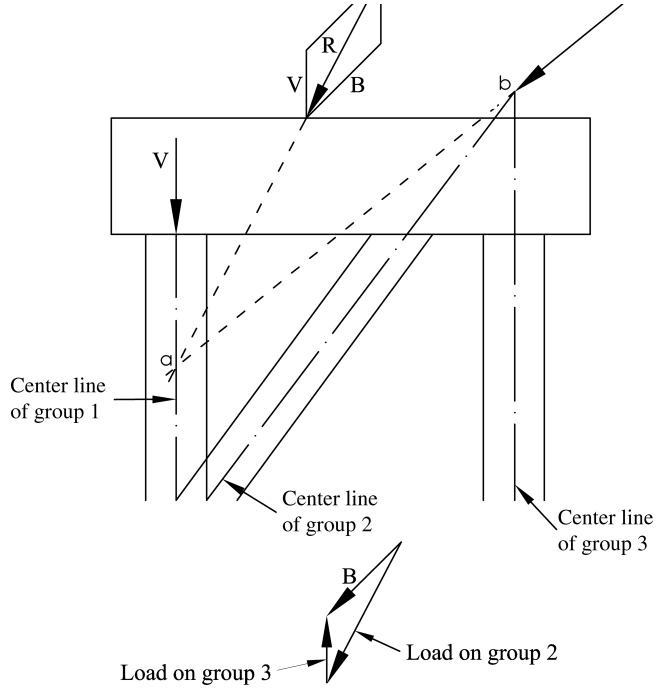

Figure 10.22 Graphical method (Culmann's method). Column base plate.

This method is statically determinate where piles are arranged in not more than three directions; some examples are given by Teng (1964).

10.13 Design of Pile Foundations

The general criteria for the design of pile groups is that:

1. The load-carrying capacity of a single pile should not be exceeded due to loads and moments coming from the superstructure.
2. The load-carrying capacity of the group should not be exceeded by the total superposed loads.
3. The settlements, both total and differential, should be within permissible limits.

The design of pile foundation may be carried out in the following steps:

1. Calculate the loads. The total load acting on the piles includes the weight of the pile cap and the soil above it. If the ground is newly filled or will be filled in the future, the additional load on piles due to negative skin friction should be included (Chapter 9).
2. Get the soil profile of the site and, superimpose the outline of the proposed foundation and substructure on this. Mark the ground water level.
3. Determine type and length of piles.
4. Determine pile capacity.
5. Establish pile spacing (Section 10.3).
6. Check stresses in lower strata (Section 10.8).

These aspects are summarized below in terms of design guidelines.

10.14 Summary of Assumptions and Guidelines for Design

The details presented in the previous sections for pile foundation design are summarized for practical applications as follows:

1. Under a concentric load the piles are assumed to take equal axial loads in proportion to their areas of cross section (Section 10.5).
2. Under an eccentric loading or a concentric loading plus a moment, the pile group is designed with the following assumptions:
   a. Pile cap is rigid.
   b. Pile heads are hinged to the pile cap and therefore no bending moment is transmitted from the pile cap to the piles directly.
   c. Piles are short elastic columns. Therefore, the deformations and stress distribution are planar.
   d. The axial and lateral loads coming on any pile are calculated as explained in Section 10.5 (Equations (10.4)–(10.8)).
3. Uplift equal to the submerged self weight of the pile can be allowed. Where the uplift is due to load, including wind load, an additional resistance due to skin friction can be allowed.
4. When the pile is close to a deep foundation, skin friction should be neglected.
5. The following loadings on the pile need to be considered:
   a. Loads as supplied by the shop/structural requirements.
   b. Full weight of the pile cap.
   c. Submerged weight of pile cap.

d. Full weight of soil above pile cap.
e. Submerged weight of soil above pile cap.
f. A surcharge on the gross area of the pile cap.

6. Combination of loads.
   a. The combination of loading for a maximum compressive load is

$$a + b + d + f + \text{maximum bending moment at the CG of the pile group due to } P_x, P_y, P_z$$

   The combination of loading for a minimum compressive or maximum tensile load is $a + c + e +$ minimum bending moment at the CG of the pile group due to P_x, P_y, P_z

   b. The bending moment at the CG of the pile group is

$$\text{Moment due to } P_x \text{ or } P_y, \text{i.e.}, M_y = P_x \times h \tag{10.32}$$

$$M_x = P_y \times h \tag{10.33}$$

   where h is the thickness of the pile cap.
   c. Torsional moments on the pile group:
   These are caused due to eccentricity of horizontal loads acting at the center line of the column and also due to eccentricity of the horizontal loads acting on the whole structure, For example

$$M_z = P_x e_y + P_y e_x + M_{zc} \tag{10.34}$$

   where e_x and e_y are eccentricities of the center line of the column with respect to CG of the pile group along x and y directions. M_{zc} is the torsional moment transmitted by the columns of the structure.

7. Pile groups in some cases have to be made eccentric with respect to the module axis (axes passing through C.G of the columns) to reduce the effect of overturning moment, keeping in view that this eccentricity deos not cause any adverse effect in any case of loadings, including reversal of direction of moment. When there is an increase of moment due to eccentricity, it has to be taken into account.
8. Torsional moment M_z is shared in proportion to the torsional stiffness I_{zz}/L of the pile where I_{zz} is the polar moment of inertia and L is the length of pile.
9. Minimum center to center spacing between piles is taken as $2.5D$ to $3.0D$ where D is the diameter of the pile.
10. Clearances from the edge of pile cap to the various members are as follows:

Piles	−15 cm
Base plate	−15 cm
Center of anchor bolts	−35 cm

    Depth of pile cap is taken as equal to the maximum length of anchor bolts in concrete with a cover of 0.25 m.
11. Bending moment in the i-th pile, M_{bi} due to horizontal force is calculated as

$$M_{bi} = P_{hi} \times \frac{L_{fi}}{2} \tag{10.35}$$

where P_{hi} is the total horizontal force coming on the i th pile (Equation 10.8), L_{fi} is the fixity length of i th pile (Section 10.5.4). This is an empirical/approximate method based on some design practices, as discussed in Sections 9.7 and 10.6. This needs to be verified by local practices and codes as well as by other methods discussed in Sections 9.7 and 10.6. As per the design practice, only the pile reinforcement is computed using BM due to lateral load and the vertical load on a pile as in a RCC column.

12. Maximum allowable stresses in steel and concrete are increased by 33% when that increase is due to wind load only.

    Usually M_{bi} is obtained by analysis of pile subjected to lateral loads or by pile load tests (Section 10.6). However to make the computation simple, M_{bi} may be calculated using Equation (10.35).

    The fixity length L_f can be taken from the graphs given in Figure 10.6 (IS: 2911–1984, 1984). In the absence of any data, it may be assumed to be around $5d$ to $10d$ where d is the diameter of the pile.
13. Batter piles: when excessive horizontal forces are encountered, batter piles could be used.
14. The axial loads and horizontal loads coming on a pile in a group are calculated using Equation (10.4) (Section 10.5).

10.15 Example

An example of the analysis and design of pile foundations is given below which essentially highlights the important steps involved, the use of specifications and assumptions and simplified approach to practical problems.

Example 10.1

Design a pile foundation with the following data. The details of column base plate and the pile group are shown in Figures 10.23 and 10.24.

Loads coming from the column to the pile group are:

$$P_z = 1663\,\text{kN},\ P_y = 0,\ M_x = 0,\ P_x = (\text{wind} = 60.62\,\text{kN},\ \text{crane} = 64.90\,\text{kN}),$$
$$M_y = (\text{wind} = 1036.8\,\text{kNm},\ \text{due to loads} = 1579.8\,\text{kNm})$$

where P_x, P_y, P_z are the loads along the x, y, z axes.

M_x, M_y, M_z are the moments about the x, y, z axes coming from the column (superstructure).

The loads and moments are considered positive if they are acting along and about the positive direction of the respective axes as per usual convention.

10.15.1 Types of Piles

Type	Diameter (m)	Capacity (kN)	$3d$ spacing (m)
A	0.50	1200	1.5

10.15.2 Concrete Data

Unit weight of concrete $= 24\,\text{kN/m}^3$
Submerged unit weight of concrete $= 14\,\text{kN/m}^3$

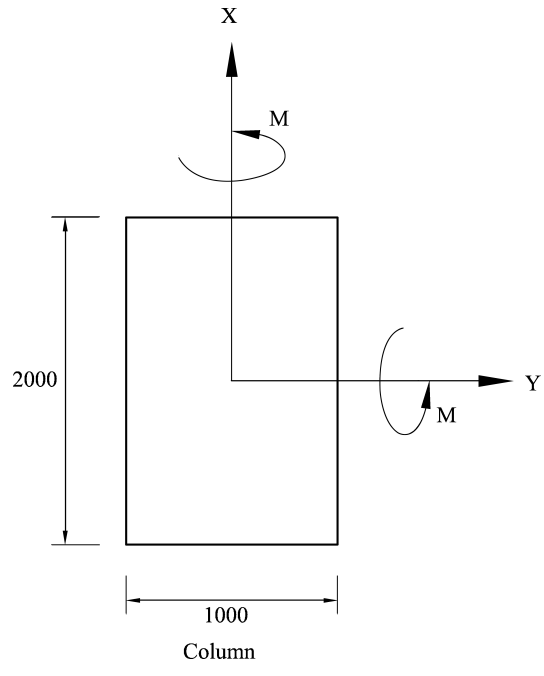

Figure 10.23 Column base plate.

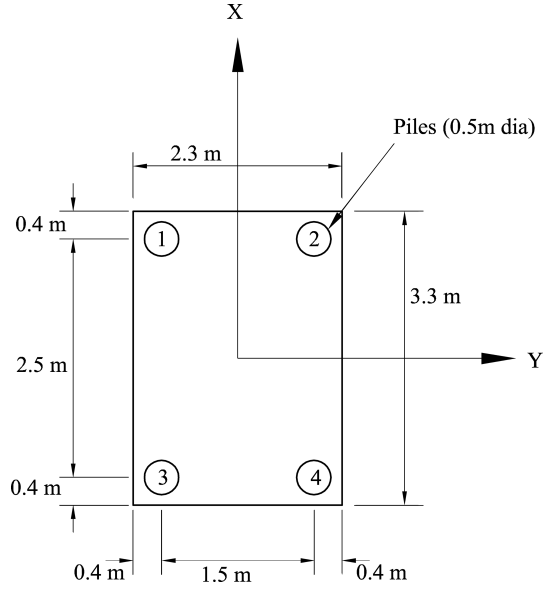

Figure 10.24 Pile group.

10.15.3 Soil Data

The soil is uniform with the following data:

Cohesion, $c = 14\,\text{kN/m}^3$
Angle of internal friction, $\phi = 34^0$
Bulk unit weight $= \gamma_t = 17.5\,\text{kN/}m^3$
Submerged unit weight $= \gamma_{\text{sub}} = 10\,\text{kN/m}^3$

10.15.4 Loads From the Superstructure

$P_x = 1663\,\text{kN}$
$P_x = 60.62\,\text{kN(wind)} + 64.90\,\text{kN(crane)} = 125.2\,\text{kN}$
$M_y = 1036.8\,\text{kNm (wind)} + 1579.8\,\text{kNm (load)} = 2616.6 \approx 2617\,\text{kNm}$
$P_y = 0, M_x = 0$
Surcharge $= 50\,\text{kN/m}^2$

Let us assume that there is no eccentricity between the module axis (column center line) and the pile group. Let us try a group of four piles.

10.15.5 Modulus of Piles About the Axes Passing Through the CG of the Pile Group

Neglecting the moment of inertia of piles about their own centroidal axes passing through the center of gravity, the moments of inertia of the pile group can be written by parallel axis theorem as follows:

About y axis, $I_{yy} = (4 \times 1.25^2)\,A = 6.25\,A$
About x axis, $I_{xx} = (4 \times 0.75^2)\,A = 2.25\,A$
About z axis, $I_{zz} = 8.50\,A$

where A is the area of the pile.

Modulus of extreme piles:

$$f_y = \frac{xA}{I_{yy}} = \frac{1.25}{(4 \times 1.25^2)} = 0.2,\ f_x = \frac{yA}{I_{xx}} = \frac{0.75}{(4 \times 0.75^2)} = 0.33$$

Approximate size of pile cap $=(2.5 + 0.5 + 0.3) \times (1.5 + 0.5 + 0.3) = 3.3\,\text{m} \times 2.3\,\text{m}$.

Take 0.75 m to be the depth of the pile cap (area $= 3.3 \times 2.3 = 7.6\,\text{m}^2$) as shown in Figure 10.24.

10.15.6 Loads

1. Column load $= 1663\,\text{kN}$.
2. Self weight of pile cap $= 3.3 \times 2.3 \times 24 \times 0.75 = 137\,\text{kN}$.

3. Submerged weight pile cap = 3.3 × 2.3 × 14 × 0.75 = 80 kN.
   Assume the top of the pile cap to be 1 m below ground level.
4. Soil weight (1 m thick) = 3.3 × 2.3 × 1.0 × 17.5 = 133 kN.
5. Submerged weight of soil = 3.3 × 2.3 × 1.0 × 10 = 76 kN.
6. Surcharge (including floor weight if any) = 3.3 × 2.3 × 50 = 380 kN.

10.15.7 Moments

1. Data = ± 2617 kNm.
2. Data (without wind) = ± 1580 kNm.
3. Moment due to horizontal load = ± 125.2 × 0.75 = ± 94 kNm.
4. Moment due to horizontal load (without wind) = ± 64.9 × 0.75 = ± 49 kNm.

10.15.8 Combination of Loads and Moments for Maximum Load on Pile

10.15.8.1 Loads

Using data listed in Section 10.15.6

$$\begin{aligned} &= \text{item 1} + \text{item 2} + \text{item 4} + \text{item 6} \\ &= 1663 + 137 + 133 + 380 \\ &= 2313\,\text{kN} \end{aligned}$$

10.15.8.2 Moments

Using data listed in Section 10.15.7

$$\begin{aligned} &= \text{item 1} + \text{item 3} \\ &= \pm 2617 \pm 97 \\ &= \pm 2711\,\text{kNm} \end{aligned}$$

10.15.8.3 Maximum Load on Piles

$$\begin{aligned} &= 2313/4 + 2711/5 \\ &= 580 + 540 \\ &= 1120\,\text{kN} \end{aligned}$$

10.15.8.4 Minimum Load on Piles

$$\begin{aligned} &= 580 - 540 \\ &= 40\,\text{kN} \end{aligned}$$

The maximum allowable load with wind is 33.33% above 1200 kN (1600 kN). Hence, it is acceptable.

10.15.9 Combination of Loads and Moments for Minimum Load on Pile

10.15.9.1 Loads

Using data listed in Section 10.15.6

$$\begin{aligned} &= \text{item 1} + \text{item 3} + \text{item 5} \\ &= 1663 + 8 + 76 \\ &= 1819\,\text{kN} \end{aligned}$$

10.15.9.2 Moments

Using data listed in Section 10.15.7

$$\begin{aligned} &= \text{item 1} + \text{item 3} \\ &= \pm 2617 \pm 97 \\ &= \pm 2711\,\text{kNm} \end{aligned}$$

10.15.9.3 Minimum Load Per Pile

$$\begin{aligned} &= 1819/4 - 2711/5 \\ &= 455 - 542 \\ &= -87\,\text{kN (tension)} \end{aligned}$$

$$\begin{aligned} \text{Allowable tensile load on the pile} &= \text{Self weight of about 18 m long pile} \\ &= 18 \times \frac{\pi}{4} \times 0.508^2 \times 24 + \text{skin friction} \\ &= 87.5\,\text{kN} + \text{skin friction} > 87\,\text{kN (tension)} \end{aligned}$$

Hence, it is acceptable.

10.15.10 Maximum Load on Pile Without Wind

10.15.10.1 Loads

Using data listed in Section 10.15.6

$$\begin{aligned} &= \text{item 1} + \text{item 2} + \text{item 4} + \text{item 6} \\ &= 2313\,\text{kN} \end{aligned}$$

10.15.10.2 Moments

$$\begin{aligned} &= \pm 1580 \pm 49 \\ &= \pm 1629\,\text{kNm} \end{aligned}$$

10.15.10.3 Maximum Load Per Pile

$$\begin{aligned} &= 2313/4 + 1629/5 \\ &= 910\,\text{kN} < 1200\,\text{kN} \end{aligned}$$

Hence, it is acceptable.

10.15.11 Design of Reinforcement in Pile

The pile has to carry a vertical load of 1120 kN (with wind).

Fixity length of pile is taken as $5d$ (2.50 m).

Horizontal load per pile = 125.2/4 = 31.3 kN (about 3% of nominal allowable load).

Hence, it is acceptable.

Bending moment to be carried by pile $= 31.3 \times 5d/2 = 31.3 \times 1.25 \approx 40$ kNm.

A proper percentage of reinforcement has to be used for a vertical load of 1120 kN and bending moment of 40 kNm.

10.15.12 Pile Cap

10.15.12.1 Longer Direction (x–Axis)

BM at the face of the base plate

$= 2 \times 1120 \times 1.25$ (due to two piles at a distance of $x_c = 1.25$ m from the CG of pile group and CL of column)
$= 2800$ kNm

Shear at the face of the base plate

$= 2 \times 1120$ (due to two piles)
$= 2240$ kN

Provide reinforcement, check the adequacy of depth for BM and check for shear and bond stress.

10.15.12.2 Shorter Direction (y–Axis)

Loads on piles = 1120 + 40 = 1160 kN (due to one pile with 1120 kN and second pile with 40 kN).

Bending moment at the face of the base plate $= 1160 \times y_c = 1160 \times 0.75 = 870$ kNm (y_c for both the piles is 0.75 m from the CG of the group and CL of column).

Shear at the face of the base plate = 1160 kN.

Provide reinforcement for the BM and check for shear and bond stress.

10.15.13 Check for Vertical Load Capacity of Pile

Pile parameters:

$$L = 18 \text{ m},\ h = 0.75 \text{ m},\ D = 0.5 \text{ m}$$

Soil parameters:

$\phi = 34^\circ$, $c = 14\ \text{kN/m}^2$, $\gamma_{\text{sub}} = 10\ \text{kN/m}^3$, assume K_o = lateral earth pressure coefficient at rest = 1.0

End bearing for $\phi = 34^\circ$, $c = 14\ \text{kN/m}^2$, $N_c = 52.64$, $N_q = 36.5$, $N_\gamma = 38.04$:

$$P_b = \frac{\pi D^2}{4}\left[1.3\,CN_c + \gamma D_F N_q + 0.3\gamma\, D\, N_\gamma\right]$$

$$P_b = \frac{\pi(0.5)^2}{4}[(1.3 \times 14 \times 52.64) + (10(18 + 0.75)36.5) + 0.3(0.5) \times 10 \times 38.04]$$

$$P_b = 1543\,\text{kN}$$

10.15.13.1 Friction and Adhesion

Shear strength of the mid depth of the pile (assuming adhesion factor of $\alpha = 1.0$) and taking $K_o = 1.0$, that is, at *L/2* (neglecting the additional effect due to *h*),

$$\begin{aligned} s &= \left[c + K_o \gamma_{\text{sub}} \left(\frac{L}{2}\right) \tan\phi\right] \\ &= \left[14 + 10\left(\frac{18}{2}\right)0.5774\right] \\ &= 66\,\text{kN/m}^2 \\ P_f &= \pi DLs = \pi \times 0.5 \times 18 \times 66 \\ P_f &= 1866\,\text{kN} \end{aligned}$$

Total pile capacity $= P_b + P_f = 1543 + 1866 = 3409$ kN
Safe capacity of vertical load on pile with factor of safety $= 3$ is

$$\frac{3409}{3} = 1136.4\,\text{kN} > 1120\,\text{kN}$$

Hence, it is safe.

10.16 Construction Guidelines

Noting that piles transfer loads from the superstructure by either end-bearing and/or by skin friction, they can be used at sites where the above load transfer mechanisms are possible in the subsoil. Construction of pile foundations require a judicious choice of piling system depending on soil conditions, loads coming from the superstructure and constraints of total and differential settlements besides special requirements. The installation of piles requires careful control on position, alignment, depth which involves skilled and experienced manpower. Pile load test (Section 9.6.7) is the most direct method to assess the above requirements and judging its performance. The details of testing are similar to the plate load test (Chapter 4) but instrumentation needs to be elaborate as described in standard text books such as Taylor (1964), Teng (1964), Terzaghi and Peck (1967) and Bowles (1996).

10.16.1 Construction Details

The construction of pile foundations involves two steps, namely construction of piles and the pile caps. The second step is a simple process similar to the construction of spread footings. Procedures and equipment required for installation of piles are described below.

Driven piles are installed by a pile driving device known as a pile hammer. The hammer may be suspended from the boom of a crane, supported on a large frame called a pile driver or carried on a barge for construction in water. In all cases, the hammer is guided between two parallel

steel members known as leads. The leads may be adjusted at various angles for driving vertical and batter piles.

Usually the information concerning the pile driving should be kept in an orderly form. It should include the details of the hammer and accessories. The behavior of the pile during the entire period of driving should be observed. It is time to stop driving a timber pile when the following phenomena are observed:

1. The pile vibrates and springs near the ground surface.
2. The pile hammer bounces.
3. The pile head shows distress under moderate driving.

Pile may be already damaged if the following behavior is noticed:

1. Penetration suddenly increases or becomes irregular, while the soil profile cannot account for it.
2. Pile suddenly changes direction.

Cast in situ piles are provided by drilling a bore hole with or without casing using drilling equipment and then placing reinforcement and concrete in the drilled bore hole (Section 9.2.2).

10.16.1.1 Alignment

Piles cannot be driven (or cast in situ) absolutely vertical and true to position. Even in ideal conditions the center of a pile head must be allowed to deviate a certain amount from the required location, and the pile at lower depth to vary from the required vertical or batter line. However, every precaution should be exercised to maintain the piles in position. The general procedure for determining the pile alignment and elevations is as follows:

1. Measure the elevation at top of piles immediately after driving of each and check the final elevations after the adjacent piles are driven or at the completion of all pile driving. If point-bearing piles are uplifted, they should be redriven.
2. Check the location of all piles after adjacent piles are driven or at the completion of all pile driving. In ordinary soil conditions an 8 cm tolerance is considered reasonable.
3. Inspect the pile shaft for verticality or required batter. In the case of heavily loaded piles measurement must be made by specially devised instruments, unless load test is made with piles having questionable verticality.

The above steps are equally applicable for cast-in-situ piles as well.

10.16.1.2 Defective Piles

A pile may be considered defective if:

1. It is damaged by driving.
2. It is driven out of position and/or is bent along its length.

To avoid damage to fresh concrete in a cast in place pile by the driving of adjacent piles, the pile should not be concreted until all piles within a certain radius are driven. The radius depends upon soil condition, length and size of pile and spacing.

A damaged or defective pile has to be withdrawn and replaced by another pile adjacent to it after checking the design with the new position of the replaced pile. Alternatively a new pile may be driven/cast while leaving the damaged pile as it is.

10.16.1.3 Effect of Pile Driving

Pile driving may introduce some of the following effects on the ground:

1. *Subsidence.* Vibration due to pile driving in loose sand may cause compaction of the sand. Consequently, the area may settle and adjacent structures may be affected. In saturated fine sand and silt, the shock may introduce large settlements.
2. *Heave.* Pile driving in clays and dense sand is commonly associated with surface heave and sometimes with lateral displacement. The heave of clay is followed by settlement immediately after driving. Piles uplifted by ground heave should be redriven. To avoid heave and lateral movement, pile driving should be started from the center of the ground and proceed outwards.
3. *Compaction.* Sand and gravel within a lateral distance of about three diameters of the pile and two diameters below the tip is largely compacted due to the displacement of pile. Consequently, a pile group in sand behaves as a rigid block of compacted soil.
4. *Disturbance.* Clayey soil surrounding the pile is greatly disturbed due to the displacement of pile. The disturbance may extend to a large lateral distance and the strength of clay is largely reduced. However, in ordinary cases it starts to regain its strength and in 30–50 days; 90% or more of its strength may be regained.

Exercise Problems

The problem assignments are mainly on pile foundation design, that is, Sections 10.13 and 10.14. Use concrete of grade M20 and steel of grade Fe450, unless stated otherwise.

10.1 Analyze a pile foundation with the following data. Pile diameter = 0.6 m, number of piles = 5. Soil data: $c = 15\ \text{kN/m}^2$, $\phi = 20^\circ$, $\gamma = 17\ \text{kN/m}^3$. Depth of pile cap surface below GL = 1 m. No ground water at site. Column size = 0.6 × 0.6 m. Length of anchor bolt in the pile cap = 0.4 m. $P_x = 1000\ \text{kN}$, $P_y = 500\ \text{kN}$, $P_z = 200\ \text{kN}$, $M_x = 1000\ \text{kNm}$, $M_y = 200\ \text{kNm}$, $M_z = 150\ \text{kNm}$, surcharge = $50\ \text{kN/m}^2$. Use five piles as shown in Figure 10.25 and find the length of pile required to get the required capacity with a Factor of safety =3. All specifications are to be satisfied.

10.2 Design a pile foundation with a group of circular piles of 0.5 m diameter with the same data for soil, top of pile cap, column, loads and moments. Also find the length of pile required with a factor of safety = 3.

10.3 Calculate the elastic and consolidation settlements of the group (Problem 10.1 and Figure 10.25) if there is a compressible layer of 10 m thick clay from 20 to 30 m from ground level, mv of compressible soil = $25 \times 10^{-3}\text{m}^2/\text{kN}$.

10.4 Analyze the pile group given in Figure 10.25 if the piles are of different diameters. P_1 and $P_2 = 0.4$ m diameter, P_3 and $P_4 = 0.6$ m diameter, $P_5 = 1.0$ m diameter. Use the same data as given in Problem 10.1 except for the diameters of piles.

10.5 Design the pile group of Problem 10.2 if the water table is at a depth of 5 m below GL.

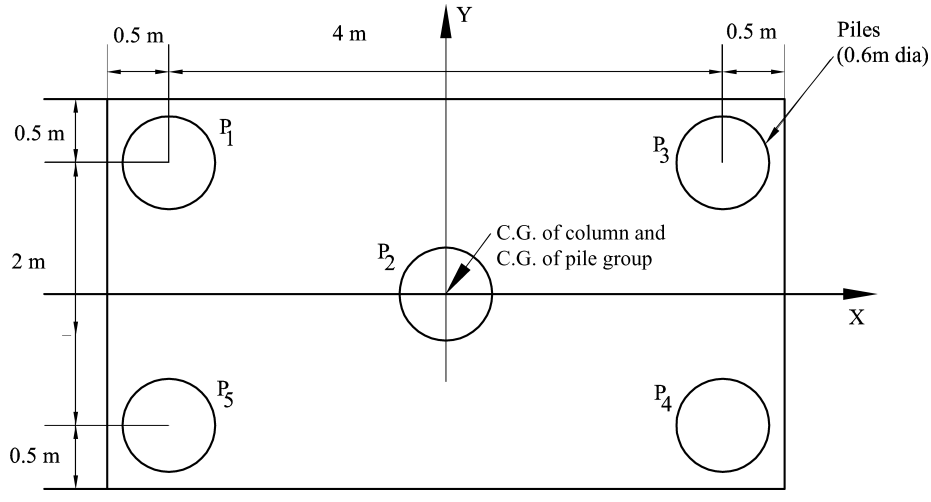

Figure 10.25 Problem 10.1.

10.6 For the pile group shown in Figure 10.26, find design loads and moments on each pile with the following data (loads in kN; moments in kNm):

$P_z = -2250$, $P_x = 200$, $P_y = -150$, $M_x = 3000$, $M_y = -2000$
Depth of pile cap = 2 m
Unit weight of concrete = 24 kN/m^2

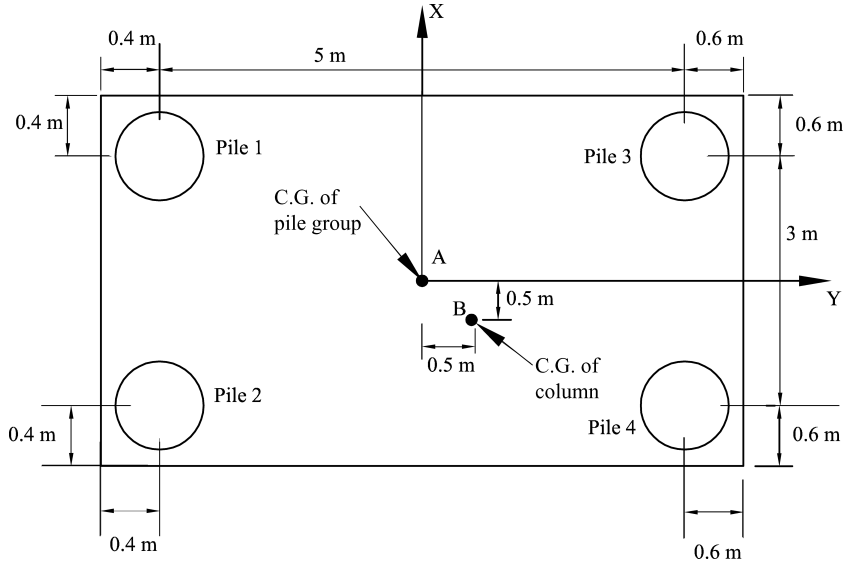

Figure 10.26 Problem 10.6.

Depth of top surface of pile cap below GL = 1.5 m
Unit weight of soil = 17.7 kN/m^3
Surcharge = 50 kN/m^2
Fixity length of pile = 6d (d is diameter of pile)
Submerged unit weight of soil = 10.5 kN/m^3
Submerged unit weight of concrete = 14 kN/m^3
Diameters of piles 1 and 2 = 0.5 m
Diameters of piles 3 and 4 = 0.75 m
Water table can rise up to GL.

10.7 Compute the permissible lateral load for the offshore circular pile shown in Figure 10.27. If the maximum permissible lateral displacement is $d/10$ where d is the diameter of pile. Diameter of pile = 0.5 m. Pile is quite long and can be analyzed as a semi-infinite beam on elastic foundation. $E_{\text{soil}} = 15$ MPa, $\nu_{\text{soil}} = 0.2$. $E_{concrete}$ may be taken appropriately. Use BEF approach.

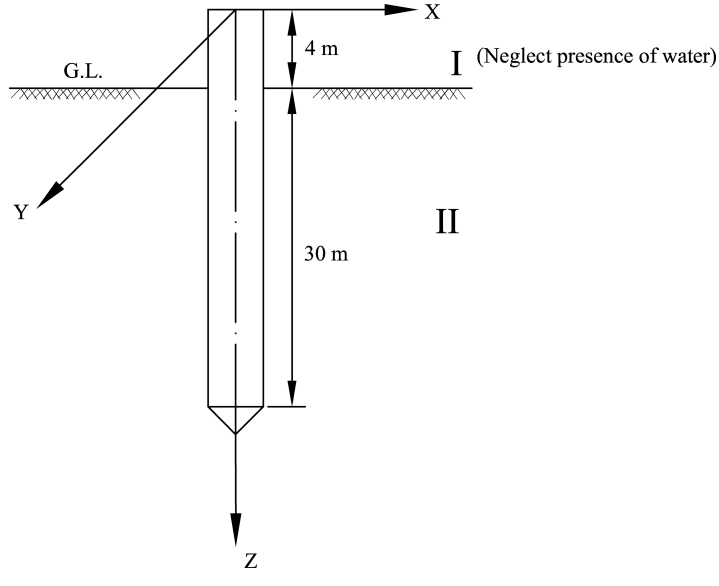

Figure 10.27 Problem 10.7.

10.8 Redo the example 10.7 with pile head at the ground level.

11

Machine Foundations

11.1 Introduction

Rapid industrialization being the key to the development of a country, engineers and technologists are adopting machines, machine tools and heavy equipment with a wide range of speeds, loads and operating conditions. Foundations to support these machines play a vital role in their operating performance besides satisfying stringent environmental stipulations. An improperly designed machine foundation impairs the efficiency of the machine itself besides creating structural, acoustic, environmental and abnormal maintenance problems, even when the machine is perfectly sound on its own. Thus technical and industrial progress has motivated the intensive study of machine foundations. Essentially in this, the engineer has to study the problems of shocks and vibrations on the foundations supporting industrial installations, as well as the laws governing the propagation of waves from these foundations through the soil.

11.1.1 Design of Foundations in a Dynamic Environment

A stepwise process for the satisfactory design of foundations in a dynamic environment can be outlined as follows:

1. Evaluation of dynamic forces and moments produced by the operating machines.
2. Definition of proper design criteria in terms of permissible limits of system responses.
3. Simplification and idealization of the physical system and its representation by appropriate mathematical models guided by relevant response mechanisms.
4. Determination of relevant system parameters characterizing the elements of the above idealized models (step 3) through field and laboratory investigations.
5. Selection of analytical methods and system parameters to compute system responses.
6. Choice of geometrical design parameters of the various components of the system which yield acceptable responses satisfying the design criteria stipulated in step 2.
7. Optimization of the design parameters.

Foundation Design: Theory and Practice N. S. V. Kameswara Rao
 ISBN: 978-0-470-82534-1

11.2 Types of Machine Foundations

Foundations for machines are generally of the following types, based on their structural shapes, as shown in Figure 11.1.

1. Block type (rigid foundations)
2. Box or caisson type
3. Wall type
4. Framed type
5. Nonrigid or flexible type

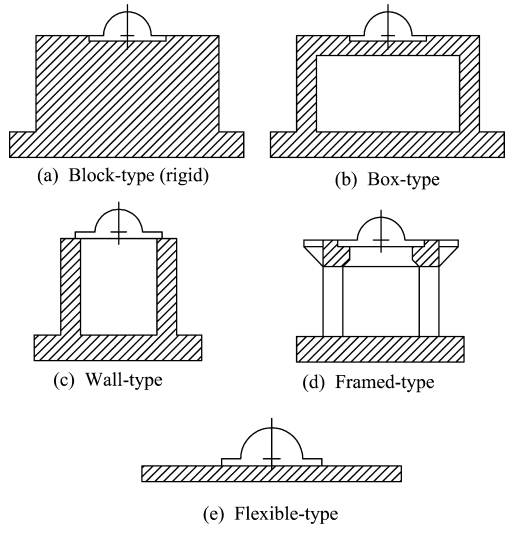

Figure 11.1 Common types of machine foundations.

In a majority of cases block type (rigid) foundations are adopted especially for machines producing periodic and impulsive forces. For rotatory machines at high speeds (such as turbo machinery) framed type foundations are preferred. In certain specific situations flexible foundations can also be effectively designed.

11.3 General Requirements of Machine Foundations and Design Criteria

Some of the important requirements of a machine–foundation–soil system (MFS) can be listed as follows (Richart, Hall and Woods, 1970; Srinivasulu and Vaidyanathan, 1976; Kameswara Rao, 1998):

1. Settlements should be within permissible limits.
2. Foundation block should be structurally adequate to carry the loads.

3. The combined center of gravity (CG) of machine and foundation and the center of contact area (with the soil) should lie on the same vertical line as far as possible.
4. Resonance should not occur. Accordingly, wherever possible, the operating frequency ω should be lower than the natural frequency of the system, ω_n, that is

$$\frac{\omega}{\omega_n} \text{ should be less than } 0.5 \tag{11.1}$$

If the operating frequency happens to be more than the natural frequency, then

$$\frac{\omega}{\omega_n} \text{ should be more than } 2.0 \tag{11.2}$$

Thus the design criterion on frequency can be written as

$$\frac{\omega}{\omega_n} \leq 0.5 \quad \text{or} \quad \frac{\omega}{\omega_n} \geq 0.2 \tag{11.3}$$

The amplitudes of displacement or velocity or acceleration of the MFS should be within permissible limits. These are generally prescribed by the machine manufacturers. Some general design criteria (IS: 2974–1966, 1966) are shown in Figures 11.2–11.4. Tolerable levels of vibration are related to:

a. human perception
b. maintenance problems and potential damage to machines or instruments
c. potential damage of structural components
d. avoidance of total failure
e. the dimensions of machine foundations.

These should conform to operational requirements of the machine in addition to the minimum clearances from the foundation bolts as stipulated by codes (IS: 2974–1966, 1966) and manufacturers. As a guideline, the approximate weights of the foundation blocks in terms of multiples of the weight of the machines being supported can be used as an initial guess and are given in Table 11.1 (Leonards, 1962).

11.4 Dynamic Loads

The foundations are generally excited by any of the following:

1. Unbalanced rotating and reciprocating parts of the machines which produce transient and steady state dynamic loads
2. Impact loads
3. Neighborhood of vibration environment
4. Earthquakes
5. Wind-induced forces
6. Other periodic and aperiodic forces and moments such as those due to blasting, mining, drilling and piling operations and sonic booms
7. Moving loads.

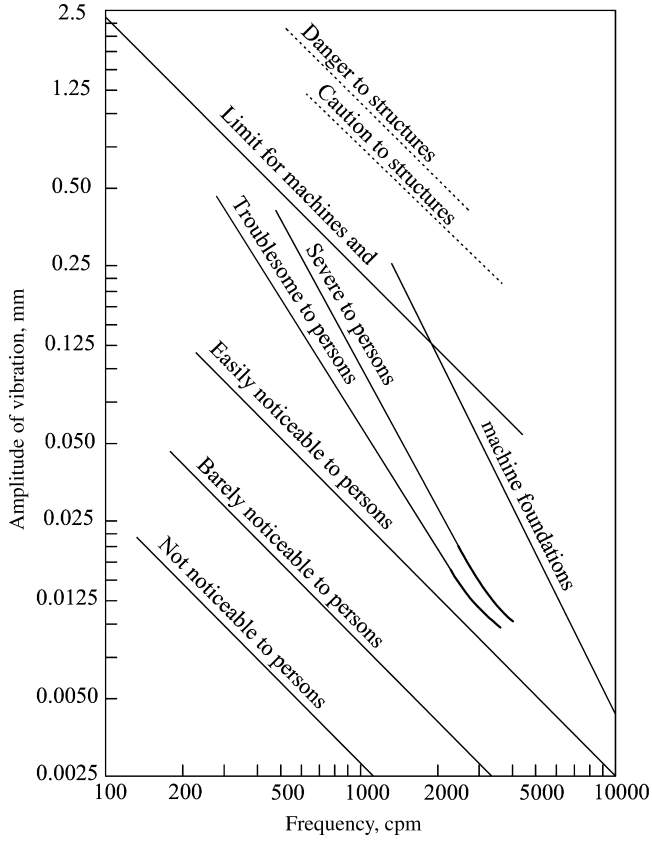

Figure 11.2 Limiting amplitudes for vertical vibration. (Richart, F.E./Hall, J.R./Woods, R.D., *Vibrations of Soils and Foundations*, 1st Edition, © 1970, p. 311. Printed and electronically reproduced by permission of Pearson Education, Inc., Upper Saddle River, New Jersey.)

Among these, situations where foundations are excited by forces and moments caused due to the machines operating on them are of great interest. The location and magnitudes of these loads and moments have to be carefully assessed (Richart, Hall and Woods, 1970) if not provided by the manufacturer. Machine details including static loads (magnitude and point of action), operating speeds and other geometrical features are usually furnished by the manufacturer.

11.5 Physical Modeling and Response Analysis

While the structural and machine components do not leave much of an alternative for idealization (hence chances of misjudgment are expected to be very limited), it is the soil medium where the study has to be intensive coupled with judgment. A brief and critical review on dynamics of soil–structure systems (Woods, 1976; Kameswara Rao, 1977) brings out the

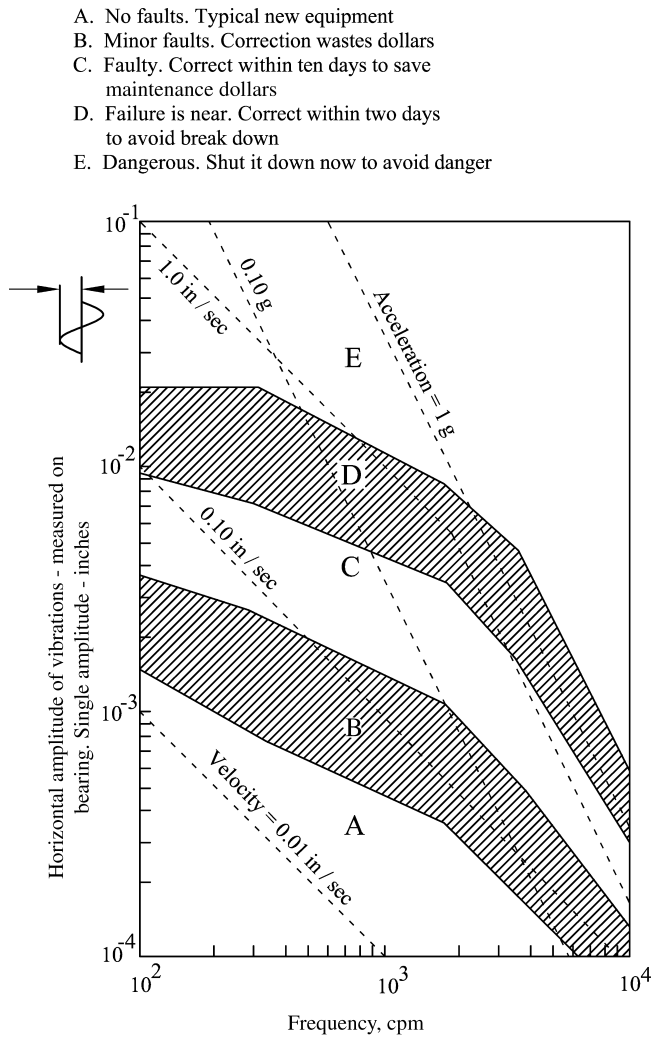

Figure 11.3 Criteria for vibrations of rotating machinery. (Reproduced from M.P. Blake, "New vibration standards for maintenance," *Journal of Hydrocarbon Processing and Petroleum Refiner*, vol. **43**, no. 1, pp. 111–114, © 1964, with permission from Gulf Publishing Company, Houston, Texas.)

status of the various methods. However, some important aspects of the approaches are highlighted below.

11.5.1 Dynamic Interaction of Rigid Foundations and Soil Media

A rigid foundation on soil medium having six degrees of freedom: three components of position (translation – vertical, longitudinal and lateral motions) and three angles defining

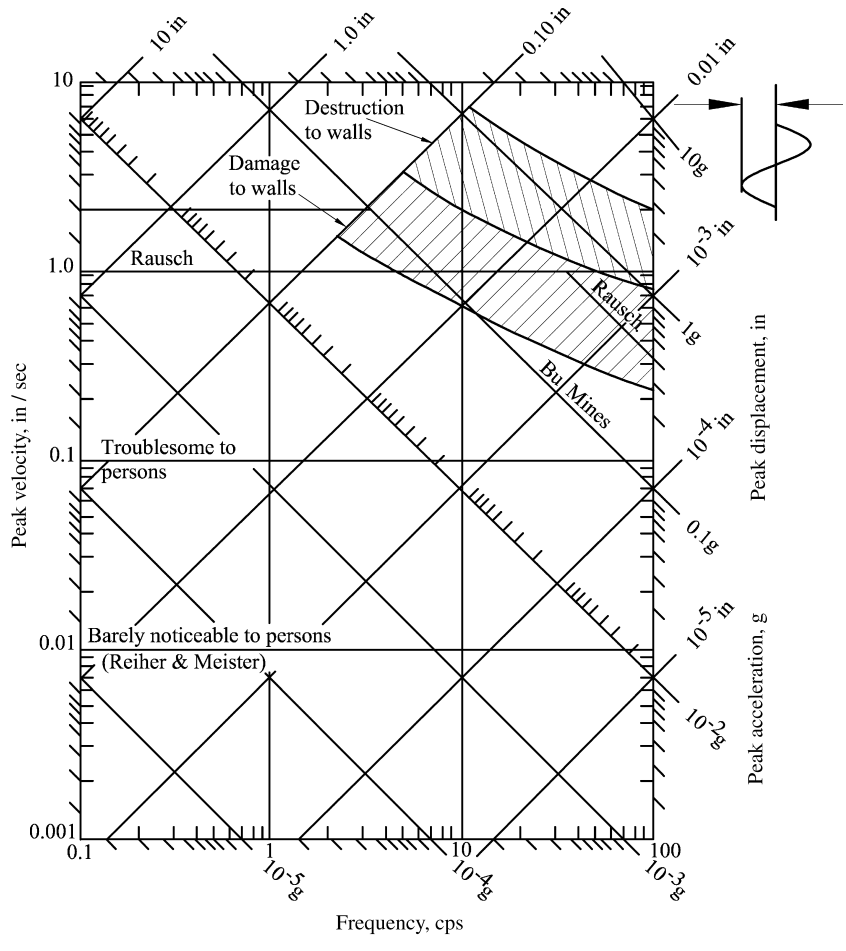

Figure 11.4 Response spectra for vibration limits. (Richart, F.E./Hall, J.R./Woods, R.D., *Vibrations of Soils and Foundations*, 1st Edition, © 1970, p. 316. Printed and electronically reproduced by permission of Pearson Education, Inc., Upper Saddle River, New Jersey.)

its orientation (rotation – yawing, pitching and rocking motions), is shown in Figure 11.5. A flexible foundation has infinite degrees of freedom. The vibratory motions can occur independently or in a coupled manner. Often the dynamics of continuous systems can be handled without much loss in accuracy by resolving them into equivalent systems with finite degrees of freedom idealizing parts of such systems as rigid bodies. In general the machine and the foundation block are idealized as rigid bodies in almost all methods of analysis in practice.

Starting from some of the approximate approaches as suggested by Barkan, Pauw, Ford and Haddow (Barkan, 1962; Kameswara Rao, 1998), the theory as well as experimental techniques have attained a high level of sophistication so as to be able to treat the soil medium either as elastic, or elastoplastic or as a viscoelastic medium. Translational as well as rotational modes

Table 11.1 Guidelines for choosing weight of foundation block.

Type of engine	Weight of foundation/weight of engine
Gas engines	
One cylinder	3.00
Two cylinders	3.00
Four cylinders	2.75
Six cylinders	2.25
Eight cylinders	2.00
Diesel engines	
Two cylinders	2.75
Four cylinders	2.10
Six cylinders	2.10
Eight cylinders	1.90
Others	
Rotary converter	0.50–0.75
Vertical compound steam engine coupled to generator	3.80
Vertical triple-expansion steam engine coupled to generator	3.50
Horizontal cross-compound engine coupled to generator	3.25
Horizontal steam turbine coupled to generator	3.00–4.00
Horizontal steam turbine coupled to generator	3.50
Vertical diesel engine coupled to generator	2.60
Vertical gas engine coupled to generator	3.50

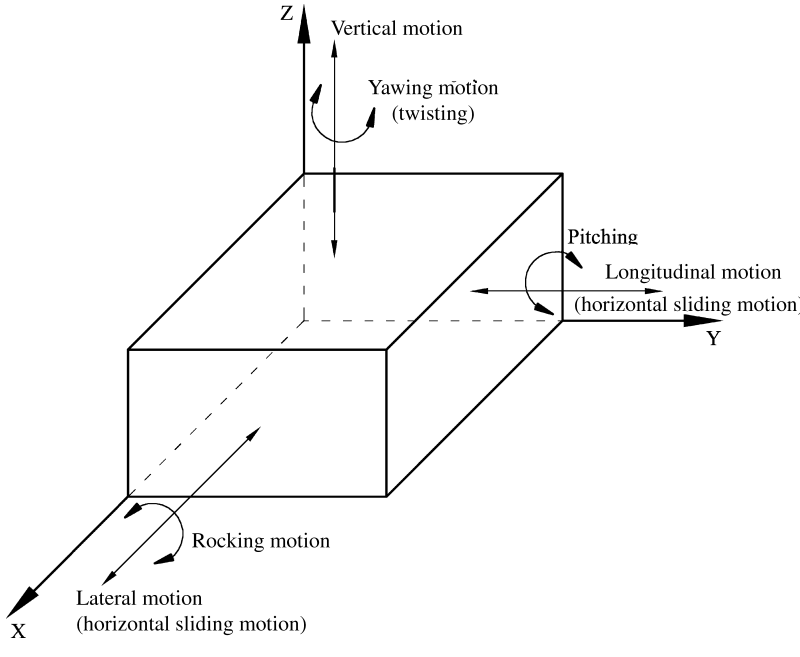

Figure 11.5 Rigid body (foundation block) on soil medium.

can be analyzed. A few important approaches among these are discussed in the following sections.

11.5.2 Idealization of Foundation Dynamics Problems

To predict the dynamic performance of a MFS, in a large number of cases the system can be conveniently and satisfactorily analyzed by idealizing it as a single degree of freedom system (SDF; Richart, Hall and Woods, 1970), for which the solutions are readily available. Depending on the situation, an idealized model consisting of a multidegree of freedom system (MDF) can also be formulated and solutions can be attempted. A few typical idealizations are shown in Figure 11.6. While the SDF appears to be a gross simplification of a real problem of MFS, experience has shown that it provides satisfactory solutions to predict the dynamic behavior. In fact, a footing resting on an elastic soil medium has been shown to be equivalent to an SDF system for dynamic analysis (Kameswara Rao, 1998).

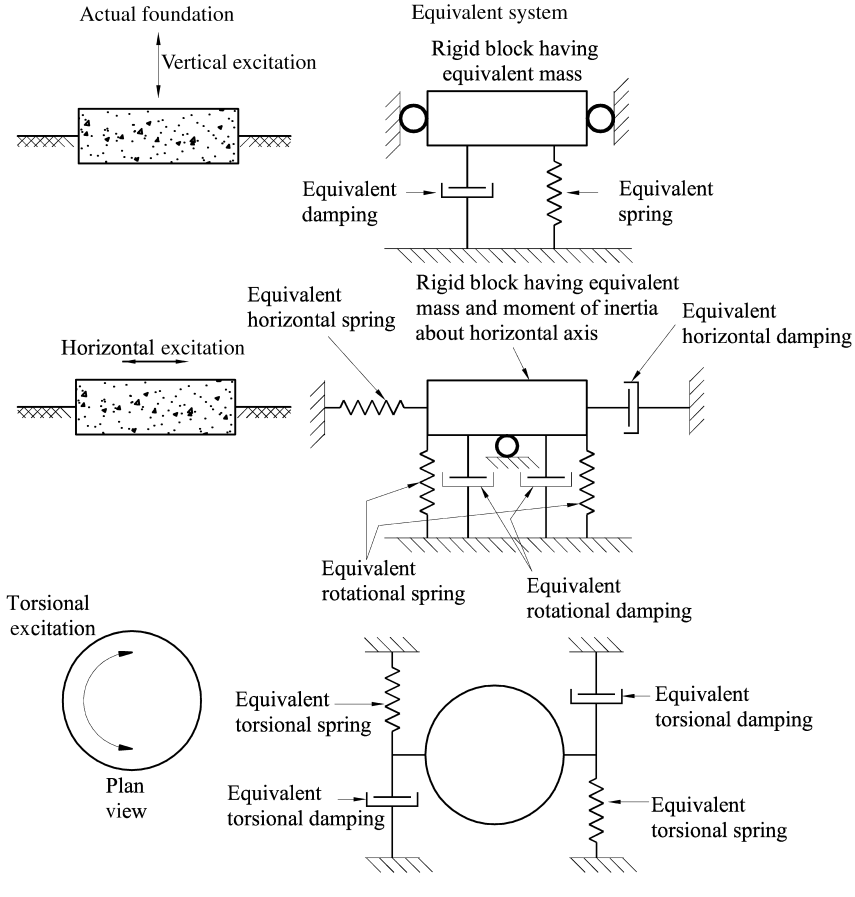

Figure 11.6 Typical equivalent multidegree of freedom systems.

The theory of vibrations of discrete systems has been presented in detail in several books on vibrations (Thomson, 1965; Rao, 1986; Kameswara Rao, 1998; Kameswara Rao, 2005). Solutions to specific problems can be readily obtained using the methods presented in these books as well as from other references. Elements of the theory and a brief summary of solutions are given in Appendix 11.A at the end of this chapter for ready reference.

Thus the spring–mass–dashpot system represents one of the theoretical models developed for an easy and direct application to the problems of machine foundations. The elastic half space model which deals with the problem of vibratory loads on semi-infinite half space using elastic theory represents another useful model and has been discussed in detail by Richart, Hall and Woods (1970) and Kameswara Rao (1998). Besides these, a number of empirical and semi-empirical approaches have been developed. These are applicable to problems of foundation vibration in a restricted sense and the degree of empiricism should be properly understood before application to specific problems. The empirical methods have been evolved based on observed behavior of foundations subjected to vibratory loads. The uncertainty regarding the mutual influence among the applied vibratory load, the geometric parameters of the foundations and the dynamic properties of the soil warrants caution in the choice of empirical relationships in machine foundation design. A few important results from these simple approaches are presented below.

11.5.3 Resonant Frequency

Referring to SDF idealization of the MFS, the natural frequency ω_n, of an undamped system is expressed as

$$\omega_n = \sqrt{\left(\frac{k}{m}\right)} \tag{11.4}$$

where

k = equivalent spring constant
m = mass of machine and foundation.

The theory of vibration for spring–mass–dashpot systems considers the spring to be weightless and accordingly Equation (11.4) has been derived. This theory can be applied to foundation vibrations only if the mass of the soil participating in the vibration can also be included. If the effect of the mass of the soil, m_s, is taken into account, the expression as shown in Equation (11.4) becomes (Kameswara Rao, 1998)

$$\omega_n = \left(\frac{k}{m+m_s}\right)^{1/2} \quad \text{and} \quad f_n = \frac{1}{2\pi}\left(\frac{k}{m+m_s}\right)^{1/2} \tag{11.5}$$

where

$f_n = \dfrac{\omega_n}{2\pi}$ = natural frequency in cps
m_s = mass of soil participating in vibration.

In the case of machine foundations, the mass of soil, m_s, participating in vibration needs to be determined. There have been several approaches suggested to determine the effective or equivalent mass of soil, m_s, in calculating the natural frequency. The choice of any one method still remains the designer's preference. Some of these methods are discussed below.

Barkan (1962), Pauw, Ford and Haddow, Converse, Newcomb, Tschebotarioff and Ward, Lorenz, Crockett and Hammond, Rao and Nagaraj (Kameswara Rao, 1998) are some of the earlier contributors for the analysis and design of machine foundations using empirical and semi-empirical methods based on tests and simple idealizations. The details of these methods are discussed by Richart, Hall and Woods (1970) and Kameswara Rao (1998). However, these approaches mainly use SDF systems and the determination of the mass (including apparent mass of soil participating in vibrations), spring constant of the soil and damping ratio. Then the natural frequencies are determined using Equations (11.4) and (11.5) and responses are computed using the available solutions of SDF (Rao, 1986; Kameswara Rao, 1998). In this context a few observations on some of these parameters, that is, apparent mass of soil participating in vibrations, spring constants and damping coefficients needed for computations are summarized below.

11.5.4 Apparent Mass of Soil

If the apparent mass of soil, m_s, participating in vibration is determined, the natural frequency of the soil can be easily obtained from Equation (11.5).

Barkan (1962) has suggested that the mass of the vibrating soil should lie between 2/3 to 1.5 times the total mass of the vibrator and foundations.

Lorenz (Kameswara Rao, 1998) reasoned from his investigations that the apparent mass of soil did not depend either on the unit contact pressure or on the size of the contact area but appeared to increase with increasing vibratory force. He also concluded that the natural frequency itself was only slightly affected by the size of the contact area.

Crockett and Hammond (Kameswara Rao, 1998) observed that the natural frequency is a function of the Rayleigh wave velocity in the medium, which depends on the density and elastic modulus of the medium. They also introduced the concept that the apparent mass of soil is equivalent to the soil contained in some bulb of pressure. Later Rao and Nagaraj (Kameswara Rao, 1998) suggested that the soil contained in the pressure bulb corresponding to ρ *psf*, where ρ is the density of the soil in *pcf*, will be equivalent to the apparent soil mass. This suggestion is based on their experimental data.

11.5.5 Spring Constants and Damping Coefficients

As brought out in the above section, computations of the resonant frequency, responses of MFS using a spring–mass–dashpot type of discrete system idealization required the determination of the spring constant, damping constant and the mass of the machine and foundation as well as apparent mass of soil participating in vibration. One of the important approaches is due to Barkan (1962) and is briefly discussed below.

11.5.6 Barkan's Approach

Barkan (1962) used the cyclic plate load tests to obtain the equivalent spring constants in various modes of vibration. A detailed presentation of these results and expressions are given by Kameswara Rao (1998) and discussed in Chapter 4. For example, by plotting the recoverable or elastic deformation against the bearing pressure from the cyclic plate load

test in the vertical mode, we can get the coefficient of elastic uniform compression, C_u, as the slope of the linear portion of the plot. Then the spring constant, k_v, in the vertical direction can be obtained as

$$k_v = C_u \times A \tag{11.6}$$

where

C_u = coefficient of elastic uniform compression in the vertical direction
A = area of the plate/foundation used for the test.

It may be noted that $C_u = k_s$, where k_s is called the modulus of subgrade reaction of the soil as discussed in Section 4.8.

C_u is also related to the elastic properties of the soil and can be obtained from theory of elasticity as

$$C_u = \frac{E}{1-v^2}\frac{C}{\sqrt{A}} \tag{11.7}$$

where

E, v = Young's modulus of elasticity and Poisson's ratio of the soil/half space respectively
A = area of the plate/foundation
C = constant depending on the shape and flexibility of the plate/foundation.

The values of C (c_f for flexible plate, c_r for rigid plate) are given by Kameswara Rao (1998, 2000) and discussed in Chapter 4.

From Equation (11.6) it can be noted that C_u is inversely proportional to the contact area of the plate. The same can be used to compute the value of C_{u2} for a plate of area A_2, knowing the value of C_{u1} for the plate of area A_1 as

$$\frac{C_{u2}}{C_{u1}} = \left(\frac{A_1}{A_2}\right)^{1/2} \tag{11.8}$$

Similar expressions for other modes of test (lateral, horizontal, rotational, etc.) can be obtained as given by Barkan (1962) and are summarized by Kameswara Rao (1998, 2000).

Since there is no direct way of obtaining Poisson's ratio, v, from the cyclic plate load test, the same has to be obtained from other relevant laboratory and/or field tests (Kameswara Rao, 1998, 2000). Since it is generally noted that the elastic response values are not very sensitive to a wide variation in the values of Poisson's ratio, usually the following values are taken in the absence of specific test results (Richart, Hall and Woods, 1970):

$$\begin{aligned} v \text{ for cohesionless soils} &= 0.25 \text{ to } 0.3 \\ v \text{ for cohesive soils} &= 0.35 \text{ to } 0.45 \end{aligned} \tag{11.9}$$

Accordingly an average value of $v = 0.3$ for cohesionless soils and 0.4 for cohesive soils could be used for computational purposes in the absence of any test data.

11.6 Analysis by Lysmer and Richart

11.6.1 Introduction

Lysmer and Richart (1966) presented in their analysis a method of finding a simplified analog for the dynamic behavior of footings on elastic half space which can be applied for all frequency

ranges of steady state motion. They also calculated the transient response caused by an arbitrary pulse loading using the steady state solutions. The components of this analog consist of mass, spring and dashpot and are independent of the frequency of the exciting force. This approach facilitates the application of classical methods of elastic theory for the study of the dynamic behavior using simpler models of mass, spring and dashpot. The investigations are limited to the case of axisymmetric dynamic vertical force on a rigid circular footing, though it can be extended to other modes. It has been assumed that the soil is elastic, homogeneous and isotropic and only normal stresses are transferred at the contact area between soil and footing. Important details of the method are also given by Richart, Hall and Woods (1970) and Kameswara Rao (1998). The components of the equivalent analog model are obtained as below. The equivalent analog is taken as SDF consisting of mass, spring and a dashpot as shown in Figure 11.7.

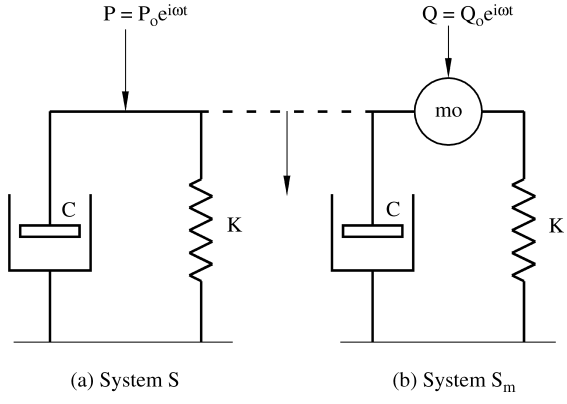

Figure 11.7 Simple damped oscillators.

Thus the simplified analog has the components as

$$m_o = \text{mass of footing} \tag{11.10}$$

$$k = \text{equivalent spring constant} = \frac{4\mu r_0}{1-v} \tag{11.11}$$

$$c = \text{equivalent damping constant} = 0.85\frac{kr_0}{V_s} = \frac{3.4}{1-v}r_0^2\left(\frac{\rho\mu}{g}\right)^{1/2} \tag{11.12}$$

where

μ = shear modulus of the soil
r_0 = radius of the circular footing
ρ = unit weight of soil
g = acceleration due to gravity
V_s = shear wave velocity in the soil medium.

The accuracy of the results using the analog model with the choice of m_o, c, and k as given in Equations (11.10)–(11.12) can be clearly noted by comparing these results with those of elastic half space theory obtained by Lysmer (1966). Lysmer and Richart also compared the results

with the field test results reported by Fry and others (Richart, Hall and Woods, 1970) and reported satisfactory agreement.

For these values of c and k, it can be shown that resonance occurs only when $b_o \geq 0.36$, where

$$b_o = \text{mass ratio} = \frac{(1-v)m_o g}{4\rho {r_0}^3} \tag{11.13}$$

Accordingly the approximate expressions for frequency and amplitude at resonance can be obtained as

$$\begin{aligned} \omega_{res} &= \frac{V_s}{r_o}\left(\frac{b_o - 0.36}{b_o}\right)^{1/2} \\ \delta_{res} &= \frac{Q_0}{k}\,\frac{b_0}{0.85(b_0 - 0.18)^{1/2}} \end{aligned} \tag{11.14}$$

where

Q_0 = amplitude of harmonic force acting on the mass m_o.

If $b_o < 0.36$, it is obvious that the resonance does not occur and the static amplitude itself is the maximum for such a system. This is similar to the situation observed for an SDF for cases of damping factor $\zeta > 1$ (Kameswara Rao, 1998).

As the steady state solutions tally well for the footing soil system and its simplified analog, it can be expected that they behave very closely in free vibrations and under transient motion. Lysmer and Richart (1966) presented analysis for the above cases also and some important results are given below.

1. Free vibrations

$$\delta_{\ln} = \text{logarithmic decrement} = \log_e\left(\frac{\delta_n}{\delta_{n+1}}\right) = \frac{2.67}{(b_0 - 0.18)^{1/2}} \tag{11.15}$$

$$\omega_d = \text{damped natural frequency} = \frac{V_s}{r_0}\,\frac{(b_0 - 0.18)^{1/2}}{b_0} \tag{11.16}$$

where δ_n and δ_{n+1} are amplitudes of motion in the nth and $(n+1)$th cycles of the free vibration motion, and $\log_e$ is the natural logarithm.

2. Frequency-dependent dynamic loads

If the dynamic load is frequency-dependent, that is, of the type

$$Q_o = m_e e \omega^2$$

where

m_e = eccentric rotating mass
e = eccentricity
ω = frequency of rotation,

then expressions for ω_{res} and δ_{res} can be obtained as

$$\omega_{res} = \frac{V_s}{r_o} \frac{1}{(b_o - 0.36)^{1/2}} \tag{11.17}$$

$$\delta_{res} = \frac{Q_0}{ka_0^2} \frac{1}{0.85(b_0 - 0.18)^{1/2}} \tag{11.18}$$

11.6.2 Other Modes

All modes of vibration of a rigid circular (or an equivalent circle for rectangular shaped) footing resting on an elastic half space can be expressed in terms of analog parameters of an equivalent single degree of freedom system, in which the parameters are frequency independent. Hall followed the approach of Lysmer (Richart, Hall and Woods, 1970) and derived analog parameters for rocking, sliding along and about horizontal direction and torsional modes. The expressions for stiffness and damping parameters are given in Table 11.B.1.

11.6.3 Analog Models for Dynamic Analysis of Single Piles

Novak (1974) analyzed the vibration of single piles in different modes of vibration. He gave the pile head stiffness and damping parameters for floating and endbearing piles. These parameters are frequency-independent. The stiffness and damping parameters are expressed in terms of nondimensional parameters. These expressions as well as the values of the nondimensional parameters are given in Kameswara Rao (1998).

Example 11.1

A rectangular RCC machine foundation of size $2.0 \times 2.0 \times 0.75$ m thick is supporting a machine of negligible weight. The machine transmits an unbalanced vertical load passing through the combined CG of the machine and foundation whose amplitude is $10\left[1 - \sin\frac{\pi}{4}t\right]$ kN. Soil medium has the following properties:

1. Young's modulus, $E = 0.6 \times 10^5$ kN/m^2.
2. Poisson's ratio, $v = 0.4$.
3. Unit weight of soil, $\gamma = 18$ kN/m^3.

Find the response of the system and natural frequency using the analog model of Lysmer and Richart.

Solution:
Assume unit weight of concrete $= 24$ kN/m^3
Then, the weight of the foundation block, $W = 2.0 \times 2.0 \times 0.75 \times 24 = 72$ kN

$$\text{Equivalent radius of the foundation block, } r_z = \left(\frac{ab}{\pi}\right)^{0.5} = \left(\frac{2.0 \times 2.0}{\pi}\right)^{0.5} = 1.13 \tag{11.19}$$

$$\text{Shear modulus, } \mu = \frac{E}{2(1+v)} = \frac{0.6 \times 10^5}{2(1+0.4)} = 0.214 \times 10^5 \text{ kN/m}^2 \tag{11.20}$$

$$\text{Velocity of the shear wave, } V_s = \left(\frac{\mu g}{\rho}\right)^{0.5} = \left[\frac{0.214 \times 10^5 \times 9.81}{18}\right]^{0.5} = 108 \text{ m/s} \tag{11.21}$$

$$\text{Mass ratio, } b_z = \frac{0.25\, mg\,(1-v)}{\rho r_z^3} = \frac{0.25 \times 72 \times (1-0.4)}{18 \times 1.13^3} = 0.416 \tag{11.22}$$

$$\text{Damping ratio, } \zeta_{zz} = \frac{0.425}{\sqrt{b_z}} = \frac{0.425}{\sqrt{0.416}} = 0.66 \tag{11.23}$$

$$\text{Spring constant, } k_{zz} = \frac{4\mu_s r_z}{(1-v)} = \frac{4 \times 0.214 \times 10^5 \times 1.13}{(1-0.4)} = 1.61 \times 10^5 \text{ kN/m} \tag{11.24}$$

$$\text{Damping constant, } c_{zz} = 2\zeta_z\sqrt{k_z m} = 2 \times 0.66 \times \sqrt{1.61 \times 10^5 \times \frac{72}{9.81}} = 1435 \text{ kN s/m} \tag{11.25}$$

$$\text{Natural frequency of the system, } \omega_n = \sqrt{\frac{k_z}{m}} = \sqrt{\frac{1.61 \times 10^5}{72/9.81}} = 148 \text{ rad/s} \tag{11.26}$$

$$\text{Operating frequency of the machine, } \omega = \frac{\pi}{4} \text{rad/s}$$

$$\text{Therefore, the frequency ratio} = \frac{\omega}{\omega_n} = \frac{\pi/4}{148} = 0.0053$$

The equation of motion in case of the underdamped vibrations is given by (Kameswara Rao, 1998)

$$m\ddot{z} + c\dot{z} + kz = F_o - F_1 \sin \omega t = 10\left(1 - \sin\frac{\pi}{4}t\right) \tag{11.27}$$

Amplitude of motion can be obtained for $F(t) = F_o$, and $F(t) = F_1 \sin \omega t$ separately and then superposing the two solutions (Kameswara Rao, 1998).
The solution for $F(t) = F_o = 10$ is

$$z_1 = \frac{F_o}{k_{zz}} = \frac{10}{1.61 \times 10^5} = 6.21 \times 10^{-5}\ \text{m} \tag{11.28}$$

The solution for $F(t) = F_1 \sin \omega t = -10 \sin \frac{\pi}{4} t$ is

$$z_2 = \frac{F_1}{k_{zz}} \frac{1}{\sqrt{\left[1-\left(\frac{\omega}{\omega_n}\right)^2\right]^2 + \left(2\zeta_z \frac{\omega}{\omega_n}\right)^2}} \sin\left(\frac{\pi}{4} t - \varphi\right) \tag{11.29}$$

where φ is the phase angle given by

$$\tan \varphi = \frac{2\zeta_z \left(\frac{\omega}{\omega_n}\right)}{1-\left(\frac{\omega}{\omega_n}\right)^2} \tag{11.30}$$

Therefore

$$\varphi = \tan^{-1}\left[\frac{2 \times 0.66 \times 0.0053}{1-0.0053^2}\right] = 6.996 \times 10^{-3}\ \text{rad}$$

Now

$$z_2 = \frac{-10}{1.61 \times 10^5}\left[\frac{1}{\sqrt{[1-0.0053^2]^2 + (2 \times 0.66 \times 0.0053)^2}}\right] \sin\left(\frac{\pi}{4} t - 6.996 \times 10^{-3}\right)$$

$$= -62.1 \times 10^{-6} \sin(0.785t - 6.996 \times 10^{-3})\text{m}$$

The steady state solution is given by

$$\begin{aligned} z &= z_1 + z_2 \\ &= 6.21 \times 10^{-5} - 6.21 \times 10^{-5} \sin(0.785t - 6.996 \times 10^{-3})\text{m} \end{aligned} \tag{11.31}$$

11.7 General Analysis of Machine–Foundation–Soil Systems Using Analog Models

Modern industrial construction practice requires solutions to many problems concerning machine foundations. The most important aspect which ensures the successful performance of machine is the proper dynamic behavior of the foundation–soil systems. Vibrations due to machines may cause damage to structures nearby or even to machines themselves. Hence a knowledge of the dynamic behavior of the foundation, the energy transmitted through soil and

the response of the foundation system is essential for proper design of the system. Machine installations can, in general, be supported either by rigid blocks directly resting on soil or by piles. The choice of the foundation system depends on the strength and compressibility characteristics of the soil and the performance criteria required.

Rational dynamic analysis of the foundation soil systems has been carried out by Sung, Quinlan, Richart, Hall and Woods, Lysmer and Richart, and Lysmer and Kuhlemeyer, Kausel, Luco and Westman, Ahmad and Banerjee and several others (Richart, Hall and Woods, 1970; Kameswara Rao, 1998). Besides methods which are either empirical or semi-empirical, the methodologies that are used for the prediction of dynamic behavior of machine foundation soil system (MFS) are: (1) elastic half space theory approach and (2) methods using discrete system representation using equivalent analog parameters. Closed form solutions have been obtained for foundations resting on a homogeneous elastic half space under different modes of vibration for regular shaped (circular, rectangular) foundations subjected to harmonic loads (Richart, Hall and Woods, 1970; Kameswara Rao, 1998). Based on elastic half space results (and making use of finite element methods with wave-absorbing boundaries and boundary element methods) some simplified (analog) models have been developed which are essentially models based on discrete representation of the system.

In general, machines transmit unbalanced dynamic loads and moments of general nature (consisting of several frequencies of different amplitudes) generated at various locations. The forces may be present in all the six modes of vibration and hence complete response analysis of MFS requires the formulation of equations of motion which are generally coupled and provide a solution in all six modes (Kameswara Rao, 1998). The coupled equations of motion of an MFS and machine–pile foundation–soil system (MPFS) are derived in the next section. A few examples of such coupled vibration problems subjected to arbitrary excitations are illustrated. Fourier analysis is used for problems involving arbitrary excitations of periodic nature. For exciting forces of general nature, solutions using numerical integration techniques can be used (Venugopala Rao, 1995). These methods give the total solution to the coupled equations of motion with arbitrary forcing functions and can be applied to any engineering system with any number of (finite) degrees of freedom, including continuous systems. However, the method is illustrated for machine–foundation–soil systems and machine–pile foundation–soil systems with six degrees of freedom (taking the foundation block to be rigid, as is normally done) subjected to dynamic forces of general nature in terms of amplitudes, directions, locations and time dependency. Total solutions can be obtained with very little computing effort and hence are easily adaptable to analyze a wide variety of problems of practical interest. These methods are particularly well suited for general machine foundation design and analysis. Lysmer's analog parameters (Richart, Hall and Woods, 1970) are used to model the soil medium while Novak's functions (Novak, 1974) are used to model pile–soil system for illustration. However, other modified parameters can also be used (if physical modeling so requires) such as those obtained by Wolf (1988), Mita and Luco (1989), Kameswara Rao (1998).

11.8 General Equations of Motion

11.8.1 Machine–Block Foundation–Soil System

A typical machine–foundation–soil system (MFS) is shown in Figure 11.8 with the foundation block supported on piles. However, for the present discussion consider the foundation block

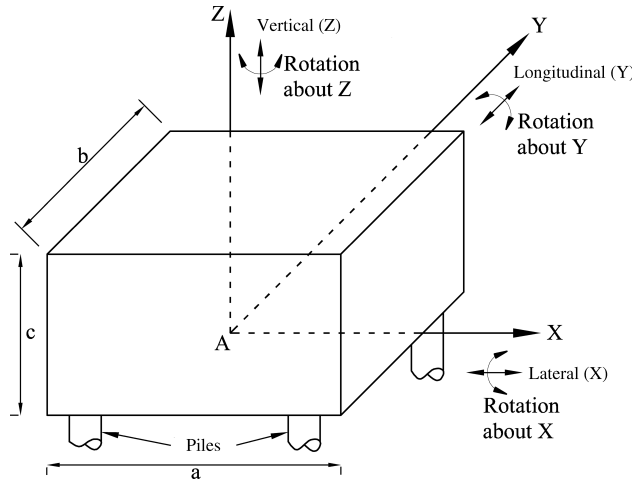

Figure 11.8 Typical machine–foundation system showing coordinate axes, forces and moments.

only (without piles). Typical views of the block with the sign convention are shown in Figure 11.9. Point *A* refers to the combined CG of the system and reference axes pass through point *A*. Now displacements at any point *s* can be expressed in terms of displacements of combined CG as

$$\begin{Bmatrix} w_s \\ u_s \\ \varphi_{ys} \\ v_s \\ \varphi_{xs} \\ \varphi_{zs} \end{Bmatrix} = \begin{Bmatrix} 1 & 0 & -x_s & 0 & y_s & 0 \\ 0 & 1 & z_s & 0 & 0 & -y_s \\ 0 & 0 & 1 & 0 & 0 & 0 \\ 0 & 0 & 0 & 1 & -z_s & x_s \\ 0 & 0 & 0 & 0 & 1 & 0 \\ 0 & 0 & 0 & 0 & 0 & 1 \end{Bmatrix} \begin{Bmatrix} w_A \\ u_A \\ \varphi_{yA} \\ v_A \\ \varphi_{xA} \\ \varphi_{zA} \end{Bmatrix} \tag{11.32}$$

where u, v, w and φ_x, φ_y, φ_z are displacements and rotations in the x, y, z directions, respectively. The subscripts A and s denote the corresponding values at locations A and s. Equation (11.32) can be written in matrix form as

$$\{d_s\} = [G_s]\{d_A\} \tag{11.33}$$

where $\{d_s\}$, $\{d_A\}$ denote displacement vectors at points s and A respectively, and $[Gs]$ is the geometric matrix of coordinates of the point s with respect to A.

Rearranging Equation (11.33), $\{d_A\}$ can also be expressed in terms $\{d_s\}$ as

$$\{d_A\} = [G_s]^{-1}\{d_s\} = [G_A]\{d_s\} \tag{11.34}$$

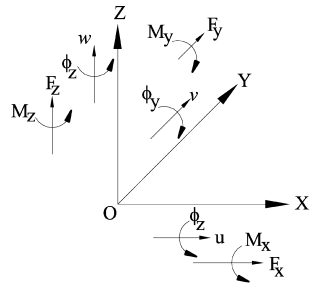

u, v, w – Displacements
ϕ_x, ϕ_y, ϕ_z – Rotations
F_x, F_y, F_z – Forces
M_x, M_y, M_z – Moments

(a) Convention sketch showing positive displacements and rotations (right handed co-ordinate system)

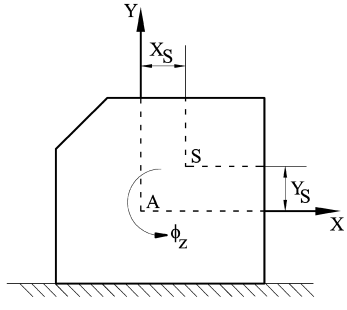

A – Combined C.G. of machine and foundation
S – Any point (X_S, Y_S, Z_S) (say center of contact pressure)

(b) Top view

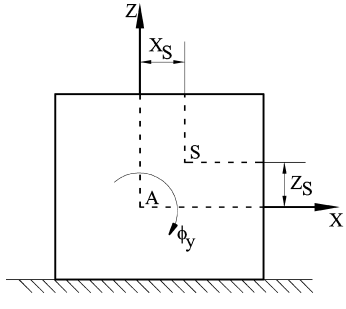

(c) Front view

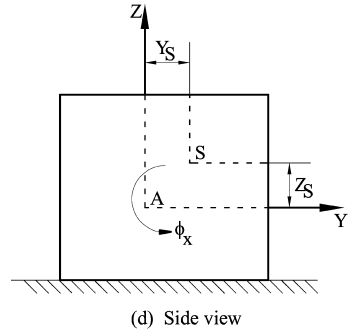

(d) Side view

Figure 11.9 Rigid foundation block supporting the machine.

where

$$[G_A] = \begin{Bmatrix} 1 & 0 & x_s & 0 & -y_s & 0 \\ 0 & 1 & -z_s & 0 & 0 & y_s \\ 0 & 0 & 1 & 0 & 0 & 0 \\ 0 & 0 & 0 & 1 & z_s & -x_s \\ 0 & 0 & 0 & 0 & 1 & 0 \\ 0 & 0 & 0 & 0 & 0 & 1 \end{Bmatrix} \tag{11.35}$$

$[G_A]$ can be identified to be the matrix of coordinates of A with respect to s.

The resultant soil reactions may be taken to be acting at point s without loss of generality (usually taken as center of contact area of the block) and consist of the forces

Pxs, *Pys*, *Pzs* and moments *Mxs*, *Mys*, *Mzs*. These quantities can be expressed (Kameswara Rao, 1998) as

$$\begin{Bmatrix} P_{zs} \\ P_{xs} \\ M_{ys} \\ P_{ys} \\ M_{xs} \\ M_{zs} \end{Bmatrix} = -\begin{bmatrix} k_{zz} & 0 & 0 & 0 & 0 & 0 \\ 0 & k_{xx} & 0 & 0 & 0 & 0 \\ 0 & 0 & k_{\varphi_{yy}} & 0 & 0 & 0 \\ 0 & 0 & 0 & k_{yy} & 0 & 0 \\ 0 & 0 & 0 & 0 & k_{\varphi_{xx}} & 0 \\ 0 & 0 & 0 & 0 & 0 & k_{\varphi_{zz}} \end{bmatrix} \begin{Bmatrix} w_s \\ u_s \\ \varphi_{ys} \\ v_s \\ \varphi_{xs} \\ \varphi_{zs} \end{Bmatrix}$$

$$-\begin{bmatrix} c_{zz} & 0 & 0 & 0 & 0 & 0 \\ 0 & c_{xx} & 0 & 0 & 0 & 0 \\ 0 & 0 & c_{\varphi_{yy}} & 0 & 0 & 0 \\ 0 & 0 & 0 & c_{yy} & 0 & 0 \\ 0 & 0 & 0 & 0 & c_{\varphi_{xx}} & 0 \\ 0 & 0 & 0 & 0 & 0 & c_{\varphi_{zz}} \end{bmatrix} \begin{Bmatrix} \dot{w}_s \\ \dot{u}_s \\ \dot{\varphi}_{ys} \\ \dot{v}_s \\ \dot{\varphi}_{xs} \\ \dot{\varphi}_{zs} \end{Bmatrix} \tag{11.36}$$

k_{xx}, c_{xx} ... and so on are the equivalent stiffness and damping parameters along the directions indicated by the subscripts and are called *analog parameters* of an equivalent mass–spring–-dashpot system. The symbol φ indicates rotation about the axis mentioned in the second subscript. Expressions derived by Richart, Hall and Woods (1970) and several others are available in literature as mentioned earlier in this chapter and are given by Kameswara Rao (1970). The commonly used analog parameters given by Richart, Hall and Woods (1970) discussed in Section 11.6 are given in Appendix 11.B (Table 11.B.1).

Equation (11.36) can be written in matrix form as

$$\{P_s\} = -[K]\{d_s\} - [C]\{d_s\} \tag{11.37}$$

The negative sign in Equations (11.36) and (11.37) indicates that the soil reactions on the foundation block are opposite in direction to the applied forces coming from the machine, and subscript *s* refers to the center of all such reactive forces usually taken as the center of contact area. These soil reactions (Equations (11.36) and (11.37)) are taken to be equal and opposite to the amplitude of contact pressure acting on the soil medium for the translational mode. Since the directions of these soil reactions are taken care of appropriately in Equations (11.36) and (11.37), they can now be vectorially added to the other forces acting on the rigid foundation block for writing down the governing equations of motion. The unbalanced forces and moments coming from various machine components/units can in general be converted into equivalent forces and moments acting at the combined CG (point *A*) of the machine–foundation system. In general these can be three forces $\bar{P}_x, \bar{P}_y, \bar{P}_z$ and three moments $\bar{M}_x, \bar{M}_y, \bar{M}_z$ acting along and about the *x*, *y*, *z* axes respectively. The soil reaction force vector $\{Ps\}$ given by Equation (11.37) can also be transformed as a vector acting at the combined CG (point *A*) as

$$\{P_A\} = [G_A]\{P_s\} \tag{11.38}$$

where $\{P_A\}$ is the equivalent force vector acting at *A* and G_A is given by Equation (11.35).

The dots over the variables denote their corresponding derivatives with respect to time.

11.8.1.1 Equations of Motion of MFS

Now dynamic equilibrium equations of rigid block can be written for all six modes of vibration of MFS as

$$\begin{aligned} m\ddot{w}_A &= \bar{P}_z + P_{zA} \\ m\ddot{u}_A &= P_x + P_{xA} \\ I_{\varphi y}\,\ddot{\varphi}_{yA} &= \bar{M}_y + M_{yA} \\ m\ddot{v}_A &= \bar{P}_y + P_{yA} \\ I_{\varphi x}\,\ddot{\varphi}_{xA} &= \bar{M}_x + M_{xA} \\ I_{\varphi z}\,\ddot{\varphi}_{zA} &= \bar{M}_z + M_{zA} \end{aligned} \tag{11.39}$$

where m is the total mass of the machine and foundation (including piles in case of pile foundation) and $I_{\varphi x}, I_{\varphi y}, I_{\varphi z}$ are mass moments of inertia of the machine and foundation about the x, y, z axes respectively.

These equations (Equation (11.39)) can be expressed in matrix form as

$$[m]\,\{\ddot{d}_A\} = \{\bar{P}\} + \{P_A\} \tag{11.40}$$

where $\{\bar{P}\}$ is the vector of forces and moments $\bar{P}_x, \bar{P}_y, \bar{P}_z, \bar{M}_z, \bar{M}_y$ and $\bar{M}_z$ acting at the combined CG of the MFS transmitted by the machine as explained above.

Substituting expression for $\{P_A\}$ from Equation (11.38) and expressions for $\{ds\}, \{Ps\}$ from Equations (11.33)–(11.37) in Equation (11.40), we get the equations of motion of machine-foundation-soil system as

$$[m]\{\ddot{d}_A\} + [G_A][C][G_S]\{\dot{d}_A\} + [G_A][K][G_S]\{d_A\} = [m]\{\ddot{d}_A\} + [C_A]\{\dot{d}_A\} + [K_A]\{d_A\} = \{\bar{P}\} \tag{11.41}$$

where m, C_A, K_A are the system mass, damping and stiffness matrices of the MFS.

11.8.2 Machine–Pile Foundation–Soil System

In the case of machine–block–pile foundation–soil system (MPFS) shown in Figure 11.8, the dynamic reactions acting on the pile cap at s*th* pile head can be expressed similarly (Kameswara Rao, 1998) as

$$\begin{Bmatrix} P_{zs} \\ P_{xs} \\ M_{ys} \\ P_{ys} \\ M_{xs} \\ M_{zs} \end{Bmatrix} = -\begin{bmatrix} k_{zzs} & 0 & 0 & 0 & 0 & 0 \\ 0 & k_{xxs} & k_{x\varphi ys} & 0 & 0 & 0 \\ 0 & k_{\varphi yxs} & k_{\varphi yys} & 0 & 0 & 0 \\ 0 & 0 & 0 & k_{yys} & k_{y\varphi xs} & 0 \\ 0 & 0 & 0 & k_{\varphi xys} & k_{\varphi xxs} & 0 \\ 0 & 0 & 0 & 0 & 0 & k_{\varphi zzs} \end{bmatrix} \begin{Bmatrix} w_s \\ u_s \\ \varphi_{ys} \\ v_s \\ \varphi_{xs} \\ \varphi_{zx} \end{Bmatrix}$$
$$-\begin{bmatrix} c_{zzs} & 0 & 0 & 0 & 0 & 0 \\ 0 & c_{xxs} & c_{x\varphi ys} & 0 & 0 & 0 \\ 0 & c_{\varphi yxs} & c_{\varphi yys} & 0 & 0 & 0 \\ 0 & 0 & 0 & c_{yys} & c_{y\varphi xs} & 0 \\ 0 & 0 & 0 & c_{\varphi xys} & c_{\varphi xxs} & 0 \\ 0 & 0 & 0 & 0 & 0 & c_{\phi zzs} \end{bmatrix} \begin{Bmatrix} \dot{w}_s \\ \dot{u}_s \\ \dot{\varphi}_{ys} \\ \dot{v}_s \\ \dot{\varphi}_{xs} \\ \dot{\varphi}_{zx} \end{Bmatrix} \tag{11.42}$$

which can be written as

$$\{P_s\} = -[K_s]\{d_s\} - [C_s]\{\dot{d}_s\} \tag{11.43}$$

The negative sign in Equations (11.42) and (11.43) indicates that the reactions on the pile cap are opposite in direction to the applied forces and subscript s indicates that the quantities refer to sth pile. k_{xxs}, c_{xxs}, and so on, are the stiffness and damping parameters of the individual piles along the directions indicated by the subscripts. Expressions for these parameters as derived by Novak (1974) are given in Kameswara Rao (1998). The reactions on the pile cap (Equations (11.42) and (11.43)) are taken to be equal and opposite to the forces due to piles acting on the soil medium. Since the directions of these reactions are taken care of appropriately in Equations (11.42) and (11.43) they can now be vectorially added to the other forces and moments acting on the rigid pile cap for writing down the governing equation of motion. The unbalanced forces and moments coming from various machine components can in general be converted into equivalent forces and moments acting at the combined CG (point A). It consists, in general, of three forces, $\bar{P}_x, \bar{P}_y, \bar{P}_z$ and three moments $\bar{M}_x, \bar{M}_y, \bar{M}_z$ denoted by vector $\{\bar{P}_A\}$. The reaction force vector $\{P_s\}$ acting at any point/pile s can be transformed to a force vector acting at point A as

$$\{P_A\} = [G_A]\{P_s\} \tag{11.44}$$

where $\{P_A\}$ is an equivalent force vector acting at point A and G_A is given by Equation (11.35).

11.8.2.1 Equations of Motion of MPFS

Equations of motion of rigid pile cap of MPFS can now be written as

$$\begin{aligned}
m\ddot{w}_A &= \bar{P}_z + \sum_s P_{zA} \\
m\ddot{u}_A &= \bar{P}_x + \sum_s P_{xA} \\
I_{\varphi y}\,\ddot{\varphi}_{yA} &= \bar{M}_y + \sum_s M_{yA} \\
m\ddot{v}_A &= \bar{P}_y + \sum_s P_{yA} \\
I_{\varphi x}\,\ddot{\varphi}_{xA} &= \bar{M}_x + \sum_s M_{xA} \\
I_{\varphi z}\,\ddot{\varphi}_{zA} &= \bar{M}_z + \sum_s M_{zA}
\end{aligned} \tag{11.45}$$

These equations can be written in matrix form as

$$[m]\,\{\ddot{d}_A\} = \{\bar{P}\} + \sum_s \{P_A\} \tag{11.46}$$

Substituting expression for $\{P_A\}$ from Equation (11.44) and expression for $\{d_s\}$ and $\{P_s\}$ from Equations (11.33) to (11.37), in Equation (11.46), results in equations of motion of MPFS system as

$$[m]\{\ddot{d}_A\} + \sum([G_A][C][G_s]\{\dot{d}_A\}) + \sum_s([G_A][K][G_s]\{d_s\})$$
$$= [m]\{\ddot{d}_A\} + [C_{Ap}]\{\dot{d}_A\} + [K_{Ap}]\{d_A\} = \{\bar{P}\} \tag{11.47}$$

where $[m]$, $[C_{Ap}]$, $[K_{Ap}]$ are the system mass, damping and stiffness matrices of the MPFS respectively.

The summation has to be carried out for all the piles in the group. It may be noted that Equations (11.41) and (11.47) are similar in form.

In Equations (11.40) and (11.46), $[m]$ is the diagonal mass matrix consisting of $m, m, I_{\varphi y}, k, I_{\varphi x}, I_{\varphi z}$ as diagonal elements and $\{\bar{P}\}$ and $\{P_A\}$ are vectors of equivalent external forces and soil reactions respectively acting at point A. m is the total mass of the machine and rigid block/pile cap including piles. $I_{\varphi x}, I_{\varphi y}, I_{\varphi z}$ are the mass moments of inertia of machine foundation block/pile cap about the x, y, z axes passing through point A respectively.

In Equation (11.45)$\{P_{zA}\}$ and so on (i.e., second terms of the right hand side of the equations) are equivalent soil reactions due to any piles converted as equivalent forces and moments acting at point A (the combined CG). In Equations (11.45) and (11.46) the summation is carried out over all s, signifying the number of piles on which the foundation block and machine assembly is supported.

Thus, Equations (11.41) have to be analyzed in case only block foundation is used while Equations (11.47) have to be analyzed if pile foundation are used.

These six coupled equations (linear) will uniquely determine the responses $u_A, v_A, w_A, \varphi_x, \varphi_y, \varphi_z$ of the rigid body subjected to dynamic loads and moments $\bar{P}_x, \bar{P}_y, \bar{P}_z, \bar{M}_x, \bar{M}_y, \bar{M}_z$. These equations are similar to those of MDF and accordingly analytical and numerical methods discussed by Kameswara Rao (1998) and Rao (1986) can be used to study the free and forced vibrations of such systems. Solutions can also be directly attempted using ordinary differential equations theory (for simultaneous variables).

11.8.3 Some Simplifications for MFS

Under some conditions of symmetry which can be easily adopted by the designer, Equation (11.41) can be considerably simplified. For example, if the center of contact area, B, can be made to lie on the vertical line passing through the combined CG of the machine and foundation, A (z axis), then it is obvious that

$$x_A = x_s = 0;\ y_B = y_s = 0;\ z_B = z_s \tag{11.48}$$

Substituting $x_s = y_s = 0$ in Equation (11.41), the resulting equations are

$$m\frac{d^2u_A}{dt^2} + c_x\frac{du_A}{dt} + k_x u_A + z_B\left[c_x\frac{d\phi_y}{dt} + k_x\varphi_y\right] = \bar{P}_x \tag{11.49}$$

$$m\frac{d^2v_A}{dt^2} + c_y\frac{dv_A}{dt} + k_y v_A - z_B\left(c_y\frac{d\varphi_x}{dt} + k_y\varphi_x\right) = \bar{P}_y \tag{11.50}$$

$$m\frac{d^2w_A}{dt^2} + c_z\frac{dw_A}{dt} + k_z w_A = \bar{P}_z \tag{11.51}$$

$$I_x\frac{d^2\varphi_x}{dt^2} + (H_x + z_B^2 c_y)\frac{d\varphi_x}{dt} + (S_x + z_B^2 k_y)\varphi_x - z_B\left(c_y\frac{dv_A}{dt} + k_y v_A\right) = \bar{M}_x \tag{11.52}$$

$$I_y\frac{d^2\varphi_y}{dt^2} + (H_y + z_B^2 c_x)\frac{d\varphi_y}{dt} + (S_y + z_B^2 k_x)\varphi_y - z_B\left(c_x\frac{du_A}{dt} + k_x u_A\right) = \bar{M}_y \tag{11.53}$$

$$I_z\frac{d^2\varphi_z}{dt^2} + H_z\frac{d\varphi_z}{dt} + S_z\varphi_z = \bar{M}_z \tag{11.54}$$

where

$k_x, k_y, k_z = k_{xxs}, k_{yys}, k_{zzs}$ respectively
$c_x, c_y, c_z = c_{xxs}, c_{yys}, c_{zzs}$ respectively
$z_B = z_s$
$I_x, I_y, I_z = I_{\varphi x}, I_{\varphi y}, I_{\varphi z}$ respectively
$H_x, H_y, H_z = c_{\varphi xxs}, c_{\varphi yys}, c_{\varphi zzs}$ respectively
$S_x, S_y, S_z = k_{\varphi xxs}, k_{\varphi yys}, k_{zzs}$ respectively.

It can be seen from Equations (11.49)–(11.54) that equations of motion for translation along the z axis (vertical direction) and rotation about the z axis (Equations (11.51) and (11.54)), are completely uncoupled, that is, the quantities w_A and φ_z can be independently solved from Equations (11.51) and (11.54) respectively. Further Equations (11.49) and (11.53) involving the quantities u_A and φ_y are coupled (the coupling now is in terms of these quantities only). Similarly Equations (11.50) and (11.52) involving v_A and φ_x are also coupled. Thus the translation of the point A (combined CG of the machine and foundation) along any horizontal axis (x or y axis) is always associated with rotation about the horizontal axis perpendicular to the axis of translation (i.e., y or x axis) and vice versa. This statement is obvious from the fact that the combined CG, A is not in the same horizontal plane as the center of contact area B (i.e., $z_B = z_s \neq 0$), as can be seen from Figure 11.9.

It can be observed that Equations (11.49)–(11.54) are considerably simplified both in the order of coupling (and hence mathematical complexities) as well as computational adaptability. Hence solutions can be conveniently attempted. This symmetry can be easily prescribed by the designer (even if x_B and/or y_B are of the order of 5% (or less) of the respective dimensions of the contact area, symmetry can be assumed; IS: 2974–1966, 1966).

In several cases the vertical distance of the combined CG, A from the horizontal contact plane (containing point B) is quite small (z_B is quite small) in comparison to the other dimensions of the machine and foundation block. In such cases, it appears to be quite reasonable to neglect z_B. Thus if $x_B = y_B = z_B = 0$, Equation (11.41) can further be simplified as

$$m\frac{d^2u_A}{dt^2} + c_x\frac{du_A}{dt} + k_x u_A = \bar{P}_x \tag{11.55}$$

$$m\frac{d^2v_A}{dt^2} + c_y\frac{dv_A}{dt} + k_y v_A = \bar{P}_y \tag{11.56}$$

$$m\frac{d^2w_A}{dt^2} + c_z\frac{dw_A}{dt} + k_z w_A = \bar{P}_z \tag{11.57}$$

$$I_x\frac{d^2\varphi_x}{dt^2} + H_x\frac{d\varphi_x}{dt} + S_x\varphi_x = \bar{M}_x \tag{11.58}$$

$$I_y\frac{d^2\varphi_y}{dt^2} + H_y\frac{d\varphi_y}{dt} + S_y\varphi_y = \bar{M}_y \tag{11.59}$$

$$I_z\frac{d^2\varphi_z}{dt^2} + H_z\frac{d\varphi_z}{dt} + S_z\varphi_z = \bar{M}_z \tag{11.60}$$

It can be noticed that Equations (11.53)–(11.60) are completely uncoupled and hence all the components of displacements and rotations of the rigid body can be independently solved. Further a close examination of these equations reveals the fact that these equations of motion are identical in form with that of a single degree of freedom system and hence all the available solutions to SDF can be readily used for analyzing the MFS. In this context the solutions to SDF are of direct significance for analysis of MFS. However, the equivalent spring and dashpot constants of the soil in various modes of vibration ($k_x, k_y, k_z, c_x, c_y, c_z, H_x, H_y, H_z, S_x, S_y, S_z$) have to be computed to directly adopt the results of SDF.

In view of the similarity of Equations (11.41) and (11.47), similar simplifications can also be made in the case of MPFS.

11.9 Methods of Solution

Equation (11.41) for MFS and Equation (11.47) for MPFS are coupled and represent motion of multi degree of freedom systems. The solution to such equations in all their generalities, that is, free and forced vibrations, arbitrary forcing functions, and so on, have been discussed in detail by Kameswara Rao (1998).

Solutions to such coupled equations can also be obtained using numerical methods Several practical examples have been discussed in detail by Richart, Hall and Woods (1970) and Kameswara Rao (1998).

11.9.1 Observations

A general methodology is presented to analyze MFS systems and MPFS systems. The present study makes use of frequency-independent foundation impedances and the total response of the machine foundation is obtained in time domain. Steady state solutions can also be obtained using Fourier analysis (Kameswara Rao, 1998) whenever the excitation forces and moments are periodic (with several periods) though the amplitudes are of general nature. The method has the following advantages:

1. The system can be modeled using as many degrees of freedom as may be appropriate.
2. Loads of general nature, acting at different locations and directions can be incorporated.
3. Analog parameters with more accurate physical modeling can be introduced.

4. Transient and impact type of loads can be easily handled.
5. Since the integration methodology is adaptive, the desired degree of accuracy can be maintained throughout the time interval of interest.
6. The presence of piles reduces the displacements significantly.

   Contrary to the normal belief, heavier block foundations do not produce lower displacements. Responses can be controlled in weak soils by providing pile foundations. The effect of thickness is strongly felt at lower moduli than at higher moduli. The analysis presented is quite general in nature and can be used to predict the response of MFS systems with all their inherent complexities in terms of general loads, locations, modeling, support conditions, interation between components and so on.

11.10 General Remarks

The empirical and semi-empirical methods mentioned in this chapter have been widely used with varying degrees of success. These may be constantly reviewed in the light of further evidences and observations. Many times, these are the only tools conveniently available to a designer and hence a foundation engineer should be familiar with the basis of their development and limitations in application. By now it is quite apparent that the continuum problem of a foundation soil system subjected to dynamic loads can be conveniently idealized and simplified in terms of simple discrete systems with mass–spring–dashpot components using analogs mentioned in the previous sections. Of these, the most logical and comprehensive models are the ones given by Lysmer and Richart (1966) and Richart, Hall and Woods (1970) for MFS, who developed them from the basic solutions of elastic continua. Even in the case of pile foundations (used in the case of weak soils), it is feasible to represent the continuum problem by equivalent simple mass–spring–dashpot systems (Kameswara Rao, 1998).

11.11 Framed Foundations

Framed foundations are generally preferred for high-speed machines such as turbo generators, compressors, dynamos, blowers and so on, as they are quite flexible, versatile for construction on any site, and cost effective. Further, they are very convenient for connecting and servicing, pipes, airvents and wiring besides providing easy access to inspection and maintenance. The analysis and design aspects are quite specialized and are given by Kameswara Rao (1998). Use of the finite element method for such foundations is also discussed in the above reference.

Exercise Problems

The problems for exercise are mainly based on Section 11.6.

11.1 Explain briefly the Lysmer and Richart's analog and derive the following in terms of the dimensionless frequency ratio and dimensionless mass ratio for machine foundation acted upon by a frequency dependent dynamic load of the type $m_1 e\omega^2 \sin \omega t$

1. Resonant frequency, ω_{mr}
2. Amplitude at operating frequency, z
3. Amplitude at resonant frequency, z_{res}.

11.2 A rigid machine foundation block of mass m, resting on a soil medium with spring constant k and damping constant c is being subjected to a dynamic vertical load of $F_0 = \sin \omega_n t$ through its CG, where $\omega_n = \sqrt{\frac{k}{m}}$. If the system starts from rest (initial displacement and velocity are zero), obtain expressions for the responses of the system for all ranges of damping.

11.3 A rectangular RCC machine foundation block of size $3.0 \times 2.0 \times 0.8$ m thick is supporting a machine weighing 15 kN. The machine is bolted at the top of the foundation block by a base plate. The machine transmits an unbalanced sinusoidal moment about the longitudinal axis (horizontal) whose amplitude is 20 kNm and frequency is $\pi/2$ rad/s. The soil medium has the following properties.

1. Young's modulus, $E = 6.0 \times 10^7$ kN/m^2
2. Poisson's ratio, $v = 0.4$
3. Unit weight, $\rho = 18$ kN/m^3.

Assuming that the combined CG of the machine is directly above the center of contact area of the foundation block, find the response of the system and the natural frequencies using analog model.

1. Unit weight of concrete = 24 kN/m^3
2. Acceleration due to gravity, $g = 9.81$ m/s^2.

11.4 For the Example 11.1, assuming that the mass of the soil participating in the vibrations to be 50% of the mass of the machine and foundation block, compute the displacements at operating frequency using soil spring analogs.

11.5 A cylindrical machine foundation block of radius r and height h is subjected to a horizontal dynamic load = $F_0 \sin \omega t$ at its top surface. Assuming that the CG of the machine foundation block is at a height of $h/2$ from the ground level, write the coupled equations of motion. The spring constant and damping constant of the soil are k_h, c_h in the horizontal direction and k_ϕ, c_ϕ in the rotational motion about the horizontal axis. Obtain the natural frequencies and steady state responses assuming no damping.

Appendix 11.A Elements of Vibration Theory

11.A.1 Introduction

Many complex practical problems can be judiciously simplified as simple discrete systems having finite degrees of freedom. Dynamic analysis of these systems can be carried out using several approaches outlined in standard books on vibrations (Thomson, 1965; Rao, 1986; Kameswara Rao, 1998, 2005). Study of an idealized simple mass–spring–dashpot provides an insight into the various steps leading to the solution to corresponding practical problems. However, it is re-emphasized that a proper idealization of the original system, which facilitates the realization of the objectives of the study, is essential though the mathematical solution is by and large a routine classical step. Hence elements of the theory and a few solutions of the SDF are summarized in this section. The formulation of multi degree of freedom systems (MDF) is also introduced. Details of analysis and design of these discrete systems are discussed in the above references.

11.A.2 SDF Translational Systems

11.A.2.1 Equation of Motion

An idealized SDF for translational motion is shown in Figure 11.A.1 in a vertical position. If the system is in horizontal position, the mass is supported on frictionless rollers and the unstretched length of the spring is l_o. From Newton's second law, the equation of motion can be written as

$$m\ddot{x} = -c\dot{x} - kx + F(t) \tag{11.A.1}$$

$$\text{(unbalanced force)} = \text{(damping force)} + \text{(spring force)} + \text{(applied force)}$$

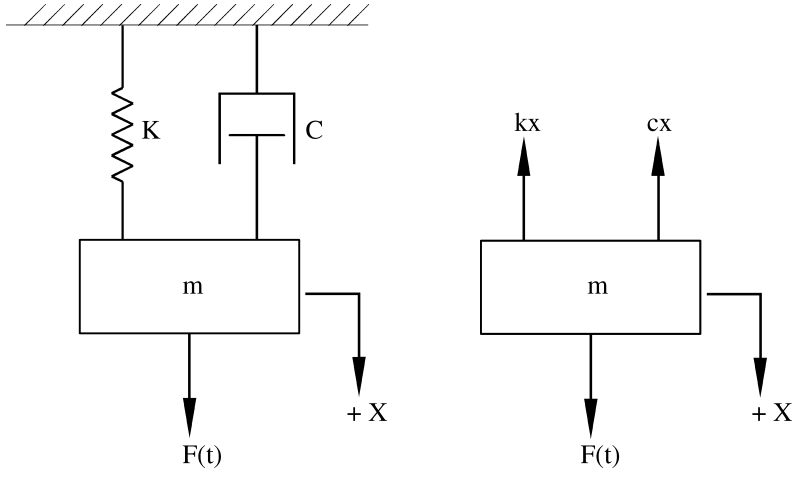

(a) (b) Free body diagram

Figure 11.A.1 A spring–dashpot system.

where

$$\dot{x} = \frac{dx}{dt},\ \ddot{x} = \frac{d^2x}{dt^2}$$

m = mass
c = viscous damping constant
k = spring constant.
Equation (11.A.1) can be rewritten as

$$m\ddot{x} + c\dot{x} + kx = F(t) \tag{11.A.2}$$

The spring is assumed to be massless or of negligible mass in comparison to the mass attached to it.

Here the displacement **x** is measured from the static equilibrium position.

Referring to Equation (11.A.2), the following types of vibrations can be useful for study:

1. Undamped free vibration (if $c = 0$; $F(t) = 0$)
2. Damped free vibrations, that is, $F(t) = 0$ with: (a) viscous damping, (b) Coulomb damping, (c) hysteretic damping. However, solutions for viscous damping only are presented in this section.
3. Forced vibrations with harmonic excitation, that is

$$F(t) \neq 0 \text{ and } F(t) = F_o \sin \omega t \text{ or } F_o e^{i\omega t}$$

4. Steady state vibrations
5. Transient vibrations, and so on.

In the following sections several useful solutions to the single degree of freedom systems such as those mentioned above are presented.

11.A.3 General Solutions

Starting from the general equation of motion for a SDF (Equation (11.A.2) and Figure 11.A.1), solutions to different cases, that is, different forms of the input parameters are summarized below.

11.A.3.1 Undamped Free Vibrations

In the absence of damping, the system can be symbolically represented as shown in Figure 11.A.1 with $c = 0$. In the absence of an external force, the motion resulting from any initial disturbance is a free vibration. The system may vibrate freely if it is subjected to initial displacement or velocity. The governing equations, solution, important results and characteristics are given below.

Equation of motion:

$$m\ddot{x} + kx = 0 \tag{11.A.3}$$

where m and k are mass and spring constants.

Solution:

The characteristic roots of the above second order ordinary differential equation are $\pm i\omega_n$ where

$$\omega_n = \sqrt{\frac{k}{m}} = \text{natural frequency of the system} \tag{11.A.4}$$

Then the solution to the differential (Equation (11.A.2) with $c = 0$) can be expressed as

$$x(t) = A_1 \cos \omega_n t + A_2 \sin \omega_n t \tag{11.A.5}$$

$$= A \cos(\omega_n t - \phi) = A_0 \sin(\omega_n t + \phi_0) \tag{11.A.6}$$

where A_1, A_2, A, φ, A_o and φ_0 are arbitrary constants. Equation (11.A.6) represents a typical harmonic motion as shown in Figure 11.A.2.

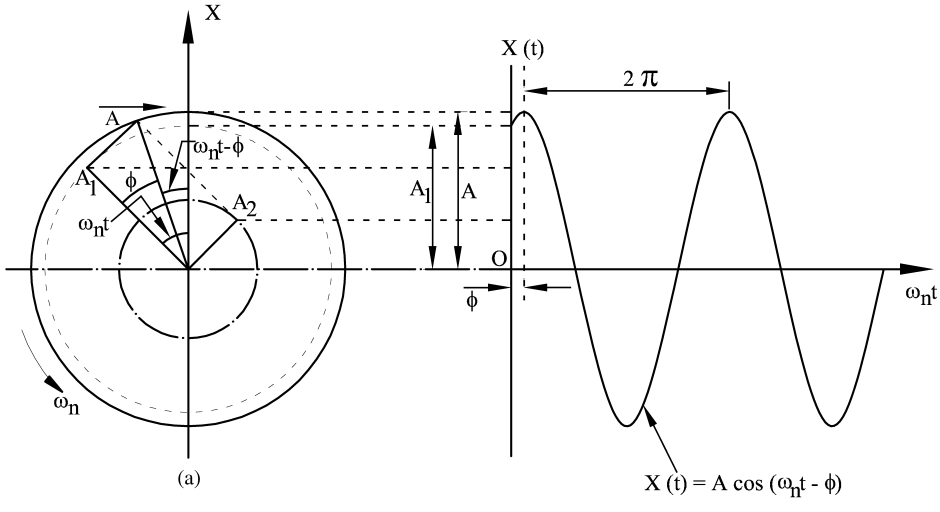

Figure 11.A.2 Graphical representation of harmonic motion.

The above solution can also be expressed in terms of initial conditions, that is, initial displacement x_0 and initial velocity v_0 as

$$x(t) = x_0 \cos \omega_n t + \frac{v_0}{\omega_n} \sin \omega_n t \tag{11.A.7}$$

The motion is shown in Figure 11.A.2.

1. Significant characteristics:

$$\text{Natural frequency of the system} = \omega_n = \sqrt{k/m} \tag{11.A.8}$$

$$\text{Amplitude of motion} = A = A_o = (A_1^2 + A_2^2)^{1/2} \tag{11.A.9}$$

$$\text{Phase angle, } \phi = \tan^{-1} \frac{A_2}{A_1} \tag{11.A.10}$$

$$\text{Phase angle, } \phi_0 = \tan^{-1} \frac{A_1}{A_2} \tag{11.A.11}$$

$$\text{Natural period, } \tau_n = \frac{2\pi}{\omega_n} \tag{11.A.12}$$

$$\text{Natural frequency in cycles per second, } f_n = \frac{\omega_n}{2\pi} \tag{11.A.13}$$

If the spring mass system is in vertical position, then

$$k = \frac{mg}{\delta_{st}} = \frac{W}{\delta_{st}} \tag{11.A.14}$$

where W is the weight, and δ_{st} is the static deflection due to weight W and g is the acceleration due to gravity.Correspondingly, the above characteristics can also be expressed in terms of the static weight and static deflection by replacing k by W/δ_{st} as given in Equation (11.A.14). For example

$$f_n = \frac{1}{2\pi}\left(\frac{g}{\delta_{st}}\right)^{1/2} \tag{11.A.15}$$

$$\tau_n = \frac{1}{f_n} = 2\pi\left(\frac{\delta_{st}}{g}\right)^{1/2} \tag{11.A.16}$$

From the solution given by Equation (11.A.6), that is, $x(t) = A\cos(\omega_n t - \varphi)$

$$\dot{x}(t) = \frac{dx}{dt} = \text{velocity} = \omega_n A \sin(\omega_n t - \varphi) = \omega_n A \cos(\omega_n t - \varphi + \pi/2) \tag{11.A.17}$$

$$\ddot{x}(t) = \frac{d^2x}{dt^2} = \text{acceleration} = -\omega_n^2 A \cos(\omega_n t - \varphi) = \omega_n^2 A \cos(\omega_n t - \varphi + \pi) \tag{11.A.18}$$

From the above expressions it can be noted that the velocity leads the displacement by $\pi/2$ and the acceleration leads the displacement by π.

2. Solutions in terms of initial disturbances given to the system:If the initial displacement $x_o = 0$, Equation (11.A.7) simplifies to

$$x(t) = \frac{\dot{x}_o}{\omega_n}\sin\omega_n t = \frac{v_o}{\omega_n}\sin\omega_n t \tag{11.A.19}$$

Alternatively, if the initial velocity $v_o = 0$, then Equation (11.A.7) becomes

$$x(t) = x_o \cos\omega_n t \tag{11.A.20}$$

It can however be noted that $x(t) = 0$, if both x_o and v_o are zero, signifying that there cannot be any free vibration with the absence of initial disturbances.

11.A.3.2 The Energy Method – Rayleigh's Method

For conservative systems, there is no dissipation of energy and at any instant of time, the energy in free vibrations is partly kinetic and partly potential. However, the total energy in the system at any instant is constant, that is,

$$T + U = \text{constant} \tag{11.A.21}$$

where T and U are the kinetic and potential energies respectively. From Equation (11.A.21) it is obvious that

$$\frac{d}{dt}(T + U) = 0 \tag{11.A.22}$$

Equation (11.A.22) can be interpreted as

$$T_{\max} = U_{\max} \tag{11.A.23}$$

Using these energy principles, the natural frequency of the system can be determined if the vibrational motion is assumed to be harmonic.

11.A.4 Damped Free Vibrations – Viscous Damping

11.A.4.1 Equations of Motion and Solutions

Referring to Figure 11.A.1, taking $F(t) = 0$, the equation of motion of the rigid body in this case can be written as

$$m\ddot{x} + c\dot{x} + kx = 0 \tag{11.A.24}$$

Seeking the solution to this homogeneous second order differential equation in the form

$$x = e^{st} \tag{11.A.25}$$

the characteristic equation can be written as

$$s^2 + \frac{c}{m}s + \frac{k}{m} = 0 \tag{11.A.26}$$

and the characteristic roots are

$$\begin{aligned} s_{1,2} &= -\frac{c}{2m} \pm \sqrt{\left(\frac{c}{2m}\right)^2 - \frac{k}{m}} \\ &= \left(-\zeta \pm \sqrt{\zeta^2 - 1}\right)\omega_n \end{aligned} \tag{11.A.27}$$

where

$$\zeta = \text{damping ratio} = \frac{c}{c_c} \tag{11.A.28}$$

$$c_c = \text{critical damping constant} = 2\sqrt{km} = 2m\omega_n \tag{11.A.29}$$

$$\omega_n = \text{natural frequency} = \sqrt{k/m} \tag{11.A.30}$$

The general solution to the homogeneous Equation (11.A.24) can be written as

$$x = A_1 e^{s_1 t} + A_2 e^{s_2 t} \tag{11.A.31}$$

The actual form of the solutions depends on the nature of roots given by Equation (11.A.27), that is, imaginary (complex conjugate) roots, real distinct ($\zeta > 1$) roots or real repeated roots ($\zeta = 1$) and are presented below.

Case 1: Underdamped ($\zeta < 1.0$)
The characteristic roots given by Equation (11.A.27) are complex conjugate in this case. The solution can be obtained as

$$x(t) = e^{-\zeta\omega n t}(A_1 \cos \omega_d t + A_2 \sin \omega_d t) \tag{11.A.32}$$

where A_1 and A_2 are arbitrary constants to be evaluated from the initial conditions of the system and ω_d is the *damped natural frequency* of the system given by

$$\omega_d = \omega_n(1 - \zeta^2)^{1/2} \tag{11.A.33}$$

It can be seen from Equation (11.A.33) that ω_d is always less than undamped natural frequency ω_n. Equation (11.A.32) can also be expressed as

$$x(t) = Xe^{-\zeta\omega nt}\sin(\omega_d t + \varphi_0) \tag{11.A.34}$$

$$= X_o e^{-\zeta\omega nt}\cos(\omega_d t - \varphi) \tag{11.A.35}$$

where A_1, A_2 and X, φ and X_o, φ_o have to be evaluated from the initial conditions.

The motion can be seen to be oscillatory with diminishing amplitude, as shown in Figure 11.A.3. For the initial conditions x (at $t = 0) = x_o$ and v (at $t = 0) = v_o$ A_1, A_2 can be obtained as

$$A_1 = x_o; \quad A_2 = \frac{\dot{x}_o + \zeta\omega_n x_o}{\omega_d} = \frac{v_o + \zeta\omega_n x_o}{\omega_d} \tag{11.A.36}$$

The solution can now be written in terms of x_0, v_0 as

$$x(t) = e^{-\zeta\omega nt}\left[x_0\cos\omega_d t + \frac{v_0 + \zeta\omega_n x_0}{\omega_d}\sin\omega_d t\right] \tag{11.A.37}$$

X, φ and X_o, φ_o can also be obtained as

$$X = X_o = (A_1^2 + A_2^2)^{1/2} \tag{11.A.38}$$

$$\varphi_0 = \tan^{-1}\frac{A_1}{A_2} \tag{11.A.39}$$

$$\varphi = \tan^{-1}\frac{A_2}{A_1} \tag{11.A.40}$$

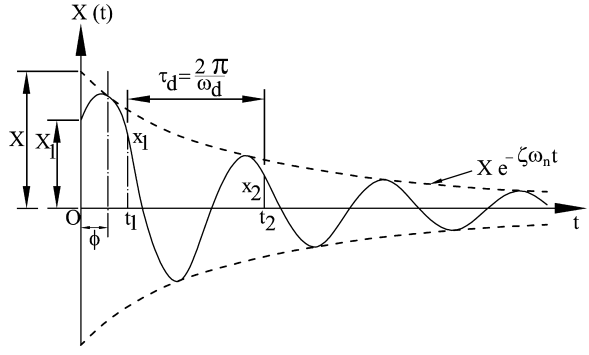

Figure 11.A.3 Solution to underdamped system: $\zeta < 1.0$.

Case 2: Overdamped ($\zeta > 1.0$)

In this case the characteristic roots given by Equation (11.A.27) are real and distinct. The solution can be expressed as

$$x(t) = A_1 e^{[-\zeta + (\zeta^2-1)^{1/2}]\omega_n t} + A_2 e^{[-\zeta - (\zeta^2-1)^{1/2}]\omega_n t} \tag{11.A.41}$$

where A_1 and A_2 are arbitrary constants to be evaluated from the initial conditions of the system. The motion as given by Equation (11.A.41) is no longer oscillatory (as shown in Figure 11.A.4) and is aperiodic. Equation (11.A.41) can also be expressed in terms of the general initial conditions x_o and v_0 (initial displacement and initial velocity) as

$$x(t) = \frac{v_o(e^{s_1 t} - e^{s_2 t}) + x_o(s_1 e^{s_2 t} - s_2 e^{s_1 t})}{(s_1 - s_2)} \tag{11.A.42}$$

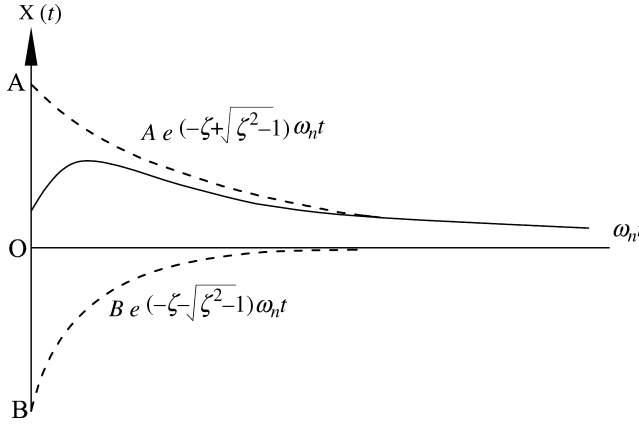

Figure 11.A.4 Solution to overdamped system: $\zeta > 1.0$.

where

$$s_1 = \{-\zeta + (\zeta^2 - 1)^{1/2}\}\omega_n < 0 \tag{11.A.43}$$

$$s_2 = \{-\zeta + (\zeta^2 - 1)^{1/2}\}\omega_n < 0 \tag{11.A.44}$$

Case 3: Critically damped ($\zeta = 1.0$)
The characteristic roots given by Equation (11.A.27) will be real but repeated in this case. The solution can be written as

$$x(t) = (A_1 + A_2 t)e^{-\omega_n t} \tag{11.A.45}$$

where A_1 and A_2 are the arbitrary constants to be evaluated in terms of the initial conditions. Equation 11.A.45 represents an aperiodic motion which is essentially a transition between the oscillatory and non-oscillatory conditions, as shown in Figure 11.A.5.

In terms of the general initial conditions x_o and v_o (initial displacement and initial velocity at $t = 0$), Equation (11.A.45) can be expressed as

$$x(t) = \left[x_0 + \left(\frac{v_0}{\omega_n} + x_0\right)\omega_n t\right] e^{-\omega_n t} \tag{11.A.46}$$

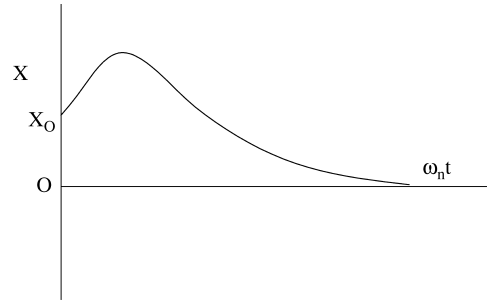

Figure 11.A.5 Solution to critically damped system: $\zeta = 1.0$.

Since critical damping represents the limit of aperiodic damping, the motion returns to rest in the shortest time without oscillation. This property can be advantageously used in many practical vibration problems such as large guns, measuring instruments and electrical meters.

A comparison of motions with different types of damping is shown in Figure 11.A.6.

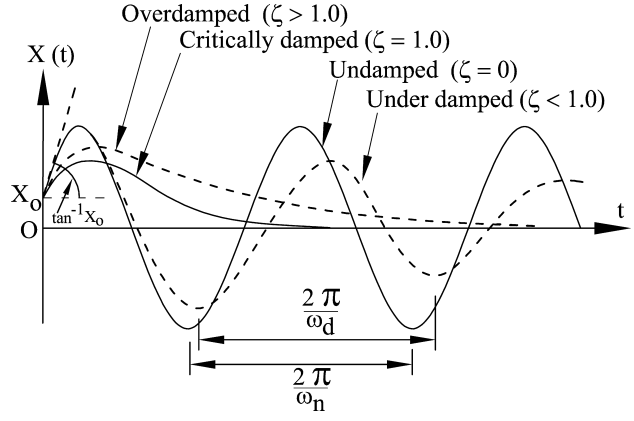

Figure 11.A.6 Comparison of motions with different types of damping.

11.A.4.2 Logarithmic Decrement

The damping present in a system can be conveniently evaluated from the free vibration response curve. However, it is of major interest only in underdamped systems which makes the motion oscillatory as shown in Figure 11.A.3. This can be easily expressed in terms of the natural logarithm of the ratio of any two successive amplitudes, generally referred to as *logarithmic decrement*. The logarithmic decrement can be expressed (using Equation (11.A.34)

and Figure 11.A.3) as

$$\delta = \ln\frac{x_1}{x_2} = \ln\left[\frac{e^{-\zeta\omega_n t_1}}{e^{-\zeta\omega_n(t_1+\tau)}}\right] = \ln\, e^{\zeta\omega_n\tau} = \zeta\omega_n\tau = \frac{2\pi\zeta}{(1-\zeta^2)^{1/2}} \tag{11.A.47}$$

For small values of ζ, Equation (11.A.47) can be approximately written as

$$\delta \approx 2\pi\zeta \tag{11.A.48}$$

The plot of logarithmic decrement versus damping ratio is shown in Figure 11.A.7. The logarithmic decrement can easily be determined from a free vibration test by taking the natural logarithm of the ratio of any two successive amplitudes of the free vibration response curve obtained from the test. The damping ratio, ζ, can than be obtained either from Equations (11.A.47) or (11.A.48). From Equation (11.A.48)

$$\zeta \approx \frac{\delta}{2\pi} \tag{11.A.49}$$

As can be seen from Equations (11.A.47) and (11.A.48), in the presence of viscous damping in the system, the decay of vibrations shows a pattern in which the ratio of amplitudes of any two successive peaks is a constant. Thus the logarithmic decrement can be obtained from any two-peak amplitudes x_1 and x_{n+1} which are separated by n cycles as

$$\delta = \frac{1}{n}\ln\frac{x_1}{x_{n+1}} \tag{11.A.50}$$

It can also be noticed from Figure 11.A.7 that the two curves represented by Equations (11.A.47) and (11.A.48) are difficult to be distinguished for $\zeta < 0.3$. The damping ratio, ζ, can also be obtained from Equation (11.A.49).

11.A.5 Forced Vibrations

11.A.5.1 Introduction

Dynamic systems are often subjected to time dependent forces or exciting functions. These forces may be harmonic (hence periodic), nonharmonic but periodic, aperiodic or nonperiodic, or random in nature. The response of a system to harmonic forces is called harmonic response and usually such forces act for a longer duration. However, nonharmonic but periodic forces can always be expressed in terms of a series of harmonic functions using Fourier series (Kameswara Rao, 1998) and are called harmonics. Such forces also may act for longer duration. Nonperiodic forces may act for a longer or a shorter duration. The response of the system to suddenly applied forces is called transient response. In view of the feasibility of expressing a general forcing function (periodic or nonperiodic) in terms of Fourier series, the harmonic analysis of a system is very useful as a means to obtain solutions to most cases involving general dynamic inputs.

The harmonic response of a single degree of freedom system is presented below. The most general forms of the forcing functions are

$$F(t) = F_o\sin(\omega t+\varphi);\quad F_o\cos(\omega t+\varphi);\quad F_o e^{i\omega t};\quad F_o\sin\omega t;\quad F_o\cos\omega t \tag{11.A.51}$$

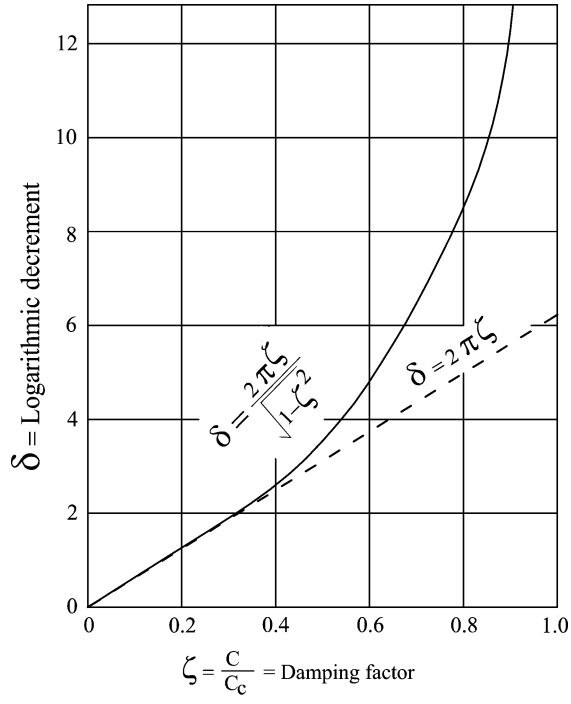

Figure 11.A.7 Logarithmic decrement versus damping.

where F_o is the amplitude of exciting force, ω is the frequency of harmonic motion, φ is the phase angle. The value of φ depends on the nature of $F(t)$ at $t = 0$ and it can be noted that there is no loss of generality if φ is taken to be zero. It may also be further noted that mathematically it may be convenient to take the forcing function as real or imaginary part of $F_o e^{i\omega t}$ and the expressions are all equivalent even though it is represented as a complex function.

11.A.5.2 Forced Vibration of SDF

A viscously damped SDF subjected to a dynamic force $F(t)$ is shown in Figure 11.A.1. The equation of motion (Equation (11.A.2)) is

$$m\ddot{x} + c\dot{x} + kx = F(t) \tag{11.A.52}$$

The general solution to the above second order ordinary differential equation consists of a homogeneous part x_h which can be recognized to be the free vibration solution dealt in Section 11.A.4, and a particular integral x_p which essentially depends on the nature of the forcing function $F(t)$ and the system parameters m, c and k.

For example x_h, x_p and the total solution $x(t) = x_h + x_p$ for a typical case of an undamped system are shown in Figure 11.A.8. It may be noted that the free vibration solution (i.e., x_h) vanishes with time for all the cases of damping, for example, underdamping, critical damping

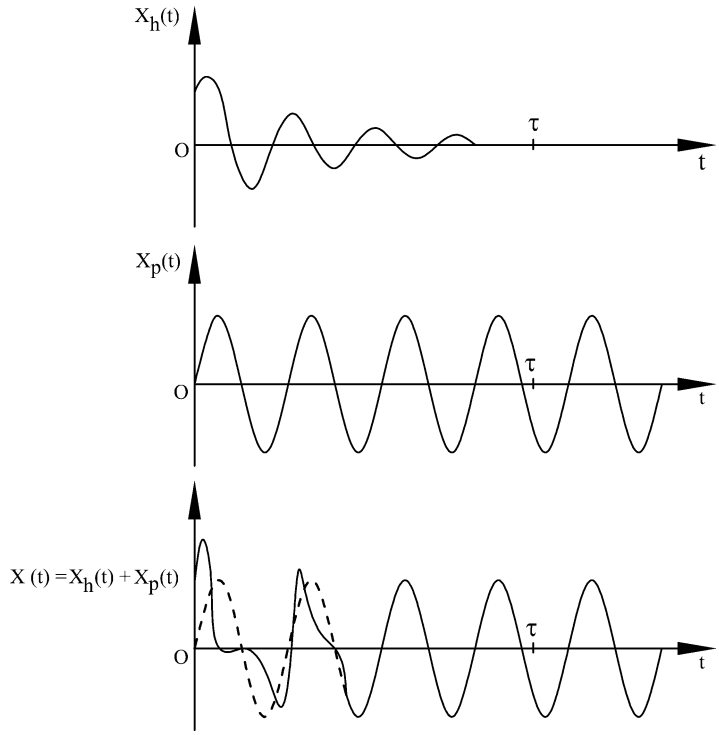

Figure 11.A.8 Homogeneous, particular, and general solutions of an underdamped MFS.

and overdamping (Section 11.A.4), or for that matter any other type of damping (e.g., Coulomb damping or hysteretic damping).

This part of the motion which vanishes with time, is also called *transient motion* and the rate of decrease of the amplitude of motion depends on k, c and m as can be seen from the response curves given in Section 11.A.4 Hence for a physical system where there is always some (however small) damping present, the general solution eventually reduces to the particular solution $x_p(t)$ which represents the steady state solution and logically exists as long as $F(t)$ is present. In view of the relatively short duration of the transient motion, steady state motion is usually of more practical interest since the system response ultimately reduces to the steady state motion (viz., turbines, blowers, compressors, machines, machine tools, machine foundations, etc.) where the systems operate under $F(t)$ for a considerable time. However, in cases where $F(t)$ exists for a short duration (viz., impact loads, blasts, wind, earthquake, etc.) the transient response becomes important and cannot be ignored while steady state motion has no practical significance. Hence except in cases where transient response considerations are important, only steady state solutions are presented in the following sections. Also, majority of solutions presented below correspond to the case when $F(t)$ is harmonic, in view of the ready extendability of these solutions for several general cases of forcing function as mentioned earlier in Section 11.A.5.1.

11.A.5.3 Forced Vibrations – Undamped Case

Taking $c = 0$, the relevant equation of motion can be written as

$$m\ddot{x} + kx = F(t) \tag{11.A.53}$$

The general solution to Equation (11.A.53) can be obtained as

$$x(t) = A_1 \cos \omega_n t + A_2 \sin \omega_n t + \int_0^t \frac{F(\xi)}{m\omega_n} \sin \omega_n (t-\xi) d\xi \tag{11.A.54}$$

where A_1 and A_2 are arbitrary constants to be evaluated from initial conditions.

The first two terms of the response Equation (11.A.54) can be identified to be the homogeneous part of the solution and is the same as the free vibration solution (Section 11.A.3.1). Depending on the nature of the exciting force, the particular integral can be obtained either using the integral in Equation (11.A.54) or directly. A few solutions are given below.

Case 1: Force $F(t) = F_o$ = constant
Substituting $F(t) = F_o$ in Equations (11.A.53) and (11.A.54), the solution can be simplified as

$$\begin{aligned} x(t) &= A_1 \cos \omega_n t + A_2 \sin \omega_n t + \frac{F_o}{k}(1 - \cos \omega_n t) \\ &= A_3 \cos \omega_n t + A_4 \sin \omega_n t + \frac{F_o}{k} \end{aligned} \tag{11.A.55}$$

The motion represented by Equation (11.A.55) corresponds to an oscillatory motion about the new equilibrium position of the rigid mass corresponding to the additional force F_o (in addition to its own weight W).

Case 2: Force $F(t) = F_o \sin \omega t$ – harmonic excitation
In this case the exciting harmonic force has a circular frequency which is independent of ω_n (the undamped natural frequency). Substituting for $F(t) = F_o \sin \omega t$ in Equation (11.A.51), the general solution can be obtained as

$$x(t) = A_1 \cos \omega_n t + A_2 \sin \omega_n t + x(t) = A_1 \cos \frac{F_o/k}{1 - \left(\frac{\omega}{\omega_n}\right)^2} \sin \omega t \tag{11.A.56}$$

$$= A_o \sin (\omega_n t + \varphi_o) + \frac{F_0/k}{1 - (\omega/\omega_n)^2} \sin \omega t \tag{11.A.57}$$

where A_o and φ_o can be determined in terms of A_1 and A_2 as explained in Section 11.A.3.1.

In terms of the general initial conditions x_o and v_o (initial displacement and velocity at $t = 0$), Equation (11.A.57) can also be expressed as

$$x(t) = \left[\frac{v_0}{\omega_n} - \frac{F_0}{k} \frac{\omega/\omega_n}{\{1 - (\omega/\omega_n)^2\}}\right] \sin \omega_n t + x_0 \cos \omega_n t + \frac{F_o/k}{1 - \left(\frac{\omega}{\omega_n}\right)^2} \sin \omega t \tag{11.A.58}$$

The last terms in Equations (11.A.56)–(11.A.58) represent the particular integral while the remaining terms represent the homogeneous solution. For a real system the homogeneous part of the solution will eventually vanish because of some damping present in the system, thus yielding the so-called steady state solution, which is the particular integral, $x_p(t)$ itself, that is

$$x_p(t) = \frac{F_o/k}{1-(\omega/\omega_n)^2}\sin \omega t = X\sin \omega t \tag{11.A.59}$$

The amplitude corresponding to the particular solution given by Equation (11.A.59) can be written as

$$X = \frac{F_o/k}{1-(\omega/\omega_n)^2}\sin \omega t \tag{11.A.60}$$

The ratio between the amplitude of motion, X, and the static displacement corresponding to the amplitude of the dynamic force, $\delta_{st}\left(=\frac{F_o}{k}\right)$, is often referred to as the magnification factor, M, and can be expressed as

$$M = \frac{X}{\delta_{st}} = \frac{X}{F_o/k} = \frac{1}{1-(\omega/\omega_n)^2} \tag{11.A.61}$$

M is also referred to as amplification factor or amplitude ratio and it is customary to represent X and M as positive. The steady state magnification factor M given by Equation (11.A.61) depends on the value of the denominator as given below.

Case 1: $0 < \dfrac{\omega}{\omega_n} < 1$

The denominator of Equation (11.A.61) is positive and the response is given by Equation (11.A.59) without change. Hence the response $x_p(t)$ can be noted to be in phase with the forcing functions. The total response can be expressed as

$$x(t) = A_o\sin(\omega_n t + \varphi_o) + \frac{\delta_{st}\sin \omega t}{1-\left(\frac{\omega}{\omega_n}\right)^2} \tag{11.A.62}$$

Case 2: $\dfrac{\omega}{\omega_n} > 1$

The denominator in Equation (11.A.61) becomes negative and Equation (11.A.59) can now be expressed as

$$x_p(t) = -X\sin \omega t = X\sin(\omega t - \pi) \tag{11.A.63}$$

and

$$M = \frac{X}{\delta_{st}} = \frac{1}{1-(\omega/\omega_n)^2} \tag{11.A.64}$$

Here, $x_p(t)$ and $F(t)$ can be seen to be of opposite sign and $x_p(t)$ lags the forcing function by π, that is, 180°.

$$\text{Further as } \frac{\omega}{\omega_n} \to \infty,\ M \to 0 \quad \text{and} \quad x \to 0 \tag{11.A.65}$$

as can be seen from Equation (11.A.64).

The total response in this case can be expressed as

$$x(t) = A_o \sin(\omega_n t + \varphi_o) - \frac{\delta_{st} \sin \omega t}{1 - (\omega/\omega_n)^2} \tag{11.A.66}$$

Case 3: $\dfrac{\omega}{\omega_n} = 1$

From Equations (11.A.60) and (11.A.61) the values of X and M become infinite.

This implies that the frequency of the exciting force, ω, is equal to the natural frequency of the system, ω_n, and is referred to as resonance. Using L'Hospital's rule, the response of the system at resonance can be obtained as

$$x(t) = x_o \cos \omega_n t + \frac{\dot{x}_o}{\omega_n} \sin \omega_n t + \frac{(\sin \omega_n t - \omega_n t \cos \omega_n t)}{2} \tag{11.A.67}$$

It can be seen from the above equation that $x(t)$ increases indefinitely with time at resonance. Variation of M and φ $(= -\varphi_o)$ with ω/ω_n is shown in Figure 11.A.9.

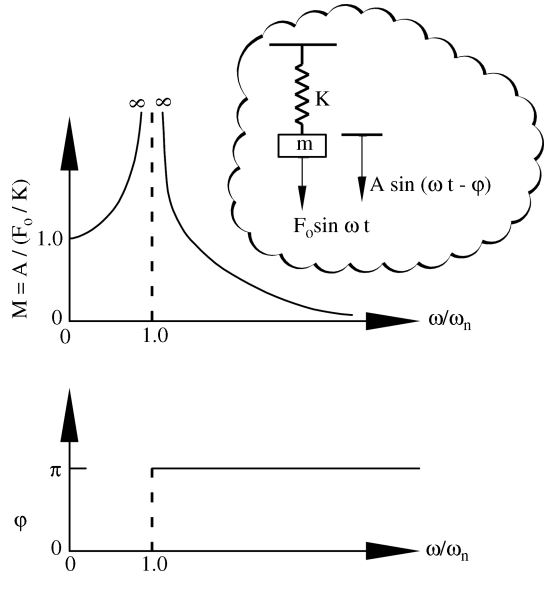

Figure 11.A.9 Magnification factor and phase angle for an undamped SDF system.

If the forcing function is of the form $F(t) = F_o \cos \omega t$ or $F_o e^{i\omega t}$ expressions can be derived in a similar manner.

11.A.5.4 Forced Vibrations with Viscous Damping

Referring to Figure 11.A.1, the equation of motion for the SDF can be written as

$$m\ddot{x} + c\dot{x} + kx = F(t) \tag{11.A.68}$$

Solutions to the above ordinary differential equation can be readily written for general expressions of $F(t)$ from theory using Green's function or convolution integral.

Since the general solutions (homogeneous solution and particular integral) depend on the damping present in the system, they can be listed as below as per the cases discussed in Section 11.A.4.1.

Case 1: Underdamped systems ($\zeta < 1.0$)
The general solution in this case can be expressed as

$$x(t) = e^{-\zeta\omega_n t}(A_1 \cos \omega_d t + A_2 \sin \omega_d t) + \int_0^t \frac{F(\xi)e^{-\zeta\omega_n(t-\xi)}}{m\omega_d} \sin \omega_d(t-\xi)d\xi \qquad (11.A.69)$$

where ζ, ω_n and ω_d are the damping ratio, natural frequency and damped natural frequency as defined earlier. A_1 and A_2 are arbitrary constants to be evaluated from the initial conditions. The first term in Equation (11.A.69) represents the homogeneous part of the solution and the second part represents the particular integral. The homogeneous part of solution vanishes with time (which represents the free vibration part), while the particular integral persists thus representing a steady state motion (after a sufficient time interval).
Case 2: Overdamped systems ($\zeta > 1.0$)
The general solution in this case can be expressed as

$$x(t) = (A_1 e^{s_1 t} + A_2 e^{s_2 t}) + \int_0^t \frac{F(\xi)\left[e^{s_1(t-\xi)} - e^{s_2(t-\xi)}\right]d\xi}{m(s_1 - s_2)} \qquad (11.A.70)$$

in which s_1 and s_2 are quantities given by Equations (11.A.43) and (11.A.44) and A_1 and A_2 are arbitrary constants to be evaluated from the initial conditions of the system.
Case 3: Critically damped systems ($\zeta = 1.0$)
The general solution to this case can be obtained as

$$x(t) = (A_1 + A_2 t)\, e^{-\omega_n t} + \int_0^t \frac{F(\xi)}{m}(t-\xi)\, e^{-\omega_n(t-\xi)}d\xi \qquad (11.A.71)$$

in which ω_n is the natural frequency and A_1 and A_2 are arbitrary constants to be evaluated from the initial conditions.
Since the homogeneous part of the solutions given by Equations (11.A.69)–(11.A.71) vanishes after sufficient duration of time, steady state solutions (represented by the particular integrals in the above equations) are presented below in detail for a variety of situations. However, the total behavior (including the transient behavior) of the system subjected to any arbitrary exciting force can be evaluated using the Equations (11.A.69)–(11.A.71).

11.A.5.5 Steady State Solutions

After a sufficiently long duration of time, steady state conditions are reached and the steady state responses of the system become important to predict the long-term behavior (beyond the transient stage). Accordingly, steady state solutions to a variety of cases are summarized below.

Case 1: Constant force, $F(t) = F_0 = \text{constant}$
The particular integral in this case can be obtained from ordinary differential equations theory as

$$x_p(t) = \frac{F_o}{k} \tag{11.A.72}$$

Hence, it can be concluded that after the transient motion vanishes, the mass m remains motionless at the new equilibrium position corresponding to the additional force F_o.
Case 2: Harmonic exciting force of constant amplitude, $F(t) = F_0 \sin \omega t$
For such a harmonic forcing function, the nonhomogeneous solution can be easily obtained using the theory of ordinary differential equations. However, the same can also be solved using vectorial representation of all the forces acting on the system. The particular solution in this case can be assumed as

$$x_p(t) = X \sin(\omega t - \varphi) \tag{11.A.73}$$

where X is the amplitude and φ is the phase angle. We can solve for X and φ by substituting the above solution in the differential equation of motion given by Equation (3.122). The expressions on substitution come out as

$$m\omega^2 X \sin(\omega t - \varphi) - c\omega_d X \sin\left(\omega t - \varphi + \frac{\pi}{2}\right) - kX \sin(\omega t - \varphi) + F_o \sin \omega t = 0 \tag{11.A.74}$$

that is

$$\text{Inertia force} + \text{damping force} + \text{spring force} + \text{external force} = 0 \tag{11.A.75}$$

These forces can be vectorially represented as shown in Figure 11.A.10. From this vector diagram X and φ can be readily obtained as

$$X = \frac{F_0/k}{\sqrt{\left\{1 - \left(\frac{\omega}{\omega_n}\right)^2\right\}^2 + \left(2\zeta \frac{\omega}{\omega_n}\right)^2}} \tag{11.A.76}$$

and

$$\tan \varphi = \frac{2\zeta\omega/\omega_n}{1 - (\omega/\omega_n)^2} = \frac{2\zeta r}{1 - r^2} \tag{11.A.77}$$

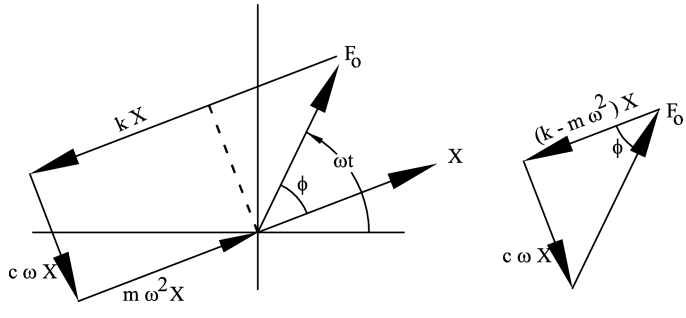

Figure 11.A.10 Vector representation of forced vibration with viscous damping.

where $r = \omega/\omega_n =$ frequency ratio. The particular solution $x_p(t)$ can then be obtained from Equation (11.A.73).

The following observations can be made from the vector diagrams (Figure 11.A.10) which help in the understanding of the physical behavior of the system:

1. There is a phase lag of φ between the exciting force and displacement response which can vary from 0 to 180°.
2. The spring force being a reactive force is opposite to the direction of the displacement.
3. The phase lag between displacment and the damping force is 90 degrees and is opposite to the direction of velocity.
4. The inertial force is in the same direction as the displacement but opposite to the direction of acceleration.

From Equation (11.A.76), the dynamic magnification factor, M can be expressed as

$$M = \frac{X}{F_0/k} = \frac{X}{\delta_{st}} = \frac{1}{[(1-(\omega/\omega_n)^2)^2 + (2\zeta\omega/\omega_n)^2]^{1/2}} = \frac{1}{[(1-r^2)^2 + (2\zeta r)^2]^{1/2}} \tag{11.A.78}$$

where $\delta_{st} = F_o/k =$ static deflection under force F_o.

The dynamic magnification factor, M and phase angle, φ are graphically shown in Figure 11.A.11 for various values of ζ (mainly for values of $\zeta \leq 1.0$, since these are the most relevant solutions to practical situations).

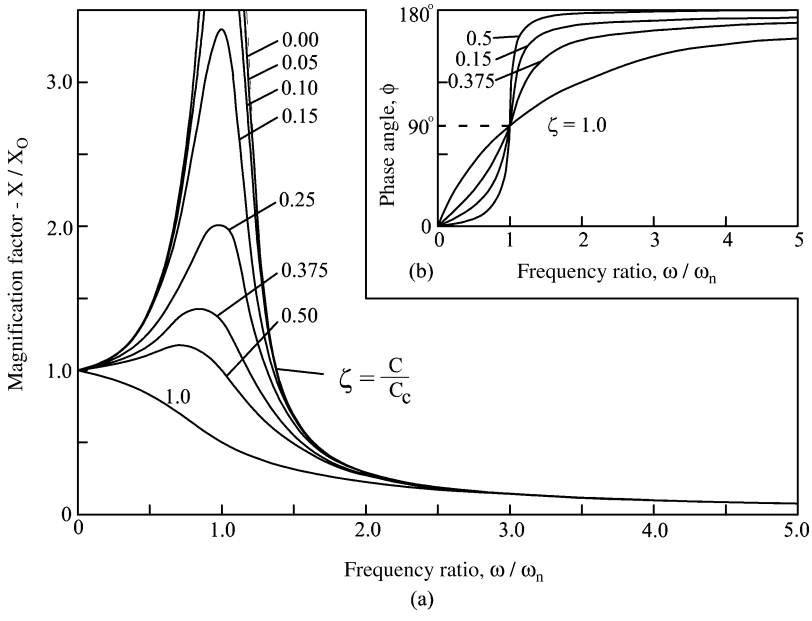

Figure 11.A.11 Forced vibration response of a viscously damped system.

It can be observed from the figures that the frequency at which the maximum amplitude occurs is less than the undamped natural frequency and is equal to

$$\omega_m = \omega_n(1-2\zeta^2)^{1/2} \tag{11.A.79}$$

ω_m is referred to as the *resonant frequency* for constant force amplitude type of exciting force. The magnification factor at this frequency can be obtained as

$$M_{\max} = \frac{1}{2\zeta(1-\zeta^2)^{1/2}} \tag{11.A.80}$$

From Equations (11.A.79) and (11.A.80), it can be inferred that for $\zeta \geq 1/\sqrt{2}$, static response itself is the maximum response. The phase angle φ [Figure 11.A.11(b)] has a value of $\pi/2$ at $\frac{\omega}{\omega_n} = 1$ for all cases of damping.

Force transmitted to the base:

To assess the safety of the base supporting the SDF it may be necessary to calculate the force transmitted to the base. This can be expressed as

$$F_T = kx_p + c\dot{x}_p \tag{11.A.81a}$$

By substituting for x_p from Equations (11.A.73) and (11.A.76), the amplitude of the force transmitted to the base can be obtained as

$$F_T = F_o\left[\frac{1+(2\zeta r)^2}{(1-r^2)^2+(2\zeta r)^2}\right]^{1/2} \tag{11.A.81b}$$

$$\text{Hence transmissibility, } T_r = \left|\frac{F_T}{F_0}\right| = \left[\frac{1+(2\zeta r)^2}{(1-r^2)^2+(2\zeta r)^2}\right]^{1/2} \tag{11.A.82}$$

The transmissibility is plotted in Figure 11.A.12.

It can be seen from Figure 11.A.12, that $T_r < 1$ for $r = \omega/\omega_n > \sqrt{2}$ for all values of damping, with T_r reducing with reduction in damping ratio, ζ.

For small values of ζ and $r > \sqrt{2}$, transmissibility can be approximated as

$$T_r \approx \frac{1}{r^2-1} \approx \frac{1}{\frac{(2\pi f)^2\delta_{st}}{g}-1} \tag{11.A.83}$$

where $f = \omega/2\pi =$ frequency in cycles per second and g is the acceleration due to gravity. Solving for f from Equation (11.A.83) and expressing it in cycles per minute, we obtain

$$f_m = 60f = 188\left[\frac{1}{\delta_{st}}\left(\frac{1}{T_r}+1\right)\right]^{1/2} = 188\left[\frac{2-R}{\delta_{st}(1-R)}\right]^{1/2} \tag{11.A.84}$$

where δ_{st} is the static deflection in inches, and R is the ratio representing the percentage reduction in the transmitted vibratory force defined as

$$R = 1-T_r \tag{11.A.85}$$

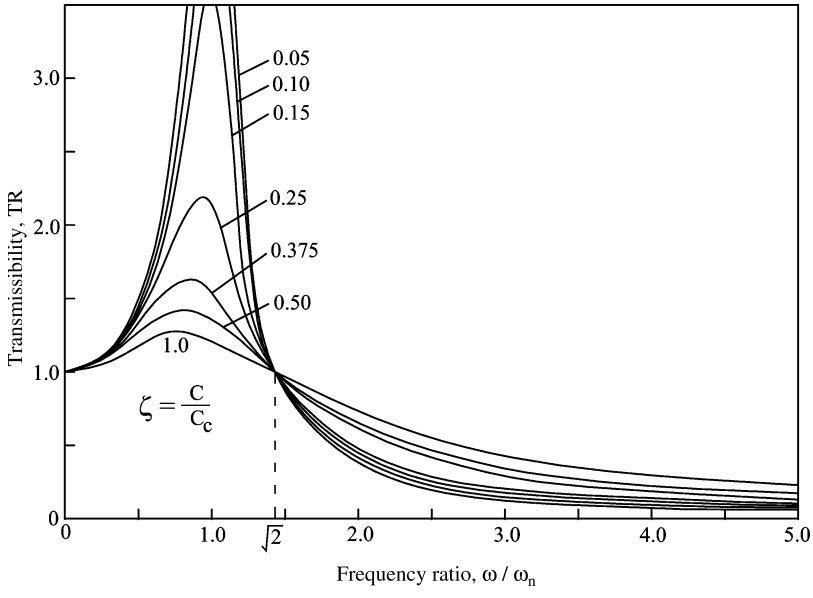

Figure 11.A.12 Transmissibility versus frequency ratio.

The same is called isolation efficiency and is shown in Figure 11.A.13 which is quite useful for practical applications in vibration isolation problems.

The following features can be noted from the above solutions and Figure 11.A.11:

1. For $\zeta = 0$, the solutions to x_p, X, M and φ are given by Equations (11.A.73)–(11.A.78) and coincide with the corresponding solutions to undamped system derived in Section 11.A.5.3. Phase angle, φ can be noted to be zero for $r < 1.0$ and $\varphi = \pi$ for $r > 1.0$.
2. Amplitude ratio, M reduces with increasing damping for all values of ω and the reduction of M is significant in the vicinity of resonance.
3. Maximum value of amplitude ratio $M_{\max} = \dfrac{1}{2\zeta\sqrt{1-\zeta^2}}$ occurs when $\omega = \omega_m = \omega_n(1-2\zeta^2)^{1/2}$ which is lower than the damped natural frequency $\omega_d = \omega_n(1-\zeta^2)^{1/2}$. At $r = 1$, $M = \dfrac{1}{2\zeta}$. These expressions can be advantageously used for the evaluation of damping in a system.
4. For $\zeta \geq 1/\sqrt{2}$, curve for M (or X) has peak value only at $r = 0$, that is, static situation. This implies that static deflection itself is the maximum amplitude for damping ratios $\geq 1/\sqrt{2}$.
5. The sharpness at resonance is qualitatively expressed as 2ζ. This also can be conveniently used for the experimental determination of the damping present in a system using a forced vibration test.
6. The total response of the system in all the above cases can be obtained by adding the corresponding homogeneous part of the solution (same as those obtained in the free vibration analysis given in Section 11.A.4) to the particular integral, that is,

$$x(t) = x_h(t) + x_p(t)$$

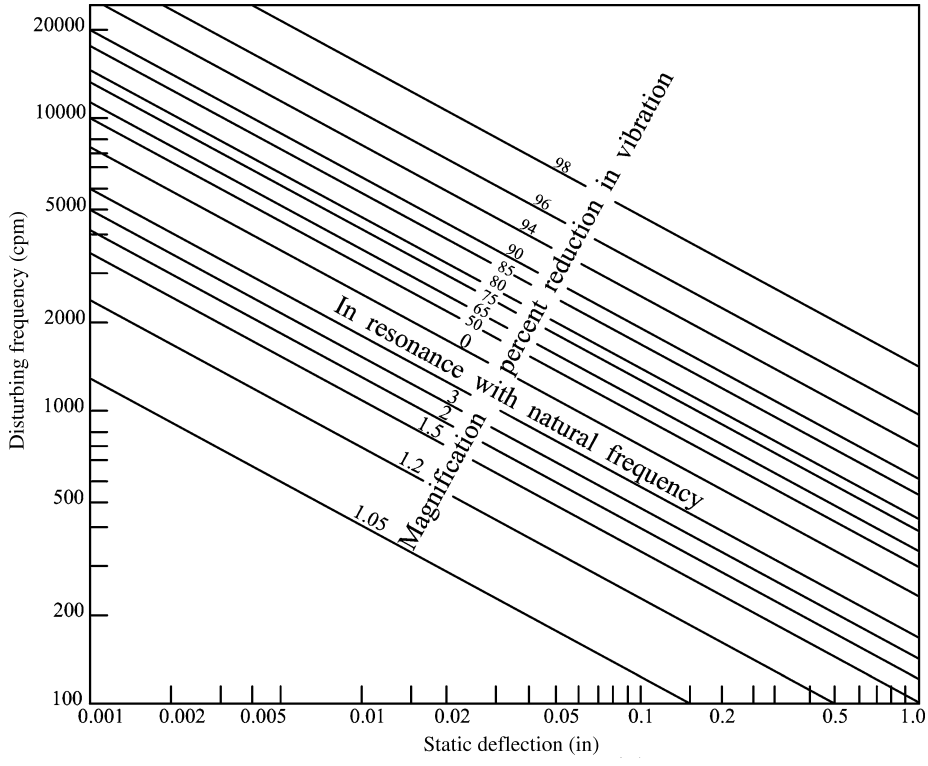

Figure 11.A.13 Isolation efficiency graphs for flexibly mounted systems.

Case 3: Harmonic exciting force – rotating mass type excitation, $F(t) = m_e e\omega^2 \sin \omega t$
Sometimes, vibrations are produced by unbalanced rotating masses such as in reciprocating and rotating engines. A typical mechanism of this type is shown in Figure 11.A.14, which consists of two counter rotating eccentric masses m_1, at an eccentricity e. The eccentric masses are positioned in such a manner, that the horizontal forces at any instant of time, balance each

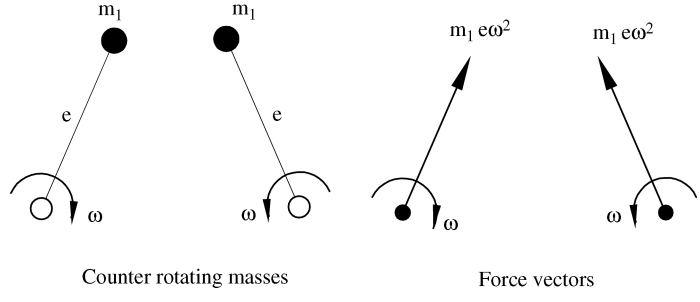

Figure 11.A.14 Forces produced by two counter rotating masses.

other and produce an unbalanced vertical harmonic force equal to

$$F(t) = 2m_1 e\omega^2 \sin \omega t = m_e e\omega^2 \sin \omega t \tag{11.A.86}$$

where

$$m_e = 2m_1 = \text{total eccentric mass} \tag{11.A.87}$$

A typical SDF subjected to reciprocating and rotating imbalance is shown in Figure 11.A.15. The equation of motion in the vertical direction for the SDF shown in Figure 11.A.15 (b) can be obtained as follows.
The vertical displacement of the eccentric mass m_e is

$$x_e = x + e \sin \omega t \tag{11.A.88}$$

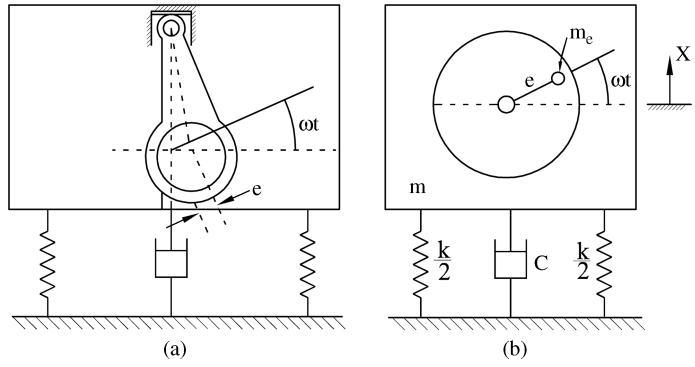

Figure 11.A.15 Periodic force from a reciprocating or rotating imbalance.

If m is the total mass of the system including the eccentric mass m_e, the equation of motion of the system can be written as

$$(m - m_e)\frac{d^2x}{dt^2} + m_e \frac{d^2}{dt^2}(x + e\sin \omega t) = -kx - c\frac{dx}{dt} \tag{11.A.89}$$

This can be written as

$$m\ddot{x} + c\dot{x} + kx = m_e e\omega^2 \sin \omega t \tag{11.A.90}$$

Equation (11.A.90) can be noted to be the same as Equation (11.A.68) where the forcing function is $F(t) = m_e e\omega^2 \sin \omega t$. Hence the solutions obtained for the case where $F(t) = F_o \sin \omega t$ can be readily used replacing F_o by $m_e e\omega^2$ in Equation (11.A.76). Accordingly, the particular integral for Equation (11.A.90) can be obtained from Equation (11.A.76) while the phase angle φ remains the same as given by Equation (11.A.77). Thus the steady state displacement can be expressed as

$$\begin{aligned} x_p(t) &= \frac{m_e e\omega^2/k}{[(1-(\omega/\omega_n)^2)^2 + (2\zeta\,\omega/\omega_n)^2]^{1/2}} \sin(\omega t - \varphi) \\ &= \frac{m_e e}{m} \frac{r^2}{[(1-r^2)^2 + (2\zeta r)^2]^{1/2}} \sin(\omega t - \varphi) = X \sin(\omega t - \varphi) \end{aligned} \tag{11.A.91}$$

Hence,

$$\frac{mX}{m_e e} = \frac{r^2}{[(1-r^2)^2 + (2\zeta r)^2]^{1/2}} \tag{11.A.92}$$

and

$$\tan \varphi = \frac{2\zeta r}{1-r^2} \tag{11.A.93}$$

A plot of $\frac{mX}{m_e e}$ with frequency ratio r $(= \omega/\omega_n)$ for different values of ζ is shown in Figure 11.A.16.

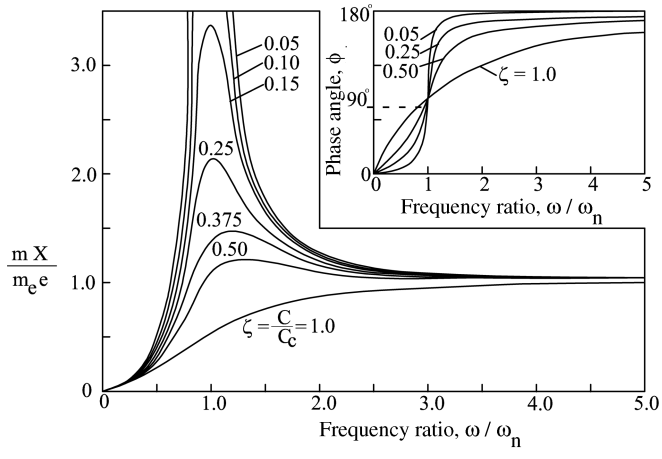

Figure 11.A.16 Response of a viscously damped system with reciprocating or rotating imbalance.

It should be noted that m is the total vibrating mass and includes the eccentric mass m_e. The resonant frequency occurs in this case when

$$\frac{\omega}{\omega_n} = \frac{1}{(1-2\zeta^2)^{1/2}} \tag{11.A.94}$$

Accordingly, denoting ω at resonance in this case as ω_{mr}, the same can be expressed from Equation (11.A.94) as

$$\omega_{mr} = \frac{\omega_n}{(1-2\zeta^2)^{1/2}} \tag{11.A.95}$$

The value of $\frac{mX}{m_e e}$ at the resonant frequency ω_{mr} can be evaluated as

$$\left(\frac{mX}{m_e e}\right)_{\max} = \frac{1}{2\zeta\sqrt{1-\zeta^2}} \tag{11.A.96}$$

It can also be observed from Figure 11.A.16 that for $\zeta \geq 1/\sqrt{2}$ no peak exists in the response curves for forced vibration of this type.

The following features can be observed from the solution to SDF subjected to rotating imbalances.

1. The response starts from zero for all values of damping. The amplitude near resonance is very sensitive to the values of damping ratio ζ.
2. As ω/ω_n goes on increasing, that is, at high speeds of rotation, $\dfrac{mX}{m_e e}$ tends to unity for all values of damping.
3. The maximum value of $\frac{mX}{m_e e}$ occurs at

$$r = \frac{\omega}{\omega_n} = \frac{1}{[1-2\zeta^2]^{1/2}} \tag{11.A.97}$$

that is, slightly to the right of resonance value of $r = 1$.

11.A.5.6 Natural Frequencies and Resonant Frequencies

As brought out in the above sections, there exist the quantities ω_n, ω_d, ω_m and ω_{mr} associated with the resonance phenomenon of a single degree of freedom system and are expressed as in Equations (11.A.8), (11.A.33), (11.A.79), and (11.A.95). These are graphically shown as functions of the damping ratio (viscous damping) in Figure 11.A.17.

11.A.5.7 SDF Subjected to Base Excitation

Several times vibrations may be produced due to the motion of the base as shown in Figure 11.A.18. If for example the base excitation is of the type

$$y = Y \sin \omega t \tag{11.A.98}$$

the equation of motion of SDF in this case can be written as

$$m\ddot{x} + c(\dot{x}-\dot{y}) + k(x-y) = 0 \tag{11.A.99}$$

where x and y are the time dependent displacements/motions of the mass and the base respectively.

Using Equations (11.A.98) and (11.A.99) we get

$$m\ddot{x} + c\dot{x} + kx = kY \sin \omega t + c\omega Y \cos \omega t \tag{11.A.100}$$

The response of the rigid mass can be expressed as

$$x_p = X \sin(\omega t - \varphi) \tag{11.A.101}$$

Then the absolute value of the ratio of amplitudes can be obtained as

$$\left|\frac{X}{Y}\right| = \left[\frac{1 + (2\zeta\omega/\omega_n)^2}{[1-(\omega/\omega_n)^2]^2 + (2\zeta\omega/\omega_n)^2}\right]^{1/2} = \left[\frac{1 + (2\zeta r)^2}{(1-r^2)^2 + (2\zeta r)^2}\right]^{1/2} \tag{11.A.102}$$

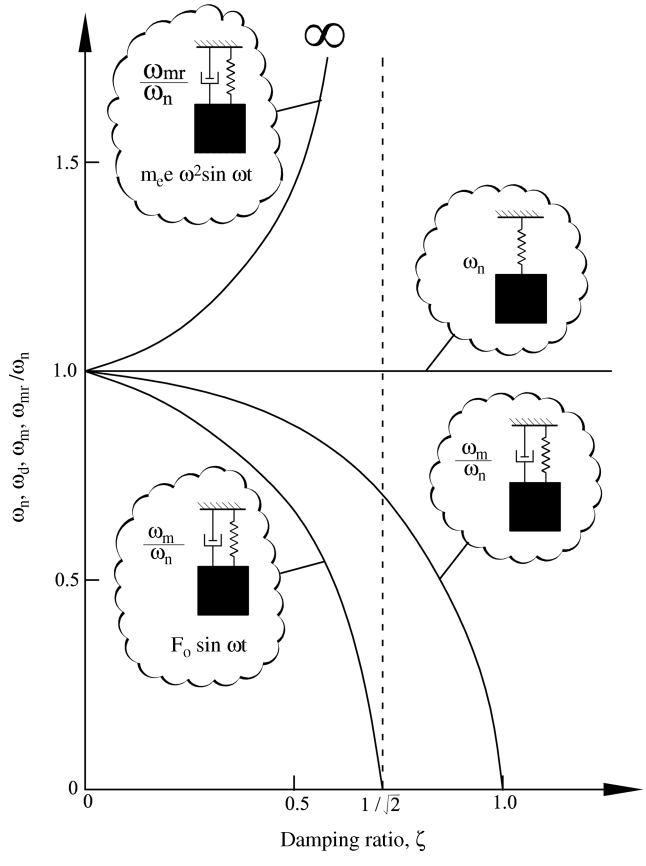

Figure 11.A.17 Frequency ratio versus damping ratio of a single degree of freedom system.

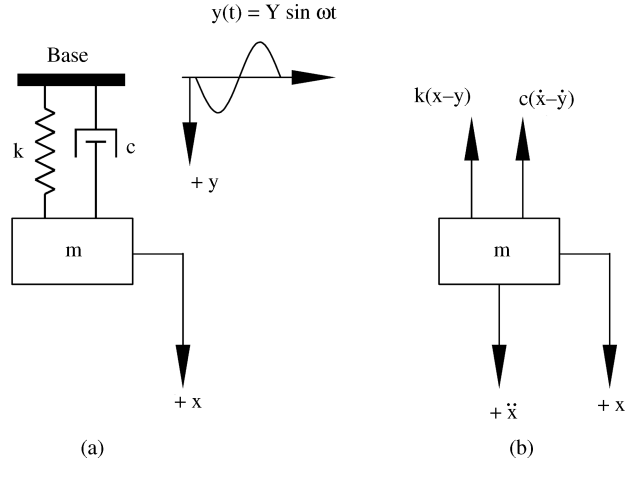

Figure 11.A.18 Single degree of freedom system subjected to base excitation.

and the phase angle, φ can be expressed as

$$\tan\varphi = \frac{2\zeta(\omega/\omega_n)^3}{1-(\omega/\omega_n)^2+(2\zeta\omega/\omega_n)^2} = \frac{2\zeta r^3}{1-r^2+(2\zeta r)^2} \tag{11.A.103}$$

where ζ and r are damping and frequency ratios. The plots of Equations (11.A.102) and (11.A.103) are shown in Figure 11.A.19.

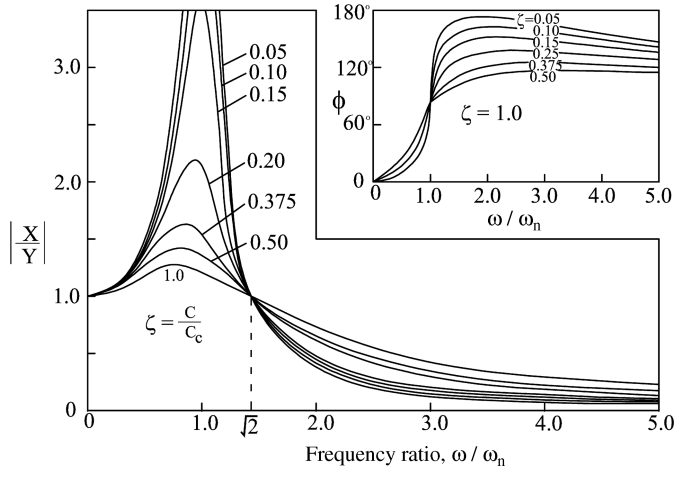

Figure 11.A.19 Response of viscously damped system subjected to base excitation.

The ratio X/Y is called transmissibility and the right hand side of Equation (11.A.102) can be noted to be identical with that of Equation (11.A.82) wherein $\frac{F_T}{F_o}$ is also called transmissibility, T_r. Thus the problem of displacement transmissibility is identical to that of force transmissibility. Accordingly all the observations made in connection with force transmissibility and isolation efficiency in Section 11.A.5.5 apply equally to the case of displacement transmissibility.

1. Force transmitted to the base
   The force transmitted to the base in this case of base motion can be similarly expressed from Figure 11.A.18 as

$$F_T = k(x-y) + c(\dot{x}-\dot{y}) = -m\ddot{x} \tag{11.A.104}$$

From Equations (11.A.101) and (11.A.102), the same can be expressed as

$$\begin{aligned} F_T &= -m\ddot{x} = m\omega^2 X\sin(\omega t-\varphi) \\ &= kYr^2\left[\frac{1+(2\zeta r)^2}{(1-r^2)^2+(2\zeta r)^2}\right]^{1/2} \end{aligned} \tag{11.A.105}$$

The variation of F_T/kY with frequency ratio r and damping ratio ζ are shown in Figure 11.A.20.

2. Relative motion
   Referring to Figure 11.A.18, it can be noted that

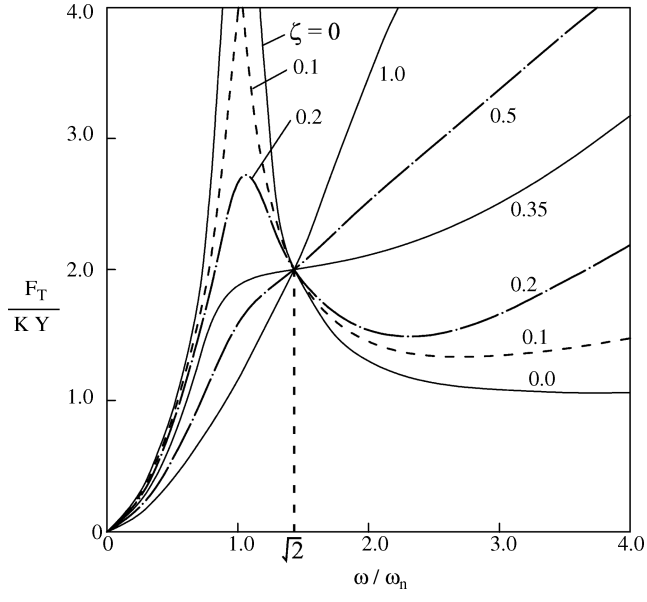

Figure 11.A.20 Force transmitted versus frequency ratio.

$$x - y = z \tag{11.A.106}$$

denotes the relative motion between the base and the mass. The equation of motion (Equation (11.A.99)) can also be expressed in terms of relative displacement z as

$$m\ddot{z} + c\dot{z} + kz = -m\ddot{y} = m\omega^2 Y \sin \omega t \tag{11.A.107}$$

where

z = relative displacement
x = displacement of the mass
y = displacement of the base.

Taking the base motion to be harmonic of the form given by Equation (11.A.98), the steady state solution to Equation (11.A.107) can readily be written as

$$z = \frac{m\omega^2 Y \sin(\omega t - \phi)}{[(k - m\omega^2)^2 + (c\omega)^2]^{1/2}} = Z \sin(\omega t - \varphi) \tag{11.A.108}$$

where the amplitude

$$Z = \frac{m\omega^2 Y}{[(k - m\omega^2)^2 + (c\omega)^2]^{1/2}} = Y \frac{r^2}{\left[(1 - r^2)^2 + (2\zeta r)^2\right]^{1/2}} \tag{11.A.109}$$

or

$$\frac{Z}{Y} = \frac{r^2}{[(1 - r^2)^2 + (2\zeta r)^2]^{1/2}} \tag{11.A.110}$$

The phase angle φ is the same as in the case of forced vibration with either constant amplitude or frequency dependent harmonic force. Results for Z/Y and φ are shown in Figure 11.A.21. These results are also applicable for computing the response of simple vibration measuring instruments which essentially measure relative motion characteristics.

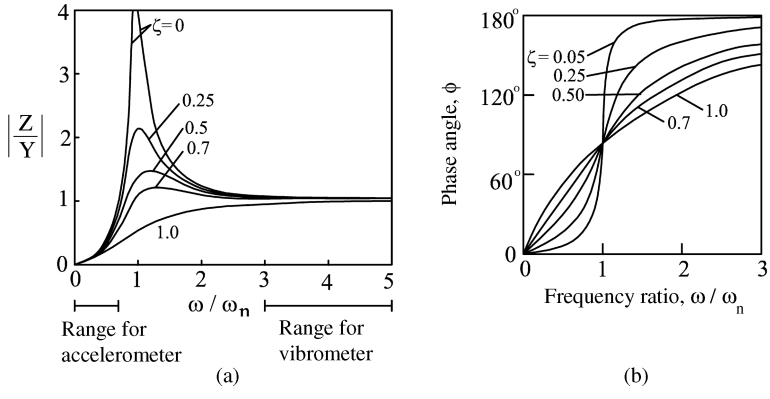

Figure 11.A.21 Relative motion versus frequency ratio.

The ratio Z/Y from Equation (11.A.110) can be seen to have identical expression with that of $\frac{mX}{m_e e}$ in the case of frequency dependent harmonic force as given by Equation (11.A.92). Hence the variation of Z/Y with frequency ratio r is identical to the variation of $\frac{mX}{m_e e}$ with r as given in Figure 11.A.16.

11.A.5.8 Other Types of Loads

The solutions for other types offloads such as general periodic loads, aperiodic loads, impact loads can be referred to Thomson (1965), Rao (1986), Kameswara Rao (1998, 2005) and other standard books on vibrations.

11.A.6 Multi Degree of Freedom Systems

11.A.6.1 Introduction

Though many physical systems can be analyzed fairly accurately using a single degree of freedom (SDF) idealization, sometimes it might become necessary to model the system, as one having more than one degree of freedom. These are called multi degree of freedom systems (MDFs). The topic has just been introduced to give a general idea of the formulation. The details can be referred to in standard text books on the subject (Thomson, 1965; Rao, 1986; Kameswara Rao, 1998, 2005).

In the system shown in Figure 11.A.22, the motion of the body moving in a horizontal plane (same for vertical orientation also if the system is in static equilibrium position, as mentioned for SDF in Section 11.A.2.1) can be specified by $x_1(t)$ and $x_2(t)$. Hence the system has two degrees of freedom. The number of degrees of freedom, n can be usually computed as $n =$ (number of masses in the system) $\times$ (number of possible types of motion of each mass).

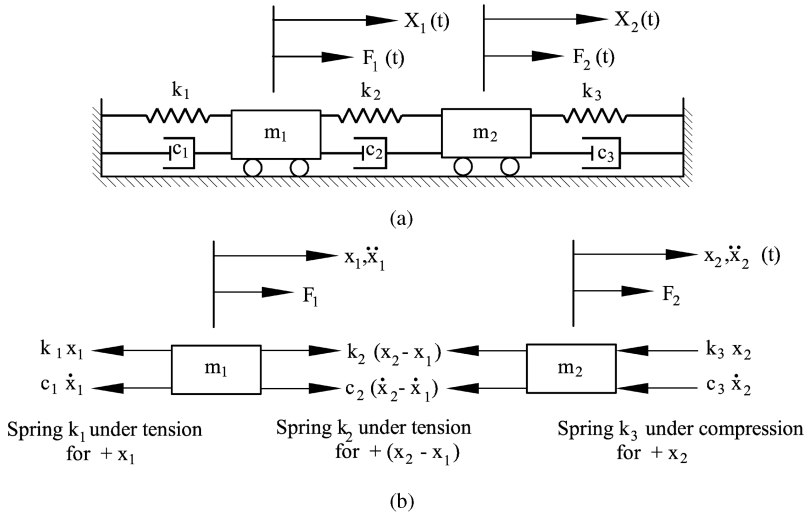

Figure 11.A.22 A two degrees of freedom spring–mass–dashpot system.

An n degree of freedom system needs n independent coordinates to describe its motion by a set of n simultaneous coupled ordinary differential equations of the second order. The system has as many natural frequencies as the degrees of freedom. A mode of vibration is associated with each natural frequency and the configuration is called a normal mode, principal mode or natural mode of vibration.

If the system is given an initial excitation, the resulting free vibrations will be the superposition of all the normal modes of vibration. However if the system vibrates under an external harmonic force, the response of the system will be at the frequency of the external force and the response tends to a maximum at any of the natural frequencies.

Although the equations of motion of an MDF are generally coupled, it may be possible to find a set of coordinates such that these are uncoupled, that is, each equation of motion involves only one independent coordinate and can be solved independently. Such a system of coordinates is called principal coordinates. Hence once the equations get uncoupled, all the solutions to a single degree of freedom system (SDF) can be conveniently used for studying the response of the MDF.

11.A.6.2 Equations of Motion

The equations of motion can be derived using either Newton's laws of motion or influence coefficients or more conveniently by using Lagrange's equation. The procedures for obtaining

the equations of motion, and solutions are essentially the same whether the system has two degrees of freedom or more. To illustrate the steps involved, a two degrees of freedom system (Figure 11.A.22(a)) is considered and equations of motion are derived using Newton's laws of motion. The motion can be described by the generalized coordinates $x_1(t)$ and $x_2(t)$ which are measured from the respective equilibrium positions of the masses, m_1 and m_2. From the free body diagrams of the masses m_1 and m_2 shown in Figure 11.A.22(b), the equations of motion can be written using Newton's second law of motion as

$$m_1\ddot{x}_1 + (c_1 + c_2)\dot{x}_1 - c_2\dot{x}_2 + (k_1 + k_2)x_1 - k_2x_2 = F_1(t) \tag{11.A.111}$$

$$m_2\ddot{x}_2 - c_2\dot{x}_1 + (c_1 + c_2)\dot{x}_2 + (k_3 + k_2)x_2 - k_2x_1 = F_2(t) \tag{11.A.112}$$

These are two coupled equations and can also be conveniently written in matrix form as

$$[m]\,\ddot{x}(t) + [c]\dot{x}(t) + [k]x(t) = F(t) \tag{11.A.113}$$

where $[m]$, $[c]$ and $[k]$ are called the mass, damping and stiffness matrices respectively and are given by

$$[m] = \begin{bmatrix} m_1 & 0 \\ 0 & m_2 \end{bmatrix}$$

$$[c] = \begin{bmatrix} c_1 + c_2 & -c_2 \\ -c_2 & c_2 + c_3 \end{bmatrix} \tag{11.A.114}$$

$$[k] = \begin{bmatrix} k_1 + k_2 & -k_2 \\ -k_2 & k_2 + k_3 \end{bmatrix}$$

and $x(t)$ and $F(t)$ are the displacement and force vectors respectively and are given by

$$x(t) = \begin{Bmatrix} x_1(t) \\ x_2(t) \end{Bmatrix}$$

$$F(t) = \begin{Bmatrix} F_1(t) \\ F_2(t) \end{Bmatrix} \tag{11.A.115}$$

It can be noted that $[m]$, $[c]$ and $[k]$ are square and symmetric matrices of second order, the order being the same as the degrees of freedom of the system. The equations of motion for any MDF will be of the same matrix form as Equation (11.A.113) and the order of the matrices will be equal to the degrees of freedom of the system under consideration. If another set of coordinates p_1, p_2 (instead of x_1, x_2) are used to describe the motion of the same system, it is obvious to see that the elements of matrices $[m]$, $[c]$, $[k]$ will differ from those shown in Equation (11.A.114). However, the system characteristics such as natural frequencies will be independent of the coordinates used to describe the motion. Hence the general form of a two degrees of freedom system can be

$$[m]\,\ddot{x}(t) + [c]\dot{x}(t) + [k]x(t) = F(t) \tag{11.A.116}$$

where

$$[m] = \begin{bmatrix} m_{11} & m_{12} \\ m_{21} & m_{22} \end{bmatrix} = \text{mass matrix}$$

$$[c] = \begin{bmatrix} c_{11} & c_{12} \\ c_{21} & c_{22} \end{bmatrix} = \text{damping matrix}$$

$$[k] = \begin{bmatrix} k_{11} & k_{12} \\ k_{21} & k_{22} \end{bmatrix} = \text{stiffness matrix} \tag{11.A.117}$$

The concept can be generalized for a multi degree of freedom system (say, n degrees). Equation (11.A.116) describes the motion where the matrices will now be of the nth order, that is

$$[m] = [m_{ij}]; [c] = [c_{ij}]; [k] = [k_{ij}]$$

$$x(t) = \begin{Bmatrix} x_1 \\ x_2 \\ \cdot \\ \cdot \\ x_n \end{Bmatrix}; \quad F(t) = \begin{Bmatrix} F_1 \\ F_2 \\ \cdot \\ \cdot \\ F_n \end{Bmatrix} \tag{11.A.118}$$

where $i, j = 1, 2 \ldots n$ and $x(t)$ and $F(t)$ are the generalized coordinates and force vector of order n.

But for the matrix form, Equations (11.A.113) and (11.A.116) can also be seen to be similar to the forced vibration equation of SDF given by Equation (11.A.2) in Section 11.A.2. The solution to Equations (11.A.111) and (11.A.112) (represented in matrix form by Equation (11.A.113) for general values of $F_1(t)$ and $F_2(t)$, that is, $F(t)$) is difficult to obtain mainly due to coupling of the variables $x_1(t)$ and $x_2(t)$ represented by the nonzero off-diagonal terms in the coefficient matrices $[c]$ and $[k]$. If the coupling exists in matrix $[m]$, it is called dynamic coupling, or inertial coupling or mass coupling. If it exists in matrix $[k]$, it is called static coupling or elastic coupling. If the coupling exists in matrix $[c]$ it is called damping or velocity coupling. It is possible to choose a different set of coordinates say $q_1(t)$and $q_2(t)$which can uncouple the equations completely thus yielding two uncoupled equations of motion resembling two SDF equations of motion. Such coordinates are called principal or natural coordinates. It is obviously advantageous to uncouple the equations of motion so that all the existing solutions to SDF can be readily used and all the equations can be solved independently of one another (Thomson, 1965; Rao, 1986; Kameswara Rao, 1998, 2005). These references give the various methods of solution using analytical and numerical approaches.

Appendix 11.B Stiffness and Damping Parameters

11.B.1 Introduction

The stiffness and damping parameters (also called analog parameters of an equivalent mass–spring–dashpot SDF model) derived by several research workers are available in literature. These are useful in analyzing MFS and MPFS as equivalent MDF systems. Lysmer and Richart's (1966) analysis which is presented in Section 11.6 is one such example of obtaining an equivalent SDF model for each mode of vibration. A few such important expressions/values for these stiffness and damping parameters commonly used in the analysis are presented in this appendix.

11.B.2 Analog Parameters of Lysmer and Richart

The stiffness and damping parameters for surface foundations derived by Lysmer and Richart (Richart, Hall and Woods, 1970; discussed in Section 11.6) are given in Table 11.B.1.

11.B.3 Other Parameters

Similar parameters for analog models for block foundations incorporating the actual field conditions as closely as possible have been derived by Gazetas and Tassoulas (1987), Wolf (1988) and Mita and Luco (1989) and are given by Kameswara Rao (1998). In the case of machine foundations with piles, Novak *et al.* derived the stiffness and damping parameters and these are presented by Kameswara Rao (1998). Their applications in the actual analysis of MPFS are discussed in Section 11.8.

11.B.4 Parameters of Machine Foundation for Computations

It has been shown clearly in this chapter that the general equations of motion of a machine foundation–soil system resemble those involving multi degree of freedom systems. Under certain conditions of symmetry, these equations simplify such that they are identical (in form) to the equations of motion of several single degree of freedom systems. This section presents the expressions for various constants that are needed for the computational purposes involving the equations discussed in this chapter.

11.B.4.1 Various Modes of Vibration

Using the elasticity solutions for the dynamic responses of a rigid foundation block resting on semi-infinite, homogeneous, isotropic, linearly elastic soil medium in all six modes of vibration (corresponding to the six degrees of freedom of a rigid body) SDF analogs have been developed by Lysmer and Richart and several others (Richart, Hall and Woods, 1970) which give the various constants (spring and dashpot constants). The expressions of these constants are listed in Table 11.B.1. The expressions of these parameters reported by several others are given by Kameswara Rao (1998). In particular, the analog parameters for pile foundations reported by Novak are also presented in the above reference of Kameswara Rao (1998).

Table 11.B.1 Analog parameters for surface foundations.

Mode	Parameters
Vertical along z axis	$r_z = \left(\frac{ab}{\pi}\right)^{0.5}; b_z = \frac{0.25m(1-v)g}{\rho_s r_z^3}; k_{zz} = \frac{4\mu_s r_z}{1-v}$
	$\zeta_z = \frac{0.425}{\sqrt{b_z}};\ c_{zz} = 2\zeta_z\sqrt{k_{zz}m}$
Horizontal along x axis	$r_x = \left(\frac{ab}{\pi}\right)^{0.5};\ b_x = \frac{(7-8v)mg}{32(1-v)\rho_s r_x^3};\ k_{xx} = \frac{32(1-v)\mu_s r_x}{7-8v}$
	$\zeta_x = \frac{0.288}{\sqrt{b_x}}; c_{xx} = 2\zeta_z\sqrt{k_{xx}m}$
Horizontal along y axis	Same as above with subscripts as y
Torsional about z axis	$r_{zz} = \left(\frac{ab(a^2+b^2)}{6\pi}\right)^{0.25}; b_{rz} = \frac{I_{\varphi z}g}{\rho_s r_{rz}^5}; k_{\varphi_{zz}} = \frac{16\mu_s r_{rz}^3}{3}$
	$\zeta_{rz} = \frac{0.5}{1+2b_{rz}}; c_{\varphi_{zz}} = 2\zeta_{rz}\sqrt{k_{\varphi_{zz}}I_{\varphi_z}}$
Rocking about x axis	$r_{rx} = \left(\frac{ab^3}{3\pi}\right)^{1/2}; b_{rx} = \frac{0.375(1-v)I_{\varphi_x}g}{\rho_s r_{rx}^5}; k_{\varphi_{xx}} = \frac{8\mu_s r_{rx}^3}{3(1-v)}$
	$\zeta_{rx} = \frac{0.15}{(1+b_{rx})\sqrt{b_{rx}}}; c_{\varphi_{xx}} = 2\zeta_{rx}\sqrt{k_{\varphi_{xx}}I_{\varphi_x}}$
Rocking about y axis	$r_{ry} = \left(\frac{a^3b}{3\pi}\right)^{0.25}; b_{ry} = \frac{0.375(1-v)I_{\varphi_y}g}{\rho_s r_{ry}^5}; k_{\varphi_{yy}} = \frac{8\mu_s r_{ry}^3}{3(1-v)}$
	$\zeta_{ry} = \frac{0.15}{(1+b_{ry})\sqrt{b_{ry}}}; c_{\varphi_{yy}} = 2\zeta_{ry}\sqrt{k_{\varphi_{yy}}I_{\varphi_y}}$
Notation used	
a, b	Dimensions of the block in x, y directions
$r_z, r_x, r_y, r_{rx}, r_{ry}, r_{rz}$	Equivalent radii for translational modes in vertical and horizontal modes, rotational modes about x, y and z directions, m mass of the footing
$I_{\phi x}, I_{\phi y}, I_{\phi z}$	Moment of inertia about x, y and z directions
$b_z, b_x, b_y, b_{rx}, b_{ry}, b_{rz}$	Mass ratios for translational modes in vertical and horizontal directions and rotational modes about x, y and z axes
$k_{zz}, k_{xx}, k_{yy}, k_{\phi xx}, k_{\phi yy}, k_{\phi zz}$	Stiffness parameters for translational modes along vertical and horizontal directions and for rotational modes about x, y and z axes
$c_{zz}, c_{xx}, c_{yy}, c_{\phi xx}, c_{\phi yy}, c_{\phi zz}$	Damping parameters for translational modes along vertical and horizontal directions and for rotational modes about x, y and z axes
$\varsigma_z, \varsigma_x, \varsigma_y, \varsigma_{rx}, \varsigma_{ry}, \varsigma_{rz}$	Damping ratios for translational modes along vertical and horizontal directions and for rotational modes about x, y and z axes
μ	Shear modulus of the soil
v	Poisson's ratio of the soil
ρ	Unit weight of the soil, and g acceleration due to gravity

11.B.4.2 Mass and Mass Moment of Inertia

In Equations (11.39)–(11.41)

$$\begin{aligned} m &= \text{total mass of machine and foundation} = \frac{W_T}{g} \\ &= m_F + \sum_i m_i \end{aligned} \tag{11.B.1}$$

where

W_T = total weight
g = acceleration due to gravity
m_F = mass of the foundation (including piles in case of pile foundations)

$m_i = m_1, m_2\ (I = 1, 2, \ldots)$ = masses of machines and accessories

I_x, I_y, I_z = total mass moment of inertia of the machine and foundation about the x, y and z axes respectively.

11.B.4.3 Rectangular Solids

For a foundation of the type shown in Figure 11.8 (rectangular parallelopiped with dimensions a, b, c along the x, y, z axes respectively) supporting machine, I_x, I_y, I_z can be expressed as

$$\begin{aligned} I_x &= m_F\left(\frac{b^2+c^2}{12}\right) + \sum_i I_{mxi} + \sum_i m_i\left(y_i^2 + z_i^2\right) \\ I_y &= m_F\left(\frac{c^2+a^2}{12}\right) + \sum_i I_{myi} + \sum_i m_i\left(z_i^2 + x_i^2\right) \\ I_z &= m_F\left(\frac{a^2+b^2}{12}\right) + \sum_i I_{mzi} + \sum_i m_i\left(x_i^2 + y_i^2\right) \end{aligned} \tag{11.B.2}$$

11.B.4.4 Right Circular Cylinder of Radius r, Length l

$$I_v\ (\text{through axis of figure}) = m_F\frac{r^2}{2} + \sum_i I_{mvi} + \sum_i m_i\left(x_i^2 + y_i^2\right) \tag{11.B.3}$$

$$\begin{aligned} &I_h(\text{through centre perpendicular to axis of figure, say along } x \text{ axis}) \\ &= m_F\left(\frac{l^2}{12} + \frac{r^2}{4}\right) + \sum_i I_{mhi} + \sum_i m_i\left(y_i^2 + z_i^2\right) \end{aligned} \tag{11.B.4}$$

x_i, y_i, z_i = coordinates of mass m_i with reference to the combined CG of mass and foundation, that is, point A in Figure 11.8; and

$I_{mvi}, I_{mhi}, I_{mxi}, I_{myi}, I_{mzi}$ = mass moment of inertia of the ith machine/accessory about its own axis parallel to the axis about which the mass moment of inertia is being calculated.

It can be noted from the above expressions that parallel axis theorem is used for computing the mass moments of inertia of other machines and accessories. Usually the mass moments of inertia of machines and accessories about their own axes may be negligible in comparison to other terms. The summation is to be taken on all the masses on the foundation such as all machines and accessories, and so on. Expressions for other shapes of foundations can be derived or taken from standard mathematical tables.

Appendix 11.C General Guidelines for Design and Construction of Machine Foundations

11.C.1 Introduction

The design and construction practices of machine foundations have evolved over several decades and are based on local codes of practice. Since the codes may not exhaustively cover all aspects, the information needed by designers and professional engineers has to be supplemented from existing books and literature. Some of these broad guidelines relevant to design and construction are highlighted in this section. The relevant codes of practice (such as IS: 456–2000 for reinforced concrete, IS: 2974–1966 for machine foundations, IS: 5249–1969 for tests to determine the dynamic parameters, IS: 1888–1982, IS: 2720–1983 for various tests on soils) provide the broad guidelines for the design and construction of machine foundations. Elaborate details on the topic are also given by Barkan (1962), Major (1962), Richart, Hall and Woods (1970), Srinivasulu and Vaidyanathan (1976) and Kameswara Rao (1998, 2000).

11.C.2 Data for Analysis and Design

1. Soil data
   Usual soil data shall be obtained from soil investigation report. In particular values of Young's modulus of elasticity, E, and Poisson's ratio, v, are needed for analysis, and coefficients of elastic uniform and/or non-uniform compression are required for analysis. The details can be seen in the above codes. Some of the above test results are complimentary and the actual tests to be carried out have to be decided based on the design problem and site conditions. The details of dynamic soil tests are also given by Barkan (1962), Richart, Hall and Woods (1970) and Kameswara Rao (1988, 2000).
2. Machine data
   All relevant data for the machines including their layout should be obtained from the manufacturer/supplier of the equipment. In particular, the static and dynamic loads, their points of application and so on must be obtained or computed from the machine data. The details needed for various types of machines are given in the above codes and references.

11.C.3 Guidelines for Design

11.C.3.1 Reciprocating Engines

1. Natural frequency
   For machines with an operating speed <300 rpm, the foundation should be designed such that the natural frequency of the foundation–soil system is much higher than 2 times the operating speed/frequency of the dynamic load. For machines with an operating speed >500 rpm, the natural frequency of the system should be less than $0.5\times$ the operating speed/frequency of the dynamic load.

2. Amplitudes
   a. The permissible amplitude of vibration shall be based on the criteria given in IS: 2974–1966 (1966) and in no case greater than 0.2 mm or the limiting amplitude specified by the manufacturer. Some guidelines are given in Figures 11.2–11.4.
   b. Any other stipulation on amplitudes or differential amplitude between two points connected by rigid members (such as shafts connecting generator and alternator etc.) specified by the manufacturer to ensure smooth operation of the machine(s), noise control and human comfort and so on.
3. Permissible stresses
   The soil stress below the foundation shall not exceed 80% of the allowable bearing pressure on soil under static loading determined in accordance with IS: 1904–1966 (1966). When seismic forces are considered the allowable stresses on soil may be increased as per IS: 1893–1984 (1984).
   M15 to M20 concrete shall be used for the foundation. The allowable stresses for concrete and steel specified in IS: 456–2000 (2000) shall be reduced to 40% for concrete and 55% for steel, if the detailed design of foundation and components is limited to static load of foundation and machine. Considering temperature or shrinkage and all other loading together these reduced stresses may be exceeded by 33.33%. If dynamic loads are separately considered in detailed design with suitable dynamic and fatigue factor, no reduction in allowable stresses as given in IS: 456–2000 (2000) is necessary.
4. Dimensional criteria
   a. The size of the foundation block in plan should be larger than base plate of the machine with a minimum all round clearance of 150 mm.
   b. The eccentricity of the CG of foundation block plus the weight of the machine should not exceed 5% of the least width of the base area of foundation unless the imbalances are accounted for in the design.
   c. According to Rausch (Kameswara Rao, 1998) the recommended weight of foundation may be 5–10 times that of machines of up to 500 rpm and 10–20 times for machines of up to 1000 rpm (see also the recommended thicknesses and weights given in Table 11.C.1 and Table 11.C.2).

Table 11.C.1 Recommended thickness of foundation for impact type of machines.

Weight of tup (kN)	Minimum thickness (m)
<10	1.00
10–20	1.25
20–40	1.75
40–60	2.25
>60	2.50

5. Reinforcement
   The amount of reinforcement in the foundation shall not be less than 250 N/m^3. Around all openings, pits, and so on, a steel reinforcement equal to 0.50–0.75% of the cross sectional area of the opening shall be provided in the form of a cage. All units of foundation shall be provided with reinforcement both ways. The minimum diameter of bars shall be 12 mm, with a maximum spacing of 200 mm in order to take care of shrinkage in concrete. The concrete cover to reinforcement shall be minimum 75 mm at the bottom and 50 mm at the sides and top.

11.C.3.2 Impact Type Machines

1. Natural frequency
   The natural frequency of the foundation system shall not be a whole number multiple of the operating frequency of impact. A natural frequency of the system of two and a half times the frequency of impact is considered satisfactory and for undertuned systems it shall be at least 30% less than the frequency of impact.
2. Amplitudes
   a. The maximum vertical vibrational amplitude of the foundation shall not be more than 1.2 mm. In case of foundations on sand below ground water table amplitude shall not be more than 0.8 mm.
   b. Vibrational amplitudes of the anvil shall not be more than 1 mm for tup weight up to 10 kN, 2 mm for tup weight 20 kN and 3–4 mm for tup weights more than 30–40 kN.
   c. Any other limits prescribed by the manufacturer should be taken into account.
3. Permissible stresses
   The stresses produced at the time of impact in the foundation base (soil, timber sleepers, cork, spring elements or piles) shall be within 0.8 times allowable static stress.
4. Dimensional criteria
   a. The CG of the system should coincide with the line of fall of the hammer tup.
   b. The depth of foundation block shall be so designed that the block is safe both in punching shear and bending. However, the minimum thickness shall be as given in Table 11.C.1.
   c. Weight of the anvil may be generally kept at 20 times the weight of the tup and weight of the foundation block generally varies from 66 to 120 times the weight of the tup depending on the type of soil as given in Table 11.C.2.

Table 11.C.2 Recommended weight of foundation.

Type of foundation/soil	Weight of foundation block: weight of tup
Pile foundations in weak soils	66–120
Block foundations on stiff clays, compact sandy deposits	75–90
Block foundations on moderately firm to soft clays, medium dense to loose sandy deposits	90–120

5. Reinforcement
   Reinforcement shall be arranged along the three axes and also diagonally under the anvil to prevent shear. Reinforcement at top may be provided in the form of layers of grills made of 16 mm diameter bars suitably spaced. The top layer should have a cover of at least 50 mm. The minimum reinforcement shall be 250 N/m^3 of concrete.

11.C.3.3 Rotary Type Machines

1. Natural frequency
   For high frequency machines with framed foundations the natural frequency of any foundation member should not preferably be within 20% of the operating speed of the

machine/frequency of the dynamic loads and moments. Foundations under low frequency machines should have their natural frequencies much higher than the operating speed of the machines/frequency of the dynamic loads and moments.

2. Amplitudes
   Permissible amplitudes at bearing level for framed foundations shall be as follows:
   a. For low to medium frequency machines:
      Vertical vibration = 0.04–0.06 mm
      Horizontal vibration = 0.07–0.09 mm
   b. For high frequency machines:
      Vertical vibration = 0.02–0.03 mm
      Horizontal vibration = 0.04–0.05 mm

   The amplitude of vibration of the foundation or any of its components shall not exceed half of the above values. Permissible amplitudes of low frequency machines with block foundations shall not exceed 0.3 mm.
3. Permissible stresses
   The soil stress below foundation shall not exceed the allowable bearing pressure. When seismic forces are considered these values may be increased as specified in IS: 1893–1984 (1984). M20 or higher grade concrete may be used for framed foundations and M15 or M20 grade concrete for block foundations of low frequency machines. The allowable stresses as specified in IS: 456–2000 (2000) shall be reduced to 40% for concrete and 55% for steel to take care of fatigue. Considering temperature or shrinkage and all other loading together, these reduced stresses may be exceeded by 33.33%.
4. Dimensional criteria
   In framed foundations the effective thickness of the base slab shall be at least one-tenth of its length or minimum width of any column. The weight of the base slab shall not be less than the total weight of the machine plus the weight of the foundation without the base slab. As far as possible the foundation shall be so dimensioned that the resultant force due to the weight of the machine, the upper deck, intermediate slabs and the base slab together with columns passes through the CG of the base area in contact with soil.
   In case of block foundations for low frequency machines, the weight of foundation should be at least 2.5 times the weight of the whole machine. The CG of machine and foundation should pass through the CG of the area in contact with the soil.
5. Reinforcement
   In case of framed foundations the vertical reinforcement of columns should reach the bottom of base slab up to 1 m thickness. In thicker slabs 50% of the reinforcement may be cut off at half the height of the base slab. All units of the foundation shall be provided with double reinforcement. Symmetric reinforcement shall be provided on the sides of cross section of beams and columns even if it is not required by calculations. The amount of reinforcement in separate foundation units shall not be less than 1 kN/m^3 of concrete.
   The minimum diameter of longitudinal steel for beams and columns should be 20 mm for machines up to 10 MW and 25 mm for machines over 10 MW. The maximum spacing of longitudinal bars in columns and beams shall not be more than 150 mm. Minimum cover to reinforcement shall be as follows:

Base slab = 100 mm all sides
Columns = 50 mm all sides
Beams = 40 mm all sides

In case of block foundations for low frequency machines reinforcement in the form of cage in three dimensions should be provided. The amount of reinforcement shall not be less than 500 N/m^3. The minimum diameter of bars shall be 12 mm and maximum spacing shall be 200 mm. Cover to reinforcement shall be minimum 75 mm at the bottom and 50 mm on sides and top.

11.C.4 Miscellaneous Guidelines

11.C.4.1 Pile Foundations

The use of piles in machine foundations subjected to vibrations and shocks may be necessary in the following cases:

a. If the total pressure on the soil, both static and dynamic, is larger than the bearing capacity of the soil, considering the dynamic action of the foundation on the soil.
b. If it is necessary to increase the natural frequency of vibrations of the foundation, but it is impossible to alter its dimensions.
c. If it is necessary to decrease the amplitude of natural or forced vibrations.
d. If it is necessary to decrease the residual dynamic settlement of the foundation.
e. Due to presence of ground water table, vibrations are frequently transmitted undamped to considerable distances. However, in cohesive soils such as clay and loam, considerable damping may take place, yet the soil may become plastic and this, in turn, may result in the transmission of harmful vibrations to the environment. In both these cases, depending upon soil characteristics, pile foundations may be resorted to. However, the pile foundations should be adopted based on the soil investigation report and the nature of machines.

11.C.4.2 Location

It should be noted that in case of important and heavy machines, it is the machine foundations that decide the layout of the building and not vice versa. It is advisable to separate at all levels, usually by means of expansion joints, machine foundations from adjacent structures. For low capacity machines separation may not be necessary. Building foundations can be constructed at a level higher than that of machine foundations; however, the possible decrease of angle of internal friction of soil due to dynamic forces should be studied. If the distance between two foundations is small they should be founded at same elevation. The machine foundation should not be used as a bearing foundation for other structures. In unavoidable circumstances suitable insulations against vibrations, such as gaskets of rubber, cork, felt and so on should be employed at the interface.

11.C.4.3 Several Machines on Common Raft

A number of similar machines erected on individual pedestals may be mounted on a common raft. The raft is designed conventionally by taking sections of raft corresponding to separate foundations and vibration computations made. Design values of permissible amplitudes of vibration can be increased by 30% in such raft foundations.

11.C.4.4 Foundations for Machine Tools

Foundations for machine tools require dynamic analysis only in special cases. Allowance for static loads is in general sufficient.

Automatic lathes, turret lathes, milling machines, gear shaping machines, drilling and boring machines and other automatic machines can be carried by concrete grade floors of 150–200 mm thickness. Vertical boring and turning machines, grinding machines, transverse planning machines as well as planers and planer type milling machines should always have separate foundations. The approximate depth required can be calculated as follows (Table 11.C.3).

Table 11.C.3 Minimum depth of foundation from surface.

Type of machine	Minimum depth of foundation below ground level (where L is length of the foundation in meters)
Milling machines, gear shaping machines, drilling machines	0.25 meters
Lathes	$0.2\sqrt{L}$
Vertical boring and turning machines	$0.6\sqrt{L}$
Grinding machines	$0.4\sqrt{L}$
Planers, planer type milling machines	$0.3\sqrt{L}$
Transverse planing machine	0.8–1.2 meters

While designing the foundations care should be taken so that the clearance between pockets for bolts and the edge of the foundation is not less than 200 mm and that between base plate/frame and edge is not less than 100 mm.

11.C.4.5 Machine Foundations on Suspended Floors

Smooth running machines such as machine tools and small electric motors can be set on suspended floors with proper vibration damping. For the determination of natural frequencies of floors/beams with different end conditions, tables are given in Major (1962).

11.C.5 Construction Guidelines

Besides the specifications given in IS: 456–2000 (2000) for RCC construction, some useful guidelines for the construction of machine foundations are outlined below.

11.C.5.1 Concrete Details

As mentioned in earlier sections, concrete grade used should be at least M15 for block foundations and M20 for framed foundations and structures. All the precautions and procedures applicable for normal concrete construction should be adopted. Cold joints in the body of the foundation should be avoided. A perfectly dense concrete should be used especially for columns and loadbearing walls. Construction joints should be judiciously chosen ensuring monolithicity of the structure at the joint. Accordingly, shear keys and suitable number of dowel bars should be provided at the joint. Epoxy cements should be used under the base plate of the machine and for filling the anchor bolt holes. The concreting of foundation should be

done in horizontal lifts without interruption, if possible. If interruption is unavoidable, it should be done at those points where superstructure walls and columns join the foundation. To simplify construction process, flat slab foundation may be preferred instead of ribbed foundations. The top surface of the machine foundation should be at least 50 mm below the floor level with provision for drainage.

11.C.5.2 Reinforcement Details

The guidelines for the reinforcement have been given in earlier sections depending on the type of machine for which the foundation is constructed. However few more details are presented in this section from practical considerations besides the specifications given in IS: 456–2000 (2000).

Reinforcement should be provided along all surfaces, around openings, conduits and so on in all the three directions in block foundations as well as base slab of framed foundations. Typical reinforcement details for a framed foundation are shown in Figure 11.C.1. As already mentioned earlier, additional reinforcement equal to 0.5–0.75% of cross sectional area of the opening should be provided in the form of a cage around openings as shown in Figure 11.C.2. Typical reinforcement details at junction of structural members are shown in Figures 11.C.3 and 11.C.4. Reinforcing bars in the proximity of say 50 cm radius of openings left for power cables should be properly insulated.

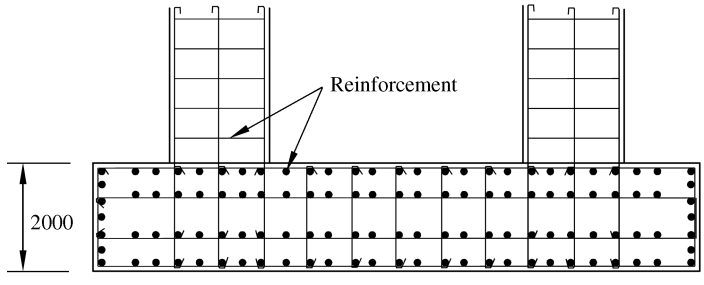

Figure 11.C.1 Typical reinforcement in a base slab of a framed foundation.

Structural steel can also be used as reinforcement for heavy foundations. Structural steel reinforcement is generally self supporting. After fabricating the steel framework, the super structure should be concreted in a single operation.

It may be expedient to use prefabricated cage reinforcement in the block type of machine foundations as well as the base slab of a framed foundation. This is feasible when the prefabricated reinforcement can be transported to the site easily.

11.C.5.3 Expansion Joints

Transmission of vibrations from machine foundations to adjoining structural components could be prevented by separating them through an expansion joint. Debris should not be

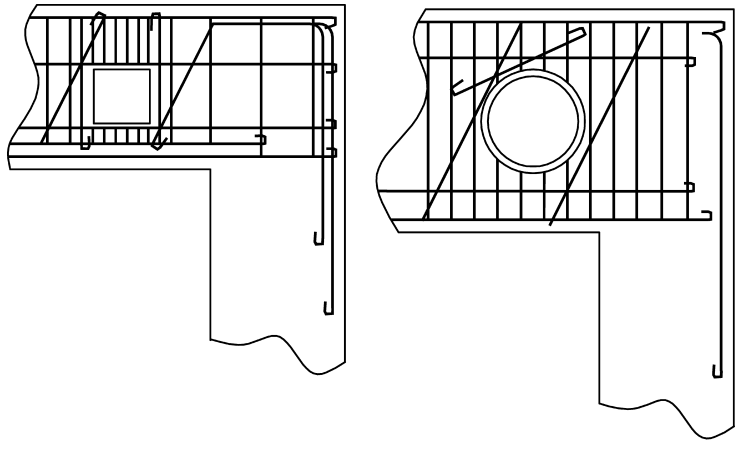

Figure 11.C.2 Reinforcement around (a) rectangular and (b) circular openings.

allowed to fill up the expansion joint for its efficient functioning. Usually the width of the expansion joints is 20–40 mm, depending on requirements.

It is advisable to provide expansion joints all around the zones to be separated including zones of adjoining structures to safeguard against failures due to differential settlement. Bituminous felt or corrugated sheets could be used at the interfaces of structural components that may be coming into contact with each other. Several examples of expansion joints are given by Major (1962).

11.C.5.4 Foundation Bolts and Fixtures

The machine is fixed to the foundation through a base plate and anchor bolts of appropriate dimensions as provided by the manufacturer. Concreting therefore should be stopped a few centimeters below the lower plane of the base plate. The gap should be filled up by cement mortar/epoxy cement and the base plate brought up to the desired level. For base plates of

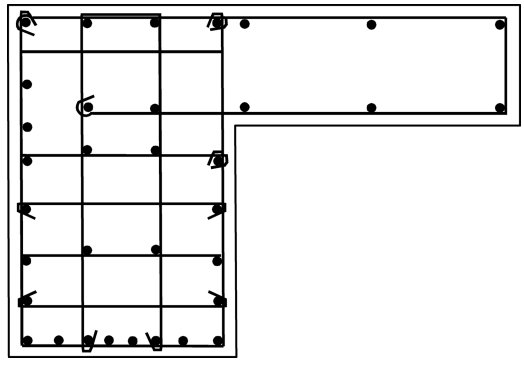

Figure 11.C.3 Typical reinforcement in longitudinal beams with cantilever projection.

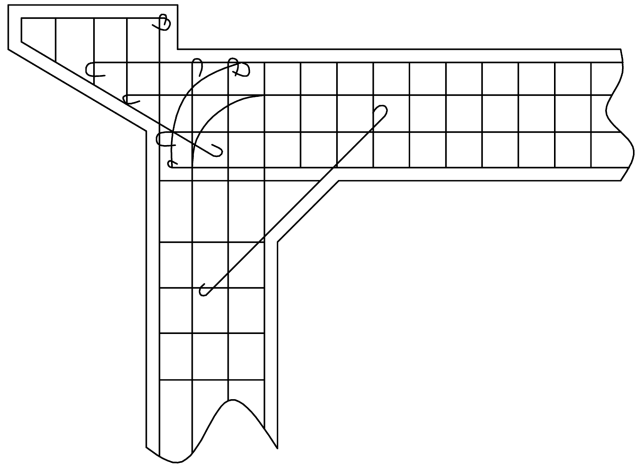

Figure 11.C.4 Detail at a beam–column junction.

30–40 cm width, the underfilling could be 2–3 cm thick. For wider base plates, the filling could be up to 5 cm thickness.

The base plates can be placed directly on concrete or on an intermediate grillage or jacks as shown in Figure 11.C.5. The leveling can be done through wedges or jacks which also support the base plate until the mortar has set in.

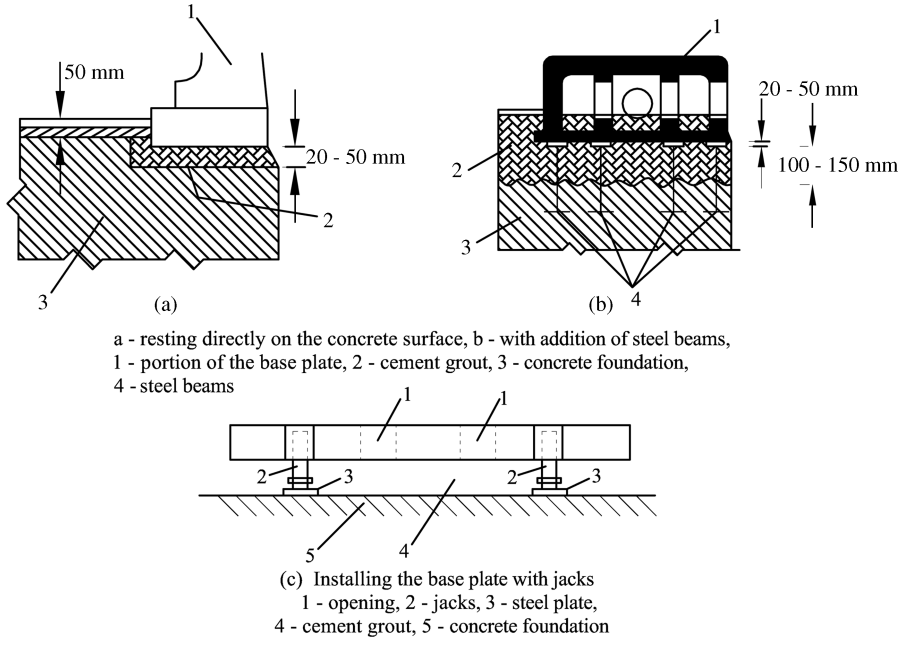

Figure 11.C.5 Positioning of base plate (a) with mortar; (b) with steel beams.

Base plates are then fixed to the foundation by anchor bolts which have to be concreted into the block in prescribed positions corresponding to the holes in the base plate. It is difficult to put the bolts in correct position and maintain them in subsequent concreting except in small machines. Hence the bolts are positioned by means of a template whose holes coincide with the holes in the base plate as shown in Figure 11.C.6. Then the concreting is done by holding the bolts in position by template and nuts. After the concrete has set in, the templates and nuts can be removed. This method however will not allow any subsequent adjustments in the position of bolts if required.

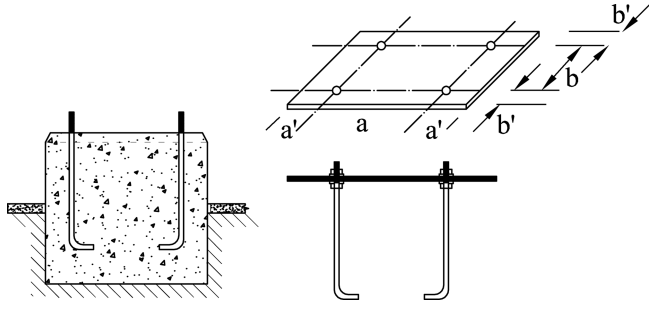

Figure 11.C.6 Fixing anchor bolts by a drilled plate, the holes of which correspond to those of steel plate.

To facilitate some adjustments while fixing the base plate, the bolt pockets holes are left in the foundation block while concreting as shown in Figure 11.C.7 and these pockets are filled with mortar/epoxy after the base plate is placed in position and the bolts are correctly aligned. The bolt holes are left such that they are accessible at the bottom through a horizontal shaft leading to the outer surface of the foundation block or extending them through the entire block. This will help in cleaning the holes while concreting and to fix the bolts correctly.

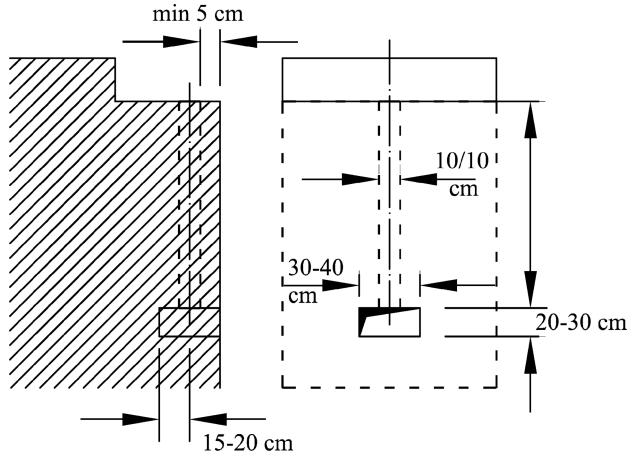

Figure 11.C.7 Bolt holes accessible from the cleaning duct.

The bolt holes should not normally be larger than 15×15 cm (to avoid dislocation of reinforcement) with a minimum clearance of 8 cm from the edge/surface of the foundation block. The length of the bolt in concrete should be sufficient to have enough bond with concrete and to hold the machine in position during operation and is usually 30–40 times the diameter of the bolt. These are supplied along with the machine by the manufacturer as per requirements. If the thickness of the foundation block is smaller than the bolt length in concrete, a washer plate and nut must be used to secure the fixity. Some usual methods of fixing the bolts in foundation pockets are illustrated in Figure 11.C.8.

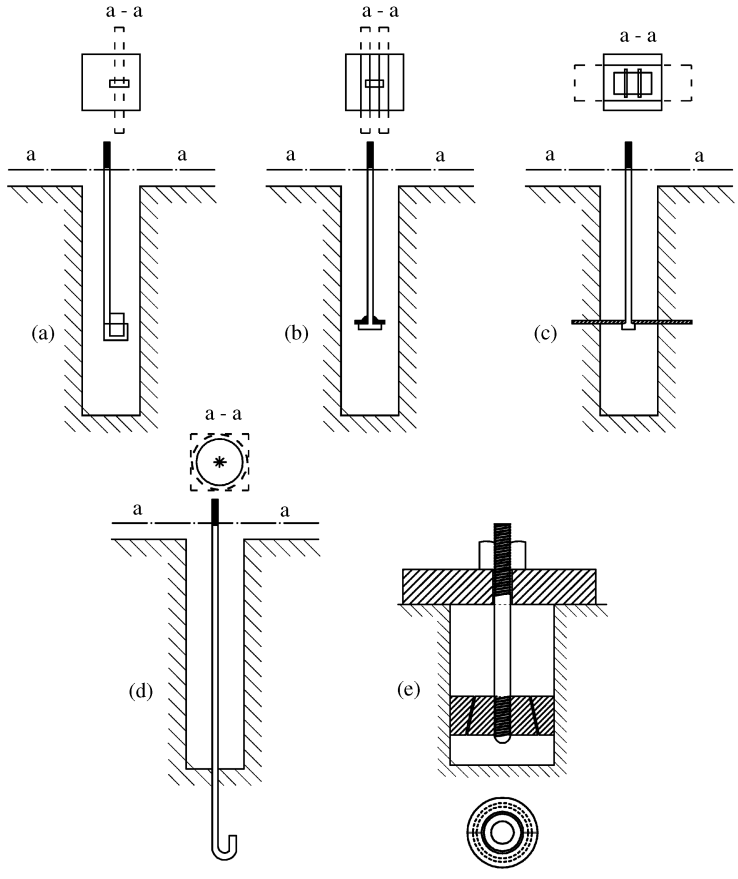

Figure 11.C.8 Details of anchor bolt fixtures. (a) Fastening anchor bolt with cast-in flat iron. (b) Fastening anchor bolt with angle iron. (c) Fastening anchor bolt with cast steel plate. (d) Anchor bolts welded to tube bottom. (e) Fixing with expanding wedge and with upper and lower threads.

The bolt holes are filled with concrete after aligning the bolts. If machines are placed directly on floors, the anchor length may not be sufficient. In such cases either washer or nuts may be used at the lower end or expansion bolts can be used as shown in Figure 11.C.8(e). Since anchor bolts transmit the vibrations without much damping, in some special cases the machines are

bonded to the foundations block through high strength special adhesives. The adhesives eliminate the drawbacks of conventional bolt holes and also damp the vibrations and noise.

To reduce excessive vibration transmission to the foundation, sometimes a shock absorbing medium may be placed below the base plate. The bolt holes should be concreted only after the shrinkage of the foundation block is complete. The underfilling below the base plate has to be done with cement mortar of 1 : 2 or epoxy cement of proper specifications. Grouting is recommended wherever possible. Machine operations can be started only after a gap of at least 15 days from installation.

11.C.5.5 Connection with Floors and Protection of Edges

Special care should be taken at the junction between floors and machine foundations to avoid cracks as illustrated in Figure 11.C.9.

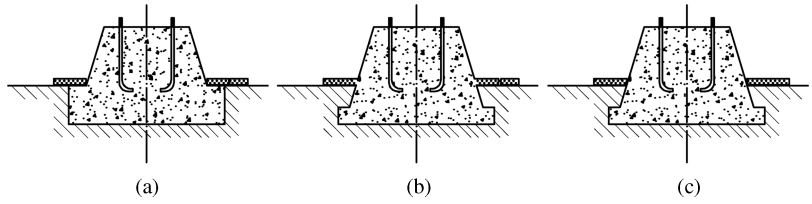

Figure 11.C.9 (a) Connection of machine foundation and floor cover: (b) incorrect; (c) correct.

Edges and openings of foundation blocks should be protected with plates, angles and lugs as shown in Figures 11.C.10 and 11.C.11. Holes should be left for the lugs and angle irons while concreting the foundation block and these holes should be concreted along with floor finish. The maximum spacing of lugs is 50 cm center to center.

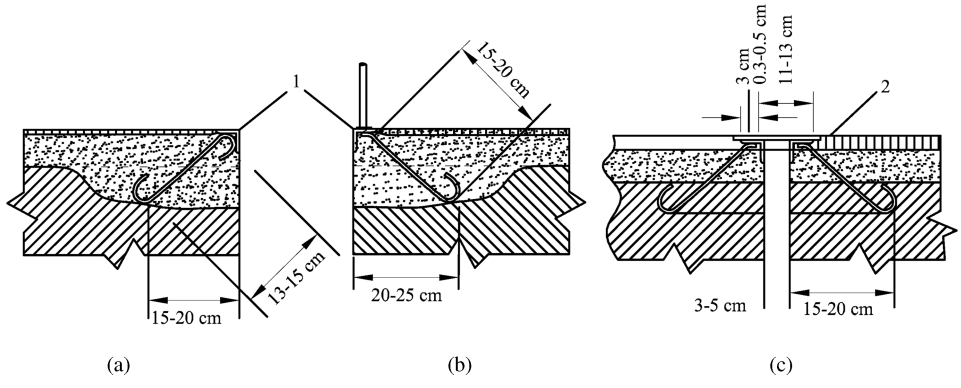

Figure 11.C.10 Edges of corner and channels. (a) Edges at corner. (b) Edges with railing on the ground. (c) Edges at expansion joint.

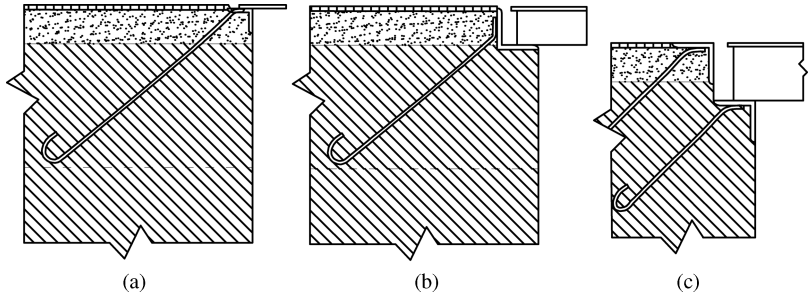

Figure 11.C.11 Edges at openings and various ways of providing support.

11.C.5.6 Prestressed Concrete Foundations

Prestressed concrete foundations can be used to support machines such as hammers. This improves fatigue behavior of materials since the material does not experience alternating tensile and compressive stresses and experiences only compression of varying intensities due to prestressing and eliminates the possibilities of cracking. A typical foundation with stressing ducts for a hammer is shown in Figure 11.C.12. However prestressed foundations can be adopted for simple cross sections and small dimensions.

11.C.5.7 Provisions for Tuning of Foundations

Due provisions in construction should be made to allow tuning of foundations, that is, changing the natural frequency as may be required to avoid resonance, at a later stage. Accordingly provisions to increase the contact area of the foundation, thus to increase the stiffness and natural frequency and reduce the amplitudes as well as to increase the mass of the foundation (to reduce the natural frequency) at a later stage should be kept during construction. Accordingly enough dowel bars on the sides of the foundation block may be kept in addition to space for enlarging the base area subsequently if needed. Similarly, few hollow spaces could be kept in the block to be filled by concrete to increase the mass later if necessary.

In the case of framed foundations desired tuning can be achieved by altering any of the following:

1. The rigidity of the frame by reducing the effective length of the columns by connecting the columns at intermediate levels and also leaving enough dowel bars in columns at appropriate levels during initial construction. The columns may also be rigidly connected to the walls by bracings.
2. Changing the rigidity of the column by changing the end conditions. For example, if the column is designed as a fixed–fixed column, the fixed end connection can be altered to a pinned or partially fixed case by removing excess concrete at the connection and relieving the fixity.
3. Changing the effective length of the column by placing the column base in a sleeve and fixing it with the base slab. By concreting the sleeve up to the desired depth, the required

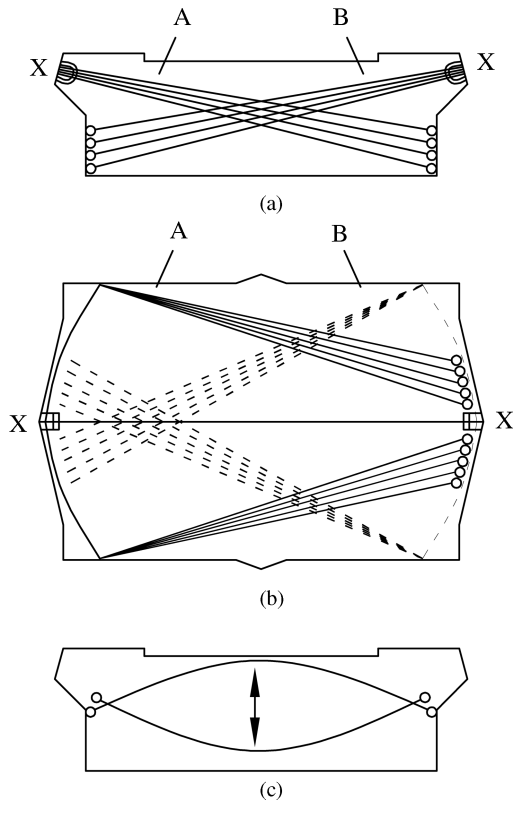

Figure 11.C.12 Part of pre-stressed concrete hammer foundation showing stressing ducts.

change in effective length can be obtained. Alternatively, the columns can be connected by an additional longitudinal beam cast on the top of base slab to reduce the effective length.

4. Enlargement of the area of columns by encasing and/or by providing additional columns.

11.C.6 Guidelines for Providing Vibration Absorbers

When the vibration characteristics can not be altered or turned using methods mentioned in Section 11.C.5.7, vibration absorbers can be employed to bring in the necessary changes. In fact, vibration absorbers may prove to be more cost effective and easy in many cases than the elaborate structural changes suggested in Section 11.C.5.7. However, maintaining these absorbers regularly to ensure their efficient performance over a reasonable period of time could prove to be difficult and costly. These absorbers are mainly used for mechanical isolation and have to be designed using proper analysis such as analysis of multi degree of freedom systems. Only a few practical applications of spring type absorbers are illustrated in this section.

11.C.6.1 Spring Type Absorbers

Two types of spring type absorbers are commonly adopted for vibration isolation: (a) the supported system and (b) the suspended system. While the principles of their analysis and functioning are similar, the difference essentially lies in the location of the springs. In the supported system, the springs are directly placed under the machine or the foundation, as shown in Figures 11.C.13–11.C.17. In the suspended system the foundation is suspended from springs which are located at or close to the floor level as shown in Figure 11.C.18. The suspended system provides easy access to the springs for regular maintenance.

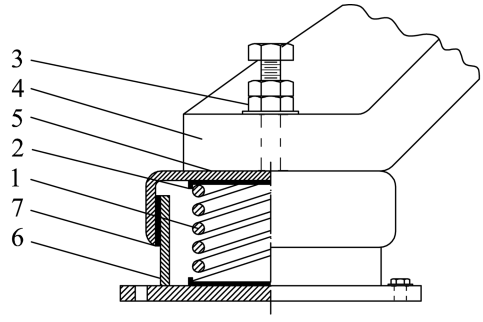

1 - Coil spring, 2 - Adjustable slab, 3 - Regulating bolt,
4 - Frame, 5 - Cover, 6 - Housing, 7 - Insulating pads

Figure 11.C.13 Small one-spring vibration absorber.

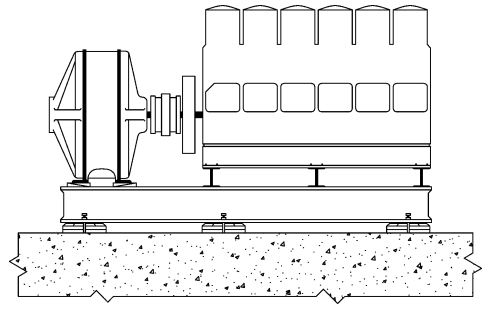

Figure 11.C.14 Supporting spring type of vibro-isolation of a six-cylinder diesel engine with generator on the shaft.

1. Supported system
   Properly designed spring absorbers can be used for machines which are well balanced with small dynamic forces generated in higher harmonics, having light weight including mountings, as shown in Figure 11.C.14. In such an installation, the machine is mounted on a rigid frame of structural steel which in turn is placed directly on the spring absorbers. Also, installation of the type shown in Figure 11.C.15 can be adopted for low frequency

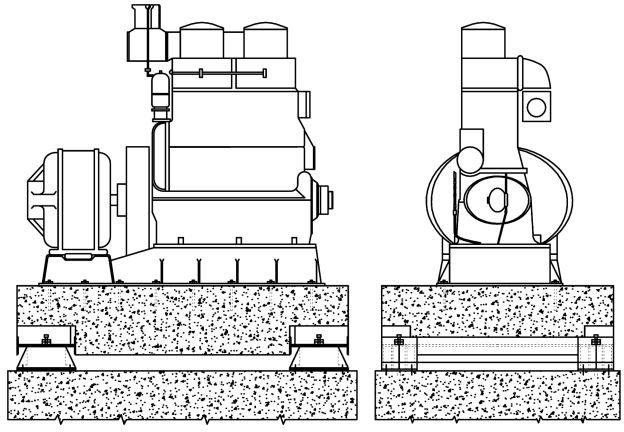

Figure 11.C.15 Vibro-isolation of high-speed two-cylinder diesel engine with generator on the same shaft. System has unbalanced first harmonic of exciting loads.

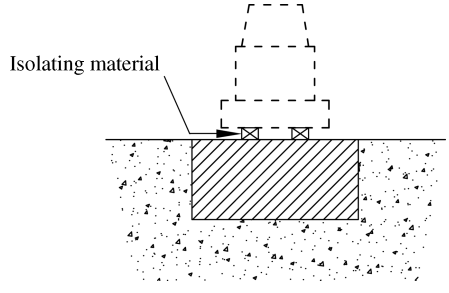

Figure 11.C.16 Supported system.

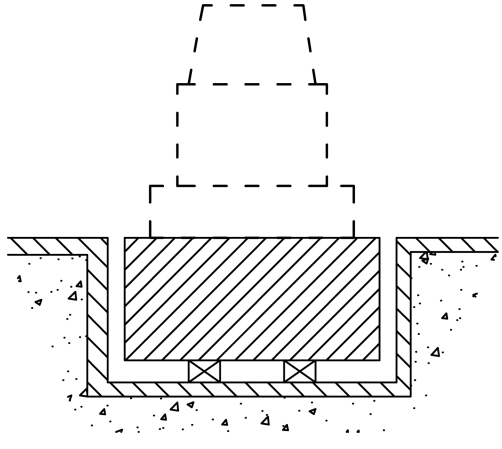

Figure 11.C.17 Supported system with additional concrete block.

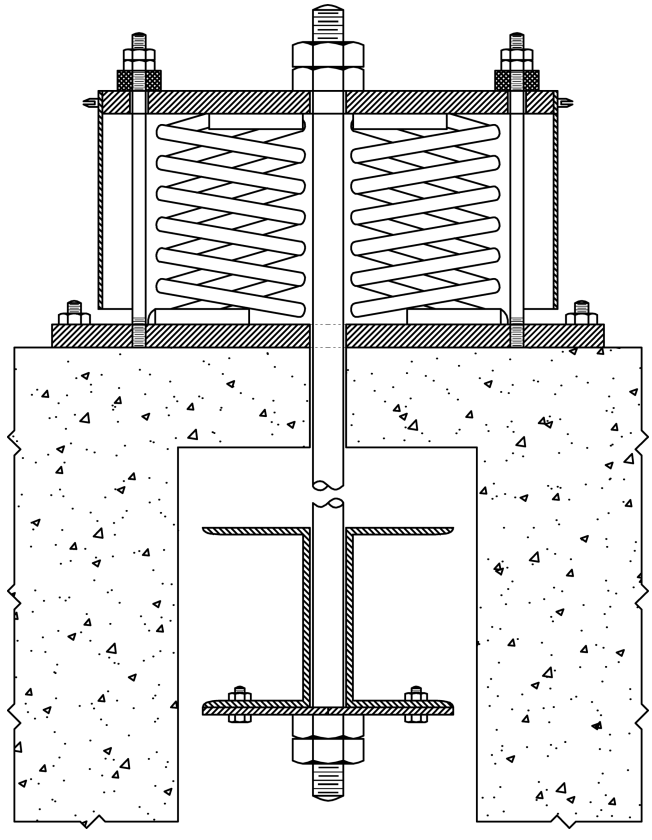

Figure 11.C.18 Suspended type absorber.

machines with large unbalanced forces necessitating an increase in weight coming onto the absorbers. As can be noted in Figure 11.C.15, an additional concrete block is added to the machine mounting which in turn is placed on the absorbers fixed to the base slab. In both the cases the absorbers are directly supporting the machine installations and hence are called supported systems.

Different types of spring absorbers such as the one shown in Figure 11.C.13 are commercially available. Construction details of such systems are given by Barkan (1962) and Kameswara Rao (1998). These absorbers are relatively inexpensive, reliable in operation and effective in decreasing the amplitudes of vibrations. For high capacity machines, absorber units with multiple springs are used.

2. Suspended system

   A schematic diagram of this system is shown in Figure 11.C.18. It differs from the supported type only by the long length of the anchor bolt passing through the absorber. The foundation is connected to the lower ends of the anchor bolts using girders and cantilever projections taken out of the foundation block needed for such a suspended connection. The absorbers are placed on the top edges of the foundation mass below the springs. This mass is designed

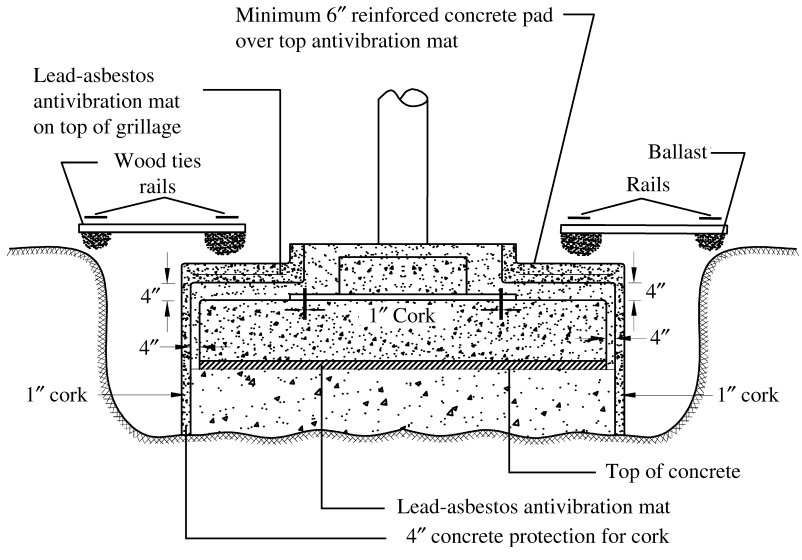

Figure 11.C.19 Passive isolation using lead-asbestos pads.

in the shape of a base in which the mass to be suspended is located. The construction procedure of the suspended type absorbers is similar to the supported type of systems. As already mentioned earlier, suspended systems provide easy access to the spring casings for frequent inspection and maintenance.

11.C.6.2 Passive Isolation Using Lead Asbestos Pads

Lead asbestos pads can be used for passive isolation of heavy column footings as illustrated in Figure 11.C.19. These pads are effective since vibrations get partially dissipated at the interfaces of different materials in contact.

11.C.6.3 Other Vibration-Absorbing Devices

The use of other materials such as cork, felt and so on for vibration absorption have been discussed by Barkan (1962), Richart, Hall and Woods (1970) and Kameswara Rao (1998).

12

Structural Design of Foundations

12.1 Introduction

In previous chapters, we discussed the various aspects that are needed for structural design of foundations. A few of these are reiterated below.

1. **Shape of the foundation:** The shape of the foundation can be square, rectangle, circular, annular, rafts and other shapes as may be decided based on the requirements of the superstructure and economy of construction.
2. **Shallow and deep foundations:** The foundations can be shallow such as the ones mentioned in (1) above or can be taken to deeper soil layers such as piles, wells and so on, depending on the loads, soils and site conditions.
3. **Design soil pressure:** This is the lower value of the allowable bearing capacity (based on failure load) and allowable soil pressure (based on allowable settlement). The net design pressure can be obtained by deducting the weight of soil removed for construction which is usually adopted in design.
4. **Depth of foundation:** A minimum depth of 50 cm below ground level is usually necessary for a foundation (IS: 1080–1962, 1962). The minimum depth of footing below the GL can be calculated by Rankine's formula as follows (Section 4.6.4)

$$h = \frac{p}{\gamma}\left[\frac{1-\sin\phi}{1+\sin\phi}\right]^2 \tag{12.1}$$

where

h = minimum depth of foundation below GL
p = gross bearing pressure from the structure
γ = unit weight of soil
ϕ = angle of internal friction of soil.

12.2 Analysis of Foundations

In the conventional analysis, the foundations are assumed to be rigid and the contact pressure to be planar. In the rational analysis using BEF approach, the foundation is assumed to be flexible

Foundation Design: Theory and Practice N. S. V. Kameswara Rao
 ISBN: 978-0-470-82534-1

and the soil is represented by Winkler model. These aspects have been discussed in detail in Chapters 4–7.

For the analysis and design of foundations the theory of bending is used as for any structural member. All relevant limit states must be considered in design to ensure adequate safety and serviceability.

12.3 Structural Design

The foundations are usually constructed using reinforced cement concrete (RCC). Working stress method (WSM) was commonly used earlier. Now limit state method (LSM) is more in use these days. In the present chapter, LSM is used for the examples. The details about these methods are available in standard text books on RCC (Punmia, Jain and Jain, 1992; Jain, 1997; IS: 456–2000, 2000). The evaluation of design parameters such as bending moments (BM) and shear forces (SF) and punching shear and critical sections where these have to be calculated are available in the above books and codes. However some of these are explained below. Some important factors needed for the design of RC structures are given in Appendix 12.A.

12.3.1 Bending Moment

The critical sections for computing maximum bending moment for design of an isolated concrete footing supporting different types of structures are given below and shown in Figure 12.1.

1. At the face of the column, pedestal or wall for footings supporting a concrete column, pedestal or wall respectively (Figures 12.1(a) and (b)).

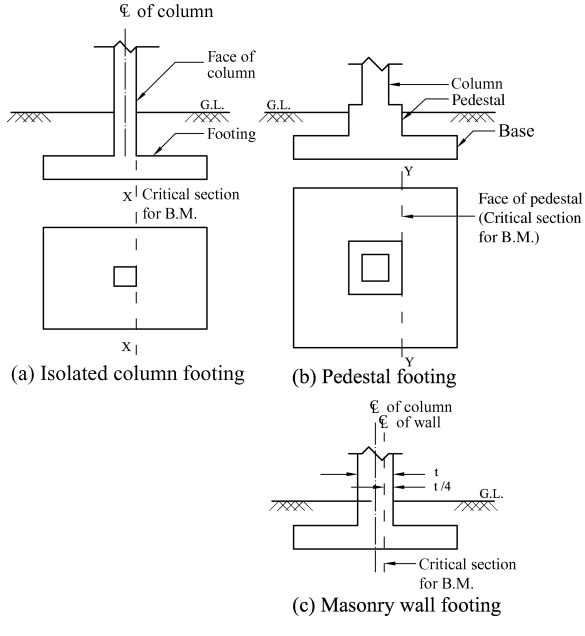

Figure 12.1 Critical sections for bending moment in isolated footings.

2. Midway between the center line and edge of the wall for footings under masonry walls (Figure 12.1(c)).
3. Midway between the face of the column or pedestal and the edge of the gusseted base for footings under gusseted bases.

The formulae for calculating effective depth, reinforcement and so on, are given in Appendix 12.A.

12.3.2 Shear Force

The shear capacity of footings is checked in one-way bending action as well as in two-way bending action in accordance with the codes. When bending is primarily one way, the footings should be checked in vertical shear. When bending is primarily two-way, the footing should be checked in punching shear. A shear failure should not occur prior to reaching the member flexural capacity. The critical sections for shear capacity are as follows:

1. Vertical shear across the full width of the base on a vertical section located from the face of the column, pedestal or wall at a distance equal to:
   a. the effective depth of footing in case of footings on soils and
   b. half the effective depth of the footing for footings on piles.
2. Punching shear around the column on a perimeter 0.5 times the effective depth away from the face of column or pedestal.

These are shown in Figures 12.2 and 12.3. For one-way shear action, the nominal shear stress is calculated as follows

$$\tau_v = \frac{V_u}{L_x d} \tag{12.2}$$

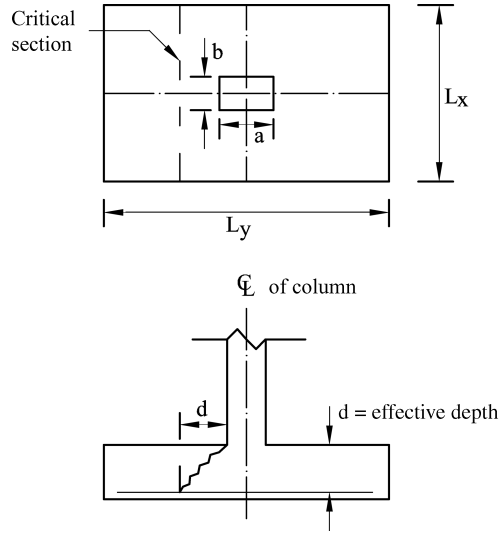

Figure 12.2 Critical section for one-way shear capacity.

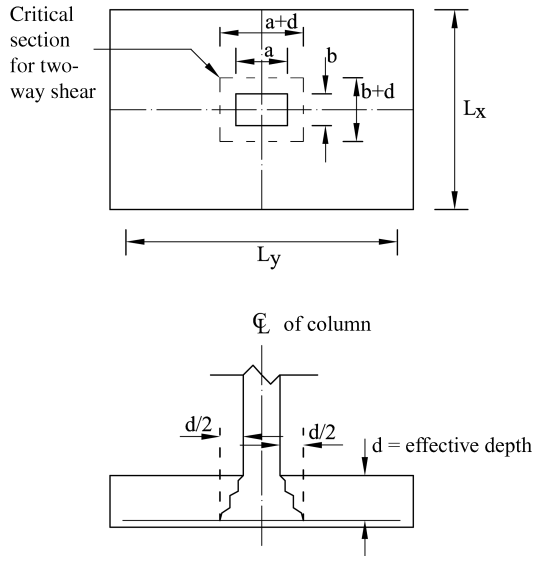

Figure 12.3 Critical section for two-way shear capacity.

where

V_u = factored vertical shear force
L_x = breadth of the critical section
d = effective depth

If shear reinforcement is not provided, the nominal shear stress at the critical section should not exceed $k\tau_c$

where

k = factor for calculating shear strength of concrete
τ_c = shear strength of concrete

The factor k depends on the overall thickness of the slab, D_s and is given in Table 12.1.

In solid slabs or footings, the nominal shear stress, $\tau_v < k\tau_c$. Shear reinforcement may be provided for slabs of depth greater than 200 mm. The development length has to be checked at the same critical sections as for beams. It is important to check deflections in slab design. For this the strip of slab may be checked against span to effective depth ratio (Jain, 1997).

Table 12.1 k values for solid slabs.

D_s (mm)	300 or more	275	250	225	200	175	150 or less
k	1.00	1.05	1.10	1.15	1.20	1.25	1.30

For two-way shear action, the nominal shear stress is calculated in accordance with codes as follows

$$\tau_v = \frac{V_u}{b_o d} \tag{12.3}$$

where b_o = periphery of the critical section

If shear reinforcement is not provided, the nominal shear stress at the critical section should not exceed $k_s\tau_c$
where

$$k_s = 0.5 + \beta_e \quad \text{(should not be greater than 1)} \tag{12.4a}$$

$$\beta_e = \frac{\text{short dimension of column or pedestal}}{\text{long dimension of column or pedestal}} \tag{12.4b}$$

and

$$\tau_c = 0.25\sqrt{\sigma_{ck}}N/mm^2 \tag{12.4c}$$

where σ_{ck} is compression strength of concrete.

It is general practice to make the base deep enough so that shear reinforcement is not required. The thickness of the foundation is usually governed by shear.

12.3.3 Development Length

The critical section for checking the development length in a footing can be assumed at the same planes as those specified for bending moments. In addition, it should also be checked at all other vertical planes where abrupt change of section occurs. In case the reinforcement is curtailed, anchorage requirements must be satisfied as in the case of beams (Jain, 1997).

12.3.4 Deflection and Cracking

There is no need to check deflection in foundations. For checking cracks, the spacing of tension bars should be the same as those for slabs. There is no need to provide side reinforcement in foundation slabs as done in the case of deeper beams.

12.3.5 Transfer of Load at Base of Column

All forces acting at the base of column or pedestal should be transferred into the footing. Tensile forces are transferred through developed reinforcement. Compressive forces are transferred through direct bearing. The permissible bearing stress on full area of concrete is given by

$$\sigma_{br} = 0.45\sigma_{ck} \tag{12.5}$$

where σ_{br} is the bearing stress and σ_{ck} is the compressive strength of concrete.

It may be noted that this stress is the allowable stress in concrete column. Since the footing area is much larger than the column area, the permissible bearing stress in the footing may be increased, thus permitting dispersion of the concentrated load. The permissible bearing stress for concrete in such situations can be specified as

$$\begin{aligned}\sigma_{br} &= 0.45\sigma_{ck}\sqrt{\frac{A_1}{A_2}} \\ &\leq 0.90\sigma_{ck}\end{aligned} \tag{12.6}$$

in which:

A_1 = maximum area of the portion of the supporting surface that is geometrically similar to and concentric with the loaded area.

A_2 = loaded area at the column base.
σ_{ck} = compression strength of concrete.

In sloped or stepped footings, area A_1 may be taken as the area of the lower base contained wholly within the footing and having for its upper base, the area actually loaded and having a side slope of one vertical to two horizontal as shown in Figure 12.4.

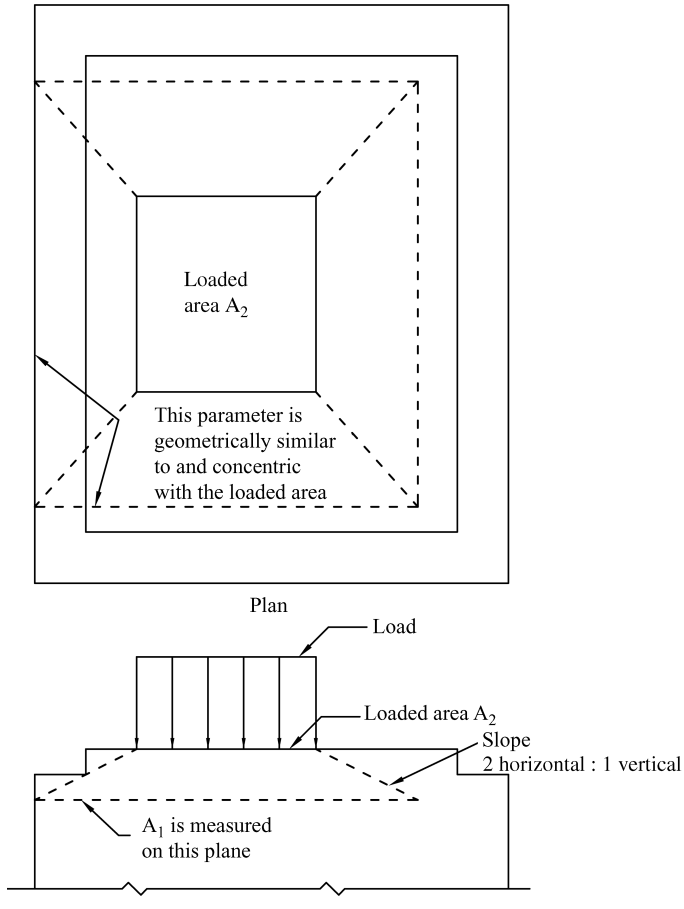

Figure 12.4 Bearing area in a stepped or sloped footing.

If the permissible bearing stress is exceeded either in column or in footing, reinforcement must be provided for developing the excess force. The reinforcement may be provided either by extending the longitudinal bars into the footing or by providing dowels (in accordance with the code) as given below:

1. Minimum area of extended longitudinal bars or dowels must be 0.5% of cross-sectional area of the supported column or pedestal.
2. A minimum of four bars must be provided.

3. If dowels are used, their diameter should not exceed the diameter of the column bars by more than 3 mm.
4. Enough development length should be provided to transfer the compression or tension to the supporting member.
5. Column bars of diameter larger than 36 mm, in compression only can be doweled into the footings with bars of smaller diameters. The dowel must extend into the column a distance equal to the development length of the column bar. At the same time, the dowel must extend vertically into the footing up to a distance equal to the development length of the dowel as shown in Figure 12.5.

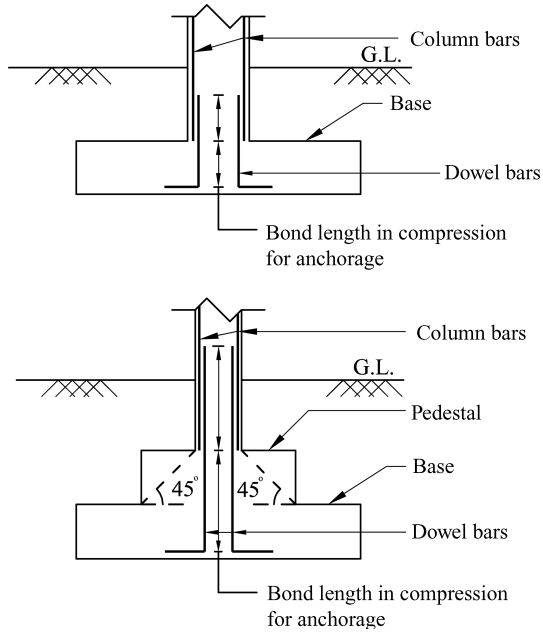

Figure 12.5 Development length of dowel bars.

12.3.6 Tensile Reinforcement

The total tensile reinforcement at any section should be adequate to resist the bending moment at the section caused by the factored forces. The tensile reinforcement should be provided in accordance with the following guidelines:

1. In one-way reinforced footings, the reinforcement must be distributed uniformly across the full width of the footing.
2. In two-way reinforced square footings, the reinforcement extending in each direction must be distributed uniformly across the full width of the footing.

3. In two-way reinforced rectangular footings, the reinforcement in the longer direction should be distributed uniformly across the full width of the footing. The reinforcement in the short direction should be provided by dividing the length in three zones as shown in Figure 12.6.

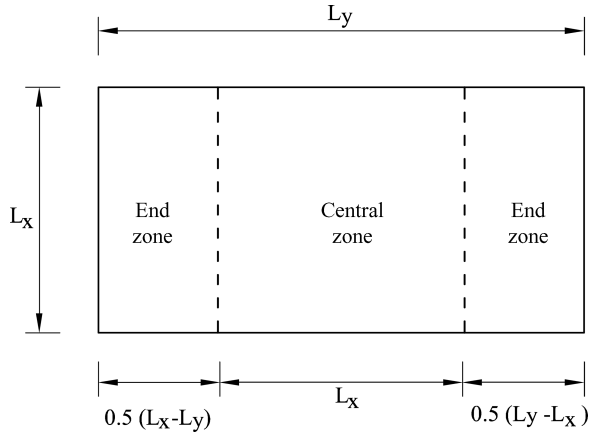

Figure 12.6 Zones for reinforcement in a rectangular footing.

The reinforcement in the central zone should be provided in accordance with the following equation

$$A_{to} = \frac{2A_t}{1 + L_y/L_x} \tag{12.7}$$

where

A_{to} = area of reinforcement in central band
A_t = total area of reinforcement in the shorter direction
L_x = length of the shorter side
L_y = length of the longer side

The reinforcement in each of the end zones should be provided in accordance with the following equation

$$A_{te} = 0.5(A_t - A_{to}) \tag{12.8}$$

where

A_{te} = area of reinforcement in one end band

The reinforcement in each of the three zones must be distributed uniformly.

12.4 Isolated Footings

These are also called spread footings. An isolated footing may be of a square, rectangular or circular shape. It may be axially loaded or eccentrically loaded. The design of square footings

amounts to calculating the size and depth of the footing and amount of main reinforcement and dowels. The bending moments and shear forces are obtained at the critical sections as discussed above. Rectangular footings may be used where space is restricted and it may not be possible to provide a square footing. Rectangular footing is also provided for rectangular columns or pedestals. The design of rectangular footings is identical to that of a square footing except that it has to be designed in both directions separately. Accordingly, bending moment and one way shear action must be considered in both directions. Once the total area required for the footing has been determined, the dimensions of the footing must be selected such that the maximum bending moment on each of the two adjacent projections is equal, that is, the projections on all sides of the column should be equal.

For the design of a circular footing which supports a circular column or pedestal, the expressions applicable for the circular slabs have to be used. These are given in Appendix 12.B. Alternatively, the circular footing is replaced by an equivalent square footing which can be inscribed within its perimeter. Then the design procedure of the footing is similar to that of a square footing.

12.4.1 Eccentrically Loaded Footings

The details regarding the evaluation of contact pressure due to eccentrically loaded footings are given in Section 4.4.5. However, a few important aspects are reiterated below for ready reference.

Columns may transmit axial loads and moments to the footing. In such cases the soil reaction below the footing will not be uniform if the column is placed centrally on the footing as shown in Figure 12.7. The moment M may be replaced by an axial load P acting at an eccentricity $e = M/P$. Hence a column may be placed at an eccentricity e so that the soil pressure becomes uniform as shown in Figure 12.8. Alternatively, the footing should be designed for the actual soil pressure distribution which depends on the amount of eccentricity. There are normally two cases for footings under uniaxial bending:

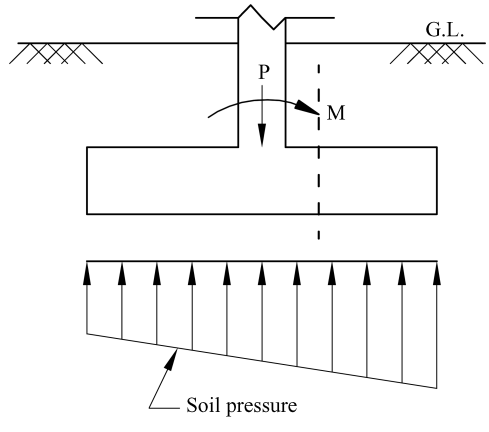

Figure 12.7 Pressure distribution under a centrally placed column subjected to vertical load and moment.

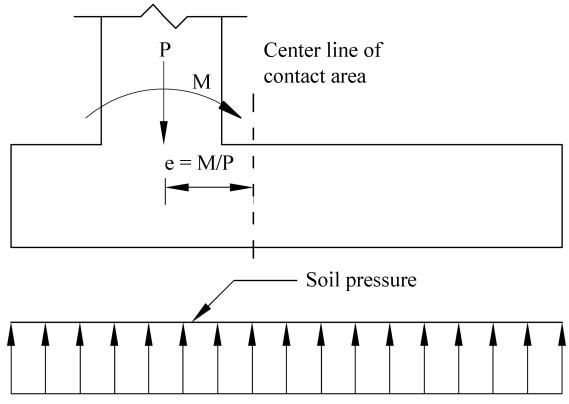

Figure 12.8 Uniform pressure distribution under an eccentrically placed column with $e = M/P$.

Case 1: Load eccentricity not greater than $L/6$ ($M/P < L/6$).
Case 2: Load eccentricity greater than $L/6$ ($M/P > L/6$).

Case 1

A section carrying axial load and bending moment or an eccentric load is subjected to uniform stresses and bending stresses. The footing is considered to be rigid and soil pressure can be computed from principles of mechanics of materials for combined axial and bending stresses assuming a planar distribution. The resultant soil pressure in this case is the algebraic sum of the uniform pressure due to axial load P and varying pressure due to moment about the center of gravity of the section as shown in Figure 12.9.

$$\text{Uniform pressure} = \frac{P}{A} \tag{12.9}$$

$$\text{Varying pressure} = \frac{M}{I}y = \frac{Pey}{I} \tag{12.10}$$

where

P = axial load
M = moment = $P\ e$
e = eccentricity measured from the center line of the footing
A = area of the footing = $L \times B$
I = moment of inertial of the footing
$= \frac{BL^3}{12}$
$y = L/2$
B = width of the footing
L = length of the footing

The resultant soil pressure, q at any section is given by

$$q = \frac{P}{A} \pm \frac{Pey}{I} \tag{12.11}$$

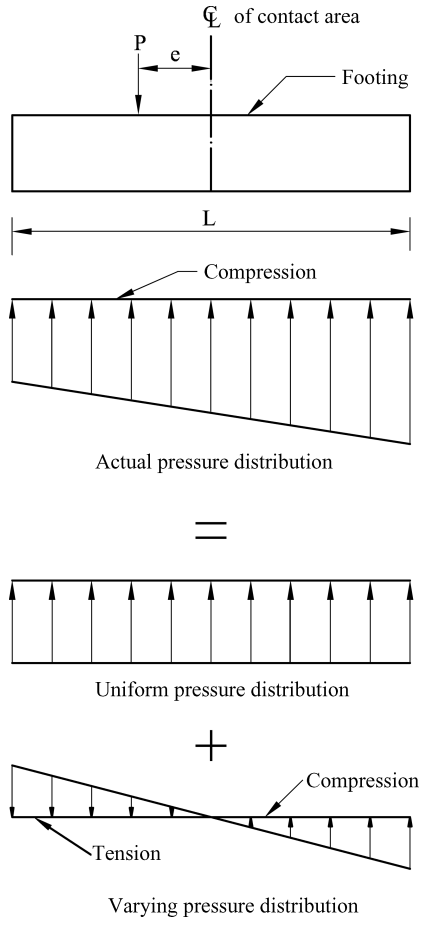

Figure 12.9 Soil pressure distribution below footings due to axial load and moment.

where

+ ve sign indicates compression

−ve sign indicates tension.

It can be shown that if e lies within $\pm L/6$ on either side of the center of footing, the resultant pressure throughout the footing is compressive. If eccentricity exceeds $L/6$, part of the footing looses contact with the ground being in tension.

For footing subjected to moments or eccentricity along both axes, the soil pressure, q at any point is given by the equation

$$q = \frac{P}{A} \pm \frac{M_y}{I_{yy}} x \pm \frac{M_x}{I_{xx}} y \tag{12.12}$$

as long as there is no tension along the contact surface.

where

I_{xx} = moment of inertia of footing about x axis.

I_{yy} = moment of inertia of footing about y axis.

x = distance from y axis to the point.
y = distance from x axis to the point.

Case 2

When eccentricity exceeds $L/6$, cracking of the structure may be allowed on the tension face provided the compressive pressure is within the safe limit and sufficient factor of safety is available against overturning. The maximum compressive pressure may be calculated as follows.

If x is the length of contact as shown in Figure 12.10, its value can be determined by the condition that the load P should lie on its outer third point so that point C may carry zero pressure. Thus

$$AB = \frac{x}{3}$$

or

$$x = 3(0.5L - e) \tag{12.13}$$

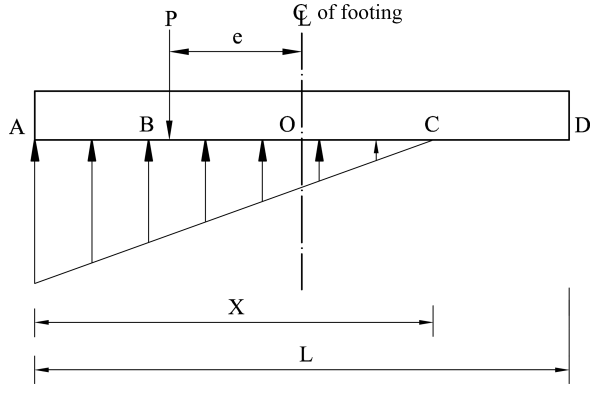

Figure 12.10 Soil pressure distribution with tension on a part of contact surface ($e > L/6$).

The maximum base pressure is now equal to twice the average pressure, that is

$$q_{\max} = \frac{2P}{Bx} = \frac{2P}{3B(0.5L - e)} \tag{12.14}$$

Thus, it is possible to design an isolated footing in plain cement concrete by using either Equations (12.11) and (12.14). The following requirement regarding the depth of such a footing is also specified by some codes.

$$\tan \alpha < 0.9\sqrt{\frac{100q_0}{\sigma_{ck}} + 1} \tag{12.15}$$

where

α = angle between the plane passing through the bottom edge of the footing and the corresponding junction edge of the column with footing and horizontal plane as shown in Figure 12.11

q_0 = calculated maximum bearing pressure at the base of the footing in N/mm^2.

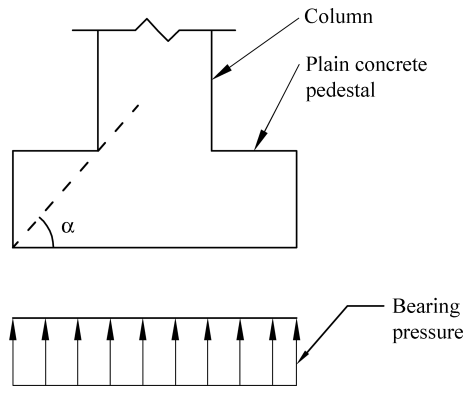

Figure 12.11 Thickness of plain concrete pedestal/footing.

However, in reinforced concrete footings sufficient steel should be provided in the tension zone and the design is done by using Equations (12.11) and (12.12) or Equation (12.14).

12.4.1.1 Unsymmetrical Footings

There are situations where a footing needs to be designed with a hole or notch and is thus unsymmetrical in plan about both the axes. The contact pressure distribution (q) in such footings can be obtained from the principles of mechanics assuming linear stress distribution as follows

$$q = \frac{P}{A} + \frac{M_y I_{xx} - M_x I_{xy}}{I_{xx} I_{yy} - I_{xy}^2}(x) + \frac{M_x I_{yy} - M_y I_{xy}}{I_{xx} I_{yy} - I_{xy}^2}(y) \tag{12.16}$$

in which

M_x = moment about x axis
M_y = moment about y axis
I_{xy} = product of inertia (may be + ve or −ve)
I_{xx}, I_{yy} = moments of inertia of footing about x and y axes respectively.

12.5 Wall Footings

Wall footings carrying direct vertical loads may be designed either in plain concrete or in reinforced concrete. Since a wall footing deflects essentially in one-way, it is analyzed by considering as a strip of unit width along its length. The critical sections for computing maximum bending moments in different types of wall footing are given in Figures 12.1 and 12.2.

12.6 Combined Footings

When two columns are too close and separate footings may overlap, a combined footing may be adopted as shown in Figure 12.12. Further if one column is close to a property line or pipe line,

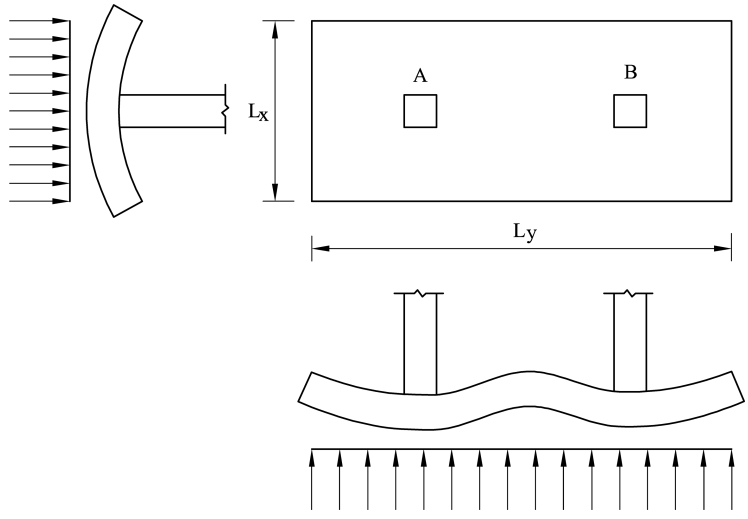

Figure 12.12 Deflections under combined footing in both directions.

the load on an isolated footing will be eccentric. It may be economical to combine this footing with that of adjacent column in such a manner that the center of gravity of the loads from the two columns coincides with the center of gravity of the combined footing. If this is not feasible, moments of forces are taken about the center of base and maximum pressure is determined from the total vertical load and moment as outlined in Section 12.4.1. In such a situation, the footing will deflect in both the directions as shown in Figure 12.12. In the longitudinal direction the cantilever portion and the portion under the columns will develop sagging moments (tension at bottom fibers), the central portion of the footing will develop hogging moment (tension at top). Thus at any section, shear force is the sum of the forces and moment is the moment of all forces on one side of section. The footing may be treated as a beam loaded on its underside and supported on columns. In the transverse direction, the footing develops sagging moments. The moments and shears are found in the same manner as for an isolated footing.

Combined footings may be rectangular or trapezoidal in plan or may consist of isolated footings connected with a narrow beam. Such a footing is called a strap footing with strap beam, connecting both the footings so that they will act in unison (Figure 12.13). Each footing must be checked for one-way shear action and two-way shear action.

12.7 Strap Footings

A strap footing consists of spread footings of two columns connected by a strap beam as shown in Figure 12.13. This type of footing can be adopted when the external column (wall column) is very near to the property line and hence its footing cannot be extended beyond the property line. If a combined trapezoidal footing is provided, the bending moment and shear force in the footing are very high since the footing is continuous under both the columns. In the case of strap footing, the individual footings have very large area under the columns, resulting in decrease in the maximum bending moment and shear force. It is assumed that the strap beam connecting the two spread

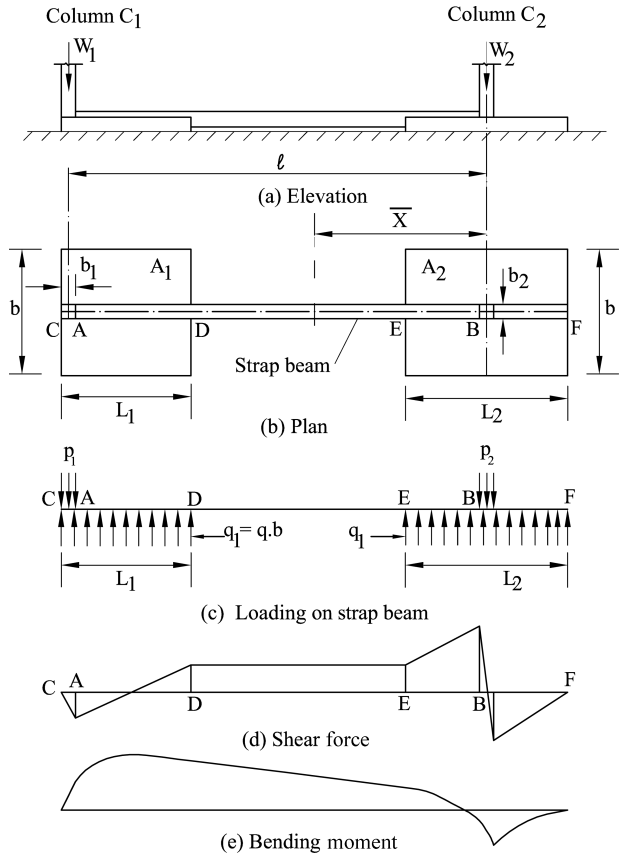

Figure 12.13 Strap footing.

footings does not transfer any load to the soil. The individual footing areas are so arranged that the center of gravity (C.G) of the combined loads of the two columns pass through the combined C.G of the two footing areas. Once this criterion is achieved the pressure distribution below each individual footing will be uniform. The function of the strap beam is to transfer the load of heavily loaded outer column to the inner one. In doing so, the strap beam is subjected to bending moment and shear force and has to be suitably designed to withstand these.

Figure 12.13 shows two columns C_1 and C_2, transmitting axial loads W_1 and W_2 with center to center (c/c) distance of l. Let W' be the total weight of both the individual footings. If A_1 and A_2 are the individual footing areas, and q_0 is the safe bearing capacity of soil, we have

$$A_1 + A_2 = \frac{W_1 + W_2 + W'}{q_0}$$

that is

$$b(L_1 + L_2) = \frac{W_1 + W_2 + W'}{q_0} \tag{12.17}$$

where b is the common width of each footings and L_1 and L_2 are the individual lengths of the footings. Length L_2 is arranged centrally under column C_2.

The C.G of the resultant load $W = W_1 + W_2$ falls at $\bar{X}$ from the center of the column C_2. Hence

$$\bar{X} = \frac{W_1 l}{W_1 + W_2} \tag{12.18}$$

Let $(b_1 \times b_1)$ and $(b_2 \times b_2)$ be the sizes of the columns C_1 and C_2 respectively. Taking moments of the footing areas about center of column C_2, we get

$$\bar{X} = \frac{(b \times L_1)\left(l + \frac{b_1}{2} - \frac{L_1}{2}\right)}{b(L_1 + L_2)} \tag{12.19}$$

From Equations (12.18) and (12.19), we get

$$\frac{L_1\left[\left(l + \frac{b_1}{2} - \frac{L_1}{2}\right)\right]}{L_1 + L_2} = \frac{W_1 l}{W_1 + W_2} \tag{12.20}$$

From Equations (12.19) and (12.20), the unknowns L_1 and L_2 can be obtained in terms of any suitable value of b.

$$\text{Net upward soil pressure, } q = \frac{W_1 + W_2}{b(L_1 + L_2)}$$

Each individual footing is designed as cantilever slab, having sagging bending moment in each of the cantilever portion.

The strap beam transfers a part of load of footing C_1 to footing C_2 in such a way that C.G of two loads coincides with the C.G of the footing areas. In doing so, it is subjected to bending moment and shear forces all along its length, Figure 12.13 shows the loading diagram on the strap beam CDEF.

The upward uniform load, q_1 per unit length, under CD and EF will be equal to $(q \times B)$. The downward load p_2 per unit length is in the portion under column $C_1 = \frac{W_1}{b_1}$ per unit length. Similarly, downward load under column C_2 is $p_2 = \frac{W_2}{b_2}$ per unit length. The bending moment diagram and SF diagram are sketched in Figures 12.13(e) and (d), respectively. For large portion of the strap beam, it will experience hogging bending moment, the maximum being at the section where SF is zero. For the cantilever portion beyond B, it also has a sagging bending moment, its maximum value being at the place where SF is zero. The rest of the design is to be done as per the codes for RCC, such as Eurocode, ACI code and Indian code IS: 456–2000 (2000).

12.8 Raft Foundations

Raft foundations are also called mat foundations. These are combined foundations supporting several columns arranged in one or more rows and columns. These may be necessary in the following situations (Chapters 1 and 8):

1. Soil strength is very poor.
2. Area of individual footings if provided, exceeds half the total area.
3. To minimize excessive differential settlements.

4. The soil is not uniform.
5. In cases when floating foundations are to be designed.
6. To support machine foundations where differential settlements need to be reduced such as in power generators, bar mills, large tanks and so on.
7. When large hydrostatic pressure is encountered at site, a mat foundation is preferable because of its structural strength and the feasibility of making it watertight.
8. To reduce the settlements and differential settlements of structures to be constructed on soils with high compressibility.

Since rafts are constructed at some depth below ground level, a large volume of excavation may be required. If weight of the excavated soil is equal to the weight of structure and that of the raft, and the centers of gravity of excavation and structure coincide, settlement should be negligible. Such foundations are called floating foundations. Where complete compensation is not feasible, a shallower raft may be acceptable if the net increase in loads is small enough to lead to tolerable settlement. A raft foundation may be rectangular or circular or annular as shown in Figures 12.14 and 12.15.

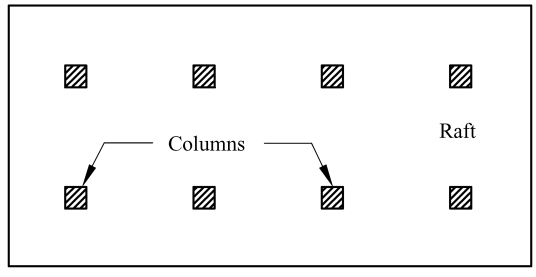

Figure 12.14 Rectangular raft.

If the columns are equally spaced and loads are not very heavy a raft may be designed as having uniform thickness. The conventional design of such a raft consists of establishing its dimensions using loads and design soil pressure. Then, the soil pressure at various points beneath the slab may be computed. The raft is divided into a series of continuous strips centered on the appropriate column rows in both directions as shown in Figure 12.16. The shear and bending moment diagrams may be drawn treating it as a continuous beam. The depth is provided to satisfy bending moment and shear force requirements. The steel requirements will vary from strip to strip. This method generally gives a conservative design since the interaction of adjacent strips is neglected.

If the columns are equally spaced and their loads are equal, the pressure on the soil will be uniform, otherwise, moments of the loads may be taken about the center of the contact area and pressure distribution determined using Equations (12.12) and (12.16). These equations are derived assuming the raft to be rigid. However, since a raft in general is not a rigid member, the pressures and resulting internal stresses may be seriously in error if the eccentricity is very large. The weight of the raft is not considered in the structural design because it is assumed to be carried directly by subsoil.

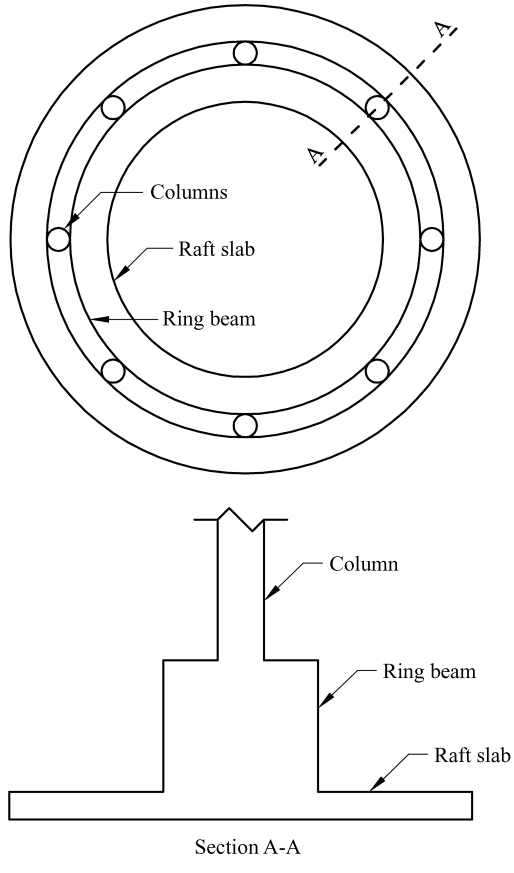

Figure 12.15 Circular raft.

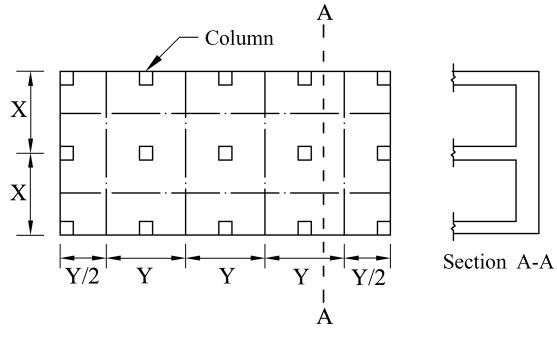

Figure 12.16 Raft foundation with strips centered on columns.

Rafts may be ribbed where the column spacing is irregular or for economy by reducing slab thickness over most of the area as shown in Figure 12.17.

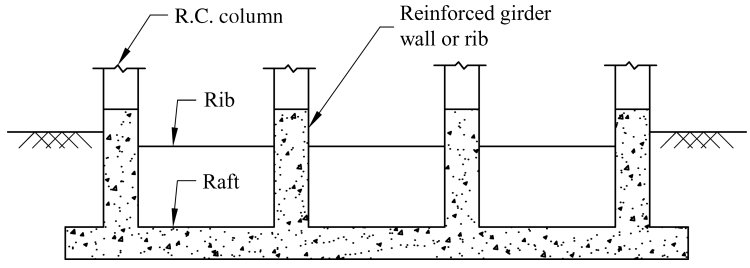

Figure 12.17 Raft foundation with wall as stiffener.

Alternatively, rafts may also be made thicker at the column for economy and depth should be made sufficient to resist shear. A ribbed raft consists of a slab acted upon by upward soil pressure and supported by beams and columns at its top which balance the upward pressure with downward column loads. It is similar to a floor slab resting on a system of beams and columns. The portion between beams is designed as a conventional one way or two way slab. If the beams are deep, they should be designed as deep beams.

If the mat rests on a soft soil, an eccentricity of loading may cause large differential settlement at extreme corners. In such cases, a computation of settlement should be made for the corners. The vertical pressure in any soil stratum under each corner of the mat may be determined by means of Newmark's influence chart (Teng, 1964; Bowles, 1966). Since a mat occupies the entire area of the building, it may not be feasible to proportion the mat so that the centroid of the mat coincides with, or is close to, the line of action of the resultant force.

12.8.1 Conventional Design of Rafts

The mat is analyzed as a whole in each of two perpendicular directions. The total shear force acting on any section of the mat is equal to the sum of all forces and reactions (due to bearing pressure) to the left or right of the section. The total bending moment acting on such section is equal to the sum of all moments to the left, or right, of this section, as per the classical bending theory of beams.

Although the total shear forces and moments can be determined by the principles of simple structures, the stress distribution along this section is a problem of highly indeterminate nature. If the column loads and spacing are almost equal, an approximate idea as to how the moment and shear are distributed along each section may be arrived at. In most cases, however, the variation of moment and shear is often far different from the average value. This point can be illustrated by a simple example shown in Figure 12.18. The total bending moment on section *a-a* is equal to the difference between the positive moment (tension on the bottom of the slab) due to the soil reaction and the negative moment due to the column load. Let us say the net total moment is positive. Then the average bending moment on section *a-a* is equal to this net moment divided by the length of section *a-a*. But it is obvious in this case that the strip *b* is subjected to a positive moment and the strip *c* is subjected to a negative moment. Thus, the

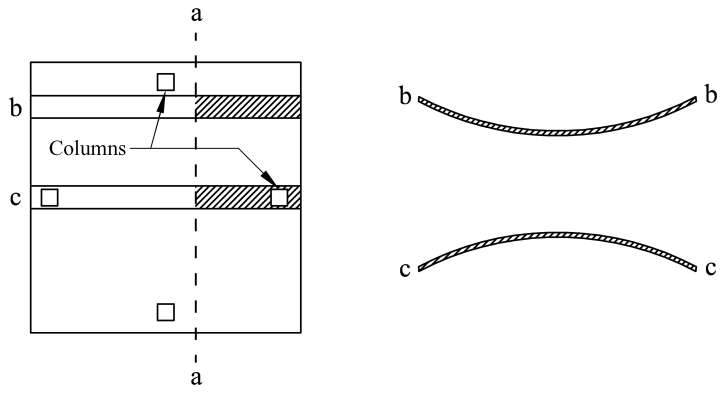

Figure 12.18 Example illustrating variation of bending moment in raft foundation.

average moment is not indicative of the sign and the magnitude of the bending moments in the individual strips.

In order to obtain some idea of the upper limit of stresses, each strip bounded by center lines of column bays may be analyzed as independent, continuous, or combined footings.

Full column loads are used and the soil reaction under each strip is determined without reference to the planar distribution determined with the mat as a whole. This method undoubtedly gives very high stresses because it ignores the two way action of the mat. Therefore certain arbitrary reductions in stresses (e.g., 15.0, 25.0, or sometimes >33.33%) are used.

In the design by conventional method, the column loads, wall loads and allowable bearing pressure are already known. The centroid of all column loads and wall loads $\sum P, \bar{x}$ and $\bar{y}$ are first determined. Then a trial size for the mat is assumed.

The eccentricity of the centroid of all loads from the columns and walls with reference to the C.G of the mat or raft can now be obtained as e_x and e_y along the x and y directions. Then, the soil pressure under the mat is determined by the general equation (Equation (12.12))

$$q = \frac{\sum P}{BL}\left(1 \pm 6\frac{e_x}{L} \pm 6\frac{e_y}{B}\right) \tag{12.21}$$

where

$\sum P$ = sum of vertical loads from all columns and walls.
L = length of the mat (along the x direction)
B = width of the mat (along the y direction)
e_x, e_y = eccentricities of the C.G of loads with respect to the C.G of the contact area of the mat along the x and y directions.

With the soil pressure determined, the mat is analyzed as individual bands along column center lines. In this analysis, a moment coefficient of 1/10 is used.

12.9 Circular and Annular Footings

Circular and annular shaped footings and mats are used as foundations for circular water tanks, transmission towers and so on. The design of such foundations is similar to the design of circular or annular slabs (Punmia, Jain and Jain, 1992; Jain, 1997; IS: 11089–1984, 1984).

The theory is presented in Chapter 5 for circular plates on elastic foundations. The expressions for axially symmetric circular and annular slabs are given in Appendix 12.B for ready reference. The same can be applied to design circular and annular foundations subjected to symmetric loads with an appropriate sign for the load as the soil reaction is vertically upwards while the loads on circular slabs are taken in the expressions (Appendix 12.B) as vertically downwards. The rest of the design details are similar to those of slabs.

12.10 Construction Guidelines for Footings

Footings are very simple to construct. The few steps to be pursued are:

1. The adequacy of subsoil conditions
2. The relative depth of footings
3. The dewatering of the excavation when necessary.

The construction of footings for buildings is usually started after the ground is leveled at surface or at 15 cm below the bottom of the lowest floor slab. Then the area is excavated. The bottom of the excavation is taken up to the required depth. The form work for the sides of footing is placed and held by stakes, and reinforcement is placed on cement block supports (and high chairs if top bars are used). Before placing the concrete, anchor bolts or column dowels have to be accurately secured on the form work. Short and straight dowels of small diameter may be placed by hand immediately after the concrete is poured. The form work for the sides may not be necessary and the concrete may be poured against the vertical sides of the excavation if the soil does not cave in.

12.10.1 Relative Depth of Footings

Adjacent footings should not be constructed at such different levels that the construction of the lower footing would disturb the soil supporting the upper footing. Also the pressure from the upper footing should not introduce large additional stress to the soil under the lower footing. This difficulty is generally avoided by keeping the difference in footing elevations not greater than one-half the clear distance between the footings. For this reason it is always a good practice to construct the lower footings first. If it is necessary to construct a lower footing at a greater depth than contemplated, the elevation of the upper footing can be adjusted accordingly (Section 4.4.1).

If adjacent footings must be constructed at largely different levels, for example, when a new basement is constructed adjacent to footings under an existing first floor, sheet pile walls/ retaining walls may be used to retain the adjacent ground when excavation is made.

12.10.2 Dewatering

The excavation should be kept dry during the construction period. In clayey soils, water tends to soften the upper portion of the soil and causes settlement of footings. The soil conditions under water cannot be readily inspected. Excavation in water is expensive and not satisfactory. Furthermore, the quality of concrete placed in water may not be up to the mark, particularly when the water is flowing.

12.11 Construction of Raft Foundations

Rafts/mats are usually constructed of RCC. Concrete is poured in small quantities to avoid excessive shrinkage cracks.

Construction joints should be carefully located at sections of low shear stress. The common practice is to locate them along the center lines between columns. A lapse of at least 24 hours is desired between concreting of adjacent areas. Reinforcing bars should be placed to run across the joints. The concrete should be strong enough to transfer the shear stress across the joint. This is commonly done by providing a shear key along the joint. The shear key, usually occupies the middle third of the thickness of the raft and should be designed for the maximum shear stress. The mat may be thickened to strengthen the joints if necessary.

12.12 Examples of Structural Design

Examples of structural design of footings and rafts discussed in this chapter are presented in Appendix 12.C for illustration. It may however be noted that the designs have to follow the standard codes specified by the local regulatory agencies.

Exercise Problems

All the problems assignments are based on Sections 12.4–12.8. Take the load factor as 1.5 unless specified.

12.1 Design a footing for a 40 cm square column carrying a load of 1050 kN and reinforced with 10–20 mm Fe 415 grade bars. One side of the footing is restricted to 1.6 m. The gross bearing capacity of the soil is 150 kN/m^2. Use M25 concrete for column and footing.

12.2 Design a stepped footing for a 50 cm square column carrying a load of 1500 kN and reinforced with eight 25 mm Fe 415 grade bars. The gross bearing capacity of the soil is 120 kN/m^2. Use M25 concrete for both column and footing.

12.3 Design a footing of a brick wall 30 cm thick which is transmitting a load of 180 kN/m per unit length. The gross bearing capacity of the soil is 100 kN/m^2. Use M20 concrete and Fe 250 steel bars.

12.4 Design a footing for a rectangular column 30 × 40 cm carrying an axial service load of 1200 kN. The net bearing capacity of the soil is 130 kN/m^2. Use M30 concrete and Fe 250 grade steel.

12.5 Design a combined footing for two columns A and B carrying axial loads of 1000 kN and 800 kN respectively. Both columns are 40 cm in diameter and spaced 4 m c/c. Columns are reinforced with 20 mm bars and consist of M25 concrete. The bearing capacity of the soil is 120 kN/m^2. Use M20 mix and Fe 415 grade steel for the footing.

12.6 Design a strap footing for the columns given in problem 12.5 if the edge of column A is on the property line.

12.7 A building contains 12 columns 40 × 40 cm in three rows of four each. The distance between the columns is 4 m. Each of the four corner columns carry a load of 600 kN, each of the exterior columns carry a load of 900 kN and each of the interior columns carry a load of 1500 kN. The net bearing capacity of the soil is 100 kN/m^2. Design a raft foundation using M30 concrete and Fe 415 grade steel.

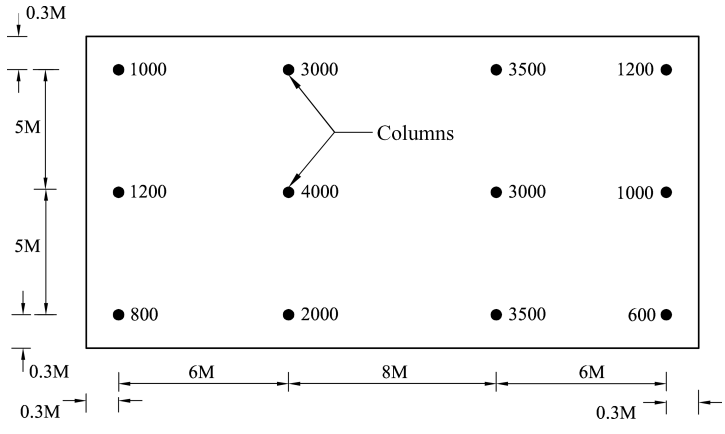

Figure 12.19 Plan layout and factored column loads.

12.8 Design a raft foundation for the layout as shown in Figure 12.19. Net bearing capacity of the soil is 60 kN/m^2, diameter of exterior columns is 50 cm and that of interior columns is 60 cm. Assume load factor = 2.

Appendix 12.A Details of RC Design

12.A.1 Introduction

As discussed in the Chapters 4–11 of this book, the analysis of foundations can be carried out using either conventional approaches (assuming the foundation to be rigid and soil reaction/contact pressure to be planar) or rational approaches such as flexible/elastic foundation approaches. Usually soil is represented as Winkler's spring model (or by two parameter models such as Vlasov, Pasternak). Both these approaches have been presented in detail in Chapters 4–11. Once the design parameters such as bending moment (BM) and shear force (SF) are known either from conventional or rational/elastic foundation approach, the rest of the design procedure is the same which uses principles of RC design (Punmia, Jain and Jain, 1992; Jain, 1997; ACI 318, UBC, Eurocode 2, IS: 456–2000). A few of these details which can be readily used for foundations are summarized in the following sections, while further details can be referred from any other standard books and codes. The following details are based on Indian standard code of practice IS: 456–2000 (2000) for plain and reinforced concrete and limit state design method. Some variations in these details in other codes (such as ACI 318, UBC, Eurocode 2) are given in Appendix 12.D for information. The parameters used in the following sections for RCC beams are shown in Figure 12.A.1 (σ_{ck} is the 28 days characteristic strength of concrete in N/mm^2 and σ_y is the yield stress of steel in N/mm^2).

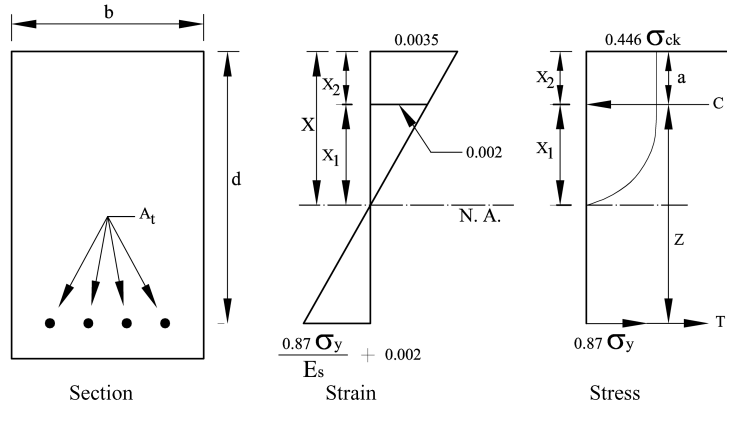

Figure 12.A.1 RC beams – parameters.

12.A.2 Factored Loads

A factored load is obtained by multiplying a characteristic load by an appropriate partial safety factor. This factored load is used to calculate factored bending moment, and shear force, thrust and so on. Alternatively, bending moment, shear force and thrust can be calculated based on the characteristic load values and then factored values can be obtained by multiplying them by an appropriate partial safety factor as given in Tables 12.A.1 and 12.A.2. The stresses in steel bars are given in Tables 12.A.3 and 12.A.4.

Table 12.A.1 Partial safety factors for loads under limit state of failure.

Load combination	DL	LL	WL
DL + LL	1.5	1.5	—
DL + WL	1.5	1.5	—
DL + WL[a]	0.9	—	1.5
DL + LL + WL	1.2	1.2	1.2

[a]This value should be considered when stability against overturning or stress reversal is critical.
DL = dead load, LL = live load, WL = wind or earthquake load.

Table 12.A.2 Partial safety factors for loads under limit state of serviceability.

Load combination	DL	LL	WL
DL + LL	1.0	1.0	—
DL + WL	1.0	—	1.0
DL + LL + WL	1.0	0.8	0.8

Table 12.A.3 Mechanical properties of structural steel marketed by the Steel Authority of India – micro alloy (SAIL-MA).

Grade	Yield stress, σ_y N/mm^2 (min)	Tensile strength N/mm^2 (min)	% elongation (min)
SAIL-MA: 300 HY	300	440–560	20
SAIL-MA: 350 HY	350	490–610	20
SAIL-MA: 410 HY	410	540–660	19
SAIL-MA: 450 HY	450	570–720	18

12.A.3 Yield Stress

The types of steels to be used in limit state design in reinforced concrete and their characteristic strengths are give in Table 12.A.4.

Table 12.A.4 Yield stress of different steels.

Type of steel	Indian standard	Yield stress or 0.2% proof stress (N/mm^2)
Mild steel	IS: 432 (part 1)	260 for bars up to 20 mm
	IS: 1139	240 for bars over 20 mm
Medium tensile steel	IS: 432 (part 1)	360 for bars up to 20 mm
	IS: 1139	345 for bars between 20–40 mm
		330 for bars over 40 mm
High yield strength steel	IS: 1139	425 for bars of all sizes
	IS: 1786	415 for bars of all sizes
		500 for bars of all sizes
SAIL-MA	IS: 8500	Given in Table 12.A.3

12.A.4 Maximum Depth of Neutral Axis

A compression failure is a brittle failure. The maximum depth of neutral axis (NA) is limited to ensure that tensile steel will reach its yield stress, σ_y, before concrete fails in compression, thus a brittle failure is avoided. The limiting values of the depth of neutral axis x_m for different grades of steel are given in Table 12.A.5.

Table 12.A.5 Maximum depth of neutral axis (NA).

σ_y (N/mm^2)	x_m
250	$0.53d$
415	$0.48d$
500	$0.46d$

12.A.5 Limiting Values of Tension Steel and Moment of Resistance

The maximum value of the moment of resistance is limited since the maximum depth of neutral axis is limited. Its value for singly reinforced rectangular section is given below while for other types of structural members, it can be referred to books on RCC.

$$M_{\text{lim}} \text{ with respect to concrete} = 0.36\sigma_{ck} b.z = 0.36\sigma_{ck} b x_m (d - 0.42x_m) \quad (12.A.1)$$

$$M_{\text{lim}} \text{with respect to steel} = 0.87\sigma_y A_t (d - 0.42x_m) \quad (12.A.2)$$

For a beam of rectangular cross-section, the limiting value of M_{lim} depends on the grade of concrete mix and the steel. The values of limiting moment of resistance M_{lim} with respect to concrete for a few grades of concrete and steel are given in Table 12.A.6

Table 12.A.6 Limiting moment of resistance values (Nmm).

Grade of concrete	Fe 250 steel	Fe 415 steel	Fe 500 steel
General	$0.148\ \sigma_{ck} bd^2$	$0.138\ \sigma_{ck} bd^2$	$0.133\ \sigma_{ck} bd^2$
M15	$2.22\ bd^2$	$2.07\ bd^2$	$2\ bd^2$
M20	$2.96\ bd^2$	$2.76\ bd^2$	$2.66\ bd^2$
M25	$3.70\ bd^2$	$3.45\ bd^2$	$3.33\ bd^2$

The percentages of tensile reinforcement corresponding to the limiting moment of resistance are obtained by equating the forces of tension and compression and are given in Table 12.A.7.

Table 12.A.7 Limiting tensile steel in rectangular sections.

Grade of concrete σ_{ck} N/mm^2	Percentage of tensile steel		
	250 N/mm^2	415 N/mm^2	500 N/mm^2
15	1.32	0.72	0.57
20	1.76	0.96	0.76
25	2.20	1.19	0.94
30	2.64	1.43	1.13

12.A.6 Maximum and Minimum Tension Reinforcement

Codes specify that the minimum area of tension reinforcement A_0 should not be less than the following

$$\frac{A_0}{bd} = \frac{0.85}{\sigma_y} \tag{12.A.3}$$

where σ_y = characteristic strength of steel in N/mm^2.

Also the maximum area of tension reinforcement should not exceed 4% of the gross cross-sectional area to avoid difficulty in placing and compacting concrete properly in the formwork.

12.A.7 Moment of Resistance

The values of moment of resistance for under reinforced, balaced and over reinforced concrete sections are summarized below (parameters are shown in Figure 12.A.1).

1. For an under-reinforced section, the value of x is less than x_m value. The moment of resistance is calculated by the following equations:

$$x = \frac{0.87\sigma_y A_t}{0.36\sigma_{ck} b} \tag{12.A.4}$$

$$z = \left(d - \frac{\sigma_y A_t}{\sigma_{ck} b}\right) \tag{12.A.5}$$

$$M_u = 0.87\sigma_y A_t z$$

that is

$$M_u = 0.87\sigma_y A_t \left(d - \frac{\sigma_y A_t}{\sigma_{ck} b}\right) \tag{12.A.6}$$

2. For a balanced section, the moment of resistance is calculated by the following equations:

$$x = x_m \tag{12.A.7}$$

$$x = d - 0.42x_m \tag{12.A.8}$$

$$M_u = 0.36\sigma_{ck} b x_m (d - 0.42x_m) \tag{12.A.9}$$

that is

$$M_u = 0.87\sigma_y A_t (d - 0.42x_m) \tag{12.A.10}$$

The value of x_m is obtained from Table 12.A.5.

3. For an over-reinforced section, the value of x is limited to x_m and the moment of resistance is computed based on concrete behavior, as follows

$$x = x_m \tag{12.A.11}$$

$$z = d - 0.42x_m \tag{12.A.12}$$

$$M_u = 0.36\sigma_{ck} b x_m (d - 0.42x_m) \tag{12.A.13}$$

12.A.8 Design Tables

It is possible to generate design curves and design tables for singly reinforced beams by making use of Equation (12.A.6), that is

$$\frac{M_u}{bd^2} = \frac{0.87\sigma_y A_t}{bd^2}\left(d - \frac{\sigma_y A_t}{\sigma_{ck} b}\right) \tag{12.A.14}$$

If p is the percentage of steel, then

$$A_t = pbd \text{ and } \frac{M_u}{bd^2} = m.$$

Therefore, $m = 0.87\sigma_y p(1 - p\sigma_y/\sigma_{ck})$
that is

$$0.87\frac{\sigma_y^2}{\sigma_{ck}}p^2 - 0.87\sigma_y p + m = 0 \tag{12.A.15}$$

For a given concrete mix and type of steel, it is possible to obtain a relation between p and m. For example, Table 12.A.8 gives percentage values of p for a given value of $\frac{M_u}{bd^2}$ for M15 mix and Fe 415 grade steel.

Table 12.A.8 Reinforcement (%) in singly reinforced beams ($\sigma_{ck} = 15$ MPa and $\sigma_y = 415$ MPa).

$\frac{M_u}{bd^2}$ N/mm^2	p%	$\frac{M_u}{bd^2}$ N/mm^2	p%
0.30	0.085	1.30	0.406
0.50	0.144	1.40	0.442
0.60	0.175	1.45	0.462
0.80	0.237	1.55	0.500
0.90	0.270	1.65	0.538
0.95	0.286	1.70	0.558
1.00	0.302	1.75	0.578
1.10	0.336	1.85	0.619
1.20	0.370	1.95	0.662
1.25	0.390	2.00	0.682

Intermediate values can be obtained by interpolation or from Equation (12.A.15).

12.A.9 Shear Reinforcement

To prevent the possibility of concrete being crushed in the web of a member, the maximum shear stress values are limited as shown in Table 12.A.9. The shear strength of concrete τ_c based on the percentage of longitudinal tensile reinforcement is shown in Table 12.A.10. The values

Table 12.A.9 Maximum shear stress in concrete section.

Concrete grade	M15	M20	M25	M30	M35	M40
$\tau_c N/mm^2$	2.5	2.8	3.1	3.5	3.7	4.0

Table 12.A.10 Design shear strength of concrete.

$\frac{100A_s}{bd}$	τ_c (N/mm^2)					
	M15	M20	M25	M30	M35	M40
0.25	0.35	0.36	0.36	0.37	0.37	0.38
0.50	0.46	0.48	0.49	0.50	0.50	0.51
0.75	0.54	0.56	0.57	0.59	0.59	0.60
1.00	0.60	0.62	0.64	0.66	0.67	0.68
1.25	0.64	0.67	0.70	0.71	0.73	0.74
1.50	0.68	0.72	0.74	0.76	0.78	0.79
1.75	0.71	0.75	0.78	0.80	0.82	0.84
2.00	0.71	0.79	0.82	0.84	0.86	0.88
2.25	0.71	0.81	0.85	0.88	0.90	0.92
2.50	0.71	0.82	0.88	0.91	0.93	0.95

Note: the term A_s is the area of longitudinal tension reinforcement which continues at least one effective depth beyond the section being considered except at supports where the full area of tension reinforcement may be used provided the detailing conforms to the specifications.

given in the table are based on the following equation

$$\tau_c = \frac{0.85}{6\beta}\sqrt{0.80\sigma_{ck}}\left(\sqrt{(1+5\beta)}-1\right) \tag{12.A.16}$$

where

$$\beta = \frac{0.8\sigma_{ck}}{6.89p_t} \lhd 1 \tag{12.A.17}$$

$$p_t = \frac{100A_t}{b_w d} \tag{12.A.18}$$

Thus when shear reinforcement is necessary, the shear strength of the beam is calculated on the following basis:

Total shear strength = shear resistance of effective concrete area as a function of longitudinal main steel bars.
+ shear resistance of vertical shear stirrups
+ shear resistance of inclined shear stirrups.

It may be noted that inclined bars alone do not provide a satisfactory solution and their contribution is limited to 50% of the net shear obtained after deducting the shear due to concrete. The balance shear resistance has to be provided by vertical stirrups. The inclined bars at an angle of 45° are considered very effective, though the angle of inclination can vary from 30° to 60°.

12.A.10 Bond and Development Length

The bond stress, τ_{bd} for mild steel bars in various grades of concrete are given in Table 12.A.11.

The code specifies that these τ_{bd} values may be increased by 60% for deformed steel bars in tension. These values may be further increased by 25% for bars in compression. In case of

Table 12.A.11 Design bond stress, τ_{bd} for mild steel bars.

Concrete	M15	M20	M25	M30	M35	M40
τ_{bd} N/mm^2	1.0	1.2	1.4	1.5	1.7	1.9

bundled bars in contact, the development length is given by that for the individual bar when increased by:

1. 10% for two bars in contact
2. 20% for three bars in contact
3. 33% for four bars in contact.

The reduction in development length of bundled bars with increase in number of bars is due to the reduced contact area between steel and concrete.

Development lengths for steel bars of different grades and different concretes are given in Table 12.A.12.

Table 12.A.12 Development lengths for single bars (ϕ is the diameter of the bar).

σ_y N/mm^2	Tension bars		Compression bars	
	M15	M20	M15	M20
250	55ϕ	46ϕ	44ϕ	37ϕ
415	56ϕ	47ϕ	45ϕ	38ϕ
500	69ϕ	58ϕ	54ϕ	46ϕ

12.A.10.1 Flexural Bond

At certain locations in a beam, high bond stress may arise due to large variation of bending moment over a short distance, that is, high shear force. These bond stresses are called flexural bond stresses and must be checked at the face of a simple support and at the points of inflection within continuous spans. At these locations, tensile capacity to be developed is usually small but the rate of change of tensile stress in the bars is high.

12.A.11 Clear Cover for Reinforcement

A reinforcing bar must be surrounded by concrete for two principal reasons:

1. To develop the desired strength of a bar by ensuring proper bond between concrete and steel throughout its perimeter.
2. To provide protection against corrosion and fire.

The clear cover to reinforcement which is nearest to the face of a member should be as follows:

1. At each end of the reinforcing bar not less than 25 mm, nor less than twice the diameter of such bar.
2. For a longitudinal bar in a beam not less than 25 mm, nor less than the diameter of such bar.

3. For tensile, compressive, shear or other reinforcement in a slab, not less than 15 mm, nor less than the diameter of such bar.
4. For a longitudinal reinforcing bar in a column, not less than 40 mm, nor less than the diameter of such bar. Such a large cover is required so as to prevent buckling of the main longitudinal bars under compression.
5. In the case of columns of minimum dimensions of 200 mm or below, whose reinforcing bars do not exceed 12 mm, a cover of 25 mm may be used.
6. For any other reinforcement, not less than 15 mm, nor less than the diameter of such bar.

12.A.12 Spacing of Reinforcement

The diameter of a round bar is referred to as its nominal diameter. In case of non circular bars or deformed bars, the diameter is taken as the diameter of a circle giving an equivalent effective area. Where minimum concrete cover and spacing limitations are based on diameter of a bar, a group of bars bundled in contact, must be treated as a single bar of diameter derived from the total equivalent area.

Maximum distance between bars:

1. The clear horizontal distance between two parallel main reinforcing bars should not be less than the greatest of the following:
   a. the diameter of the bar if the diameters are equal
   b. the diameter of the larger bar if the diameters are unequal
   c. 5 mm more than the nominal maximum size of coarse aggregate.
2. If needle vibrators are used, the horizontal distance between bars of a group may be reduced to two-thirds the nominal maximum size of the coarse aggregate provided that sufficient space is left between groups of bars to permit the vibrator to be operated.
3. The clear vertical distance between two parallel main reinforcing bars should not be less than the greatest of the following:
   a. 15 mm
   b. the diameter of the larger bar if the diameters are unequal
   c. two-thirds the nominal maximum size of the coarse aggregate.

Maximum distance between bars in tension:

In tension, the maximum distance between bars is restricted to control cracking of concrete which depends on the stress in the reinforcing bars and the distance between bars. In normal environments, the crack widths should not exceed 0.3 mm. This value decreases for aggressive environments.

Beams:

The maximum clear horizontal distance between parallel reinforcement bars or groups, near the tension face of a beam should not exceed the values given in Table 12.A.13. These values depend on the amount of redistribution of moment carried out in the analysis and the characteristic strength of the reinforcement.

Table 12.A.13 Maximum clear distance between reinforcement bars.

σ_y N/mm^2	% redistribution to or from section considered				
	−30	−15	0	15	30
250	215	260	300	300	300
415	125	155	180	210	235
500	105	130	150	175	195

Reinforcement in slabs:

1. The horizontal distance between parallel main reinforcement bars should not be more than three times the effective depth of a solid slab or 450 mm whichever is smaller.
2. The horizontal distance between parallel reinforcement bars provided against shrinkage and temperature should not be more than five times the effective depth of a solid slab or 450 mm whichever is smaller.

Tolerance on placing reinforcement:

The code specifies the following tolerances on placing reinforcement in concrete members:

1. for an effective depth of 200 mm or less: tolerance of $\pm$ 10 mm
2. for an effective depth more than 200 mm: tolerance of $\pm$ 15 mm.

The clear cover should not be reduced by more than one-third of the specified cover or 5 mm whichever is less.

12.A.13 Reinforcement Requirements in Beams and Slabs

Beams:

a. **Minimum tension reinforcement:** The minimum area of tension reinforcement should not be less than that given by Equation (12.A.3).
b. **Maximum reinforcement:** The maximum reinforcement in tension or compression should not exceed $0.04bD$ where, D = overall depth of section (i.e., 4%).
c. **Side face reinforcement:** If the depth of the web in a beam exceeds 750 mm, side face reinforcement should be provided along the two faces. The total area of such reinforcement should not be less than 0.1% of the web area. It should be equally distributed on each of the two faces. The spacing of such reinforcement should not exceed 300 mm or web thickness whichever is less. However, there is no need to provide side reinforcement in footings (Section 12.3.4).
d. **Spacing of shear reinforcement:** For vertical shear stirrups, maximum spacing measured along the axis of the member is restricted to $0.75d$. For inclined shear bars, maximum spacing measured along the axis of the member should not exceed the effective depth d. In any case, the maximum spacing of shear stirrups is limited to 450 mm.
e. **Minimum shear reinforcement:** Even if calculations show that a beam has sufficient shear strength and shear stirrups are not required, a small quantity of shear stirrups is still provided. The reason is that tensile forces may be induced into a beam through shrinkage or some restraint which will reduce the shear strength of the concrete in the compression zone. Shear

failures in concrete beams without secondary reinforcement are essentially brittle which should be avoided. The spacing of minimum shear reinforcement is computed as

$$x = \frac{\sigma_y A_0}{0.4b}$$

where

A_0 = total cross-sectional area of stirrups effective in shear
b = width of the beam
σ_y = characteristic strength of stirrup reinforcement (not greater than 415 N/mm^2).

Slabs – Minimum Reinforcement:

Certain minimum reinforcement is provided in slabs to prevent excessive local curvature and provide some resistance to shear forces. It also helps provide resistance to some unforeseen forces applied during construction. The minimum reinforcement in either direction in slabs should not be less than 0.15% of the total cross-sectional area when using mild steel reinforcement, and 0.12% of the total cross-sectional area when using high yield strength reinforcement or welded wire fabric. The maximum diameter of reinforcing bars should not exceed one-eighth of the total thickness of the slab.

12.A.14 Reinforcement in Piles

Longitudinal reinforcement:

The minimum longitudinal reinforcement in piles is given as follows:

1. In piles whose length is less than 30 times the least lateral dimension, the minimum reinforcement should be 1.25%.
2. In piles whose length is 30–40 times the least lateral dimension, the minimum reinforcement should be 1.5%.
3. In piles whose length exceeds 40 times the least lateral dimension, the minimum reinforcement should be 2%.

Lateral reinforcement:

The minimum lateral reinforcement in a pile should be as follows:

1. The diameter of bars of lateral reinforcement should not be less than 5 mm.
2. In the body of the pile, minimum reinforcement should be 0.2% of the gross volume of the pile.
3. At each end of a pile for a length of about three times the least lateral dimension, the minimum reinforcement should be 0.6% of the gross volume of the pile.

Cover:

Longitudinal bars should normally be provided with a clear cover of 40 mm.

12.A.15 Under-Reamed Piles

Part III of IS: 2911–1984 (1984) provides a readymade table for the design of under-reamed piles. It gives safe load carrying capacity in bearing, uplift, and lateral thrust and reinforcement details in the piles of various sizes.

12.A.16 Pile Caps

Pile caps are structural elements that tie a group of piles together. Pile caps may support bearing walls, isolated columns or groups of several columns. Pile caps are used to transmit forces from the columns or walls to the piles. Plan dimensions of a pile cap depend on the closest allowable spacing of the piles which is generally 1 m. Its depth is based on the shear and/or development length for the column bars. Details of pile cap design are given in Chapter 10. Additional general guidelines for the design of pile caps are given below:

1. The pile cap along with column pedestal should be deep enough to allow for the necessary anchorage of the column and pile reinforcement.
2. The clear overhang of the pile cap beyond the outermost pile in the group should be within 10–15 cm.
3. A leveling course of mass concrete of about 8 cm thickness may be provided under the pile cap.
4. Reinforcement from pile must be properly tied to the pile cap.
5. Clear cover to the main reinforcement from bottom of the cap should not be less than 60 mm.
6. Computations of moments and shears may be based on the assumption that the reaction from any pile is concentrated at the center of the pile.
7. In computing the external shear on any section c–c through a footing supported on piles as shown in Figure 12.A.2, the entire reaction from any pile of diameter D_P whose center x_1 is located at $0.5D_P$ or more outside the section will be assumed as producing shear on the section. The shear force will be zero at a section $c'-c'$, due to reaction from a pile whose center x_2 is at $0.5D_P$ or more inside the section. For intermediate positions of the pile center, the portion fo the pile reaction to be assumed as producing shear on the section is based on a straight line interpolation between full value (when the pile center is at $x_1 = 0.5D_P$ outside the section c–c) and zero value (when the pile center is at $x_2 = 0.5D_P$ inside the section $c'-c'$).
8. Minimum thickness of pile cap at edges should not be less than 30 cm.

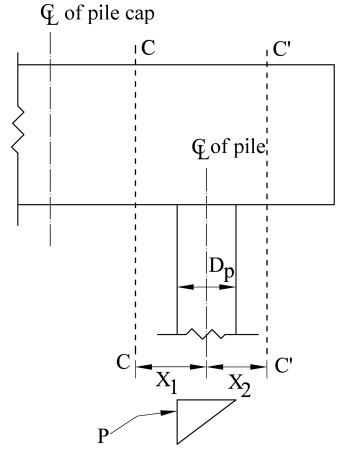

Figure 12.A.2 Critical section for shear in pile cap.

Appendix 12.B Expressions for BM and SF for Circular and Annular Slabs, and Foundations

12.B.1 Introduction

Circular slabs and foundations are used for the following purposes:

1. Shape of structures is circular in plan.
2. Floor of circular water tanks or towers.

The bending of such a slab is essentially different from a rectangular slab where bending takes place in distinctly two perpendicular directions along the two spans. When a circular slab, simply supported at the edge is loaded with uniformly distributed load, it bends in the form of a saucer, due to which stresses are developed both in the radial as well as in circumferential directions. The tensile, radial and circumferential stresses develop towards the convex side of the saucer, and hence reinforcement has to be provided at the convex face of the slab. Theoretically, reinforcement should be provided both in the radial and circumferential directions, but this arrangement would cause congestion and anchoring problem at the center of the slab. Hence, an alternative method of providing reinforcement in the form of a mesh of bars having an equal area of cross-section in both the directions can be adopted, the area being equal to that required for the bigger of the radial and circumferential moments. However, if the stresses near the edge are not negligible, or if the edge is fixed, radial and circumferential reinforcement near the edge has to be provided.

The exact analysis of slab, based on theory of elasticity and assuming Poisson's ratio equal to zero is given by Timoshenko and Woinowsky-Krieger (1959). The expressions can also be used for symmetrically loaded circular and annular foundations noting that the applied load on footings is from soil reaction and hence the applied load is in the opposite direction to that of the load applied on slabs. Sometimes, empirical formulae are used for bending moments and shear forces and so on.

Expressions are given for following cases for ready reference and application (Punmia, Jain and Jain 1992):

1. Plate/slab freely supported at edges carrying uniformly distributed load (UDL)
2. Slab fixed at edges and carrying UDL
3. Slab simply supported at the edges, with load W uniformly distributed along the circumference of a concentric circle
4. Slab simply supported at the edges with UDL, inside a concentric circle
5. Slab simply supported at the edges with a central hole and carrying UDL
6. Slab simply supported at the edges, with a central hole and carrying W distributed along the circumference of a concentric circle.

12.B.2 Slab Freely Supported at the Edges and Carrying UDL

This is shown in Figure 12.B.1.

The parameters are:

w = uniformly distributed load
a = radius of slab

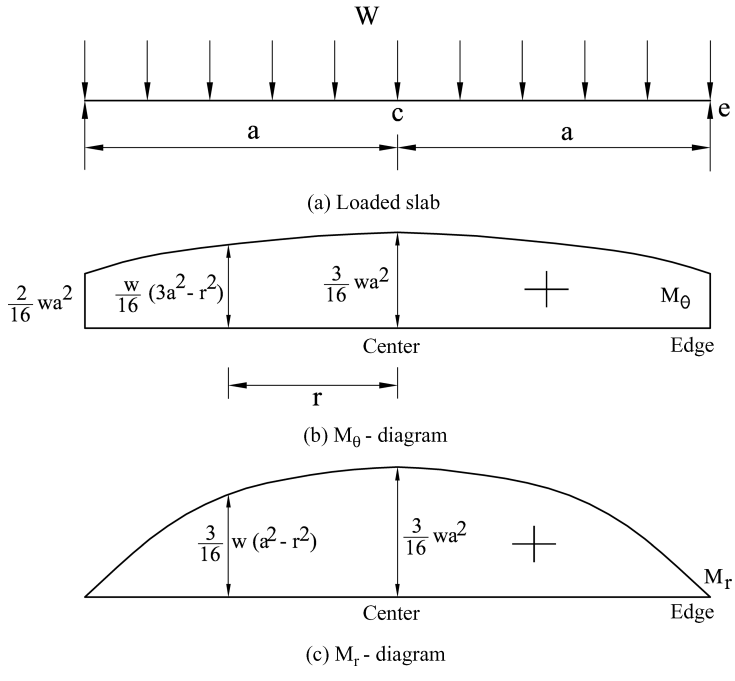

Figure 12.B.1 Slab with UDL.

M_r= radial bending moment at any point at radius r from the center of the slab
$(M_r)_c$ and $(M_r)_e$ = radial moments at center and edge respectively
M_θ = circumferential bending moment at any point at radius r from the center of the slab
$(M_\theta)_c$ and $(M_\theta)_e$ = circumferential moments at center and edge respectively.

The circumferential moment (M_θ) distribution diagram along any diameter is shown in Figure 12.B.1. The moment varies parabolically with a maximum value of $\frac{3}{16}wa^2$ at the middle to a minimum value of $\frac{2}{16}wa^2$ at the edges. Similarly, the radial moment (M_r) distribution along any diameter is shown in Figure 12.B.1(c). The moment varies from $\frac{3}{16}wa^2$ at the middle to zero at the edges.

The values of various moments, per unit width, are given below:

$$(M_\theta)_c = + \frac{3}{16}wa^2 \tag{12.B.1}$$

$$(M_\theta)_e = + \frac{2}{16}wa^2 \tag{12.B.2}$$

$$M_\theta = + \frac{w}{16}(3a^2 - r^2), \text{at any radius } r \tag{12.B.3}$$

$$(M_r)_c = + \frac{3}{16}wa^2 \tag{12.B.4}$$

$$(M_r)_e = 0 \tag{12.B.5}$$

$$M_r = \frac{3}{16}w(a^2 - r^2) \tag{12.B.6}$$

The radial shear force F_r, at any radius r is given by

$$F_r = \frac{1}{2} w.r \quad \text{(per unit width)} \tag{12.B.7}$$

The circumferential shear force is zero everywhere. Assuming redistribution of moments in the slab due to plasticity of materials, during failure, Reynolds and Steadman (1981) recommend maximum values of M_θ and M_r as $\frac{1}{9} wa^2$ instead of $\frac{3}{16} wa^2$ given above.

12.B.3 Slabs Fixed at Edges and Carrying UDL

The slab is shown in Figure 12.B.2. Figure 12.B.2(b) shows the circumferential moment distribution diagram, where M_θ varies parabolically from a maximum value at center to zero at the edge. The moment is positive throughout. Figure 12.B.2(c) shows the radial moment distribution diagram. M_r varies from a maximum positive value at the center to zero at a distance $\frac{a}{\sqrt{3}} = 0.577a$ from the center and then becomes negative at the edges. The various values of moments and shear per unit width are:

$$(M_\theta)_c = + \frac{1}{16} wa^2 \tag{12.B.8}$$

$$M_\theta = + \frac{1}{16} w(a^2 - r^2) \tag{12.B.9}$$

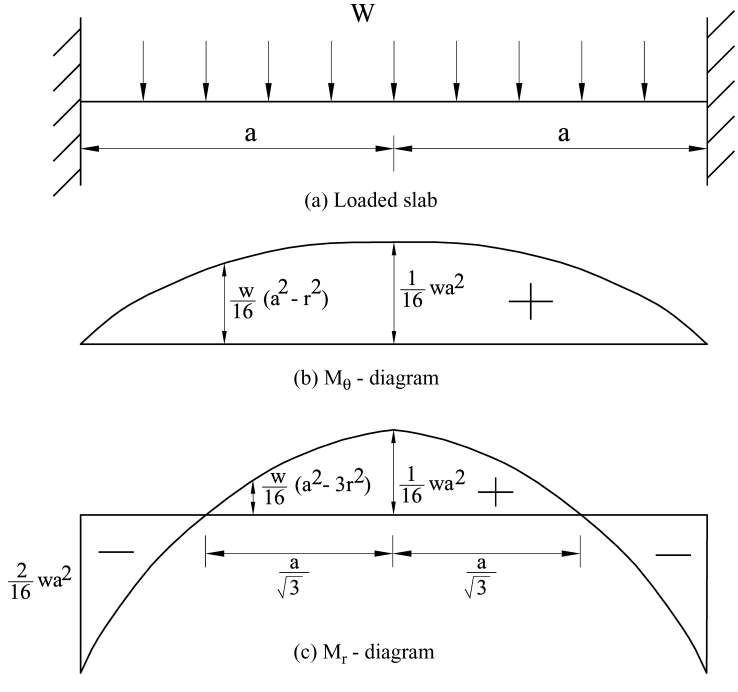

Figure 12.B.2 Slab with fixed edges.

$$(M_\theta)_e = 0 \tag{12.B.10}$$

$$(M_r)_c = + \frac{1}{16} wa^2 \tag{12.B.11}$$

$$M_r = + \frac{1}{16} w(a^2 - 3r^2) \tag{12.B.12}$$

$$(M_r)_e = -\frac{2}{16} wa^2 \tag{12.B.13}$$

$$F_r = \frac{1}{2} w.r \quad \text{(per unit width)} \tag{12.B.14}$$

Slabs partially fixed at the edges:

This case is in between the cases of a freely supported slab and a fixed slab. Hence, the moments may be assumed to be the average of the corresponding moment of the two cases. For radial moment the point of contraflexure occurs at a radius $r = a\sqrt{2/3}$. The various moments per unit width are:

$$(M_r)_c = (M_\theta)_c = + \frac{2}{16} wa^2 \tag{12.B.15}$$

$$(M_r)_e = -\frac{1}{16} wa^2 \tag{12.B.16}$$

$$(M_\theta)_e = + \frac{1}{16} wa^2 \tag{12.B.17}$$

12.B.4 Slab Simply Supported at the Edges with Load W Uniformly Distributed Along the Circumference of a Concentric Circle

The slab is shown in Figure 12.B.3. Here M_r as well as M_θ are constant from $r = 0$ to $r = b$. When r is greater than b (i.e., outside the load circle), both M_θ and M_r decrease parabolically, to values $(M_\theta)_e$ and zero respectively at the edges. Various values of moments and so on, per unit width are as follows:

For $r < b$

$$M_r = (M_r)_b = M_\theta = (M_\theta)_b = \frac{W}{8\pi}\left[2\log_e\left(\frac{a}{b}\right) + 1 - \left(\frac{b}{a}\right)^2\right] \tag{12.B.18}$$

$$F_r = 0 \tag{12.B.19}$$

For $r > 0$

$$M_\theta = \frac{W}{8\pi}\left[2\log_e\left(\frac{a}{r}\right) - \left(\frac{b}{r}\right)^2 + 2 - \left(\frac{b}{a}\right)^2\right] \tag{12.B.20}$$

$$M_r = \frac{W}{8\pi}\left[2\log_e\left(\frac{a}{r}\right) - \left(\frac{b}{a}\right)^2 + \left(\frac{b}{r}\right)^2\right] \tag{12.B.21}$$

$$F_r = \frac{W}{2\pi r} \tag{12.B.22}$$

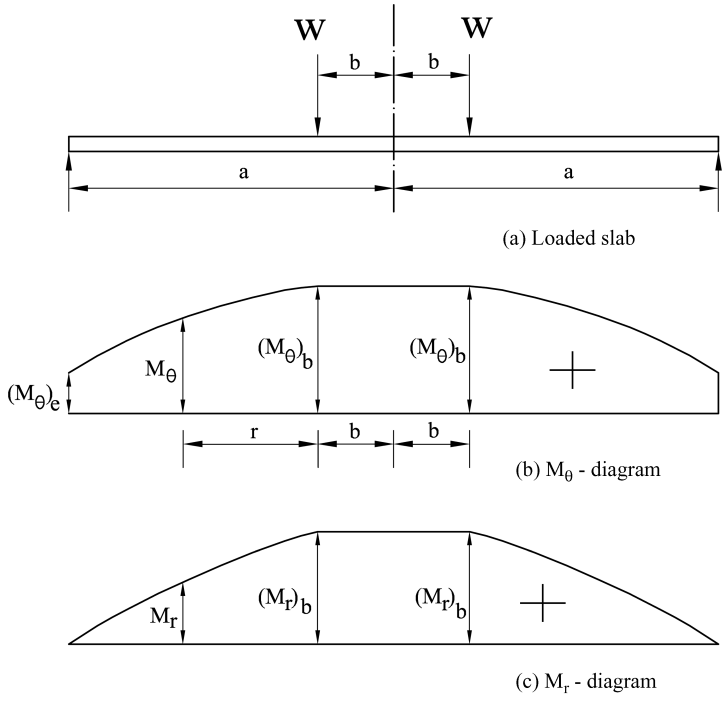

Figure 12.B.3 Simply supported slab.

12.B.5 Slab Simply Supported at Edges, with UDL Inside a Concentric Circle

This case is shown in Figure 12.B.4. Let b be the radius of concentric circle carrying UDL per unit area. The bending moment (M_θ and M_r) diagrams are shown in Figures 12.B.4(b) and (c), respectively. The various values of moments per unit width are as follows:

For $r < b$

$$M_r = -\frac{3}{16}wr^2 + \frac{1}{4}wb^2\left[1-\log_e\left(\frac{b}{a}\right)-\frac{b^2}{4a^2}\right] \tag{12.B.23}$$

$$M_\theta = -\frac{1}{16}wr^2 + \frac{1}{4}wb^2\left[1-\log_e\left(\frac{b}{a}\right)-\frac{b^2}{4a^2}\right] \tag{12.B.24}$$

$$(M_r)_c = + \frac{1}{4}wb^2\left[1-\log_e\left(\frac{b}{a}\right)-\frac{b^2}{4a^2}\right] \tag{12.B.25a}$$

$$(M_r)_b = (M_r)_e = \frac{3}{16}wb^2 \tag{12.B.25b}$$

$$(M_\theta)_c = + \frac{1}{4}wb^2\left[1-\log_e\left(\frac{b}{a}\right)-\frac{b^2}{4a^2}\right] \tag{12.B.26a}$$

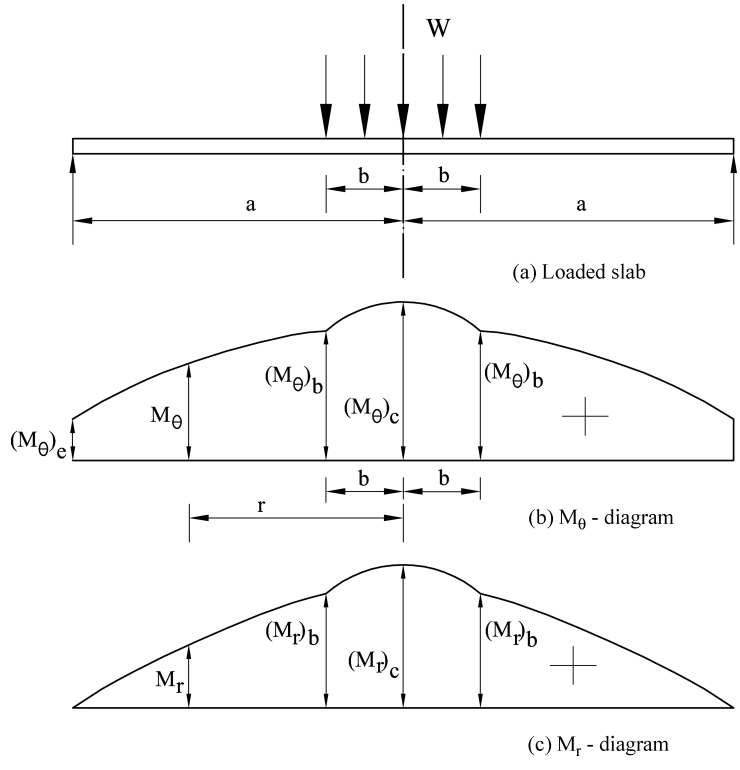

Figure 12.B.4 Slab with concentric load.

$$(M_\theta)_b = (M_\theta)_c = -\frac{1}{16} wb^2 \tag{12.B.26b}$$

$$F_r = \frac{wr}{2} \tag{12.B.27}$$

For $r > b$

$$M_r = -wb^2 \left[\frac{1}{4} \log_e \left(\frac{r}{a} \right) + \frac{b^2}{16} \left(\frac{1}{a^2} - \frac{1}{r^2} \right) \right] \tag{12.B.28}$$

$$M_\theta = -wb^2 \left[\frac{1}{4} \log_e \left(\frac{r}{a} \right) - \frac{1}{4} + \frac{b^2}{16} \left(\frac{1}{a^2} + \frac{1}{r^2} \right) \right] \tag{12.B.29}$$

$$(M_r)_e = 0 \tag{12.B.30}$$

$$(M_\theta)_e = -wb^2 \left[-\frac{1}{4} + \frac{b^2}{8a^2} \right] \tag{12.B.31}$$

$$F_r = \frac{wb^2}{2r} \tag{12.B.32}$$

12.B.6 Slab Simply Supported at Edges, with a Central Hole and Carrying UDL

The slab is shown in Figure 12.B.5. Let b be the radius of the hole. The BM diagrams are shown in Figures 12.B.5(b) and (c). The various values of the moments per unit width are:

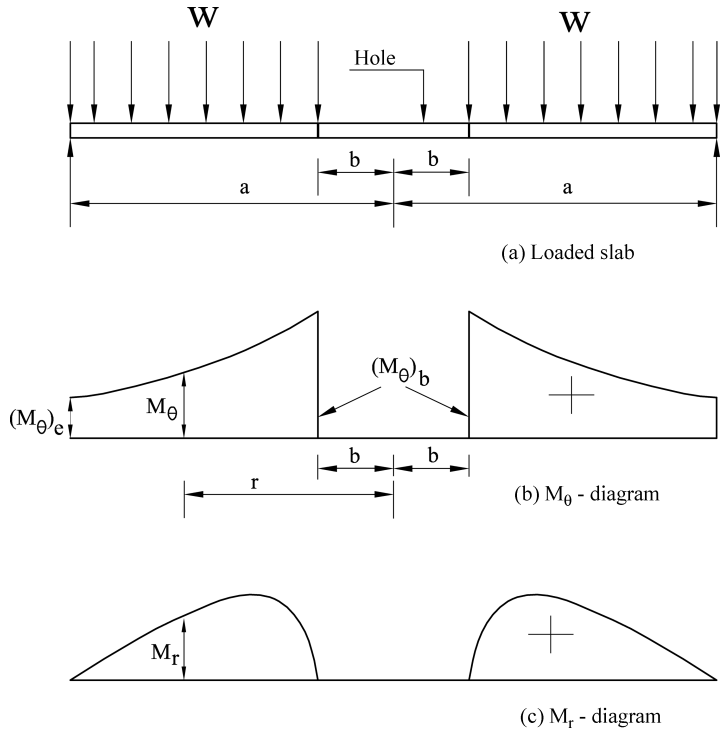

Figure 12.B.5 Annular slab.

$$M_\theta = -\frac{1}{16}wr^2 + \frac{wb^2}{4}\left[\log_e\left(\frac{r}{a}\right) + \frac{3}{4}\left(-\frac{1}{3} + \frac{a^2}{b^2} + \frac{a^2}{r^2}\right) - \frac{a^2 + r^2}{r^2} \rightleftarrows \frac{a^2}{a^2 - b^2}\log_e\left(\frac{a}{b}\right)\right] \tag{12.B.33}$$

$$M_r = -\frac{3}{16}wr^2 + \frac{wb^2}{4}\left[\log_e\left(\frac{r}{a}\right) + \frac{3}{4}\left(1 + \frac{a^2}{b^2} - \frac{a^2}{r^2}\right) + \frac{a^2 - r^2}{r^2} - \rightleftarrows \frac{b^2}{a^2 - b^2}\log_e\left(\frac{a}{b}\right)\right] \tag{12.B.34}$$

$$F_r = \frac{wr}{2} - \frac{wb^2}{2r} \tag{12.B.35}$$

12.B.7 Slab Simply Supported at the Edges with a Central Hole and Carrying W Distributed Along the Circumference of a Concentric Circle

The slab is shown in Figure 12.B.6. Let $b =$ radius of the hole and $c =$ radius of load circle.

The bending moment (M_θ and M_r) diagrams are shown in Figures 12.B.6(b) and (c), respectively. Various values per unit width are given below.

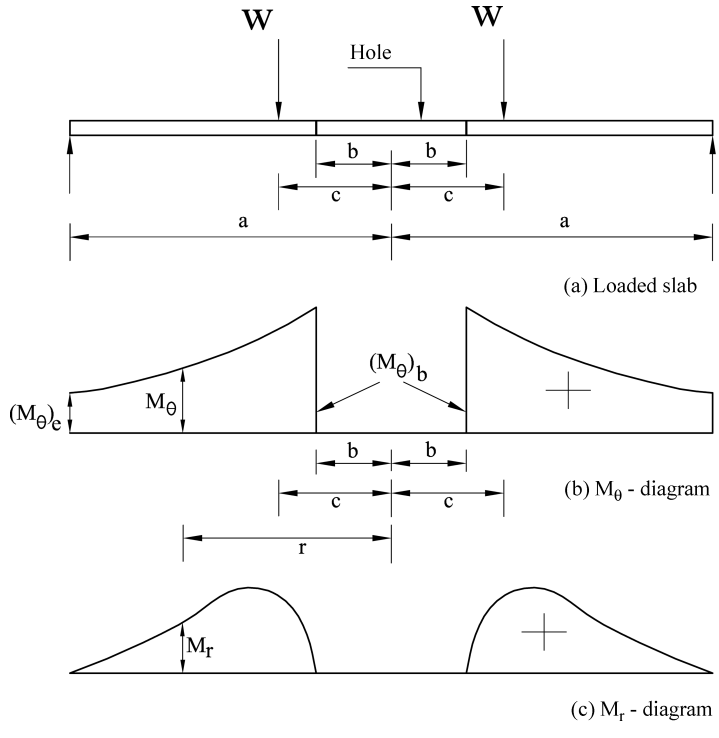

Figure 12.B.6 Slab with concentric line load.

For $r < c$

$$M_\theta = \frac{W}{4\pi}\frac{a^2}{a^2-b^2}\left(1 + \frac{b^2}{r^2}\right)\left[\log_e\frac{a}{c} + \frac{1}{2} - \frac{c^2}{2a^2}\right] \tag{12.B.36}$$

$$M_r = \frac{W}{4\pi}\frac{a^2}{a^2-b^2}\left(1 - \frac{b^2}{r^2}\right)\left[\log_e\frac{a}{c} + \frac{1}{2} - \frac{c^2}{2a^2}\right] \tag{12.B.37}$$

$$F_r = 0 \tag{12.B.38}$$

For $r > c$

$$M_\theta = \frac{W}{4\pi}\left[\log_e\left(\frac{c}{r}\right) + \frac{1}{2} + \frac{a^2}{a^2-b^2}\frac{r^2+b^2}{r^2}\left(\log_e\left(\frac{a}{c}\right) + \frac{1}{2} - \frac{c^2}{2a^2}\right) - \frac{c^2}{2r^2}\right] \tag{12.B.39}$$

$$M_r = \frac{W}{4\pi}\left[\log_e\left(\frac{c}{r}\right) - \frac{1}{2} + \frac{a^2}{a^2-b^2}\frac{r^2-b^2}{r^2}\left(\log_e\left(\frac{a}{c}\right) + \frac{1}{2} - \frac{c^2}{2a^2}\right) + \frac{c^2}{2r^2}\right] \quad (12.B.40)$$

$$F = \frac{W}{2\pi r} \quad (12.B.41)$$

12.B.8 Application of Expressions to Foundations

As mentioned in Section 12.B.1, all the above expressions can be used for foundation design by noting that the loads are vertically upwards due to soil reactions while in the case of slabs, they are vertically downwards. Hence by inserting a negative sign for the loads (w), that is, by replacing w by –w, the expressions given in Sections 12.B.2–12.B.7, the BM, SF and so on, can be computed. The rest of the design procedure will be similar to that of any concrete structure.

Appendix 12.C Structural Design of Shallow Foundations

12.C.1 Introduction

Several examples of structural design of commonly used foundations of reinforced cement concrete (RCC) are presented below. The examples are worked out using the limit state method (LSM) based on IS: 456–2000 (2000). The design parameters for the footing, such as shear forces, bending moments, deflections, and soil reactions or contact pressures, are obtained using both the conventional method as well as the beams on elastic foundation (BEF) method. Once these values are available from either of these methods the rest of the design procedure is the same following LSM and IS: 456–2000 (2000) or other codes which are followed in the country/city where the structure is being designed and constructed. The structural designs are presented in detail using the values obtained from conventional method for illustration. In view of using LSM for structural design, the design parameters for conventional method have been calculated for factored loads, that is, design loads multiplied by the load factor. These results for factored as well as design loads are compared, with the BEF responses for design loads only (without multiplying with the load factor). However comparison of these design parameters obtained from both the conventional and BEF methods are qualitative in nature as explained below.

The important features of IS: 456–2000 (2000) relevant to foundation design are presented in Chapter 12 and Appendices 12.A and 12.B. Also, comparative features of other commonly used codes, such as Eurocode, ACI and so on, are given in Appendix 12.D, along with a design example using these codes for illustration and easy understanding.

12.C.2 Input of Soil Parameters for Structural Design

The soil data needed for conventional design is the design soil pressure (q; based on the lower of the two values, that is, bearing capacity and allowable soil pressure, as explained in Chapters 3 and 8). In contrast, the data input for BEF solution is Young's modulus (E) of soil, Poisson's ratio (v) of soil, modulus of subgrade reaction (k_s) and spring constant (k) derived from these values as outlined in the INPUT section of WINBEF solutions. Essentially these values have to be obtained from laboratory and field tests as discussed in Chapters 3 and 4 and are site-specific. They also may not have any correlation in view of the variations in testing objectives and procedures besides being site specific. Hence the comparison of soil–foundation responses based on the conventional and BEF methods presented at the end of the design are only qualitative and indicative of the likely differences in the response parameters, such as deflections, bending moments, shear forces and bearing pressures and so on. Further, factored loads are used for conventional design while design loads only are used for calculating BEF responses (for illustration) as mentioned above.

12.C.3 Modulus of Subgrade Reaction for the Analysis

The conventional approach for obtaining a solution for foundations resting on elastic half space utilizes Winkler-based models such as proposed by Vesic (1961), Vlasov and Leontev (1966) and so on (see Chapters 4 and 5 for details). In such a case, an appropriate subgrade modulus needs to be assumed both for linear elastic and nonlinear analyses. In linear elastic analysis the subgrade modulus is usually determined by means of the expression given by Vesic (1961) and/

or other approaches discussed in Chapters 4 and 5. Vesic's expression essentially allows a beam on a Winkler foundation to exhibit similar displacements and moments to that of a beam on an elastic half space when loaded with the same load. Therefore, Vesic's expression given by Equation (4.41) is used for the evaluation of the modulus of subgrade reaction (k_s) in this chapter.

12.C.4 BEF Solutions for Circular and Annular Rafts

It is possible to analyze circular and annular rafts using BEF by considering a sector of any angular dimension with the loads and treating it as a beam with its width varying from zero to the chord length at its periphery (for full raft) and inner chord width to outer chord width for an annular sector. This is possible as the circular raft or annular raft can be seen as an assemblage of these sectors which are axially symmetric. However BEF analysis of these sectors is feasible only when the load is also axially symmetric. This condition makes BEF somewhat restrictive for applications, though some improvizations can be made (Jones, 1997). Hence for examples of circular rafts (Examples 12.8 and 12.9), BEF solutions are not included in this appendix.

12.C.5 Examples of Structural Design

The detailed design of most commonly used foundations, such as isolated footings, combined footings, strap footings, rafts of rectangular as well as circular shape and so on, are presented in the following pages. Area of steel reinforcement is calculated as per the expressions given in Appendix 12.A and are summarized below.

The bending moment at any section is equated to the resisting moment given by (Equation (12.A.6))

$$M = 0.87 f_y A_{st}\left(d - \frac{f_y A_{st}}{f_{ck} B}\right) \tag{12.C.1}$$

where

M = bending moment
$f_{ck} = \sigma_{ck}$ = compressive/characteristic strength of concrete
$f_y = \sigma_y$ = characteristic/yield strength of steel.
d = effective depth of the cross-section of the footing
B = width of the footing
A_{st} = area of steel reinforcement

The area of tension steel (A_{st}) can be obtained by solving the above quadratic equation in A_{st} (Punmia, Jain and Jain, 1992; IS: 456–2000, 2000) as

$$A_{st} = 0.5\frac{f_{ck}}{f_y}\left[1 - \sqrt{1 - \frac{4.6 \times M \times 10^6}{f_{ck} B d^2}}\right] Bd \tag{12.C.2}$$

Example 12.1 Spread Footing – Square Shape

Design a square footing (Figure 12.C.1(a)) to carry a load of 800 kN transmitted through a 40 cm square column reinforced with 20 mm steel bars in the longitudinal direction. The design soil pressure (DSP) is 100 kN/m^2. The footing is based at 1.0 m below ground level. The unit weight of

soil (γ_s) is 18 kN/m^3. Use concrete with $f_{ck} = 20\,\text{N/mm}^2$ (MPa), steel with $f_y = 415\,\text{N/mm}^2$ and load factor = 1.5.

A. Soil Pressure

$$\text{Axial load} = 800\,\text{kN}$$

$$\text{Approximate area of footing required} = \frac{800}{100} = 8\,\text{m}^2$$

$$\text{Weight of the footing including earth (approximate)} = 18 \times (1 \times 8) = 144\,\text{kN}$$

$$\text{Total weight on soil} = 800 + 144 = 944\,\text{kN}$$

$$\text{Actual area of footing required} = \frac{944}{100} = 9.44\,\text{m}^2$$

$$\text{Provide } 3.2\,\text{m} \times 3.2\,\text{m square footing giving total area} = 10.24\,\text{m}^2 \Rightarrow 10\,\text{m}^2$$

B. Bending Moment: The net earth pressure acting upward due to factored loads is

$$q = \frac{800 \times 1.5}{10} = 120\,\text{kN/m}^2$$

where 1.5 is the partial safety factor.

Bending moment about an axis *x*–*x* passing through the face of the column as shown in Figure 12.C.1(a) is

$$M = 120 \times 3.2 \times \left(\frac{3.2-0.40}{2}\right)^2 \times \frac{1}{2} = 376.32\,\text{kNm} \tag{12.C.3}$$

Bending moment at any section is given by

$$M = 0.138 f_{ck} B d^2 \tag{12.C.4}$$

where B = breadth of the beam.

The effective depth required is

$$d = \sqrt{\frac{M}{0.138 f_{ck} B}} \tag{12.C.5}$$

$$d = \sqrt{\frac{376.32 \times 10^6}{0.138 \times 20 \times 3200}} = 206\,\text{mm}$$

Adopt 560 mm effective depth and 600 mm overall depth. Increased depth is taken due to shear requirements.

Bending moment at any section is given by (Equations (12.A.6) and (12.C.1))

$$M = 0.87 f_y A_{st}\left(d - \frac{f_y A_{st}}{f_{ck} B}\right) \tag{12.C.6}$$

where $f_{ck} = \sigma_{ck}$ = compressive/characteristic strength of concrete and $f_y = \sigma_y$ = characteristic/yield strength of steel.

The area of tension steel (A_{st}) can be obtained by solving the above quadratic equation in A_{st} (Punmia, Jain and Jain, 1992; IS: 456–200, 2000) as given in Equation (12.C.2). Accordingly

$$A_{st} = 0.5\frac{f_{ck}}{f_y}\left[1-\sqrt{1-\frac{4.6 \times M \times 10^6}{f_{ck}Bd^2}}\right]Bd \tag{12.C.7}$$

$$A_{st} = 0.5\frac{20}{415}\left[1-\sqrt{1-\frac{4.6 \times 376.32 \times 10^6}{20 \times 3200 \times 560^2}}\right]3200 \times 560 = 1904\,\text{mm}^2$$

$$\text{Percent reinforcement}, p_r = \frac{1904 \times 100}{3200 \times 560} = 0.11\%$$

Use 10 mm bars @ 120 mm c/c ($A_{st} = 2094.3 > 1904\,\text{mm}^2$).

C. Shear – One-Way Action: The critical section is taken at distance d away from the face of the column as shown in Figure 12.C.1(a).

$$\text{Shear force}, V_u = 120 \times 3.2\left[\left(\frac{3.2-0.40}{2}\right)-0.56\right] = 322.56\,\text{kN}$$

$$\text{Nominal shear stress}, \tau_v = \frac{V_u}{Bd} = \frac{322560}{3200 \times 560} = 0.18\,\text{N/mm}^2$$

Shear strength of M20 concrete with 0.11% steel, $\tau_c = 0.20\,\text{N/mm}^2 > \tau_v$ – OK.

D. Shear – Two-Way Action: The critical section is taken at a distance $0.5d$ away from face of column as shown in Figure 12.C.1(b).

$$\text{Shear force}, V_u = 120\left[3.2^2-(0.40 + 0.56)^2\right] = 1118.208\,\text{kN}$$

$$\text{Nominal shear stress}, \tau_v = \frac{V_u}{b_o d} = \frac{1118.208 \times 1000}{4(400 + 560)560} = 0.5546\,\text{N/mm}^2 \tag{12.C.8}$$

$$\text{Shear strength of M20 concrete}, \tau_c^{|} = k_s\tau_c \tag{12.C.9}$$

where

$$k_s = 0.5 + \beta_c \Rightarrow \beta_c = \frac{a}{b} \tag{12.C.10}$$

where a = length of shorter side of column, b = length of longer side of column$k_s = 0.5 + 1 = 1.5$ (should not be greater than one)

$$\therefore k_s = 1.0$$

$$\tau_c^{|} = \tau_c = 0.25\sqrt{\sigma_{ck}} = 0.25\sqrt{20} = 1.118\,\text{N/mm}^2 > 0.5546\,\text{N/mm}^2 \quad \text{OK.}$$

This shows that a footing having as effective depth of 206 mm would not be safe in shear. Reinforcement details are shown in Figures 12.C.1(c) and (d).

E. Development Length of Reinforcement: Development length for 10 mm bars

$$L_d = \frac{\sigma_s \phi}{4\tau_{bd}} = \frac{0.87 \times 415\phi}{4 \times (1.6 \times 1.0)} = 56\phi \qquad (12.C.11)$$

where 1.6 is a factor due to deformed bars.

$$\therefore L_d = 560\,\text{mm}$$

Actual embedment provided from the face of the column is $= \left(\frac{3200-400}{2} - 50\right)$

$= 1350\,\text{mm} > L_d$ OK

F. Load Transfer from Column to Footing: Nominal bearing stress in the column concrete

$$\sigma_{cr} = \frac{P_u}{A_c} = \frac{1.5 \times 800 \times 1000}{400 \times 400} = 7.5\,\text{N/mm}^2$$

where 1.5 is the partial safety factor.

Allowable bearing stress $= 0.45\sigma_{ck} = 0.45 \times 20 = 9.0\,\text{N/mm}^2 > 7.5\text{N/mm}^2$ OK

Hence it is safe. Thus no separate dowel bars are required for the transfer of load. However it is advisable to continue all the bars of the column into the foundation.

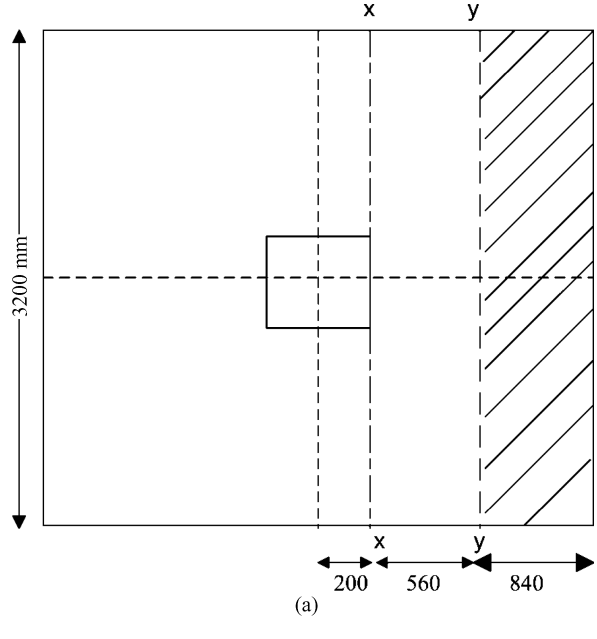

Figure 12.C.1 (a) Critical section for moment and one-way shear; (b) critical section for two-way shear; (c) reinforcement in the footing base; and (d) sectional elevation showing reinforcement (Example 12.1).

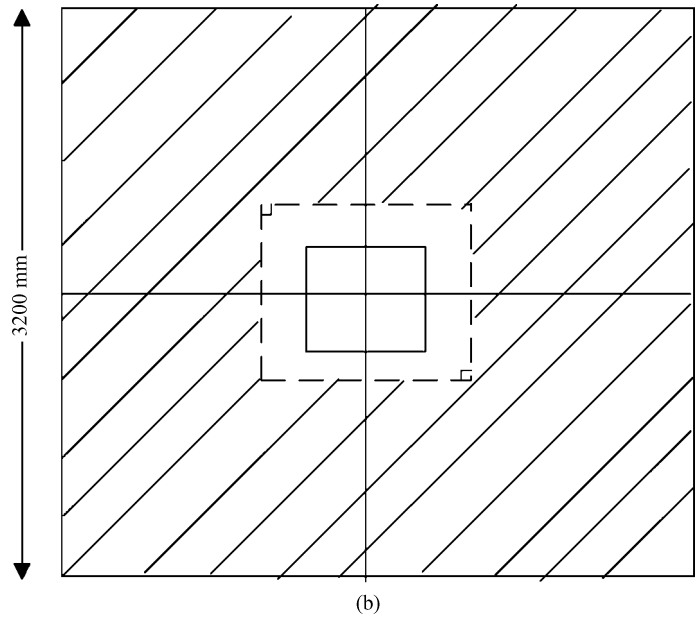

Figure 12.C.1 (*Continued*)

WINBEF Solution (BEF Method):

WINBEF Input

Young's modulus of soil: $E_s = 10^5\ \text{kN/m}^2$
Unit weight of soil: $\gamma_{soil} = 18\ \text{kN/m}^3$
Poisson's ratio of soil: $v_s = 0.3$

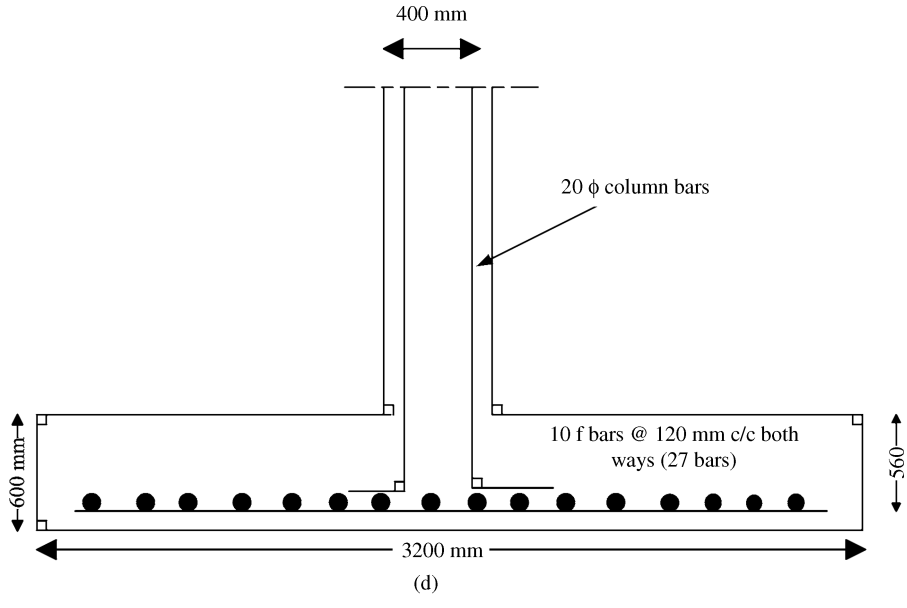

Figure 12.C.1 *(Continued)*

Young's modulus of concrete:

$$E_f = 5000\sqrt{\sigma_{ck}} = 5000\sqrt{20} = 22360\,\text{N/mm}^2 = 2.236 \times 10^7\,\text{kN/m}^2$$

Moment of inertia of the concrete beam:

$$I_f = \frac{Bd^3}{12} = \frac{3.2 \times 0.560^3}{12} = 0.0468\,\text{m}^4$$

Modulus of subgrade reaction is given by

$$k_s = \frac{1}{B(\text{mm})}\left[0.65\sqrt[12]{\frac{E_s B^4}{E_f I_f}}\right]\frac{E_s}{1-v_s^2} = \frac{86547.72}{3200} = 27.04\,\text{kN/m}^2/\text{mm}$$

The length of the beam = 3200 mm, breadth of the beam = 3200 mm and the other details are given below.

Loading Data for WINBEF and Results

The loading data is shown in Figure 12.C.2. The deflections, shear force, bending moment and bearing pressure obtained from BEF analysis are shown in Figure 12.C.3. Table 12.C.1 shows the comparative study of the results.

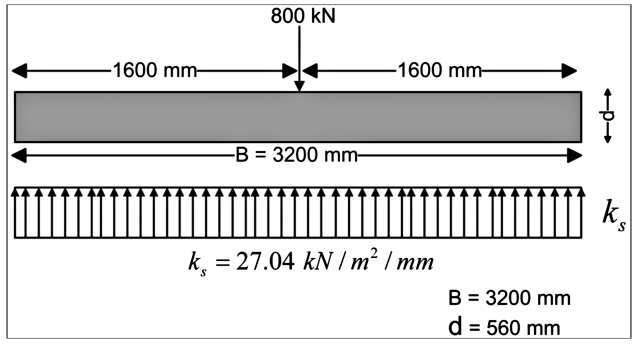

Figure 12.C.2 Details of loading and modulus of the subgrade reaction of a beam resting on an elastic foundation (Example 12.1).

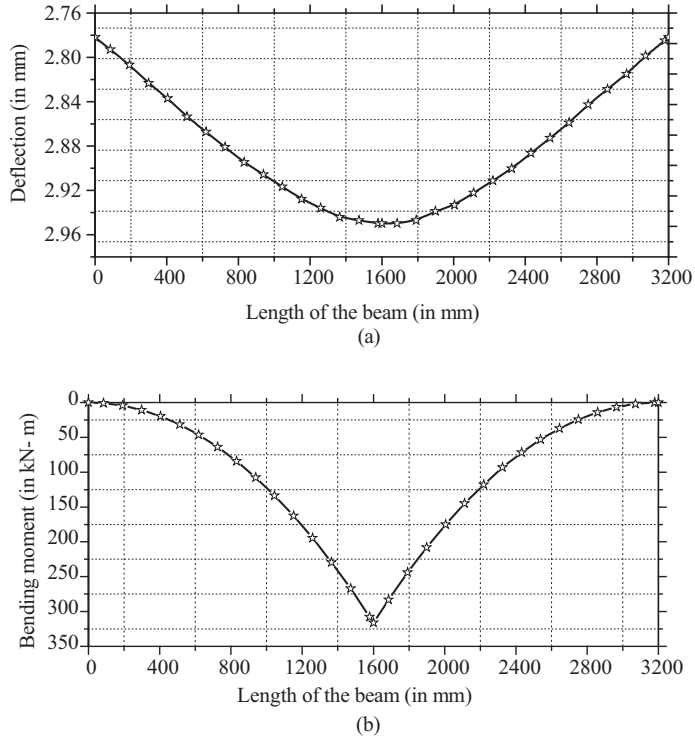

Figure 12.C.3 (a) BEF deflection diagram; (b) BEF bending moment diagram; (c) BEF shear force diagram; and (d) BEF bearing pressure diagram (Example 12.1).

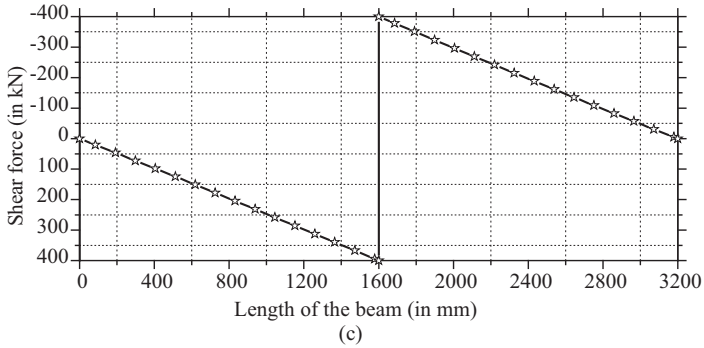

(c)

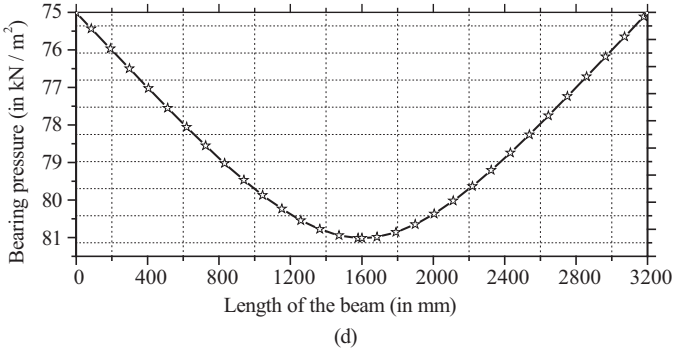

(d)

Figure 12.C.3 (*Continued*)

Table 12.C.1 Comparative study (see comments in Section 12.C.2).

		Maximum bearing pressure (kN/m^2)	Maximum bending moment (kNm)	Maximum shear force (kN)	Maximum deflection (mm)
Conventional design	With factored load	120	376.32	322.56	$120/k_s = 4.436$
	With design load	120/1.5 = 80	376.32/1.5 = 250.88	322.56/1.5 = 215.04	4.436/1.5 = 2.97
Design using BEF (with design load only)		80.21	316.21	400.00	2.96

Example 12.2 Rectangular Footing

Design a rectangular footing with length/breadth ratio = 1.5 to carry a load of 800 kN transmitted through a 40 cm square column reinforced with 20 mm steel bars in the longitudinal direction. The design soil pressure (DSP) is 100 kN/m^2. The footing is based at 1.0 m below

ground level. The unit weight of soil, γ_s, is 18 kN/m^3. Use concrete with $\sigma_{ck} = 15$ N/mm^2 (MPa), and steel with $\sigma_y = 415$ N/mm^2 and load factor = 1.5. (This is the same column as given in the above Example 12.1. However, a rectangular footing is to be designed instead of square footing with M_{15} concrete.)

A. Soil Pressure

$$\text{Axial load} = 800\,\text{kN}$$

$$\text{Approximate area of footing required} = \frac{800}{100} = 8\,\text{m}^2$$

$$\text{Weight of the footing including earth(approximate)} = 18 \times (1 \times 8) = 144\,\text{kN}$$

$$\text{Total weight on soil} = 800 + 144 = 944\,\text{kN}$$

$$\text{Actual area of footing required} = \frac{944}{100} = 9.44\,\text{m}^2$$

Length/breadth ratio = 1.5

$$L = 1.5B \tag{12.C.12}$$

$$B \times L = 9.44\,\text{m}^2$$

$$1.5B^2 = 9.44$$

$$B = 2.5\,\text{m and } L = 3.76\,\text{m}.$$

Adopt 4.0 m × 2.5 m rectangular footing giving total area = 10.0 m^2

B. Bending Moment: The net earth pressure acting upward due to factored load is

$$q = \frac{800 \times 1.5}{10} = 120\,\text{kN/m}^2$$

where 1.5 is the partial safety factor.

Bending moment (M_1) about an axis x–x passing through the face of the column as shown in Figure 12.C.4(a). The column dimensions are $a = b = 0.4\,m$.

$$M_1 = qB\left(\frac{L-a}{2}\right)^2 \times \frac{1}{2} \tag{12.C.13}$$

$$M_1 = 120 \times 2.5 \times \left(\frac{4.0-0.40}{2}\right)^2 \times \frac{1}{2} = 486\,\text{kN}$$

$$\text{The effective depth required is, } d = \sqrt{\frac{M_1}{0.138 f_{ck} L}} \tag{12.C.14}$$

$$d = \sqrt{\frac{486 \times 10^6}{0.138 \times 15 \times 4000}} = 243\,\text{mm}$$

Bending moment, M_2, about an axis y–y passing through the face of the column as shown in Figure 12.C.4(a) is given by

$$M_2 = qL\left(\frac{B-b}{2}\right)^2 \times \frac{1}{2}$$

$$M_2 = 120 \times 4.0 \times \left(\frac{2.5-0.40}{2}\right)^2 \times \frac{1}{2} = 264.6\,\text{kN} \tag{12.C.15}$$

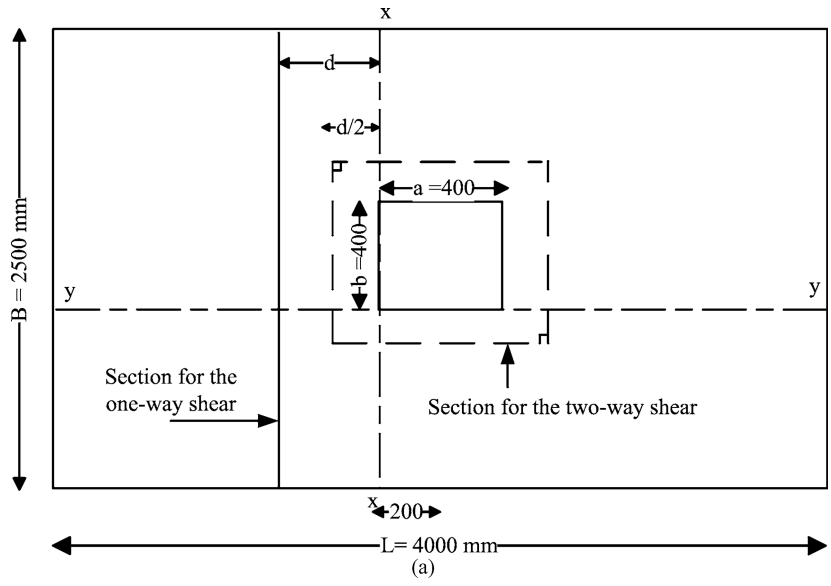

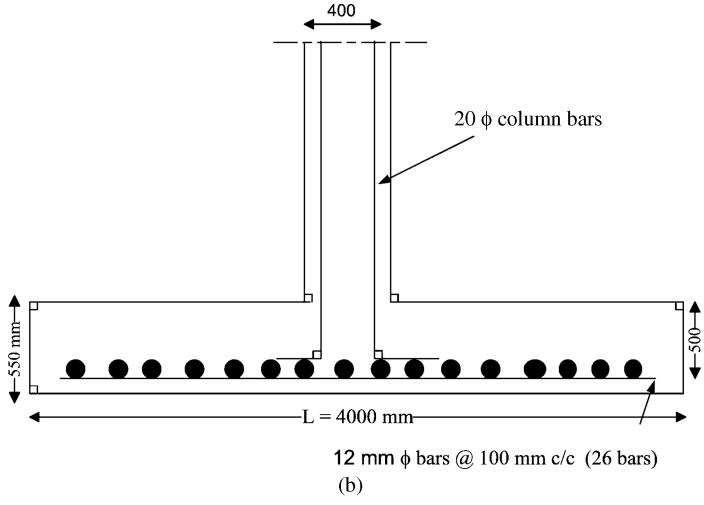

Figure 12.C.4 (a) Critical section for one- and two-way shear; (b) sectional elevation showing reinforcement; and (c) reinforcement in the footing base (Example 12.2).

Thus, $M_2 < M_1$, the effective depth found above has to be checked for shear.

Keep $d = 500$ mm and total depth $= 550$ mm for shear requirements.

C. Design for Reinforcement: Area of reinforcement (A_{st1}) of long bars calculated for moment M_1 is given by

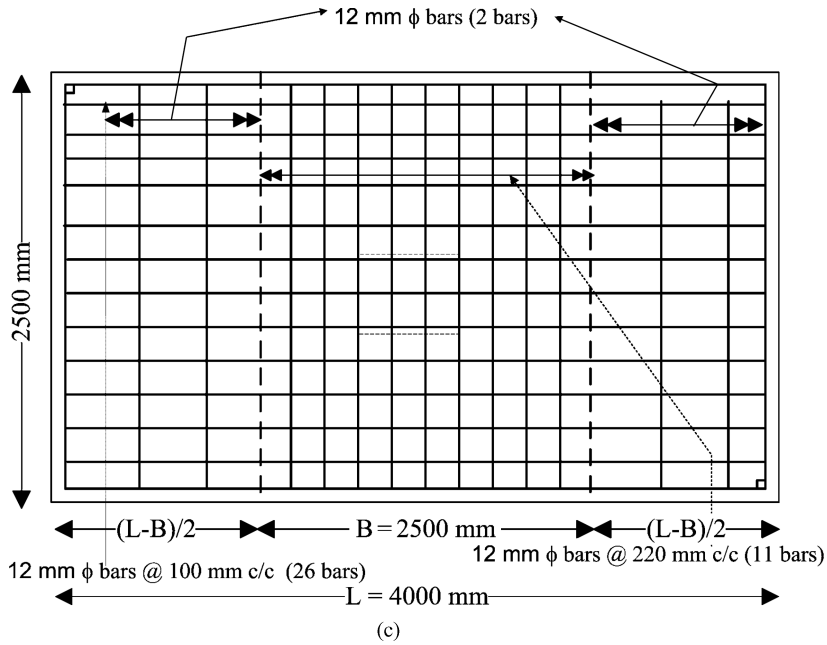

Figure 12.C.4 *(Continued)*

$$A_{st1} = 0.5\frac{f_{ck}}{f_y}\left[1-\sqrt{1-\frac{4.6\times M_1\times 10^6}{f_{ck}Bd^2}}\right]Bd \tag{12.C.16}$$

$$A_{st1} = 0.5\frac{15}{415}\left[1-\sqrt{1-\frac{4.6\times 486\times 10^6}{15\times 2500\times 500^2}}\right]2500\times 500 = 2876.64\,\text{mm}^2$$

Area of steel (%)

$$p_r = \frac{2876.64}{2500\times 500}\times 100 = 0.23\%$$

Use 12 mm bars, area of reinforcement bar $(A_\phi) = (\pi/4)d^2 = 113.09\,\text{mm}^2$
Number of bars = 2876.64/113.09 = 25.43 ≈ 26 bars
Spacing of long bars = 2500/26 = 96.15 mm ≈ 100 mm
Use 12 mm Φ bars for longitudinal reinforcement @ 100 mm c/c.
Area of reinforcement (A_{st2}) of short bars calculated for moment, M_2 is given by

$$A_{st2} = 0.5\frac{f_{ck}}{f_y}\left[1-\sqrt{1-\frac{4.6\times M_2\times 10^6}{f_{ck}Ld^2}}\right]Ld \tag{12.C.17}$$

$$A_{st1} = 0.5\frac{15}{415}\left[1-\sqrt{1-\frac{4.6\times 264.6\times 10^6}{15\times 4000\times 500^2}}\right]4000\times 500 = 1497.47\,\text{mm}^2$$

This area is to be provided in two distinct band widths. Area $A_{st2(B)}$ in central band of width $B = 2.5$ m is given by

$$A_{st2(B)} = \frac{2A_{st2}}{\frac{L}{B}+1} = \frac{2\times 1497.47}{\frac{4.0}{2.5}+1} = 1151.9\,\text{mm}^2 \tag{12.C.18}$$

Number of 12 mm Φ bars = 1151.9/113.09 ≈ 11, to be provided in the central band width $(B) = 2.5$ m. Remaining area in each end band strip = $\frac{1}{2}(1497.47-1151.9) = 172.78\,\text{mm}^2$
Number of 12 mm Φ bars = 172.78/113.09 ≈ 2
These two bars provided in each end band of width $\frac{1}{2}(L-B) = \frac{1}{2}(4-2.5) = 0.75$ m.
Spacing of short bars in each end band = 750/2 = 350 mm
The reinforcement details are shown in Figures 12.C.4(b) and (c).

D. Shear – One-Way Action: The critical section is taken at a distance, d, away from the face of the column (size $a \times b$) as shown in Figure 12.C.4(a).

$$\text{Shear force, } V_u = qB\left[\left(\frac{L-a}{2}\right)-d\right] \tag{12.C.19}$$

$$V_u = 120\times 2.5\left[\left(\frac{4.0-0.40}{2}\right)-0.50\right] = 390\,\text{kN}$$

$$\text{Nominal shear stress, } \tau_v = \frac{V_u}{Bd} = \frac{390000}{2500\times 500} = 0.312\,\text{N/mm}^2 \tag{12.C.20}$$

Shear strength of M15 concrete with 0.23% steel, $\tau_c = 0.34\,\text{N/mm}^2 > \tau_v$ OK.

E. Shear – Two-Way Action: The critical section is taken at a distance $d/2$ away from face of column as shown in Figure 12.C.4(a).

$$\begin{aligned}\text{Net shear force at the periphery, } \quad F &= q[BL-(a+d)(b+d)]\\ &= 120[2.5\times 4.0-(0.40+0.50)(0.40+0.50)]\\ &= 1102.8\,\text{kN}\end{aligned} \tag{12.C.21}$$

$$\begin{aligned}\text{Nominal shear stress, } \quad \tau_v &= \frac{F}{2[(a+d)+(b+d)]d}\\ &= \frac{1102.8\times 1000}{2[(400+500)+(400+500)]500} = 0.6126\,\text{N/mm}^2\end{aligned} \tag{12.C.22}$$

$$\text{Shear strength of M15 concrete, } \quad \tau_c^{|} = k_s\tau_c \tag{12.C.23}$$

where

$$k_s = 0.5+\beta_c, \quad \beta_c = \frac{a}{b} \tag{12.C.24}$$

a = length of shorter side of column
b = length of longer side of column
$k_s = 0.5 + 1 = 1.5$ (should not be greater than one)

$$\therefore k_s = 1.0$$

$$\tau_c^{\downarrow} = \tau_c = 0.25\sqrt{f_{ck}} = 0.25\sqrt{15} = 0.9682\,\text{N/mm}^2 > 0.6126\,\text{N/mm}^2 \quad \text{OK.}$$

This shows that a footing having as effective depth of 243 mm would not be safe in shear. Reinforcement details are shown in Figure 12.C.4(c).

F. Development Length of Reinforcement: Development length for 12 mm bars

$$L_d = \frac{\sigma_s \Phi}{4\tau_{bd}} = \frac{0.87 \times 415\Phi}{4 \times (1.6 \times 1.0)} = 56\Phi \qquad (12.C.25)$$

where 1.6 is a factor due to deformed bars and Φ = diameter of the steel bar.

$$\therefore L_d = 56\Phi = 56 \times 12 = 672\,\text{mm}$$

Providing 50 mm side cover, actual embedment provided from the face of the column is given by $\left(\frac{2500-400}{2} - 50\right) = 1000\,\text{mm} > L_d$ OK.

G. Load Transfer from Column to Footing: Nominal bearing stress in the column concrete

$$\sigma_{br} = \frac{P_u}{A_c} = \frac{1.5 \times 800 \times 1000}{400 \times 400} = 7.5\,\text{N/mm}^2$$

where 1.5 is the partial safety factor

$$\text{Permissible bearing stress} = 0.45\sigma_{ck}\sqrt{\frac{A_1}{A_2}} \qquad (12.C.26)$$

where A_1 = maximum area of the portion of the supporting surface that is geometrically similar to and concentric with the loaded area (used 2: 1 method for the load distribution).

$$A_1 = [400 + 2(2 \times 550)]^2 = 6.76 \times 10^6\,\text{mm}^2$$

$$A_2 = \text{Loaded area at the column base} = 400 \times 400 = 160000\,\text{mm}^2$$

$$\text{Permissible bearing stress} = 0.45 \times 15\sqrt{\frac{6.76 \times 10^6}{160000}}$$
$$= 43.875\,\text{N/mm}^2 > 7.5\,\text{N/mm}^2, \text{ hence it is satisfactory.}$$

WINBEF Solution (BEF Method):

WINBEF Input

Young's modulus of soil, $E_s = 10^5\,\text{kN/m}^2$
Unit weight of soil, $\gamma_{soil} = 18\,\text{kN/m}^3$
Poisson's ratio of soil, $v_s = 0.3$

$$\text{Young's modulus of concrete,} \quad E_f = 5000\sqrt{\sigma_{ck}} = 5000\sqrt{15}$$
$$= 19364.92\,\text{N/mm}^2 = 1.9364 \times 10^7\,\text{kN/m}^2$$

$$\text{Moment of inertia of the concrete beam,} \quad I_f = \frac{Bd^3}{12} = \frac{2.5 \times 0.55^3}{12} = 0.03466\,\text{m}^4$$

$$\text{Modulus of subgrade reaction,} \quad k_s = \frac{1}{B(\text{mm})}\left[0.65\sqrt[12]{\frac{E_s B^4}{E_f I_f}}\right]\frac{E_s}{1-v_s^2} \qquad (12.\text{C}.27)$$

$$k_s = \frac{0.65}{2500}\frac{10^5}{(1-0.3^2)}\sqrt[12]{\frac{10^5 \times 2.5^4}{1.9364 \times 10^7 \times 0.02604}} = \frac{82721.17}{2500} = 33.08\,\text{kN/m}^2/\text{mm}.$$

Loading Data for WINBEF and Results

The loading data is shown in Figure 12.C.5. The details of deflection, bending moment, shear force and bearing pressure are shown in Figure 12.C.6. Table 12.C.2 shows the comparative study of the results.

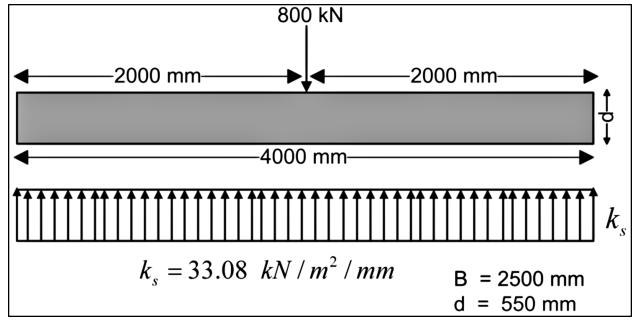

Figure 12.C.5 Details of loading and modulus of the subgrade reaction of a beam resting on an elastic foundation (Example 12.2).

Table 12.C.2 Comparative study (see comments in Section 12.C.2).

		Maximum bearing pressure (kN/m^2)	Maximum bending moment (kNm)	Maximum shear force (kN)	Maximum deflection (mm)
Conventional design	With factored load	120	486	390	$120/k_s = 3.636$
	With design load	120/1.5 = 80	486/1.5 = 324.1	390/1.5 = 260	3.636/1.5 = 2.424
Design using BEF (with design load only)		87.45	383.50	400.00	2.60

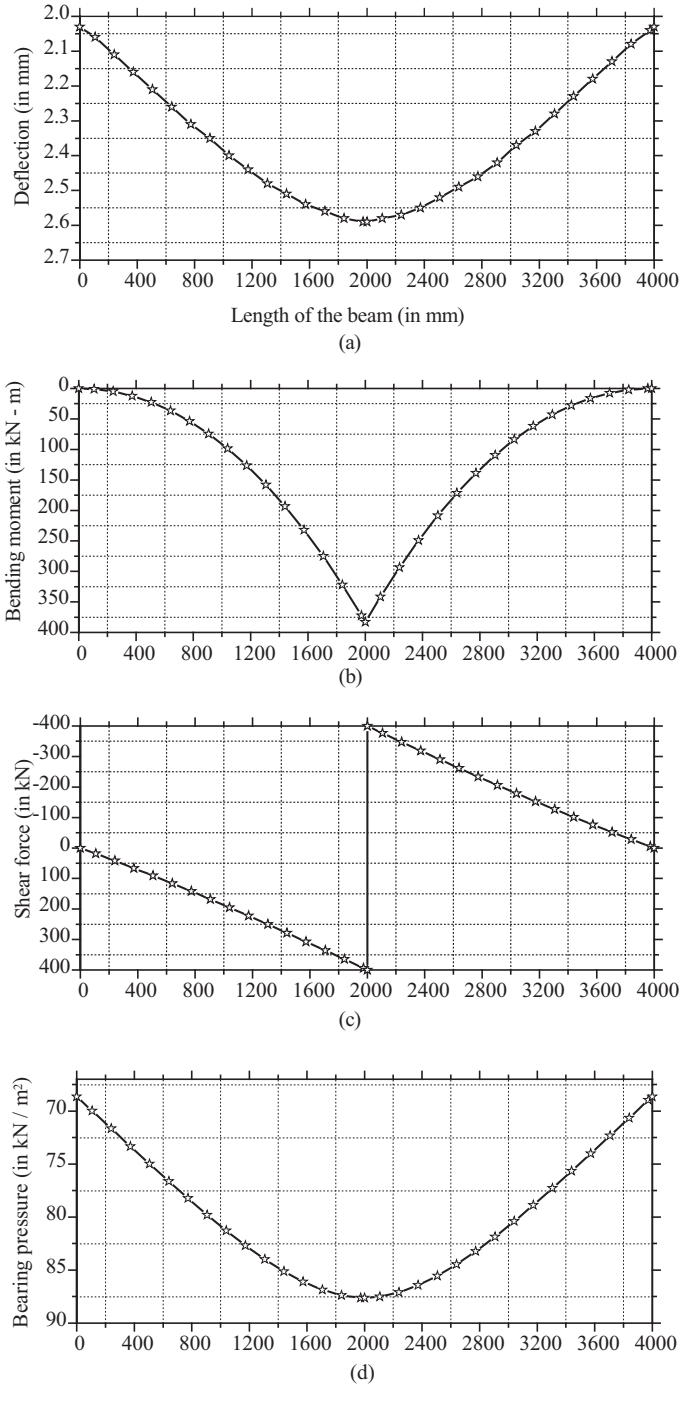

Figure 12.C.6 (a) BEF deflection diagram; (b) BEF bending moment diagram; (c) BEF shear force diagram; and (d) BEF bearing pressure diagram (Example 12.2).

Example 12.3 Continuous Footing

Design a continuous footing for a brick wall of 40 cm thick transmitting a load of 150 kN/m. The allowable design soil pressure (ADSP) is 100 kN/m^2. Assume unit weight of soil (γ_s) is 17 kN/m^3. Use concrete with $\sigma_{ck} = 15$ MPA and load factor = 1.5.
Assume base of the footing to be 0.5 m below the ground level.

$$\text{Axial load} = 150\ \text{kN/m}$$

$$\text{Width of the footing required} = \frac{150}{100} = 1.5\ \text{m}$$

Approximate weight of the footing including earth above it $= (1.5 \times 1 \times 0.50) \times 17 = 12.75$ kN/m $\approx$ 20 kN/m

$$\text{Total weight on soil} = 150 + 20 = 170\ \text{kN/m}$$

$$\text{Actual width of the footing required} = \frac{170}{100} = 1.7\ \text{m}$$

Therefore, use $B = 1.7$ m wide footing. Consider 1 m length for design, that is, $L = 1.0$ m.

$$\text{Applying the load factors,} \quad w_u = 150 \times 1.5 = 225\ \text{kN/m}$$

$$\text{Net soil pressure acting upward, } q = \frac{225}{1.7} = 133\ \text{kN/m}^2/\text{m}$$

The critical section for bending moment in footing under masonry wall occurs half way between the middle and the edge of the wall.

$$\therefore\ M = 133 \times \frac{0.85^2}{2} = 48.05\ \text{kNm}$$

The effective depth required is given by

$$d = \sqrt{\frac{M}{0.138 f_{ck} L}} \tag{12.C.28}$$

$$d = \sqrt{\frac{48.046 \times 10^6}{0.138 \times 15 \times 1000}} = 152.35\ \text{mm}$$

Let us adopt an overall depth as 300 mm and effective depth as 270 mm.

A. Design for Reinforcement: Area of steel bars, A_{st}, calculated for moment, M, is given by

$$A_{st} = 0.5 \frac{f_{ck}}{f_y} \left[1 - \sqrt{1 - \frac{4.6 \times M \times 10^6}{f_{ck} L d^2}}\right] Ld \tag{12.C.29}$$

$$A_{st} = 0.5 \frac{15}{250} \left[1 - \sqrt{1 - \frac{4.6 \times 48.046 \times 10^6}{15 \times 1000 \times 270^2}}\right] 1000 \times 270 = 864.72\ \text{mm}^2$$

$$\text{Percent area of steel, } p_r = \frac{864.72}{1000 \times 270} \times 100 = 0.32\%$$

Use 10 mm diameter bars, then area of steel bar $(A_\phi) = (\pi/4)10^2 = 78.5398\ \text{mm}^2$

$$\text{Number of bars} = \frac{864.72}{78.5398} = 11\ \text{bars}$$

$$\text{Spacing of long bars} = 1000/11 = 90.90 \approx 90\ \text{mm}$$

Use 10 mm Φ bars for reinforcement @ 90 mm c/c.

B. Development Length of Reinforcement: The development length for 10 mm bars is given by

$$L_d = \frac{\sigma_s \Phi}{4\tau_{bd}} = \frac{0.87 \times 250\Phi}{4 \times (1.0)} = 34\Phi = 34 \times 10 = 340\ \text{mm}$$

Actual embedment provided from the face of the column

$$= \left(\frac{1700-400}{2}\right) = 650\ \text{mm} > L_d, \quad \text{OK.}$$

Provide longitudinal reinforcement for shrinkage equal to 0.15% sectional area $= \frac{0.15}{100} \times 1700 \times 300 = 765\ \text{mm}^2$

Use 10 mm bars, $A_\phi = 78.5398\ \text{mm}^2$

$$\text{Number of bars} = \frac{765}{78.5398} = 9.74 \approx 10\ \text{bars}$$

$$\text{Spacing of long bars} = 1700/10 = 170\ \text{mm}$$

Use 10 mm Φ bars for reinforcement @ 170 mm c/c.

C. Shear – One-Way Action: The critical section is taken at distance d away from the face of the column (side dimension of square column, $a = 0.4$ m).

$$\text{Shear force, } V_u = q\left[\left(\frac{B-a}{2}\right) - d\right] \tag{12.C.30}$$

$$V_u = 133 \times 1 \times \left[\left(\frac{1.7-0.40}{2}\right)\right] = 86.45\ \text{kN}$$

$$\text{Nominal shear stress, } \tau_v = \frac{V_u}{Bd} = \frac{86450}{1000 \times 270} = 0.32\ \text{N/mm}^2 \tag{12.C.31}$$

$$\%\ \text{area of steel, } p_r = \frac{864.72}{1000 \times 270} \times 100 = 0.32\%$$

Shear strength of M15 concrete with 0.32% steel, $\tau_c = 0.38\ \text{N/mm}^2 > \tau_v$ OK

Reinforcement details are shown in Figures 12.C.7(a) and (b).

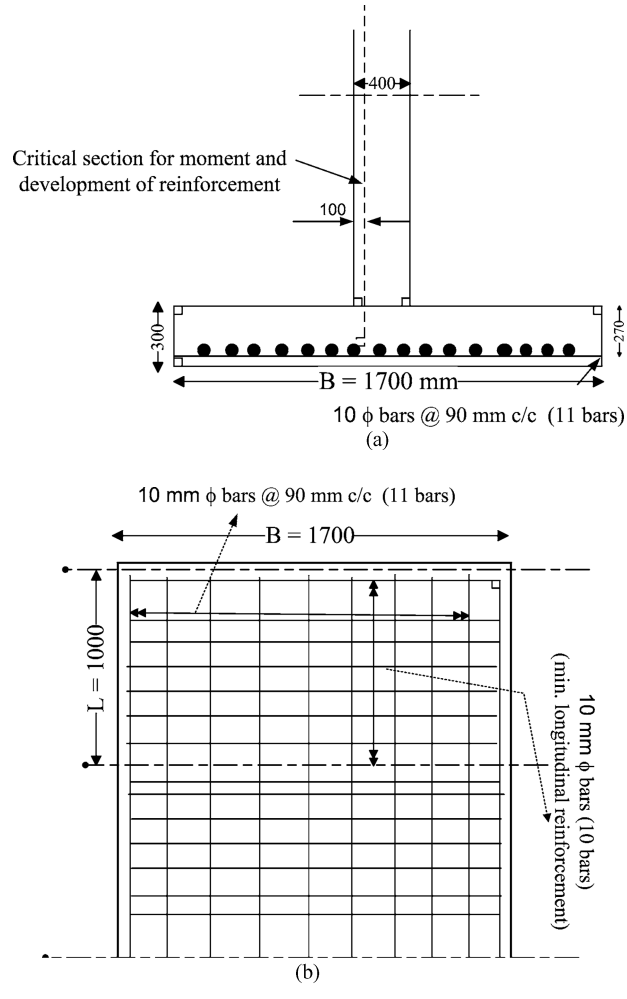

Figure 12.C.7 (a) Sectional elevation showing reinforcement; and (b) Reinforcement in the footing base (Example 12.3).

WINBEF Solution (BEF Method):

WINBEF Input

$$\text{Young's modulus of soil, } E_s = 10^5\ \text{kN/m}^2$$
$$\text{Unit weight of soil, } \gamma_{soil} = 17\ \text{kN/m}^3$$
$$\text{Poisson's ratio of soil, } v_s = 0.3$$

Young's modulus of concrete, $E_f = 5000\sqrt{15} = 19364.92\ \text{N/mm}^2 = 1.9364 \times 10^7\ \text{kN/m}^2$
Moment of inertia of the concrete beam, $I_f = \frac{Ld^3}{12} = \frac{1.0 \times 0.30^3}{12} = 0.0022\ \text{m}^4$

where L = breadth of foundation = 1.0 m (perpendicular to plane of the paper, that is, along the length of the continuous footing)

$$\text{Modulus of subgrade reaction,} \quad k_s = \frac{1}{L(\text{mm})}\left[0.65\sqrt[12]{\frac{E_s L^4}{E_f I_f}}\right]\frac{E_s}{1-\nu_s^2} \qquad (12.C.32)$$

$$k_s = \frac{0.65}{1000}\frac{10^5}{\left(1-0.3^2\right)}\sqrt[12]{\frac{10^5 \times 1.0^4}{1.9364 \times 10^7 \times 0.0022}} = \frac{76692}{1000} = 76.69\,\text{kN/m}^2/\text{mm}$$

Loading Data for WINBEF and Results

The loading data is shown in Figure 12.C.8. The details of deflection, bending moment, shear force and bearing pressure are shown in Figure 12.C.9. Table 12.C.3 shows the comparative study of the results.

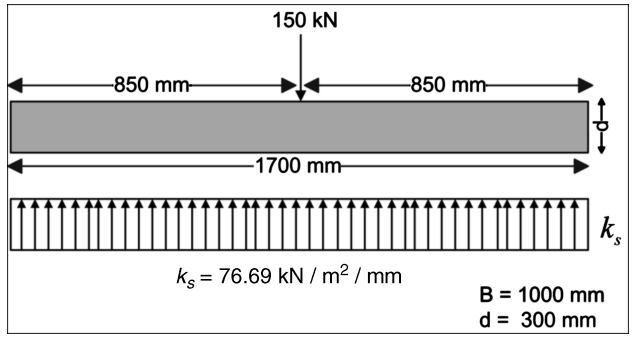

Figure 12.C.8 Details of loading and modulus of the subgrade reaction of a beam resting on an elastic foundation (Example 12.3).

Table 12.C.3 Comparative study (see comments in Section12.C.2).

		Maximum bearing pressure (kN/m^2)	Maximum bending moment (kNm)	Maximum shear force (kN)	Maximum deflection (mm)
Conventional design	With factored load (150 kN)	133	48.046	86.45	133/ks = 1.76
	With design load (100 kN)	133/1.5 = 88.67	48.04/1.5 = 32.03	86.45/1.5 = 55.63	1.76/1.5 = 1.173
Design using BEF (with design load only)		61.41	20.84	50.00	0.81

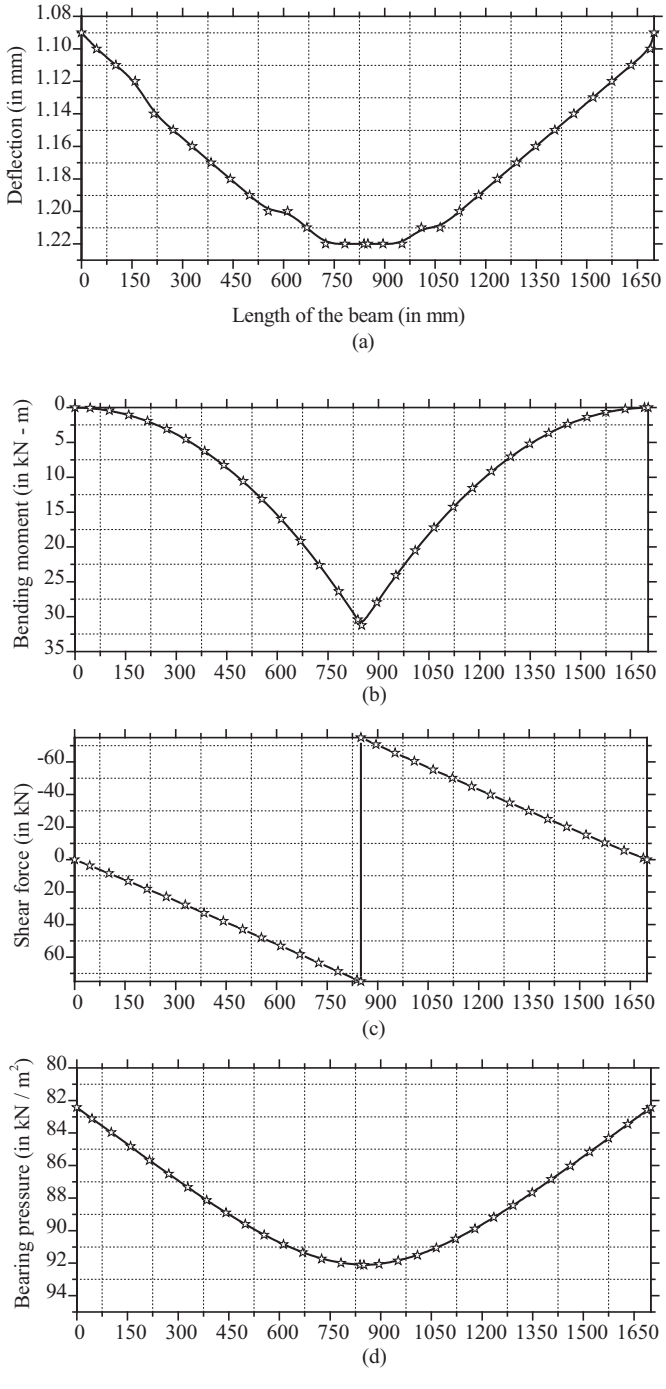

Figure 12.C.9 (a) BEF deflection diagram; (b) BEF bending moment diagram; (c) BEF shear force diagram; and (d) BEF bearing pressure diagram (Example 12.3).

Example 12.4 Combined Footing

Design a combined footing for two square columns A (40×40 cm) and B (50×50 cm) respectively carrying axial loads of 900 kN and 1200 kN with a spacing of 4 m c/c. They are reinforced longitudinally with 20 mm bars. The property line is at a distance of 0.5 m from the center line of the column A. ADSP of soil is 140 kN/m^2. Assume weight of footing and earth above as 10% of the total loads carried by the columns. Use M_{20} concrete mix and Fe 460 grade steel.

A. Length and Width of Footing: Center of gravity of loads from the property line

$$x = \frac{900 \times 0.5 + 1200 \times 4.5}{900 + 1200} 2.79 \text{ m} \cong 2.80 \text{ m}$$

$$\therefore \text{Length of the footing} = 2 \times 2.8 = 5.6 \text{ m}.$$

Use 5.6 m length of the footing. There will be a slight eccentricity of $5.6 - 5.58 = 0.02$ which will cause a moment of $2100 \times 0.02 = 42$ kNm with respect to the centroid of the footing. But this effect can be neglected and pressure beneath the footing will be assumed to be uniform. Assume weight of footing and earth above it as 10% of the total weight.

$$\text{Total load on soil} = 2100 \times 1.1 = 2310 \text{ kN}$$

$$\therefore \text{ Footing width, B} = \frac{2310}{5.6 \times 140} = 2.946 \text{ m} \cong 3.0 \text{ m}.$$

Adopt 3.0 m width of footing. The columns and loads are shown in Figure 12.C.10(a).

B. Longitudinal Bending Moment and Shear:

$$\text{Factored load on column A} = 1.5 \times 900 = 1350 \text{ kN}$$

$$\text{Factored load on column B} = 1.5 \times 1200 = 1800 \text{ kN}$$

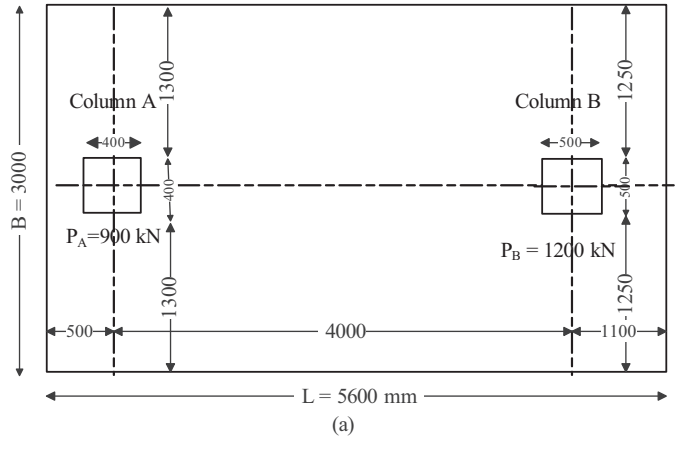

Figure 12.C.10 (a) Combined footing in plan; (b) shear force and bending moment diagrams; (c) plan of top reinforcement; and (d) plan of bottom reinforcement (Example 12.4).

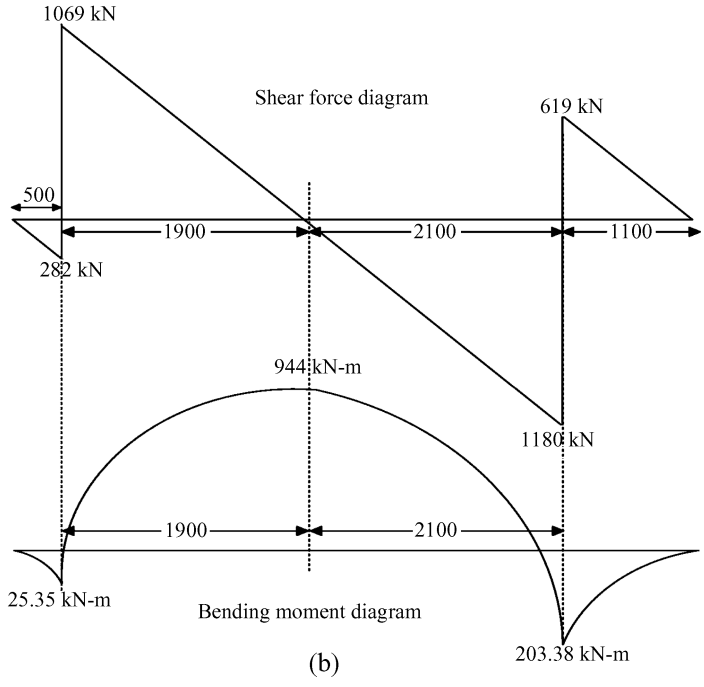

(b)

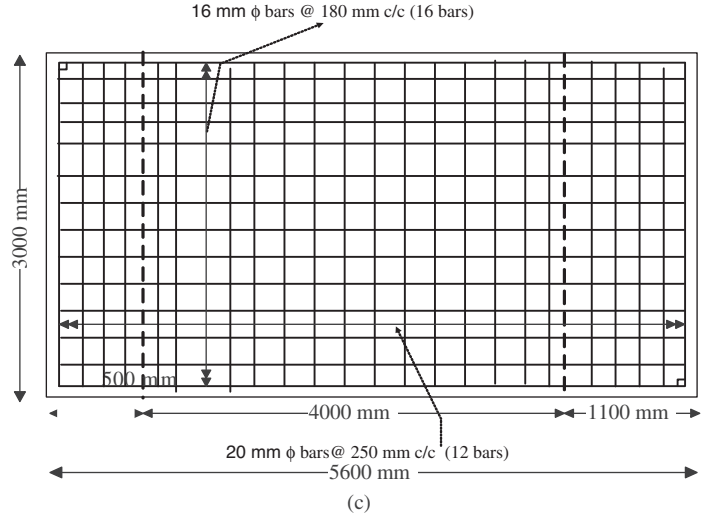

(c)

Figure 12.C.10 (*Continued*)

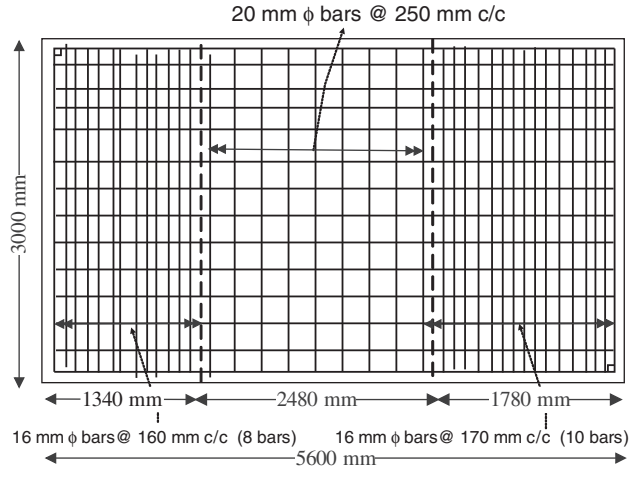

Figure 12.C.10 (*Continued*)

Net upward soil pressure, $q = \frac{1350 + 1800}{5.6 \times 3.0} = 187.5\,\text{kN/m}^2$

$$\text{Net upward soil pressure per unit length of footing} = 187.5 \times 3.0 = 562.5\,\text{kN/m} \cong 563\,\text{kN/m}$$

Maximum shear force at the center line of column A

$$V_1 = -563 \times 0.5 = -281.5\,\text{kN} \tag{12.C.33}$$

$$V_2 = -281.5 + 1350 = 1068.5\,\text{kN} \tag{12.C.34}$$

Maximum shear force at the center line of column B

$$V_3 = 563 \times 1.1 = 619.3\,\text{kN} \tag{12.C.35}$$

$$V_4 = -619.3 + 1800 = 1180.7\,\text{kN} \tag{12.C.36}$$

Point of zero shear force from the center line of column A

$$\frac{1069}{x} = \frac{1180}{4-x} \Rightarrow x = 1.90\,\text{m} \tag{12.C.37}$$

$$\text{Maximum BM computed from left side } M = 563 \times \frac{(0.5 + 1.90)^2}{2} - 1350 \times 1.90 = -943.56\,\text{kN}$$

$$\text{Maximum BM computed from right side} = 563 \times \frac{(1.1 + 2.1)^2}{2} - 1800 \times 2.1 = -897.44\,\text{kN}$$

There is a slight difference in the maximum BM computed at the same section with respect to the two sides of the footing. This is because of the slight eccentricity of the

resultant of the two footings. Take larger moment for computing depth of footing and reinforcement. The resulting shear force and bending moment diagrams are shown in Figure 12.C.10(b).

The effective depth required is $$d = \sqrt{\frac{M}{0.138 f_{ck} B}}$$

$$d = \sqrt{\frac{944 \times 10^6}{0.138 \times 20 \times 3000}} = 337.653 \text{ mm} \tag{12.C.38}$$

Adopt overall depth as 700 mm and effective depth as 660 mm.

C. Main Negative Longitudinal Reinforcement: Area A_{st1} of long bars calculated for moment, M_1 is given by

$$A_{st1} = 0.5 \frac{f_{ck}}{f_y} \left[1 - \sqrt{1 - \frac{4.6 \times M \times 10^6}{f_{ck} B d^2}}\right] Bd \tag{12.C.39}$$

$$A_{st1} = 0.5 \frac{20}{460} \left[1 - \sqrt{1 - \frac{4.6 \times 944 \times 10^6}{20 \times 3000 \times 660^2}}\right] 3000 \times 660 = 3738.07 \text{ mm}^2$$

$$\text{No of bars} = \frac{3738.06}{314.151} = 11.89 \cong 12$$

$$\text{Spacing of long bars} = \frac{3000}{12} = 250 \text{ mm}$$

Use 12–20 mm Φ bars for longitudinal reinforcement @ 250 mm c/c.

$$\text{Development length for } M_{20} \text{ concrete and Fe 460 grade steel} = L_d = \left(\frac{0.87 f_y}{4 \tau_{bd}}\right) \Phi \tag{12.C.40}$$

where $\tau_{bd} = 1.92$ for M_{20} concrete.

$$L_d = \left(\frac{0.87 \times 460}{4 \times 1.92}\right) \Phi = 52.11 \Phi$$

D. Shear – One-Way Action (Column B): The shear at a distance, d, from the face of the support is

$$V_u = 1180 + \left(\frac{0.5}{2} + 0.66\right) 563 = 667.67 \text{ kN}$$

$$\text{Nominal shear stress,} \quad \tau_v = \frac{V_u}{Bd} = \frac{668 \times 1000}{3000 \times 660} = 0.33 \text{N/mm}^2$$

$$\%\text{ area of steel}, \quad p_r = \frac{3738.06}{3000 \times 700} \times 100 = 0.178\%$$

Shear strength of M_{20} concrete with 0.178% steel, $\tau_c = 0.36\,\text{N/mm}^2 > \tau_v$ OK.

E. Shear – Two-Way Action: The critical section is taken at a distance $0.5d$ away from face of column.

$$\text{Net shear force at the periphery}, = 1800 - \left[\frac{0.5}{2} + \frac{d}{2}\right]^2 187.5$$

$$= 1800 - \left[\frac{0.5}{2} + \frac{0.66}{2}\right]^2 \times 187.5 = 1735.44\,\text{kN}$$

$$\text{Nominal shear stress}, \quad \tau_v = \frac{1735.44 \times 1000}{4\left[\left(0.5 + \frac{d}{2}\right)\right]d} = \frac{1735.44 \times 1000}{4\left[\left(0.5 + \frac{0.66}{2}\right)\right] \times 1000 \times 0.66}$$

$$= 0.792\,\text{N/mm}^2$$

Shear strength of M_{20} concrete

$$\tau_c^{\downarrow} = k_s \tau_c$$

$$k_s = 0.5 + \beta_c, \quad \beta_c = \frac{a}{b} \tag{12.C.41}$$

where

a = length of shorter side of column

b = length of longer side of column

$k_s = 0.5 + 1 = 1.5$ (should not be greater than one)

$$\therefore k_s = 1.0$$

$$\tau_c^{\downarrow} = \tau_c = 0.25\sqrt{f_{ck}} = 0.25\sqrt{20} = 1.12\,\text{N/mm}^2 > 0.792\,\text{N/mm}^2 \quad \text{OK.}$$

F. Points of Inflection: Let us assume that zero bending moment occurs at a distance, x, from the center of column A. Then taking moments about the point of inflection,

$$563 \times \frac{(0.5 + x)^2}{2} - 1350x = 0 \Rightarrow x = 0.067\,\text{m} \tag{12.C.42}$$

Similarly the point of inflection near column B can be obtained, that is

$$563 \times \frac{(1.1 + x)^2}{2} - 1800x = 0 \Rightarrow x = 0.311\,\text{m} \tag{12.C.43}$$

The shear force and bending moment diagrams are shown in Figure 12.C.10(b).Let us check development length at points of inflection. All the 12–20 mm bars extend through the inflection points.At column A inflection point:

$$M_1 = 944 \times 10^6 \left(\frac{3769.91}{3738.06}\right) = 951.83 \times 10^6\,\text{kNm}$$

$$V = 1069\,\text{kN} \quad (\text{at column A})$$
$$L_o = 500 + 65 - 25 = 540\,\text{mm}$$
$$L_d = 52.11\Phi$$
$$L_d \leq \frac{M_1}{V} + L_o \quad \text{or} \tag{12.C.44}$$
$$52.11\Phi \leq \frac{951.83 \times 10^6}{1069 \times 10^3} + 540$$

$1042.2\,\text{mm} \leq 1430.4\,\text{mm}$, hence it is OK.

At column B, inflection point

$$M_1 = 951.83 \times 10^6$$
$$V = 1180\,\text{kN}$$
$$L_o = d = 660 = 660\,\text{mm}$$
$$L_d = 52.11\Phi$$
$$L_d \leq \frac{M_1}{V} + L_o \quad \text{or}$$
$$52.11\Phi \leq \frac{951.83 \times 10^6}{1180 \times 10^3} + 660$$
$$1042.2\,\text{mm} \leq 1466.63\,\text{mm} \quad \text{Hence it is} \quad \text{OK.}$$

G. Positive Longitudinal Reinforcement at Bottom of Footing Beyond Column Faces

$$\text{Bending moment at the face of column A} = 563 \times \frac{0.3^2}{2} = 25.335\,\text{kNm}$$

$$\text{Bending moment at the face of column B} = 563 \times \frac{(1.1 - 0.5/2)^2}{2} = 203.383\,\text{kNm}$$

Area of tension steel is given by

$$A_t = 0.5\frac{f_{ck}}{f_y}\left[1 - \sqrt{1 - \frac{4.6 \times M \times 10^6}{f_{ck}Bd^2}}\right]Bd \tag{12.C.45}$$

$$A_{st1} = 0.5\frac{20}{460}\left[1 - \sqrt{1 - \frac{4.6 \times 203.383 \times 10^6}{20 \times 3000 \times 660^2}}\right]3000 \times 660 = 779.4783\,\text{mm}^2$$

$$\text{Minimum steel} = 0.15\% = \frac{0.15}{100}(3000 \times 700) = 3150\,\text{mm}^2$$

Use 16 mm bars

$$A_\phi = 201.06\,\text{mm}^2$$

$$\text{Number of bars} = \frac{3150}{201.06} = 15.66 \cong 16$$

$$\text{Spacing of long bars} = \frac{3000}{16} = 187.5\ \text{mm}$$

Use 16–16 mm Φ bars near the bottom of the slab for longitudinal reinforcement @ 180 mm c/c eight bars are curtailed at L_d (≅1500 mm) away from the point of maximum bending moment near column A. Similarly eight bars are curtailed at L_d (≅1500 mm) away from the point of maximum bending moment near column B ($1100 - \frac{500}{2} = 850$ mm).

The reinforcement details are shown in Figures 12.C.10(c) and (d).

H. Transverse Reinforcement: It is suggested that transverse reinforcement should be provided into groups proportionate in sectional area to the column loads. The transverse reinforcement under each column should be provided within a band having a width equal to the width of the column plus two times the effective depth of the foundation. The effective column band widths are shown in Figure 12.C.10(c).

Effective depth

$$\text{d} = 700 - 40(\text{cover}) - 20(\text{bar}) = 640\ \text{mm}.$$

$$\text{Width of bending strip at column A} = 400 + 2(640) = 1680\ \text{mm}.$$

However, width available to the left of outer face of column A = 500 − 200 = 300 mm only instead of 640 mm. Hence available band width (B_1) = 300 + 400 + 640 = 1340 mm.

$$\text{Factored upward pressure under column A} = \frac{1350}{3.0} = 450\ \text{kN/m}$$

$$\text{Bending moment at the face of column A} = 450 \times \frac{1.3^2}{2} = 380.25\ \text{kN-m}$$

Area of tension steel is given by

$$A_t = 0.5\frac{f_{ck}}{f_y}\left[1 - \sqrt{1 - \frac{4.6 \times M \times 10^6}{f_{ck} B_1 d^2}}\right] B_1 d$$

$$A_{st1} = 0.5\,\frac{20}{460}\left[1 - \sqrt{1 - \frac{4.6 \times 380.235 \times 10^6}{20 \times 1340 \times 640^2}}\right] 1340 \times 640 = 1549.76\ \text{mm}^2$$

Use 16 mm bars

$$A_\phi = 201.06\ \text{mm}^2$$

$$\text{Number of bars} = \frac{1549.6}{201.06} = 7.70 \cong 8$$

$$\text{Spacing of long bars} = \frac{1340}{8} = 167.5\ \text{mm}$$

Use 8–16 mm Φ bars in 1.34 m width under column A at the bottom of the slab @ 160 mm c/c.

$$\text{Factored upward pressure under column B} = \frac{1800}{3.0} = 600\,\text{kN/m}$$

$$\text{Bending moment at the face of column A} = 600 \times \frac{1.25^2}{2} = 468.75\,\text{kNm}$$

$$\text{Width of bending strip at column } B_2 = 500 + 2(640) = 1780\,\text{mm}.$$

Area of tension steel is given by

$$A_t = 0.5\frac{f_{ck}}{f_y}\left[1-\sqrt{1-\frac{4.6 \times M \times 10^6}{f_{ck}B_2d^2}}\right]B_2d$$

$$A_t = 0.5\frac{20}{460}\left[1-\sqrt{1-\frac{4.6 \times 468.75 \times 10^6}{20 \times 1780 \times 640^2}}\right]1780 \times 640 = 1904.26\,\text{mm}^2$$

Use 16 mm bars

$$A_\phi = 201.06\,\text{mm}^2$$

$$\text{Number of bars} = \frac{1904.26}{201.06} = 9.47 \cong 10$$

$$\text{Spacing of long bars} = \frac{1780}{10} = 178\,\text{mm}$$

Use 10–16 mm Φ bars in 1.78 m width under column B at the bottom of the slab @ 170 mm c/c. Full development length of L_d(≅1500 mm) for 20 mm bars is available in the transverse direction. In the remaining central portion provide temperature reinforcement consisting of 12 mm bars @ 250 mm c/c. The reinforcement details are shown in Figures 12.C.10(c) and (d).

WINBEF Solution (BEF Method):

WINBEF Input

$$\text{Young's modulus of soil, } E_s = 10^5\,\text{kN/m}^2$$

$$\text{Unit weight of soil, } y_{soil} = 20\ kN/m^3$$

$$\text{Poisson's ratio of soil, } v_s = 0.3$$

Young's modulus of concrete,

$$E_f = 5000\sqrt{20} = 22360.68\,\text{N/mm}^2 = 2.236 \times 10^7\,\text{kN/m}^2$$

$$\text{Moment of inertia of the concrete beam, } I_f = \frac{Bd^3}{12} = \frac{5.6 \times 0.660^3}{12} = 0.07187\,\text{m}^4$$

$$\text{Modulus of subgrade reaction, } k_s = \frac{1}{B(\text{mm})}\left[0.65\sqrt[12]{\frac{E_sB^4}{E_fI_f}}\right]\frac{E_s}{1-v_s^2}$$

$$k_s = \frac{0.65}{3000}\frac{10^5}{\left(1-0.3^2\right)}\sqrt[12]{\frac{10^5 \times 3.0^4}{2.236 \times 10^7 \times 0.07187}} = \frac{81735.50}{3000} = 27.245\,\text{kN/m}^2/\text{mm}$$

Loading Data for WINBEF and Results

The loading data is shown in Figure 12.C.11. The details of deflection, bending moment, shear force and bearing pressure are shown in Figure 12.C.12. Table 12.C.4 shows the comparative study of the results.

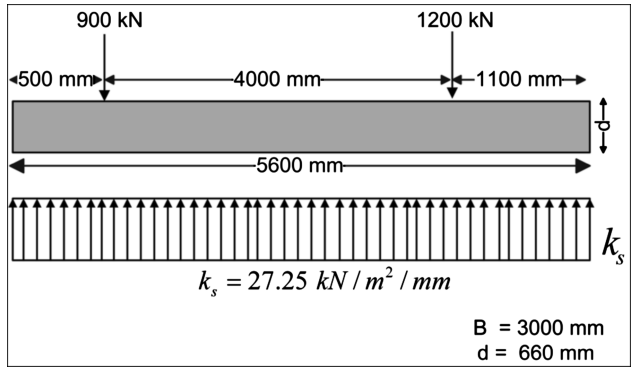

Figure 12.C.11 Details of loading and modulus of the subgrade reaction of a beam resting on an elastic foundation (Example 12.4).

Example 12.5 Combined Footing – Trapezoidal Shape

Design a combined footing (trapezoidal shape) for two square columns A (40 × 40 cm) and B(50 × 50 cm) respectively carrying axial loads of 900 kN and 1200 kN with a spacing of 4 m c/c with width of footing towards column A as 0.6 times the width of the footing on the side of column B. They are reinforced with 20 mm bars longitudinally. The property line is at a distance of 0.5 m from the left face of column A. ADSP of soil is 140 kN/m^2. Assume weight of footing and earth above as 10% of the total loads carried by the columns. Use M 20 concrete mix and Fe 460 grade steel. (The data is the same as for Example 12.4.)

Thus, factored load of Column A = 1350 kN and factored load of Column B = 1800 kN.

Weight of footing and earth above = (1200 × 900) × 0.1 = 210 kN

The footing is shown in Figure 12.C.13(a).

Let the widths of footing be B_1 and B_2 as shown in Figure 12.C.13(a). The values of B_1 and B_2 should be such that C.G of footing coincides with the C.G of the column loads.

Total area required for the footing

$$\frac{(B_1 + B_2)L}{2} = \frac{W_1 + W_2 + 10\%(W_1 + W_2)}{q_o} \tag{12.C.46}$$

where $W_1 = P_A = 900$ kN and $W_2 = P_B = 1200$ kN.

$$\text{It is given that } B_1 = 0.6\,B_2 \tag{12.C.47}$$

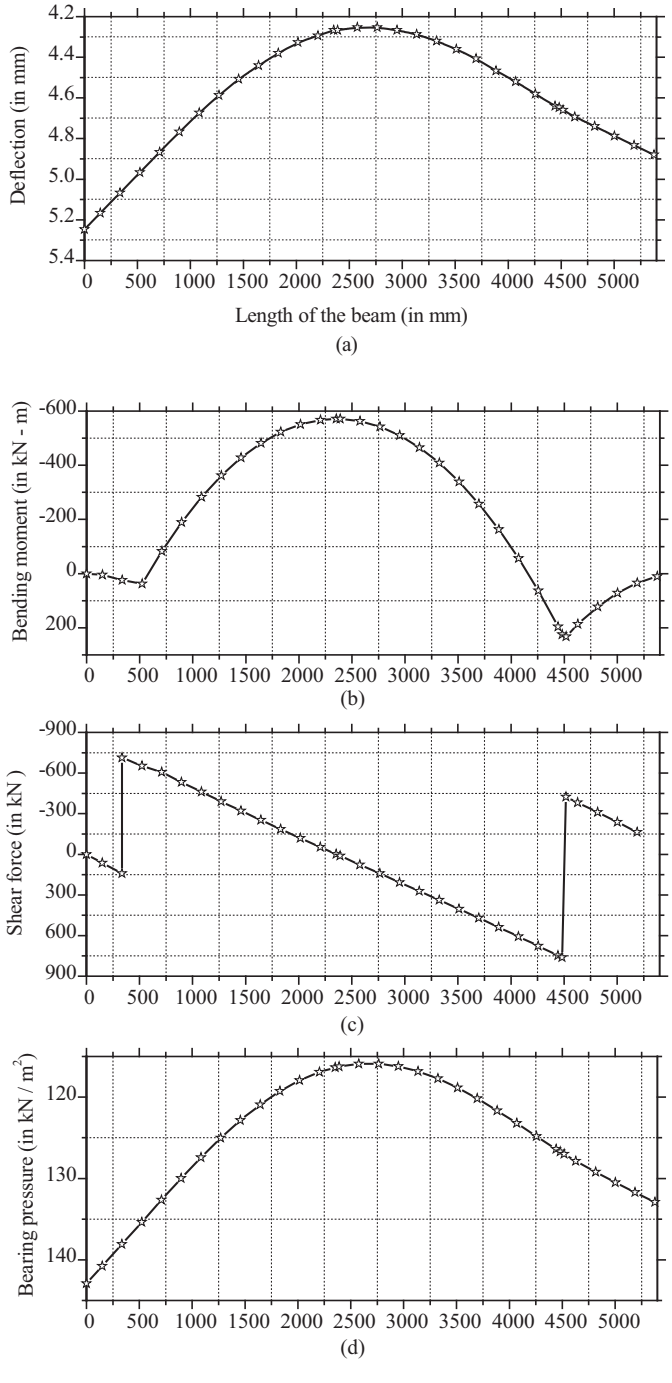

Figure 12.C.12 (a) BEF deflection diagram; (b) BEF bending moment diagram; (c) BEF shear force diagram; and (d) BEF bearing pressure diagram (Example 12.4).

Table 12.C.4 Comparative study (see comments in Section 12.C.2).

		Maximum bearing pressure (kN/m^2)	Maximum bending moment (kNm)	Maximum shear force (kN)	Maximum deflection (mm)
Conventional design	With factored load	187.5	944 at $x = 2400$ mm	1180 at $x = 4500$ mm; -1069 at $x = 500$ mm	$187.5/k_s = 6.88$
	With design load	$187.5/1.5 = 125$	$944/1.5 = 629.33$ @ $x = 2400$ mm	$1180/1.5 = 786.67$ at $x = 4500$ mm $-1069/1.5 = 712.67$ at $x = 500$ mm	$6.88/1.5 = 4.60$
Design using BEF (with design load only)		142.921 kN/m^2 at $x = 0$ mm	232.135 kNm at $x = 4517$ mm; -571.211 kNm at $x = 2352$ mm	760.936 kN at $x = 4480$ mm; -681.810 kN at $x = 523$ mm	5.25

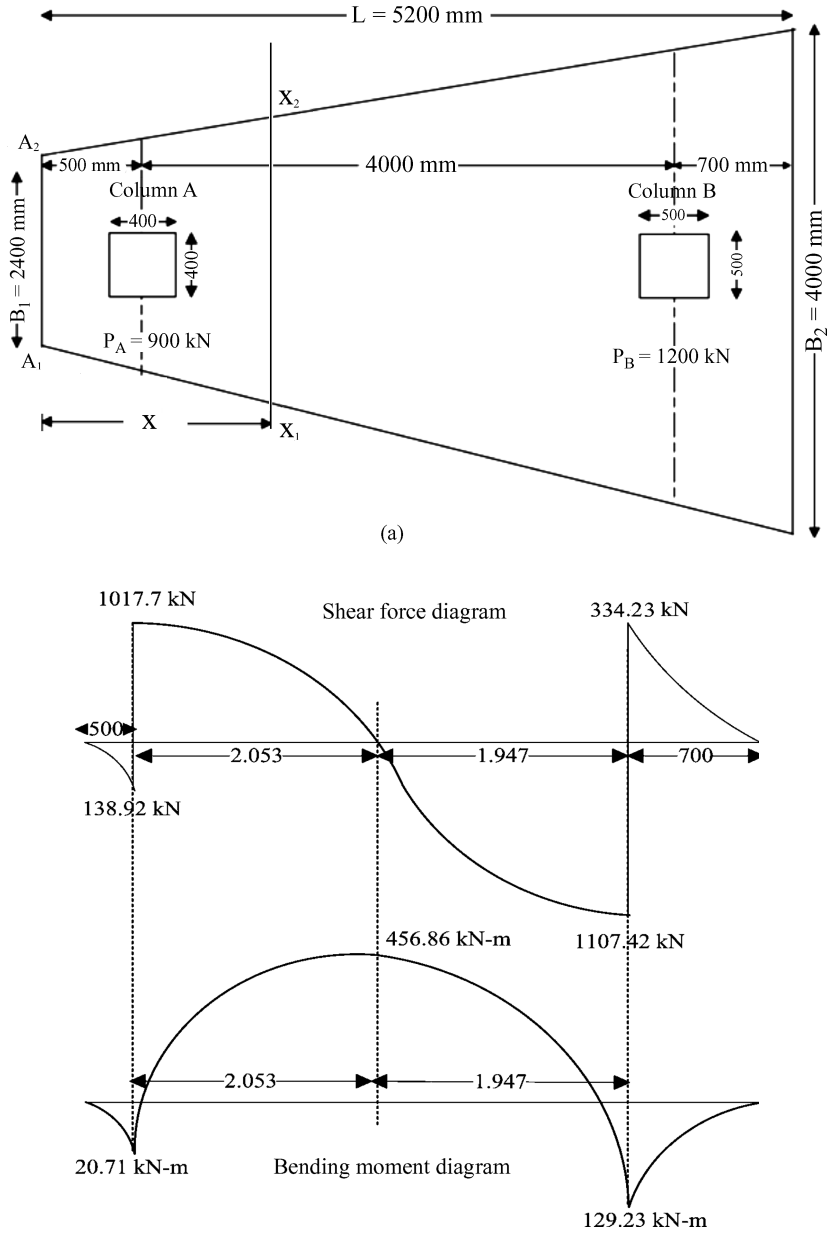

Figure 12.C.13 (a) Combined footing in plan (with design loads); (b) shear force and bending moment diagrams (with factored loads); and (c) reinforcement details (Example 12.5).

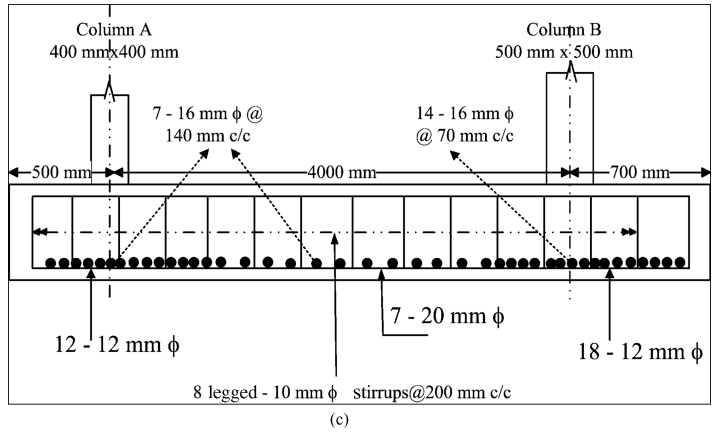

Figure 12.C.13 (*Continued*)

$$\frac{(B_1 + B_2)L}{2} = \frac{(900 + 1200 + 210)}{140}$$

$$\frac{1.6B_2L}{2} = 16.5$$

$$B_2L = 20.625$$

$$\text{Distance of C.G of load} = \frac{W_2 l}{W_1 + W_2} = \frac{1200 \times 4}{900 + 1200} = 2.285 \cong 2.3\,\text{m}$$

$$\text{Distance of C.G of load from the edge } B_1 = 0.5 + 2.3 = 2.8\,\text{m} \tag{12.C.48}$$

$$\text{Distance of C.G of footing from edge } B_1 = \frac{L}{3}\left(\frac{B_1 + 2B_2}{B_1 + B_2}\right) = 2.8 \tag{12.C.49}$$

From Equation (12.C.49), we get $\frac{L}{3}\left(\frac{2.6B_2}{1.6B_2}\right) = 2.8$
Hence, $L = 5.1692\,\text{m} \cong 5.2\,\text{m}$

$$B_2 = 3.966\,\text{m} \cong 4.0\,\text{m}; \quad B_1 = 2.4\,\text{m}$$

Net upward soil pressure intensity is given by (taking factored loads into consideration)

$$p_o = \frac{(W_1 + W_2)}{\frac{1}{2}(B_1 + B_2)L} = \frac{(900 + 1200)1.5}{\frac{1}{2}(2.4 + 4)5.2} = 189.30\,\text{kN/m} \tag{12.C.50}$$

A. Bending Moment and Shear Force: Consider the bending of the footing in the longitudinal direction. At any distance, x from the face A_1A_2 (Figure 12.C.13(a)), the width of section X_1X_2 is given by

$$B_x = B_1 + \left(\frac{B_2 - B_1}{L}\right)x = 2.4 + \left(\frac{4 - 2.4}{5.2}\right)x = 2.4 + 0.308x$$

$$\therefore \text{ Area } A_x \text{ to the left of section } X_1X_2 \text{ is given by} = \frac{1}{2}(B_1 + B_x)x$$

$$A_x = \frac{1}{2}(2.4 + (2.4 + 0.308x))x = \frac{x}{2}(4.8 + 0.308x)$$

$$\text{Distance of C.G from section } X_1X_2 = \frac{x}{3}\left(\frac{2B_1 + B_x}{B_1 + B_x}\right) = \frac{x}{3}\left(\frac{2 \times 2.4 + (2.4 + 0.308x)}{2.4 + (2.4 + 0.308x)}\right)$$

$$= \frac{x}{3}\left(\frac{7.2 + 0.308x}{4.8 + 0.308x}\right)$$

$$\text{Hence, total upward force to the left of } X_1X_2 = \frac{p_o x}{2}(4.8 + 0.308x)$$

$$= \frac{189.3x}{2}(4.8 + 0.308x)$$

$$= 94.65x(4.8 + 0.308x)$$

$\therefore$ Shear force (SF) at outer face of column of A, where $x = 0.3$ is given by

$$F_1 = 94.65 \times 0.3 \times (4.8 + 0.308 \times 0.3) = 138.92 \text{ kN}$$

$$\text{SF at } x \text{ to the right of A} = 1350 - 94.65x(4.8 + 0.308x) \tag{12.C.51}$$

SF at inner face of column A, where $x = 0.5 + 0.2 = 0.7$ m, is given by

$$F_2 = 1350 - 94.65 \times 0.7 \times (4.8 + 0.308 \times 0.7) = 1017.70 \text{ kN}$$

To find the position of the section where SF is zero, equate Equation (12.C.51) to zero, that is

$$1350 - 94.65x(4.8 + 0.308x) = 0.0 \tag{12.C.52}$$

$$1350 - (454.32x + 29.152x^2) = 0.0$$

$$29.152x^2 + 454.32x - 1350 = 0.0 \;\Rightarrow\; x = 2.553 \text{ m}$$

Bending moment (BM) at section X_1X_2 is given by

$$M_2 = 1350(x-1) - (\text{upward force} \times \text{distance of its C.G})$$

$$= 1350(x-1) - \left\{94.65x(4.8 + 0.308x)\left[\frac{2 \times 2.4 + (2.4 + 0.308x)}{2.4 + (2.4 + 0.308x)}\right]\frac{x}{3}\right\} \tag{12.C.53}$$

$$= 1350(x-1) - 31.55x^2(7.2 + 0.308x)$$

The maximum hogging bending moment (M_1) occurs at $x = 2.553$ m, where SF is zero.

$$\therefore M_1 = 1350(2.55-1) - 31.55(2.55)^2[7.2 + 0.308(2.55)] = 456.86 \text{ kN-m}$$

To find the value of x when M_x is zero, equate Equation (12.C.53) to zero, that is

$$\begin{aligned} M_x &= 1350(x-1) - 31.55x^2(7.2 + 0.308x) = 0.0 \\ &= 9.7174x^3 + 227.16x^2 - 1350x + 1350 = 0.0 \end{aligned} \tag{12.C.54}$$

Solving this by trial and error, we get $x = 1.30$ m and 3.76 m.

Thus the position of both the points of contraflexure is known. For getting the value of SF (F_3) at the first point of contraflexure, put $x = 1.30$ m in Equation (12.C.51) that is

$$F_3 = 1350 - 94.65 \times 1.30 \times (4.8 + 0.308 \times 1.30) = 709.90\,\text{kN}$$

Similarly, SF (F_4) at $x = 3.76$ m is

$$F_4 = 1350 - 94.65 \times 3.76 \times (4.8 + 0.308 \times 3.76) = -768.566\,\text{kN}$$

SF at the inner face of column of B, at $x = 4.25$ m is

$$F_5 = 1350 - 94.65 \times 4.25 \times (4.8 + 0.308 \times 4.25) = -1107.42\,\text{kN}$$

SF at the outer face of column of B, at $x = 4.75$ m is

$$F_6 = 1350 - 94.65 \times 4.75 \times (4.8 + 0.308 \times 4.75) + 1800 = 334.23\,\text{kN}$$

Sagging bending moment (M_2) at the outer face of column A is obtained by putting $x = 0.3$ m in the second term of Equation (12.C.53) and neglecting the first term, that is

$$M_2 = 31.55(0.3)^2[7.2 + 0.308(0.3)] = 20.71\text{kNm}$$

Sagging bending moment for the cantilever portion to the right of column of B is given by

$$M_x = 31.55(0.3)^2[7.2 + 0.308(0.3)] - 1350(x - 0.5) - 1800(x - 4.5)$$

Putting $x = 4.75$ m, we get BM (M_3) at the outer face of column B, as shown below

$$M_3 = 31.55(4.75)^2[7.2 + 0.308(4.75)] - 1350(4.75 - 0.5) - 1800(4.75 - 4.5) = 129.23\,\text{kN-m}$$

The BM and SF diagrams are shown in Figure 12.C.13(b).

The SF diagram differs slightly at the column centerlines as the values calculated above are at the inner and outer faces of the columns though they are shown at the centerlines of columns in the SF diagram where the actual jump discontinuities are 1350 kN and 1800 kN.

The effective depth is determined on the basis of the hogging moment, $M_1 = 456.86$kNm, which is the maximum bending moment in the footing. It occurs at a section distant, $x = 2.553$ m from edge A_1A_2. The width B_x at that section is given by

$$B_x = 2.4 + 0.308(2.55) = 3.1854\,\text{m}$$

$$\therefore\ d = \sqrt{\frac{M_1}{0.138 f_{ck} B_x}} \tag{12.C.55}$$

$$d = \sqrt{\frac{456.86 \times 10^6}{(0.138 \times 20 \times 3185.4)}} = 227.96\,\text{mm}$$

This depth should be sufficient from punching shear point of view. Punching shear will be maximum near column B, where load $W_2 = 1800$ kN.

Side $b_o = b + d = (500 + d)$ mm where b is the width of the column.

$$\text{Punching shear } F = W_2 - p_o b_o^2 \tag{12.C.56}$$

$$F = 1800 - \frac{189.3(500+d)^2}{1000}\ \text{kN}$$

$$\tau_v = \frac{\left[1800\times 10^3 - 0.1893(500+d)^2\right]}{[4(500+d)d]}$$

$$\text{Permissible shear stress} = k_s\tau_c = 1\times\tau_c = 0.25\sqrt{f_{ck}} = 1.118\text{N/mm}^2$$

$$\tau_v = \frac{\left[1800\times 10^3 - 0.1893(500+d)^2\right]}{[4(500+d)d]} = 1.118\,\text{N/mm}^2$$

Rearranging the above terms, we get $4.6613d^2 + 2425.3d - 1758675.00 = 0.0$

From which we can obtain $d = 405.96$ mm which is greater than the one found from bending compression. Anyhow, keep $D = 500$ mm.

Using 60 mm cover, effective depth, $d = 500 - 60 = 440$ mm.

B. Reinforcement in the Longitudinal Direction

1. Reinforcement for hogging bending moment, M_1

Area A_{st1} of long bars calculated for moment, M_1, is given by

$$A_{st1} = 0.5\frac{f_{ck}}{f_y}\left[1 - \sqrt{1 - \frac{4.6\times M_1\times 10^6}{f_{ck}B_x d^2}}\right]B_x d$$

The width of the section at $x = 2.553$ m, $B_x = 2.4 + 0.308\times 2.55 = 3185.40$ mm

$$A_{st1} = 0.5\frac{20}{460}\left[1 - \sqrt{1 - \frac{4.6\times 456.86\times 10^6}{20\times 3185.40\times 440^2}}\right]3185.40\times 440 = 2047.03\,\text{mm}^2$$

Use 20 mm bars, $A_\phi = 314.151$ mm^2

$$\text{Number of bars} = \frac{2047.03}{\frac{\pi}{4}20^2} = 6.52 \cong 7$$

$$\text{Spacing of long bars} = \frac{3185.40}{7} = 455\ \text{mm}$$

Use 7–20 mm Φ bars for longitudinal reinforcement @ 450 mm c/c.

Thus, provide seven bars at the top face of the footing. These bars should be checked for development length at each point of contraflexure, to satisfy the criteria

$$\frac{M_1}{V} + L_o \geq L_d \tag{12.C.57}$$

Out of these two points of contraflexure in the hogging bending moment range, the one near column B, has maximum shear force $V = F_4 = 768.566\,\text{kN}$

$$M_1 = 468.80\,\text{kNm}$$

$$L_o = 12\Phi(240\,\text{mm}) \text{ or } d(440\,\text{mm}) \text{ whichever is more} = 440\,\text{mm}$$

$$L_d = \left(\frac{0.87 f_y}{4\tau_{bd}}\right)\Phi = \left(\frac{0.87 \times 460}{4 \times 1.92}\right)\Phi = 52.11\Phi$$

$$L_d = 1042.2\,\text{mm}$$

$$\frac{468.80 \times 10^6}{768.566 \times 10^3} + 440 \geq 52.11 \times 20$$

$$1046.576 \geq 1042.2 \quad \text{Hence it is OK.}$$

So all *seven* bars are taken up to the point of contraflexure. These bars are to be taken beyond this point for a distance of 12Φ (240 mm) or 440 mm, whichever is more. After that, curtail four bars and continue three bars straight up to edge of the footing, so that these may serve as anchorage bars for shear stirrups.

2. Reinforcement for sagging bending moment, M_3, near outer face of column

The width of the section at $x = 4.75$ m is $B_x = 2.4 + 0.308 \times 4.75 = 3863$ mm

$$A_{st3} = 0.5\frac{20}{460}\left[1 - \sqrt{1 - \frac{4.6 \times 20.77 \times 10^6}{20 \times 3863 \times 440^2}}\right] 3863 \times 440 = 73.445\,\text{mm}^2$$

$$\therefore \text{ Minimum reinforcement @ } 0.12\% = \left(\frac{0.15}{100}\right) \times 3863 \times 440 = 2039.66\,\text{mm}^2$$

Use 12 mm bars, $A_\phi = 113.09\,\text{mm}^2$

$$\text{Number of bars} = \frac{2039.66}{\frac{\pi}{4}12^2} \cong 18 \text{ bars}$$

$$\text{Spacing of long bars} = \frac{3863}{18} = 214.611\,\text{mm}$$

Use 18–12 mm Φ bars for longitudinal reinforcement @ 200 mm c/c.

This reinforcement should be checked for development length at the point of contraflexure, near inner face of column B, so as to satisfy the criteria

$$1.3\left(\frac{M_3}{V}\right) + L_o \geq L_d$$

$M_3 = 129.23\,\text{kNm}, L_o = 12\Phi(144\,\text{mm})$ or $d(440\,\text{mm})$ whichever is more $= 440\,\text{mm}$

$$1.3\left(\frac{129.23 \times 10^6}{768.5 \times 10^3}\right) + L_o \geq L_d$$

$$V = F_4 = 768.5\,\text{kN}$$

$$1.3\left(\frac{129.23\times10^6}{768.5\times10^3}\right)+440\geq L_d=\left(\frac{0.87f_y}{4\tau_{bd}}\right)\Phi=\left(\frac{0.87\times460}{4\times1.92}\right)\Phi=52.11\Phi$$

$$658.36\geq 625.20.$$

Hence it is safe, provided all the 18 bars are available at the point of contraflexure. However, these bars are to be taken beyond this point for a distance of 12Φ (144 mm) or 440 mm, whichever is more. After that curtail ten bars and continue eight bars straight up to edge of the footing so that these may serve as anchorage bars for shear stirrups.

3. Reinforcement for sagging bending moment, M_2, near other face of column A

The width of the section at $x = 0.3$ m is $B_x = 2.4 + 0.308\times0.3 = 2500$ mm

$$A_{st2}=0.5\frac{20}{460}\left[1-\sqrt{1-\frac{4.6\times20.71\times10^6}{20\times2500\times440^2}}\right]2500\times440=117.961\ \text{mm}^2$$

$$\therefore\ \text{Min reinforcement @}\ 0.12\%=\left(\frac{0.12}{100}\right)\times2500\times440=1320\ \text{mm}^2$$

Use 12 mm bars, $A_\phi = 113.09\ \text{mm}^2$

$$\text{Number of bars}=\frac{1320}{\frac{\pi}{4}12^2}\cong 12\ \text{bars}$$

$$\text{Spacing of long bars}=\frac{2500}{12}=208.33\ \text{mm}$$

Use 12–12 mm Φ bars for longitudinal reinforcement @ 200 mm c/c.

This reinforcement should be checked for development length at the point of contraflexure, near column A, so as to satisfy the criteria

$$1.3\left(\frac{M_2}{V}\right)+L_o\geq L_d \tag{12.C.58}$$

$$M_2=0.87f_yA_{st}\left(d-\frac{\sigma_yA_{st}}{\sigma_{ck}B}\right) \tag{12.C.59}$$

$$M_2=0.87\times460\times1320\times\left(440-\frac{460\times1320}{20\times2500}\right)=230.29\,\text{kNm}$$

$$L_o=12\Phi(144\ \text{mm})\ \text{or}\ d(440\ \text{mm}),\ \text{whichever is more}\ =440\ \text{mm}$$

$$1.3\left(\frac{230.29}{V}\right)+L_o\geq L_d$$

$$V=F_3=709.90\,\text{kN}$$

$$1.3\left(\frac{230.29\times10^6}{709.90\times10^3}\right)+440\geq L_d=\left(\frac{0.87f_y}{4\tau_{bd}}\right)\Phi=\left(\frac{0.87\times460}{4\times1.92}\right)\Phi=52.11\Phi$$

$$861.717\geq 625.20.\quad \text{Hence it is safe.}$$

However extend the bars up to $L_o = d$(i.e., 440 mm) from the point of contraflexure, that is, 0.5 + 0.2 + 0.440 = 1.140 m from the edge of the footing. After that curtail four bars but continue the remaining eight bars.

C. Check for Diagonal Tension: Test for the diagonal tension should be made in the cantilever portion at a distance d from the column face. In the present case, $d = 400$ mm = 0.4 m. At 0.4 m from the outer face of column B, distance $x = 4 + 0.7 + 0.2 + 0.44 =$ 5.34 m. At this section shear force is extremely small and available width B_x is large. Hence shear stress will be small. Similarly, for the cantilever portion to the left of the column A, shear force and hence shear stress will be small.

For diagonal tension between A and B, near column B, crack can occur at the bottom of the footing (i.e., for hogging BM) at a distance $d = 440$ mm, or at the top of footing (i.e., hogging BM) at the point of contraflexure distant from the center of column B. When the point of contraflexure is nearer, more SF are at the point. SF at point of contraflexure $= F_4 =$ 768.566 kN.

At the point of contraflexure $x = 3.75$, $B_x = 2.4 + 0.308 \times 3.75 = 3555$ mm

$$\tau_v=\frac{768.566\times10^3}{3555\times440}=0.4913\ \text{N/mm}^2$$

$$\frac{100A_s}{Bd}=\frac{100\times2047}{3555\times440}=0.13\%$$

Hence for 0.13% steel $\tau_c = 0.36\ \text{N/mm}^2$(for M_{20} concrete).

.Thus, actual shear stress is more than the permissible one, and shear reinforcement is necessary.

$$V_c=\tau_cBd=0.36\times3555\times440=563112\ \text{N}=563.112\ \text{kN}$$

$$V_s=V-V_c=768.566-563.112=205.454\ \text{kN}$$

Using 10 mm Φ 8-legged stirrups $A_{sv}=8\times\frac{\pi}{4}(10^2)=628.318\ \text{mm}^2$

$$S_v=\frac{0.87f_yA_{sv}d}{V_{us}}=\frac{0.87\times460\times628.318\times440}{205.454\times10^3}=538.511\ \text{mm}$$

Maximum spacing of nominal stirrups is given by

$$S_{v\max}=\frac{2.5A_{sv}f_y}{B}=\frac{2.5\times628.318\times460}{3555}=203.253\ \text{mm}$$

$S_{v\min}$ = 0.75d or 450 mm whichever is less

= 330 or 450 mm whichever is less

$S_{v\min}$ = 330 mm

Hence provide these nominal stirrups @ 200 mm c/c throughout the length.

D. Transverse Reinforcement: The footing will bend transversely near column face. Projection $a_2^{|}$ beyond the face of the column

$$B = \frac{1}{2}(B_x - b_2) \tag{12.C.60}$$

where B_x is the width of footing at the center of the column B, where $x = 4.5$ and $b_2 =$ column width $= 0.5$ m.

$$B_x = 2.4 + 0.308 \times 4.5 = 3.786 \text{ m}$$

$$a_2^{|} = \frac{1}{2}(3.786 - 0.5) = 1.6430 \text{ m}$$

$$\text{Width of bending strip near column B} = 440 + 500 + 440 = 1380 \text{ mm}$$

$$\therefore \text{ Average area of bending strip} = 3.786 \times 1.380 = 5.2246 \text{ m}^2$$

$$\text{Net upward pressure } p_o^{|} = \frac{1800}{5.2246} = 344.52 \text{ kN/m}^2$$

(This is approximately double the value of average pressure, p_o.)

Maximum bending moment at the face of the column is

$$M = 344.52 \times \frac{(1.6430)^2}{2} = 465 \text{ kNm}$$

$$d_{\text{required}} = \sqrt{\frac{465 \times 10^6}{0.138 \times 20 \times 3.786 \times 1000}} = 210.95 \text{ mm}$$

Actual d available is 440 mm. Hence the transverse beam, of width $= 1.38$ m will be of the same thickness as the remaining footing. The transverse reinforcement is given by

$$A_{st} = 0.5 \frac{20}{460} \left[1 - \sqrt{1 - \frac{4.6 \times 465 \times 10^6}{20 \times 3786.40 \times 440^2}}\right] 3786 \times 440 = 2741.81 \text{ mm}^2$$

Use 16 mm bars, $A_\phi = 201.061$ mm^2

$$\text{Number of bars} = \frac{2741.81}{\frac{\pi}{4}16^2} \cong 14$$

$$\text{Spacing of long bars} = \frac{3786}{14} = 73.33 \text{ mm}$$

Use 14–16 mm Φ bars for transverse reinforcement @ 70 mm c/c

Similarly for column A, width $B_x$at the center of column, where $x = 0.5$

$$B_x = 2.4 + 0.308 \times 0.5 = 2.55 \text{ m}$$

$$\text{Projection } a_1^{|} = \frac{1}{2}(2.55 - 0.4) = 1.075$$

$$\text{Width of bending strip} = 2 \times 440 + 400 = 1280\,\text{mm}$$

$$\therefore \text{Area of bending strip} = 2.55 \times 1.28 = 3.264\,\text{m}^2$$

$$\text{Net upward pressure } p_o^{\downarrow} = \frac{1352}{3.264} = 413.60\,\text{kN/m}^2$$

Maximum bending moment at the face of the column is given by

$$M = 413.60 \times \frac{1.075^2}{2} = 238.98\,\text{kNm}$$

The available depth $d = 440\,\text{mm}$ is sufficient. Area of transverse reinforcement is

$$A_{st} = 0.5\frac{20}{460}\left[1-\sqrt{1-\frac{4.6 \times 238.98 \times 10^6}{20 \times 2550 \times 440^2}}\right]2550 \times 440 = 1396.21\,\text{mm}^2$$

Use 16 mm bars, $A_\phi = 201.061\,\text{mm}^2$

$$\text{Number of bars} = \frac{1396.21}{\frac{\pi}{4}16^2} \cong 7\,\text{bars}$$

$$\text{Spacing of long bars} = \text{s} = \frac{1000\left(\frac{\pi}{4}16^2\right)}{1396.21} = 143.98\,\text{mm}$$

Use 7–16 mm Φ bars for transverse reinforcement @ 140 mm c/c in the strip of width 1.28 m. For the remaining portion, provide 16 mm Φ bars @ 140 mm c/c, so that this reinforcement at any section is not less than 0.12% of the cross-sectional area. The details of reinforcement and so on are shown in Figure 12.C.13(c).

WINBEF Solution (BEF Method):

WINBEF Input

Young's modulus of soil, $E_s = 10^5\,\text{kN/m}^2$, Unit weight of soil, $\gamma_{soil} = 20\,\text{kN/m}^3$
Poisson's ratio of soil, $v_s = 0.3$
Young's modulus of concrete, $E_f = 5000\sqrt{20} = 22360.68\,\text{N/mm}^2 = 2.236 \times 10^7\,\text{kN/m}^2$
Moment of inertia of the concrete beam, $I_{f1} = \frac{Bd^3}{12} = \frac{2.4 \times 0.440^3}{12} = 0.01703\,\text{m}^4$

$$I_{f2} = \frac{Bd^3}{12} = \frac{4.0 \times 0.440^3}{12} = 0.02839\,\text{m}^4$$

Modulus of subgrade reaction

$$k_s = \frac{1}{B(\text{mm})}\left[0.65\sqrt[12]{\frac{E_s B^4}{E_f I_f}}\right]\frac{E_s}{1-v_s^2}$$

$$k_{s1} = \frac{0.65}{2400}\frac{10^5}{(1-0.3^2)}\sqrt[12]{\frac{10^5 \times 2.4^4}{2.236 \times 10^7 \times 0.01703}} = \frac{85550}{2400} = 35.64\,\text{kN/m}^2/\text{mm}$$

$$k_{s2} = \frac{0.65}{4000}\frac{10^5}{(1-0.3^2)}\sqrt[12]{\frac{10^5 \times 4.0^4}{2.236 \times 10^7 \times 0.02839}} = \frac{97201.32}{4000} = 24.30\,\text{kN/m}^2/\text{mm}$$

The data is shown below in Figure 12.C.14.

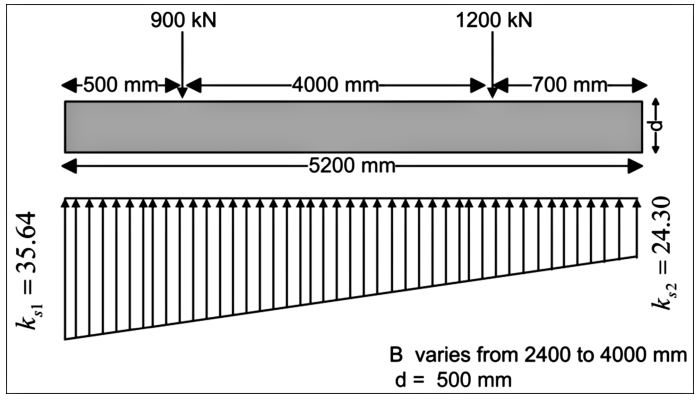

Figure 12.C.14 Details of loading and modulus of the subgrade reaction of a beam resting on an elastic foundation (Example 12.5).

Loading Data for WINBEF and Results

The loading data is shown in Figure 12.C.14. The details of deflection, bending moment, shear force and bearing pressure are shown in Figure 12.C.15. Table 12.C.5 shows the comparative study of the results.

Example 12.6 Strap Footing

Design a strap footing for two square columns A (40×40 cm) and B (50×40 cm) carrying axial loads of 900 kN and 1200 kN with a c/c spacing of 6 m. The columns are reinforced with 20 mm bars longitudinally and are to be supported by square footings. The property line is at a distance of 0.5 m from the left face of column A. ADSP of soil = 140 kN/m^2. Assume weight of footing and earth above is 10% of the total loads carried by the columns. Use M_{20} concrete mix and Fe 460 grade steel. (This example is similar to Example 12.4 but a strap footing has to be designed now.)

Figure 12.C.16(a) shows the general arrangement of the footing.

Let the width of footings be B_1 and B_2 as shown in Figure 12.C.16(a). The values of B_1 and B_2 should be such that the C.G of the footing coincides with the C.G of the column loads. Length of footing under A = B_1 and length of footing under B = B_2 centrally arranged under A and B

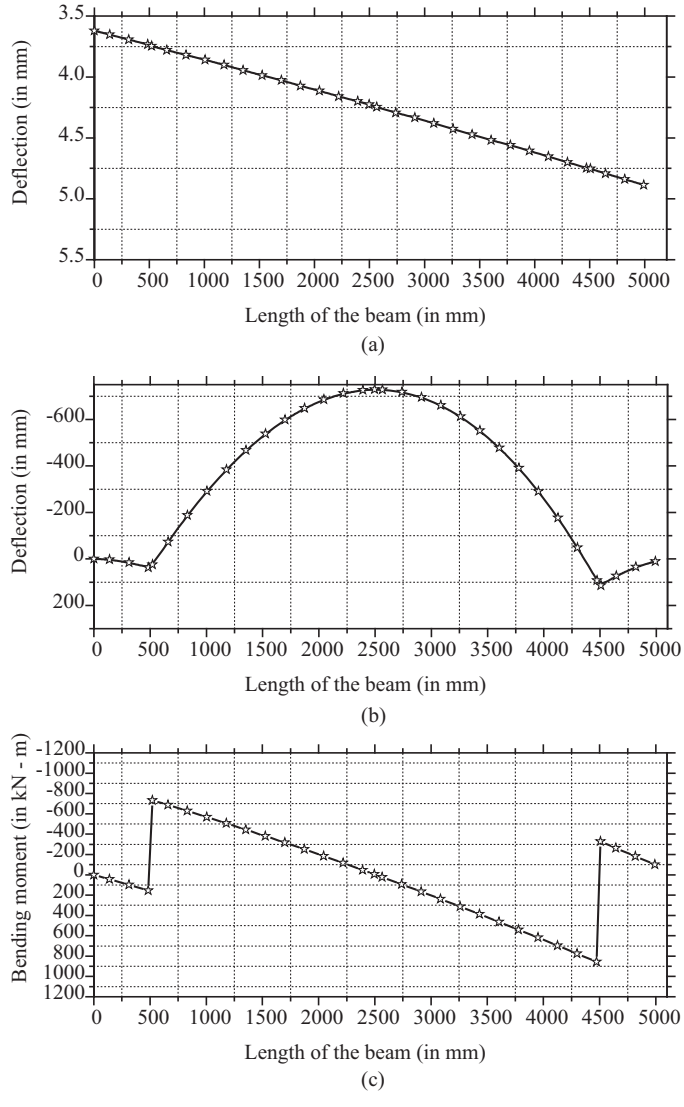

Figure 12.C.15 (a) BEF deflection diagram; (b) BEF bending moment diagram; (c) BEF shear force diagram; and (d) BEF bearing pressure diagram (Example 12.5).

(square footings).

$$\therefore \left(B_1^2 + B_2^2\right) = \frac{W_1 + W_2 + 10\%(W_1 + W_2)}{q_o}$$

$$\left(B_1^2 + B_2^2\right) = \frac{(900 + 1200 + 210)}{140}$$

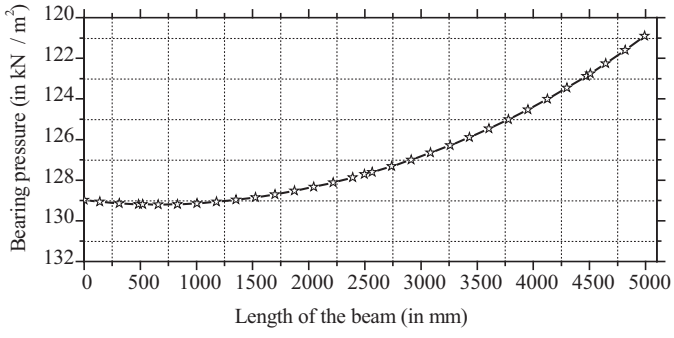

(d)

Figure 12.C.15 (*Continued*)

$$\left(B_1^2 + B_2^2\right) = 16.5 \tag{12.C.61}$$

Let $\bar{x}$ = distance of C.G of loads from center of column B, as given by

$$\bar{x} = \frac{W_1 l}{W_1 + W_2} = \frac{900 \times 6}{900 + 1200} = 2.571 \cong 2.6\,\text{m}$$

If $\bar{x}$ is also the distance of C.G of areas from the center of column B, we have

$$\bar{x} = \frac{B_1^2\left(l + \frac{b_1}{2} + \frac{B_1}{2}\right)}{\left(B_1{}^2 + B_2{}^2\right)} = 2.5713$$

where l = distance between center lines of columns and b_1 = width of column A.
Substituting the values of $\bar{x}$, b_1 and l_1, we get

$$B_1^2\left(6 + 0.2 + \frac{B_1}{2}\right) = 2.5713\left(B_1^2 + B_2^2\right)$$

$$B_1^3 + 12.4B_1^2 - 84.84 = 0 \Rightarrow B_1 = 2.4\,\text{m}$$

$$\left(2.4^2 + B_2^2\right) = 16.5 \Rightarrow B_2 = 3.3\,\text{m}$$

Net upward soil pressure intensity is given by

$$p_o = \frac{(W_1 + W_2)}{\left(B_1^2 + B_2^2\right)} = \frac{(900 + 1200)1.5}{16.5} = 190.90\,\text{kN/m}$$

A. Design of Footing Slab for Column A: Cantilever projection beyond the beam is

$$a = \frac{1}{2}(3.3 - 0.5) = 1.4\,\text{m}$$

Maximum bending moment

Table 12.C.5 Comparative study (see comments in Section 12.C.2).

		Maximum bearing pressure (kN/m^2)	Maximum bending moment (kNm)	Maximum shear force (kN)	Maximum deflection (mm)
Conventional design	With factored load	189.3	456.86	1107.42	$189.3/k_s = 7.88$
	With design load	$189.3/1.5 = 126.2$	$456.86/1.5 = 304.57$	$1170.42/1.5 = 780.28$	$7.88/1.5 = 5.25$
Design using BEF (with design load only)		$176.396\ kN/m^2$ at $x = 0$ mm	135.092 kNm at $x = 4507$ mm; −618.301 kNm at $x = 2496$ mm	801.353 kN at $x = 4472$ mm; −687.080 kN at $x = 520$ mm	6.03

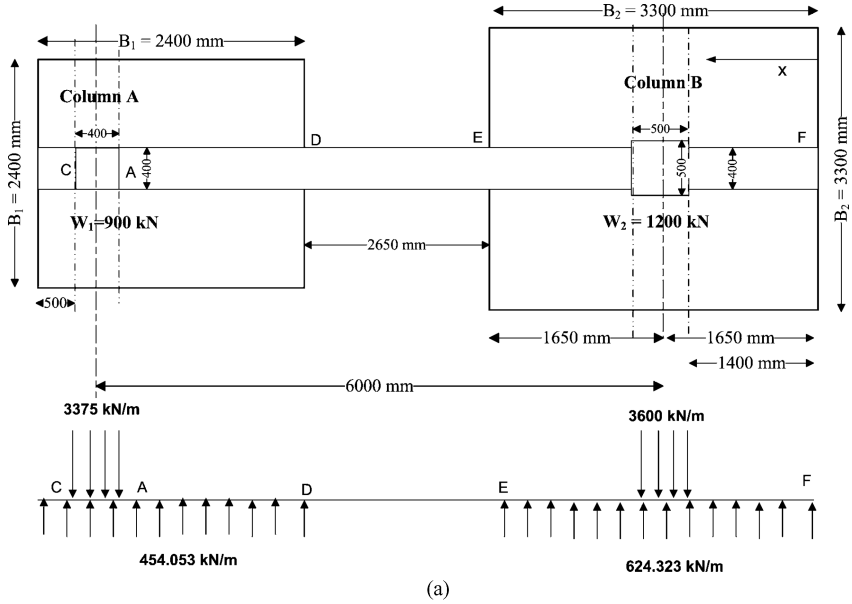

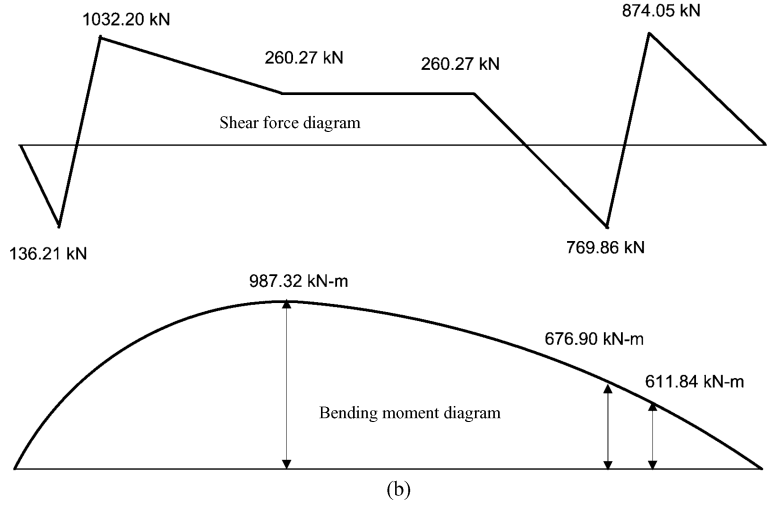

Figure 12.C.16 (a) Strap footing in plan; (b) shear force and bending moment diagrams; (c) section of the strap beam; (d) section of the strap beam details; (e) plan of square footing (2.4 × 2.4 m) with reinforcement details; and (f) plan of square footing (3.3 × 3.3 m) with reinforcement details (Example 12.6).

$$M = p_o \frac{a^2}{2} = 190.90 \times \frac{0.5^2}{2} = 23.86 \text{ kN-m}$$

$$\therefore d = \sqrt{\frac{M}{0.138 f_{ck} B_1}} = \sqrt{\frac{23.86 \times 10^6}{0.138 \times 20 \times 2400}} = 60.02 \text{ mm}$$

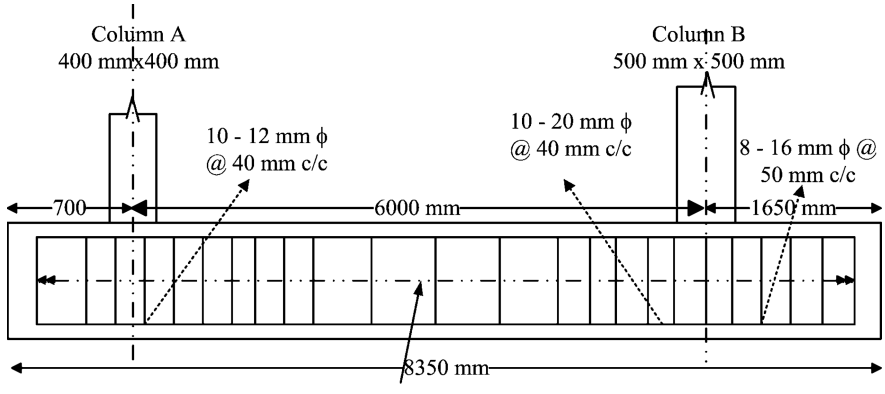

(c)

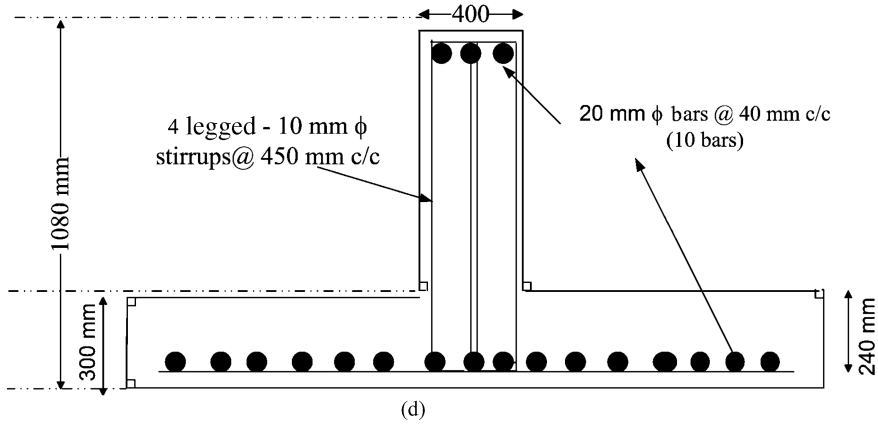

(d)

Figure 12.C.16 (*Continued*)

Keeping the cover to the center of the steel = 60 mm. $D = 60 + 40 = 100$ mm, However keep $D = 150$ mm and $d = 110$ mm

$$A_{st} = 0.5\frac{f_{ck}}{f_y}\left[1-\sqrt{1-\frac{4.6\times M\times 10^6}{f_{ck}B_1d^2}}\right]B_1d \tag{12.C.62}$$

$$A_{st1} = 0.5\frac{20}{460}\left[1-\sqrt{1-\frac{4.6\times 23.86\times 10^6}{20\times 2400\times 110^2}}\right]2400\times 110 = 570.64\,\text{mm}^2$$

Use 16 mm bars, $A_\phi = 201.62\,\text{mm}^2$

$$\text{Number of reinforcement bars} = \frac{570.64}{\frac{\pi}{4}12^2} = 5.045 \cong 6\,\text{bars}$$

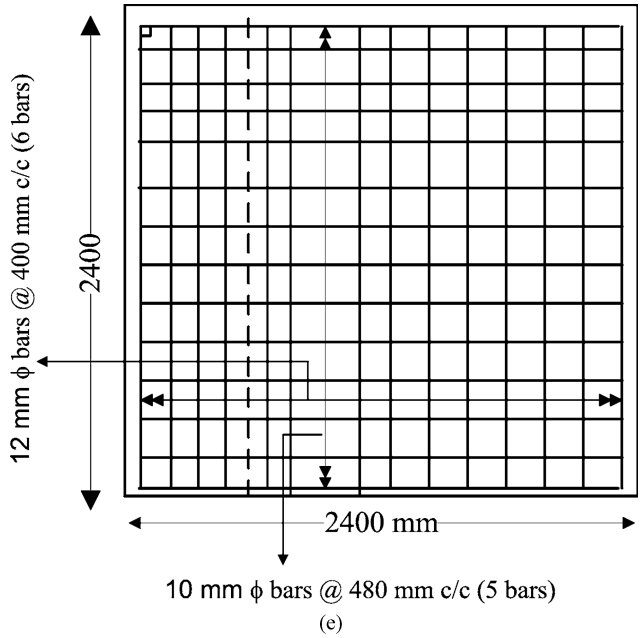

(e)

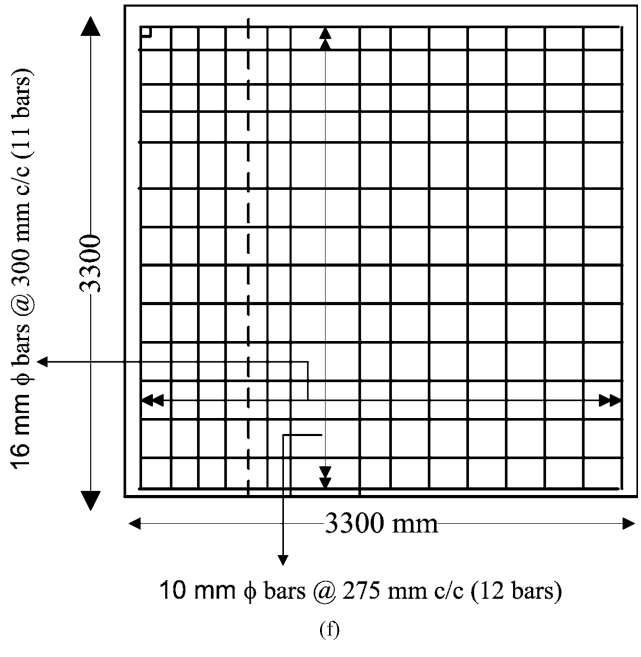

(f)

Figure 12.C.16 (*Continued*)

$$\text{Spacing of long bars} = \frac{2400}{6} = 400\,\text{mm}$$

Use 6–12 mm Φ bars for longitudinal reinforcement @ 400 mm c/c.

As per (IS: 456–2000 (2000)), the HYSD steel reinforcement in either direction in footings shall not be less than 0.12% of the total cross-sectional area ($B_1 d$).

$$\text{Therefore distribution reinforcement} = \frac{0.12}{100}(2400 \times 110) = 316.8\,\text{mm}^2$$

Use 10 mm bars, $A_\phi = 78.54\,\text{mm}^2$

$$\text{Number of reinforcement bars} = \frac{316.8}{\frac{\pi}{4}10^2} = 4.03 \cong 5\,\text{bars}$$

$$\text{Spacing of long bars} = \frac{2400}{5} = 480\,\text{mm}$$

Use 5–10 mm Φ bars for distribution reinforcement @ 480 mm c/c.

B. Design of Footing Slab for Column B: Let the width of strap beam = 400 mm.

∴ Cantilever projection, beyond the beam is

$$a = \frac{1}{2}(3.3 - 0.5) = 1.4\,\text{m}$$

$$\text{Maximum bending moment,} \quad M = p_o \frac{a^2}{2} = 190.90 \times \frac{1.4^2}{2} = 185.4052\,\text{kNm}$$

$$\therefore d = \sqrt{\frac{M}{(0.138 f_{ck} B_2)}} = \sqrt{\frac{185.4052 \times 10^6}{(0.138 \times 20 \times 3300)}} = 142.67\,\text{mm}$$

Keeping the cover to the center of the steel = 60 mm. $D = 142.67 + 60 = 202.67$ mm. However keep $D = 300$ mm and $d = 240$ mm.

$$A_{st} = 0.5 \frac{f_{ck}}{f_y} \left[1 - \sqrt{1 - \frac{4.6 \times M \times 10^6}{f_{ck} B_2 d^2}}\right] B_2 d \qquad (12.C.63)$$

$$A_{st1} = 0.5 \frac{20}{460} \left[1 - \sqrt{1 - \frac{4.6 \times 185.40 \times 10^6}{20 \times 3300 \times 240^2}}\right] 3300 \times 240 = 2053.80\,\text{mm}^2$$

Use 16 mm bars, $A_\phi = 201.62\,\text{mm}^2$

$$\text{Number of reinforcement bars} = \frac{2053.80}{\frac{\pi}{4}16^2} = 10.25 \cong 11\,\text{bars}$$

$$\text{Spacing of long bars} = \frac{3300}{11} = 300\,\text{mm}$$

Use 11–16 mm Φ bars for longitudinal reinforcement @ 300 mm c/c

As per (IS: 456–2000 (2000)), the HYSD steel reinforcement in either direction in footings shall not be less than 0.12% of the total cross-sectional area ($B_2 d$).

$$\text{Therefore distribution reinforcement} = \frac{0.12}{100}(3300 \times 240) = 950.4\,\text{mm}^2$$

Use 10 mm bars, $A_\phi = 78.54\,\text{mm}^2$

$$\text{Number of reinforcement bars} = \frac{950.4}{\frac{\pi}{4}10^2} = 12.10 \cong 12\,\text{bars}$$

$$\text{Spacing of long bars} = \frac{3300}{12} = 275\,\text{mm}$$

Use 12–10 mm Φ bars for distribution reinforcement @ 275 mm c/c

C. Bending Moment and Shear Force Diagrams for Strap Beam: Upward load w per meter run on the strap beams is given by

$$w_1 = p_o B = 189.189 \times 2.4 = 454.053\,\text{kN/m}$$

$$w_2 = p_o B = 189.189 \times 3.3 = 624.323\,\text{kN/m}$$

$$\text{Downward load of column A} = w_1 = \frac{1350}{0.4} = 3375\,\text{kN/m}$$

$$\text{Downward load of column B} = w_2 = \frac{1800}{0.5} = 3600\,\text{kN/m}.$$

The loading diagram on the strap beam is shown in Figure 12.C.16(a).

The shear force and bending moment diagrams for the strap beam are shown in Figure 12.C.16(b).

SF at the inner face of column A

$$F_1 = 454.053 \times (0.5{-}0.2) = 136.22\,\text{kN}$$

SF at the outer face of column A

$$F_2 = 1350{-}454.053 \times (0.5 + 0.2) = 1032.20\,\text{kN}$$

$$\text{SF at the edge D} = F_4 = 1350{-}454.053 \times (2.4) = 260.27\,\text{kN}$$

SF at the edge E

$$F_4 = 1350{-}454.053 \times (2.4) = 260.27\,\text{kN}$$

$$\text{S.F. at the inner edge face of column B} = F_5 = 624.323 \times (1.65){-}1800 = -769.86\,\text{kN6}$$

$$\text{S.F. at the outer edge of column B} = F_6 = 624.323 \times (1.4) = 874.052\,\text{kN}$$

In the range EF shear force is zero at a distance x from F and its value is given by

$$769.86{-}624.323 \times (x{-}1.9) = 0.0 \Rightarrow x = 3.133\,\text{m}$$

The bending moment diagram for the strap beam is shown in Figure 12.C.16(b).

The hogging bending moment is maximum at this section, its value given by

$$M_1 = 624.323 \times \left(\frac{3.133^2}{2}\right){-}3600 \times 0.5 \times \left(3.133{-}\frac{0.5}{2}{-}1.4\right) = 394.68\,\text{kNm}$$

Bending moment at the edge D is given by

$$M_2 = 454.053 \times \left(\frac{2.4^2}{2}\right) - 3375 \times 0.4 \times (2.4 - 0.5 - 0.2) = 987.327\,\text{kNm}$$

Bending moment at the outer face of column B is given by

$$M_3 = 624.323 \times \left(\frac{1.4^2}{2}\right) = 611.836\,\text{kNm}$$

D. Depth of Strap Beam: Let the width of strap beam $(b_s) = 400\,\text{mm}$.

Maximum bending moments in the strap beam are

$M_1 = 394.680\,\text{kN-m}$, $M_2 = 987.32736\,\text{kN-m}$, consider M_2 which is $> M_1$

$$d = \sqrt{\frac{M}{0.138\, f_{ck} b_s}} \tag{12.C.64}$$

$$d = \sqrt{\frac{987.33 \times 10^6}{0.138 \times 20 \times 400}} = 945.683\,\text{mm} \cong 1000\,\text{mm}$$

E. Reinforcement in the Strap Beam: For bending moment, $M_1 = 394.680\,\text{kNm}$

$$A_{st1} = 0.5\frac{20}{460}\left[1 - \sqrt{1 - \frac{4.6 \times 394.68 \times 10^6}{20 \times 400 \times 1000^2}}\right] 400 \times 1000 = 1050.10\,\text{mm}^2$$

For bending moment, $M_2 = 987.32736\,\text{kNm}$

$$A_{st2} = 0.5\frac{20}{460}\left[1 - \sqrt{1 - \frac{4.6 \times 987.33 \times 10^6}{20 \times 400 \times 1000^2}}\right] 400 \times 1000 = 2978.4\,\text{mm}^2$$

So provide reinforcement for $A_{st2} = 2978.36 > A_{st1}$.

Use 20 mm bars, $A_\phi = 314.151\,\text{mm}^2$.

$$\text{Number of bars} = \frac{2978.4}{\frac{\pi}{4}20^2} = 9.48 \cong 10\,\text{bars}$$

$$\text{Spacing of long bars} = \frac{400}{10} = 40\,\text{mm}$$

Use 10–20 mm Φ bars for longitudinal reinforcement @ 40 mm c/c.

These bars should be checked for development length to satisfy the criteria $\frac{M_2}{V} + L_o \geq L_d$

$$V = F_4 = 260.27\,\text{kN}$$

$$L_o = 12\Phi(240\,\text{mm}) \text{ or } d(1000\,\text{mm}) \text{ whichever is more } = 1000\,\text{mm}$$

$$L_d = \left(\frac{0.87 f_y}{4\tau_{bd}}\right)\Phi = \left(\frac{0.87 \times 460}{4 \times 1.92}\right)\Phi = 52.11\Phi$$

$$L_d = 1042.2\,\text{mm}$$

$$\left(\frac{987.33 \times 10^6}{260.27 \times 10^3}\right) + 1000 \geq L_d = \left(\frac{0.87 f_y}{4\tau_{bd}}\right)\Phi = \left(\frac{0.87 \times 460}{4 \times 1.92}\right)\Phi = 52.11\Phi$$

$$4973.472 \geq 1042 \quad \text{Hence it is OK.}$$

Near support B

$$M_2 = 987.327\,\text{kNm}$$

S.F. at the inner edge face of column B $= V = 624.323 \times (1.65) - 1800 = -769.86\,\text{kN}$

$$L_o = \frac{b}{2} - \text{cover} + \text{anchorage} = \frac{400}{2} - 60 + 13\Phi = \frac{400}{2} - 60 + 13\Phi$$

$$L_d = \left(\frac{0.87 f_y}{4\tau_{bd}}\right)\Phi = \left(\frac{0.87 \times 460}{4 \times 1.92}\right)\Phi$$

$$\left(\frac{987.33 \times 10^6}{769.86 \times 10^3}\right) + 400 \geq L_d$$

$$1682.47 \geq 1042 \quad \text{Hence, it is satisfactory.}$$

Hence, 10 bars of 20 mm Φ is sufficient. These are the bars arranged in two layers, keeping a clear distance of 20 mm between the two layers. Hence, the required total depth $D = d + 10 + \Phi/2 + \text{cover} = 1000 + 10 + 20/2 + 60 = 1080\,\text{mm}$.

Similarly at the outer face of column B, $M_3 = 611.386\,\text{kNm}$

$$A_{st} = 0.5\frac{20}{460}\left[1 - \sqrt{1 - \frac{4.6 \times 611.386 \times 10^6}{20 \times 400 \times 1080^2}}\right] 400 \times 1080 = 1543.05\,\text{mm}^2$$

Use 16 mm bars, $A_\phi = 201.06\,\text{mm}^2$

$$\text{Number of bars} = \frac{1543.05}{\frac{\pi}{4}16^2} = 7.67 \cong 8\,\text{bars}$$

$$\text{Spacing of long bars} = \frac{400}{8} = 50\,\text{mm}$$

Use 8–16 mm Φ bars for longitudinal reinforcement in the strap beam @ 50 mm c/c.

These bars should be checked for development length to satisfy the criteria $1.3\left(\frac{M_3}{V}\right) + L_o \geq L_d$

$$M_3 = 611.386\,\text{kNm}$$

V = SF at the outer edge of column B $= F_6 = 624.323 \times (1.4) = 874.052\,\text{kN}$

The required total depth at outer face of column B

$$D = 1000 + 10 + \frac{20}{2} + 60 = 1080\,\text{mm}$$

$$L_o = 12\Phi(240\,\text{mm}) \text{ or } D(1080\,\text{mm}) \text{ whichever is more} = 1080\,\text{mm}$$

$$1.3\left(\frac{611.386 \times 10^6}{874.05 \times 10^3}\right) + 1080 \geq L_d = 52.11 \times 16$$

$$1989.99 \geq 833.60 \quad \text{Hence it is satisfactory.}$$

F. Reinforcement for Diagonal Tension

$$\text{Reinforcement} = \frac{1000 \times 14 \times \frac{\pi}{4}(16)^2}{400 \times 1000} = 0.7037\%.$$

Hence, for 0.7037% steel $\tau_c = 0.544\,\text{N/mm}^2$ (for M_{20} concrete)

$$V_c = \tau_c bd = 0.544 \times 400 \times 1000 = 217.600\,\text{kN}$$

Hence, shear reinforcement is necessary wherever shear force exceeds 217.600 kN.

$$\text{Shear force } F_1 \text{ @ } A = 1032.20\,\text{kN}$$

$$V_{us} = F_1 - V_c = 1032.20 - 217.60 = 814.40\,\text{kN}$$

$$10\,\text{mm}\ \Phi\ 4\text{-legged stirrups } A_{sv} = 4 \times \frac{\pi}{4}(10^2) = 314.16\,\text{mm}^2$$

$$S_v = \frac{0.87 f_y A_{sv} d}{V_{us}} = \frac{0.87 \times 460 \times 314.16 \times 1000}{814.40 \times 10^3} = 154.376\,\text{mm} \cong 150\,\text{mm}$$

$$\text{At the point B,} \quad S_v = \frac{0.87 \times 460 \times 314.16 \times 1000}{(769.86 - 217.5) \times 10^3} = 227.65\,\text{mm} \cong 220\,\text{mm}.$$

At the outer face of B

$$S_v = \frac{0.87 \times 460 \times 314.16 \times 1000}{(874.052 - 217.5) \times 10^3} = 191.51\,\text{mm} \cong 190\,\text{mm}$$

Maximum spacing of nominal stirrups is given by

$$S_{v\,\min} = \frac{2.5 A_{sv} f_y}{b} = \frac{2.5 \times 314.16 \times 460}{400} = 903.19\,\text{mm}$$

$$S_{v\,\max} = 0.75\text{d or } 450\,\text{mm whichever is less}$$

$$= 750 \text{ or } 450\,\text{mm whichever is less}$$

$$S_{v\,\max} = 450\,\text{mm}$$

Hence provide these nominal stirrups @ 450 mm c/c throughout the length.

The details of the reinforcement are shown in Figures 12.C.16(c)–(f).

WINBEF Solution (BEF Method):

WINBEF Input

For a 2.4 × 2.4 m square column:

Young's modulus of soil, $E_s = 10^5\ \text{kN/m}^2$
Unit weight of soil, $\gamma_{soil} = 20\ \text{kN/m}^3$
Poisson's ratio of soil, $v_s = 0.3$
Young's modulus of concrete,
$E_f = 5000\sqrt{20} = 22360.68\ \text{N/mm}^2 = 2.236 \times 10^7\ \text{kN/m}^2$

The cross sectional details of the footings and strap beam are given in Table 12.C.6.

Table 12.C.6 Cross-section details of footings and strap beam (non-prismatic beam).

Length of beam, x (mm)	Width of beam, B (mm)	Depth of beam, d (mm)
0	2400	500
2400	2400	500
2400	400	1080
5050	400	1080
5050	3300	500
8350	3300	500

B_1 = breadth of foundation which is 2.4 m from 0 to 2.4 m (distance from left edge of the footing towards right hand side) and with subgrade modulus k_{s1} and moment of inertia of the concrete beam $I_{f1} = \frac{B_1 d^3}{12} = \frac{2.4 \times 0.500^3}{12} = 0.025\ \text{m}^4$

$$\text{Modulus of subgrade reaction,} \quad k_s = \frac{1}{B(\text{mm})}\left[0.65\sqrt[12]{\frac{E_s B^4}{E_f I_f}}\right]\frac{E_s}{1-v_s^2}$$

$$k_{s1} = \frac{0.65}{2400}\frac{10^5}{\left(1-0.3^2\right)}\sqrt[12]{\frac{10^5 \times 2.4^4}{2.236 \times 10^7 \times 0.025}} = \frac{82547.72}{2400} = 34.52\ \text{kN/m}^2/\text{mm}$$

For a 3.3 × 3.3 m square column:

B_2 = breadth of foundation which is 3.3 m from 5.05 m (that is, 2.4 + 2.65) to 8.35 m (distance from left edge of the footing towards right hand side) and with subgrade modulus k_{s2}.

B_2 = breadth of foundation = 3.3 m

$$I_{f2} = \frac{B_2 d^3}{12} = \frac{3.3 \times 0.500^3}{12} = 0.03438\ \text{m}^4$$

$$k_{s2} = \frac{0.65}{3300}\frac{10^5}{\left(1-0.3^2\right)}\sqrt[12]{\frac{10^5 \times 3.3^4}{2.236 \times 10^7 \times 0.03438}} = \frac{89721.213}{3300} = 27.188\ \text{kN/m}^2/\text{mm}$$

Breadth of the footing is 400 mm from 2.4 m to 5.05 m (which is 2.4 + 2.65) with $k_s = 0\ \text{kN/m}^2/\text{mm}$. The details are shown in the Figure 12.C.17.

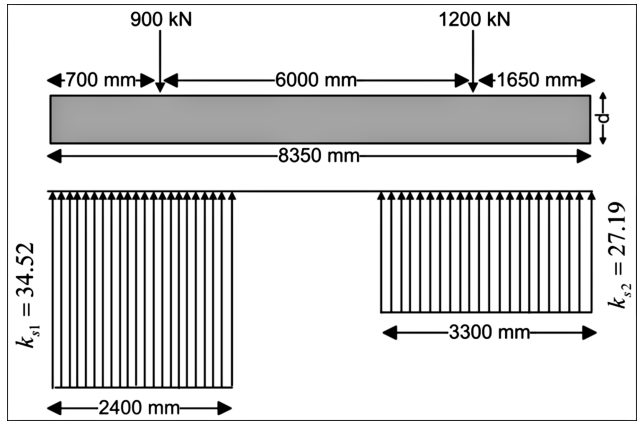

Figure 12.C.17 Details of loading and modulus of the subgrade reaction of the beam resting on the elastic foundation (Example 12.6).

Loading Data for WINBEF and Results

Loading data is shown in Figure 12.C.17. The details of deflection, bending moment, shear force and bearing pressure are shown in Figure 12.C.18. Table 12.C.7 shows the comparative study of the results.

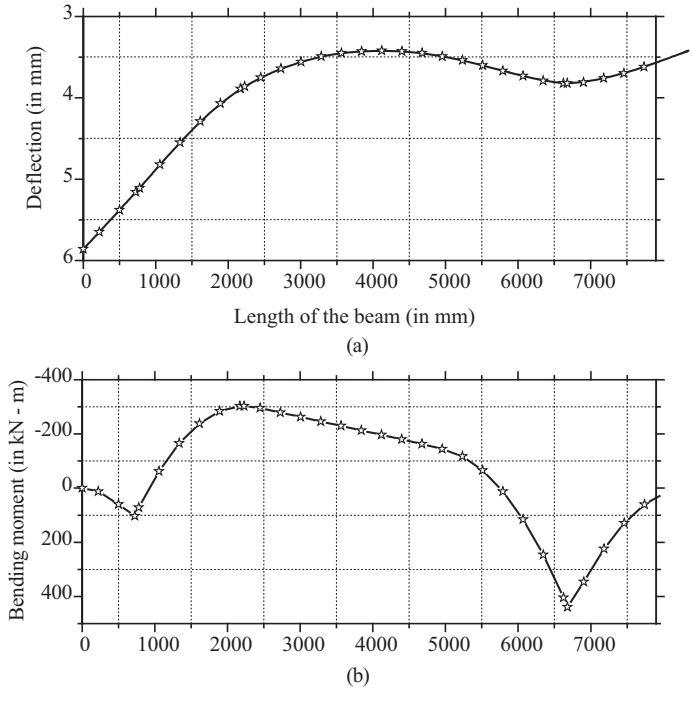

Figure 12.C.18 (a) BEF deflection diagram; (b) BEF bending moment diagram; (c) BEF shear force diagram; and (d) BEF bearing pressure diagram (Example 12.6).

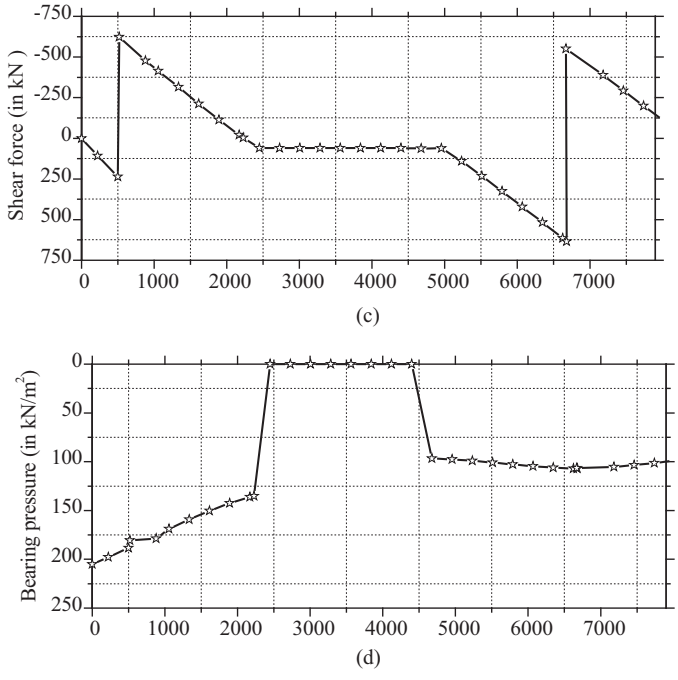

Figure 12.C.18 (*Continued*)

Example 12.7 Raft Foundation

Design a raft foundation for the layout of columns shown in Figure 12.C.19(a). All columns are of square shape of size 40×40 cm. ADSP $= 80$ kN/m^3. Use M 15 concrete and Fe 415 steel. Assume 10% as the load of raft and soil above.

A. Design of Raft Slab

$$\text{Total vertical column load} = (600 + 1600 + 2000 + 600 + 800 + 1800 + 2000 + 1000 + 800 + 1000 + 1200 + 600) = 14000$$

Eccentricity along the x direction is obtained by taking moment of column loads about the grid 1–1

$$\overline{x} = \frac{[6(1600 + 1800 + 1000) + 12(2000 + 2000 + 1200) + 18(600 + 1000 + 600)]}{14000}$$

$$= 9.1714 \text{ m}$$

$$e_x = 9.1714 - (6 + 3) = 0.1714 \text{ m}$$

Eccentricity along the y direction is obtained by taking moment of column loads about the grid C–C

Table 12.C.7 Comparative study (see comments in Section 12.C.2).

		Maximum bearing pressure (kN/m^2)	Maximum bending moment (kNm)	Maximum shear force (kN)	Maximum deflection (mm)
Conventional design	With factored load	624.323	987.323	1032.20	624.323/28 = 18.08
	With design load	624.323/1.5 = 416.22	987.323/1.5 = 658.22	1032.20/1.5 = 688.13	18.08/1.5 = 12.05
Design using BEF (with design load only)		205.050 kN/m^2 at $x = 0$ mm	440.576 kNm at $x = 6680$ mm; −299.937 kNm at $x = 2227$ mm	631.628 kN at $x = 6680$ mm; −564.406 kN at $x = 724$ mm	5.86 mm at $x = 0$ mm

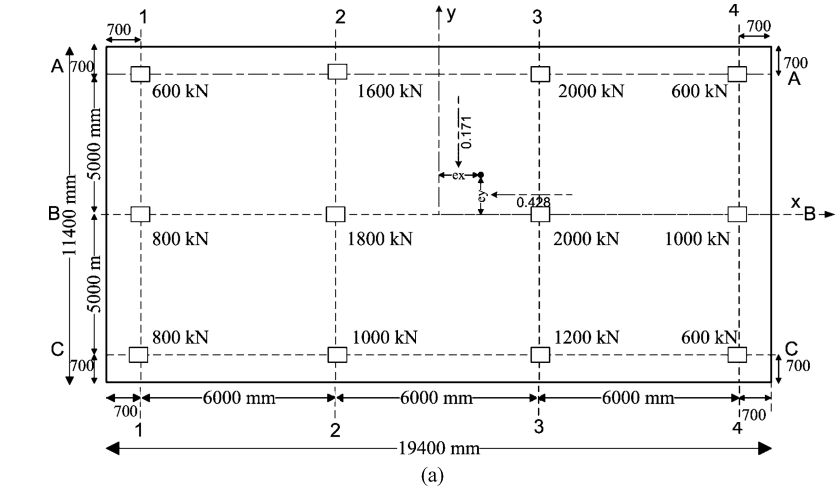

(a)

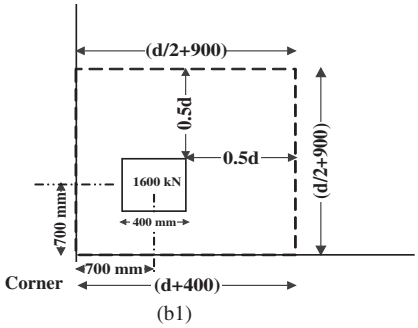

(b1)

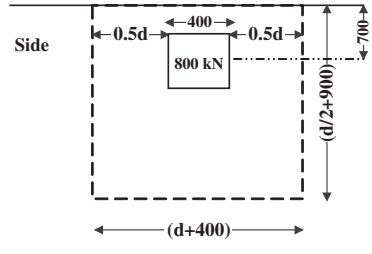

(b2)

Critical sections in shear

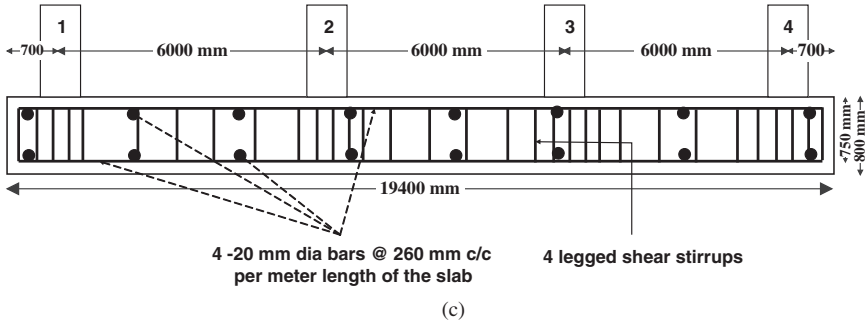

(c)

Figure 12.C.19 Raft layout and column loads; (b1) critical section in shear; (b2) critical section in shear; and (c) details of reinforcement along the longitudinal section (Example 12.7).

$$\overline{y} = \frac{[5(800 + 1800 + 2000 + 1000) + 10(600 + 1600 + 2000 + 600)]}{14000} = 5.4285\,\text{m}$$

$$e_y = 5.4285 - 5 = 0.4285\,\text{m}$$

$$I_x = \frac{19.4 \times 11.4^3}{12} = 2395.16\,\text{m}^4$$

$$I_y = \frac{11.4 \times 19.4^3}{12} = 6936.31\,\text{m}^4$$

$$A = 19.4 \times 11.4 = 221.16\,\text{m}^2$$

$$M_x = pe_y = 14000 \times 0.4285 = 6000\,\text{kNm} \tag{12.C.65}$$

$$M_y = pe_x = 14000 \times 0.1714 = 2400\,\text{kNm} \tag{12.C.66}$$

$$\frac{P}{A} = \frac{14000}{221.16} = 63.302\,\text{kN/m}^2$$

Soil pressure at different points is as follows

$$\sigma = \frac{P}{A} \pm \frac{M_y}{I_y}x \pm \frac{M_x}{I_x}y \tag{12.C.67}$$

$$\sigma = 63.302 \pm \frac{2400}{6936.31}x \pm \frac{6000}{2395.16}y = 63.158 \pm 1.5269x \pm 0.4745y$$

At corner A–4

$$\sigma_{A-4} = 63.158 + 0.346 \times 9.7 + 2.505 \times 5.7 = 80.93 \cong \text{BC of soil}\,(80\,\text{kN/m}^2)$$

At corner C–4

$$\sigma_{C-4} = 63.158 + 0.346 \times 9.7 - 2.505 \times 5.7 = 74.225\ \text{kN/m}^2$$

At corner A–1

$$\sigma_{A-1} = 63.158 - 0.346 \times 9.7 + 2.505 \times 5.7 = 52.38\,\text{kN/m}^2$$

At corner C–1

$$\sigma_{C-1} = 63.158 - 0.346 \times 9.7 - 2.505 \times 5.7 = 45.67\,\text{kN/m}^2$$

At corner B–4

$$\sigma_{B-4} = 63.158 + 0.346 \times 9.7 = 66.658\,\text{kN/m}^2$$

At corner *B*–1

$$\sigma_{B-1} = 63.158 - 0.346 \times 9.7 = 59.943\,\text{kN/m}^2$$

In the *x* direction, the raft is divided in three strips, that is three equivalent beams:

1. Beam *A*–*A* with 3.2 m width and soil pressure of $80\,\text{kN/m}^2$
2. Beam *B*–*B* with 5.0 m width and soil pressure of $\frac{(80 + 66.65)}{2} = 73.32\,\text{kN/m}^2$
3. Beam *C*–*C* with 5.0 m width and soil pressure of $\frac{(66.65 + 52.38)}{2} = 59.52\,\text{kN/m}^2$.

The bending moment is obtained by using a coefficient 1/10 and *L* as the center to center of column distance

$$+M = -M = \frac{wL^2}{10} \tag{12.C.68}$$

For strip *A*–*A*

$$\text{Maximum moment} = \frac{80 \times 6^2}{10} = 288\,\text{kNm/m}$$

For strip *B*–*B*

$$\text{Maximum moment} = \frac{73.32 \times 6^2}{10} = 263.95\,\text{kNm/m}$$

For strip *C*–*C*

$$\text{Maximum moment} = \frac{59.52 \times 6^2}{10} = 214.272\,\text{kNm/m}$$

For any strip in the *y* direction, take $M = \frac{wL^2}{8}$ since there is only a two-span equivalent beam.
For strip 4–4

$$\text{Maximum moment} = \frac{80 \times 5^2}{8} = 250\,\text{kNm/m}$$

The depth of the raft is governed by two-way shear at one of the exterior columns. If the location of critical shear is not obvious, it may be necessary to check all possible locations.

Shear strength of concrete, $\tau_c = 0.25\sqrt{f_{ck}} = 0.25\sqrt{15} = 0.97\text{N/mm}^2$

For a corner column (say *C*–1)

Perimeter $b_o = 2\left(\frac{d}{2} + 900\right) = d + 1800\,\text{mm}$ (Figure 12.C.19(b))

$$\tau_v = \frac{V_u}{b_o d} = \frac{1.5 \times 800 \times 1000}{(d + 1800)d} = 0.97$$

$$= \frac{1200000}{(d + 1800)d} = 0.97$$

$$\Rightarrow d^2 + 1800d - 1237113.40 = 0$$

$$d = \frac{-1800 \pm \sqrt{(1800^2 + 4 \times 1 \times 1237113.40)}}{2 \times 1} = 530.773\,\text{mm}$$

For a corner column (say *A*–2)

$$\text{Perimeter } b_o = 2\left(\frac{d}{2} + 900\right) + (d + 400) = 2d + 2200\,\text{mm}$$

$$\tau_v = \frac{V_u}{b_o d} = \frac{1.5 \times 1600 \times 1000}{(2d + 2200)d} = 0.97$$

$$d^2 + 1100d - 1237113.40 = 0 \tag{12.C.69}$$

$$\Rightarrow d = \frac{-1100 \pm \sqrt{(1100^2 + 4 \times 1 \times 1237113.40)}}{2 \times 1} = 690.811\,\text{mm}$$

However, adopt an effective depth of 750 mm and overall depth of 800 mm

Reinforcement in the longitudinal direction is given by (considering a 1 m wide strip)

$$A_t = 0.5\frac{15}{415}\left[1 - \sqrt{1 - \frac{4.6 \times 288 \times 10^6}{15 \times 1000 \times 750^2}}\right] 1000 \times 750 = 1109.51\,\text{mm}^2$$

Use 20 mm bars, $A_\phi = 314.151\,\text{mm}^2$

$$\text{Number of bars} = \frac{1109.51}{\frac{\pi}{4}20^2} = 3.531 \cong 4\,\text{bars}$$

$$\text{Spacing of long bars} = \frac{1000 \times \frac{\pi}{4}20^2}{1109.51} = 283.152\,\text{mm}$$

Provide 4–20 mm Φ bars for reinforcement @ 260 mm c/c at top and bottom in both directions.

$$\begin{aligned}\text{Minimum reinforcement in the slabs} &= 0.12\% \\ &= \frac{0.12}{100} \times 800 \times 1000 \\ &= 960\,\text{mm}^2/\text{m} < 1109.51\,\text{mm}^2/\text{m}\end{aligned}$$

Minimum steel governs in the remaining raft. Critical sections in shear.

WINBEF Solution:

WINBEF Input

Young's modulus of soil, $E_s = 10^5\,\text{kN/m}^2$, unit weight of soil, $\gamma_{soil} = 20\,\text{kN/m}^3$.

Poisson's ratio of soil, $v_s = 0.3$.
Young's modulus of concrete

$$E_f = 5000\sqrt{\sigma_{ck}} = 5000\sqrt{15} = 19364.92\,\text{N/mm}^2 = 1.9364 \times 10^7\,\text{kN/m}^2$$

B = breadth of foundation = 1.0 m (considering a 1 m wide strip for design).
Moment of inertia of the concrete beam $I_f = \frac{Bd^3}{12} = \frac{1.0 \times 0.8^3}{12} = 0.04267\,\text{m}^4$.
Modulus of subgrade reaction, $k_s = \frac{1}{B(\text{mm})}\left[0.65\sqrt[12]{\frac{E_s B^4}{E_f I_f}}\right]\frac{E_s}{1-v_s^2}$.

$$k_s = \frac{0.65}{1000}\frac{10^5}{\left(1-0.3^2\right)}\sqrt[12]{\frac{10^5 \times 1.0^4}{1.9364 \times 10^7 \times 0.04267}} = \frac{59902}{1000} = 59.902\,\text{kN/m}^2/\text{mm}.$$

Loading Data for WINBEF and Results

The loading data is shown in Figure 12.C.20.

Note: In the loading diagram, the load coming on to the beam is taken as maximum of A, B and C strip loads as explained below (see Figure 12.C.19(a)).

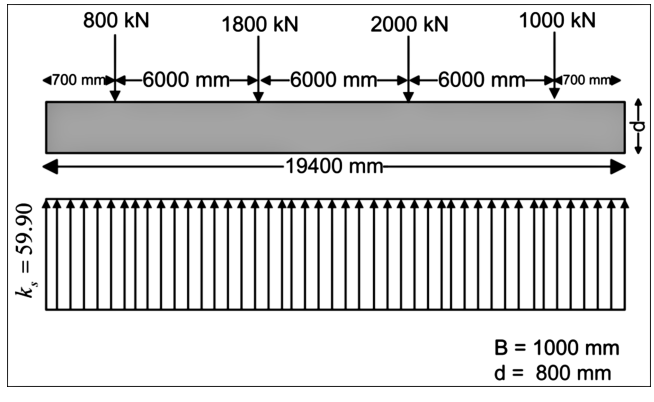

Figure 12.C.20 Loading data for WINBEF solution (Example 12.7).

The maximum load on strip 1–1: maximum of A1 (600 kN), B1 (800 kN) and C1 (800 kN), which is 800 kN.

The maximum load on strip 2–2: maximum of A2 (1600 kN), B2 (1800 kN) and C2 (1000 kN), which is 1800 kN.

The maximum load on strip 3–3: maximum of A3 (2000 kN), B3 (2000 kN) and C3 (1200 kN), which is 2000 kN.

The maximum load on strip 4–4: maximum of A4 (600 kN), B4 (1000 kN) and C4 (1000 kN), which is 1000 kN.

The details of deflection, bending moment, shear force and bearing pressure are shown in Figure 12.C.21. Please see also comments given in Section 12.C.2.

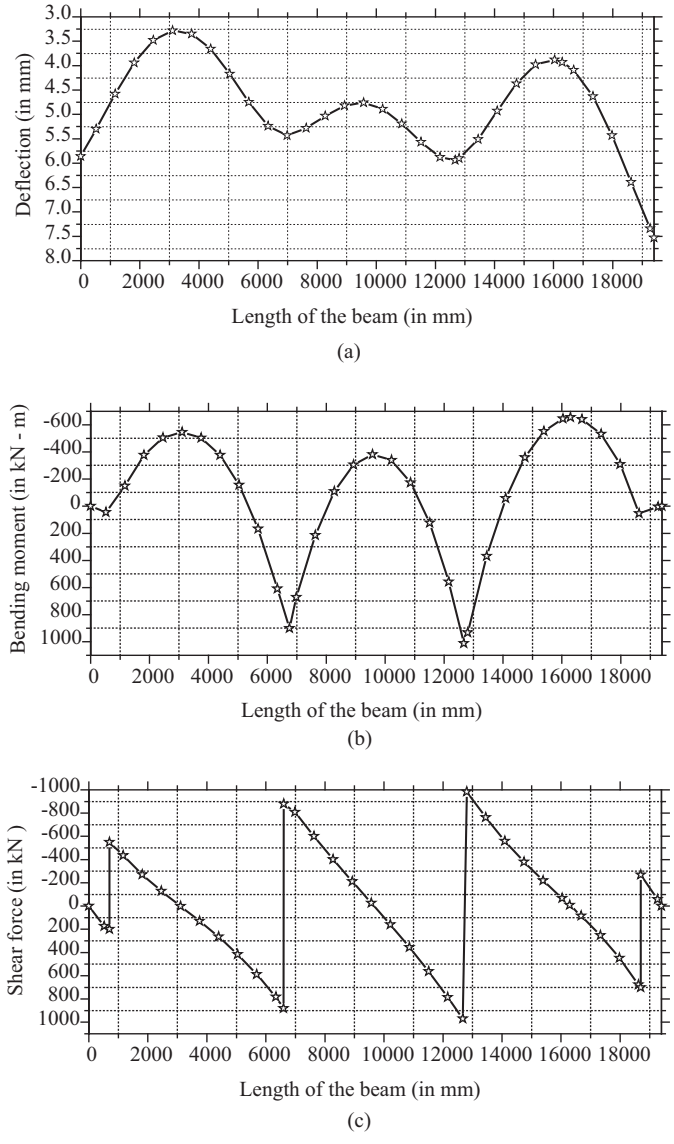

Figure 12.C.21 (a) BEF deflection diagram; (b) BEF bending moment diagram; (c) BEF shear force diagram; and (d) BEF bearing pressure diagram (Example 12.7).

Example 12.8 Annular Raft Foundation

Design an annular (circular) raft for a circular tank whose outer diameter is 12 m and is supported by a ring beam of 9 m diameter. The inner diameter of the annulus is 8 m. The factored soil pressure under the raft is 80 kN/m^2 and a linearly varying soil pressure due to

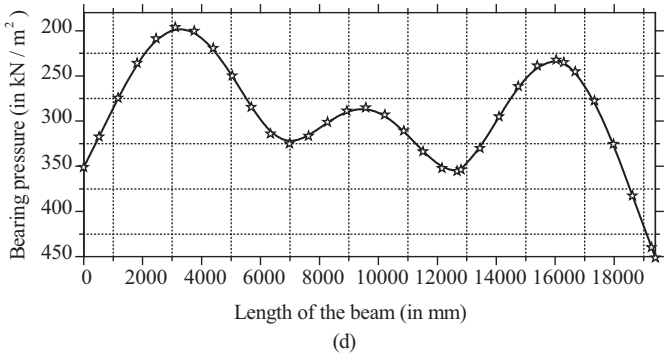

(d)

Figure 12.C.21 (*Continued*)

wind/earthquake $= \pm 30\,\text{kN/m}^2$, as shown in Figure 12.C.22(a). Use M_{20} concrete and Fe 460 grade steel.

A. Design of Annular Raft Slab

Let the thickness of the raft slab be 20 cm. The self weight of raft slab and that of the earth directly above it are not considered for the design of raft slab itself as these are directly

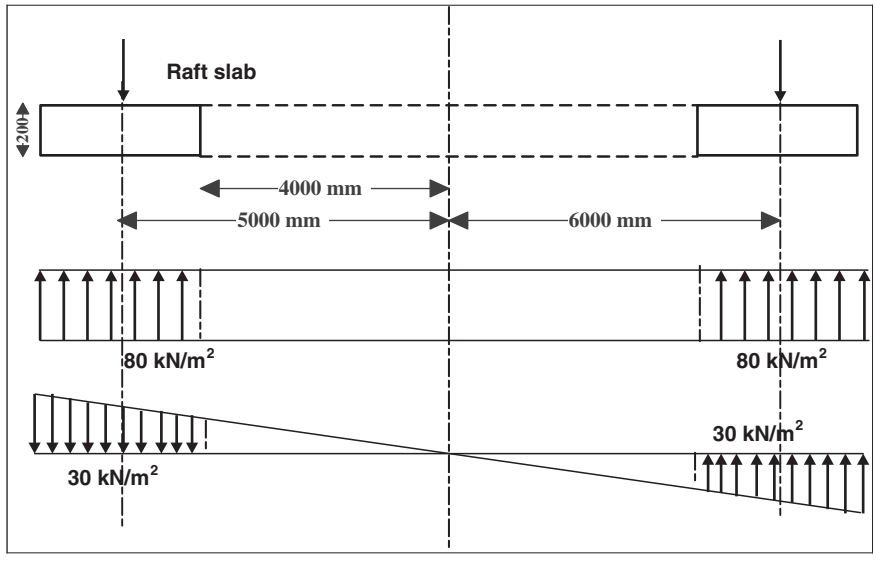

(a)

Figure 12.C.22 (a) Sectional elevation of raft with opening and pressure distribution; and (b) reinforcement in raft slab (Example 12.8).

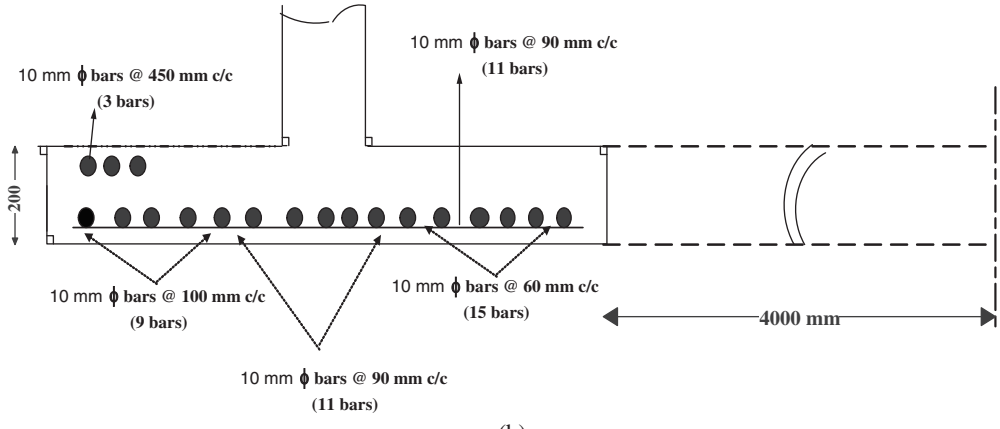

(b)

Figure 12.C.22 (*Continued*)

supported by the soil below it (see Figure 12.C.22(a) for details).

For the purpose of analysis of the base raft slab, it may be assumed to be supported on fictitious supports at the outer periphery and loaded with:

1. A uniformly distributed load of $+60\,\text{kN/m}^2$ acting upward.
2. A uniformly varying factored load of -30 to $+30\,\text{kN/m}^2$ due to reversible earthquake load.
3. A downward load of $\frac{\pi}{4}(12^2-8^2)\times 80 = 5026.5\,\text{kN}$ acting on the periphery of a concentric circle of 9.0 m diameter.

The moments due to each of these three types of load may be computed as follows.

1. **Moments due to uniformly distributed load acting upward**
   The radial and circumferential moments are given as follows:

$$M_r = \frac{3}{16}wr^2 - \frac{wb^2}{4}\left\{\log_e\left(\frac{r}{a}\right) + \frac{3}{4}\left(1 + \frac{a^2}{b^2} - \frac{a^2}{r^2}\right) + \left(\frac{a^2-r^2}{a^2-b^2}\right)\left(\frac{b}{r}\right)^2\left[\log_e\left(\frac{a}{b}\right)\right]\right\} \tag{12.C.70}$$

$$M_\theta = \frac{1}{16}wr^2 - \frac{wb^2}{4}\left\{\log_e\left(\frac{r}{a}\right) + \frac{3}{4}\left(-\frac{1}{3} + \frac{a^2}{b^2} + \frac{a^2}{r^2}\right) - \left(\frac{a^2+r^2}{a^2-b^2}\right)\left(\frac{b}{r}\right)^2\left[\log_e\left(\frac{a}{b}\right)\right]\right\} \tag{12.C.71}$$

   where

$$w = 80\,\text{kN/m}^2,\ a = 12/2 = 6\,\text{m}, b = 8/2 = 4\,\text{m}$$

   The values of M_r and M_θ for different values of r are given in Table 12.C.8
2. **Moments due to uniformly varying load $\pm p$ per unit area**
   The radial and circumferential moments are given as follows:

Table 12.C.8 Moments due to uniformly distributed load.

r	4.0	5.0	6.0
M_r (kNm/m)	0	−46.72	0
M_θ (kNm/m)	−452.90	−368.98	−312.40

Assuming Poisson's ration $\mu = 0$

$$M_r = \frac{pa^2}{48\delta^3}\left[5\left(\delta^4 - \delta^6 - \frac{\alpha^4}{\alpha^2+1}\right) + 3\left(\frac{\alpha^6}{\alpha^2+1} - \alpha^4\delta^2\right) + \frac{8\alpha^4\delta^4}{\alpha^2+1}\right]\cos\theta \quad (12.C.72)$$

$$M_\theta = -\frac{pa^2}{48\delta^3}\left\{\left[\delta^6 - \frac{8}{3}\left(\frac{\alpha^4\delta^4}{\alpha^2+1}\right)\right] + 3\left(\frac{\alpha^6}{\alpha^2+1} + \alpha^4\delta^2\right) - 5\left(\frac{\delta^4}{3} + \frac{\alpha^4}{\alpha^2+1}\right)\right\}\cos\theta \quad (12.C.73)$$

where

$$b = \alpha a \text{ or } \alpha = \frac{b}{a} = \frac{4}{6} = 0.667$$

$$r = \delta a \text{ or } \delta = \frac{r}{a} = \frac{r}{6}$$

$$\cos\theta = 1.0 \text{ for } \theta = 0,\ p = 30\,\text{kN/m}^2$$

The values of M_r and M_θ for different values of r are given in Table 12.C.9.

Table 12.C.9 Moments due to uniformly varying pressure.

r	±4.0	±5.0	±6.0
M_r (kNm/m)	0	±13.66	0
M_θ (kNm/m)	±41.88	±28.56	±21.15

3. **Moments due to concentric load**

The radial and circumferential moments are given as follows:

For $r \Leftarrow c$

$$M_r = \frac{P}{4\pi}\frac{a^2}{(a^2-b^2)}\left(1 - \frac{b^2}{r^2}\right)\lambda \quad (12.C.74)$$

$$M_\theta = \frac{P}{4\pi}\frac{a^2}{(a^2-b^2)}\left(1 + \frac{b^2}{r^2}\right)\lambda \quad (12.C.75)$$

For $r > c$

$$M_r = \frac{P}{4\pi}\left[\log_e\left(\frac{c}{r}\right) - 0.5 + \left(\frac{r^2-a^2}{a^2-b^2}\right)\left(\frac{a}{r}\right)^2\lambda + \frac{c^2}{2r^2}\right] \quad (12.C.76)$$

$$M_\theta = \frac{P}{4\pi}\left[\log_e\left(\frac{c}{r}\right) + 0.5 + \left(\frac{r^2 + b^2}{a^2 - b^2}\right)\left(\frac{a}{r}\right)^2 \lambda - \frac{c^2}{2r^2}\right] \tag{12.C.77}$$

where

$$\lambda = \log_e\left(\frac{a}{c}\right) + 0.5 - \frac{c^2}{2a^2}, c = 5$$

$P = 5026.5$ kN acting on the periphery of concentric circle.

The values of M_r and M_θ for different values of r are given in Table 12.C.10.

Table 12.C.10 Moments due to concentric load.

r	4.0	5.0	6.0
M_r (kNm/m)	0	86.86	0
M_θ (kNm/m)	482.54	395.68	336.68

The net moments in the slab can be obtained by adding algebraically the moments due to each type of loads. The net moments are given in Table 12.C.11.

Table 12.C.11 Net moments in raft slab.

r	± 4.0	± 5.0	± 6.0
M_r (kNm/m)	0	53.78 26.47	0
M_θ (kNm/m)	+ 71.52 −12.24	55.53 −1.86	45.43 3.13

The depth of slab will be based on a maximum moment of 71.52 kNm/m. It can be seen that radial moments are sagging throughout. Circumferential moments are hogging in one half of the slab, with sagging in the other half. Since the earthquake loading on the tank is reversible, circumferential steel should be provided for sagging as well as hogging moments in each half of the raft slab. Consider a 1 m wide strip for design, $B = 1$ m.

Effective depth d is given by

$$d = \sqrt{\frac{M}{0.138 f_{ck} B}} \tag{12.C.78}$$

$$d = \sqrt{\frac{71.524 \times 10^6}{(0.138 \times 20 \times 1000)}} = 160.98 \text{ mm}$$

Note that stresses are not increased by 33.33% in the limit state design method in the case of earthquake loading. Adopt effective depth as $d = 180$ mm and overall depth as $D = 200$ mm. The code requires a minimum depth of raft equal to 150 mm.

B. Design for Reinforcement:

1. **Radial steel for a moment of 53.785 kNm/m**

$$A_{st1} = 0.5\frac{20}{460}\left[1-\sqrt{1-\frac{4.6\times 53.785\times 10^6}{20\times 1000\times 180^2}}\right]1000\times 180 = 836.41\ \text{mm}^2$$

Use 10 mm bars, $A_\phi = 78.5398\ \text{mm}^2$

$$\text{Number of bars} = n = \frac{836.41}{\frac{\pi}{4}10^2} = 10.64 \cong 11\ \text{bars}$$

$$\text{Spacing of long bars} = s = \frac{1000\times 78.5398}{836.41} = 93.90\ \text{mm} \cong 90\ \text{mm}$$

Use 11–10 mm Φ bars @ 90 mm c/c radially.

2. **Circumferential steel for a sagging moment of 71.52 kNm/m @ $r = 4$ m**

$$A_{st} = 0.5\frac{f_{ck}}{f_y}\left[1-\sqrt{1-\frac{4.6\times M_\theta\times 10^6}{f_{ck}Bd^2}}\right]Bd$$

$$A_{st1} = 0.5\frac{20}{460}\left[1-\sqrt{1-\frac{4.6\times 71.524\times 10^6}{20\times 1000\times 180^2}}\right]1000\times 180 = 1167.6\ \text{mm}^2$$

Use 10 mm bars, $A_\phi = 78.5398\ \text{mm}^2$

$$\text{Number of bars} = \frac{1167.6}{\frac{\pi}{4}10^2} = 14.86 \cong 15\ \text{bars}$$

$$\text{Spacing of long bars} = s = \frac{1000\times 78.5398}{1167.6} = 67.266\ \text{mm} \cong 60\ \text{mm}$$

Use 15–10 mm Φ bars for circumferential steel reinforcement sagging moment (@ $r = 4$ m) @ 60 mm c/c.

3. **Circumferential steel for a sagging moment of 55.25 kNm/m @ $r = 5$ m**

$$A_{st1} = 0.5\frac{20}{460}\left[1-\sqrt{1-\frac{4.6\times 55.2563\times 10^6}{20\times 1000\times 180^2}}\right]1000\times 180 = 862.5042\ \text{mm}^2$$

Use 10 mm bars, $A_\phi = 78.5398\ \text{mm}^2$

$$\text{Number of bars} = n = \frac{862.50}{\frac{\pi}{4}10^2} = 10.98 \cong 11\ \text{bars}$$

$$\text{Spacing of long bars} = s = \frac{1000\times 78.5398}{862.50} = 91.06\ \text{mm} \cong 90\ \text{mm}$$

Use 11–10 mm Φ bars for circumferential steel reinforcement sagging moment (@ $r = 5$ m) @ 90 mm c/c.

4. **Circumferential steel for sagging moment of 45.43 kNm/m @ $r = 6$ m**

$$A_{st1} = 0.5\frac{20}{460}\left[1-\sqrt{1-\frac{4.6\times 45.4345\times 10^6}{20\times 1000\times 180^2}}\right]1000\times 180 = 692.2708\ \text{mm}^2$$

Use 10 mm bars, $A_\phi = 78.5398\ \text{mm}^2$

$$\text{Number of bars} = n = \frac{692.27}{\frac{\pi}{4}10^2} = 8.81 \cong 9\ \text{bars}$$

$$\text{Spacing of long bars} = s = \frac{1000\times 78.5398}{692.27} = 113.45\ \text{mm} \cong 100\ \text{mm}$$

Use 9–10 mm Φ bars for circumferential steel reinforcement for sagging moment (@ $r = 6$ m) @ 100 mm c/c.

5. **Circumferential steel for hogging moment of 12.24 kNm/m**

$$A_{st1} = 0.5\frac{20}{460}\left[1-\sqrt{1-\frac{4.6\times 12.24\times 10^6}{20\times 1000\times 180^2}}\right]1000\times 180 = 173.86\ \text{mm}^2$$

Use 10 mm bars, $A_\phi = 78.5398\ \text{mm}^2$

$$\text{Number of bars} = n = \frac{173.86}{\frac{\pi}{4}10^2} = 2.21 \cong 3\ \text{bars}$$

$$\text{Spacing of long bars} = s = \frac{1000\times 78.5398}{173.86} = 451.74\ \text{mm} \cong 450\ \text{mm}$$

Use 3–10 mm Φ bars for circumferential steel reinforcement for hogging moment (at the top of the slab thought) @ 450 mm c/c. The raft can be checked for shear and development length.

The reinforcement details are shown in Figure 12.C.22(b).

Example 12.9 Circular Raft Foundation

Design a circular raft for a circular tank whose outer diameter is 12 m and is supported by a ring beam of 9 m diameter. The inner diameter of the annulus is 8 m. The factored soil pressure under the raft is 80 kN/m^2 and a linearly varying soil pressure due to wind/earthquake = ± 30 kN/m^2. Use M 15 concrete and Fe 415 grade steel.

A. Design of Circular Raft Slab

The raft and loading details are shown in Figure 12.C.23(a).

The self weight of raft slab and that of the earth directly above it are not considered for the design of raft slab itself as these are directly supported by the soil below it. For the purpose of analysis of the base raft slab, it may be assumed to be supported on factious supports at the outer periphery and loaded with:

1. A uniformly distributed load of + 80 kN/m^2 acting upward.
2. A uniformly varying factored load of −30 to + 30 kN/m^2 due to reversible earthquake load.

The moments due to each of these two types of load may be computed as follows (Kurian, 1992).

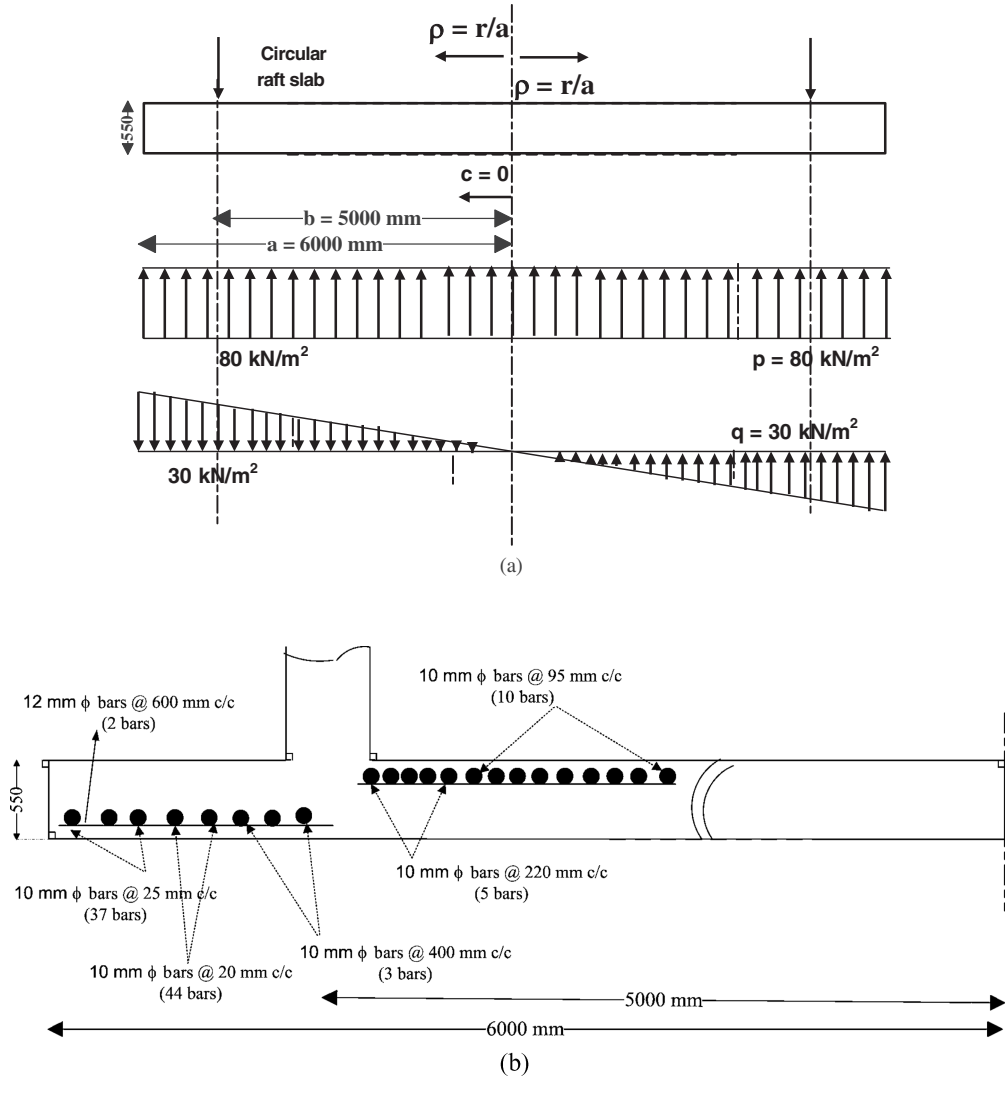

Figure 12.C.23 (a) Sectional elevation of circular raft and pressure distribution; and (b) reinforcement in raft slab (Example 12.9).

1. **Moments due to uniformly distributed load acting upward**
   The radial and circumferential moments are given as follows.

$$\text{Let } \alpha = \frac{c}{a}, \beta = \frac{b}{a}, \rho = \frac{r}{a}$$

If $r \leq b$

$$\begin{cases} K_1 = 2(1+\alpha^2)\left[\dfrac{3+\mu}{1+\mu}\right] - \dfrac{8\alpha^4 \log_e \alpha}{1-\alpha^2} - 4\beta^2\left[\dfrac{1-\mu}{1+\mu}\right] - 8[1+\log_e(1+\beta)] \\ K_2 = 4\alpha^2\left[\dfrac{3+\mu}{1-\mu}\right] - \dfrac{16\alpha^4 \log_e \alpha}{1-\alpha^2}\left[\dfrac{1+\mu}{1-\mu}\right] - 16\alpha^2\left[\dfrac{1+\mu}{1-\mu}\right][1+\log_e(1+\beta)] - 8\alpha^2\beta^2 \end{cases} \tag{12.C.79}$$

$$VM_{r1} = \frac{pa^2}{64}\left[4(3+\mu)\rho^2 - 16\alpha^2(1+\mu)\log_e\rho - 8\alpha^2(3+\mu) + 2(1+\mu)K_1 - (1-\mu)K_2\rho^{-2}\right] \tag{12.C.80}$$

$$VM_{\theta 1} = \frac{pa^2}{64}\left[4(1+3\mu)\rho^2 - 16\alpha^2(1+\mu)\log_e\rho - 8\alpha^2(1+3\mu) + 2(1+\mu)K_1 + (1-\mu)K_2\rho^{-2}\right] \tag{12.C.81}$$

If $r > b$

$$K_q^{|} = K_1 + 8[1+\log_e(1+\beta)](1-\alpha^2) \tag{12.C.82}$$

$$K_2^{|} = K_2 - 8\beta^2(1-\alpha^2) \tag{12.C.83}$$

$$VM_{r2} = \frac{pa^2}{64}\left[4(3+\mu)\rho^2 - 16(1+\mu)\log_e\rho - 8(3+\mu) + 2(1+\mu)K_1^{|} - (1-\mu)K_2^{|}\rho^{-2}\right] \tag{12.C.84}$$

$$VM_{\theta 2} = \frac{pa^2}{64}\left[4(1+3\mu)\rho^2 - 16(1+\mu)\log_e\rho - 8(1+3\mu) + 2(1+\mu)K_1^{|} + (1-\mu)K_2^{|}\rho^{-2}\right] \tag{12.C.85}$$

$$VQ_{r2} = \frac{pa}{2}(\rho - \rho^{-1}) \tag{12.C.86}$$

2. **Moments due to uniformly varying load $\pm$q per unit area**
The radial and circumferential moments are given as follows.

If $r <= b$

$$\begin{cases} K_3 = \dfrac{3}{\beta^2} - 3\beta^2\left(\dfrac{1-\mu}{3+\mu}\right) - 8\left(1+\dfrac{\alpha^4}{1+\alpha^2}\right)\left(\dfrac{2+\mu}{3+\mu}\right) \\ K_4 = 3\beta^2\alpha^4 - \dfrac{3\alpha^4}{\beta^2}\left(\dfrac{3+\mu}{1-\mu}\right) + 8\left(\dfrac{\alpha^4}{1+\alpha^2}\right)\left(\dfrac{2+\mu}{1-\mu}\right) \\ K_5 = 12\alpha^4 \end{cases} \tag{12.C.87}$$

$$MM_{r1} = \frac{qa^2}{192}\left[4(5+\mu)\rho^3 + 2(3+\mu)K_3\rho + 2(1-\mu)K_4\rho^{-3} + (1+\mu)K_5\rho^{-1}\right]\cos\theta \tag{12.C.88}$$

$$MM_{\theta 1} = \frac{qa^2}{192}\left[4(1+5\mu)\rho^3 + 2(1+3\mu)K_3\rho - 2(1-\mu)K_4\rho^{-3} + (1+\mu)K_5\rho^{-1}\right]\cos\theta \tag{12.C.89}$$

$$MQ_{r1} = \frac{qa}{192}(72\rho^2 + 8K_3 - 2K_5\rho^{-2})\cos\theta \tag{12.C.90}$$

If $r > b$

$$\begin{cases} K_3^{|} = K_3 - \dfrac{3}{\beta^2}(1-\alpha^4) \\ K_4^{|} = K_4 + 3\beta^2(1-\alpha^4) \\ K_5^{|} = 12.0 \end{cases} \tag{12.C.91}$$

The expressions for $MM_{r1}{}^{|}$ and so on, are the same as for $r \Leftarrow b$ with $K_3{}^{|}$, $K_4{}^{|}$ and $K_5{}^{|}$ replacing K_3, K_4 and K_5 respectively. The details of various terms in the above expression are as follows:

$a = 12/2 = 6$ m, $b = 10/2 = 5$ m, $\alpha = \frac{c}{a} = 0$, $\beta = \frac{b}{a} = \frac{5}{6}$, $\rho = \frac{r}{a} = \frac{r}{6}$, $\cos\theta = 1.0$ for $\theta = 0$, $q = \mp 30\,\text{kN/m}^2$, r varies from 0 to 6 m.

The depth of slab will be based on a maximum moment of $M = 499.18$ kNm/m (M_θ @ $\rho = 1.0$; see Tables 12.C.12–12.C.15). Considering a 1 m strip for design, $B = 1$ m. Effective depth d is given by

$$d = \sqrt{\frac{M}{0.138 f_{ck} B}} \tag{12.C.92}$$

Table 12.C.12 Radial moments and steel reinforcement due to uniformly distributed load and uniformly varying pressure.

M_r (kNm/m)	$\rho = 0{\cdot}0$	$\rho = 0.1$	$\rho = 0.2$	$\rho = 0.3$	$\rho = 0.4$	$\rho = 0.5$
(1) Due to UDL 80 kN/m^2	−346.35	−340.41	−322.59	−292.89	−251.31	−197.85
(2) Due to UVL + 30 kN/m^2	0.00	−6.18	−11.65	−15.69	−17.58	−16.61
(3) Due to UVL − 30 kN/m^2	0.00	6.18	11.65	15.69	17.58	16.61
(4) = (1) + (2)	−346.35	−346.59	−334.24	−308.58	−268.89	−214.45
(5) = (1) − (2)	−346.35	−334.22	−310.94	−277.20	−233.73	−181.24
Maximum design value from (4) and (5)	−346.35	−346.59	−334.24	−308.58	−268.89	−214.45
Radial steel reinforcement, A_{st} (mm^2/m)	2183.30 @ top	2185.00 @ top	2095.40 @ top	1912.60 @ top	1638.80 @ top	1279.00 @ top
Number of steel bars (12 mm dia bars; n)	20		19	17	15	12
Spacing (S; mm c/c radially)	50		55	60	70	90

Table 12.C.13 Radial moments and steel reinforcement due to uniformly distributed load and uniformly varying pressure.

M_r (kNm/m)	$\rho = 0.6$	$\rho = 0.7$	$\rho = 0.8$	$\rho = 0.9$	$\rho = 1.0$
(1) Due to UDL 80 kN/m^2	−132.51	−55.29	33.81	26.81	0.00
(2) Due to UVL + 30 kN/m^2	−12.06	−3.22	10.64	−4.67	0.00
(3) Due to UVL −30 kN/m^2	12.06	3.22	−10.64	4.67	0.00
(4) = (1) + (2)	−144.56	−58.50	44.45	22.13	0.00
(5) = (1) − (2)	−120.45	−52.07	23.18	31.48	0.00
Maximum design value from (4) and (5)	−144.56	−58.50	44.45	31.48	0.00
Radial steel reinforcement, A_{st} (mm^2/m)	840.20 @ top	330.30 @ top	249.80 @ bottom	176.20 @ bottom	0.00 @ bottom
Number of steel bars (12 mm dia bars; n)	8	3	3	2	0.00
Spacing (S) (mm c/c radially)	130	340	450	600	—

Table 12.C.14 Circumferential moments and steel reinforcement due to uniformly distributed load and uniformly varying pressure.

M_θ (kNm/m)	$\rho = 0.0$	$\rho = 0.1$	$\rho = 0.2$	$\rho = 0.3$	$\rho = 0.4$	$\rho = 0.5$
(1) Due to UDL 80 kN/m^2	−346.35	−340.41	−322.59	−292.89	−251.31	−197.85
(2) Due to UVL + 30 kN/m^2	0.00	−3.57	−6.81	−9.37	−10.92	−11.11
(3) Due to UVL −30 kN/m^2	0.00	3.57	6.81	9.37	10.92	11.11
(4) = (1) + (2)	−346.35	−343.98	−329.39	−302.25	−262.22	−208.96
(5) = (1) − (2)	−346.35	−336.83	−315.78	−283.52	−240.39	−186.73
Maximum design value from (4) and (5)	−346.35	−343.98	−329.39	−302.25	−262.22	−208.96
Circumferential steel reinforcement, A_{st} (mm^2/m)	2183.30 @ top	2166.00 @ top	2060.50 @ top	1868.30 @ top	1593.80 @ top	1243.70 @ top
Number of steel bars (10 mm dia rings; n)	28	28	27	24	21	16
Spacing (S; mm)	30	30	35	40	50	60

$$d = \sqrt{\frac{499.18 \times 10^6}{(0.138 \times 15 \times 1000)}} = 491.07 \text{ mm}$$

Note that stresses are not increased by 33.33% in the limit state design method in the case of earthquake loading. Adopt effective depth as $d = 500$ mm and overall depth as

Table 12.C.15 Circumferential moments and steel reinforcement due to uniformly distributed load and uniformly varying pressure.

M_θ (kNm/m)	$\rho = 0.6$	$\rho = 0.7$	$\rho = 0.8$	$\rho = 0.9$	$\rho = 1.0$
(1) Due to UDL 80 kN/m^2	−132.51	−55.29	33.81	−405.29	−350.00
(2) Due to UVL + 30 kN/m^2	−9.62	−6.11	−0.23	93.89	91.31
(3) Due to UVL − 30 kN/m^2	9.62	6.11	0.23	−93.89	−91.31
(4) = (1) + (2)	−142.13	−61.39	33.58	−311.40	−258.69
(5) = (1) − (2)	−122.88	−49.18	34.04	−499.18	−441.31
Maximum design value from (4) and (5)	−142.13	−61.39	34.04	−499.18	−441.31
Circumferential steel reinforcement, A_{st} (mm^2/m)	825.40 @ top	346.90 @ top	190.70 @ bottom	3409.90 @ bottom	2916.50 @ bottom
Number of steel bars (10 mm dia rings; n)	10	5	3	44	37
Spacing (S; mm)	95	220	400	20	25

$D = 550$ mm. The code requires a minimum depth of raft equal to 150 mm. Radial and circumferential steel reinforcement can be calculated by using the following equation

$$A_{st} = 0.5\frac{f_{ck}}{f_y}\left[1-\sqrt{1-\frac{4.6\times M\times 10^6}{f_{ck}Bd^2}}\right]Bd \qquad (12.C.93)$$

$$A_{st} = 0.5\frac{15}{415}\left[1-\sqrt{1-\frac{4.6\times 346.35\times 10^6}{15\times 1000\times 500^2}}\right]1000\times 500 = 2183.30\,\text{mm}^2$$

Use 12 mm bars, $A_\phi = 113.09$ mm^2

$$\text{Number of bars} = n = \frac{A_{st}}{A_\Phi} = 20\,\text{bars}$$

$$\text{Spacing of long bars } (S) = \frac{1000\times A_\Phi}{A_{st}} \cong 50\,\text{mm}$$

Use 20–10 mm Φ bars for radial steel reinforcement for hogging moment (@ $\rho = 0.0$) @ 50 mm c/c. Similarly we can calculate the radial and circumferential steel reinforcement for other ρ values. The details are shown in Tables 12.C.12–12.C.15
The raft can be checked for shear and development length.

The reinforcement is shown in Figure 12.C.23(b).

Appendix 12.D Comparative Features of Concrete Codes for Foundation Design

12.D.1 Introduction

Engineering design in general and foundation design in particular is an iterative process involving detailed analysis based on appropriate modeling, conceptualization, evaluation of input parameters for computation and satisfying the design criteria. Foundation design criteria and final choice of the dimensions and specifications may have to comply with local practices, building codes, design codes, and standards. Cities, countries, and regions have developed these codes and standards depending on the local conditions, materials, and practices and are updated regularly to keep pace with the technical developments. While the modeling and analysis is a major component of the design process, the final choice of design parameters and specifications (which is the concluding part of the design process) is essential and has to be based on the local codes and standards. Thus a major portion of the design process is common to all codes but the final design dimensions have to be decided as per the local codes and standards. Thus the structural design examples presented in this book (mainly Appendix 12.C) are based on Indian codes such as IS: 456–2000 (2000) to present a complete design though most of the analysis used is general and universal. Thus the designs presented in this book (Appendix 12.C) can be easily modified to suit applications based on local codes in the final phase since the analysis is general.

To facilitate this final process of foundation design, the comparative features of a few commonly used structural concrete design codes, that is, Indian code, BS code, Eurocode, and ACI Code are summarized in this Appendix. The information presented below is considered relevant to RCC foundation design and is not exhaustive. For further details, the presently active codes applicable to the geographical location of the site have to be referred to.

All the information given in this Appendix is summarized from the following codes, except for those mentioned specifically in the text. Symbols not defined here can be taken as those given in Appendix 12.A or referred to the relevant code mentioned:

1. Indian Standard refers to IS: 456–2000 (2000).
2. British Standard refers to BS 8110-1 (1997).
3. Eurocode refers to DD ENV 1992-1-1:1992 (Eurocode, 1992).
4. ACI code refers to ACI 318M-95 (ACI, 1995).

12.D.2 Partial Safety Factors and Load Combinations

Table 12.D.1 lists partial safety factors. For Eurocode, see Table 12.D.2.

Table 12.D.1 Partial safety factors for loads under ultimate limit states.

Load combination	Indian standard	British standard	ACI code
DL + LL	1.5DL + 1.5LL	1.4DL + 1.6LL	1.4DL + 1.7LL
DL + WL	1.5DL + 1.5WL	1.4DL + 1.4WL.	0.9DL + 1.3WL
	[a]0.9DL + 1.5WL	[a]1.0DL + 1.4WL	
DL + LL + WL	1.2DL + 1.2LL + 1.2WL		0.75(1.4DL + 1.7LL + 1.7WL)

[a]This value should be considered if stability against overturning or stress reversal is critical.

Table 12.D.2 Load combinations and values of partial safety factors for the ultimate limit state according to Eurocode.

Load combination	Load type					
	Permanent		Variable		Earth and water pressure	Wind
	Adverse	Beneficial	Adverse	Beneficial		
Permanent and variable (and earth and water pressure)	1.35 (1.40)	1.0 (1.0)	1.50 (1.60)	0 (0)	1.35 (1.40)	—
Permanent and wind (and earth and water pressure)	1.35 (1.40)	1.0 (−)	—	—	1.35 (1.40)	1.50 (1.40)
Permanent and variable and wind (and earth and water pressure)	1.35 (1.2)	1.0 (−)	1.35 (1.2)	0 (−)	1.35 (1.2)	1.35 (1.2)

Note: figures in brackets refer to British standard BS8110 values.

12.D.3 Steel Details

Table 12.D.3 lists steel details.

12.D.4 Concrete Details

Table 12.D.4 lists concrete details, Table 12.D.5 lists grades of concrete and steel, and Table 12.D.6 lists the elastic modulus for concrete and steel.

12.D.5 Maximum Depth of Neutral Axis

Table 12.D.7 lists depth data given by the four codes.

12.D.6 Limiting Moment of Resistance and Tensile Reinforcement Area

1. From Indian Standard
   a. If $\frac{x_m}{d} < \frac{x_{m,\max}}{d}$, the resistance moment of the section is

$$\begin{aligned} M_{\lim} \text{ with respect to steel} &= 0.87\sigma_y A_t(d-0.42x_m) \\ &= 0.87\sigma_y A_t d\left(1-\frac{A_t}{bd}\frac{\sigma_y}{\sigma_{ck}}\right) \end{aligned}$$

Table 12.D.3 Yield stress of different steels.

Types of steels	Indian standard	Eurocode	ACI code	British standard
Mild steel (MPa)	From IS: 432 (part 1), for bar up to 20 mm, 260 From IS: 1139, for bar over 20 mm, 240	—	—	Hot rolled mild steel, 250
High-yield steel (MPa)	From IS: 1139, 425	500	—	Hot rolled or cold worked, 460
Medium tensile steel (MPa)	From IS: 1786, 415: for bars up to 20 mm, 360 For bars between 20–40 mm, 345 For bars over 40 mm, 330	—	—	—
SAIL-MA (MPa)	300HY, 300 350HY, 350 410HY, 410 450HY, 450	—	—	—
Billet steel (MPa)	—	—	Grade 40, 276 Grade 60, 414 Grade 75, 518	—
Rail steel (MPa)	—	—	Grade 50, 345 Grade 60, 414	—
Deformed wire (MPa)	—	—	Reinforcing, 518 Fabric, 483	—
Cold-drawn wire (MPa)	—	—	Reinforcing, 483 Fabric, 448 or 386	—

Table 12.D.4 Shape of test specimen for concrete strength.

Code and clause	Clause and contents
Indian standard (IS: 456–2000)	Cube $150 \times 150 \times 150$ mm
ACI-318	Cylinder 152.4×304.8 mm
Eurocode	Cylinder 152.4×304.8 mm
British standard (BS 1881:1983)	Cube $150 \times 150 \times 150$ mm or $100 \times 100 \times 100$ mm

where
A_t = area of tension reinforcement
b = breath of beam or breath of web of T-beam.

$$At = 0.5\frac{\sigma_{ck}}{\sigma_y}\left[1-\sqrt{1-\frac{4.6M_{\lim}\times 10^6}{\sigma_{ck}bd^2}}\right]$$

Table 12.D.5 Available grades of concrete and steel.

Code and clause	Material	Clause and contents
Indian standard IS: 456–2000	Grades of concrete (in the designation of concrete mix M refers to the mix and the number to the specified compressive strength of 150 mm size cube at 28*d*, expressed in N/mm^2)	Ordinary concrete: M 10, M 15 and M 20
		Standard concrete: M 25, M 30, M 35, M40, M 45, M 50 and M 55
		High-strength concrete: M 60, M 65, M 70, M 75 and M 80
	Grades of steel	The grades of steel recommended in the Indian code are: mild steel bars and high yield strength deformed (HYSD) bars, that is, MS 250, Fe 415 and Fe 500. The number indicates the yield strength of the steel (σ_y).
ACI-318	Grades of concrete	Sampling concrete – ASTM C 172
		Strength testing standards – ASTM C 31, C 39, C 78, C 617 and C 1231
		Air content tests – ASTM C 173, C 231
		Slump – ASTM C 143
		Density – ASTM C 138
		Temperature – ASTM C 1064
		Specification of ready mixed concrete – ASTM C 94
	Grades of steel	ASTM A 615/A 615M
		Bars are of three minimum yield strength levels: namely, 40 000, 60 000, and 75 000 psi (280, 420, and 520 MPa), designated as grade 40 [280], grade 60 [420], and grade 75 [520], respectively.

(continued)

Table 12.D.5 *(Continued)*

Eurocode	Grades of concrete [for example: grade C25/30 denotes a designed mix for which cylinder strength of 25 MPa or cube strength of 30 MPa is guaranteed. In addition, C25/30 means characteristic compressive cylinder strength of concrete at $28d$ in N/mm^2 $(\sigma_{ck}) = 25\ N/mm^2$ and mean value of compressive cylinder strength of concrete at $28d$ $(\sigma_{cm}) = \sigma_{ck} + 8 = 33\ N/mm^2$]	Available grades of concrete are: C 12/15, C 16/20, C 20/2, C 25/30, C 30/37, C 35/45, C 40/50, C 45/55, C 50/60, C 55/65, C 60/75, C 70/85, C 80/95, C 90/105 and C 100/1155
	Grades of steel	The grade of steel recommended in the European code is S 500, that is, high yield steel (hot rolled or cold worked), with a yield strength (σ_{yk}) of 500 MPa.
British standard code	Grades of concrete	For reinforced concrete, the lowest grade that should be used is C15 for concrete made with lightweight aggregate and C 25 for concrete made with normal-weight aggregates. Design should be based on the $28d$ characteristic strength unless there is evidence to justify a higher strength for a particular structure. The available grades of concrete are: C 30, C 35, C 40, C 45 and C 50
	Grades of steel	The grades of steel recommended in the British standard code are: mild steel bars and high yield strength deformed (HYSD) bars, that is, MS 250, Fe 460, the number indicates the yield strength of the steel (σ_y).

Table 12.D.6 Elastic modulus for concrete and steel.

Standard	Elastic modulus
IS: 456–2000 (6.2.3.1)	Elastic modulus of concrete $E_c = 5000\sqrt{f_{ck}}$ (in N/mm^2) where f_{ck} = characteristic compressive strength of concrete in N/mm^2 Yield strength of steel, $E_s = 200 \times 10^3$ (in N/mm^2)
ACI-318 (23.2.1)	$E_c = 4700\sqrt{f'_c}$ (in N/mm^2) where f_{ck} = specified compressive strength of concrete, (in N/mm^2) $E_s = 200 \times 10^3$ (in N/mm^2)
Eurocode	Mean value of secant modulus of elasticity of concrete, $E_{cm} = 9500(f_{ck} + 8)^{1/3}$ (in N/mm^2) $E_s = 200 \times 10^3$ (in N/mm^2)
British standard code (BS 8110-2 1985)	$E_c = 5.5\sqrt{\frac{f_{cu}}{\gamma_m}}$(in N/mm^2) where f_{cu} = characteristic strength of concrete and γ_m is partial safety factor for strength of materials Mean values for normal-weight concrete $E_{c,28} = K_0 + 0.2f_{cu,28}$ where $E_{c,28}$ = static modulus of elasticity at 28d $f_{cu,28}$ = characteristic cube strength at 28 d (in N/mm^2) K_o = constant closely related to the modulus of elasticity of the aggregate (taken as 20 kN/mm^2 for normal-weight concrete) At an age t $E_{c,t} = E_{c,28}(0.4 + 0.6f_{cu,t}/f_{cu,28})$ $E_s = 200 \times 10^3$ (in N/mm^2) Test for dynamic modulus can be used to obtain an estimated value for the static modulus of elasticity of natural aggregate concrete from the following formula $E_c = 1.25E_{cq} - 19$ where E_{cq} is the dynamic modulus of elasticity

b. If $\frac{x_m}{d} = \frac{x_{m,\max}}{d}$, the resistance moment of the section is

$$M_{\lim} = 0.36\frac{x_{m,\max}}{d}\left(1 - 0.42\frac{x_{m,\max}}{d}\right)bd^2\sigma_{ck}$$

c. If $\frac{x_m}{d} > \frac{x_{m,\max}}{d}$, the section should be redesigned.

2. From Eurocode

For a concrete class less than C 50/60

$$M_{\lim} \text{ with respect to steel} = 0.95\sigma_y A_t z$$

Table 12.D.7 Maximum depth of neutral axis.

	Indian standard	Eurocode	ACI code	British standard
Maximum depth of neutral axis, x_m	$\sigma_y = 250\,\text{N/mm}^2$, $x_m = 0.53d$	$\sigma_{cu} \leq 45\,\text{N/mm}^2$, $x_m = 0.45d$	$\sigma_y = 40$ ksi (276 MPa), $x_m = 0.685d$	For all values of σ_{cu}, $x_m = 0.5d$
	$\sigma_y = 415\,\text{N/mm}^2$, $x_m = 0.48d$	$\sigma_{cu} > 45\,\text{N/mm}^2$, $x_m = 0.35d$	$\sigma_y = 50$ ksi (345 MPa), $x_m = 0.635d$	
	$\sigma_y = 500\,\text{N/mm}^2$, $x_m = 0.46d$		$\sigma_y = 56$ ksi (386 MPa), $x_m = 0.608d$	
	(d = effective depth of steel)		$\sigma_y = 60$ ksi (414 MPa), $x_m = 0.592d$	
			$\sigma_y = 65$ ksi (448 MPa), $x_m = 0.572d$	
			$\sigma_y = 70$ ksi (483 MPa), $x_m = 0.554d$	
			$\sigma_y = 75$ ksi (518 MPa), $x_m = 0.537d$	

where

$$z = \frac{d}{2}(1 + \sqrt{1-3.53k}) \leq 0.95d$$

$$k = \frac{M}{bd^2 f_{ck}}$$

and $k' = 0.60\delta - 0.18\delta^2 - 0.21$

Redistribution ratio, $\delta \leq 1.0$

If $k \leq k'$, single tension reinforcement is required.

$$A_t = \frac{M_{\text{lim}}}{0.95\sigma_y z}$$

where

A_t = area of tension reinforcement

b = breath of beam or breath of Web of T-beam.

3. From British Standard

$$M_{\text{lim}} \text{ with respect to steel} = 0.95\sigma_y A_t z$$

where

$$z = (0.5 + \sqrt{(0.25 - k/0.9)})d \leq 0.95d$$

and

$$k = \frac{M}{bd^2\sigma_{cu}} < 0.156$$

M_{lim} = design ultimate moment, σ_{cu} = characteristic strength of concrete

$$A_t = \frac{M_{\lim}}{0.95\sigma_y z}$$

4. From ACI Code

$$M_{\lim} \text{ with respect to steel} = \phi A_t \sigma_y (d - (A_t \sigma_y / 1.7\sigma_{cu} b))$$

where

Design consideration	φ
Moment, without axial load	0.90
Two-way action, bond and anchorage	0.85
Compression members, spiral	0.75
Compression members, tied	0.70
Unreinforced footings	0.65
Bearing on concrete	0.70

$$\text{Steel ratio at cross section,} \quad \rho = \frac{0.85\sigma_{cu}}{\sigma_y}\left[1 - \sqrt{1 - \frac{4M_{\lim}}{1.7\phi\sigma_{cu} b d^2}}\right]$$

Tension steel area, $A_s = \rho bd$

Equation A (for Table 12.D.8)

$$Mu = \phi b d^2 \sigma_{ck} q(1 - 0.59q)$$

For balance design, steel ratio at cross-section

$$P_{\max} = 0.75 P_b$$

$$P_b = \frac{0.85\beta\sigma_{ck}}{\sigma_y}\frac{600}{\sigma_y + 600} \quad \text{(for S.I. units)}$$

Since $q = p_{\max}\frac{\sigma_y}{\sigma_{ck}}$

$$q = \frac{0.75 \times 0.85\beta\sigma_{ck}}{\sigma_y}\left(\frac{600}{\sigma_y + 600}\right)\frac{\sigma_y}{\sigma_{ck}} \text{ and } \beta_1 = 0.85 \text{ (for concrete with } \sigma_{ck} < 30\,\text{N/mm}^2).$$

12.D.7 Limiting Tensile Steel in Rectangular Sections

Table 12.D.9 lists the data provided by all four codes.

12.D.8 Minimum Tension Reinforcement

1. From Indian Standard
   a. *Beams*

   The minimum area of tension reinforcement shall be not less than that given by the following equation

Table 12.D.8 Limiting moment of resistance values, N/mm^2.

	Indian standard	Eurocode	ACI code	British standard
General equations	For Fe 250 steel, $0.148\sigma_{ck}bd^2$	For $\sigma_{ck} \leq 45$ N/mm^2, $0.136\sigma_{ck}bd^2$	Equation A (from Section 12.D.5)	$0.156\sigma_{ck}bd^2$
	For Fe 415 steel, $0.138\sigma_{ck}bd^2$	For $\sigma_{ck} > 45$ N/mm^2, $0.11\sigma_{ck}bd^2$		
	For Fe 500 steel, $0.133\sigma_{ck}bd^2$			
For concrete – grade 15	For Fe 250 steel, $2.22bd^2$	$2.04bd^2$	For grade 40 steel (276 MPa, 40 ksi) $4.349\phi\ bd^2$	$2.34bd^2$
	For Fe 415 steel, $2.07bd^2$		For grade 50 steel, (345 MPa, 50 ksi) $4.113\phi\ bd^2$	
	For Fe 500 steel, $2bd^2$		For grade 60 steel, (414 MPa, 60 ksi) $3.900\phi\ bd^2$	
For concrete – grade 20	For Fe 250 steel, $2.96bd^2$	$2.72bd^2$	For grade 40 steel (276 MPa, 40 ksi) $5.798\phi\ bd^2$	$3.12bd^2$
	For Fe 415 steel, $2.76bd^2$		For grade 50 steel, (345 MPa, 50 ksi) $5.484\phi\ bd^2$	
	For Fe 500 steel, $2.66bd^2$		For grade 60 steel, (414 MPa, 60 ksi) $5.199\phi\ bd^2$	
For concrete – grade 25	For Fe 250 steel, $3.70bd^2$	$3.40bd^2$	For grade 40 steel (276 MPa, 40 ksi) $7.247\phi\ bd^2$	$3.90bd^2$
	For Fe 415 steel, $3.45bd^2$		For grade 50 steel, (345 MPa, 50 ksi) $6.855\phi\ bd^2$	
	For Fe 500 steel, $3.33bd^2$		For grade 60 steel, (414 MPa, 60 ksi) $6.499\phi\ bd^2$	

$$\frac{A_{\text{minimum}}}{bd} = \frac{0.85}{\sigma_y}$$

A_{minimum} = minimum area of tension reinforcement, b = breadth of beam or the breadth of the web of the T-beam, d = effective depth, and σ_y = characteristic strength of reinforcement in N/mm^2.

b. *Slabs and Footings*

The mild steel reinforcement in either direction in slabs shall not be less than 0.15% of the total cross-sectional area. However, this value can be reduced to 0.12% when high strength deformed bars or welded wire fabric are used.

Table 12.D.9 Limiting tensile steel in rectangular sections (%).

	Indian standard	Eurocode	ACI code	British standard
For concrete – grade 15	For Fe 250 steel, 1.32 For Fe 415 steel, 0.72 For Fe 500 steel, 0.57	—	For Fe 250 steel, 2.30 For Fe 415 steel, 1.16 For Fe 500 steel, 0.89	For Fe 250 steel, 1.27 For Fe 415 steel, 0.77 For Fe 500 steel, 0.64
For concrete – grade 20	For Fe 250 steel, 1.76 For Fe 415 steel, 0.96 For Fe 500 steel, 0.76	For Fe 250 steel, 1.9 For Fe 460 steel, 1.0 For Fe 500 steel, 0.9	For Fe 250 steel, 3.06 For Fe 415 steel, 1.54 For Fe 500 steel, 1.18	For Fe 250 steel, 1.70 For Fe 415 steel, 1.02 For Fe 500 steel, 0.85
For concrete – grade 25	For Fe 250 steel, 2.20 For Fe 415 steel, 1.19 For Fe 500 steel, 0.94	For Fe 250 steel, 2.4 For Fe 460 steel, 1.3 For Fe 500 steel, 1.2	For Fe 250 steel, 3.83 For Fe 415 steel, 1.93 For Fe 500 steel, 1.48	For Fe 250 steel, 2.12 For Fe 415 steel, 1.28 For Fe 500 steel, 1.06
For concrete – grade 30	For Fe 250 steel, 2.64 For Fe 415 steel, 1.43 For Fe 500 steel, 1.13	For Fe 250 steel, 2.8 For Fe 460 steel, 1.5 For Fe 500 steel, 1.4	For Fe 250 steel, 4.59 For Fe 415 steel, 2.32 For Fe 500 steel, 1.77	For Fe 250 steel, 2.54 For Fe 415 steel, 1.53 For Fe 500 steel, 1.27

2. From British Standard

$$A_{\text{minimum}} = 0.0024bd \text{ (For } \sigma_y = 250 \text{ MPa)}$$

$$A_{\text{minimum}} = 0.0013bd \text{ (For } \sigma_y = 460 \text{ MPa)}$$

3. From ACI Code
   a. *Flexural Members*

   At every section of a flexural member where tensile reinforcement is required by analysis, the minimum area of reinforcement (A_{minimum}) provided shall not be less than that given by:

$$A_{\text{minimum}} = \frac{\sqrt{\sigma_{cu}}}{4\sigma_y} bd \geq 1.4bd$$

   b. *Slabs and Foundation*

$$A_{\text{minimum}} = 0.14\%$$

   For grade 300 or 350 deformed bars steel – 0.2%.
   For grade 420 deformed bars steel – 0.18%.
4. From Eurocode

$$A_{\text{minimumn}} = \frac{0.26\sigma_{ctm}bd}{\sigma_{yk}} \leq 0.0013bd \ (\sigma_{ctm} = 0.3\sigma_{ck}^{2/3} \text{ for } \sigma_{ck} \leq 50 \text{ MPa})$$

12.D.9 Maximum Tension Reinforcement

From Indian Standard, Eurocode, and British Standard, the maximum area of tension reinforcement is limited to 4% of gross cross-sectional area to avoid difficulty in placing and compacting concrete properly in formwork.

From ACI Code, the maximum area of tension reinforcement is

$$A_{\max} = 0.75\rho_b$$

where

$$P_b = \frac{0.85\beta\sigma_{ck}}{\sigma_y}\frac{600}{\sigma_{ck} + 600}$$

12.D.10 Shear Reinforcement

From Eurocode, the maximum permissible shear stress of concrete is

$0.243\left(0.7-\frac{\sigma_{cu}}{247}\right)\sigma_{cu}$ if $\sigma_{cu} \leq 50\,\mathrm{N/mm^2}$.

From British Standard, the nominal shear stress of concrete must not exceed $0.8\sqrt{\sigma_{cu}}$ or $5\,\mathrm{N/mm^2}$.

From ACI, the allowable value of shear stress of concrete should not be more than $\frac{\phi\sqrt{\sigma_{cu}}}{3}$ and $\phi = 0.85$ (for S.I. units).

Table 12.D.10 lists the data provided by all four codes.

Table 12.D.10 Maximum shear stress.

Concrete grade	Maximum shear stress, V_{cm} ($\mathrm{N/mm^2}$)			
	Indian standard	Eurocode	ACI code	British standard
Grade 15	2.5	2.33	1.1	3.10
Grade 20	2.8	3.01	1.3	3.58
Grade 25	3.1	3.64	1.4	4.00
Grade 30	3.5	4.22	1.6	4.38
Grade 35	3.7	4.75	1.7	4.73
Grade 40	4.0	5.23	1.8	5.06

The shear strength of concrete $= v_c$.

From Indian Code

$$v_c = \frac{0.85}{6\beta}\sqrt{0.80\sigma_{ck}}\left(\sqrt{(1 + 5\beta)}-1\right)$$

$$\beta = \frac{0.80\sigma_{ck}}{6.89p_t}$$

$$p_t = \frac{100A_t}{b_w d}$$

where b_w = average web width of a flanged beam

From Eurocode

$$v_c = 0.03\sigma_{cu}^{(2/3)}\left(1.6-\frac{d}{1000}\right)\left[1.2 + 0.4\left(100\frac{A_t}{bd}\right)\right]$$

From British Code

$$v_c = \frac{0.79\left(\frac{100A_t}{b_v d}\right)^{1/3}\left(\frac{400}{d}\right)^{1/4}}{\gamma_m}$$

where

$$\gamma_m = 1.25$$

$\frac{100A_t}{b_v d}$ should not be taken as greater than 3.0
$\left(\frac{400}{d}\right)^{1/4}$ should not be taken as less than 0.67 for members without shear reinforcement
$\left(\frac{400}{d}\right)^{1/4}$ should not be taken as less than 1.0 for members with shear reinforcement

where b_v = breath of section (for a flanged beam, this should be taken as the average width of the rib below the flange).
From ACI code, $v_c = 0.17\sqrt{\sigma_{cu}}$ (for S.I. units).
Take into account the effect of ultimate moment and shear at critical section, as follows.

$$v_c = \left[0.16\sqrt{\sigma_{cu}} + \left(17.2\rho_w \frac{V_u d}{M_u}\right)\right] \leq 0.29\sqrt{\sigma_{cu}} \quad \text{(for S.I. units)}$$

$$\rho_w = \frac{A_t}{b_w d} \quad \text{and} \quad \frac{V_u d}{M_u} \leq 1.0 \quad (\text{where } V_u = \text{design shear}).$$

12.D.11 Punching Shear

Punching shear occurs around the column on a perimeter away from the face of the column or pedestal. Table 12.D.11 shows values of the perimeter.

Nominal shear stress at the critical section:

From Indian Standard:

For one-way shear action, the nominal shear stress is calculated as follows

$$\tau_v = \frac{v_u}{bd}$$

where

v_u = factored vertical shear force
b = breadth of the critical section
d = effective depth

When shear reinforcement is not provided, the nominal shear stress at critical section should not exceed $k\tau_c$, where

Table 12.D.11 Value of the critical section.

Indian standard or ACI code		Eurocode or British standard	
One-way shear	Two-way shear	One-way shear	Two-way shear
The effective depth away from the face of column or pedestal	0.5 times the effective depth away from the face of column or pedestal	The effective depth away from the face of column or pedestal	1.5 times the effective depth away from the face of column or pedestal

k = factor for calculating shear strength of concrete,
τ_c = shear strength of concrete.
The factor k depends on the overall thickness of the slab, D_s, and is given in Table 12.D.12.

Table 12.D.12 k values for solid slabs.

D_s (mm)	300	275	250	225	200	175	150
k	1.00	1.05	1.10	1.15	1.20	1.25	1.30

On solid slabs, the nominal shear stress, $\tau_v = k\,\tau_c$. Shear reinforcement may be provided for slabs of depth greater than 200 mm. The development length has to be checked at the same critical sections as for beams. It is important to check deflections in slab design. For this, the strip of slab may be checked against span to effective depth ratio (Jain, 1997).

For two-way shear action, the nominal shear stress is calculated as follows

$$\tau_v = \frac{v_u}{b_o d}$$

where b_o = periphery of the critical section.

When shear reinforcement is not provided, the nominal shear stress at the critical section should not exceed $k_s\tau_c$, where

$$k_s = 0.5 + \beta_c < 1 \quad \text{and} \quad \beta_c = \frac{\text{short dimension of column or pedestal}}{\text{long dimension of column or pedestral}}$$

$$\tau_c = 0.25\sqrt{\sigma_{ck}}\ \text{N/mm}^2$$

From Eurocode:

1. The method for punching shear design set out is based on three values of the design shear resistance at the critical perimeter, as follows:
   a. V_{Rd1} = the design shear resistance per unit length of the critical perimeter, for a slab without shear reinforcement.
   b. V_{Rd2} = the maximum design shear resistance per unit length of the critical perimeter, for a slab with shear reinforcement.
   c. V_{Rd3} = the design shear resistance per unit length of the critical perimeter, for a slab with shear reinforcement.
2. No shear reinforcement is required if $V_{sd} \le V_{Rd1}$
3. If V_{sd} exceeds V_{Rd1}, then shear reinforcement or other forms of shear connector, where their application can be justified, should be provided such that $V_{sd} \le V_{Rd3}$
4. In the case of a concentrated load or support reaction, the applied shear per unit length is

$$V_{sd} = \frac{V_{sd}\beta}{u}$$

where
V_{sd} is total design shear force developed. In a slab this is calculated along the perimeter u. For a foundation this is calculated along the perimeter of the base of the truncated punching shear cone, assumed to form at 33.7°, provided this falls within the foundation.
u is the perimeter of the critical section.

β is a coefficient which takes into account of the effects of eccentricity of loading. In cases where no eccentricity of loading is possible, β may be taken as 1.0. In other cases:
$\beta = 1.50$ for corner column.
$\beta = 1.40$ for edge column.
$\beta = 1.15$ for internal column.

Based on more rigorous analysis, other values for β may be used, when associated with appropriate methods for ensuring the anchorage of the reinforcement at the edge of the slab.

From ACI code:

1. One-way shear
   For footing with bending action in one direction, the allowable shear is equal to
   a. $v_c = 2\sqrt{\sigma_{ck}}bd$ (for US customary units)
   b. $v_c = 0.17\sqrt{\sigma_{ck}}bd$ (for S.I. units)
   where $\phi = 0.85$ and $b =$ width of critical section.
2. Two-way shear
   ACI Code, Section 11.12.2, allows shear strength (v_c) in footings without shear reinforcement for two-way shear action. The smallest of the following is to be taken.
   a. For US customary units:
      i. $v_{c1} = 4\sqrt{\sigma_{ck}}b_o d$
      ii. $v_{c2} = \left(2 + \frac{4}{\beta_c}\right)\sqrt{\sigma_{ck}}b_o d$
      iii. $v_{c3} = \left(\frac{\alpha_s d}{b_o} + 2\right)\sqrt{\sigma_{ck}}b_o d$
   b. For S.I. units:
      i. $v_{c1} = \frac{1}{3}\sqrt{\sigma_{ck}}b_o d$
      ii. $v_{c2} = \left(1 + \frac{2}{\beta_c}\right)\frac{\sqrt{\sigma_{ck}}b_o d}{6}$
      iii. $v_{c3} = \left(\frac{\alpha_s d}{b_o} + 2\right)\frac{\sqrt{\sigma_{ck}}b_o d}{12}$

   where
   $\beta_c =$ ratio of long side to short side of rectangular area
   $b_o =$ perimeter of the critical section taken at $d/2$ from the loaded area
   d = effective depth of footing

$$\begin{aligned} \text{For interior column,} \quad & \alpha_s = 40 \\ \text{For edge column,} \quad & \alpha_s = 30 \\ \text{For corner column,} \quad & \alpha_s = 20 \end{aligned}$$

12.D.12 Bond Stress and Development Length

Table 12.D.13 lists design bond stress data.

From Indian Standard:

τ_{bd} may increase by 60% for deformed steel bars in tension. These values may be further increased by 25% for bars in compression. In case of bundled bars in contact, the development length is given by that for the individual bar and can be increased by 10% for two bars in contact, 20% for three bars in contact and 33% for four bars in contact.

From Eurocode:

These values are derived from the following formulae: (with $\gamma_m = 1.5$)

Table 12.D.13 Design bond stress for mild steel bars.

Concrete	Design bond stress, τ_{bd} (N/mm^2)		
	Indian standard	Eurocode	
		Plain bars	High bond bars
Grade 12	—	0.9	1.6
Grade 15	1.0	0.93	1.9
Grade 16	—	1.0	2.0
Grade 20	1.2	1.1	2.3
Grade 25	1.4	1.2	2.7
Grade 30	1.5	1.3	3.0
Grade 35	1.7	1.4	3.4
Grade 40	1.9	1.5	3.7
Grade 45	—	1.6	4.0
Grade 50	—	1.7	4.3

For plain bars, $\tau_{bd} = \frac{0.36\sqrt{\sigma_{ck}}}{\gamma_m}$ and for high bond bars, $\tau_{bd} = \frac{2.25\sqrt{\sigma_{ck0.05}}}{\gamma_m}$
($\sigma_{ctk\ 0.05}$ is lower characteristic tensile strength (5% fractile), that is, $\sigma_{ctk0.05} = 0.21\sigma_{ck}^{2/3}$.)
From ACI Code:

This code permits the use of simplified expression to calculate the development length, L_d. This is based on the fact that current practical construction cases utilize spacing and cover values along with confining reinforcement, such as stirrups and ties that produced values of $\frac{(C + K_{tr})}{d_b} \geq 1.5$, where C is a factor which represents the smallest of the side cover, cover over the bar or wire (in both cases measured to the center of the bar or wire) or one-half the center to center spacing of the bars or wires, d_b = nominal diameter of bar, wire (in mm), and K_{tr} is a factor which represents the contribution of confining reinforcement across potential splitting planes. Moreover, tests indicated that the development length L_d can be reduced by 20% for no.6 and smaller bars.

Based on the ACI Code assumptions and assuming $\frac{(C + K_{tr})}{d_b} \geq 1.5$, the following equations are adopted for computing the development length.

	No. 19 and smaller bars and deformed wires	No. 22 and larger bars
Clear spacing of bars being developed or spliced not less than d_b, clear cover not less than d_b, and stirrups or ties throughout L_d not less than the code minimum	$\frac{L_d}{d_b} = \frac{12\sigma_y bcm}{25\sqrt{\sigma_c}}$	$\frac{L_d}{d_b} = \frac{3\sigma_y bcm}{5\sqrt{\sigma_c}}$
Clear spacing of bars being developed or spiced not less than $2d_b$ and clear cover not less than d_b		
Other cases	$\frac{L_d}{d_b} = \frac{18\sigma_y bcm}{25\sqrt{\sigma_c}}$	$\frac{L_d}{d_b} = \frac{9\sigma_y bcm}{10\sqrt{\sigma_c}}$

Note: The entire notations are defined as below.

b = reinforcement location factor
$b = 1.3$ when the horizontal reinforcement is so placed that more than 300 mm of fresh concrete is cast in the member below the development length or splice
$b = 1.0$ for other reinforcement
c = coating factor
$c = 1.5$ when epoxy-coated bars or wires with cover less than $3d_b$, or clear spacing less than $6d_b$
$c = 1.2$ for all other epoxy-coated bars or wires
$c = 1.0$ for uncoated reinforcement
the product of b c need not be taken greater than 1.7
m = lightweight aggregate concrete factor
$m = 1.3$ when lightweight aggregate concrete is used
$m = 1.0$ when normal weight concrete is used.

Table 12.D.14 lists data for development length.

Table 12.D.14 Development length for single bar.

σ_y (N/mm^2)	Concrete grade 15			Concrete grade 20		
	Indian standard		Eurocode	Indian standard		Eurocode
	Tension bars	Compression bars		Tension bars	Compression bars	
250 (plain bars)	55 φ	44 φ	58 φ	46 φ	37 φ	49 φ
415	56 φ	47 φ	47 φ	47 φ	38 φ	39 φ
500	69 φ	58 φ	57 φ	58 φ	46 φ	47 φ

12.D.13 Clear Cover for Reinforcement

From Indian Standard, the clear cover to reinforcement which is nearest to the face of a member should be as follows:

1. At each end of reinforcing bar, not less than 25 mm, nor less than twice the diameter of such bar.
2. For longitudinal bar in a beam, not less than 25 mm, nor less than the diameter of such bar.
3. For tensile, compression, shear or other reinforcement in a slab, not less than 15 mm, nor less than the diameter of such bar.
4. For a longitudinal reinforcing bar in a column, not less than 40 mm, nor less than the diameter of such bar. Such a large cover is required so as to prevent buckling of the main longitudinal bars under compression. In the case of columns of minimum dimension of 200 mm or under, whose reinforcing bars do not exceed 12 mm, a cover of 25 mm may be used.
5. For any other reinforcement, not less than 15 mm, nor less than the diameter of such bar.

From Eurocode:

1. To transmit bond forces safely, and to ensure adequate compaction, the concrete cover, to the bar or tendon being considered, should never be less than:

a. φ = diameter of the bar, diameter of a tendon or of the duct (post-tensioning)
b. φ_n = equivalent diameter for a bundle
c. (φ + 5 mm) or (φ_n + 5 mm) if $d_g > 32$ mm where d_g = largest nominal maximum aggregate size.

2. The minimum concrete cover to all reinforcement including links and stirrups should not be less than the appropriate values given in Table 12.D.15.

Table 12.D.15 Minimum cover for reinforcement according to Eurocode.

Exposure class	Minimum cover for reinforcement (mm)
Dry environment	15
Humid environment without frost	20
Humid environment with frost	25
Humid environment with frost and de-icing salts	40
Seawater environment without frost	40
Seawater environment with frost	40
Slightly aggressive chemical environment	25
Moderately aggressive chemical environment	30
Highly aggressive chemical environment	40

.

From ACI Code, for cast in place concrete, the minimum concrete cover provided for reinforcement shall conform with data in Table 12.D.16.

Table 12.D.16 Minimum cover for reinforcement according to ACI code.

Exposed condition	Member type	Bar type	Minimum cover (mm)
Concrete cast against permanently exposed earth	—	All	70
Concrete exposed to earth or weather	—	No. 19 through no. 57 bars	50
		No. 16 bar, W31 or D31 wire and smaller	40
Concrete not exposed to weather or in contact with ground	Slabs, walls, joists	No. 43 and no. 57 bars	40
		No. 36 bar and smaller	20
	Beams, columns	Primary reinforcement, ties, stirrups, spirals	40
	Shells, folded plate members	No. 19 bar and larger	20
		No. 16 bar, W31 or D31 wire, and smaller	15

12.D.14 Spacing of Reinforcement

From Indian Standard:

1. Minimum distance between bars
   a. The clear horizontal distance between two parallel main reinforcing bars should not be less than the greatest of the following:
      i. the diameter of the bar if the diameters are equal
      ii. the diameter of the larger bar if the diameters are unequal and
      iii. 5 mm more than the nominal maximum size of coarse aggregate.
      If needle vibrators are used, the horizontal distance between bars of a group may be reduced to two-thirds the nominal maximum size of the coarse aggregate provided that sufficient space is left between groups of bars to permit the vibrator to be immersed.
   b. The clear vertical distance between two parallel main reinforcing bars should not be less than the greatest of the following:
      i. 15 mm
      ii. The diameter of the larger bar if the diameters are unequal and two-thirds the nominal maximum size of the coarse aggregate.
2. Maximum distance between bars in tension
   The maximum distance between bars is restricted in order to control cracking of concrete which depends on the stress in the reinforcing bars and the distance between bars. In normal environments, the crack widths should not exceed 0.3 mm. This value decreases for aggressive environments.
3. Beams
   The horizontal distance between parallel reinforcement bars, or groups, near the tension face of a beam should not exceed the values given in Table 12.D.17. These values depend on the amount of redistribution of moment carried out in the analysis and the characteristic strength of the reinforcement.

Table 12.D.17 Maximum clear distance between bars.

σ_y (N/mm^2)	Code	% redistribution to or from section considered								
		−30	−20	−15	−10	0	+ 10	+ 15	+ 20	+ 30
250	Indian standard	215	—	260	—	300	—	300	—	300
	British standard	200	225	—	225	280	300	—	300	300
415	Indian standard	125	—	155	—	180	—	210	—	235
460	British standard	110	125	—	140	155	170	—	185	200
500	Indian standard	105	—	130	—	150	—	175	—	195
	British standard	—	—	—	—	—	—	—	—	—

From ACI code:

A. Minimum spacing for reinforcement

1. The minimum clear spacing between parallel bars in a layer shall be:
   i. d_b = nominal diameter of bar, wire or prestressing strand, mm
   ii. but not less than 25 mm.
2. Where parallel reinforcement is placed in two or more layers, bars in the upper layers shall be placed directly above bars in the bottom layer with clear distance between layers not less than 25 mm.
3. In spirally reinforced or tied reinforced compression members, clear distance between longitudinal bars shall be not less than $1.5d_b$ nor 40 mm.
4. Clear distance limitation between bars shall apply also to the clear distance between a contact lap splice and adjacent splices and bars.

B. Maximum spacing for reinforcement

1. In walls and slabs other than concrete joist construction, primary flexural reinforcement shall be spaced not farther apart than three times the wall or slab thickness, or 500 mm.

From Eurocode

A. Spacing of reinforcement bars

1. The clear distance (horizontal and vertical) between individual parallel bars or horizontal layers of parallel bars should be not less than:
   i. maximum bar diameter or 20 mm
   ii. $d_g + 5$ mm if $d_g > 32$ mm (where d_g is largest nominal maximum aggregate size).
2. Where bars are positioned in separate horizontal layers, the bars in each layer should be located vertically above each other and the space between the resulting columns of bars should permit the passage of an internal vibrator.
3. Lapped bars may touch one another within the lap length.

12.D.15 Design Examples Using Different Codes

Design a square footing to carry a dead load of 500 kN and an imposed load of 300 kN through a 400 mm square column reinforced with 20 mm steel bars in a longitudinal direction. The design soil pressure (DSP) is 100 kN/m^2. The footing is based at 1 m below ground level, unit weight of soil, γ_s is 18 kN/m^3. Design the footing according to difference concrete code.

Solution:

Size of bases

Approximate area of footing required (without including self weight)

$$= \frac{500 + 300}{100} = \frac{800}{100} = 8\ \text{m}^2$$

Assume the area of footing = 10 m^2

Weight of footing including earth $= 10 \times 1 \times 18 = 180$ kN

Total weight of footing on soil = imposed load + died load + self weight

$= 500 + 300 + 180$

$= 980$ kN

Actual area of footing required $= \frac{980}{100} = 9.8\ \text{m}^2$

Provide 3.2×3.2 m footing (total area $= 10\,m^2$).

1. Net upward pressure
   a. According to Indian Standard code (Table 12.D.1)

$$\begin{aligned}\text{Ultimate load} &= 1.5DL + 1.5LL \\ &= 1.5 \times 500 + 1.5 \times 300 \\ &= 1200\,kN\end{aligned}$$

Net soil bearing pressure acting upward due to factored load

$$= \frac{1200}{3.2 \times 3.2}$$
$$= 118\,kN/m^2$$

   b. According to Eurocode (Table 12.D.2)

$$\begin{aligned}\text{Ultimate load} &= 1.35 \times \text{Permanent load} + 1.5 \times \text{Variable load} \\ &= 1.35 \times 500 + 1.5 \times 300 \\ &= 1125\,kN\end{aligned}$$

Net soil bearing pressure acting upward due to factored load

$$= \frac{1125}{3.2 \times 3.2}$$
$$= 110\,kN/m^2$$

   c. According to ACI code (Table 12.D.1)

$$\begin{aligned}\text{Ultimate load} &= 1.4DL + 1.7LL \\ &= 1.4 \times 500 + 1.7 \times 300 \\ &= 1210\,kN\end{aligned}$$

Net soil bearing pressure acting upward due to factored load

$$= \frac{1210}{3.2 \times 3.2}$$
$$= 119\,kN/m^2$$

2. Moment calculation
   The critical section due to moment is at the face of the column on pad footing or at wall in a strip footing, as shown in the Figure 12.D.1.
   a. According to Indian Standard

Bending moment, M

$$= \left[118 \times 3.2 \times \left(\frac{3.2-0.4}{2}\right) \times \left(\frac{3.2-0.4}{2} \times \frac{1}{2}\right)\right]$$
$$= 370.05\,kNm$$

   b. According to Eurocode

Bending moment, M

$$= \left[110 \times 3.2 \times \left(\frac{3.2-0.4}{2}\right) \times \left[\frac{3.2-0.4}{2} \times \frac{1}{2}\right]\right]$$
$$= 345\,kNm$$

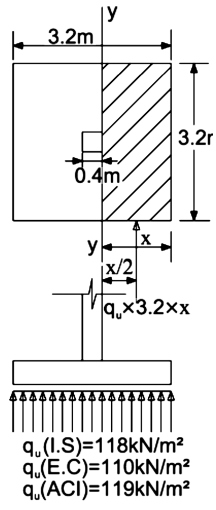

Figure 12.D.1 Critical section due to moment.

c. According to ACI code

Bending moment, M

$$= \left[119 \times 3.2 \times \left(\frac{3.2-0.4}{2}\right) \times \left[\frac{3.2-0.4}{2} \times \frac{1}{2}\right]\right]$$

$$= 373 \text{ kNm}$$

3. Effective depth

a. According to Indian Standard code (using Fe 415 steel and grade 20 concrete):
For Fe 415 steel, $M_u = 0.138\sigma_{ck}bd^2$ (Table 12.D.8)

$$d = \sqrt{\frac{M_u}{0.138\sigma_{ck}b}} = \sqrt{\frac{370.05 \times 10^6}{0.138 \times 20 \times 3200}} = 205 \text{ mm}$$

Adopt 560 mm as effective depth and 600 mm as overall depth. This increased depth is taken due to shear requirements.

b. According to Eurocode (using Fe 415 steel and grade 20 concrete):
For $\sigma_{ck} < 45 \text{ N/mm}^2$, $M_u = 0.136\sigma_{ck}bd^2$ (Table 12.D.8)

$$d = \sqrt{\frac{M_u}{0.136\sigma_{ck}b}} = \sqrt{\frac{345 \times 10^6}{0.136 \times 20 \times 3200}} = 199 \text{ mm}$$

Adopt 560 mm as effective depth and 600 mm as overall depth. This increased depth is taken due to shear requirements.

c. According to ACI code [using grade 60 steel (equivalent to Fe 415 steel) and grade 20 concrete], for grade 60 steel (414 MPa) and grade 20 concrete, $M_u = 5.199\phi bd^2$ (Table 12.D.8)

$$d = \sqrt{\frac{M_u}{5.199 \times \phi \times b}} = \sqrt{\frac{373 \times 10^6}{5.199 \times 0.9 \times 3200}} = 157 \text{ mm}$$

Adopt 560 mm as effective depth and 600 mm as overall depth. This increased depth is taken due to shear requirements.

4. Design for tension reinforcement

a. According to Indian Standard code, from Section 12.D.5

$$\begin{aligned} A_s &= 0.5\frac{\sigma_{ck}}{\sigma_y}\left[1-\sqrt{1-\frac{4.6 \times M \times 10^6}{\sigma_{ck} bd^2}}\right]bd \\ &= 0.5\frac{20}{415}\left[1-\sqrt{1-\frac{4.6 \times 370.05 \times 10^6}{20 \times 3200 \times 560^2}}\right] \times 3200 \times 560 \\ &= 1871.71 \text{ mm}^2 \end{aligned}$$

Use 10 mm bars at 130 mm c/c. Area of steel provided = 1885 mm^2.

b. According to Eurocode, from Section 12.D.5

$$k = \frac{M}{bd^2\sigma_{ck}} = \frac{345 \times 10^6}{3200 \times 560^2 \times 20} = 0.017$$

Assume $\delta = 1$

$$\begin{aligned} k' &= 0.60\delta - 0.18\delta^2 - 0.21 \\ &= 0.60(1) - 0.18(1)^2 - 0.21 \\ &= 0.21 \end{aligned}$$

Since $k < k'$, no compression steel is required.

$$\begin{aligned} z &= \frac{d}{2}\left[1 + \sqrt{1-3.53k}\right] \leq 0.95d \\ &= \frac{560}{2}\left[1 + \sqrt{1-3.53 \times 0.0171}\right] \\ &= 551.4 \text{ mm} > 0.95d(532 \text{ mm}) \end{aligned}$$

$$\therefore A_s = \frac{M}{0.95\sigma_y z} = \frac{345 \times 10^6}{0.95 \times 415 \times 532} = 1645 \text{ mm}^2$$

Use 10 mm bars at 150 mm c/c. Area of steel provided = 1649 mm^2.

c. According to ACI code, from Section 12.D.5

$$\begin{aligned}\rho &= \frac{0.85\sigma_{ck}}{\sigma_y}\left[1-\sqrt{1-\frac{4M_u}{1.7\phi\sigma_{ck}bd^2}}\right]\\ &= \frac{0.85\times 20}{414}\left[1-\sqrt{1-\frac{4\times 373\times 10^6}{1.7\times 0.85\times 21\times 3200\times 560^2}}\right]\\ &= 1.02\times 10^{-3}\end{aligned}$$

$$\begin{aligned}A_s &= \rho bd\\ &= 1.02\times 10^{-3}\times 3200\times 560\\ &= 1827.84\,\text{mm}^2\end{aligned}$$

Use 10 mm bar at 130 mm c/c. Area of steel provided = 1885 mm^2.

5. Shear
   a. According to Indian Standard code:
      i. One-way shearThe critical section is taken as effective depth, *d*, away from face of column, as shown in Figure 12.D.2.

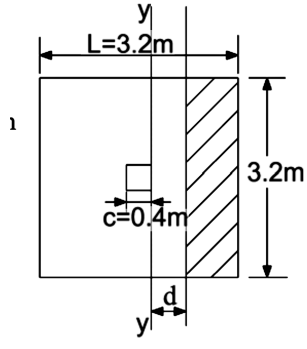

Figure 12.D.2 Critical section of one-way shear.

Shear force

$$V_u = q_u b\left(\frac{L}{2}-\frac{c}{2}-d\right)$$

$$\begin{aligned}V_u &= 118\times 3.2\times\left(\frac{3.2}{2}-\frac{0.4}{2}-0.56\right)\\ &= 317.18\,\text{kN}\end{aligned}$$

Nominal shear stress

$$\tau_v = \frac{V_u}{bd} = \frac{317.18\times 10^3}{3.2\times 0.56} = 0.177\,\text{N/mm}^2.$$

From Section 12.D.9

Shear strength of M20 concrete with 0.11% steel

$$P_t = \frac{100A_t}{b_w d} = \frac{100 \times 1885}{3200 \times 560} = 0.1052$$

$$\beta = \frac{0.80\sigma_{ck}}{6.89P_t} = \frac{0.80 \times 20}{6.89 \times 0.1052} = 22.07$$

$$v_c = \frac{0.85}{6\beta}\sqrt{0.80\sigma_{ck}}\left(\sqrt{(1 + 5\beta)}-1\right)$$

$$= \frac{0.85}{6 \times 22.07}\sqrt{0.80 \times 20}\left(\sqrt{(1 + 5 \times 22.07)}-1\right)$$

$$= 0.25\,\text{N/mm}^2$$

$\therefore \tau_v < v_c \rightarrow$ ok.

ii. Two-way shear.

The critical section is taken at $0.5d$ away from the face of the column, as shown in Figure 12.D.3.

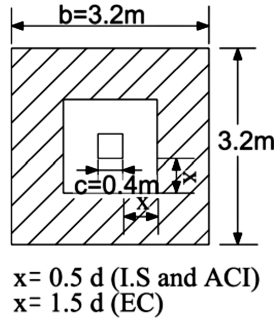

Figure 12.D.3 Critical section of two-way shear.

Shear force, $V_u = P_u\left(b^2-(d + c)^2\right)$

$$= 118\left(3.2^2-(0.4 + 0.56)^2\right)$$

$$= 1100\,\text{kN}$$

From Section 12.D.10

Nominal shear stress, $\tau_v = \frac{V_u}{b_o d} = \frac{1100 \times 10^3}{[4 \times (400 + 560)] \times 560} = 0.52\,\text{N/mm}^2$

Shear strength of concrete $= k_s \tau_c$

$$k_s = 0.5 + \beta_c \rightarrow \beta_c = \frac{\text{length of short side of column}}{\text{length of longert side of column}}$$

$$k_s = 0.5 + 1 = 1.5 \leq 1.0$$
$$\therefore k_s = 1.0$$

$$\tau_c = 0.25\sqrt{\sigma_{ck}} = 0.25 \times \sqrt{20} = 0.52$$

Shear strength of concrete $= k_s \tau_c = 1.0 \times 0.52 = 1.118\,\text{N/mm}^2 > 0.52\,\text{N/mm}^2 \rightarrow$ ok.

b. According to Eurocode:

i. One-way shear

The critical section is taken at an effective depth, d, away from face of column, as shown in Figure 12.D.2.

Shear force

$$V_u = q_u b\left(\frac{L}{2} - \frac{c}{2} - d\right)$$

$$V_u = 110 \times 3.2 \times \left(\frac{3.2}{2} - \frac{0.4}{2} - 0.56\right)$$
$$= 295.68\,\text{kN}$$

Nominal shear stress

$$\tau_v = \frac{V_u}{bd} = \frac{295.68 \times 10^3}{3.2 \times 0.56} = 0.165\,\text{N/mm}^2$$

From Section 12.D.9, shear strength of concrete

$$v_c = 0.03\sigma_{ck}^{(2/3)}\left(1.6 - \frac{d}{1000}\right)\left(1.2 + 0.4\left(100\frac{A_t}{bd}\right)\right)$$
$$= 0.03 \times (20)^{(2/3)} \times \left(1.6 - \frac{560}{1000}\right)\left(1.2 + 0.4\left(100\frac{1649}{3200 \times 560}\right)\right)$$
$$= 0.284\,\text{N/mm}^2$$

$$\therefore \tau_v < v_c \rightarrow \text{ok.}$$

ii. Two-way shear

The critical section is taken at $1.5d$ away from face of column, as shown in Figure 12.D.3.

Shear force

$$V_u = P_u\left(b^2 - (1.5d + c)^2\right)$$
$$= 110\left(3.2^2 - (1.5 \times 0.56 + 0.4)^2\right)$$
$$= 957\,\text{kN}$$

From Section 12.D.10

$$b_o = 4 \times (1.5d \times 2 + c) = 4 \times (3 \times 560 + 400) = 8320\,\text{mm}$$

Nominal shear stress

$$\tau_v = \frac{V_u}{b_o d} = \frac{957 \times 10^3}{[8320] \times 560} = 0.21\ \text{N/mm}^2$$

Shear strength of concrete, $v_c = 0.284\ \text{N/mm}^2$

$\therefore \tau_v < v_c \rightarrow$ ok.

c. According to ACI code:

i. One-way shear

The critical section is taken at an effective depth, d away from the face of the column, as shown in Figure 12.D.2.

Shear force

$$V_u = q_u b\left(\frac{L}{2} - \frac{c}{2} - \frac{d}{2}\right)$$

$$V_u = 119 \times 3.2 \times \left(\frac{3.2}{2} - \frac{0.4}{2} - 0.56\right)$$

$$= 319.87\ \text{kN}$$

Nominal shear stress

$$\tau_v = \frac{V_u}{bd} = \frac{319.87 \times 10^3}{3.2 \times 0.56} = 0.178\ \text{N/mm}^2$$

From Section 12.D.9

Shear strength of grade 20 concrete

$$v_c = 0.17\sqrt{f_{ck}} = 0.17 \times \sqrt{20} = 0.76\ \text{N/mm}^2 \quad \therefore \tau_v < v_c \rightarrow \text{ok.}$$

ii. Two-way shear

The critical section is taken at $0.5d$ away from the face of the column, as shown in Figure 12.D.3.

Shear force

$$V_u = P_u\left(b^2 - (d + c)^2\right)$$

$$= 119\left(3.2^2 - (0.4 + 0.56)^2\right)$$

$$= 1109\ \text{kN}$$

Nominal shear stress

$$\tau_v = \frac{V_u}{b_o d} = \frac{1109 \times 10^3}{[4 \times (400 + 560)] \times 560} = 0.516\ \text{N/mm}^2$$

From Section 12.D.10

$$v_{c1} = \frac{1}{3}\sqrt{f_{ck}} = \frac{1}{3} \times \sqrt{20} = 1.49\ \text{N/mm}^2$$

$$\beta_c = \frac{\text{long side of rectangular area}}{\text{short side of rectangular area}} = 1,$$

$$v_{c2} = \left(1 + \frac{2}{\beta_c}\right)\frac{\sqrt{f_{ck}}}{6} = \left(1 + \frac{2}{1}\right)\frac{\sqrt{20}}{6} = 2.24\ \text{N/mm}^2$$

Assume $\alpha_s = 20$ (corner column)

$$v_{c3} = \left(\frac{\alpha_s d}{b_o} + 2\right)\frac{\sqrt{\sigma_{ck}}}{12} = \left(\frac{20 \times 560}{3840} + 2\right)\frac{\sqrt{20}}{12} = 1.83\,\text{N/mm}^2$$

$\therefore \tau_v < v_{c1}, v_{c2}, v_{c3} \rightarrow$ ok.

6. Development length of reinforcement

Actual embedment provided at the face of the column $= \left(\frac{3200-400}{2}\right) - 50 = 1350\,\text{mm}$

a. According to Indian Standard code:

From Table 12.D.14, for $\sigma_y = 415\,\text{N/mm}^2$, $\sigma_{cu} = 20\,\text{N/mm}^2$, $\phi = 10\,\text{mm}$ deformed bars, development length for single bar, $L_d = 47\phi = 47 \times 10 = 470\,\text{mm}$

$\therefore L_d <$ actual embedment $\rightarrow$ ok.

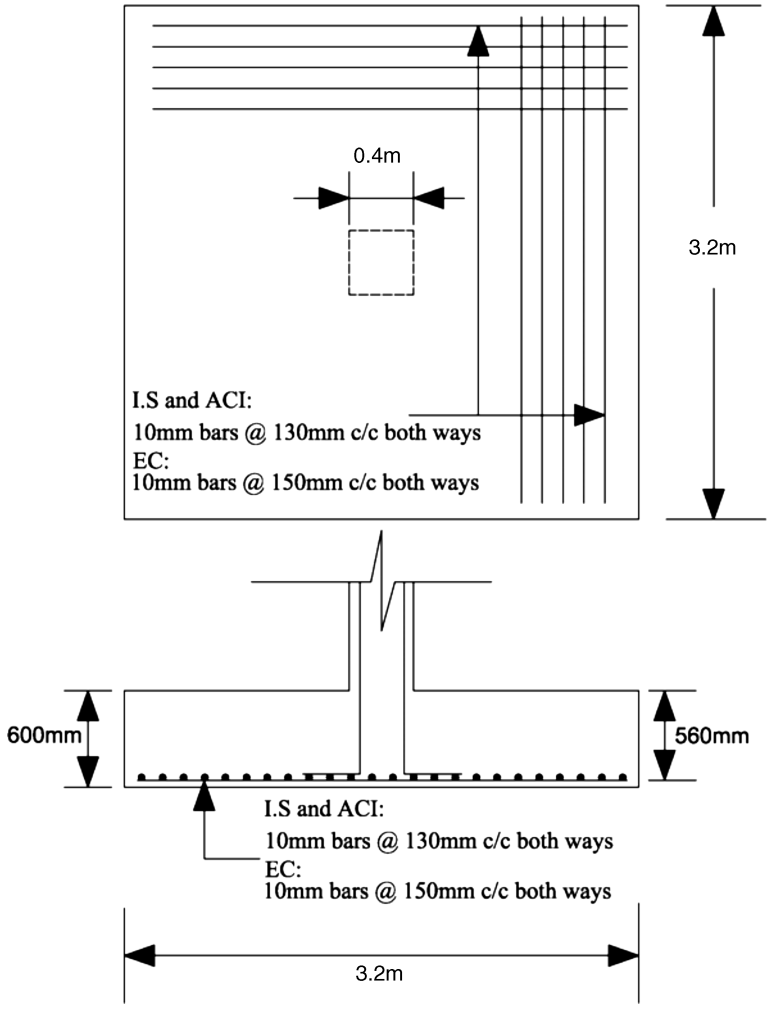

Figure 12.D.4 Reinforcement details of footing.

b. According to Eurocode:
From Table 12.D.14, for $\sigma_y = 415\ \text{N/mm}^2$, $\sigma_{cu} = 20\ \text{N/mm}^2$, $\phi = 10$ mm deformed bars, development length for single bar, $L_d = 39\phi = 39 \times 10 = 390$ mm

$\therefore L_d <$ actual embedment $\rightarrow$ ok.

c. According to ACI code:
From Section 12.D.11, for clear spacing of bars (130 mm) > diameter of bar (d_b; 10 mm)

$$\frac{L_d}{d_b} = \frac{12\sigma_y bcm}{25\sqrt{\sigma_c}}$$

b = reinforcement location factor = 1.3(horizontal reinforcement)
c = coating factor = 1.2(for expoxy-coated bars or wires)
m = lightweight aggregate concrete factor = 1.0(for normal weight concrete)

Development length for single bar

$$L_d = \frac{12\sigma_y bcm}{25\sqrt{\sigma_c}} d_b = \frac{12 \times 414 \times 1.3 \times 1.2 \times 1.0}{25\sqrt{20}} \times 10 = 693\ \text{mm}$$

$\therefore L_d <$ actual embedment $\rightarrow$ ok.

Table 12.D.18 shows how the codes compare.

Table 12.D.18 Comparison of results according to different codes.

Result	Code		
	Indian Standard code	Eurocode	ACI code
1. Net upward pressure	118 kN/m^2	110 kN/m^2	119 kN/m^2
2. Moment	370.05 kNm	345 kNm	373 kN/m^2
3. Effective depth	205 mm (560 mm)	199 mm (560 mm)	157 mm (560 mm)
4. Tension			
(a) Tension reinforcement required	1871.71 mm^2	1645 mm^2	1827.84 mm^2
(b) Tension reinforcement provided	10 mm bars at 130 mm c/c (1885 mm^2)	10 mm bars at 150 mm c/c (1649 mm^2)	10 mm bars at 130 mm c/c (1885 mm^2)
5. Shear			
(a) One-way shear			
(i) Shear force	317.18 kN	295.68 kN	319.87 kN
(ii) Nominal shear stress	0.177 N/mm^2	0.165 N/mm^2	0.178 N/mm^2
(iii) Shear strength of concrete	0.25 N/mm^2	0.284 N/mm^2	0.76 N/mm^2
(b) Two-way shear			
(i) Shear force	1100 kN	957 kN	1109 kN
(ii) Nominal shear stress	0.52 N/mm^2	0.21 N/mm^2	0.516 N/mm^2
(iii) Shear strength of concrete	1.118 N/mm^2	0.284 N/mm^2	1.49 N/mm^2
6. Development length of reinforcement required	470 mm	390 mm	693 mm

The reinforcement details, designed according to these three codes are shown in Figure 12.D.4. From Table 12.D.18, it can be clearly seen that according to Indian Standard and ACI codes, the net upward pressure (118 and 119 kN/m^2), moment (370.05 and 373 kN/m^2), tension reinforcement required (1871.71 and 1827.84 mm^2) and shear force (317.18 and 319.87 kN for one way, 1100 and 1109 kN for two ways) are comparable. However, according Eurocode all these values are slightly smaller than the values obtained using IS and ACI codes. This is due to the lower values of partial load factors used in Eurocode.

Whereas for effective depth, the values computed from Indian Standard and Eurocodes are similar (205 and 199 mm), but from ACI codes the value obtained is much smaller (157 mm). However, this value usually will be as per the critical shear force on footing. Therefore, for ACI code, the effective depth is usually governed by the critical shear force requirement.

From Table 12.D.18, it can also be seen that the shear strength of concrete due to one way shear according to Indian Standard and Eurocode (0.25 and 0.284 N/mm^2) are similar but the value according to ACI code (0.76 N/mm^2) is much higher. For development length of reinforcement required, Indian Standard and Eurocode provided similar values (470 and 390 mm). These values are much smaller if compared to those obtained from ACI code (693 mm). Since the development lengths provide from the footing is much higher than these values, it may not influence the design.

References

ACI (1995) ACI 318 M-95 *Building Code Requirement for Structural Concrete*, American Concrete Institute, USA.

AREA (1958) Manual of Recommended Practice, Chicago Construction and Maintenance Section, Engineering Division, Association of American Rail Roads.

Barkan, D.D. (1962) *Dynamics of Bases and Foundations*, McGraw-Hill Book Co., New York, USA.

Becker, A.A. (1992) *The Boundary Element Method in Engineering*, McGraw-Hill Book Co., New York, USA.

Blake, M. (1964) New vibration standards for maintenance. *Hydrocarbon Processing and Petroleum Refiner*, **43**, (1),111–114.

Bowles, J.E. (1996) *Foundation Analysis and Design*, McGraw-Hill International Book Company.

Brady, B.H.G. and Brown, E.T. (2006) *Rock Mechanics*, Springer, The Netherlands.

Brinch Hansen, J. and Christensen, N.H. (1961) The ultimate resistance of rigid piles against transversal forces. *Danish Geotechnical Institute Bulletin*, **12**, 5–9.

Broms, B.B. (1964) Lateral resistance of piles in cohesioless soils. *Journal of Soil Mechanics and Foundation Engineering, Proc. ASCE*, **90**(2), 123–156.

Broms, B.B. (1964) Lateral resistance of piles in cohesive soils. *Journal of Soil Mechanics and Foundation Engineering, Proc. ASCE*, **90**(2), 27–63.

BS 8110-1 (1997) *Structural Use of Concrete-Part1: Code of Practice for Design and Construction*, British Standard Institute, UK.

Budhu, M. (2006) *Soil Mechanics and Foundations*, 2nd edn, John Wiley & Sons, Ltd., Chichester, UK.

Butterfield, R. and Banerjee, P.K. (1971) A rigid disc embedded in an elastic half-space. *Geotechnical Engineering*, **2**(1), 35–52.

Butterfield, R. and Banerjee, P.K. (1971) The elastic analysis of compressible piles and pile groups. *Geotechnique*, **21**(1), 43–46.

Canale, S.C. and Chapra, R.P. (1989) *Numerical Methods for Engineers*, McGraw-Hill Book Co., USA.

Cemica, J.N. (1994) *Geotechnical Engineering: Foundation Design*, Wiley-VCH Verlag, Weinheim.

Clancy, P. and Randolph, M.F. (1996) Simple design tools for piled raft foundations. *Geotechnique*, **46**(2), 312–318.

Coduto, D.P. (2001) *Foundation Design: Principles and Practices*, Prentice-Hall, USA.

Coyle, H.M. and Reese, L.C. (1966) Load transfer for axially loaded piles in clay. *Journal of Soil Mechanics and Foundation Engineering, Proc. ASCE*, **92**(2), 1–26.

Crandall, S.H. (1956) *Engineering Analysis*, McGraw-Hill Inc., USA.

Foundation Design: Theory and Practice N. S. V. Kameswara Rao

ISBN: 978-0-470-82534-1

Crandall, S.H., Dahl, N.C., and Lardener, T.J. (1972) *Mechanics of Solids*, McGraw-Hill Kogokusha Ltd., New Delhi, India.

Das, B.M. (2002) *Principles of Geotechnical Engineering*, Thomson, Brooks/Cole, New York, USA.

Das, B.M. (2007) *Principles of Foundation Engineering*, 6th edn, Thomson, New York, USA.

Desai, C.S. and Abel, J.F. (1972) *Introduction to the Finite Element Method*, Affiliated East–West Press Ltd., New Delhi, India.

Duncan, J.M., Evans, L.T., and Ooi, P.S.K. (1994) Lateral load analysis of single piles and drilled shafts. *Journal of Geotechnical Engineering, ASCE*, **122**, 1088–1033.

Eurocode (1992) *Eurocode 2, Design of Concrete Structures – Part 1: General Rules and Rules for Building Authority of Standard Board*, British Standard Institution, London.

Eurocode (2005) *Eurocode 2 (Part I), Design of Concrete Structures, General –Common Rules for Building and Civil Engineering Structures*, Institute of Civil/Structural Engineers, London.

Gazetas, G. and Tassoulas, J.L. (1987) Horizontal stiffness of arbitrary shaped embedded foundations. *Journal of GT Division, ASCE*, **113**(5), 458–475.

Goodman, R.E. (1989) *Introduction to Rock Mechanics*, John Wiley & Sons, Ltd., Chichester, UK.

Gorbunov-Posadov, M.I. (1949) Beams and Plates on an Elastic Base, (in Russian), Stroizdat, Moscow, USSR.

Harr, M.E. (1966) *Foundations of Theoretical Soil Mechanics*, McGraw-Hill Book Co., USA.

Hertz, H. (1884) Uber das gleichgewicht schwimmender elasticher platten. *Wiedemmanns Annalen der Physik und Chemie*, **22**, 255.

Hetenyi, M. (1946) *Beams on Elastic Foundations*, The University of Michigan Press, Ann Arbor, Mich., USA.

Hetenyi, M. (1950) A general solution for the bending of beams on an elastic foundation of arbitrary continuity. *Journal of Applied Physics*, **21**, 55–58.

Hooper, J.A. (1973) Observations on the behavior of a pile-raft foundation in london clay. *Proceedings of the Institute of Civil Engineers*, **55**, 855–877.

Hooper, J.A. (1979) Review of the Behavior of Piled Raft Foundations, Construction Industry Research and Information Association, Report 83.

Hvorslev, M.J. (1949) *Subsurface Exploration and Sampling of Soil for Civil Engineering Purposes*, Waterways Experiment Station, Vicksburg, USA.

IS: 1080–1962 (1962) *I.S. Code of Practice for Design and Construction of Simple Spread Foundations*, Indian Standards Institution, New Delhi, India.

IS: 1904–1966 (1966) *I.S. Code of Practice for Structural Safety of Buildings: Foundations, First Revision*, Indian Standards Institution, New Delhi, India.

IS: 2974–1966 (1966) *I.S. Codes of Practice for Design and Construction of Machine Foundations, Parts I–V*, Indian Standards Institution, New Delhi, India.

IS: 5249–1969 (1969) *I.S. Method of Test for Determination of In Situ Dynamic Properties of Soils, First Reprint*, Indian Standards Institution, New Delhi, India.

IS: 8009–1976 (1976) *I.S. Code of Practice for Calculation of Settlement of Foundations Subjected to Symmetrical Vertical Loads: Part I, Shallow Foundations*, Indian Standards Institution, New Delhi, India.

IS: 1904–1978 (1978) *I.S. Code of Practice for the Structural Safety of Buildings – Shallow Foundations*, New Delhi, India.

IS: 2950–1981 (1981) *I.S. Code of Practice for Design and Construction of Raft Foundations*, Indian Standards Institution, New Delhi, India.

IS: 6403–1981 (1981) *I.S. Code of Practice for Determination of Bearing Capacity of Shallow Foundations*, Indian Standards Institution, New Delhi, India.

IS: 1888–1982 (1982) *I.S. Method of Load Test on Soils, Second Revision*, Indian Standards Institution, New Delhi, India.

IS: 2720–1983 (1983) *I.S. Methods of Tests for Soils, Parts III, XXVIII, XXXIX, XXXII*, Indian Standards Institution, New Delhi, India.
IS: 11089–1984 (1984) *I.S. Code of Practice for Design and Construction of Ring Foundations*, Bureau of Indian Standards, New Delhi, India.
IS: 1893–1984 (1984) *I.S. Criteria for the Earthquake Resistant Design of Structures*, Bureau of Indian Standards, New Delhi, India.
IS: 2911–1984 (1984) *I.S. Code of Practice for Design and Construction of Pile Foundations: Load Test on Piles, Parts I–V*, Bureau of Indian Standards, New Delhi, India.
IS: 456–2000 (2000) *I.S. Code of Practice for Plain and Reinforced Concrete*, Bureau of Indian Standards, New Delhi, India.
Iyengar, K.T.S.R. and Ramu, S. (1979) *Design Tables for Beams on Elastic Foundations and Related Structural Problems*, Applied Science Publishers Ltd., London.
Iyer, A.N. (1995) PILEAN: An Expert System for Pile Foundation Design M.Tech Thesis, IIT, Kanpur, India.
Jaeger, J. and Cook, N. (2007) *Fundamentals of Rock Mechanics*, Blackwell Publishing, New York, USA.
Jain, A.K. (1997) *Reinforced Concrete – Limit State Design*, 4th edn, Nem Chand and Bros, Roorkee, India.
Janbu, N. (1957) Earth pressure and bearing capacity calculations by generalized procedure of slices. Proceedings of the 4th International Conference on Soil Mechanics and Foundation Engineering, II, London, pp. 207–213.
Jones, G. (1997) *Analysis of Beams on Elastic Foundations using Finite Difference Theory*, Thomas Telford, London, UK.
Kameswara Rao, N. S.V. (1969) Variational Approach to Beams and Plates on Elastic Foundations, Ph.D Thesis, IIT, Kanpur, India.
Kameswara Rao, N. S. V. (1971) Variational approach to beams on elastic foundations. *Journal of EM Division, ASCE, USA*, **97**, 271–294.
Kameswara Rao, N. S. V. (1977) Dynamics of Soil-Structure Systems – A Brief Review. *Journal of Structural Engineering*, **4**, 149–153.
Kameswara Rao, N. S. V. (1998) *Vibration Analysis and Foundation Dynamics*, A. H. Wheeler and Co., New Delhi, India.
Kameswara Rao, N. S. V. (2000) *Dynamic Soil Tests and Applications*, Wheeler Publishing, New Delhi, India.
Kameswara Rao, N. S. V. (2006) *Mechanical Vibrations of Elastic Systems*, Asian Books, New Delhi, India.
Kreyszig, E. (1967) *Advanced Engineering Mathematics*, Wiley Eastern Pvt. Ltd, New Delhi, India.
Kurian, N.P. (1992) *Design of Foundation Systems – Principles and Practices*, vol. **1**, Narosa Publishing House, New Delhi, India.
Lambe, T.W. (1951) *Soil Testing for Engineers*, John Wiley & Sons, Inc., New York, USA.
Lambe, T.W., and Whitman, R.V. (1969) *Soil Mechanics*, John Wiley & Sons, Inc., New York, USA.
Lambe, T.W. (1973) Predictions in soil engineering, 13th Rankine Lecture, *Geotechnique*, **23**(2), June, pp. 148–202.
Leonards, G.A. (1962) *Foundation Engineering*, McGraw-Hill Book Co., Inc., New York, USA.
Lysmer, J. and Richart, F.E. (1966) Dynamic response of footings to vertical loading. *Journal of SM Division, ASCE*, **92**(SM1), 65–91.
Major, A. (1962) *Vibration Analysis and Design of Foundations for Machines and Turbines*, Collet's Holding Ltd., London.
Malter, H. (1958) Numerical solutions for beams on elastic foundations. *Journal of SM Division, ASCE*, **84**(2), Part I.

Meyerhof, G.G. (1953) The bearing capacity of foundations under eccentric and inclined loads. Procedures of the 3rd International Conference on Soil Mechanics and Foundation Engineering, I, Geneva, pp. 440–445.

Meyerhof, G.G. (1957) The ultimate bearing capacity of foundations on slopes. Proceedings of the 4th International Conference on Soil Mechanics and Foundation Engineering, I, London, pp. 384–386.

Mita, A. and Luco, J.E. (1989) Impedance functions and input motions for embedded square foundations. *Journal of Geotechnical Engineering, ASCE*, **115**(4), 491–503.

Novak, M. (1974) Dynamic stiffness and damping of piles. *Canadian Geotechnical Journal*, **11**, 574–598.

Peck, R.B., Hanson, W.E., and Thornburn, T.H. (1974) *Foundation Engineering*, 2nd edn, John Wiley & Sons, Inc., New York, USA.

Poulos, H.G. and Davis, E.H. (1980) *Pile Foundation Analysis and Design*, John Wiley & Sons, Ltd., Chichester, UK.

Poulos, H.G. (2001) Piled raft foundations: design and applications. *Geotechnique*, **51**(2), 95–113.

Punmia, B.C., Jain, Ashok K. and Jain, Arum K. (1992) *Reinforce Concrete Structures*, 7th edn, Laxmi Publications, New Delhi, India.

Ramiah, B.K. and Chickanagappa, L.S. (1981) *Soil Mechanics and Foundation Engineering*, Oxford and IBH Publishing Co., New Delhi, India.

Randolph, M.F. and Wroth, C.P. (1978) Analysis of deformation of vertically loaded piles. *Journal of the Geotechnical Engineering Division, ASCE*, **104**(12), 1465–1488.

Randolph, M.F. (1981) The response of flexible piling to lateral loading. *Geotechnique*, **34**(2), 247–259.

Randolph, M.F. *et al.* (1992) *Piling Engineering*, 2nd edn, Blackie and Co., London.

Rao, S.S. (1982) *The Finite Element Method in Engineering*, Pergamon Press, Oxford, U.K.

Rao, S.S. (1986) *Mechanical Vibrations*, Addison-Wesley Publishing Co., USA.

Reese, L.C., Isenhower, W.M., and Wang, S.T. (2005) *Analysis and Design of Shallow and Deep Foundations*, John Wiley & Sons, Inc., New York, USA.

Reissner, E. (1937) On the theory of beams resting on yielding foundations. *Proceedings of the National Academy of Sciences of the United States of America*, **23**, 328–333.

Reynolds, C.E. and Steadman, J.C. (1981) *Reinforced Concrete Designer's Handbook*, Cement and Concrete Association, London.

Richart, F.E., Hall, J.R., and Woods, R.D. (1970) *Vibrations of Soils and Foundations*, Prentice-Hall Inc., New Jersey.

Rijhsinghani, A. (1961) Plates Subjected to Concentrated Loads and Moments, M.S. Thesis, Illinois Institute of Technology, Chicago.

Salgado, R. (2007) *The Engineering of Foundations*, 1st edn, McGraw-Hill, USA.

Salvadori, M.G. and Baron, M.L. (1952) *Numerical Methods in Engineering*, Prentice-Hall, New York, USA.

Salvadurai, A.P.S. (1979) Elastic analysis of soil-foundation interaction, *Developments in Geotechnical Engineering*, vol. **17**, Elsevier, Amsterdam.

Scott, R.F. (1963) *Principles of Soil Mechanics*, Addison-Wesley Publishing Co., USA.

Seed, H.B. and Reese, L.C. (1957) The Action of Soft clay along Friction piles. *Transactions ASCE*, **72**, 731.

Seely, F.B. and Smith, J.O. (1952) *Advanced Mechanics of Materials*, John Wiley & Sons, Inc., New York, USA.

Sharma, H.D. and Prakash, S. (1990) *Pile Foundations in Engineering Practice*, John Wiley & Sons, Inc., New York, USA.

Skempton, A.W. (1953) Discussion on settlement of pile group in sand. Proceedings of the 3rd International Conference on Soil Mechanics and Foundation Engineering, Geneva, p. 172.

Skempton, A.W. and MacDonald, D.H. (1956) The allowable settlements of buildings. Proceedings of the Institution of Civil Engineers, III, **5**, London, pp. 759–760.

Skempton, A.W. and Bjerrum, L. (1957) A contribution to the settlement analysis of foundations on clay. *Geotechnique*, VII, 4, London, 168.
Southwell, R.V. (1946) *Relaxation Methods in Theoretical Physics*, Oxford University Press, London.
Sridhar, P. (1999) RADD-SF: Integrated Software Package for Rational Analysis, Design and Drafting of Shallow Foundations, M.Tech Thesis, Dept. of Civil Engineering, IIT, Kanpur, India.
Srinivasulu, P. and Vaidyanathan, C.V. (1976) *Handbook of Machine Foundations*, Tata McGraw-Hill Publishing Company Ltd., New Delhi, India.
Taylor, D.W. (1964) *Fundamentals of Soil Mechanics*, Asia Publishing House, New Delhi, India.
Teng, W.C. (1964) *Foundation Design*, Prentice-Hill, New Delhi, India.
Terzaghi, K. (1943) *Theoretical Soil Mechanics*, John Wiley & Sons, Inc., New York, USA.
Terzaghi, K. (1955) Evaluation of coefficient of sub grade reaction. *Geotechnique*, **5**(4), 297–326.
Terzaghi, K. and Peck, R.B. (1967) *Soil Mechanics in Engineering Practice*, John Wiley & Sons, Inc., New York, USA.
Thomson, W.T. (1965) *Vibration Theory and Applications*, Prentice-Hall Inc., New Jersey, USA.
Timoshenko, S. and Goodier, J.N. (1951) *Theory of Elasticity*, McGraw-Hill, New York, USA.
Timoshenko, S. and Woinowsky-Krieger, S. (1959) *Theory of Plates and Shells*, McGraw-Hill Book Co. Inc., New York, USA.
Tomlinson, M.J. (1977) *Pile Design and Construction Practice*, Viewpoint Publications, London, UK.
Tomlinson, M.J. (2001) *Foundation Design and Construction*, Prentice-Hall, Singapore.
UB Code – The Uniform Building Code, Structural Design Requirements, 1997.
Vesic, A.S. (1961) Bending of beams resting on isotropic elastic solid. *Journal of the Engineering Mechanics Division, ASCE* **87**, EM 2, 35–53.
Vlasov, V.Z. and Leontev, U.N. (1966) Beams, Plates and Shells on Elastic Foundations, (Translated from Russian), NASA TT F-357.
Wieghardt, K. (1922) Uber den balken auf nachgiebiger unterlage. *Zeitschrift fur Angewandte Mathematik und Mechanik*, **2**, 165–184.
Winkler, E. (1867) *Die Lehre von der elasticitaet und festigkeit*, Prag Dominicus, Berlin, p. 182.
Wolf, J.P. (1988) *Soil Structure Interaction in Time Domain*, Prentice-Hall Inc., Eaglewood Cliffs, NJ, USA.
Woods, R.D. (1976) Foundation Dynamics. *Applied Mechanics Reviews*, **29**, 1253–1258.
Zienkiewicz, O.C. (1971) *The Finite Element Method in Engineering Science*, McGraw-Hill Publishing Co., London, UK.
Zienkiewicz, O.C. and Taylor, R.L. (1989) *The Finite Element Method*, McGraw-Hill, London, UK.
Zimmermann, H. (1888) *Die Berechnung des Eisenbahnober-baues*, Berlin, Germany.

Author Index

Foundation Design: Theory and Practice N. S. V. Kameswara Rao

ISBN: 978-0-470-82534-1

Subject Index

Foundation Design: Theory and Practice N. S. V. Kameswara Rao

ISBN: 978-0-470-82534-1